NUREG/CR-5493
MEA-2376

Influence of Fluence Rate on Radiation-Induced Mechanical Property Changes in Reactor Pressure Vessel Steels

Final Report on Exploratory Experiments

Prepared by J. R. Hawthorne, A. L. Hiser

Materials Engineering Associates, Inc.

Prepared for
U.S. Nuclear Regulatory Commission

AVAILABILITY NOTICE

Availability of Reference Materials Cited in NRC Publications

Most documents cited in NRC publications will be available from one of the following sources:

1. The NRC Public Document Room, 2120 L Street, NW, Lower Level, Washington, DC 20555

2. The Superintendent of Documents, U.S. Government Printing Office, P.O. Box 37082, Washington, DC 20013-7082

3. The National Technical Information Service, Springfield, VA 22161

Although the listing that follows represents the majority of documents cited in NRC publications, it is not intended to be exhaustive.

Referenced documents available for inspection and copying for a fee from the NRC Public Document Room include NRC correspondence and internal NRC memoranda; NRC Office of Inspection and Enforcement bulletins, circulars, information notices, inspection and investigation notices; Licensee Event Reports; vendor reports and correspondence; Commission papers; and applicant and licensee documents and correspondence.

The following documents in the NUREG series are available for purchase from the GPO Sales Program: formal NRC staff and contractor reports, NRC-sponsored conference proceedings, and NRC booklets and brochures. Also available are Regulatory Guides, NRC regulations in the *Code of Federal Regulations*, and *Nuclear Regulatory Commission Issuances*.

Documents available from the National Technical Information Service include NUREG series reports and technical reports prepared by other federal agencies and reports prepared by the Atomic Energy Commission, forerunner agency to the Nuclear Regulatory Commission.

Documents available from public and special technical libraries include all open literature items, such as books, journal and periodical articles, and transactions. *Federal Register* notices, federal and state legislation, and congressional reports can usually be obtained from these libraries.

Documents such as theses, dissertations, foreign reports and translations, and non-NRC conference proceedings are available for purchase from the organization sponsoring the publication cited.

Single copies of NRC draft reports are available free, to the extent of supply, upon written request to the Office of Information Resources Management, Distribution Section, U.S. Nuclear Regulatory Commission, Washington, DC 20555.

Copies of industry codes and standards used in a substantive manner in the NRC regulatory process are maintained at the NRC Library, 7920 Norfolk Avenue, Bethesda, Maryland, and are available there for reference use by the public. Codes and standards are usually copyrighted and may be purchased from the originating organization or, if they are American National Standards, from the American National Standards Institute, 1430 Broadway, New York, NY 10018.

AVAILABILITY NOTICE

Availability of Reference Materials Cited in NRC Publications

Most documents cited in NRC publications will be available from one of the following sources:

1. The NRC Public Document Room, 2120 L Street, NW, Lower Level, Washington, DC 20555

2. The Superintendent of Documents, U.S. Government Printing Office, P.O. Box 37082, Washington, DC 20013-7082

3. The National Technical Information Service, Springfield, VA 22161

Although the listing that follows represents the majority of documents cited in NRC publications, it is not intended to be exhaustive.

Referenced documents available for inspection and copying for a fee from the NRC Public Document Room include NRC correspondence and internal NRC memoranda; NRC Office of Inspection and Enforcement bulletins, circulars, information notices, inspection and investigation notices; Licensee Event Reports; vendor reports and correspondence; Commission papers; and applicant and licensee documents and correspondence.

The following documents in the NUREG series are available for purchase from the GPO Sales Program: formal NRC staff and contractor reports, NRC-sponsored conference proceedings, and NRC booklets and brochures. Also available are Regulatory Guides, NRC regulations in the *Code of Federal Regulations*, and *Nuclear Regulatory Commission Issuances*.

Documents available from the National Technical Information Service include NUREG series reports and technical reports prepared by other federal agencies and reports prepared by the Atomic Energy Commission, forerunner agency to the Nuclear Regulatory Commission.

Documents available from public and special technical libraries include all open literature items, such as books, journal and periodical articles, and transactions. *Federal Register* notices, federal and state legislation, and congressional reports can usually be obtained from these libraries.

Documents such as theses, dissertations, foreign reports and translations, and non-NRC conference proceedings are available for purchase from the organization sponsoring the publication cited.

Single copies of NRC draft reports are available free, to the extent of supply, upon written request to the Office of Information Resources Management, Distribution Section, U.S. Nuclear Regulatory Commission, Washington, DC 20555.

Copies of industry codes and standards used in a substantive manner in the NRC regulatory process are maintained at the NRC Library, 7920 Norfolk Avenue, Bethesda, Maryland, and are available there for reference use by the public. Codes and standards are usually copyrighted and may be purchased from the originating organization or, if they are American National Standards, from the American National Standards Institute, 1430 Broadway, New York, NY 10018.

NUREG/CR-5493
MEA-2376

Influence of Fluence Rate on Radiation-Induced Mechanical Property Changes in Reactor Pressure Vessel Steels

Final Report on Exploratory Experiments

Manuscript Completed: January 1990
Date Published: March 1990

Prepared by
J. R. Hawthorne, A. L. Hiser

Materials Engineering Associates, Inc.
9700-B Martin Luther King, Jr. Highway
Lanham, MD 20706

Prepared for
Division of Engineering
Office of Nuclear Regulatory Research
U.S. Nuclear Regulatory Commission
Washington, DC 20555
NRC FIN B8900

NUREG/CR-5493

INFLUENCE OF FLUENCE RATE ON RADIATION-INDUCED MECHANICAL PROPERTY CHANGES IN REACTOR PRESSURE VESSEL STEELS

MARCH 1990

ABSTRACT

This report describes a set of experiments undertaken using a 2 MW test reactor, the UBR, to qualify the significance of fluence rate to the extent of embrittlement produced in reactor pressure vessel steels at their service temperature. The test materials included two reference plates (A 302-B, A 533-B steel) and two submerged arc weld deposits (Linde 80, Linde 0091 welding fluxes). Charpy-V (C_v), tension and 0.5T-CT compact specimens were employed for notch ductility, strength and fracture toughness (J-R curve) determinations, respectively. Target fluence rates were 8×10^{10}, 6×10^{11} and 9×10^{12} $n/cm^2 \cdot s^{-1}$. Specimen fluences ranged from 0.5 to 3.8×10^{19} n/cm^2, E > 1 MeV.

The data describe a fluence-rate effect which may extend to power reactor surveillance as well as test reactor facilities now in use. The dependence of embrittlement sensitivity on fluence rate appears to differ for plate and weld deposit materials. Relatively good agreement in fluence-rate effects definition was observed among the three test methods.

CONTENTS

Page

ABSTRACT iii
LIST OF FIGURES vii
LIST OF TABLES xi
FOREWORD xiii
ACKNOWLEDGMENT xix

1. INTRODUCTION 1

2. OBJECTIVE 3

3. MATERIALS AND IRRADIATION MATRIX 4

4. MATERIALS IRRADIATION 7

5. EXPERIMENTAL RESULTS 34

5.1 Notch Ductility and Tensile Strength Determinations ... 34
5.2 Fracture Toughness (J-R Curve) Determinations 45
5.3 Comparison of Transition Temperature Elevations by K_{Jc} and Charpy-V Test Methods 60

6. DISCUSSION 70

7. CONCLUSIONS 71

REFERENCES 72

Appendix A Neutron Dosimetry Determinations: Irradiation Assemblies UBR-38, UBR-44, UBR-45, UBR-46, UBR-65 UBR-75, UBR-76, and UBR-77 .... A-1

Appendix B Reactor Operations History: Irradiation Assemblies UBR-38, UBR-44, UBR-45, UBR-46, UBR-65 UBR-75, UBR-76, and UBR-77 .... B-1

Appendix C Tabulations of Charpy-V Notch Ductility Tests Results C-1

Appendix D Computer Curve-Fits of Charpy-V Test Results (Specimen Energy Absorption vs. Temperature) D-1

Appendix E Fracture Toughness Determinations E-1

Appendix F Computer Curve-Fits of Transition Regime Fracture Toughness Data F-1

LIST OF FIGURES

Figure		Page
1	Schematic illustration showing the locations of the irradiation facilities used in the UBR reactor	8
2	Placement of C_V and tension test specimens in Irradiation Assembly UBR-38 (Capsule A)	9
3	Placement of 0.5T-CT compact specimens in Irradiation Assembly UBR-38 (Capsule B)	10
4	Placement of C_V and tension test specimens in Irradiation Assembly UBR-44 (Capsule A)	11
5	Placement of 0.5T-CT compact specimens in Irradiation Assembly UBR-44 (Capsule B)	12
6	Placement of C_V and tension test specimens in Irradiation Assembly UBR-45 (Capsule A)	13
7	Placement of 0.5T-CT compact specimens in Irradiation Assembly UBR-45 (Capsule B)	14
8	Placement of C_V and tension test specimens in Irradiation Assembly UBR-46 (Capsule A)	15
9	Placement of 0.5T-CT compact specimens in Irradiation Assembly UBR-46 (Capsule B)	16
10	Placement of 0.5T-CT compact specimens in Irradiation Assembly UBR-65 (Capsule A)	17
11	Placement of C_V and tension test specimens in Irradiation Assembly UBR-65 (Capsule B)	18
12	Placement of 0.5T-CT compact specimens in Irradiation Assembly UBR-75 (Capsule A)	19
13	Placement of C_V and tension test specimens in Irradiation Assembly UBR-75 (Capsule B)	20
14	Placement of 0.5T-CT compact specimens in Irradiation Assembly UBR-76 (Capsule A)	21
15	Placement of C_V and tension test specimens in Irradiation Assembly UBR-76 (Capsule B)	22
16	Placement of C_V and tension test specimens in Irradiation Assembly UBR-77 (Capsule A)	23
17	Placement of 0.5T-CT compact specimens in Irradiation Assembly UBR-77 (Capsule B)	24

LIST OF FIGURES

Figure		Page
18	Irradiation Assembly UBR-38 showing thermocouple placements	26
19	Irradiation Assembly UBR-44 showing thermocouple placements	27
20	Irradiation Assembly UBR-45 showing thermocouple placements	28
21	Irradiation Assembly UBR-46 showing thermocouple placements	29
22	Irradiation Assembly UBR-65 showing thermocouple placements	30
23	Irradiation Assembly UBR-75 showing thermocouple placements	31
24	Irradiation Assembly UBR-76 showing thermocouple placements	32
25	Irradiation Assembly UBR-77 showing thermocouple placements	33
26	C_v notch ductility of the A 302-B Plate 23F after 288°C irradiation at the intermediate fluence rate	35
27	C_v notch ductility of the A 302-B Plate 23F after 288°C irradiation at the high fluence rate	36
28	C_v notch ductility of the A 302-B Plate 23F after 288°C irradiation at the low fluence rate	37
29	C_v notch ductility of the Linde 80 Weld W8A after 288°C irradiation at the intermediate fluence rate	38
30	C_v notch ductility of the Linde 80 Weld W8A after 288°C irradiation at the high fluence rate	39
31	C_v notch ductility of the A 533-B Plate 23G after 288°C irradiation at the low fluence rate	40
32	C_v notch ductility of the Linde 0091 Weld W9A after high fluence rate irradiation	41
33	Comparison of C_v 41-J transition temperature elevations observed for the Linde 80 Weld W8A, the A 302-B Plate 23F and the A 533-B Plate 23G	44

LIST OF FIGURES

Figure		Page
34	Fracture toughness data from the low fluence rate irradiation of A 3C2-B Plate 23F	47
35	Fracture toughness data from the intermediate fluence rate irradiations of A 302-B Plate 23F	48
36	Fracture toughness data from the high fluence rate irradiations of A 302-B Plate 23F	49
37	Fracture toughness data from the intermediate fluence rate irradiations of Linde 80 Weld W8A	50
38	Fracture toughness data from the high fluence rate irradiations of Linde 80 Weld W8A	51
39	Fracture toughness data from the irradiations of A 533-B Plate 23G	52
40	Fracture toughness data from the irradiation of Linde 0091 Weld W9A	53
41	Transition regime data trends for the intermediate fluence rate irradiations	54
42	Transition regime data trends for the high fluence rate irradiations	55
43	Transition temperature increase as a function of fluence for the program materials	57
44	Transition regime data for all three fluence rates	58
45	Transition regime data for the low and the high fluence rates	59
46	J-R curves for A 302-B Plate 23F	61
47	J-R curves for A 533-B Plate 23G	62
48	J-R curves for Linde 80 Weld W8A	63
49	J-R curves for Linde 0091 Weld W9A	64
50	Comparison of ΔT from C_v and ΔT from K_{Jc} for the plates	66
51	Comparison of ΔT from C_v and ΔT from K_{Jc} for the welds	67
52	Comparison of J levels at 288°C with correlation estimates	69

LIST OF TABLES

Tables		Page
1	Chemical Compositions of the Reference Plates and Submerged Arc Weld Deposits	5
2	Irradiation Matrix	6
3	Postirradiation Tensile Strengths (Ambient Temperature Tests)	42
4	Comparison of Transition Temperature Shifts (ΔT) from C_v and K_{Jc}	65

FOREWORD

The work reported here was performed at Materials Engineering Associates (MEA) under the program, Structural Integrity of Water Reactor Pressure Boundary Components, F. J. Loss, Program Manager. The program is sponsored by the Office of Nuclear Regulatory Research of the U. S. Nuclear Regulatory Commission (NRC). The technical monitor for the NRC is Alfred Taboada.

Prior reports under the current contract are listed below:

1. J. R. Hawthorne, "Significance of Nickel and Copper Content to Radiation Sensitivity and Postirradiation Heat Treatment Recovery of Reactor Vessel Steels," USNRC Report NUREG/CR-2948, Nov. 1982.

2. "Structural Integrity of Water Reactor Pressure Boundary Components, Annual Report for 1982," F. J. Loss, Ed., USNRC Report NUREG/CR-3228, Vol. 1, Apr. 1983.

3. J. R. Hawthorne, "Exploratory Assessment of Postirradiation Heat Treatment Variables in Notch Ductility Recovery of A 533-B Steel," USNRC Report NUREG/CR-3229, Apr. 1983.

4. W. H. Cullen, K. Torronen, and M. Kemppainen, "Effects of Temperature on Fatigue Crack Growth of A 508-2 Steel in LWR Environment," USNRC Report NUREG/CR-3230, Apr. 1983.

5. "Proceedings of the International Atomic Energy Agency Specialists' Meeting on Subcritical Crack Growth," Vols. 1 and 2, W. H. Cullen, Ed., USNRC Conference Proceeding NUREG/CP-0044, May 1983.

6. W. H. Cullen, "Fatigue Crack Growth Rates of A 508-2 Steel in Pressurized, High-Temperature Water," USNRC Report NUREG/CR-3294, June 1983.

7. J. R. Hawthorne, B. H. Menke, and A. L. Hiser, "Light Water Reactor Pressure Vessel Surveillance Dosimetry Improvement Program: Notch Ductility and Fracture Toughness Degradation of A 302-B and A 533-B Reference Plates from PSF Simulated Surveillance and Through-Wall Irradiation Capsules," USNRC Report NUREG/CR-3295, Vol. 1, Apr. 1984.

8. J. R. Hawthorne and B. H. Menke, "Light Water Reactor Pressure Vessel Surveillance Dosimetry Improvement Program: Postirradiation Notch Ductility and Tensile Strength Determinations for PSF Simulated Surveillance and Through-Wall Specimen Capsules," USNRC Report NUREG/CR-3295, Vol. 2, Apr. 1984.

9. A. L. Hiser and F. J. Loss, "Alternative Procedures for J-R Curve Determination," USNRC Report NUREG/CR-3402, July 1983.

10. A. L. Hiser, F. J. Loss, and B. H. Menke, "J-R Curve Characterization of Irradiated Low Upper Shelf Welds," USNRC Report NUREG/CR-3506, Apr. 1984.

11. W. H. Cullen, R. E. Taylor, K. Torronen, and M. Kemppainen, "The Temperature Dependence of Fatigue Crack Growth Rates of A 351 CF8A Cast Stainless Steel in LWR Environment," USNRC Report NUREG/CR-3546, Apr. 1984.

12. "Structural Integrity of Light Water Reactor Pressure Boundary Components -- Four-Year Plan 1984-1988," F. J. Loss, Ed., USNRC Report NUREG/CR-3788, Sep. 1984.

13. W. H. Cullen and A. L. Hiser, "Behavior of Subcritical and Slow-Stable Crack Growth Following a Postirradiation Thermal Anneal Cycle," USNRC Report NUREG/CR-3833, Aug. 1984.

14. "Structural Integrity of Water Reactor Pressure Boundary Components: Annual Report for 1983," F. J. Loss, Ed., USNRC Report NUREG/CR-3228, Vol. 2, Sept. 1984.

15. W. H. Cullen, "Fatigue Crack Growth Rates of Low-Carbon and Stainless Piping Steels in PWR Environment," USNRC Report NUREG/CR-3945, Feb. 1985.

16. W. H. Cullen, M. Kemppainen, H. Hanninen, and K. Torronen, "The Effects of Sulfur Chemistry and Flow Rate on Fatigue Crack Growth Rates in LWR Environments," USNRC Report NUREG/CR-4121, Feb. 1985.

17. "Structural Integrity of Water Reactor Pressure Boundary Components: Annual Report for 1984," F. J. Loss, Ed., USNRC Report NUREG/CR-3228, Vol. 3, June 1985.

18. A. L. Hiser, "Correlation of C_v and K_{Ic}/K_{Jc} Transition Temperature Increases Due to Irradiation," USNRC Report NUREG/CR-4395, Nov. 1985.

19. W. H. Cullen, G. Gabetta, and H. Hanninen, "A Review of the Models and Mechanisms For Environmentally-Assisted Crack Growth of Pressure Vessel and Piping Steels in PWR Environments," USNRC Report NUREG/CR-4422, Dec. 1985.

20. "Proceedings of the Second International Atomic Energy Agency Specialists' Meeting on Subcritical Crack Growth," W. H. Cullen, Ed., USNRC Conference Proceeding NUREG/CP-0067, Vols. 1 and 2, Apr. 1986.

21. J. R. Hawthorne, "Exploratory Studies of Element Interactions and Composition Dependencies in Radiation Sensitivity Development," USNRC Report NUREG/CR-4437, Nov. 1985.

22. R. B. Stonesifer and E. F. Rybicki, "Development of Models for Warm Prestressing," USNRC Report NUREG/CR-4491, Jan. 1987.

23. E. F. Rybicki and R. B. Stonesifer, "Computational Model for Residual Stresses in a Clad Plate and Clad Fracture Specimens," USNRC Report NUREG/CR-4635, Oct. 1986.

24. D. E. McCabe, "Plan for Experimental Characterization of Vessel Steel After Irradiation," USNRC Report NUREG/CR-4636, Oct. 1986.

25. E. F. Rybicki, J. R. Shadley, and A. S. Sandhu, "Experimental Evaluation of Residual Stresses in a Weld Clad Plate and Clad Test Specimens," USNRC Report NUREG/CR-4646, Oct. 1986.

26. "Structural Integrity of Water Reactor Pressure Boundary Components: Annual Report for 1985," F. J. Loss, Ed., USNRC Report NUREG/CR-3228, Vol. 4, June 1986.

27. G. Gabetta and W. H. Cullen, "Application of a Two-Mechanism Model for Environmentally-Assisted Crack Growth," USNRC Report NUREG/CR-4723, Oct. 1986.

28. W. H. Cullen, "Fatigue Crack Growth Rates in Pressure Vessel and Piping Steels in LWR Environments," USNRC Report NUREG/CR-4724, Mar. 1987.

29. W. H. Cullen and M. R. Jolles, "Fatigue Crack Growth of Part-Through Cracks in Pressure Vessel and Piping Steels: Air Environment Results, USNRC Report NUREG/CR-4828, Oct. 1988.

30. D. E. McCabe, "Fracture Evaluation of Surface Cracks Embedded in Reactor Vessel Cladding: Unirradiated Bend Specimen Results," USNRC Report NUREG/CR-4841, May 1987.

31. H. Hanninen, M. Vulli, and W. H. Cullen, "Surface Spectroscopy of Pressure Vessel Steel Fatigue Fracture Surface Films Formed in PWR Environments," USNRC Report NUREG/CR-4863, July 1987.

32. A. L. Hiser and G. M. Callahan, "A User's Guide to the NRC's Piping Fracture Mechanics Data Base (PIFRAC)," USNRC Report NUREG/CR-4894, May 1987.

33. "Proceedings of the Second CSNI Workshop on Ductile Fracture Test Methods (Paris, France, April 17-19, 1985)," F. J. Loss, Ed., USNRC Conference Proceeding NUREG/CP-0064, Aug, 1988.

34. W. H. Cullen and D. Broek, "The Effects of Variable Amplitude Loading on A 533-B Steel in High-Temperature Air and Reactor Water Environments," USNRC Report NUREG/CR-4929, Apr. 1989.

35. "Structural Integrity of Water Reactor Pressure Boundary Components: Annual Report for 1986," F. J. Loss, Ed., USNRC Report NUREG/CR-3228, Vol. 5, July 1987.

36. F. Ebrahimi, et al., "Development of a Mechanistic Understanding of Radiation Embrittlement in Reactor Pressure Vessel Steels: Final Report," USNRC Report NUREG/CR-5063, Jan. 1988.

37. J. B. Terrell, "Fatigue Life Characterization of Smooth and Notched Piping Steel Specimens in 288°C Air Environments," USNRC Report NUREG/CR-5013, May 1988.

38. A. L. Hiser, "Tensile and J-R Curve Characterization of Thermally Aged Cast Stainless Steels," USNRC Report NUREG/CR-5024, Sept. 1988

39. J. B. Terrell, "Fatigue Strength of Smooth and Notched Specimens of ASME SA 106-B Steel in PWR Environments," USNRC Report NUREG/CR-5136, Sept. 1988.

40. D. E. McCabe, "Fracture Evaluation of Surface Cracks Embedded in Reactor Vessel Cladding: Material Property Evaluations" USNRC NUREG/CR-5207, Sept. 1988.

41. J. R. Hawthorne and A. L. Hiser, "Experimental Assessments of Gundremmingen RPV Archive Material for Fluence Rate Effects Studies," USNRC Report NUREG/CR-5201, Oct. 1988.

42. J. B. Terrell, "Fatigue Strength of ASME SA 106-B Welded Steel Pipes in 288°C Air Environments," USNRC Report NUREG/CR-5195, Dec. 1988.

43. A. L. Hiser, "Post-Irradiation Fracture Toughness Characterization of Four Lab-Melt Plates," USNRC Report NUREG/CR-5216, Rev. 1, June 1989.

44. R. B. Stonesifer, E. F. Rybicki, and D. E. McCabe, "Warm Prestress Modeling: Comparison of Models and Experimental Results," USNRC Report NUREG/CR-5208, Apr. 1989.

45. A. L. Hiser and J. B. Terrell, "Size Effects on J-R Curves for A 302-B Plate," USNRC Report NUREG/CR-5265, Jan. 1989.

46. D. E. McCabe, "Fracture Evaluation of Surface Cracks Embedded in Reactor Vessel Cladding," USNRC Report NUREG/CR-5326, Mar. 1989.

47. J. R. Hawthorne, "An Exploratory Study of Element Interactions and Composition Dependencies in Radiation Sensitivity Development: Final Report," USNRC Report NUREG/CR-5357, Apr. 1989

48. J. R. Hawthorne, "Steel Impurity Element Effects on Postirradiation Properties Recovery by Annealing: Final Report," USNRC Report NUREG/CR-5388, Aug. 1989.

49. J. R. Hawthorne, "Irradiation-Anneal-Reirradiation (IAR) Studies of Prototypic Reactor Vessel Weldments," USNRC Report NUREG/CR-5469, Nov. 1989.

50. J. R. Hawthorne and A. L. Hiser, "Investigations of Irradiation-Anneal-Reirradiation (IAR) Properties Trends of RPV Welds: Phase 2 Final Report," USNRC Report NUREG/CR-5492, Jan. 1990.

51. H. H. Hanninen and W. H. Cullen, "Slow Strain Rate Testing of a Cyclically Stabilized A-516 Gr. 70 Piping Steel in PWR Conditions," USNRC Report NUREG/CR-5327, Nov. 1989.

52. A. L. Hiser, "Fracture Toughness Characterization of Nuclear Piping Steels," USNRC Report NUREG/CR-5188, Nov. 1989.

Prior reports dealing with the specific topic of this report are listed below:

J. R. Hawthorne and A. L. Hiser, "Experimental Assessments of Gundremmingen RPV Archive Material for Fluence Rate Effects Studies," USNRC Report NUREG/CR-5201, Oct. 1988.

ACKNOWLEDGMENT

The authors express their appreciation to J. W. Rogers of EG&G Idaho, Inc. for his personal efforts in neutron dosimetry determinations for the MEA irradiation assemblies.

The authors thank W. E. Hagel, L. LaMont, B. H. Menke, C. L. Miller, K. C. Miller, D. Schaffer and G. Lohr for their individual contributions to the irradiation and postirradiation phases of the program and E. D'Ambrosio for her contributions in preirradiation material properties determinations. The assistance of T. Ramey in the reduction of the fracture toughness test data, E. Martinez for her C_v data curve fittings and G. Carlson for his preparation of graphics for this report are also acknowledged with gratitude.

1. INTRODUCTION

The present investigation was undertaken with the objective of qualifying, under closely controlled experimental conditions, the influence of radiation exposure rate on embrittlement accrual in reactor pressure vessel (RPV) steels. The question of fluence-rate or dose-rate effects on radiation-induced embrittlement in nuclear service has its origins in the 1950's when accelerated irradiation exposures were first applied to study end-of-life (EOL) nuclear service effects. Materials testing reactors such as the MTR and ETR in Idaho, the LITR and ORR in Tennessee and the UBR and UCRR in New York have been vehicles for high fluence-rate exposures of reactor structural materials including RPV steels. In these reactors, radiation exposures of a few weeks or a few months in duration can equal projected EOL fluences for commercial power reactor vessels or internals. Whether or not the same magnitude of "damage" would be exhibited by materials irradiated under "fast" versus "slow" fluence accumulation conditions was a recognized uncertainty by the 1960's. This uncertainty was one key reason that power reactor vessel surveillance programs were undertaken. To guide such efforts, ASTM E 185: Standard Practice for Conducting Surveillance Tests for Light-Water-Cooled Nuclear Power Reactor Vessels was drafted.

Early investigations of fluence-rate effects, using test reactor experiments, did not reveal a significant influence of this exposure variable on steel property changes. For example, Harries and Eyre (Ref. 1) compared the effects of a 100:1 difference in exposure rate at an irradiation temperature of less than 200°C and found no apparent difference in the strength elevation with increasing fluence rate. The use of a low exposure temperature precluded thermal contributions from modifying the result. The fluence was on the order of 3×10^{17} n/cm^2. Nonetheless, strength changes were appreciable and sufficient for their analyses. One limitation of the data set was the short time frame of the lowest fluence-rate exposure (about 200 hours). Unlike the indication of these data, data derived from power reactor surveillance programs compared recently to test reactor data banks do provide indications of a fluence-rate effect or a time-at-temperature effect, or a combination of both. In most instances, the data bank information does not offer a 1:1 comparison for a specific material. Rather, the fluence-rate effect is inferred from comparisons of material trends depicting embrittlement tendencies for exposures in the two reactor types. In a few cases, correlation-monitor materials such as the ASTM A 302-B reference plate (Ref. 2) or plates of the Heavy Section Steel Technology Program (HSST Plates 01, 02 or 03) were included in the surveillance program and permit a bridge to other irradiation tests. Unfortunately, such data do not cover a broad fluence range. In turn, a basis for a critical test of fluence-rate contributions is not provided.

A further impediment to testing for fluence-rate effects is the general tie between fluence-rate level and neutron spectrum. Decoupling these two factors experimentally is, difficult if not impossible. (Harries and Eyres solved this problem by having their reactor operated at three power levels.) Progress made in neutron metrology in recent years offers partial solutions to this problem. Calculations of actual neutron spectra conditions, for example, are now available. Their use replaces the former practice of assuming a fission spectrum neutron energy distribution. Also, the exposure unit: displacements per atom (dpa) has been developed as a measure of damage production potential and is an alternative to non-weighted measures such as fluence E > 1 MeV or fluence E > 0.1 MeV for irradiation comparisons and descriptions. To the extent possible, both measures of neutron exposure are reported here. One reason is that significant portions of data in existing banks are referenced to fluence, E > 1 MeV, only. The reporting of neutron exposure in both frameworks is consistent with ASTM recommendations (Ref. 3)

This report presents MEA findings to date from its exploratory study for validating fluence rate as an exposure variable. It is noted here that one long term (3.7 year) experiment of the original matrix is still under irradiation for the NRC; results from this experiment are expected in 1991.

2. OBJECTIVE

The general objective was to clarify and confirm the significance of fluence rate for the NRC's projection of fracture resistance changes in RPV steels by irradiation at their service temperature, nominally 288°C (550°F). The research plan was to test the influence for three fluence levels: one (herein termed "low") corresponding to early vessel life; a second (termed "intermediate") corresponding approximately to the inflection of the embrittlement versus fluence curve, and the last (termed "high") corresponding to mid-vessel life measured at the inner wall surface of the vessel. (Target fluence levels were dictated in part by the fluence obtainable in a four year program.) Target fluence rates were: $8\text{-}9 \times 10^{10}$, $5\text{-}6 \times 10^{11}$ and $8\text{-}9 \times 10^{12}$ $n/cm^2 \cdot s^{-1}$. The lowest target value corresponds approximately to the upper end of the range for PWR vessel service; the highest target value corresponds to that level equated with in-core experiments in many materials testing reactors.

Fluence-rate effects were to be judged independently from: (1) relative change in notch ductility determined with the Charpy-V (C_v) test method, (2) the relative change in tensile strength determined with 5.74 mm gage diameter tensile specimens, and (3) relative change in fracture toughness (K_{Jc} and J-R curve) as defined with 12.7 mm thick (0.5T-CT) compact specimens.

The plan called for the use of reference plates and welds having a high copper content to assure a relatively-high radiation embrittlement sensitivity. High copper content materials are commonly found in older-vintage RPV's and primarily are the source of present concerns over the fracture resistance of these structures.

3. MATERIALS AND IRRADIATION MATRIX

Four materials were selected for investigation (Table 1). The A 302-B plate is the ASTM correlation-monitor material which has seen extensive use in test and power reactor irradiation programs as a reference material. The A 533-B plate represents the steel composition chosen for more recent RPV construction in the U.S.A. and abroad. Copper contents (~ 0.2% Cu) are illustrative of "high copper content" plates from non-improved steelmaking production (Ref. 4). The plates were arbitrarily coded 23F and 23G, respectively, for ready identification.

The submerged arc welds were made with Linde 80 welding flux or Linde 0091 welding flux and were coded W8A and W9A, respectively. These fluxes represent the two generic types used in RPV construction in the U.S.A. Welds made with Linde 80 tend to have a low as-fabricated C_v upper shelf energy (USE) level (80-120 J); welds made with Linde 0091 or Linde 124 tend to have a high as-fabricated C_v USE (greater than 150 J). Both welds were made commercially, using the same lot of welding wire. Only the welding flux (ϕ) type differed. Accordingly, a direct test of the significance of welding flux type to irradiation behavior could be accomplished. Copper contents of the weld deposits (~ 0.35% Cu, target) were derived primarily from the copper cladding of the welding wire.

Specimens were removed from the A 302-B plate and the A 533-B plate to represent the L-T (longitudinal, strong) and T-L (transverse, weak) test orientation, respectively. Those from the welds were aligned to have the plane of fracture parallel to the welding direction and perpendicular to the weldment surface. The weld sampling region was in accordance with ASTM Standard Practice E 185. Depending on specimen type, the A 533-B samples were removed in two or three layers bracketing the 1/4T thickness plane. For the A 302-B plate, the C_v and tensile specimens were taken from one layer located just above the 1/2T plane of the plate. The CT specimens were removed in one layer immediately beneath the C_v and tensile specimens. The use of the 3/8 to 5/8T location material, instead of the preferred 1/4T location material was with NRC concurrence and was dictated by the current shortage of ASTM reference plate material worldwide. (Note: The adjoining 1/4T and 3/4T material was consumed in the performance of the NRC's LWR-SDIP Study (Ref. 5)).

Table 2 shows the irradiation test matrix for the materials. To date, data have been developed for all experiment assemblies except UBR-49 whose irrdiation is still underway.

TABLE I Chemical Compositions of the Reference Plates and Submerged Arc Weld Deposits

Material	Code	Chemical Composition (Weight-Percent) C	Mn	Si	P	S	Ni	Cr	Mo	Cu	Sn
A 302-B Plate	23F	0.24	1.34	0.23	0.011	0.023	0.18	0.11	0.51	0.21	0.037
A 533-B Plate	23G	0.22	1.40	0.19	0.017	0.008	0.63	0.19	0.54	0.20	...[a]
S/A Weld (Linde 80 ϕ)	W8A	0.079(min)[b] 0.096(max)	1.27 1.36	0.71 0.79	0.010 0.017	0.012 0.019	0.55 0.68	0.10 0.13	0.42 0.50	0.37 0.42	0.002 0.004
S/A Weld (Linde 0091 ϕ)	W9A	0.19 (min) 0.19 (max)	1.21 1.27	0.23 0.23	0.008 0.012	0.005 0.010	0.64 0.77	0.10 0.11	0.49 0.50	0.35 0.43	0.003 0.004

[a] Not analyzed

[b] Range (min/max) observed, multiple test locations in 1.83-m long weld seam

TABLE 2 Irradiation Matrix

Material	Target Fluence[a] ($\times 10^{19}$)	Neutron Fluence Rate[b]: High (9×10^{12})	Intermediate (6×10^{11})	Low (8×10^{10})
A 302-B	0.5	UBR-65[c]	UBR-44	UBR-38
	1.0	UBR-75	UBR-46	...
	2.0	UBR-76	UBR-45	...
S/A Weld (Linde 80 ϕ)	0.5	UBR-65	UBR-44	UBR-49[d]
	1.0	UBR-75	UBR-46	...
	2.0	UBR-76	UBR-45	...
A 533-B	0.5	UBR-77	...	UBR-38
S/A Weld (Linde 0091 ϕ)	0.5	UBR-77	...	UBR-49[d]
		(In-Core)	(Core-Edge)	(Reflector)

[a] n/cm^2, $E > 1$ MeV

[b] $n/cm^2 \cdot s^{-1}$, $E > 1$ MeV

[c] Irradiation assembly number

[d] UBR-49 (irradiation in progress).

4. MATERIALS IRRADIATION

The reactor chosen for the irradiations was the UBR reactor at the Buffalo Materials Research Center (BMRC). The BMRC is located on the campus of the State University of New York at Buffalo. The UBR is a 2 MW pool-type test reactor having a low fuel enrichment (~ 6 percent) comparable to that of power reactors. Easy access for instrumented (lead-type) experimental assemblies and a capability for irradiating several assemblies at different fluence rates simultaneously were factors in its choice. The general arrangement of the MEA experiment facilities relative to the fuel core is illustrated in Fig. 1.

The in-core facilities (B4 and C2) provide a nominal fluence rate of 8-9 x 10^{12} n/cm^2·s^{-1}; those at the core edge provided the intermediate fluence rate of 5-6 x 10^{11} n/cm^2·s^{-1}. MEA experiments for the in-core and the core-edge facilities are designed to use gamma heating to attain the desired specimen irradiation temperature, in this case 288°C. Accordingly, sample temperatures drop automatically (to about 50°C) whenever the reactor is shut down. The reflector region facility (a dry standpipe) provided the lowest fluence rate. Here, the target temperature is achieved primarily by resistance heaters located external to the specimen assembly. The control instrumentation reduces specimen temperatures during reactor outages. Proper standpipe position relative to the fuel lattice for the target fluence rate was established in advance using a "dummy" assembly.

Irradiation periods to attain a fluence of 0.5 x 10^{19} n/cm^2 are about 2, 27 and 175 weeks for the three respective exposure locations. Because of the slow fluence accumulation in the standpipe, only a target fluence of 0.5 x 10^{19} n/cm^2 was included in the irradiation matrix. Each assembly typically was rotated by 180 deg in the irradiation facility at least once during the in-reactor residence period for fluence balancing across the specimen array.

Neutron spectrum conditions in the three facilities have been calculated for MEA (NRC) by outside laboratories. Calculations by Hanford Engineering Development Laboratory (HEDL) for the in-core facilities are given in Ref. 6 and 7. Those by the Institut fur Kerntechnik und Energiewandlung eV (IKE) for the core-edge and reflector region facilities are given in Ref. 8. Fluence (E > 1 MeV) measurements employed iron and nickel wire dosimeters placed within the specimen arrays. Most assemblies also included cobalt-aluminum, silver-aluminum and uranium dosimeters to supplement the results from iron and nickel. Irradiated dosimeters are analyzed routinely for MEA by EG&G Idaho, Inc. (J. W. Rogers). The levels of uncertainty it assigns to fluence rates by iron, nickel and ^{238}U analyses are, respectively, ± 8, ± 7 and ± 5 percent at the 1σ confidence level, exclusive of uncertainties associated with the actual spectrum averaged cross sections of the irradiation fields or burnout of the reaction products of interest.

Figure 2 through 17 show the specimen loadings in the individual capsules of each irradiation assembly. Neutron fluences, n/cm^2

(text continues on pg. 25)

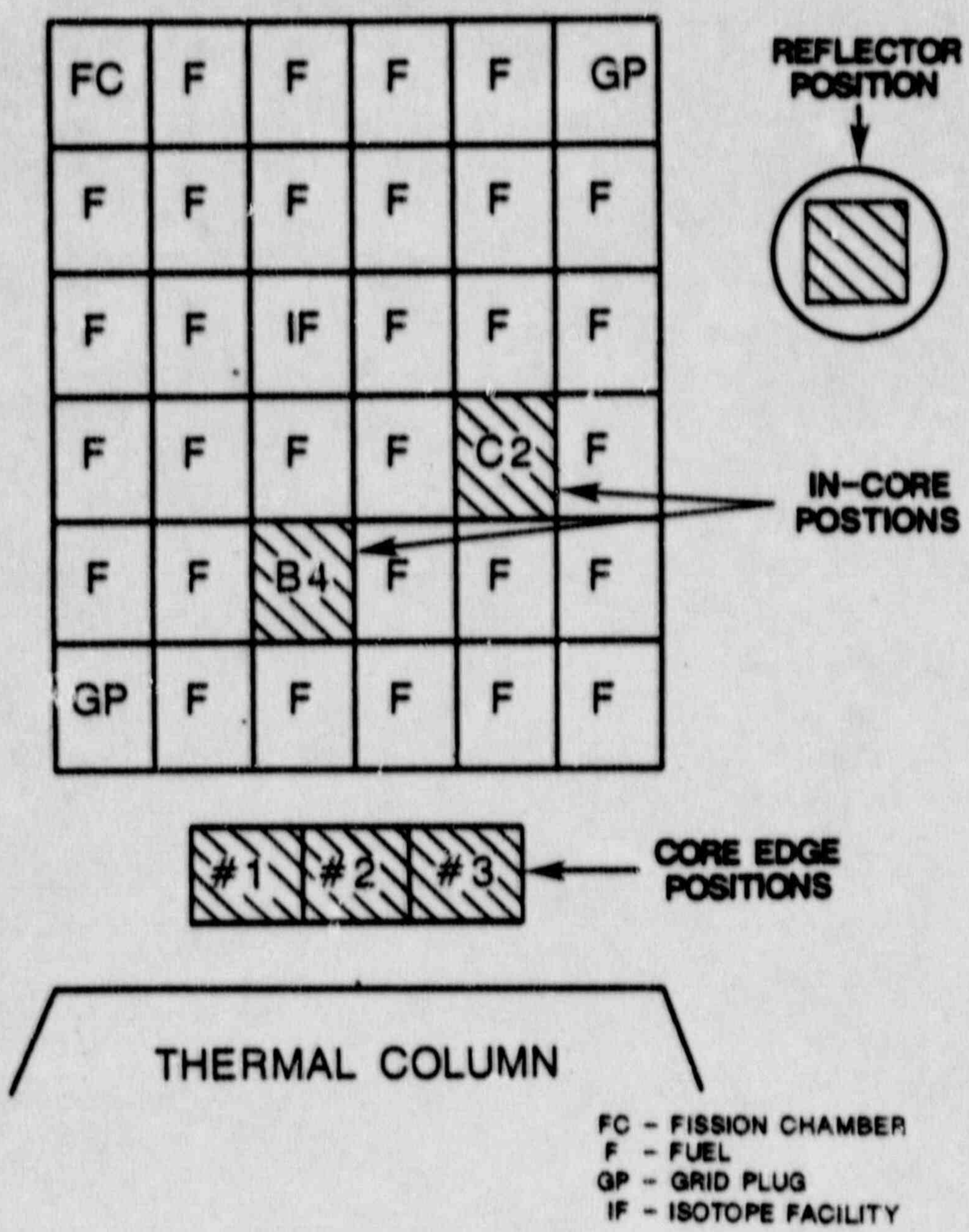

Fig. 1 Schematic illustration showing the locations of the irradiation facilities used for fluence-rate effects qualification experiments in the UBR reactor.

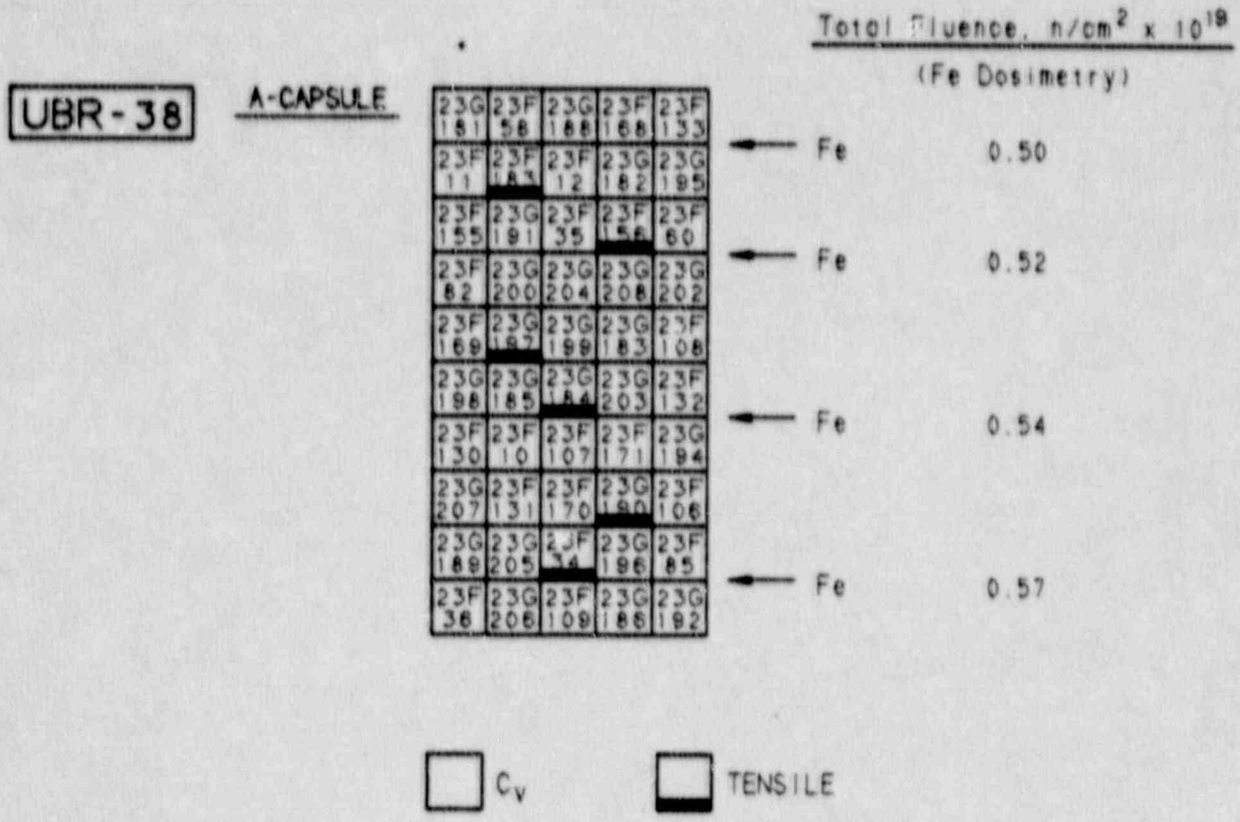

Fig. 2 Placement of C_v and tension test specimens in Irradiation Assembly UBR-38 (Capsule A; elevation view). Average neutron fluence values, based on iron dosimetry, are shown in this figure and Figure 3 to Figure 17. Determinations based on ^{238}U dosimetry, are also shown where available.

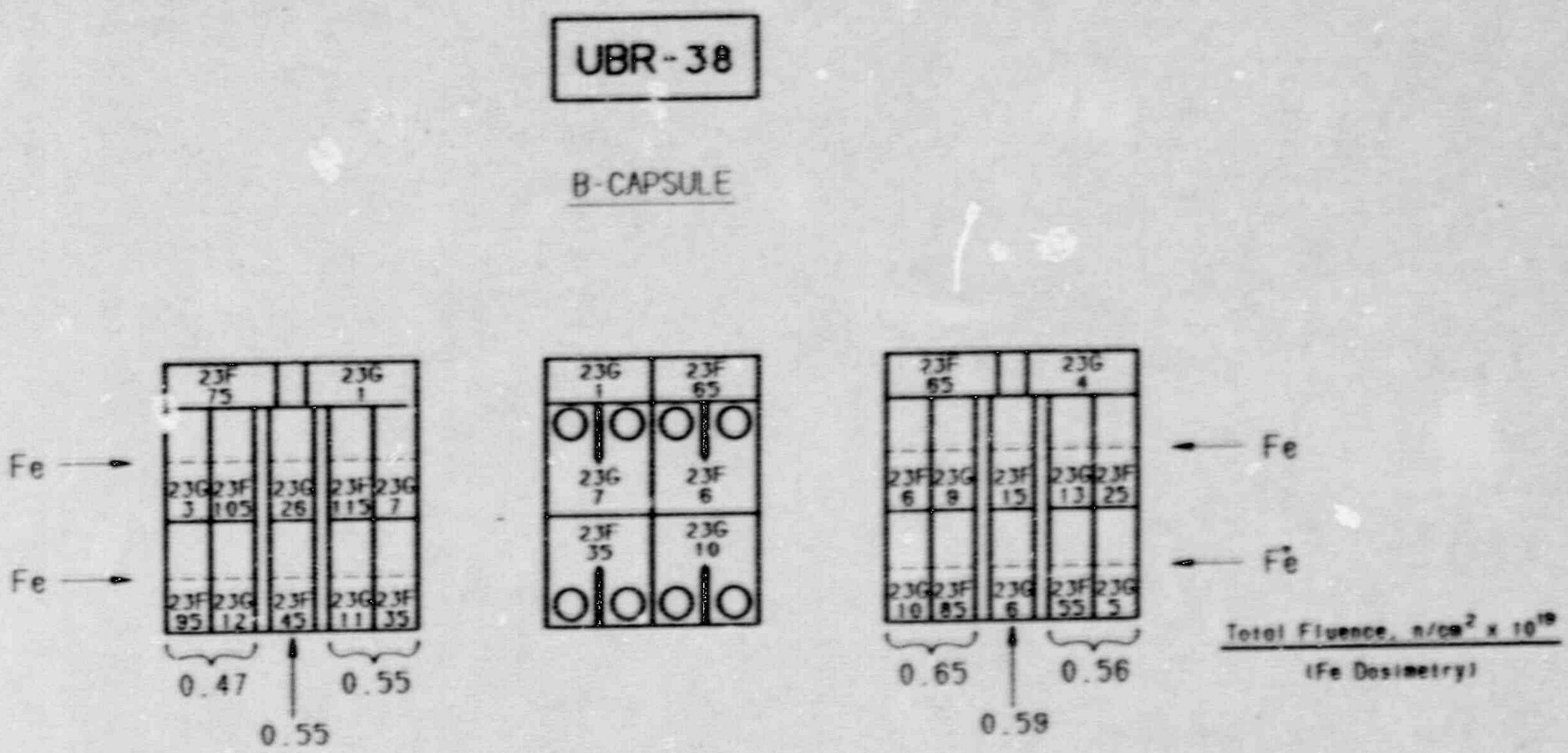

Fig. 3 Placement of 0.5T-CT compact specimens in Irradiation Assembly UBR-38 (Capsule B; elevation view).

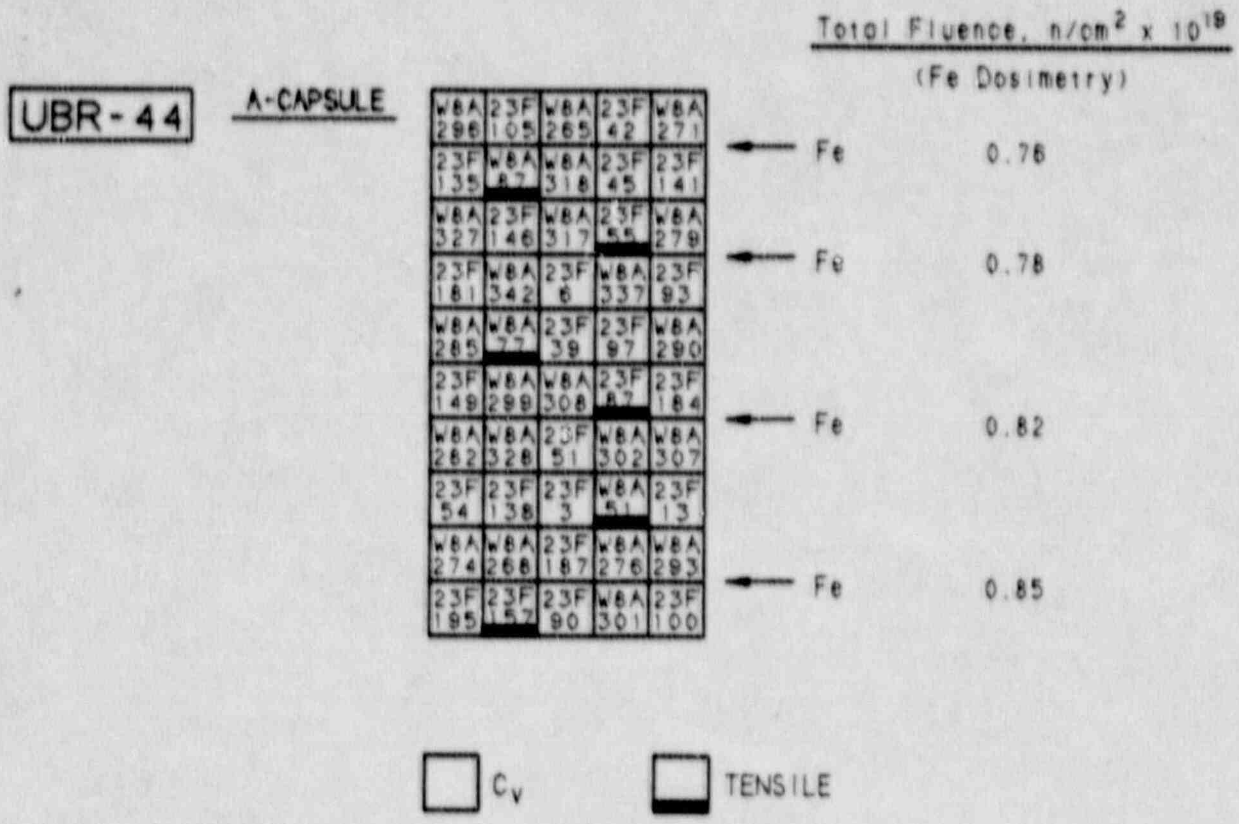

Fig. 4 Placement of C_v and tension test specimens in Irradiation Assembly UBR-44 (Capsule A; elevation view).

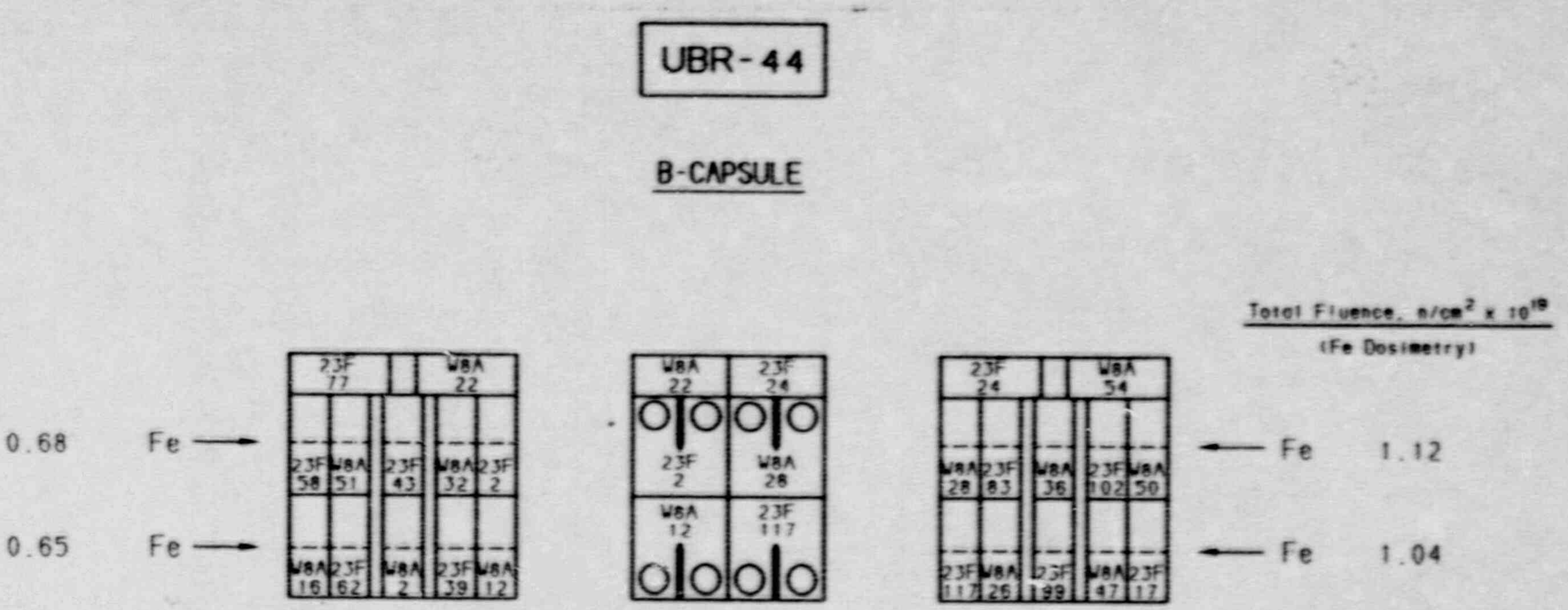

Fig. 5 Placement of 0.5T-CT compact specimens in Irradiation Assembly UBR-44 (Capsule B; elevation view).

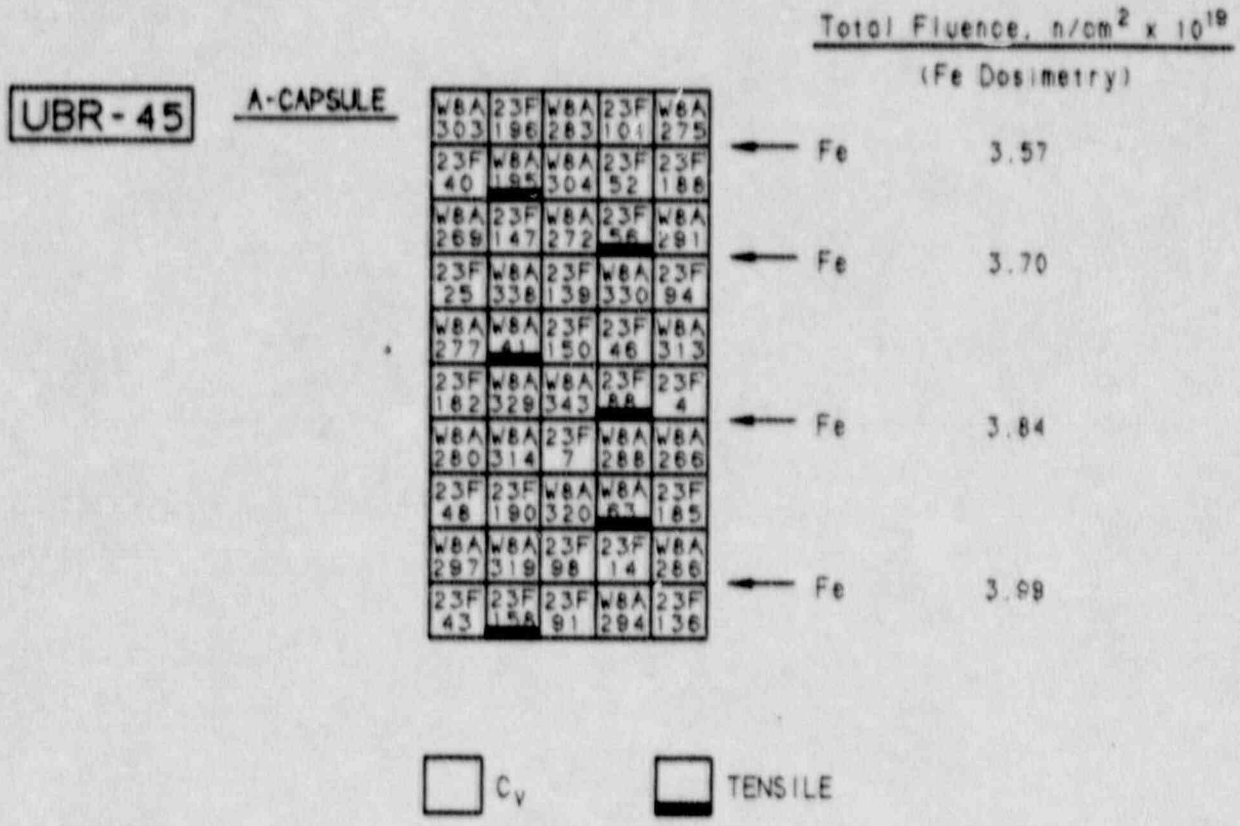

Fig. 6 Placement of C_v and tension test specimens in Irradiation Assembly UBR-45 (Capsule A; elevation view).

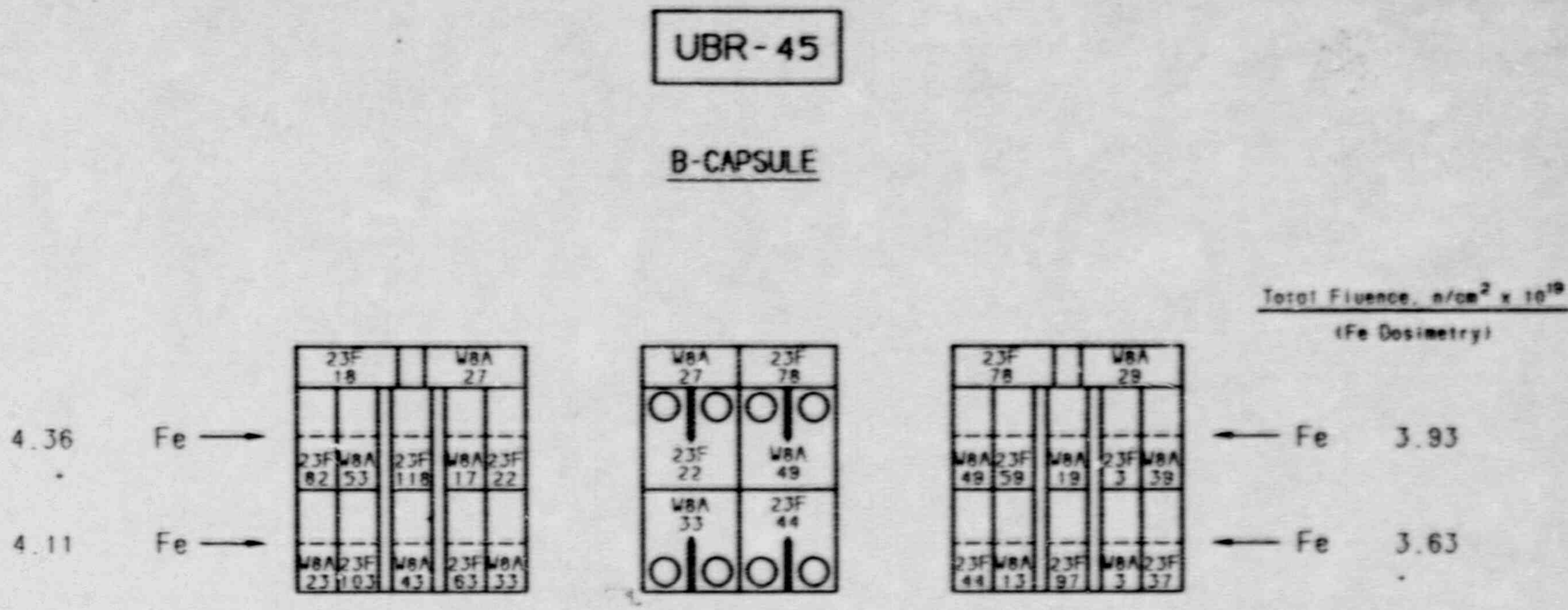

Fig. 7 Placement of 0.5T-CT compact specimens in Irradiation Assembly UBR-45 (Capsule B; elevation view).

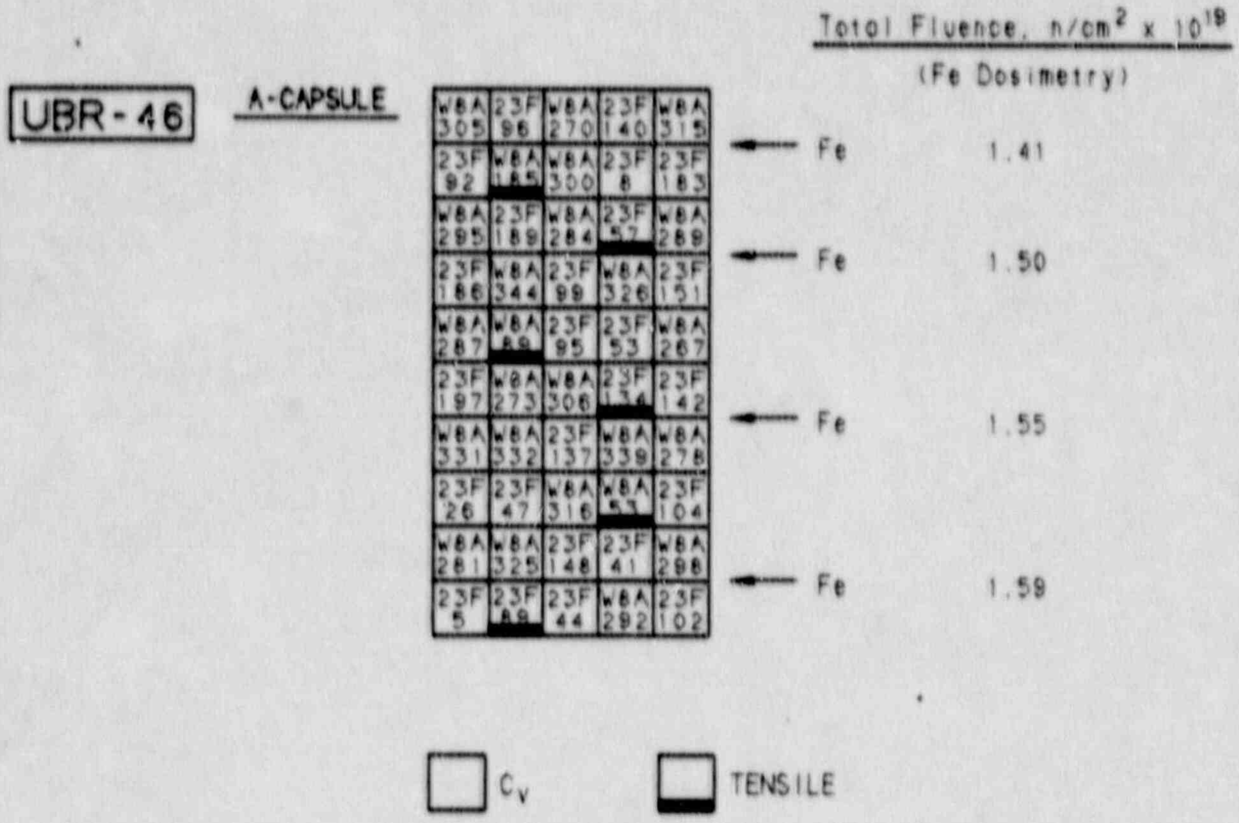

Fig. 8 Placement of C_v and tension test specimens in Irradiation Assembly UBR-46 (Capsule A; elevation view).

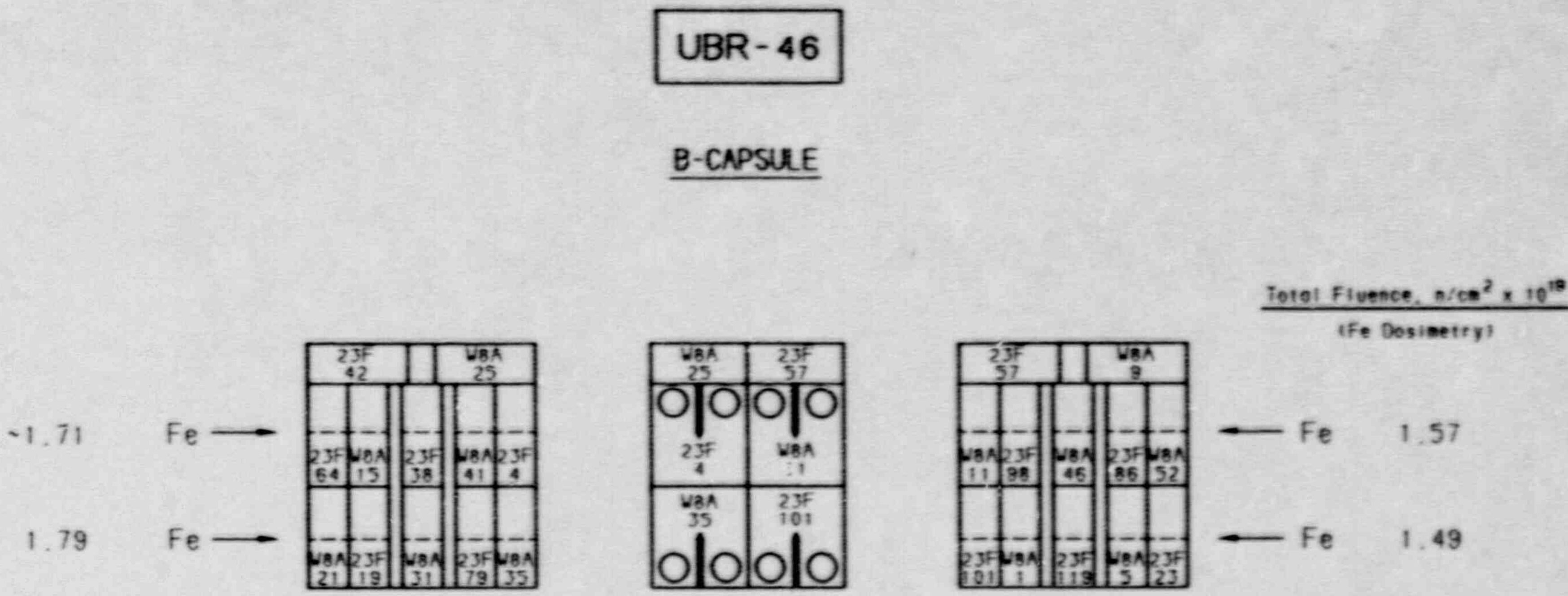

Fig. 9 Placement of 0.5T-CT compact specimens in Irradiation Assembly UBR-46 (Capsule B; elevation view).

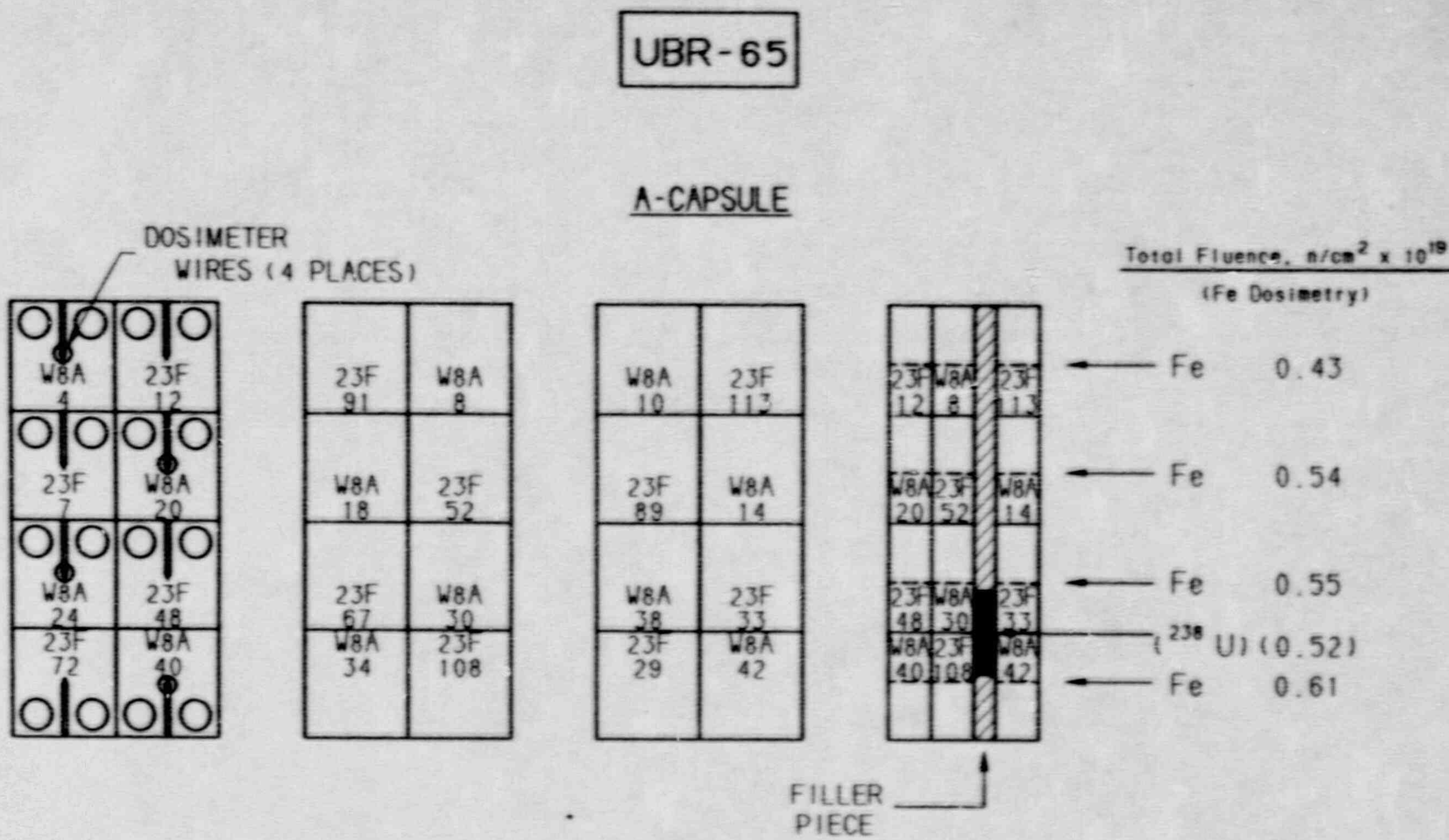

Fig. 10 Placement of 0.5T-CT compact specimens in Irradiation Assembly UBR-65 (Capsule A; elevation view).

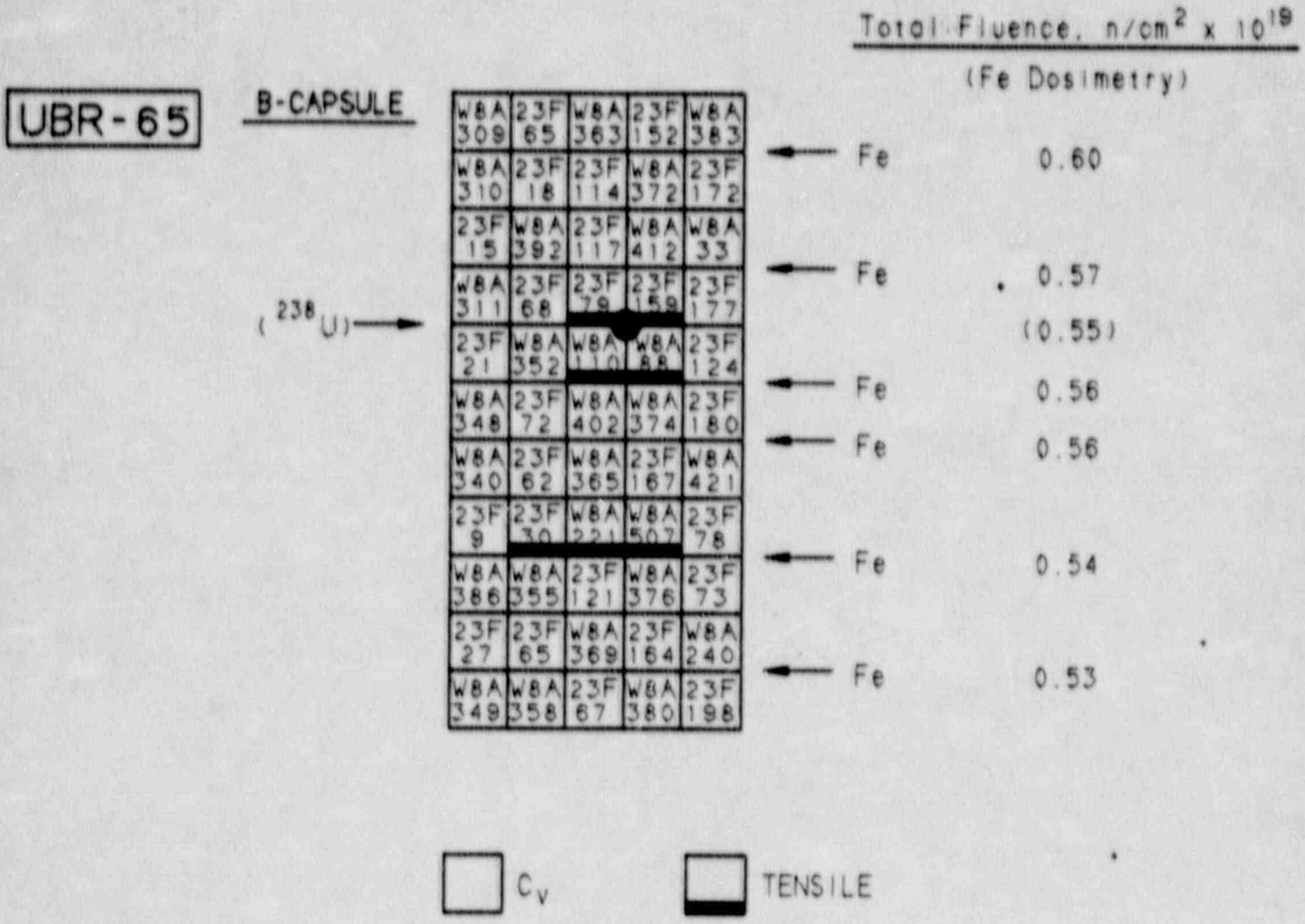

Fig. 11 Placement of C_v and tension test specimens in Irradiation Assembly UBR-65 (Capsule B; elevation view).

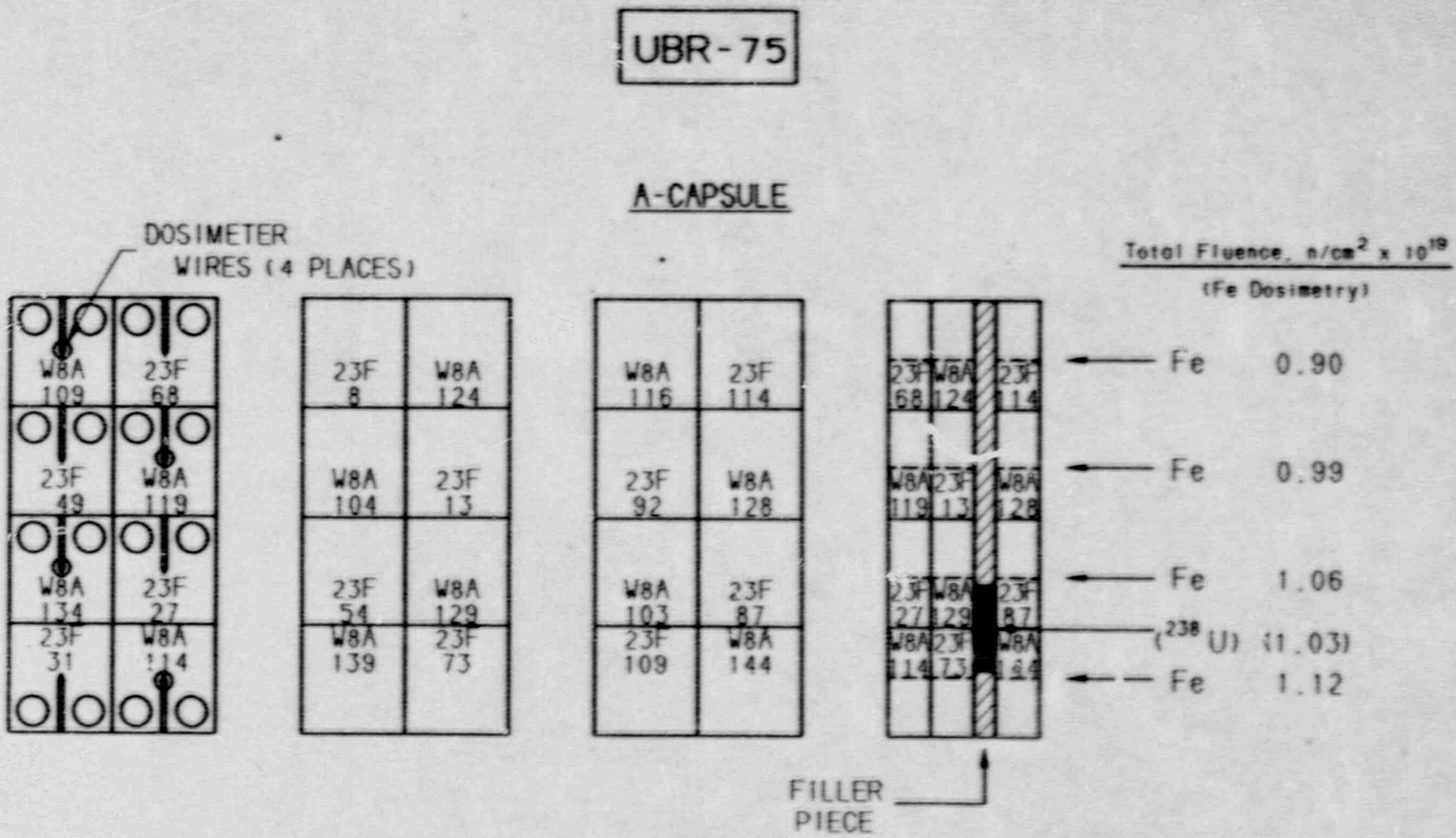

Fig. 12 Placement of 0.5T-CT compact specimens in Irradiation Assembly UBR-75 (Capsule A; elevation view).

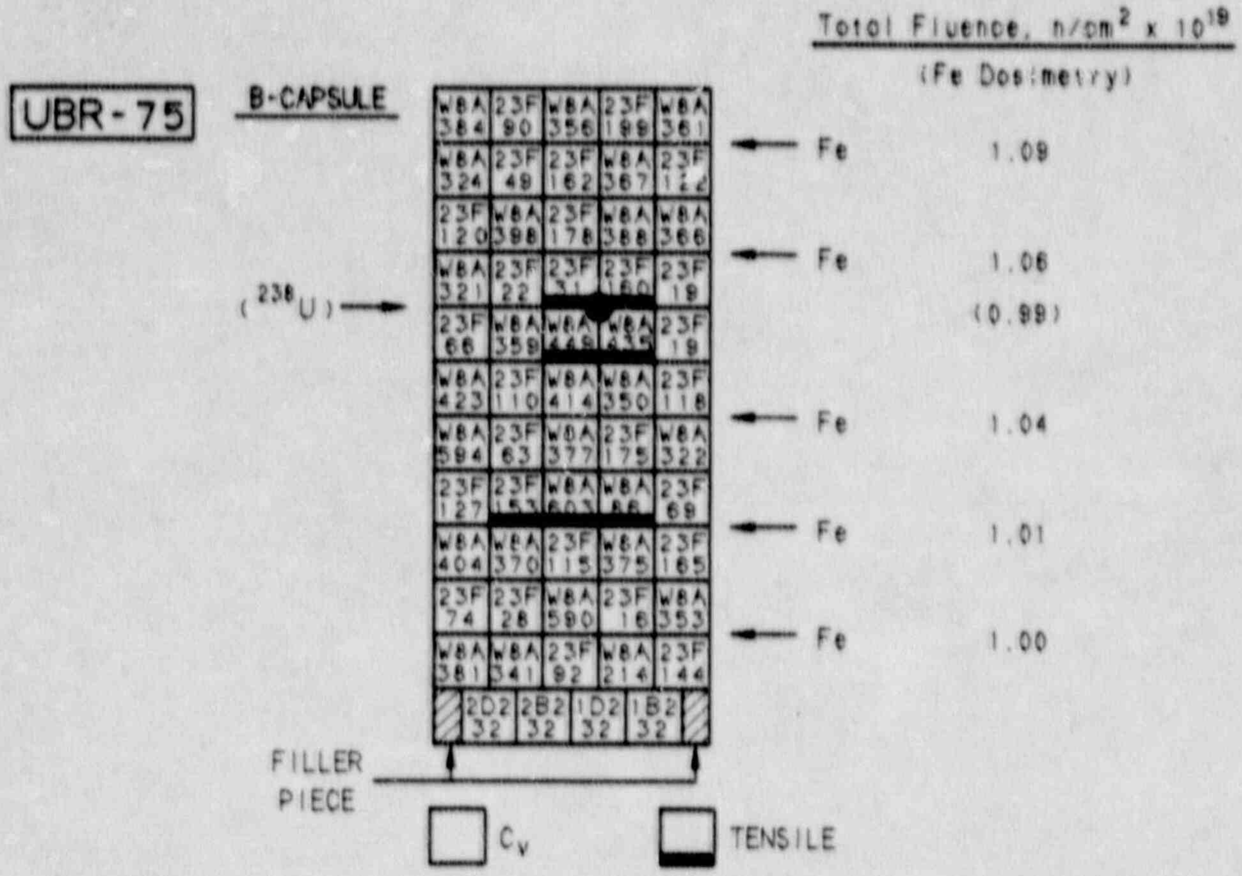

Fig. 13 Placement of C_v and tension test specimens in Irradiation Assembly UBR-75 (Capsule B; elevation view).

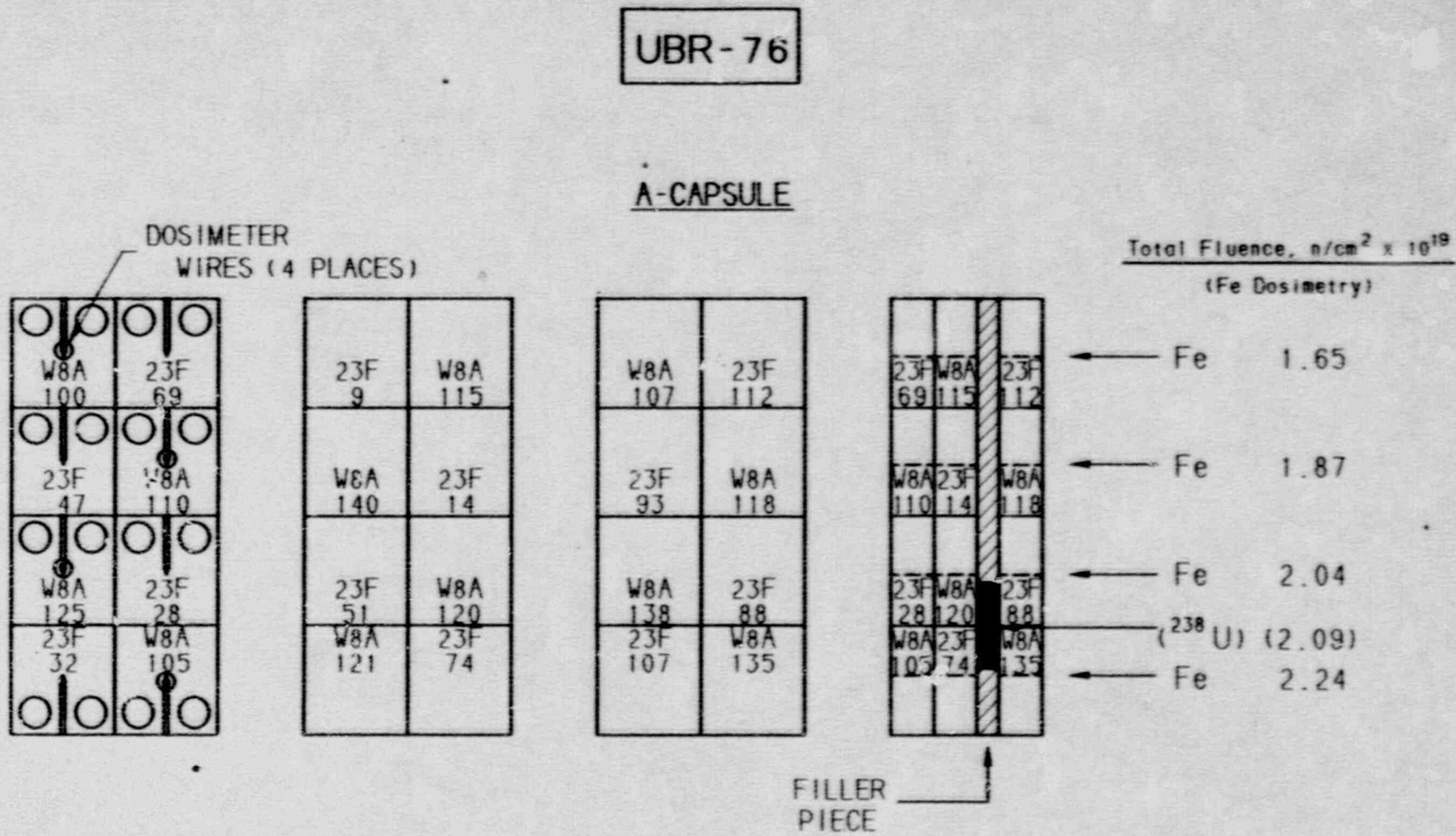

Fig. 14 Placement of 0.5T-CT compact specimens in Irradiation Assembly UBR-76 (Capsule A; elevation view).

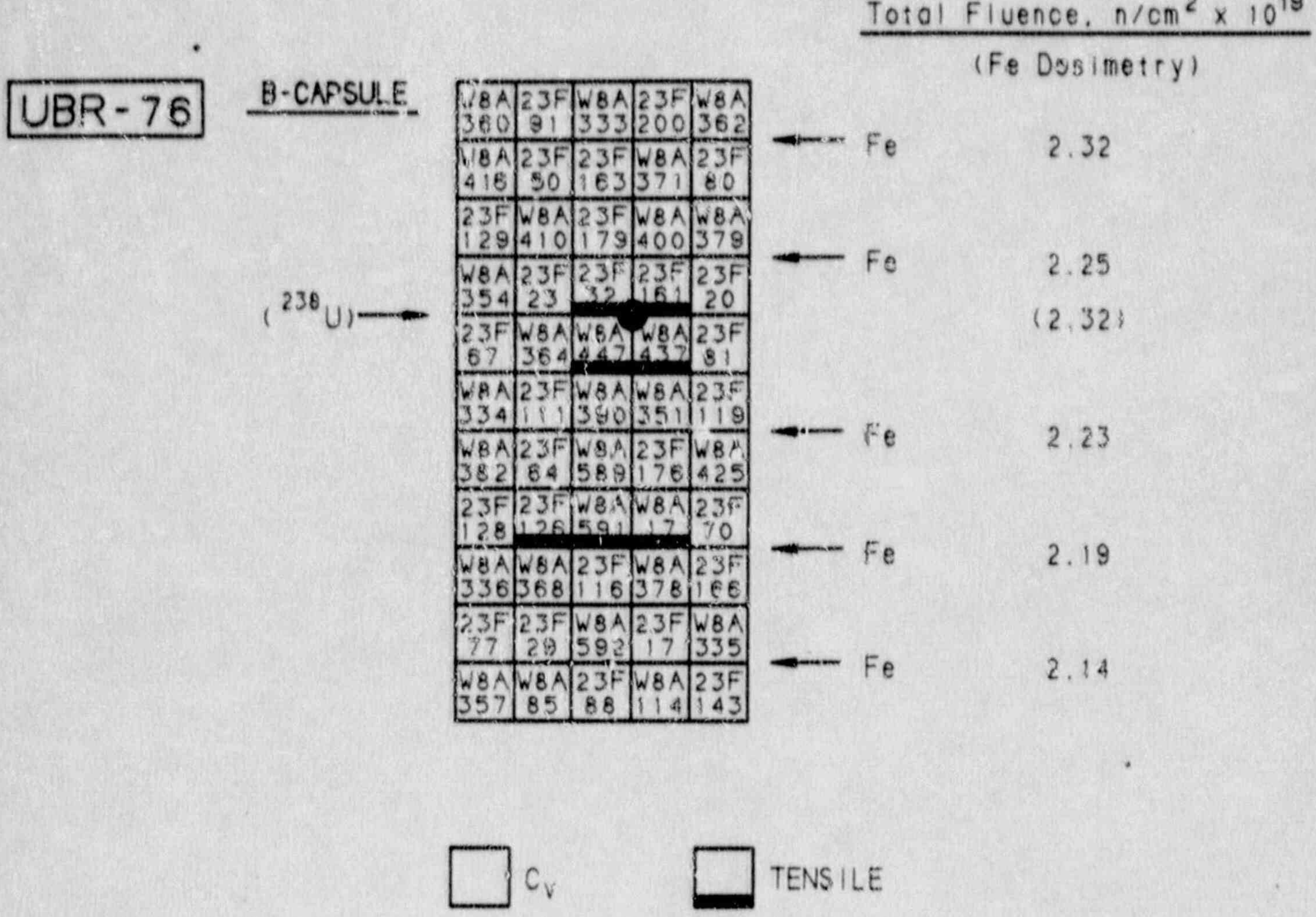

Fig. 15 Placement of C_v and tension test specimens in Irradiation Assembly UBR-76 (Capsule B; elevation view).

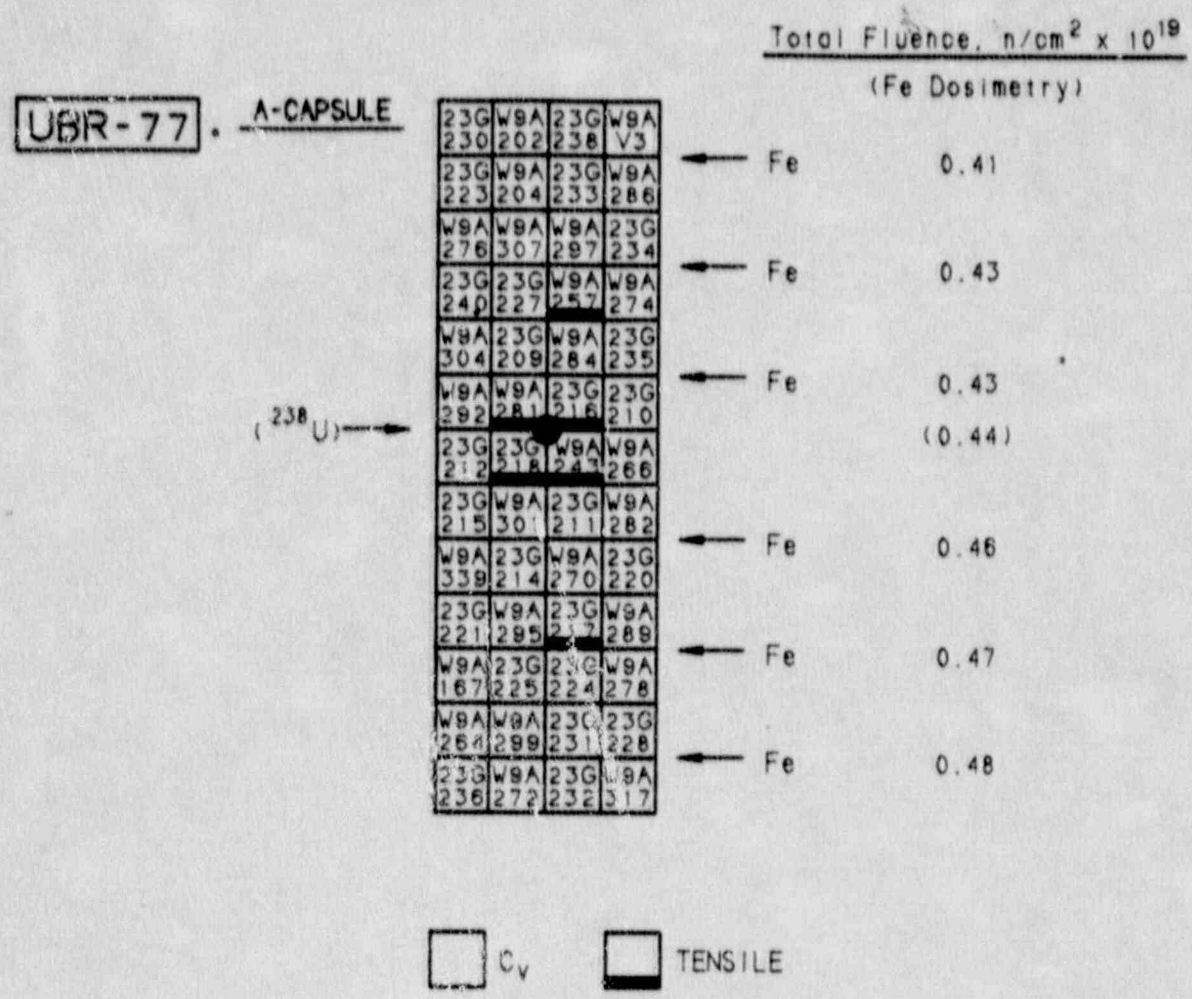

Fig. 16 Placement of C_v and tension test specimens in Irradiation Assembly UBR-77 (Capsule A; elevation view).

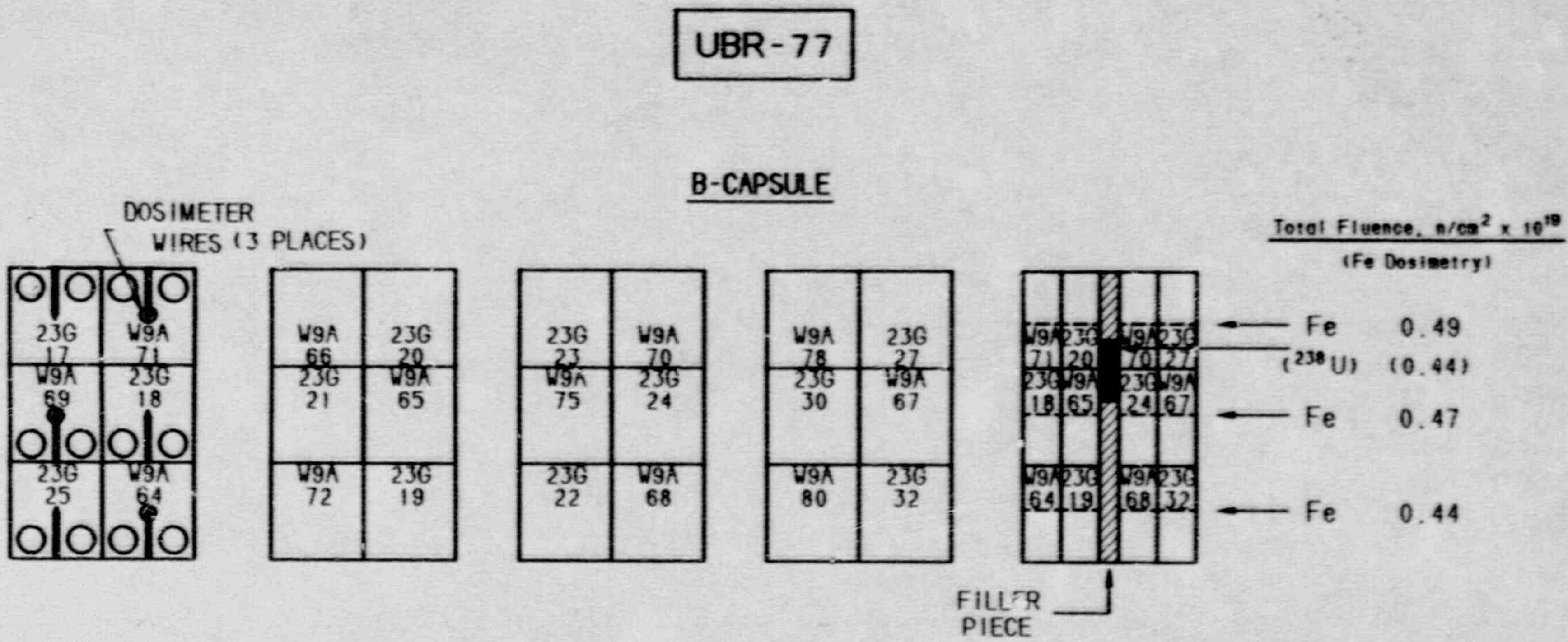

Fig. 17 Placement of 0.5T-CT compact specimens in Irradiation Assembly UBR-77 (Capsule B; elevation view).

(E > 1 MeV), at various positions in the specimen arrays are indicated. Figures 18 through 25 illustrate the placements of thermocouples within the specimen arrays. The thermocouples were welded to the specimens in the test region. Unless indicated otherwise, measured temperatures were within 11°C (20°F) of the target temperature of 288°C (550°F). Appendix A provides listings of average fluence rates obtained from the individual dosimeters: Appendix B provides detailed reactor operations history for the irradiation assemblies.

(text continues on pg. 34)

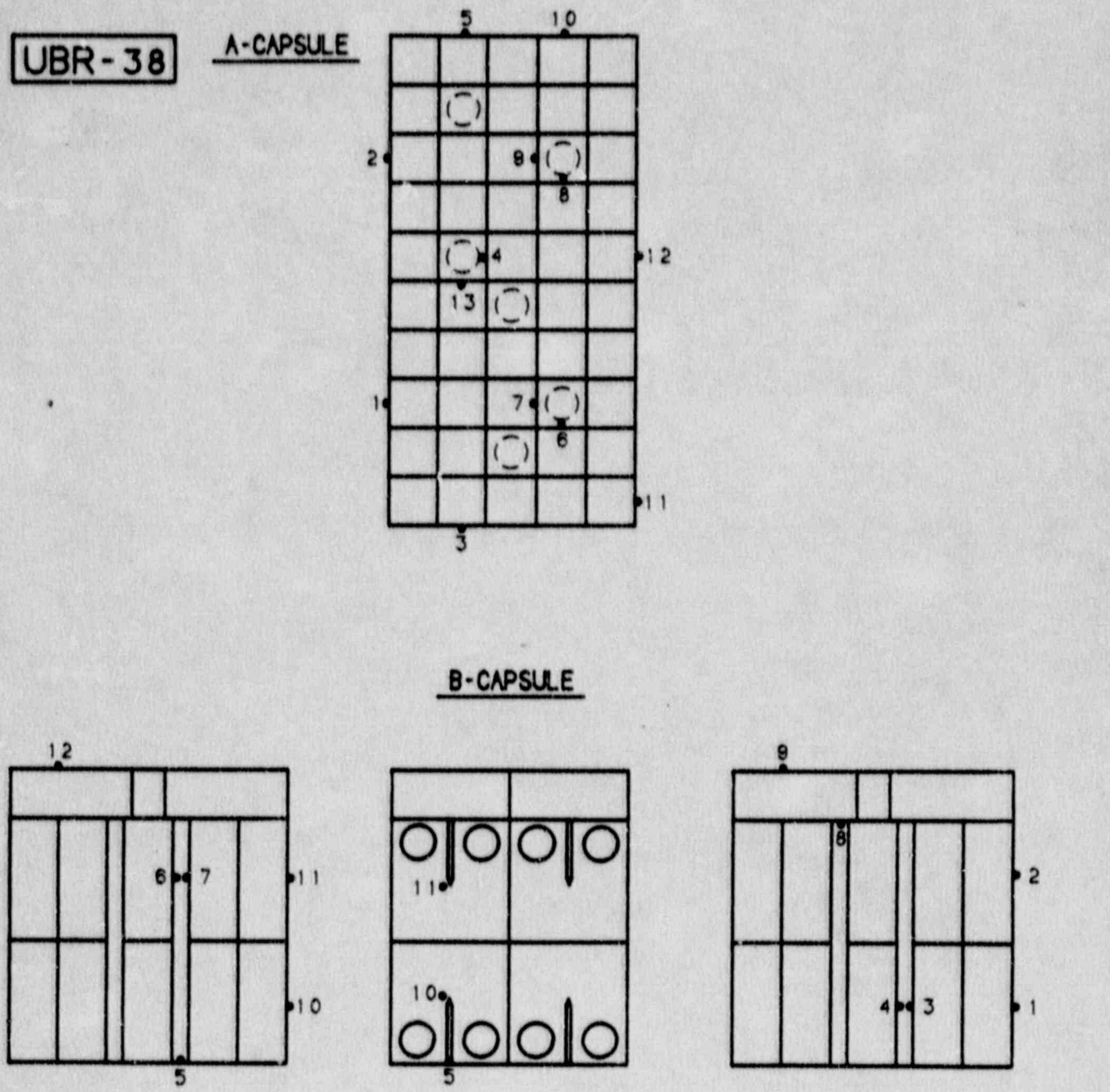

Fig. 18 Irradiation Assembly UBR-38 showing thermocouple placements in the specimen arrays.

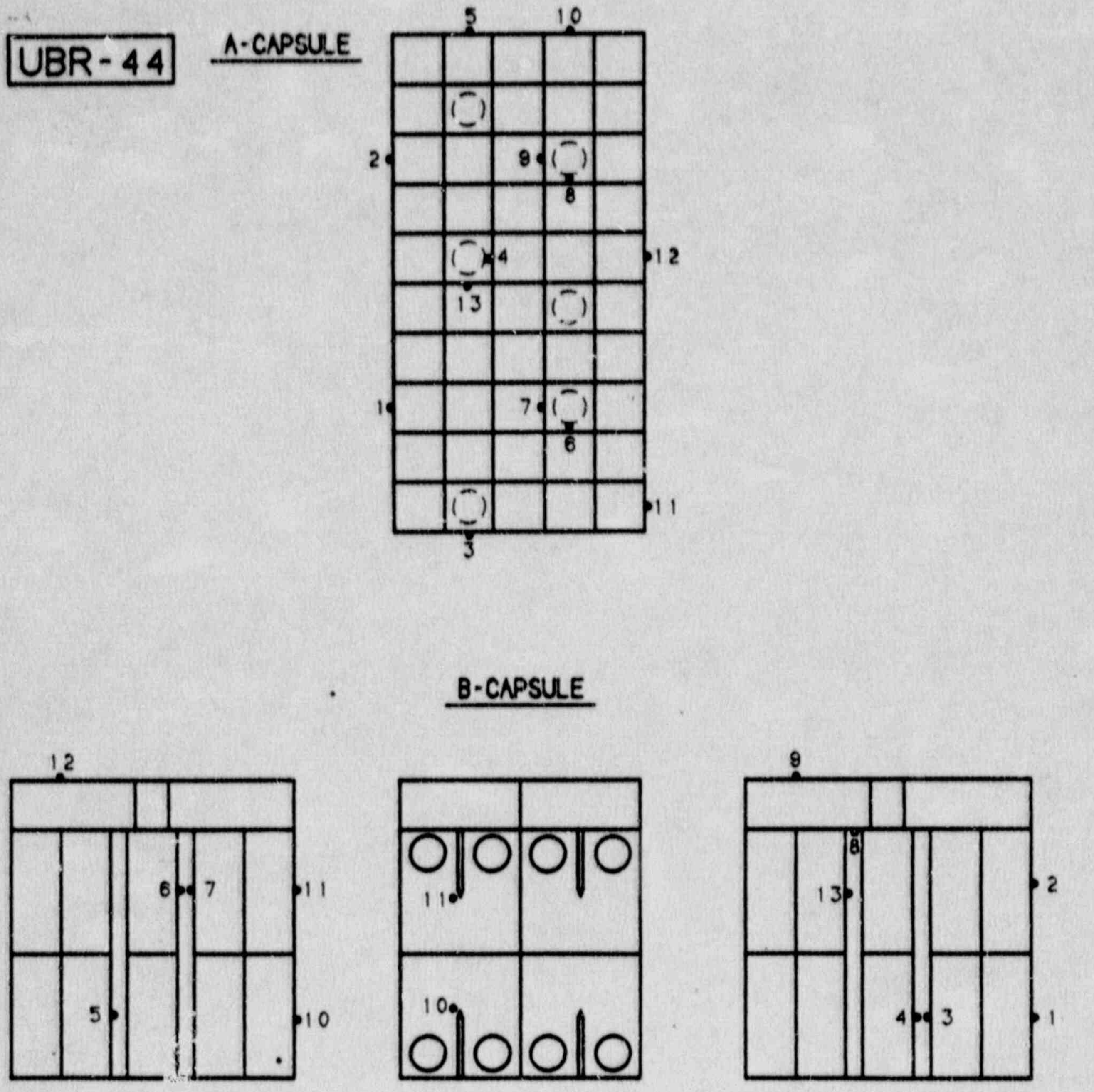

Fig. 19 Irradiation Assembly UBR-44 showing thermocouple placements in the specimen arrays.

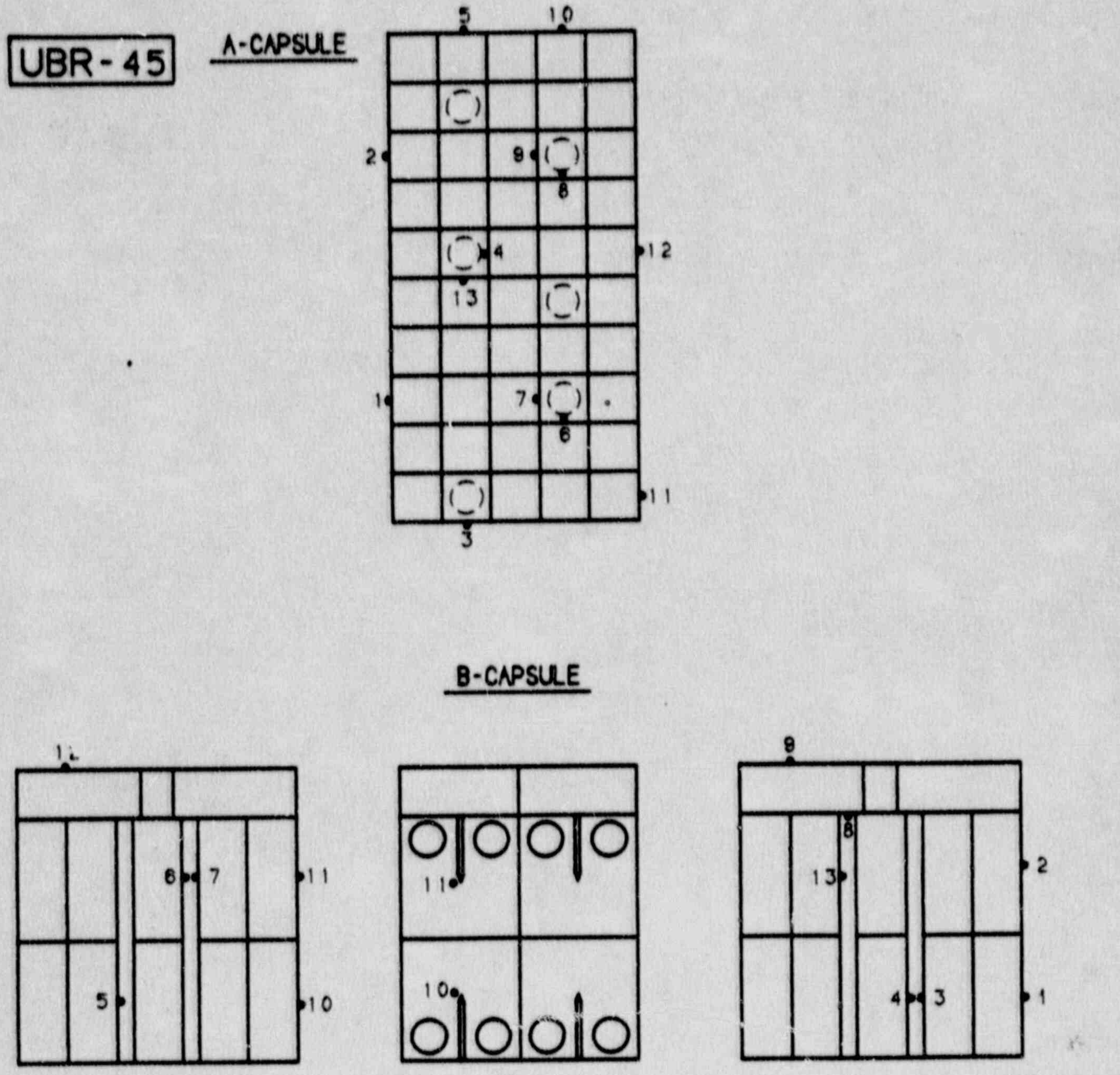

Fig. 20 Irradiation Assembly UBR-45 showing thermocouple placements in the specimen arrays.

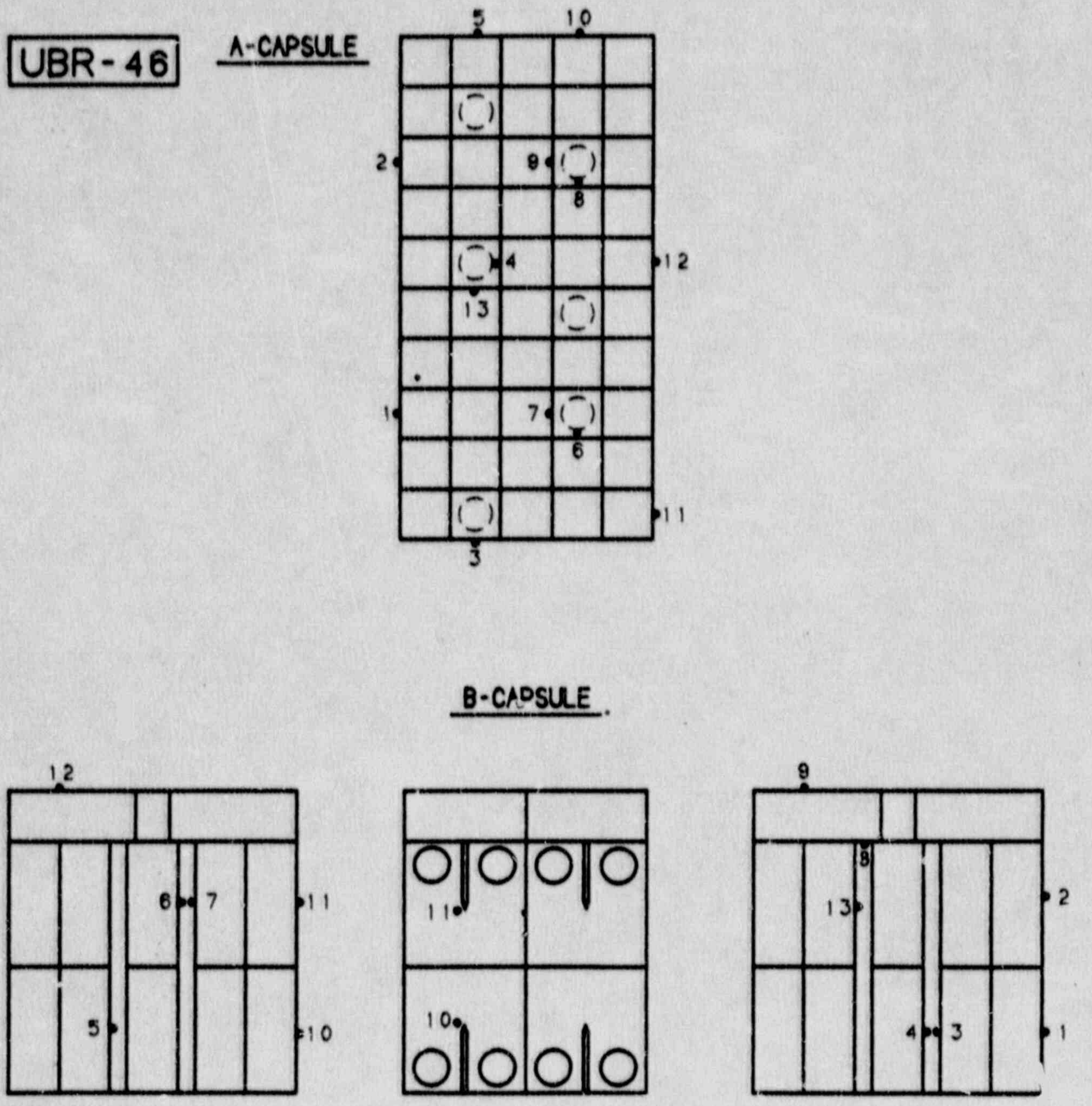

Fig. 21 Irradiation Assembly UBR-46 showing thermocouple placements in the specimen arrays.

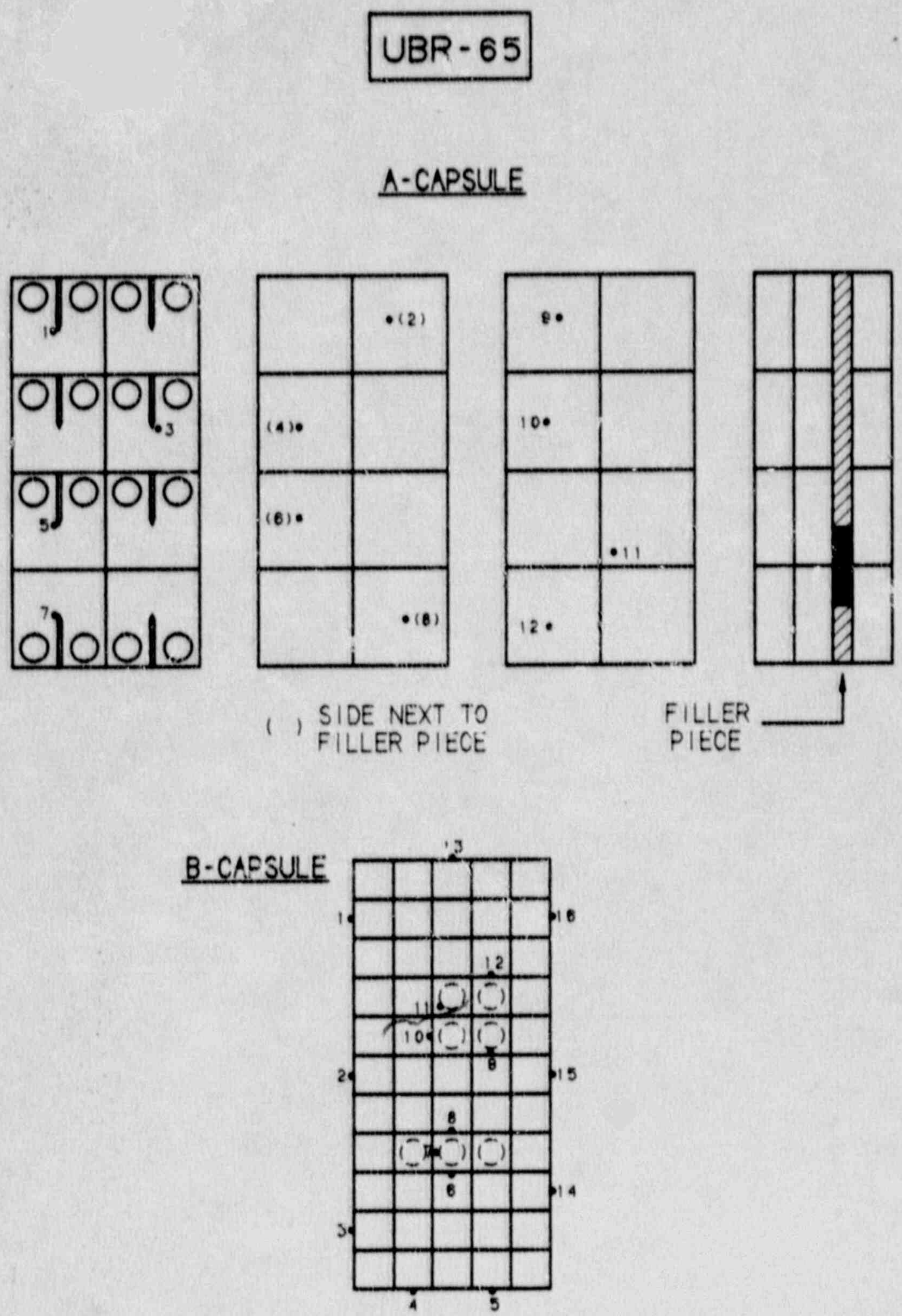

Fig. 22 Irradiation Assembly UBR-65 showing thermocouple placements in the specimen arrays.

UBR-75

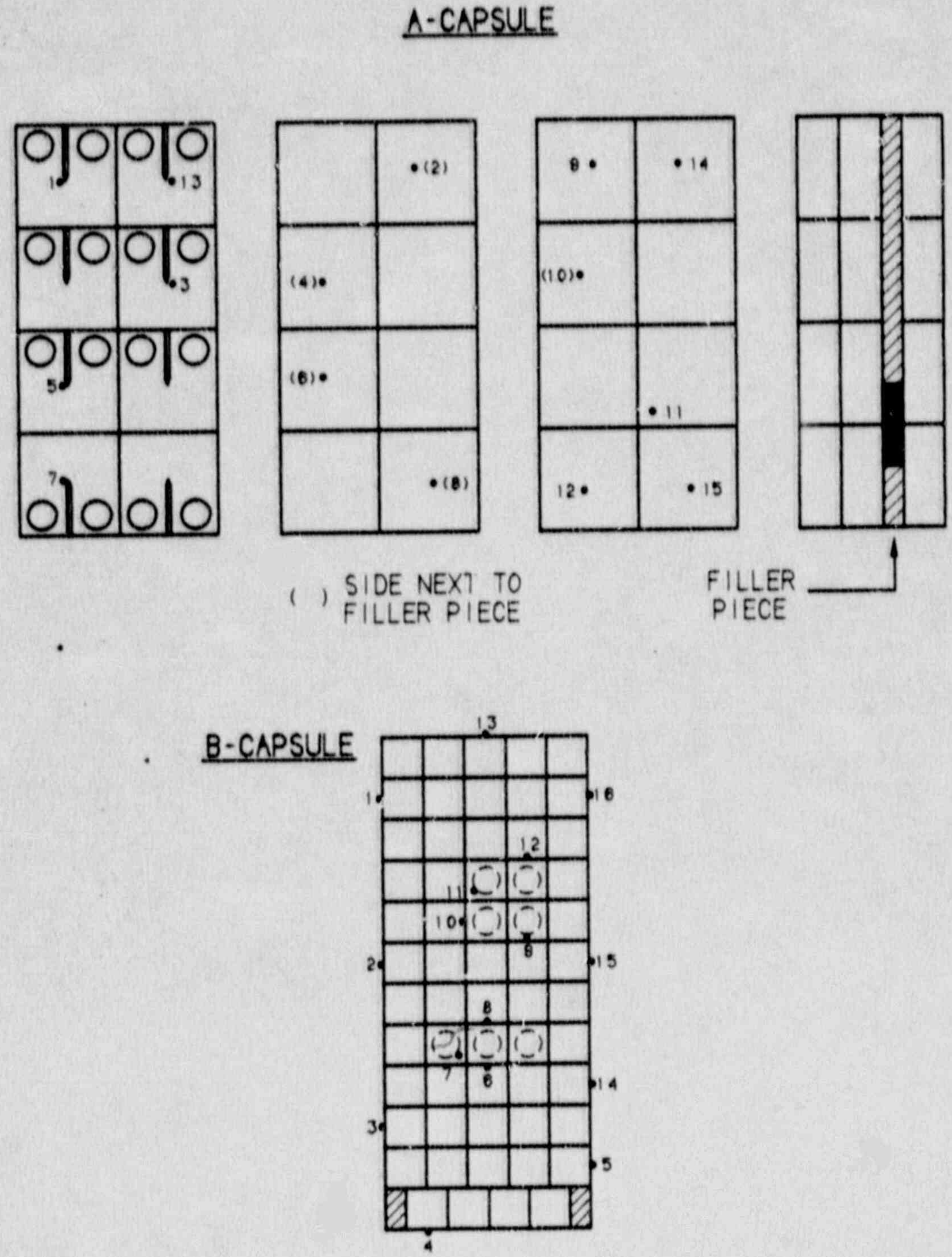

Fig. 23 Irradiation Assembly UBR-75 showing thermocouple placements in the specimen arrays.

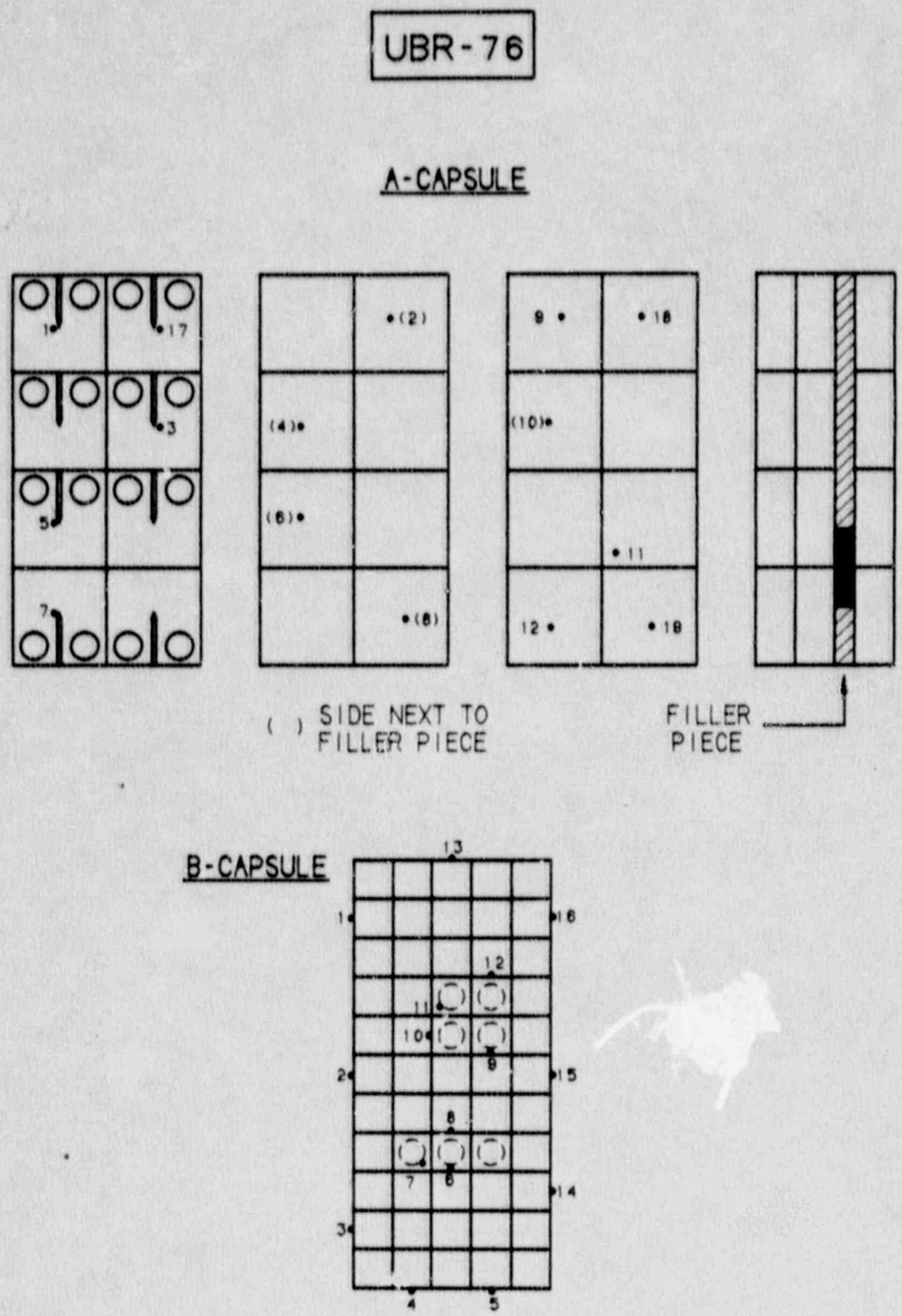

Fig. 24 Irradiation Assembly UBR-76 showing thermocouple placements in the specimen arrays.

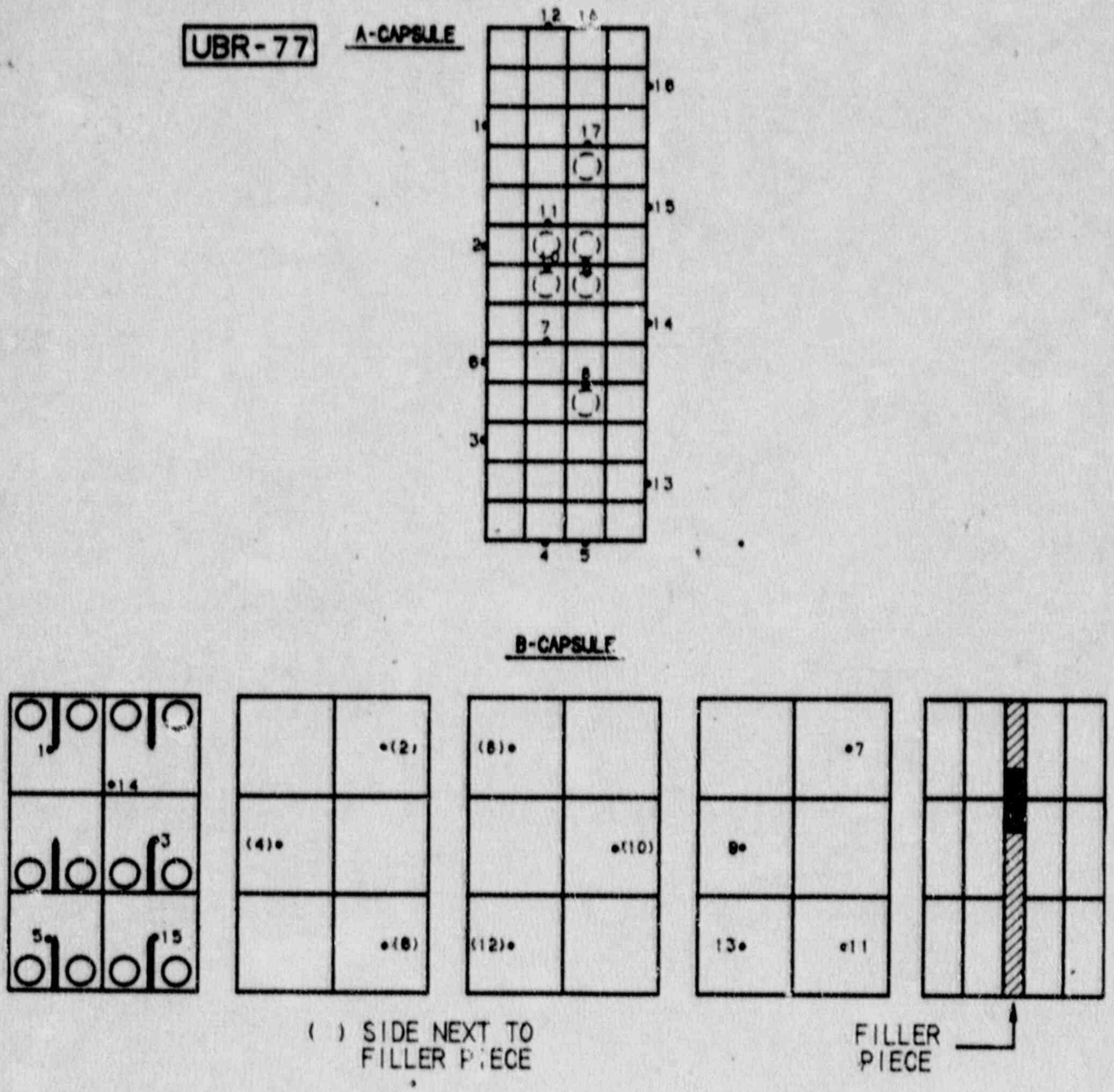

Fig. 25 Irradiation Assembly UBR-77 showing thermocouple placements in the specimen arrays.

5. EXPERIMENTAL RESULTS

5.1 Notch Ductility and Tensile Strength Determinations

5.1.1 Overview

The C_v test results for the A 302-B plate (Plate 23F) are illustrated in Fig. 26, 27 and 28; those for the Linde 80 submerged arc weld (Weld W8A) are shown in Fig. 29 and 30. C_v test results for the A 533-B plate (Plate 23G) and the Linde 0091 submerged arc weld (Weld W9A) are shown in Fig. 31 and 32, respectively. For the weld materials, data from the companion low fluence-rate irradiation are not yet available (UBR-49). Individual C_v test values from the irradiation assemblies are provided in Appendix C. Computer curve fits of the data and values of curve fitting parameters are given in Appendix D. In the text below, comparisons are based on 41-J transition temperature and upper shelf energy (USE) values from the hand-drawn curves. Determinations on strength increase with irradiation are listed in Table 3. Tensile test results for Weld W8A from other high fluence rate tests (in-core irradiations) are also listed in Table 3 to extend the data base. Expected from its higher copper and nickel content, the Weld W8A consistently showed a greater radiation embrittlement sensitivity than the Plate 23F.

Three general comments on the data for the Plate 23F and the Weld W8A are appropriate. Figure 26 shows preirradiation notch ductility properties of the plate at the 1/4T location. This thickness layer was used for the NRC's Light Water Reactor-Surveillance Dosimetry Improvement Program (LWR-SDIP) irradiations in the Pool Side Facility (PSF) of the Oak Ridge Research Reactor (Ref. 5). Comparison of the properties of this layer versus those of the present study indicates a small difference in 41-J transition temperature (about 11°C, 20°F) and a relatively large difference in C_v USE (about 16 J, 12 ft-lb). The differences point up the need for check testing when more than one thickness layer of a plate is employed for specimen stock. In Fig. 29 and 30, the data for the weld depict a very shallow ductile-to-brittle transition trend and at the higher fluences, a low C_v USE as well. These characteristics made identification of the 41-J temperature elevation by irradiation difficult. The cited characteristics are not unusual for Linde 80 welds; on the other hand, 41-J temperature identification for Linde 0091 welds generally is not hampered by either aspect (see Fig. 32 example). It is further noted that fairly high data scatter is present in certain regions in some Weld W8A curves. The cause of the scatter is not known but local weld inhomogeneity is suspected. In this regard, test specimens were taken randomly through the weld thickness. Lastly, the postirradiation tensile strength values listed in Table 3 are duplicate test values in most cases. Typically, values for a given irradiation condition were within 20 MPa (3 ksi).

Actual (measured) neutron fluences for the in-core experiments were close to target values in all cases; however, actual values for the core-edge experiments exceeded the target levels, especially that of Assembly CE-3. This precluded a 1:1 matching of data sets for the two

(text continues on pg. 43)

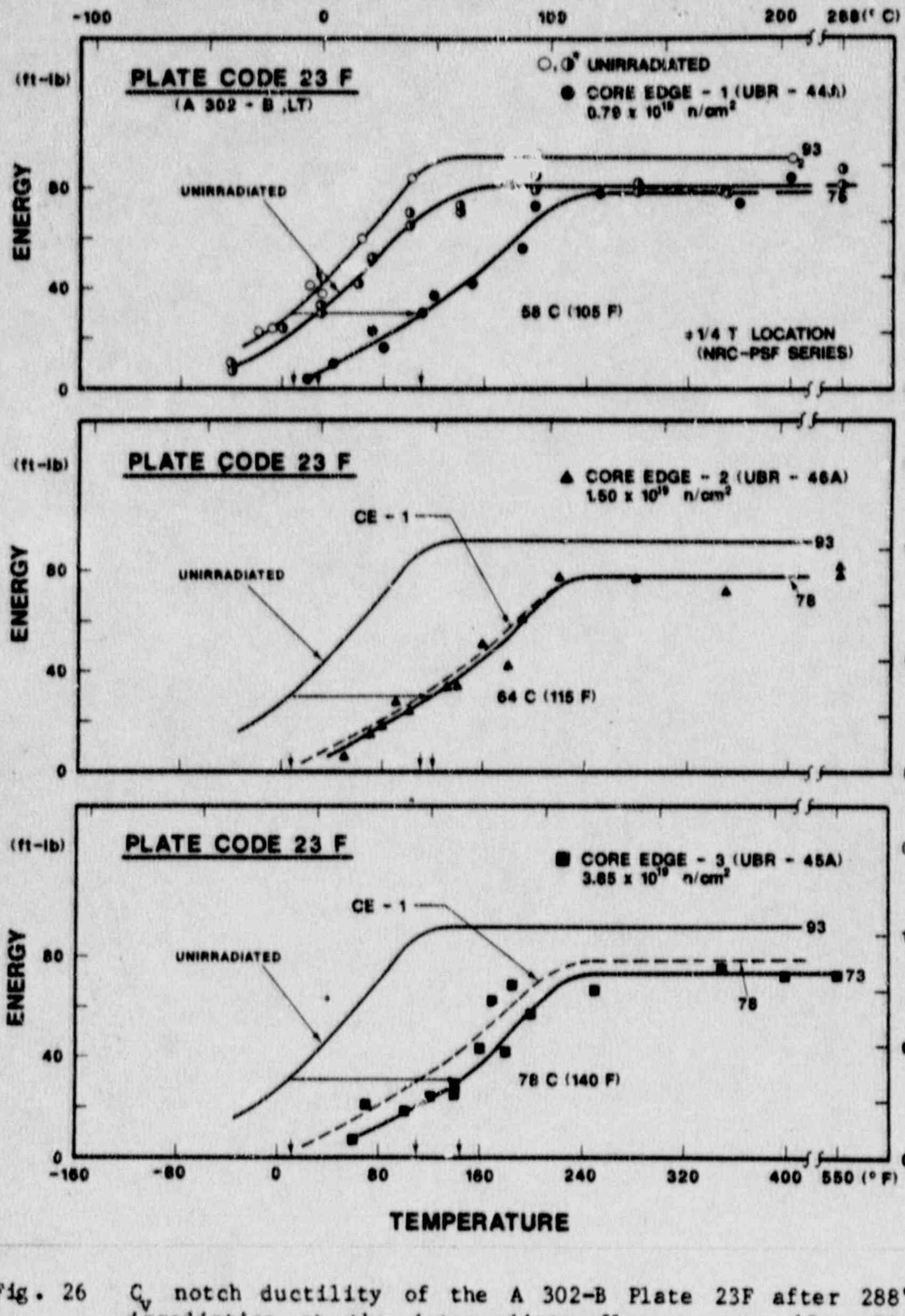

Fig. 26 C_v notch ductility of the A 302-B Plate 23F after 288°C irradiation at the intermediate fluence rate (Core-Edge Assemblies Nos. 1, 2, 3). The irradiated condition trend curve of the upper graph (CE-1) is reproduced in the middle and lower graphs for ease in making comparisons. The open and half filled circle points are for 3/8T to 5/8T and 1/4T thickness locations in the original 152-mm-thick plate, respectively.

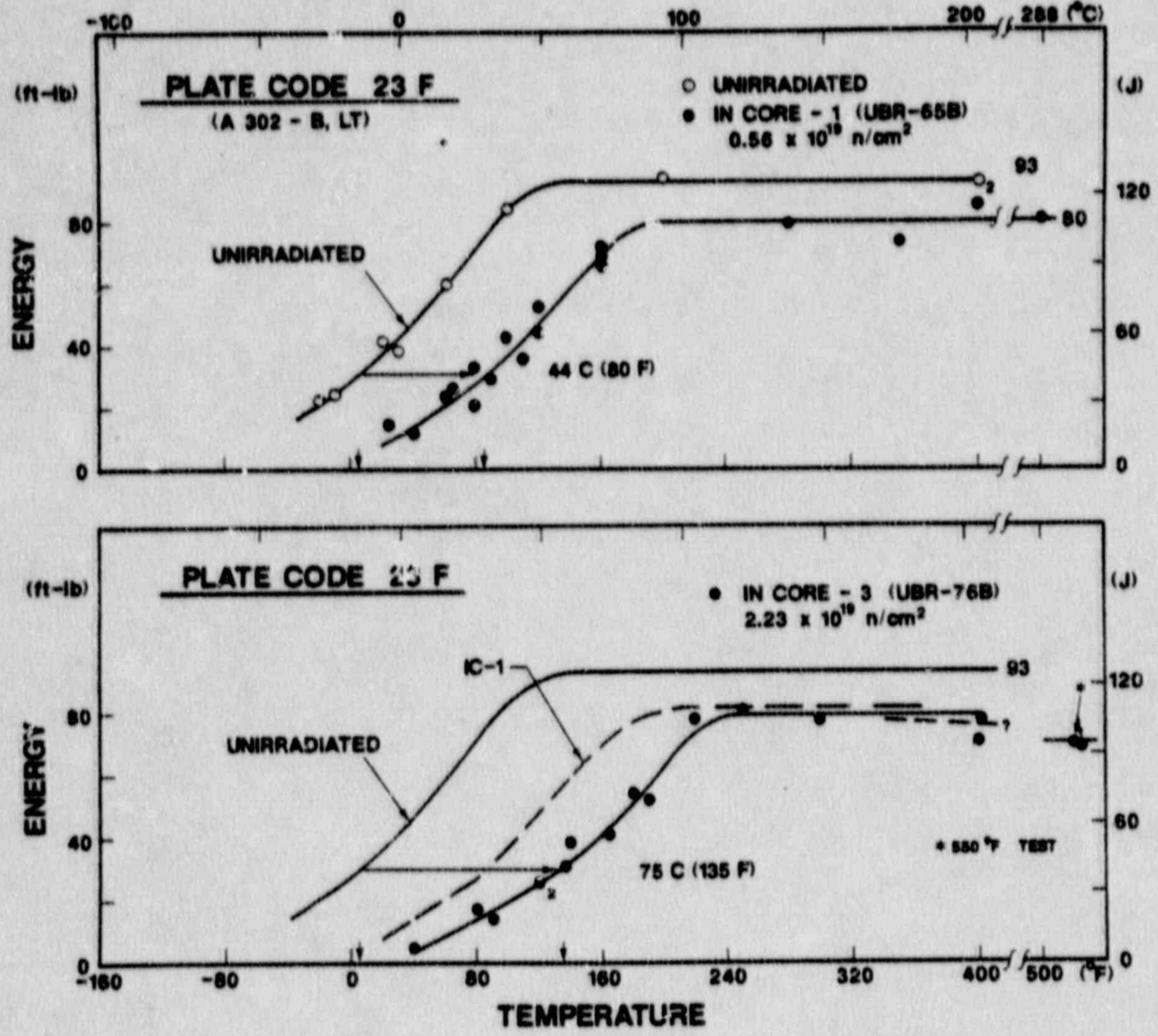

Fig. 27 C_v notch ductility of the A 302-B Plate 23F after 288°C irradiation at the high fluence rate (In-Core Assemblies Nos. 1 and 3).

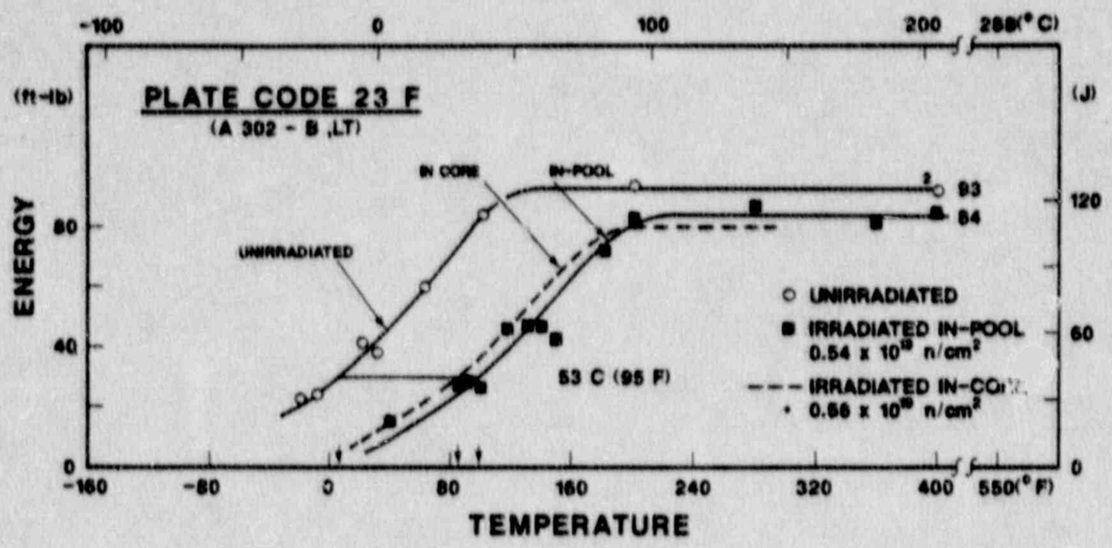

Fig. 28 C_v notch ductility of the A 302-B Plate 23F after 288°C irradiation at the low fluence rate (Reflector Region Assembly No. 1). The dashed curve depicts the notch ductility of this material after a high fluence rate irradiation to about the same fluence.

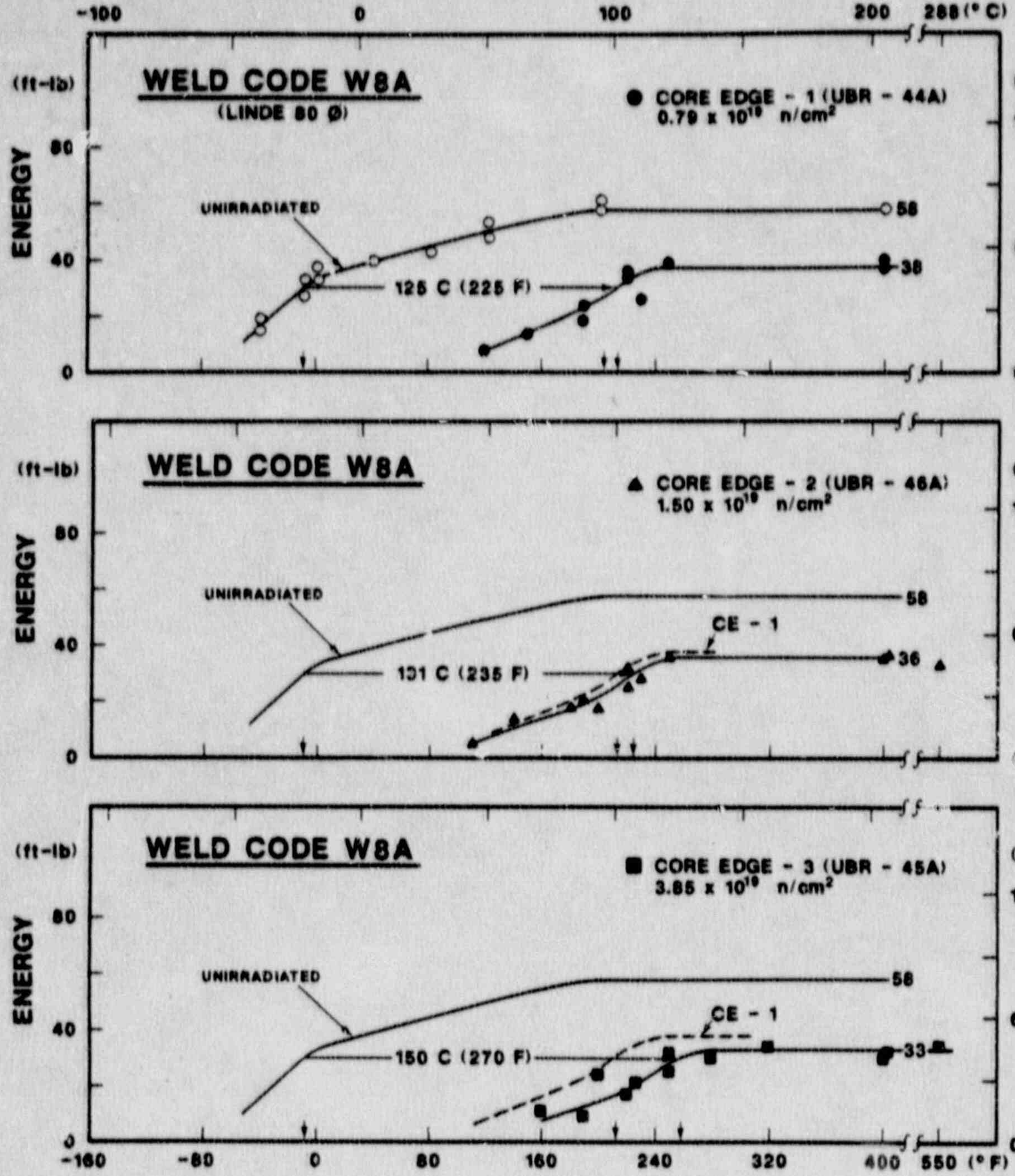

Fig. 29 C_v notch ductility of the Linde 80 Weld W8A after 288°C irradiation at the intermediate fluence rate (Core-Edge Assemblies Nos. 1, 2, 3). The irradiated condition trend curve of the upper graph (CE-1) is reproduced in the middle and lower graphs for ease in making comparisons.

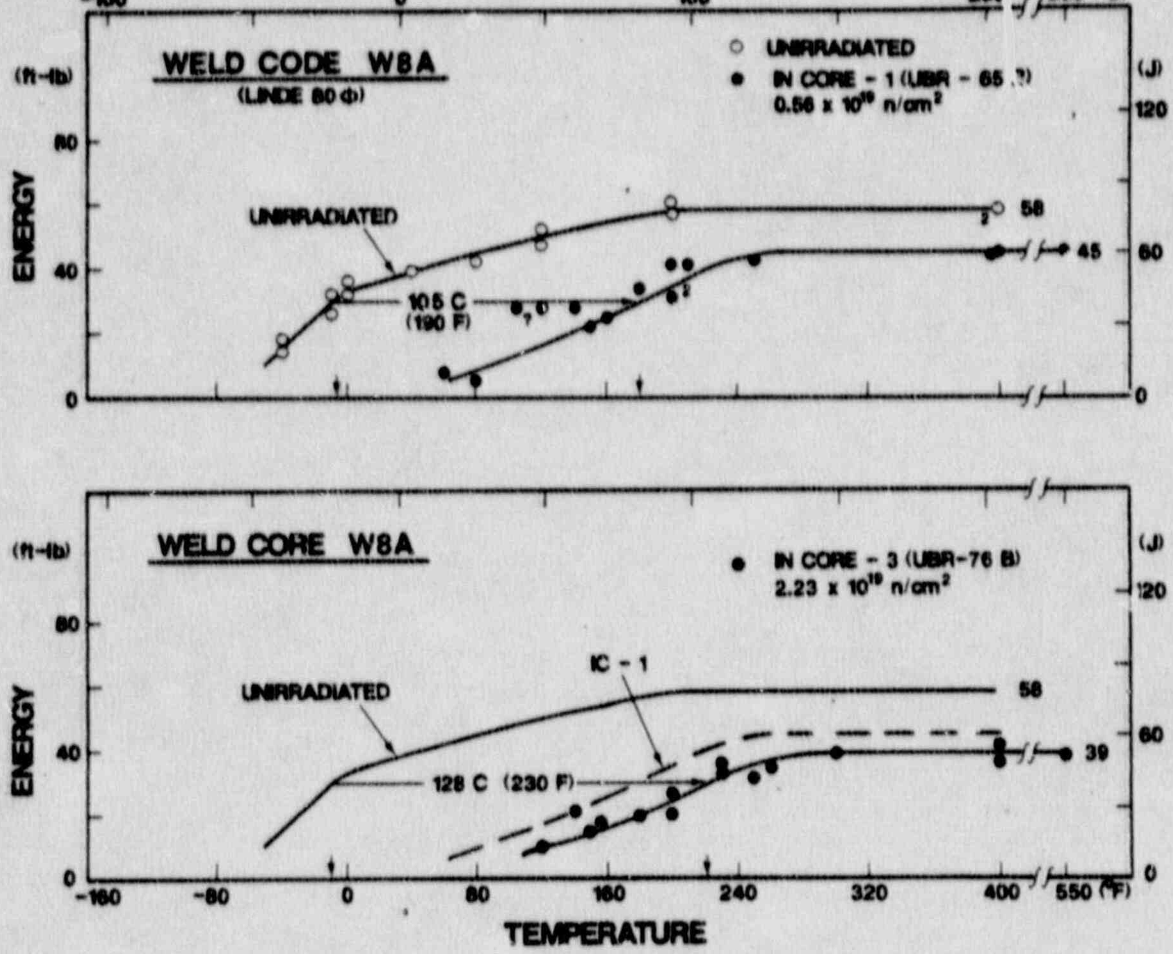

Fig. 30 C_v notch ductility of the Linde 80 Weld W8A after 288°C irradiation at the high fluence rate (In-Core Assemblies Nos. 1 and 3).

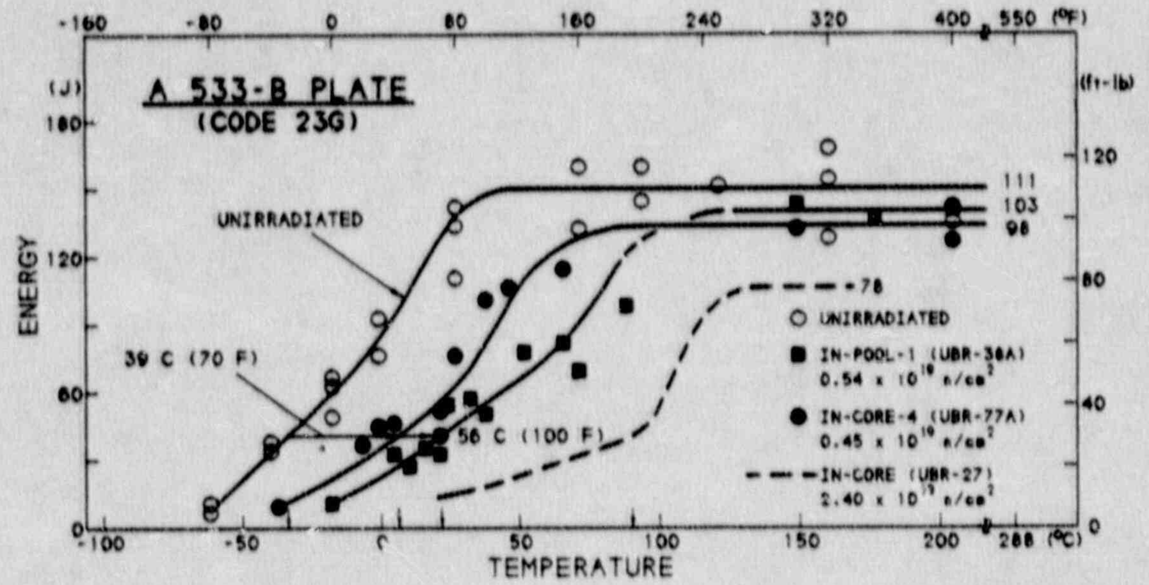

Fig. 31 C_v notch ductility of the A 533-B Plate 23G after 288°C irradiation to ~ 0.5×10^{19} n/cm^2 at the low fluence rate (Reflector Region Assembly No. 1) and at the high fluence rate (In-Core Assembly No. 4). Results from a prior high fluence rate irradiation are also illustrated (see dashed curve).

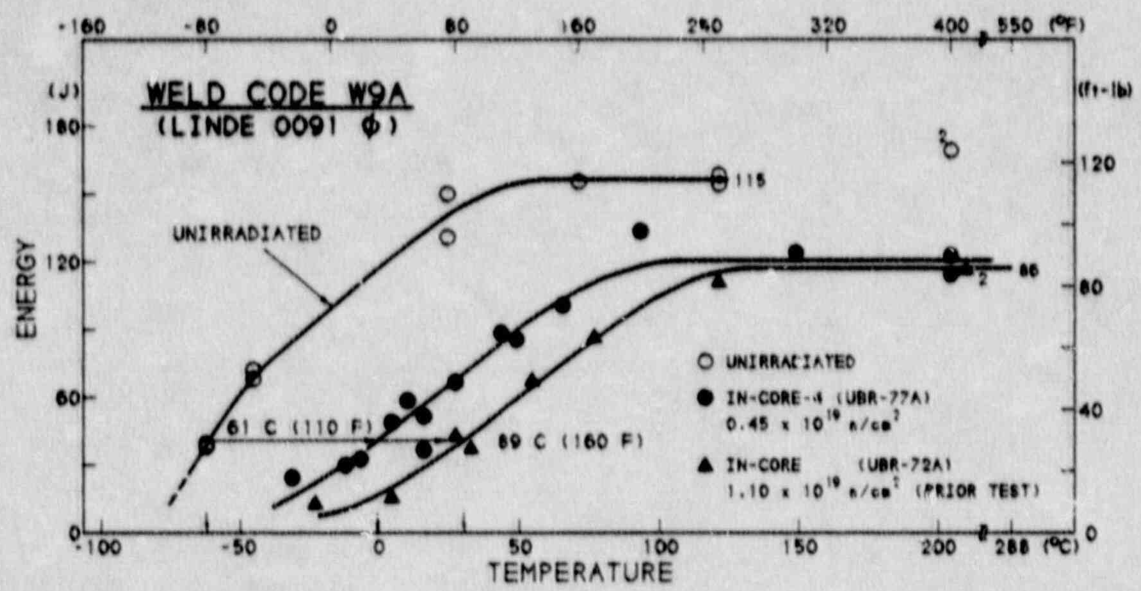

Fig. 32 C_v notch ductility of the Linde 0091 Weld W9A after high fluence rate irradiations to two fluence levels (In-Core Assembly No. 4 and a prior test).

TABLE 3 Postirradiation Tensile Strengths (Ambient Temperature Tests)

Material	Irradiation Assembly	Fluence x 10^{19} n/cm^2	dpa	Yield Strength[a] MPa	ksi	ΔMPa	Ultimate Tensile Strength MPa	ksi	ΔMPa
Plate 23F (A 302-B)	Unirradiated	...	...	447	64.74	...	589	85.35	...
	IC-1 (UBR-65B)	0.56	0.0091	517	74.93	70	647	93.79	58
	IC-2 (UBR-75B)	1.04	~ 0.0198	538	78.06	91	668	96.85	79
	IC-3 (UBR-76B)	2.23	0.0361	564	81.73	117	691	100.22	102
	CE-1 (UBR-44A)	0.79	0.0111	550	79.81	103	680	98.68	91
	CE-2 (UBR-46A)	1.50	0.0212	554	80.32	107	683	99.08	94
	CE-3 (UBR-45A)	3.85	0.0545	566	82.14	119	696	100.91	107
	IP-1 (UBR-38A)	0.54	0.0076	529	76.68	82	661	95.93	72
Plate 23G (A 533-B)	Unirradiated	...	...	431	62.47	...	581	84.33	...
	IC-4 (UBR-77A)	0.45	0.0073	493	71.46	62	641	92.91	60
	IP-1 (UBR-38A)	0.54	0.0076	550	79.74	119	699	101.34	118
Weld W8A (Linde 80)	Unirradiated	...	...	481[b]	69.76	...	604	87.59	...
				498[c]	72.18	...	617	89.50	...
	Thermal Aged[d]	...	...	483	70.06	...	604	87.56	...
	IC-1 (UBR-65B)	0.56	0.0091	592	85.86	111	699	101.44	95
	IC-2 (UBR-75B)	1.04	~ 0.0198	624	90.53	143	726	105.26	122
	IC-3 (UBR-76B)	2.23	0.0361	659	95.59	178	747	108.26	143
	UBR-72[e,f]	1.06	0.0172	625	90.62	144	721	104.62	117
	UBR-55C[e,f]	3.25	0.0527	706	102.40	260	778	112.90	189
	CE-1 (UBR-44A)	0.79	0.0111	650	94.31	169	741	107.54	137
	CE-2 (UBR-46A)	1.50	0.0212	659	95.53	178	751	108.91	147
	CE-3 (UBR-45A)	3.85	0.0545	684	99.26	203	767	111.23	163
Weld W9A (Linde 0091)	Unirradiated	...	...	564[b]	81.81	...	659	95.55	...
				565[c]	81.99	...	617	89.54	...
	Thermal Aged[d]	...	...	561	81.32	...	653	94.77	...
	IC-4 (UBR-77A)	0.45	0.0073	667	96.70	103	740	107.37	81

[a] Average of duplicate tests unless noted
[b] Specimen set no. 1 (reference set)
[c] Specimen set no. 2
[d] 288°C-1000 hours; corresponds to specimen set no. 1
[e] Prior HEA study
[f] Single determination

exposure locations. Nonetheless, sufficient overlap exists for trend definition.

5.1.2 Assessment of Fluence-Rate Effect

Figure 33 summarizes observed transition temperature elevations for the two plates and the Weld W8A to illustrate the influence of fluence rate on apparent embrittlement sensitivity. The open circle points depict results from the core-edge irradiation experiments at $5\text{-}6 \times 10^{11}$ $n/cm^2 \cdot s^{-1}$; the filled circle points signify results from the in-core irradiation experiments at the high fluence rate of $8\text{-}9 \times 10^{12}$ $n/cm^2 \cdot s^{-1}$. The filled square points refer to the low fluence-rate irradiation of the reference plates in the reflector region. To aid the identification of embrittlement trends for the in-core exposure condition, data obtained from prior in-core irradiation tests of Weld W8A have been included in Fig. 33. A reference trend band and two high fluence test points for the 1/4T thickness location of the Plate 23F are also shown for this purpose.

Referring first to the A 302-B Plate 23F, the C_v findings show no discernable effect of fluence rate on radiation sensitivity in the low target fluence regime. Furthermore, the in-core (IC) and core-edge (CE) results are in good agreement up to a fluence of about 2.0×10^{19} n/cm^2. Above this value, the data trends diverge with the intermediate fluence rate appearing to have a lesser damage-producing potential than the high fluence rate. In support of this analysis, notice the positions of the data trend for the 1/4T thickness layer of the plate versus the datum for the CE-3 Assembly. The observed fluence-rate effect for the A 533-B Plate 23G agrees well with that for the A 302-B Plate 23F in the low target fluence region. While the 41-J transition temperature elevations for the in-core and the reflector-region irradiations of this plate are not the same, the difference (17°C) can be attributed in part to the fluence difference between the two specimen sets and the observed data scatter. Considering these factors, the fluence-rate effect does not appear large for the Plate 23G - unless viewed on a percentage basis. The radiation-induced elevations in transition temperature for the two plates from the low fluence-rate experiment are essentially the same. Likewise, the transition temperature elevations from the in-core experiments at ~ 0.5×10^{19} n/cm^2 are not markedly different. This is not the case for the high fluence irradiations condition. The high fluence datum shown for Plate 23G is from an earlier MEA study. Yield strength elevations by the low fluence-rate irradiation were also very similar. It is noted from Table 1 that the nickel contents of the plates differ (0.18% vs. 0.63%) but not their copper contents (~ 0.21%). The Plate 23G has a significantly lower sulfur content (0.023% vs. 0.008%) as well.

In contrast to the apparent fluence-rate effect for the Plate 23F, the data trends for the Weld W8A indicate a fluence-rate influence in the low but not the high fluence regime. That is, the data points for core-edge and in-core tests are separated by approximately 15°C (25°F) at ~ 1×10^{19} n/cm^2 but tend toward convergence with increasing fluence. The scatter in the 41-J transition temperature elevation

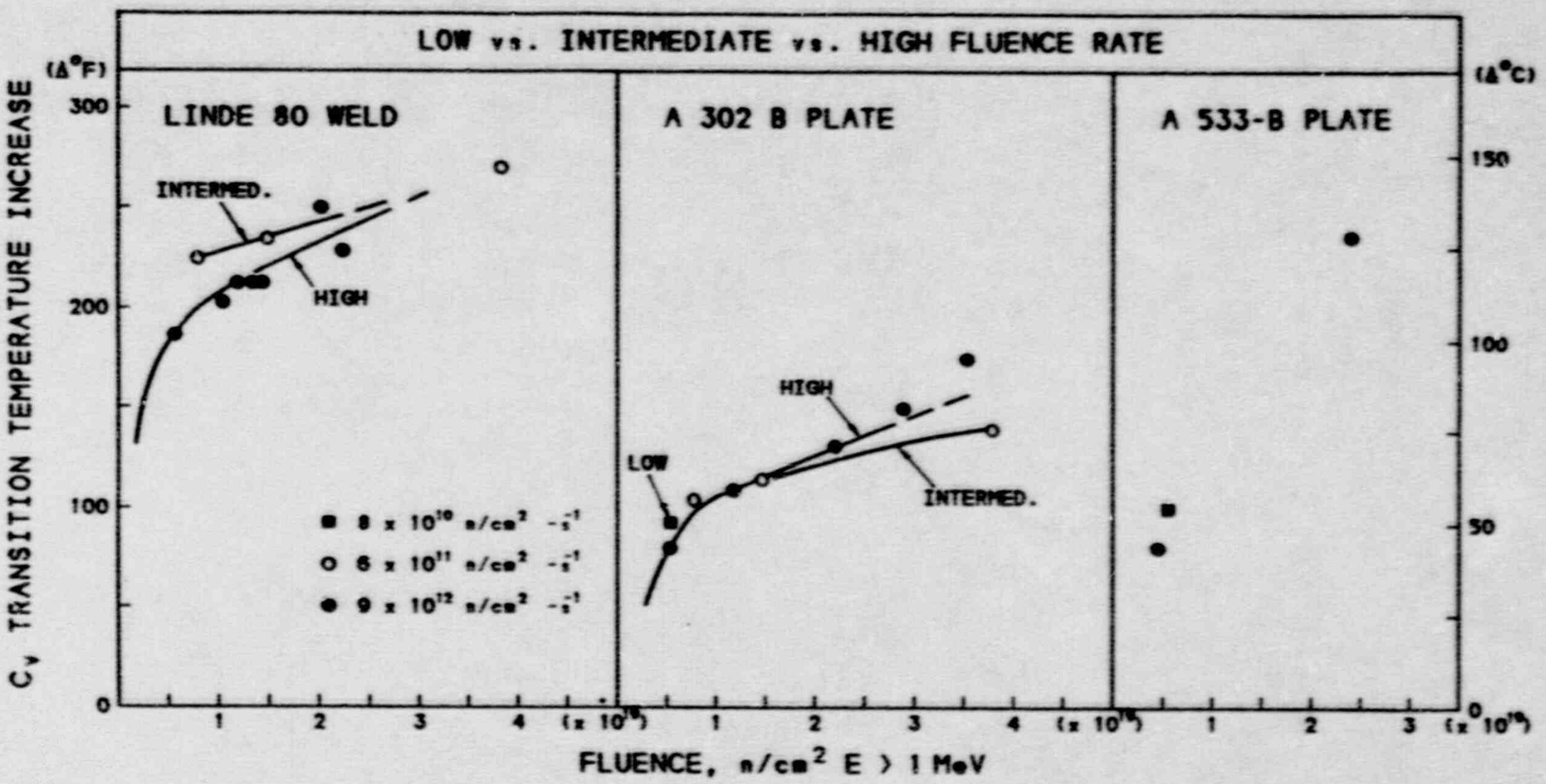

Fig. 33 Comparison of C_v 41-J transition temperature elevations observed for the Linde 80 Weld W8A (Left panel), the A 302-B Plate 23F (center panel) and the A 533-B Plate 23G (Right Panel).

values at fluences above 2 x 10^{19} n/cm^2 precludes a clear assessment of the effect. For the weld, it can be concluded however that the embrittlement condition achieved by specimens in the CE-3 Assembly is no worse than the embrittlement condition described by specimens irradiated in-core to about the same fluence level. Secondly, the determinations for the plate versus weld permit a conclusion that the fluence-rate effect is dependent on material type (or composition). Further comparisons are planned which will provide separate tests of composition effects.

The tensile test results for the Plate 23F support the cited C_v data comparisons at fluences greater than ~ 1.2 x 10^{19} n/cm^2. Noting that the fluence of Assembly CE-2 is between those of Assembly IC-2 and IC-3, the postirradiation yield strength elevation (107 MPa) is intermediate to the elevations found for specimens in Assemblies IC-2 and IC-3 (91 MPa and 117 MPa, respectively). Extrapolation of the in-core irradiation trend to 3.85 x 10^{19} n/cm^2 indicates a much greater strength elevation at this fluence than that shown by the Assembly CE-3 specimens. Relative to the fluence interval between 0.6 and 1.2 x 10^{19} n/cm^2, the yield strength elevation for Assembly CE-1 is somewhat greater than that expected (by about 25 MPa) from the C_v trends. For the low fluence condition of Weld W8A, data for the two fluence rates show a much greater difference, that is, ~ 45 MPa (~ 6 ksi) - and are considered significant. For this material, data from a prior in-core irradiation test at high fluence are available (see UBR-55C, Table 3) for comparison with the Assembly CE-3 data. Here, the yield strength elevations are within 22 MPa (~ 3 ksi).

5.2 Fracture Toughness Determinations

5.2.1 Overview

Fracture toughness data were developed for the materials in both the transition and the upper shelf regimes. Details on the test procedures and the data analysis procedures, and a detailed description of the results (including tabulated results from individual tests) are given in Appendix E. This section summarizes the most important information.

For both the transition and the upper shelf regimes, K_{Jc} values were determined from each test. For the transition region, K_{Jc} was computed from

$$K_{Jc} = \sqrt{J_{Crit}\ E / (1 - \nu^2)} \qquad (1)$$

where J_{Crit} is the critical J value at the fast fracture point (determined from the Merkle-Corten formulation, Ref. 9) , E is the elastic modulus and ν is Poisson's ratio (taken to be 0.3). Individual test points in the transition region were fitted to an exponential equation of the form

$$K_{Jc} = C_1 + C_2\ \mathrm{EXP}\ [(T-T_o)/C_3] \qquad (2)$$

where the coefficients C_1, C_2 and C_3 are determined from a non-linear regression analysis, and T_o is 0°C or 32°F, depending on the units of T. The use of confidence bounds (95%-95%) is described in Appendix E, and the curve-fit results are documented in Appendix F.

For the upper shelf region, a J resistance or J-R curve was obtained from each test. For this report, the modified form of J (J_M) per Ernst (Ref. 10) has been used for all J-R curve evaluations. For calculation of K_{Jc}, the J_{Ic} or J_Q value for each test is substituted for J_{Crit} in Eq. 1. (For the purposes of this report, upper shelf K_{Jc} values are used to compare results for the different irradiation conditions only.) As described in Appendix E, the J_{Ic} or J_Q value is determined from a power law analysis, whereby the power law intersection with the 0.15 mm offset exclusion line is termed J_Q. This definition of J_Q is similar to the ASTM E 813-87 method, where the J-R curve intersection with a 0.2 mm offset exclusion line is used. The method applied in this report is preferred to the ASTM method due to the lower, and hence more conservative values which result from this definition. The K_{Jc} values are independent of the J formulation used, since the various formulations tend to give identical values at small crack growth increments.

Plots of K_{Jc} as a function of temperature are given in Figs. 34 to 36 for the A 302-B Plate 23F, in Figs. 37 and 38 for the Linde 80 Weld W8A, in Fig. 39 for the A 533-B Plate 23G and in Fig. 40 for the Linde 0091 Weld W9A. In all cases the indicated trend lines are from computer curve-fits to the data, using Eq. 2.

In general, the K_{Jc} data for each irradiated condition data set are characterized by moderate to high amounts of scatter. This characteristic is particularly evident for the Linde 80 weld (W8A), but is true to some extent for the plates as well. Possible causes for the scatter include inherent material variability, irradiation temperature differences and to a small extent the fluence differences within the specimen set.

For the Plate 23F and for the Weld W8A, the data from the three core-edge (CE) assemblies indicate similar fracture toughness trends in the transition region for all three fluence levels, as illustrated in Fig. 41. More specifically, data for all three CE assemblies indicate about the same 100 MPa$\sqrt{m}$ transition temperature, chosen as an indexing level for making comparisons. This finding was unexpected, and is generally not supported by either the C_v or the tensile strength data, for which higher fluence equates to a greater transition temperature elevation or strength increase. The differences in the strength and transition temperature increases were not great among the various CE assemblies however. In contrast, the three in-core (IC) experiments indicate a progressive increase in transition temperature with fluence (Fig. 42). As shown in Appendix E, the J-R curve trends do not necessarily agree with the fracture toughness trends in the transition regime, as higher fluence tends to result in reduced J levels in most cases.

(text continues on pg. 56)

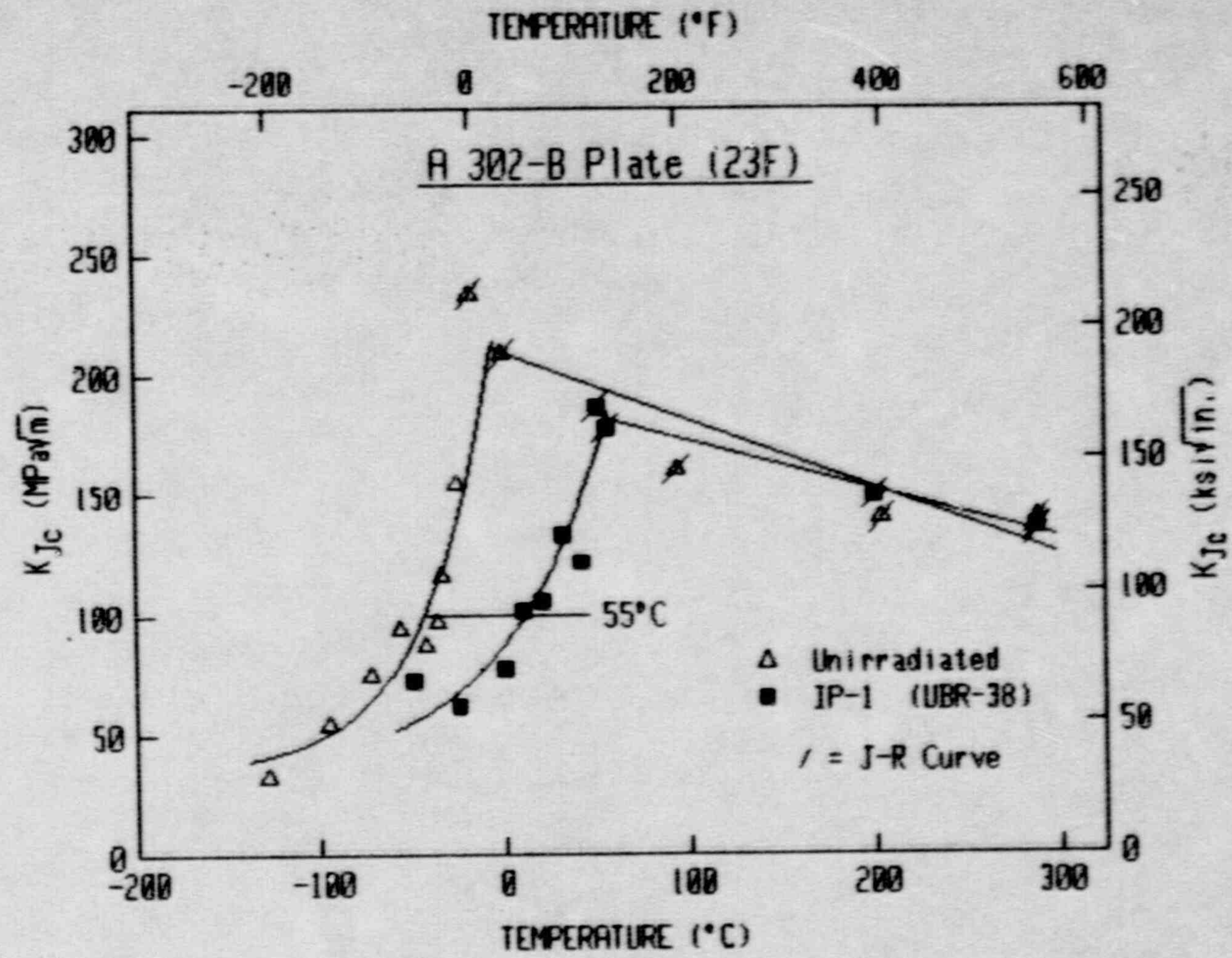

Fig. 34 **Fracture toughness data from the low fluence rate irradiation (IP-1) of A 302-B Plate 23F.**

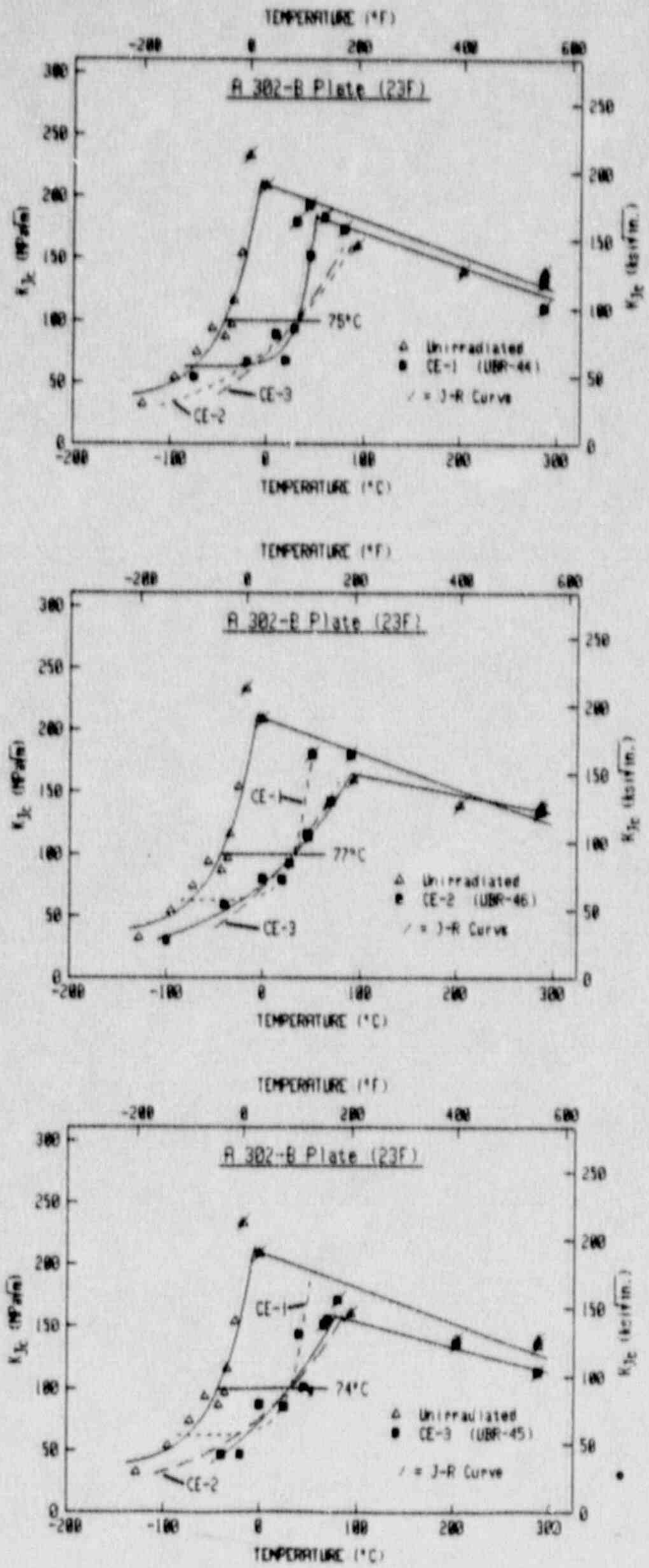

Fig. 35 Fracture toughness data from the intermediate fluence rate (CE) irradiations of A 302-B Plate 23F.

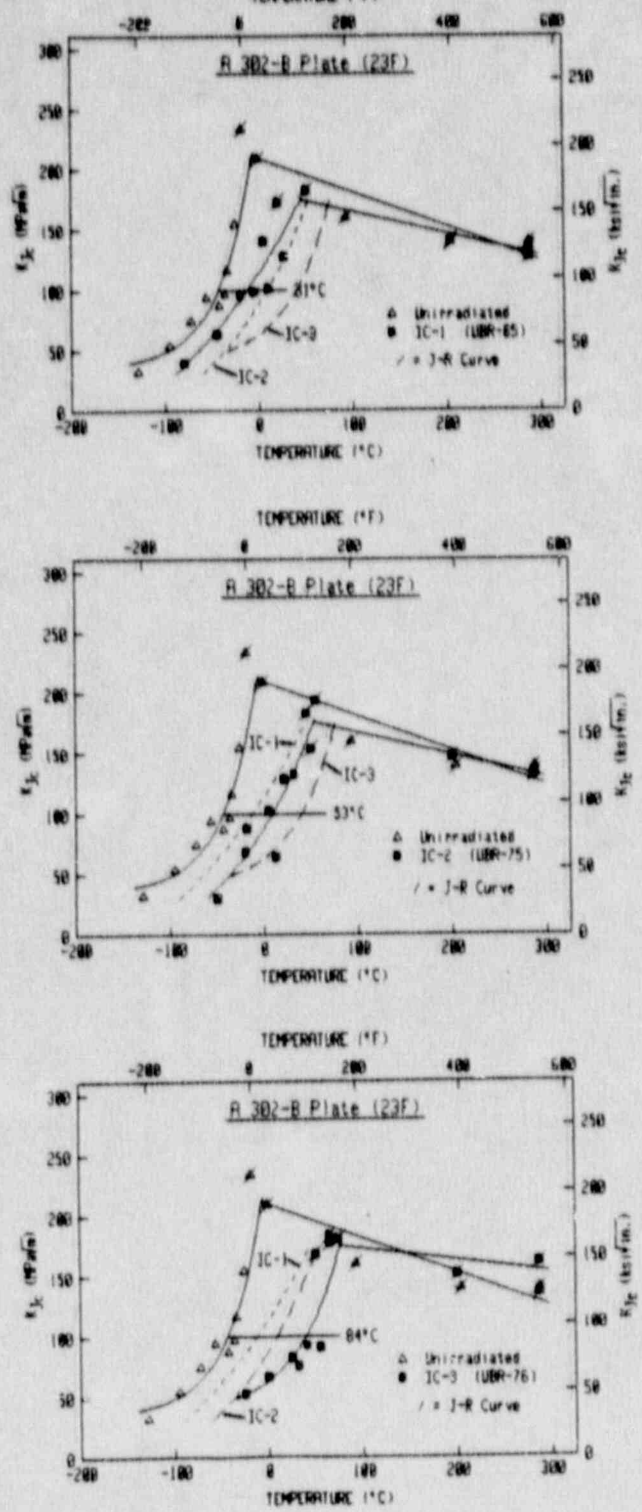

Fig. 36 Fracture toughness data from the high fluence rate (IC) irradiations of A 302-B Plate 23F.

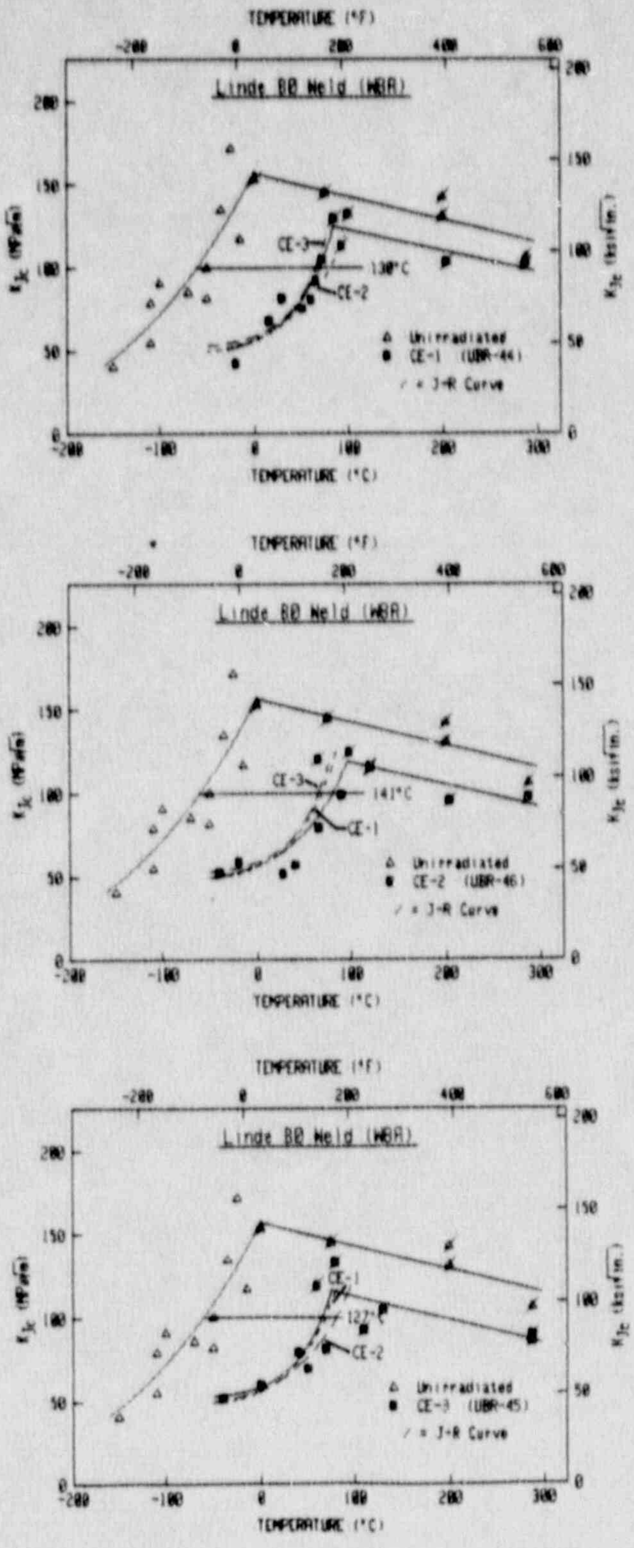

Fig. 37 **Fracture toughness data from the intermediate fluence rate (CE) irradiations of Linde 80 Weld W8A.**

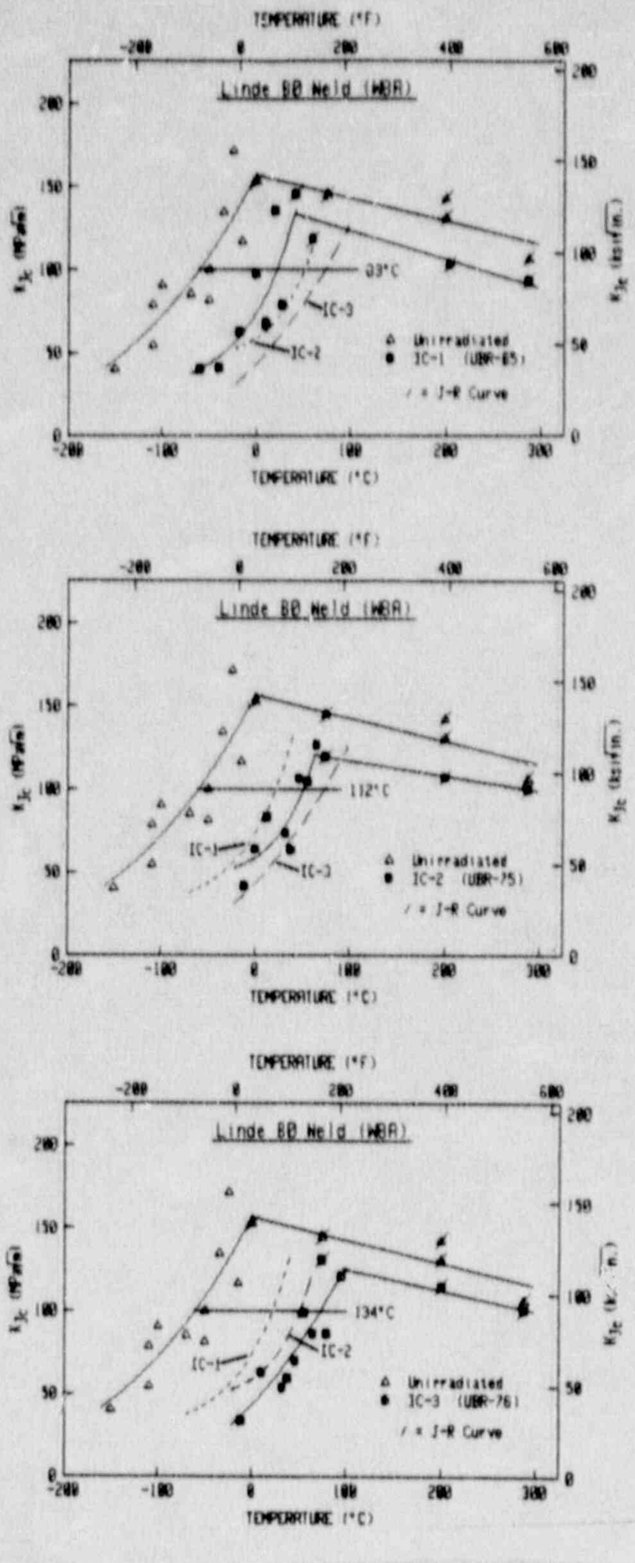

Fig. 38 Fracture toughness data from the high fluence rate (IC) irradiations of Linde 80 Weld W8A.

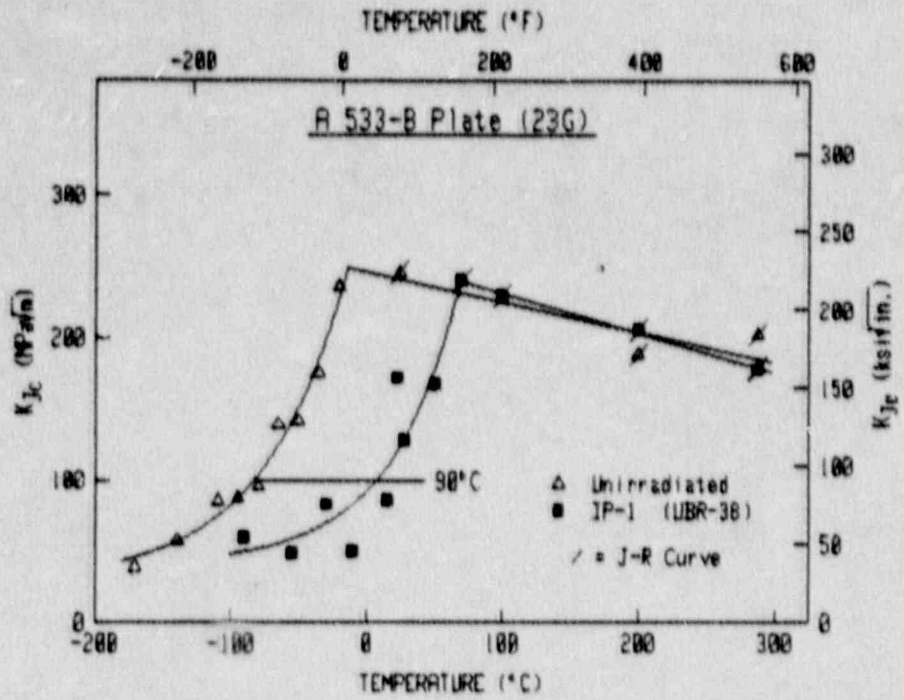

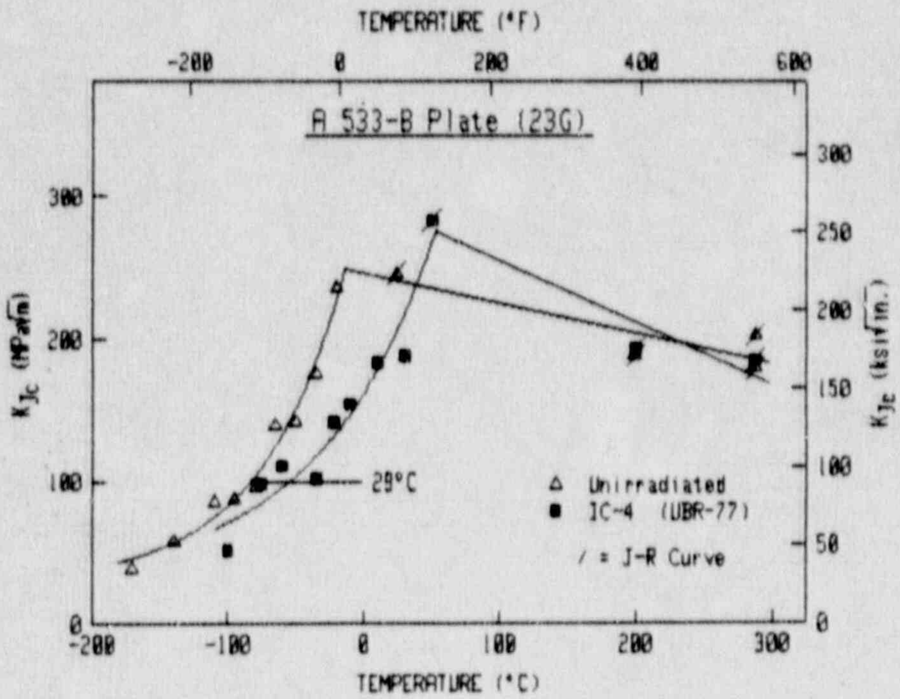

Fig. 39 Fracture toughness data from the irradiations of A 533-B Plate 23G.

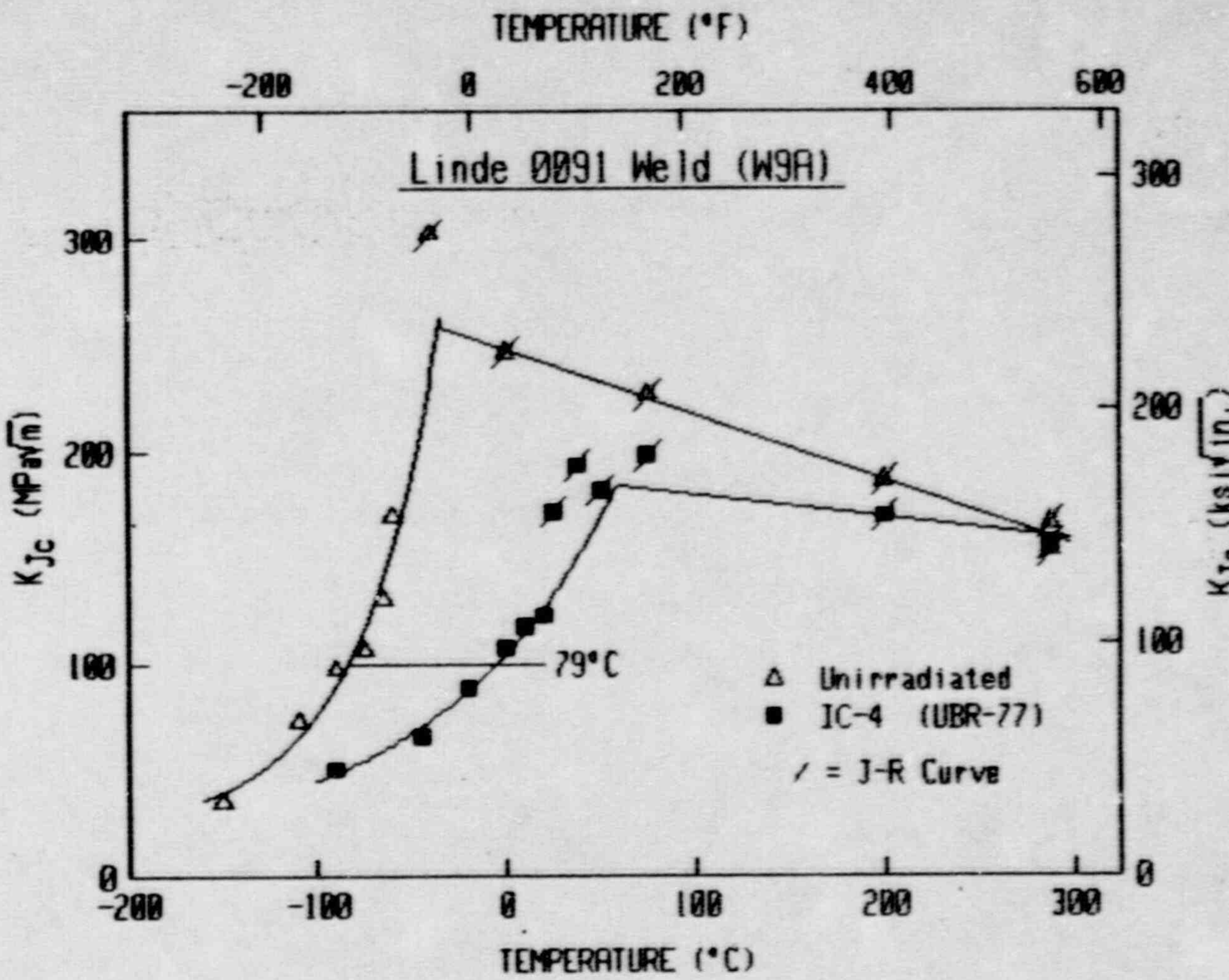

Fig. 40 **Fracture toughness data from the irradiation of Linde 0091 Weld W9A.**

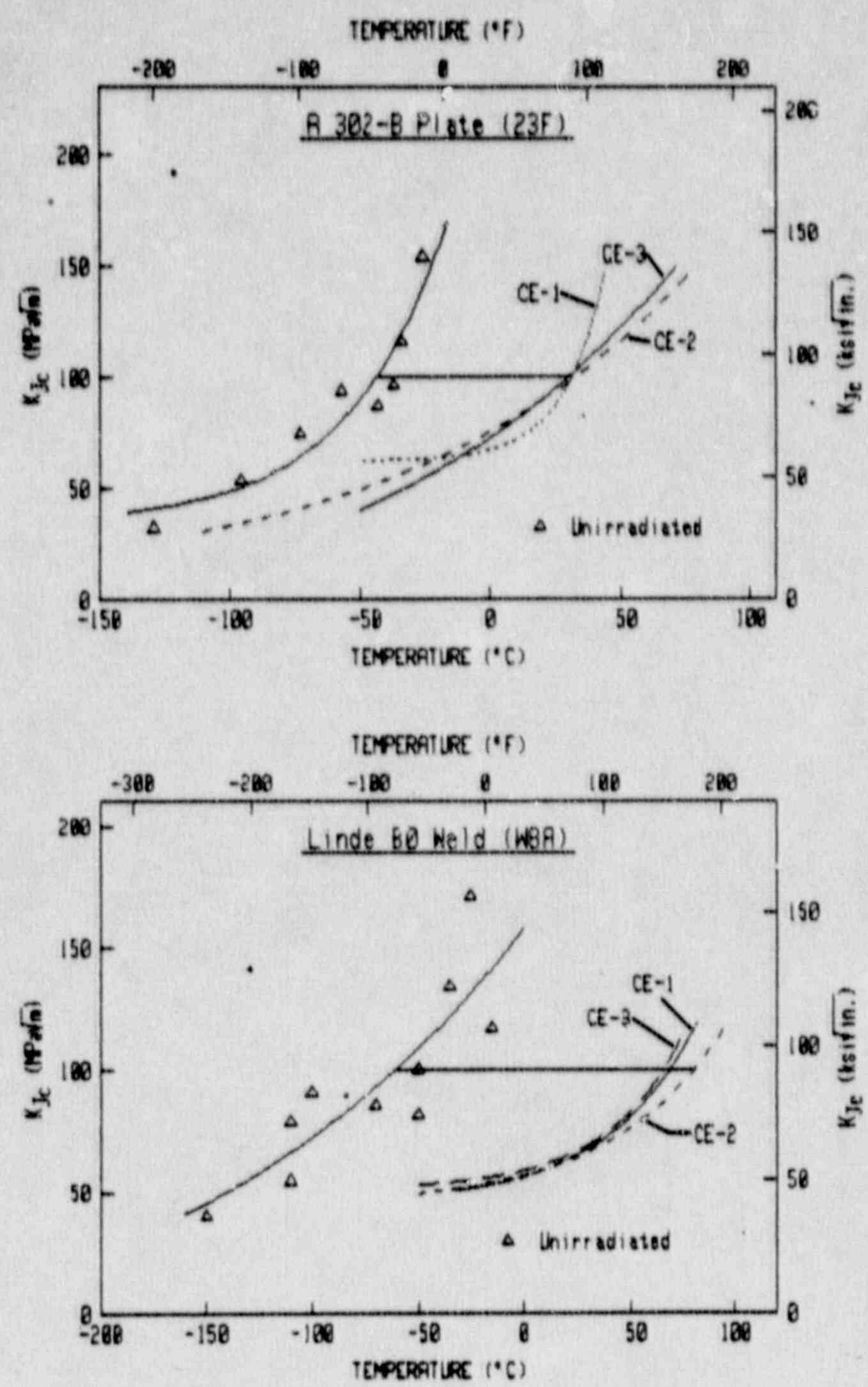

Fig. 41 **Comparison of transition regime data trends for the intermediate fluence rate irradiations of Linde 80 Weld W8A and A 302-B Plate 23F.**

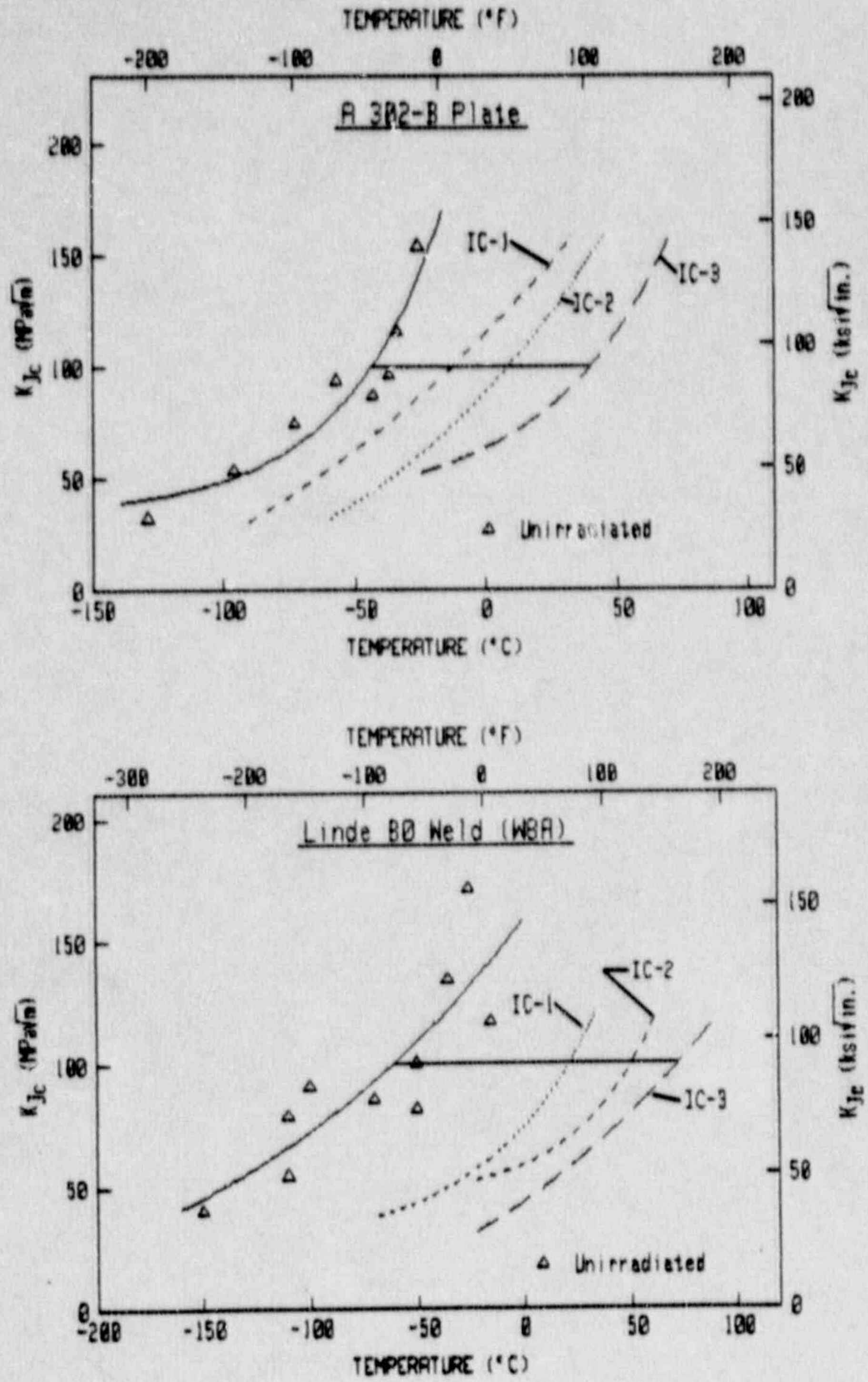

Fig. 42 Comparison of transition regime data trends for the high fluence rate irradiations of Linde 80 Weld W8A and A 302-B Plate 23F.

5.2.2 Assessment of Fluence Rate Effect

Comparisons of the transition temperature increases (at 100 MPa$\sqrt{m}$) for each material are given in Fig. 43. The Linde 0091 weld (W9A) is included in this figure for completeness. It is re-emphasized that the determinations were hampered by high data scatter in many cases. For the A 302-B Plate 23F, data from the NRC's LWR-SDIP (Ref. 5) and an EPRI-sponsored program (Ref. 11) are also shown. The fluence rate for specimens from the LWR-SDIP Simulated Surveillance Capsules (SSC) is slightly lower than the fluence rate experienced by the in-core assemblies (~ 7 vs. ~ 9 x 10^{12} n/cm^2·s^{-1}); the LWR-SDIP In-Wall capsules have fluence rates which span those of the core-edge (CE) assemblies (2-8 vs. 5-6 x 10^{11} n/cm^2·s^{-1}). The EPRI-sponsored irradiation was an in-core irradiation at UBR. For the two welds, additional in-core irradiation data are obtained from Ref. 12. For the A 533-B Plate 23G, data (of a limited nature) from a previous in-core irradiation (Ref. 13) are given to estimate embrittlement at high fluence.

For the A 302-B plate, the data from the three in-core irradiations, the SSC irradiations and the EPRI-sponsored in-core irradiation form a single data trend as a function of fluence. In comparison, the core-edge irradiations and the LWR-SDIP in-wall irradiations indicate less embrittlement at high fluences and greater embrittlement at low fluences. However, with the core-edge irradiations, no significant difference in fracture toughness was found with the fluence levels examined. Data trends for the two fluence rates (CE and IC) appear to cross-over at a fluence of ~ 2 x 10^{19} n/cm^2. For the lowest fluence rate, achieved with the in-pool (IP) facility, the indicated shift is much greater than the shift by a comparable fluence in-core. However, it is also lower than that for a somewhat higher core-edge fluence exposure. This trend is more clearly seen in Fig. 44, where the individual data points and curve-fits are illustrated for each fluence rate. (Some acknowledgement of the fluence differences among these three sets is necessary.)

Many of the observations for the A 302-B Plate 23F are found to apply to the Linde 80 weld as well. Specifically, the in-core irradiations of the Linde 80 weld in this program and previous in-core irradiations indicate a distinct dependence on the total fluence, within the range of fluences from 0.5 to 2.1 x 10^{19} n/cm^2. As well, data for the core-edge irradiations do not indicate significant differences in spite of a large fluence difference. The data trend with fluence for the in-core irradiations crosses that for the core-edge irradiations at ~ 2 x 10^{19} n/cm^2. A disturbing aspect of the results for this weld is that previous in-core data (Ref. 12) indicated much less embrittlement than the present IC data for a given fluence. Since the same irradiation facility was used for all of the in-core irradiations, the difference may be due to some weld inhomogeneity along the weld seam. This is being investigated and will be the subject of a future report.

For the A 533-B Plate 23G, the IP irradiation produced greater embrittlement than the IC irradiation (Fig. 45). In this case, the fluence differences could explain some of the difference. This trend is consistent with that observed for the A 302-B Plate 23F.

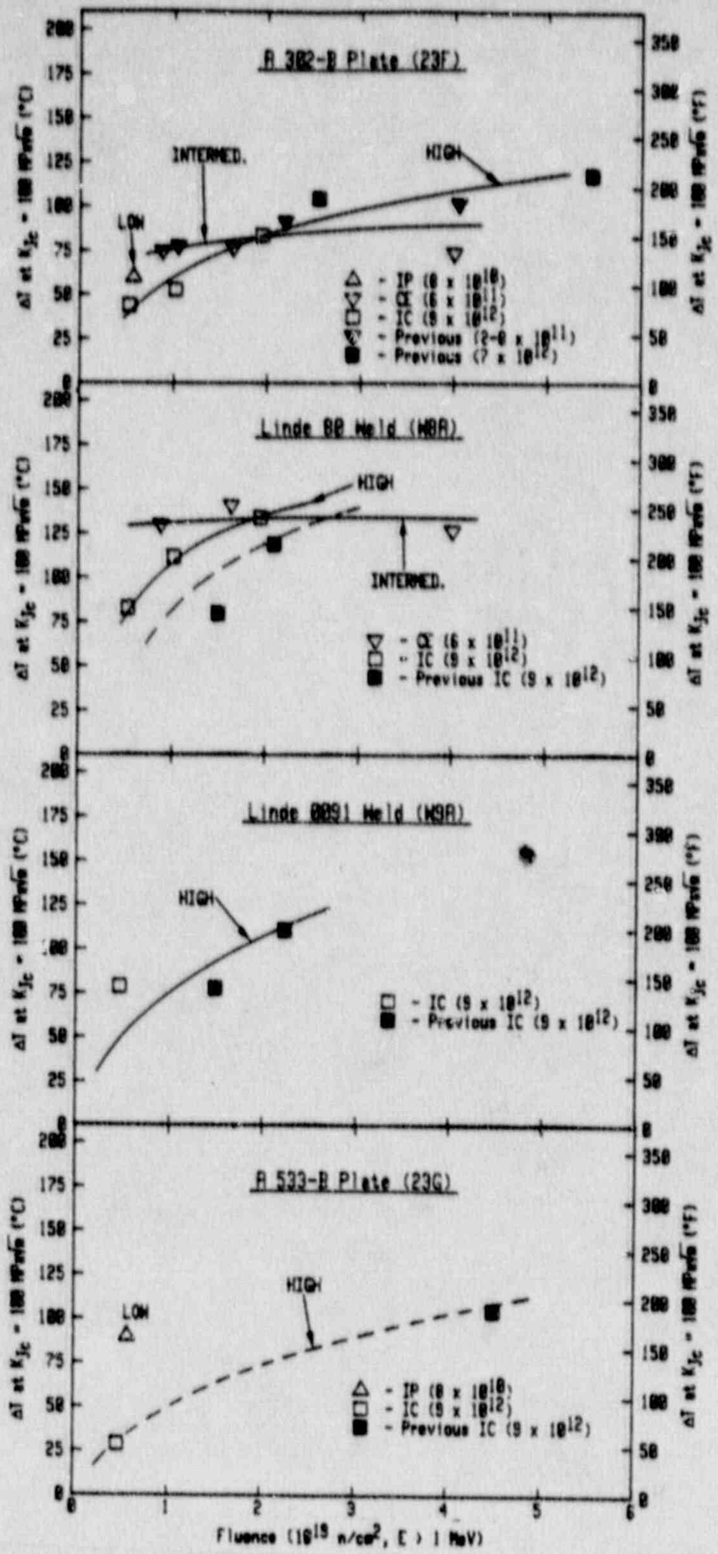

Fig. 43 Transition temperature increase as a function of fluence for the program materials.

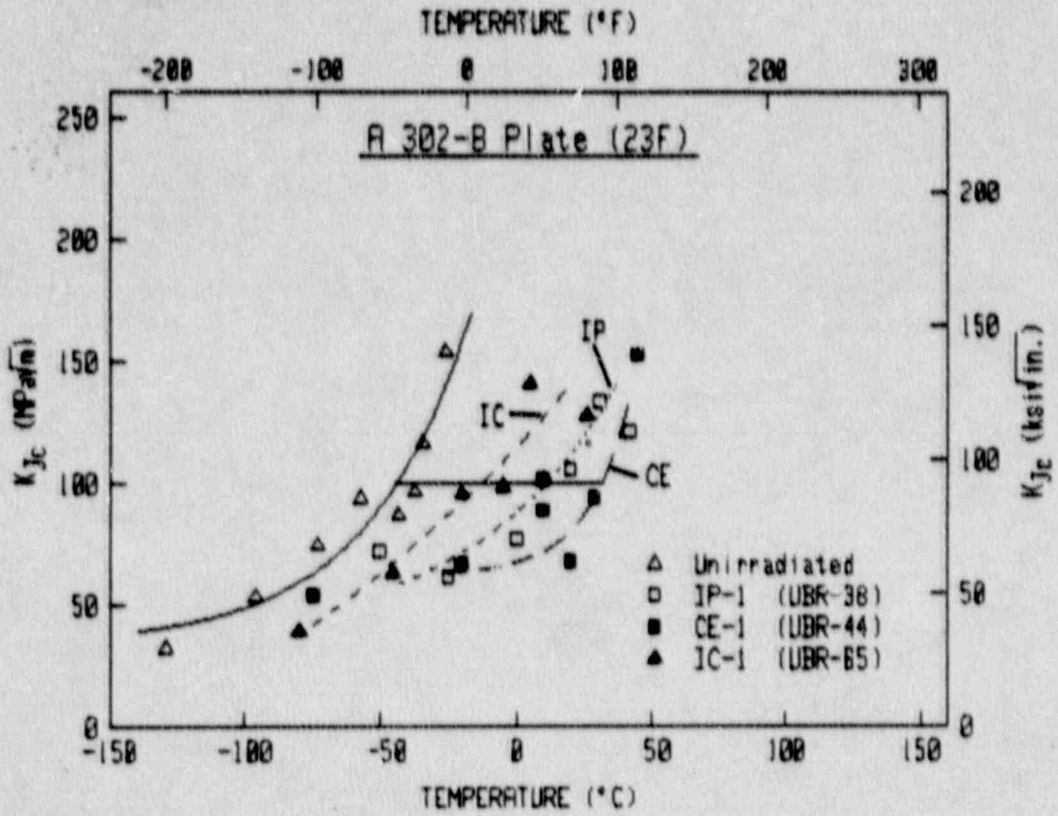

Fig. 44 For the A 302-B Plate 23F, comparison of transition regime data for all three fluence rates, at the lowest target fluence level of ~ 0.5 x 10^{19} n/cm^2.

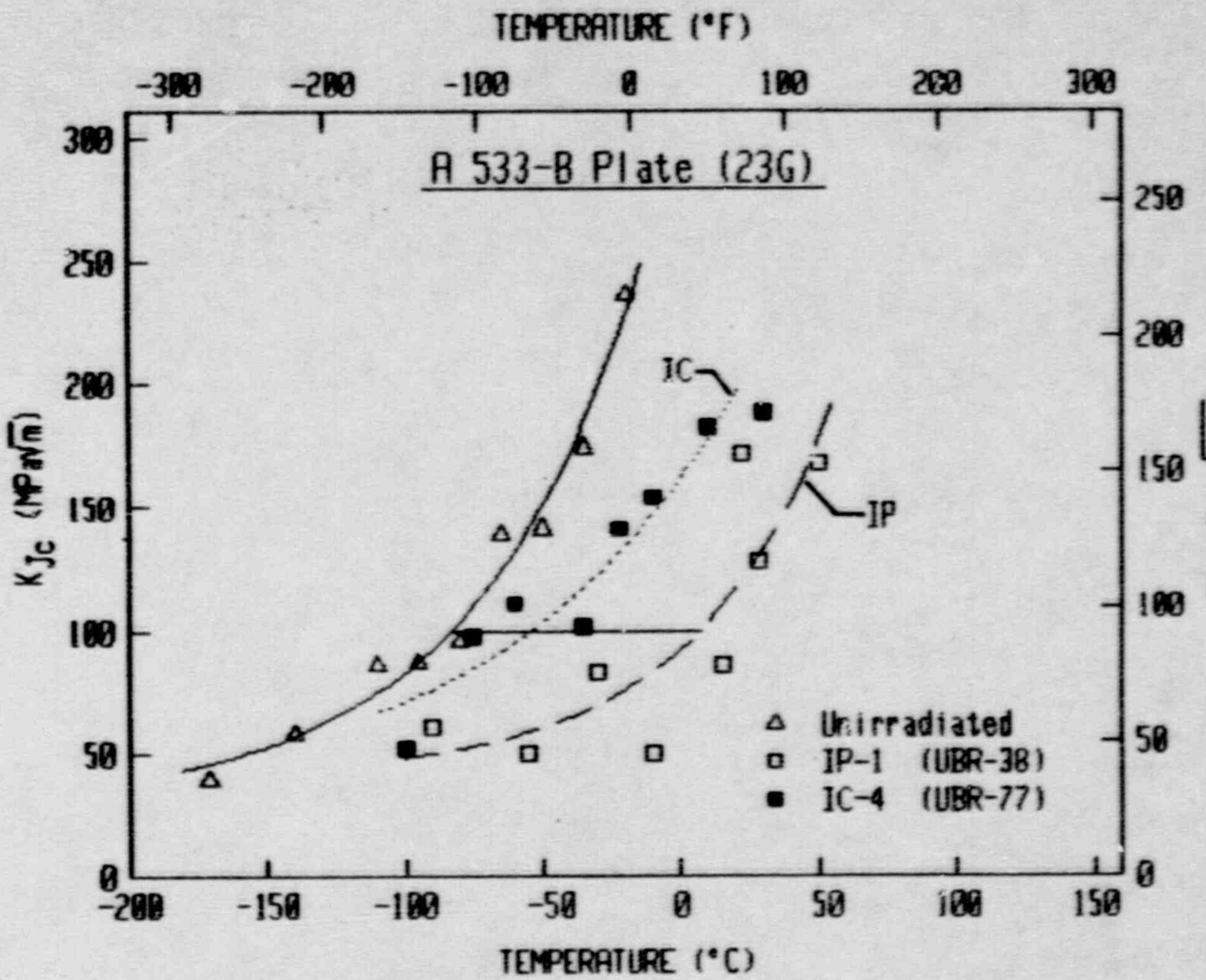

Fig. 45 For the A 533-B Plate 23G, comparison of transition regime data for the low and the high fluence rates.

For the Linde 0091 Weld 0091, no comparisons of data from different fluence rates is possible. The shift resulting from the present in-core irradiation (IC-4) is similar to that from previous in-core irradiations to a much higher fluence (0.5 vs. 1.5 x 10^{19} n/cm^2), paralleling the observations for the Linde 80 Weld W8A.

In terms of degradation in upper shelf properties, small decreases in J levels occur for the plates (Figs. 46 and 47), with moderate decreases for the welds (Figs. 48 and 49). For any of the fluence rates, higher total fluences tend to result in reduced J levels. For the A 302-B Plate 23F and the Linde 80 Weld W8A, the lowest curves overall are for the highest fluence irradiation overall, from CE-3 (UBR-45).

To summarize, fluence rate effects were seen for the fracture toughness data. In contrast to degradation from a high fluence rate exposure, a low fluence rate appeared more detrimental at low fluence, but the converse appears true for high fluence. A clearer picture is precluded by the scatter encountered in this data.

5.3 Comparison of Transition Temperature Elevations by K_{Jc} and Charpy-V Test Methods

One important consideration in the evaluation of fluence-rate effects is the relative effect on notch ductility (C_v) vs. fracture toughness correlation. Since the upper shelf fracture toughness trends are not easily quantified using a single parameter, the focus of this discussion will be on the transition temperature elevation (ΔT). Data for the transition regime are summarized in Table 4 for both the C_v and K_{Jc} data.

In Ref. 14, the ΔT from C_v data was found to underestimate somewhat the ΔT from K_{Jc} data for base metals. For weld metals, the two measures of ΔT were found to be in good overall agreement. Similar comparisons are made in Figs. 50 and 51 for the materials of the present study. Also illustrated in each case are data from previous irradiations of the same materials. For all four materials of the present study, the ΔT from C_v is found to give reasonable estimates of the ΔT from K_{Jc}. The one noteworthy exception is the somewhat large difference in ΔT's for the low fluence rate (IP) irradiation of the A 533-B Plate 23G.

For the A 302-B Plate 23F, all three fluence rates from this program yielded a similar ΔT relationship for the two test methods. In contrast, the "Previous" data (from Ref. 5) indicate a disagreement (on average 24°C) between the ΔT from C_v and that from K_{Jc}. The previous data on this plate were from the nominal 1/4T and 3/4T thickness locations, whereas specimens for the current study were taken from the plate mid-thickness (1/2T) location. On examining the data for the unirradiated condition (see Fig. 26), the C_v data for the 1/2T location shows a 41-J transition temperature which is 11°C (20°F) lower than that for the 1/4T or 3/4T location, that is -15°C vs. -4°C. In contrast, the K_{Jc} data for the 1/2T location indicate a 100 MPa$\sqrt{m}$ transition temperature (-44°C) that is 12°C (22°F) higher

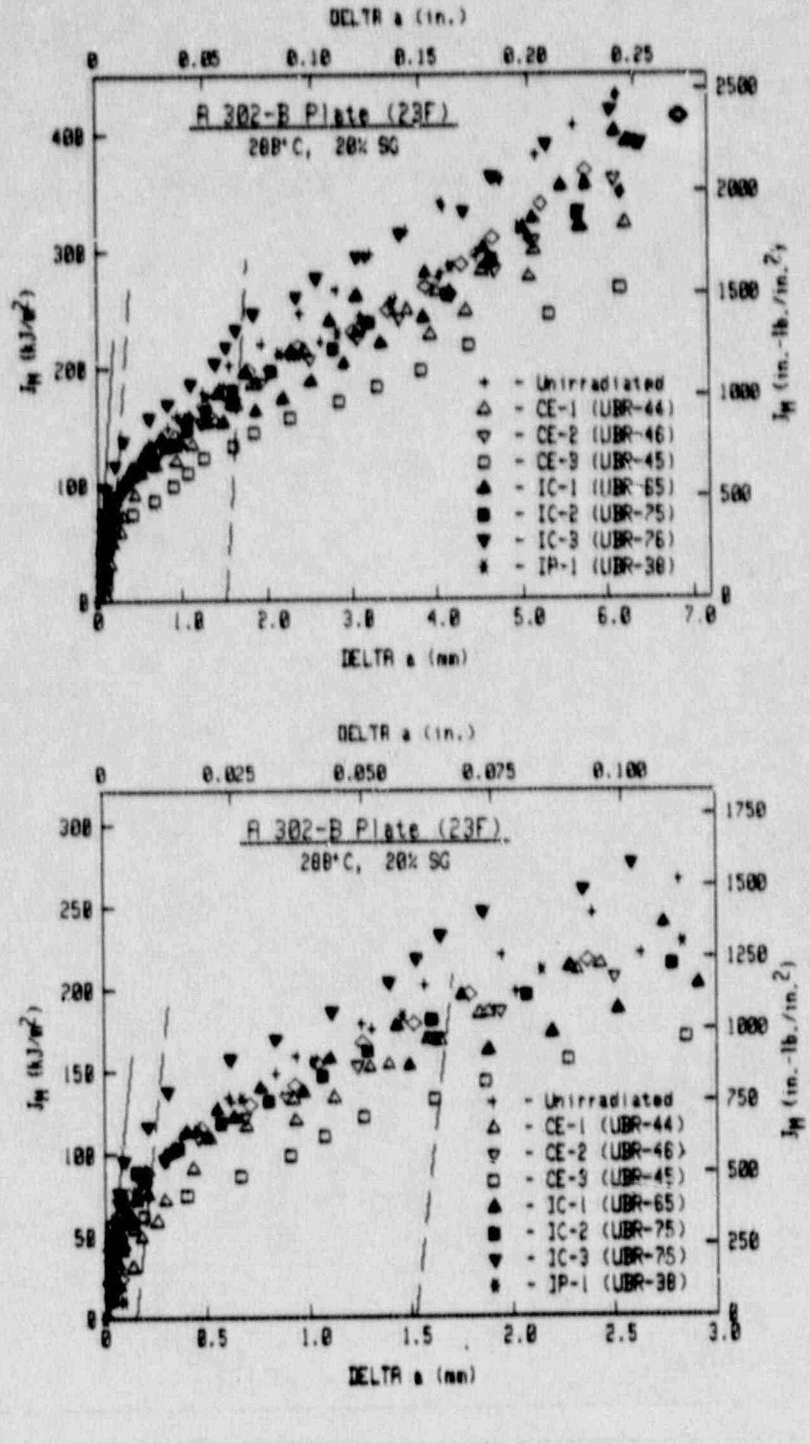

Fig. 46 Comparison of J-R curves for A 302-B Plate 23F from the various irradiation assemblies.

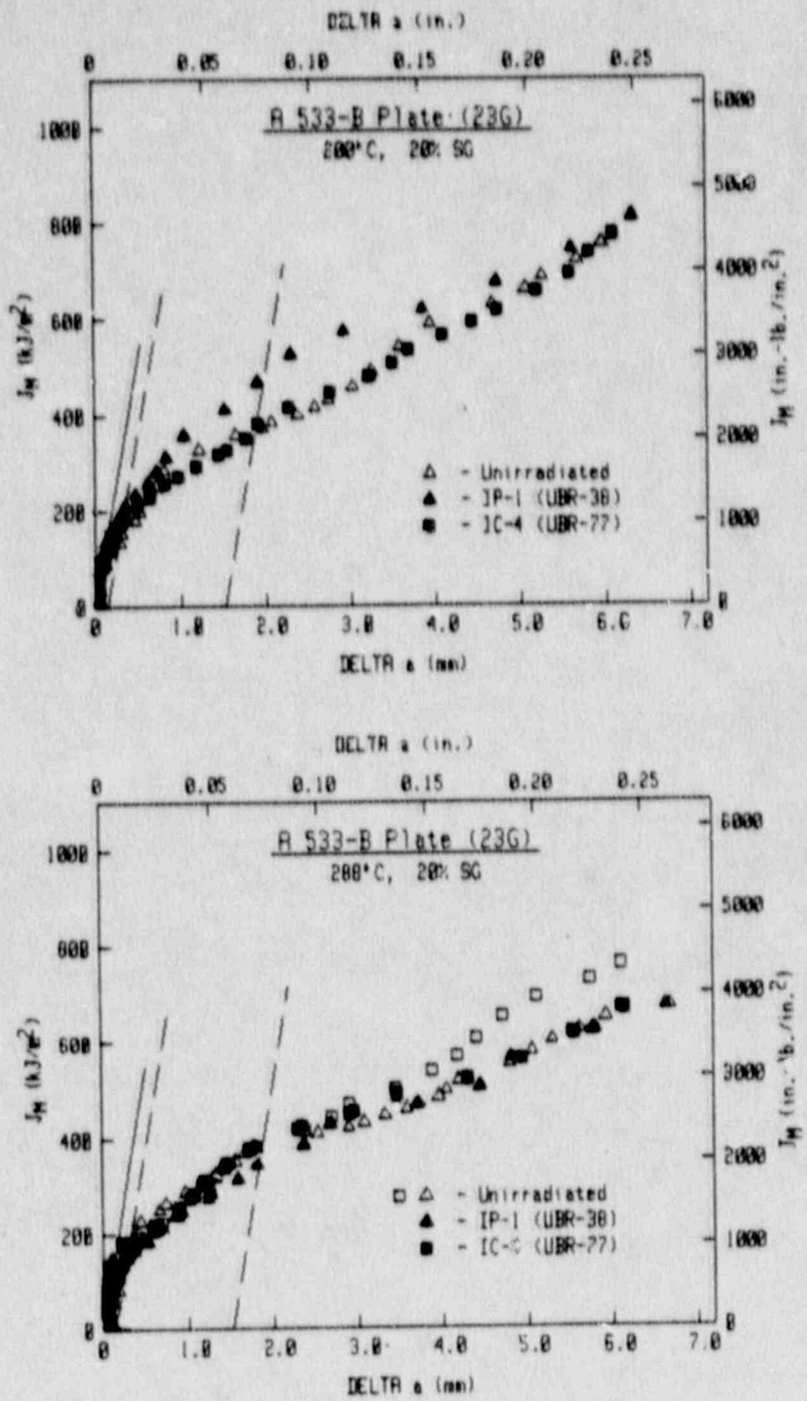

Fig. 47 **Comparison of J-R curves for A 533-B Plate 23G from the various irradiation assemblies.**

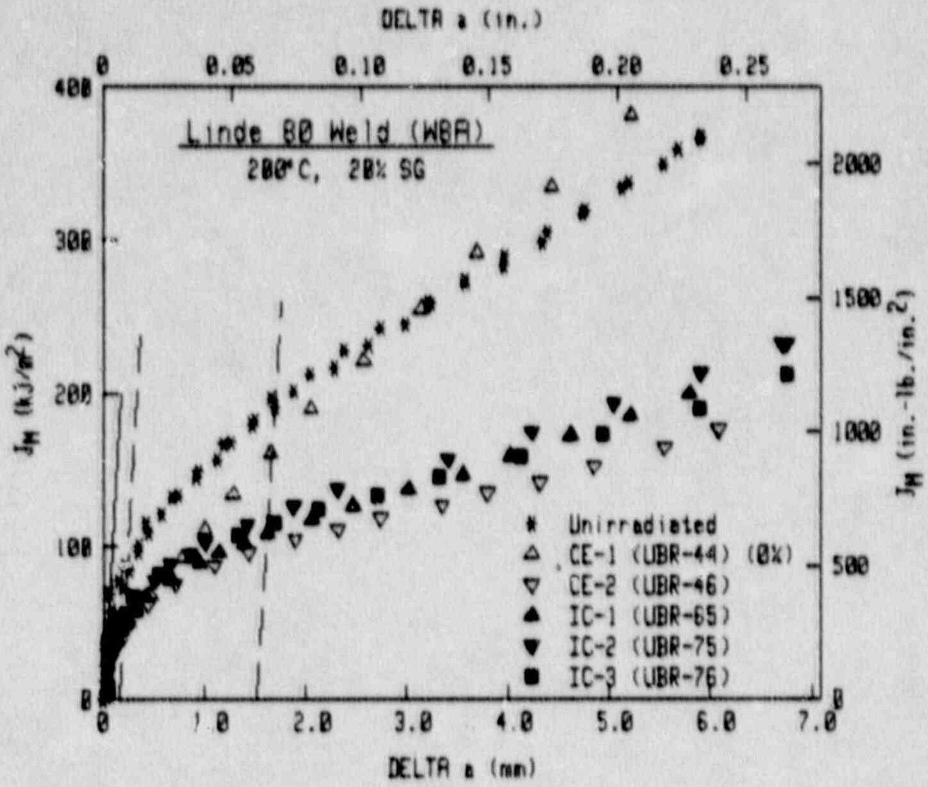

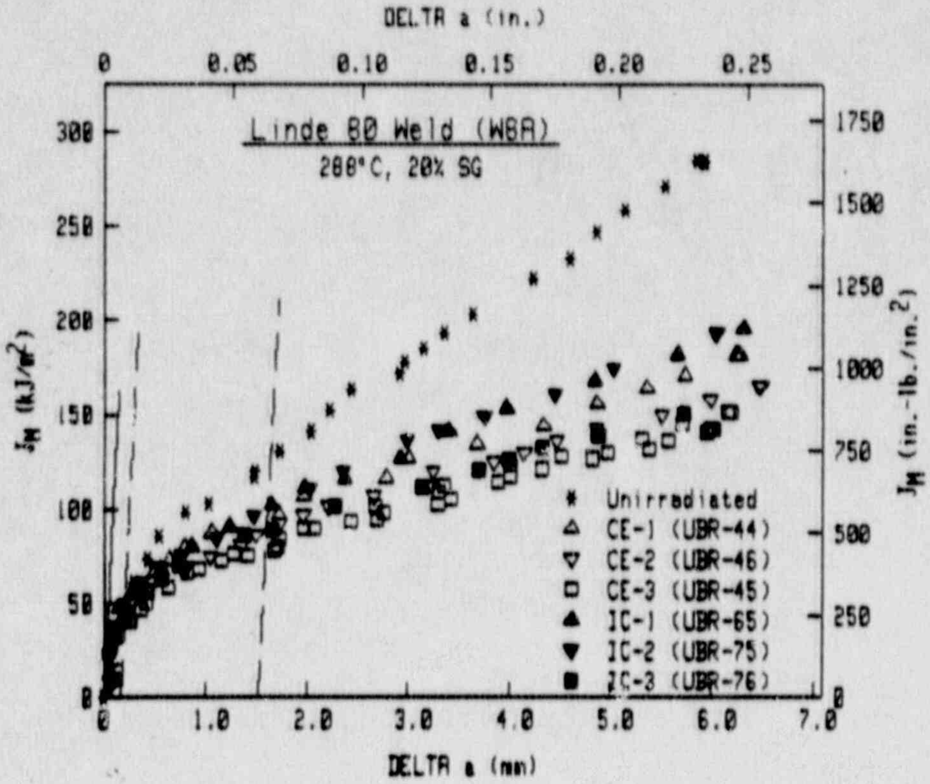

Fig. 48 Comparison of J-R curves for Linde 80 Weld W8A from the various irradiation assemblies.

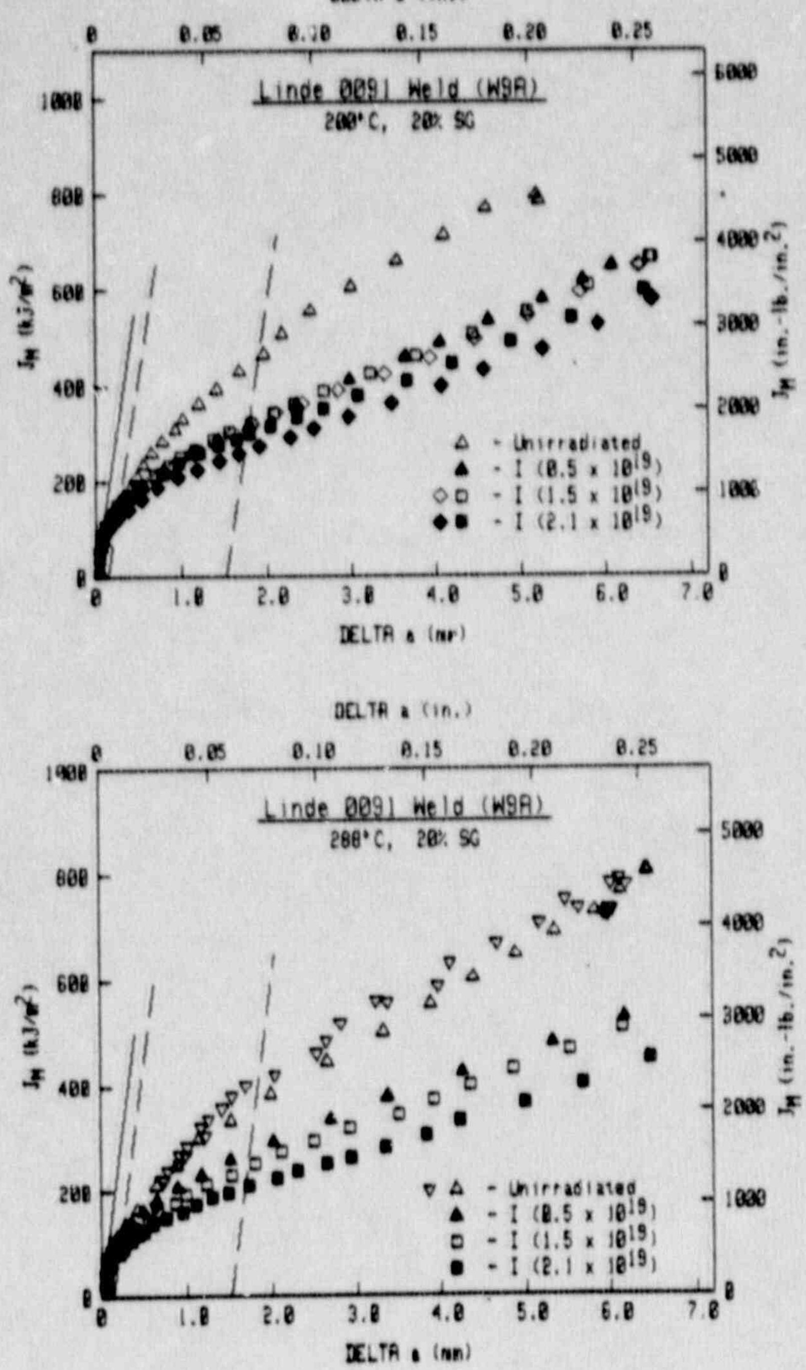

Fig. 49 Comparison of J-R curves for Linde 0091 Weld W9A from the various irradiation assemblies.

Table 4 Comparison of Transition Temperature Shifts (ΔT) from C_v and K_{Jc}

Capsule	UBR-	Fluence [a]	Temperature at 41 J (°C)	Temperature at 100 MPa$\sqrt{m}$ (°C)	Temperature Shifts at 41 J (°C)	Temperature Shifts at 100 MPa$\sqrt{m}$ (°C)
			A 302-B Plate 23F			
Unirrad.	--	----/----	-15	-44	--	--
CE-1	44	0.79/0.88	43	31	58	75
CE-2	46	1.50/1.64	49	33	64	77
CE-3	45	3.85/4.01	63	30	78	74
IC-1	65	0.56/0.53	29	-13	44	31
IC-2	75	1.22/1.02	46	9	61	53
IC-3	76	2.23/1.95	57	40	72	84
IP-1	38	0.54/0.57	38	16	53	60
			Linde 80 Weld W8A			
Unirrad.	--	----/----	-23	-61	---	---
CE-1	44	0.79/0.88	102	69	125	130
CE-2	46	1.50/1.64	107	80	130	141
CE-3	45	3.85/4.01	127	66	150	127
IC-1	65	0.56/0.53	82	22	105	83
IC-2	75	1.22/1.02	96	51	119	112
IC-3	76	2.23/1.95	104	73	127	134
			A 533-B Plate 23G			
Unirrad.	--	----/----	-34	-83	--	--
IC-4	77	0.45/0.47	5	-54	39	29
IP-1	38	0.54/0.57	21	7	55	90
			Linde 0091 Weld W9A			
Unirrad.	--	----/----	-62	-84	--	--
IC-4	77	0.45/0.47	-1	-5	61	79

[a] 10^{19} n/cm^2 (E > 1MeV), with C_v/K_{Jc}.

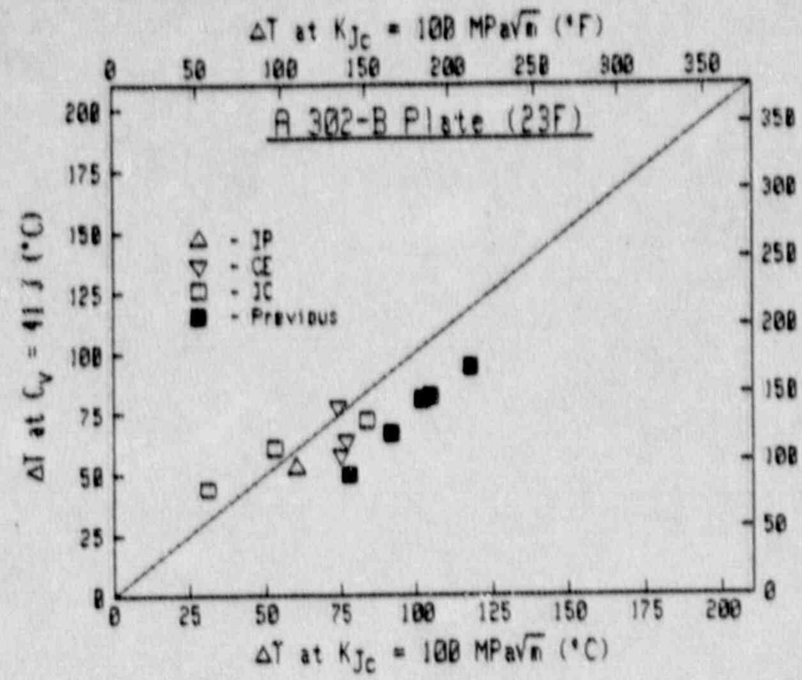

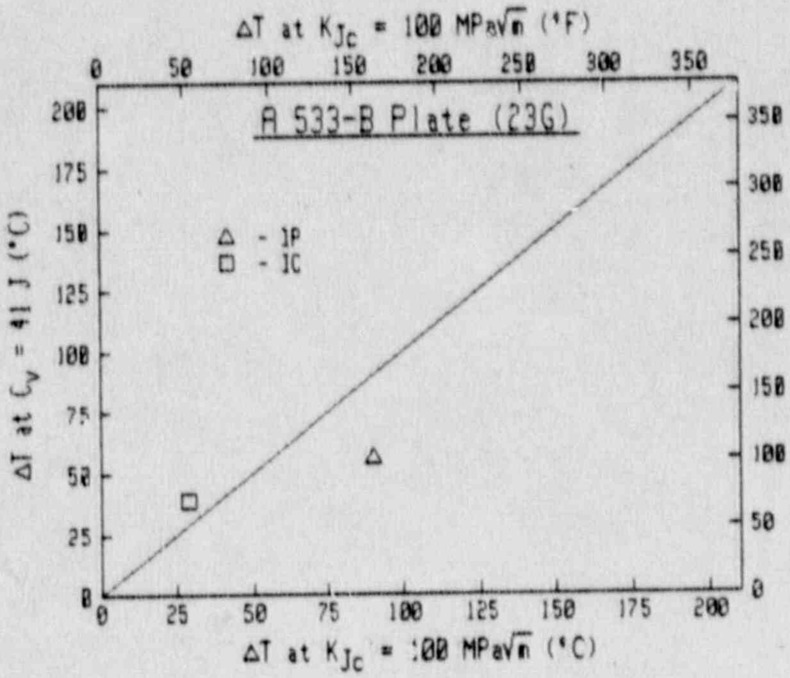

Fig. 50 Comparison of ΔT from C_v and ΔT from K_{Jc} for the A 302-B Plate 23F and the A 533-B Plate 23G.

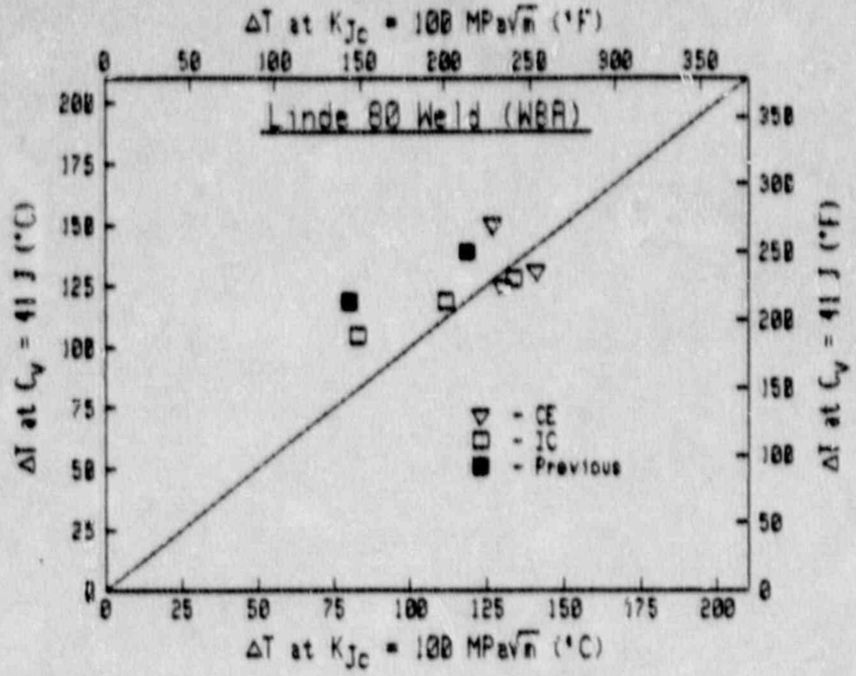

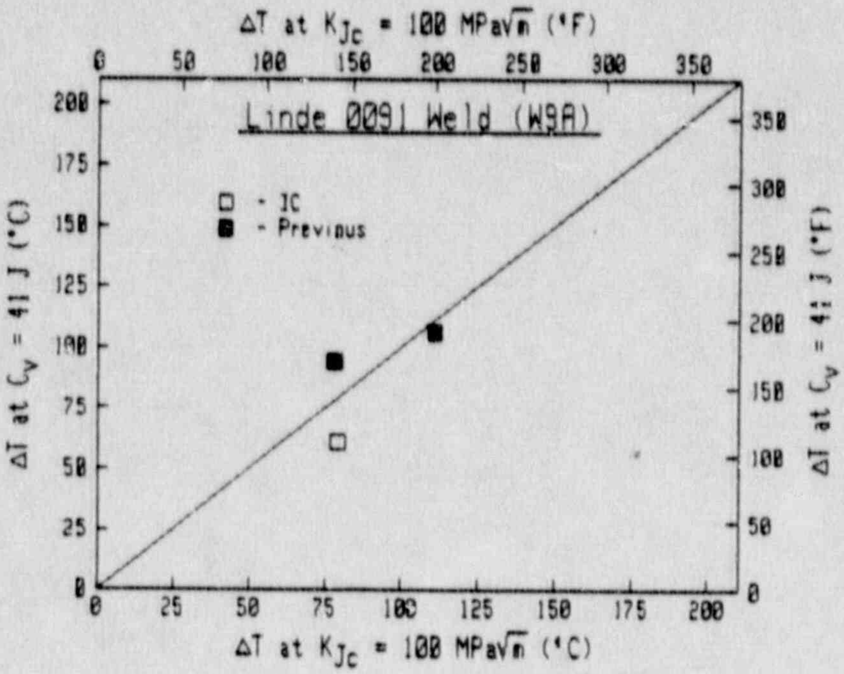

Fig. 51 **Comparison of ΔT from C_v and ΔT from K_{Jc} for the Linde 80 Weld W8A and the Linde 0091 Weld W9A.**

than that for the 1/4T or 3/4T location (-56°C). Causes for this mismatch are not known. One would expect both test methods to indicate a change in properties in the same direction. An accounting of the 23°C total offset (11°C + 12°C) in the baseline properties would bring both sets into better agreement.

In terms of upper shelf toughness, correlations have been developed relating J-R curve trends to C_vUSE levels (Ref. 15). The cited correlations were developed using Linde 80 weld materials only. As illustrated in Fig. 52, data from this program correspond well with the correlations from Ref. 15, further validating the utility of the correlations.

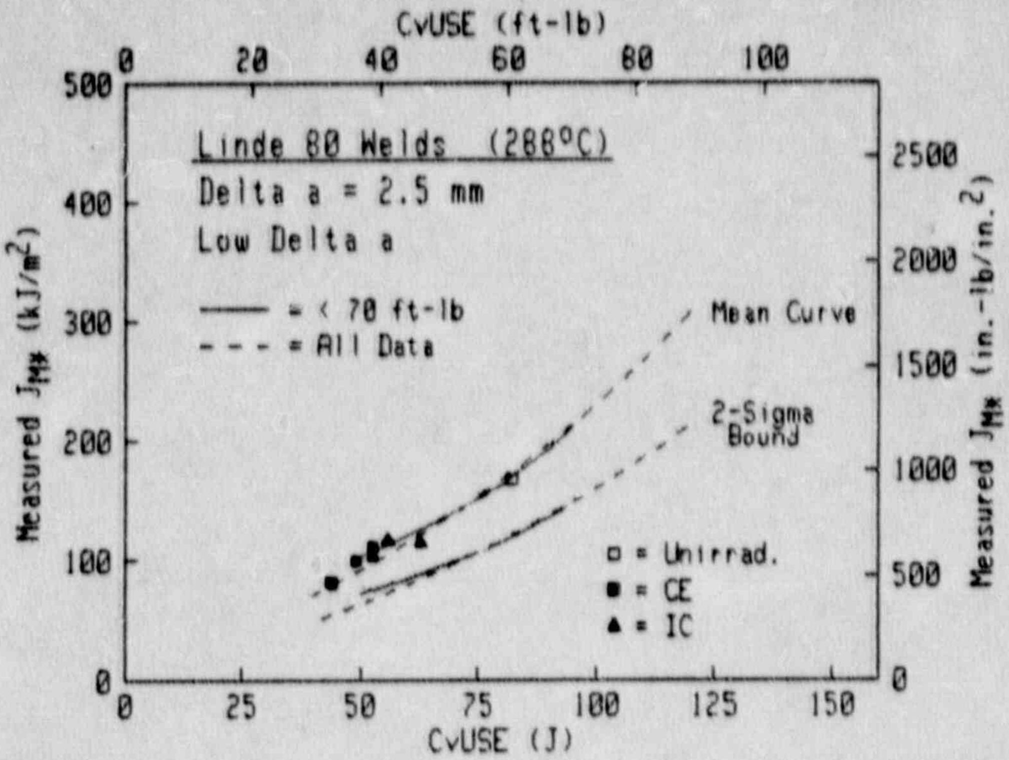

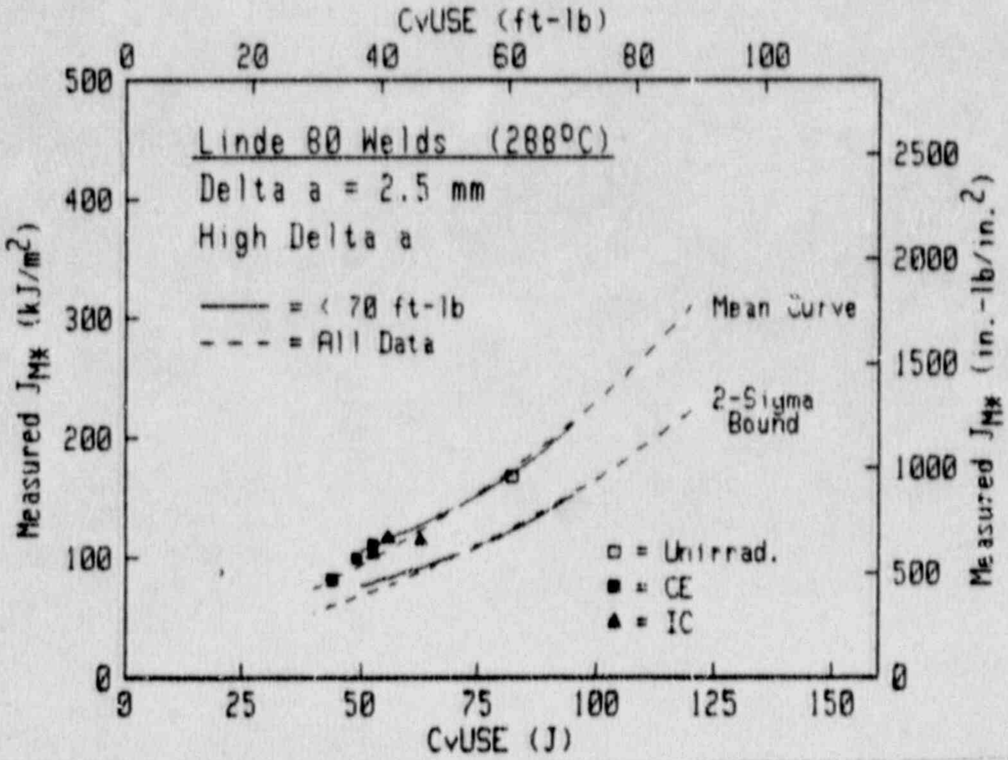

Fig. 52 For the Linde 80 Weld W8A at 288 °C, comparison of J levels with correlation estimates at 2.5mm as a function of C_vUSE. Similarly good correspondence has been found at other Δa levels.

6. DISCUSSION

The observed levels of difference in notch ductility change (or yield strength change) by an "intermediate" versus "high" fluence rate were not large. However, the differences appear to be of sufficient magnitude to warrant consideration in making judgments of material servicability or the setting of operating parameters. The influence of composition on the relative susceptibility of steels and weld metals to fluence-rate effects should be qualified. Until this variable is properly explored, the full importance of the present observations to embrittlement projection methods such as NRC Regulatory Guide 1.99 will not be known.

Additional tests of fluence-rate effects in welds should be pursued for low fluences, that is, the fluence interval of about 1 to 5 x 10^{18} n/cm^2, since here slow fluence accumulations (service) appear more damaging than fast fluence accumulations (test reactors). The magnitude of the fluence-rate effect seen to date is not so large as to preclude the use of accelerated (test reactor) irradiations for screening metallurgical, irradiation or postirradiation annealing variables.

The reduction of the C_v USE of weld W8A to a level of 50 J (and less), while hampering the establishment of 41-J temperature, demonstrates that such levels are possible with fluences less than 4 x 10^{19} n/cm^2. The development of J-R curve data at such low fluences helps to validate correlations developed for Linde 80 welds as a function of C_vUSE (Ref. 15).

The study has demonstrated the value of including tensile specimens along with C_v specimens, especially if low postirradiation C_vUSE levels result. Trends in yield strength with fluence may offer an acceptable alternative to 41-J temperature trend information in such cases.

One somewhat surprising result was the very low apparent sensitivity of the A 302-B Plate 23F and the Linde 80 Weld W8A to fluence levels above ~ 0.5 x 10^{19} n/cm^2 in the intermediate fluence rate irradiation series (CE). Such an embrittlement "plateau" was not described by the data for the materials when irradiated at the high fluence rate. Whether or not this behavior is generic to these two material types is uncertain at present.

7. CONCLUSIONS

The following observations and conclusions have been obtained from the investigations to date:

- Fluence-rate effects on the notch ductility and tensile strength properties of the ASTM A 302-B reference plate and a high copper, high nickel content Linde 80 submerged arc weld deposit were observed.

- The fluence-rate effect was apparent for the plate at high fluence but not low fluence. The converse was observed for the weld. At high fluence, the intermediate fluence rate produced less embrittlement than a high fluence rate for the A 302-B plate. At low fluence, the intermediate fluence rate produced more embrittlement than the high fluence rate for the Linde 80 weld..

- From conclusion 2, the data suggest that the fluence-rate effect is dependent on material type (plate or weld) or material composition, including copper content and nickel content.

- The apparent radiation embrittlement sensitivities of the 0.2% Cu content reference plates were about the same at ~ 0.5×10^{19} n/cm^2 but differed significantly at ~ 3×10^{19} n/cm^2. Their similarity at the lower fluence level was independent of fluence rate (high or low).

- Fluence-rate effect indications from the C_v test results are consistent with those found in tensile tests and K_{Jc} and J-R curve tests.

- Observed differences in property change attributable to a fluence rate of $5\text{-}6 \times 10^{11}$ n/cm^2·s^{-1} versus a fluence rate of $8\text{-}9 \times 10^{12}$ n/cm^2·s^{-1} are not considered large but could influence data interpretations within the framework of NRC Regulatory Guide 1.99.

- An inconsistency was found in the baseline data (unirradiated condition) for the A 302-B Plate 23F; specifically, the 1/4T and 3/4T locations exhibit a higher transition temperature in C_v tests but a lower transition temperature in fracture toughness tests compared to the 1/2T location. This observation will be investigated further in the continuing MEA program for the NRC.

REFERENCES

1. D. R. Harries and B. L. Eyre, "Effects of Irradiation in Iron and Steels," Flow and Fracture of Metals and Alloys in Nuclear Environments, ASTM STP 380, American Society for Testing and Materials, 1965, p. 105.

2. J. R. Hawthorne, "Radiation Effects Information Generated on the ASTM Reference Correlation-Monitor Steels," DS 54, American Society for Testing and Materials, 1974.

3. "Standard Practice for Characterizing Neutron Exposures in Ferritic Steels in Terms of Displacements per Atom (DPA)," ASTM E 693-79, ASTM Book of Standards, Section 12, Vol. 12.02, 1983, p. 402.

4. J. R. Hawthorne, J. J. Koziol and S. T. Byrne, "Evaluation of Commercial Production A 533-B Steel Plates and Weld Deposits with Extra-Low Copper Content for Radiation Resistance," Effects of Radiation on Structural Materials, ASTM STP 683, American Society for Testing and Materials, J. A. Sprague and D. Kramer, Eds., 1979, pp. 235-251.

5. J. R. Hawthorne, B. H. Menke and A. L. Hiser, "Notch Ductility and Fracture Toughness Degradation of A 302-B and A 533-B Reference Plates from PSF Simulated Surveillance and Through-Wall Irradiation Capsules," USNRC Report NUREG/CR-3295, Apr 1984.

6. E. P. Lippincott, "The Buffalo Light Water Reactor Calculation," Letter Communication Serial No. 7754997, Hanford Engineering Development Laboratory, Richland, WA, to J. R. Hawthorne, dated November 16, 1977.

7. E. P. Lippincott, L. S. Kellogg, W. Y. Matsumoto, W. N. McElroy and C. A. Baldwin, "Evaluation of Neutron Exposure Conditions for the Buffalo Reactor," Proceedings 5th International ASTM-Euratom Symposium on Reactor Dosimetry, Geesthacht, Federal Republic of Germany, September 24-28, 1984.

8. G. Prillinger, E. D. McGarry and J. R. Hawthorne, "Neutron Spectra Calculations for Ex-Core Irradiation Experiments at the Buffalo Reactor," presented at the ASTM Fourteenth International Symposium on Effects of Radiation on Material, Andover, MA, June 1988.

9. G. A. Clarke and J. D. Landes, "Evaluation of J for the Compact Specimen," Journal of Testing and Evaluation, Vol. 7(5), Sept. 1979, pp. 264-269.

10. H. A. Ernst, "Material Resistance and Instability Beyond J-Controlled Crack Growth," Elastic-Plastic Fracture, ASTM STP 803 Vol. 1, American Society for Testing and Materials, 1983, pp. 191-213.

11. J. R. Hawthorne, et al., "Evaluation and Prediction of Neutron Embrittlement in Reactor Pressure Vessel Materials," EPRI NP-2782, The Electric Power Research Institute, Dec. 1982.

12. J. R. Hawthorne and A. L. Hiser, "Investigations of Irradiation-Anneal-Reirradiation (IAR) Properties Trends of RPV Welds: Phase 2 Final Report," USNRC Report NUREG/CR-5492, Nov. 1989.

13. D. E. McCabe, "Fracture Evaluation of Surface Cracks Embedded in Reactor Vessel Cladding: Material Property Evaluations," USNRC NUREG/CR-5207, Sept. 1988.

14. A. L. Hiser, "Correlation of C_v and K_{Ic}/K_{Jc} Transition Temperature Increases Due to Irradiation," USNRC Report NUREG/CR-4395, Nov. 1985.

15. A. L. Hiser, "Evaluation of Upper Shelf Toughness Requirements for Reactor Pressure Vessels," EPRI NP-6790M Volume 1 Summary Report, Electric Power Research Institute, March 1990.

APPENDIX A

Neutron Dosimetry Determinations:
Irradiation Assemblies UBR-38, UBR-44, UBR-45
UBR-46, UBR-65, UBR-75, UBR-76 and UBR-77

Neutron Fluence-Rate Determinations

Based on Fission Spectrum Assumption

For Assembly UBR-38 (Reflection Region Irradiation)

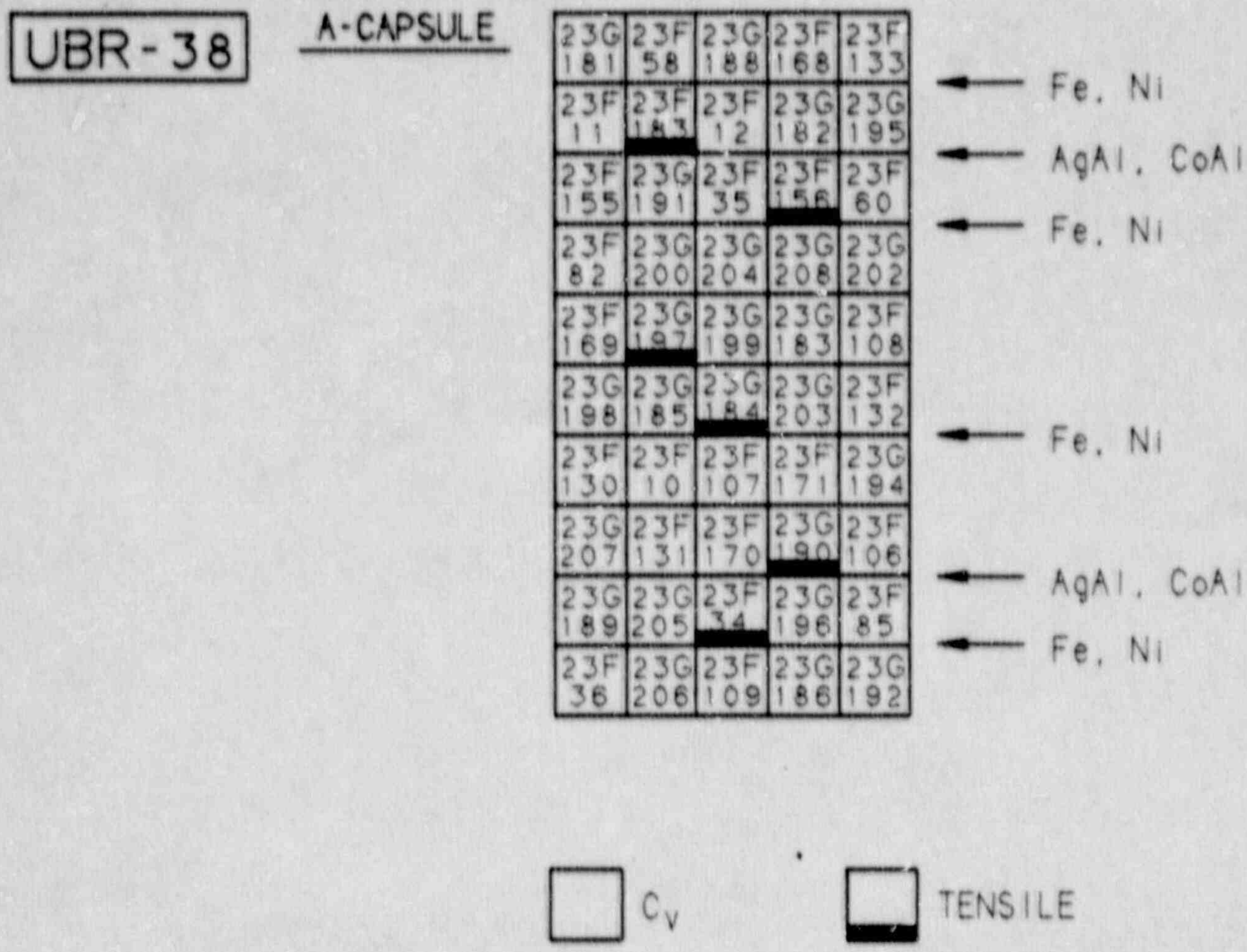

Fig. A-1 Irradiation Assembly UBR-38 (Capsule A) showing neutron fluence-rate monitor locations.

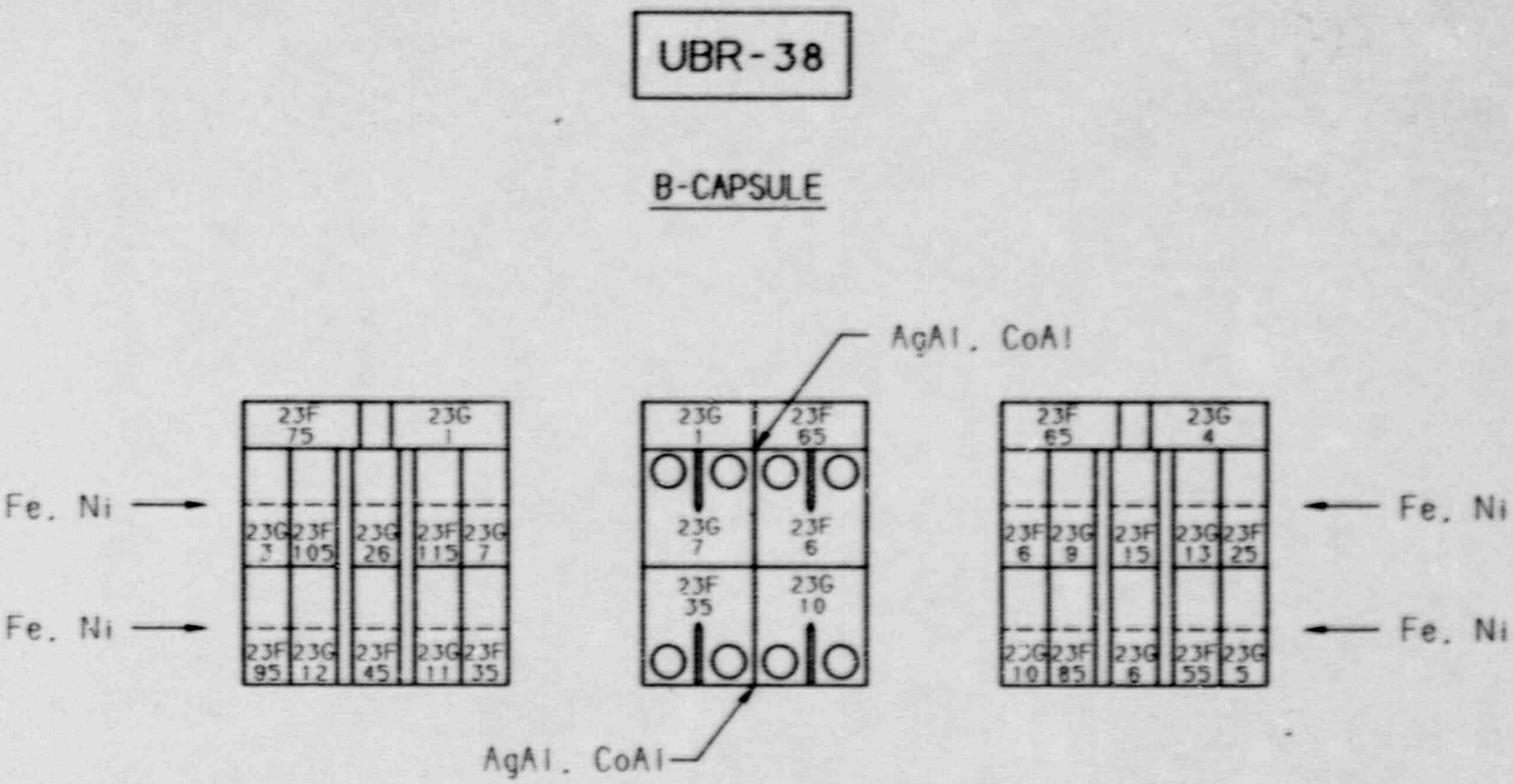

Fig. A-2   Irradiation Assembly UBR-38 (Capsule B) showing neutron fluence-rate monitor locations.

Table A-1 Irradiation Assembly UBR-38 Capsule A Fluence-Rate Monitor Results (Ref. 1)

Monitor/Segment[a]		Fluence Rate[b,c] x 10^{10} (Average)	Monitor Location in Specimen Array
A14	(Fe)	7.33	Between layers 1 and 2
	(Ni)	7.48	
A15	(AgCo)	4.36[d]	Between layers 2 and 3
A16	(Fe)	~ 7.61[e]	Between layers 3 and 4
	(Ni)	7.09	
A17	(Fe)	7.96	Between layers 6 and 7
	(Ni)	~ 6.75[e]	
A18	(AgCo)	- [f]	Between layers 8 and 9
A19	(Fe)	7.95	Between layers 9 and 10
	(Ni)	~ 7.74[e]	

[a] See Figure A-1 for monitor locii. The Fe and Ni results are based on > 1 MeV ^{235}U fission spectrum-averaged cross sections of 115.2 and 156.8 millibarns, respectively.

[b] Fission spectrum assumption; $n/cm^2 \cdot s^{-1}$ (E > 1 MeV) unless noted.

[c] Values obtained from Ni segments are suspect because of very long irradiation time of this assembly (years).

[d] Thermal fluence rate corrected for epithermal neutron contributions based on ^{109}Ag and ^{59}Co reaction rates and their cross sections.

[e] Approximate value based on two of three wire segments; one segment lost in hot cell operation.

[f] Not available.

Total time of irradiation: 17,354 hours

Table A-2 Irradiation Assembly UBR-38 Capsule B Fluence-Rate Monitor Results (Ref. 1)

Monitor/Segment[a]		Fluence Rate[b,c] x 10^{10} (Average)	Monitor Location in Specimen Array
B14	(Fe-1,2)(Ni-1,2)	8.09(15.8)	Specimens 23G-7 and 23F-115
	(Fe-3)(Ni-3)	7.24(11.9)	Specimen 23G-26
	(Fe-4,5)(Ni-4,5)	6.90(9.2)	Specimens 23F-105 and 23G-3
B13	(Fe-1,2)(Ni-1,2)	9.84(20.1)	Specimens 23F-6 and 23G-9
	(Fe-3)(Ni-3)	8.85(16.9)	Specimen 23F-15
	(Fe-4,5)(Ni-4,5)	8.39(13.0)	Specimens 23G-13 and 23F-25
B17	(Fe-1,2)(Ni-1,2)	7.90(15.5)	Specimens 23F-35 and 23G-1
	(Fe-3)(Ni-3)	6.90(11.6)	Specimen 23F-45
	(Fe-4,5)(Ni-4,5)	6.86(9.0)	Specimens 23G-12 and 23F-95
B15	(Fe-1,2)(Ni-1,2)	9.39(19.6)	Specimens 23G-10 and 23F-85
	(Fe-3)(Ni-3)	8.43(15.4)	Specimen 23G-6
	(Fe-4,5)(Ni-4,5)	8.11(12.3)	Specimens 23F-55 and 23G-5
B12	(AgCo)	~ 5.02[d,e]	Between specimens 23G-1 and 23F-65 and between specimens 23F-75 and 23G-4
B16	(AgCo)	~ 3.90[d]	On capsule centerline immediately below bottom specimen layer

[a] See Figure A-2 for monitor locii. The Fe and Ni results are based on > 1 MeV ^{235}U fission spectrum-averaged cross sections of 115.2 and 156.8 millibarns, respectively.

[b] Fission spectrum assumption; $n/cm^2 \cdot s^{-1}$ (E > 1 MeV) unless noted.

[c] Values obtained from Ni segments are suspect because of very long irradiation time of this assembly (years).

[d] Thermal fluence rate corrected for epithermal neutron contributions based on ^{109}Ag and ^{59}Co reaction rates and their cross sections.

[e] Range of measured values: 3.77 to 6.88

Total time of irradiation: 17,354 hours

Neutron Fluence-Rate Determinations

Based on Fission Spectrum Assumption

For Assembly UBR-44 (Core-Edge Irradiation)

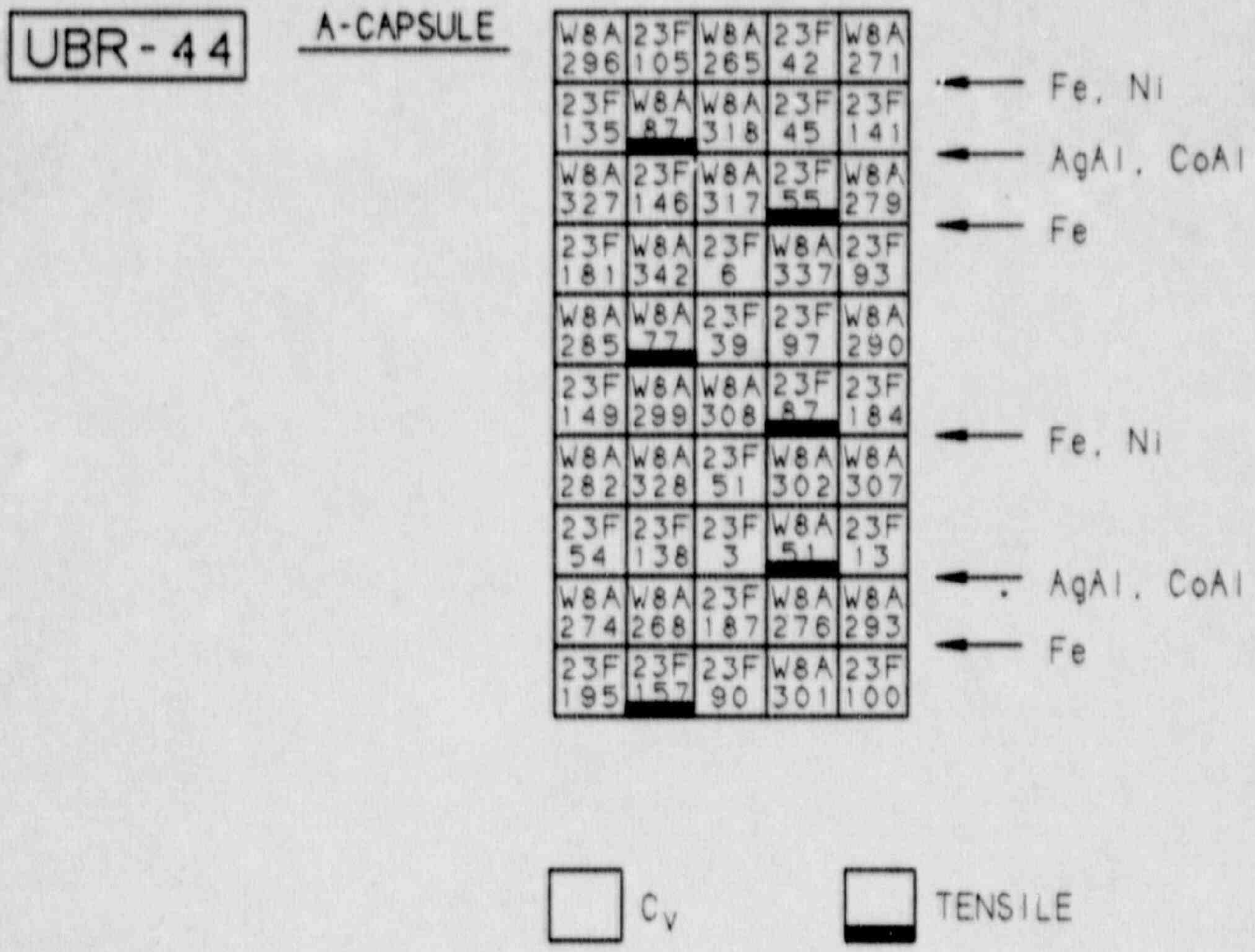

Fig. A-3 Irradiation Assembly UBR-44 (Capsule A) showing neutron fluence-rate monitor locations.

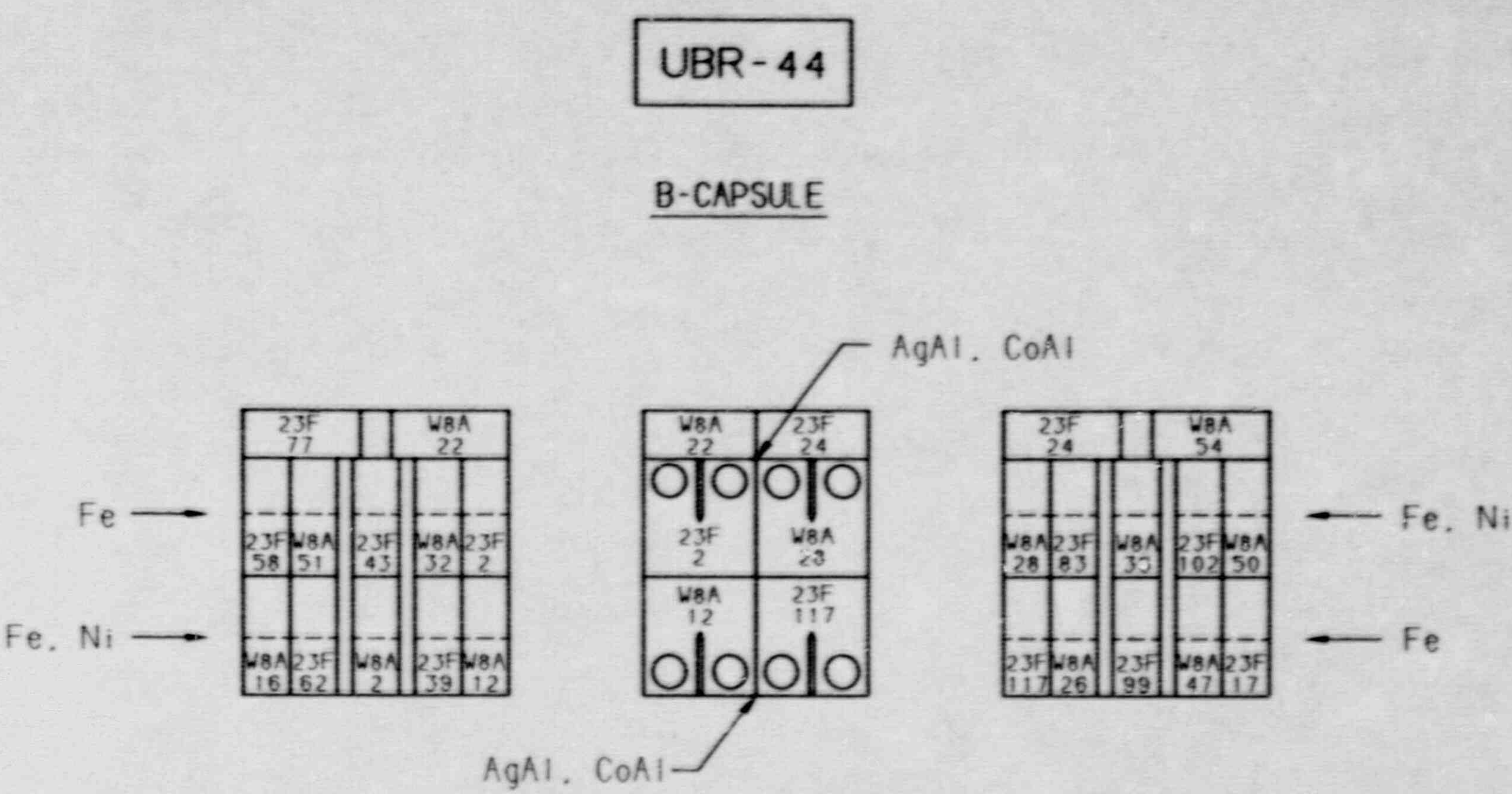

Fig. A-4 Irradiation Assembly UBR-44 (Capsule B) showing neutron fluence-rate monitor locations.

Table A-3 Irradiation Assembly UBR-44 Capsule A Fluence-Rate Monitor Results (Ref. 2)

Monitor/Segment[a]		Fluence Rate[b] x 10^{11} (Average)	Monitor Location in Specimen Array
A16	(Fe)	6.09	Between layers 1 and 2
	(Ni)	6.24	
A14	(AgCo)	11.07[c]	Between layers 2 and 3
A17	(Fe)	6.27	Between layers 3 and 4
A18	(Fe)	6.57	Between layers 6 and 7
	(Ni)	6.57	
A15	(AgCo)	13.00[c]	Between layers 8 and 9
A20	(Fe)	6.82	Between layers 9 and 10

[a] See Figure A-3 for monitor locii. The Fe and Ni results are based on > 1 MeV ^{235}U fission spectrum-averaged cross sections of 115.2 and 156.8 millibarns, respectively.

[b] Fission spectrum assumption; $n/cm^2 \cdot s^{-1}$ (E > 1 MeV) unless noted.

[c] Thermal fluence rate corrected for epithermal neutron contributions based on ^{109}Ag and ^{59}Co reaction rates and their cross sections.

Total time of irradiation: 2,775.4 hours

Table A-4 Irradiation Assembly UBR-44 Capsule B Fluence-Rate Monitor Results (Ref. 2)

Monitor/Segment[a]		Fluence Rate[b,c] x 10^{11}	Monitor Location in Specimen Array
B23	(Fe-1)	4.77	Specimens W8A-32 and 23F-2
	(Fe-2)	5.56	Specimen 23F-43
	(Fe-3)	6.06	Specimens W8A-51 and 23F-58
B22	(Fe-1), (Ni-1)	7.77, (7.74)[d]	Specimens W8A-28 and 23F-83
	(Fe-2), (Ni-2)	9.20, (8.85)[d]	Specimen W8A-36
	(Fe-3), (Ni-3)	10.00, (9.67)[d]	Specimens 23F-102 and W8A-50
B26	(Fe-1), (Ni-1)	4.77, (4.23)[d]	Specimens W8A-12 and 23F-39
	(Fe-2), (Ni-2)	5.56, (5.14)[d]	Specimen W8A-2
	(Fe-3), (Ni-3)	6.06, (5.76)[d]	Specimens 23F-2 and W8A-16
B24	(Fe-1)	7.12	Specimens 23F-117 and W8A-26
	(Fe-2)	8.47	Specimen 23F-99
	(Fe-3)	9.42	Specimens W8A-47 and 23F-17
B21	(AgCo)	11.57[e]	Between specimens W8A-22 and 23F-24 and between specimens 23F-77 and W8A-54
B27	(AgCo)	12.29[e]	On capsule centerline immediately below bottom specimen layer

[a] See Figure A-4 for monitor locii. The Fe and Ni results are based on > 1 MeV ^{235}U fission spectrum-averaged cross sections of 115.2 and 156.8 millibarns, respectively.

[b] Fission spectrum assumption; $n/cm^2 \cdot s^{-1}$ (E > 1 MeV) unless noted.

[c] Single determination value.

[d] Nickel monitor value.

[e] Thermal fluence rate corrected for epithermal neutron contributions based on ^{109}Ag and ^{59}Co reaction rates and their cross sections.

Total time of irradiation: 2,775.4 hours

Neutron Fluence-Rate Determinations

Based on Fission Spectrum Assumption

For Assembly UBR-45 (Core-Edge Irradiation)

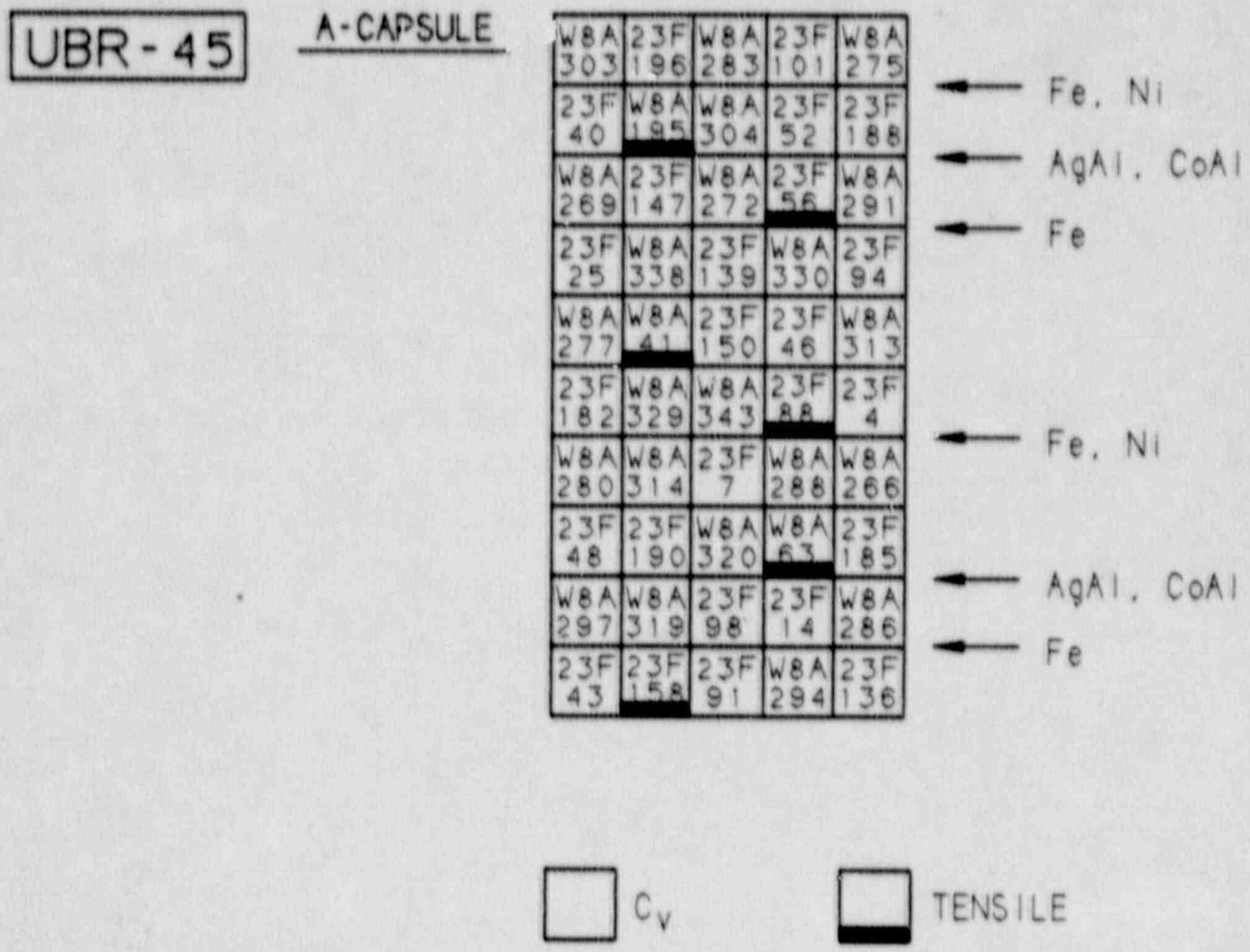

Fig. A-5 Irradiation Assembly UBR-45 (Capsule A) showing neutron fluence-rate monitor locations.

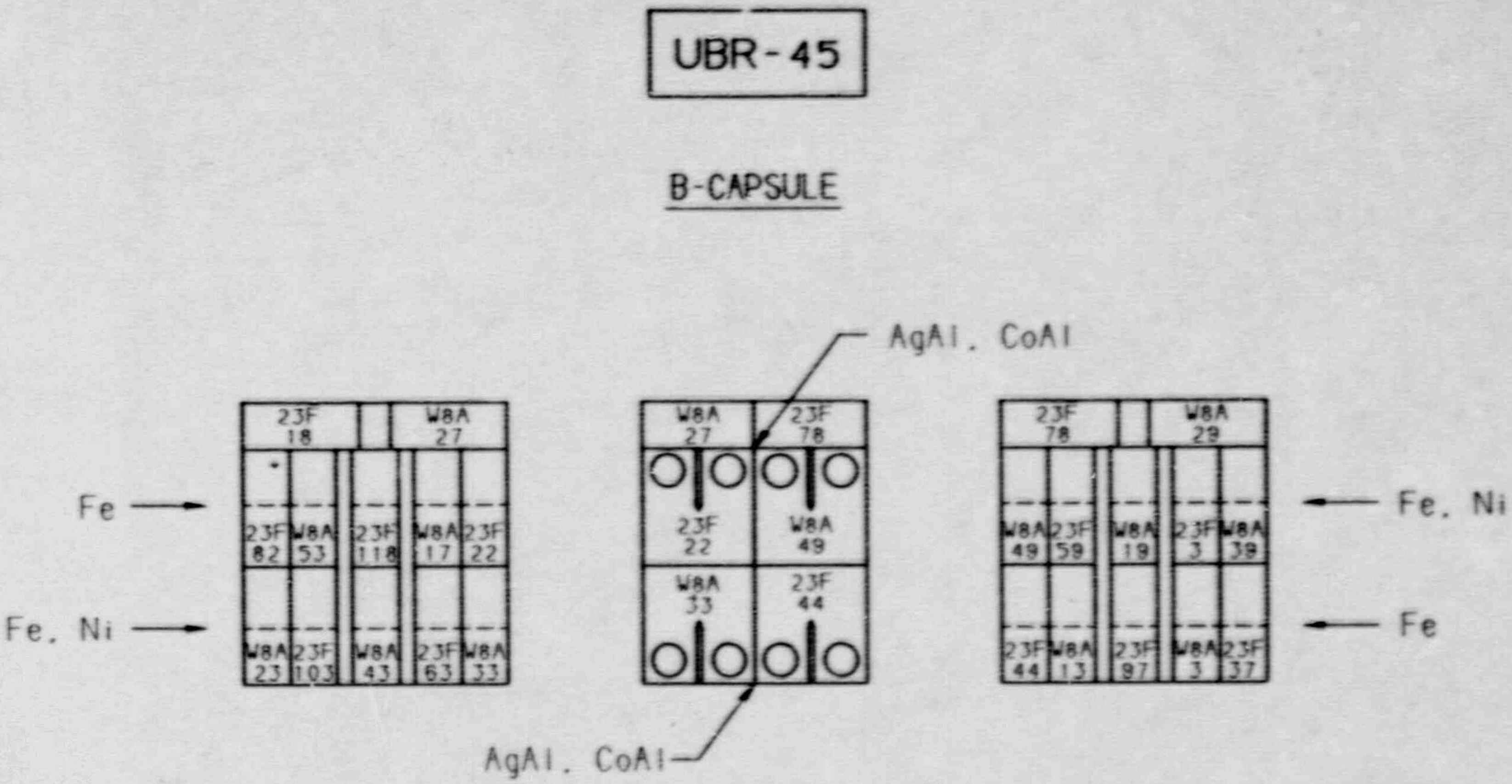

Fig. A-6 Irradiation Assembly UBR-45 (Capsule B) showing neutron fluence-rate monitor locations.

Table A-5 Irradiation Assembly UBR-45 Capsule A Fluence-Rate Monitor Results (Ref. 3)

Monitor/Segment[a]		Fluence Rate[b] x 10^{11} (Average)	Monitor Location in Specimen Array
A7	(Fe)	7.19	Between layers 1 and 2
	(Ni)	7.07	
A8	(AgCo)	19.00[c,d]	Between layers 2 and 3
A9	(Fe)	7.44	Between layers 3 and 4
A10	(Fe)	7.73	Between layers 6 and 7
	(Ni)	7.56	
A11	(AgCo)	14.43[c]	Between layers 8 and 9
A12	(Fe)	8.03	Between layers 9 and 10

[a] See Figure A-5 for monitor locii. The Fe and Ni results are based on > 1 MeV ^{235}U fission spectrum-averaged cross sections of 115.2 and 156.8 millibarns, respectively.

[b] Fission spectrum assumption; $n/cm^2 \cdot s^{-1}$ (E > 1 MeV) unless noted.

[c] Thermal fluence rate corrected for epithermal neutron contributions based on ^{109}Ag and ^{59}Co reaction rates and their cross sections.

[d] Single determination value.

Total time of irradiation: 11,106 hours

Table A-6 Irradiation Assembly UBR-45 Capsule B Fluence-Rate Monitor Results (Ref. 3)

Monitor/Segment[a]		Fluence Rate[b] x 10^{11} (Average)	Monitor Location in Specimen Array
B4	(Fe)	8.78	Specimens 23F-22 to 23F-82
B6	(Fe)	7.92	Specimens W8A-49 to W8A-39
	(Ni)	7.58	
B2	(Fe)	8.27	Specimens W8A-33 to W8A-23
	(Ni)	7.17	
B1	(Fe)	7.30	Specimens 23F-44 to 23F-37
B5	(AgCo)	16.96[c]	Between specimens W8A-27 and 23F-78 and between specimens 23F-18 and W8A-29
B3	(AgCo)	14.78[c]	On capsule centerline immediately below bottom specimen layer

[a] See Figure A-6 for monitor locii. The Fe and Ni results are based on > 1 MeV ^{235}U fission spectrum-averaged cross sections of 115.2 and 156.8 millibarns, respectively.

[b] Fission spectrum assumption; $n/cm^2 \cdot s^{-1}$ (E > 1 MeV) unless noted.

[c] Thermal fluence rate corrected for epithermal neutron contributions based on ^{109}Ag and ^{59}Co reaction rates and their cross sections.

Total time of irradiation: 11,106 hours

Neutron Fluence-Rate Determinations

Based on Fission Spectrum Assumption

For Assembly UBR-46 (Core-Edge Irradiation)

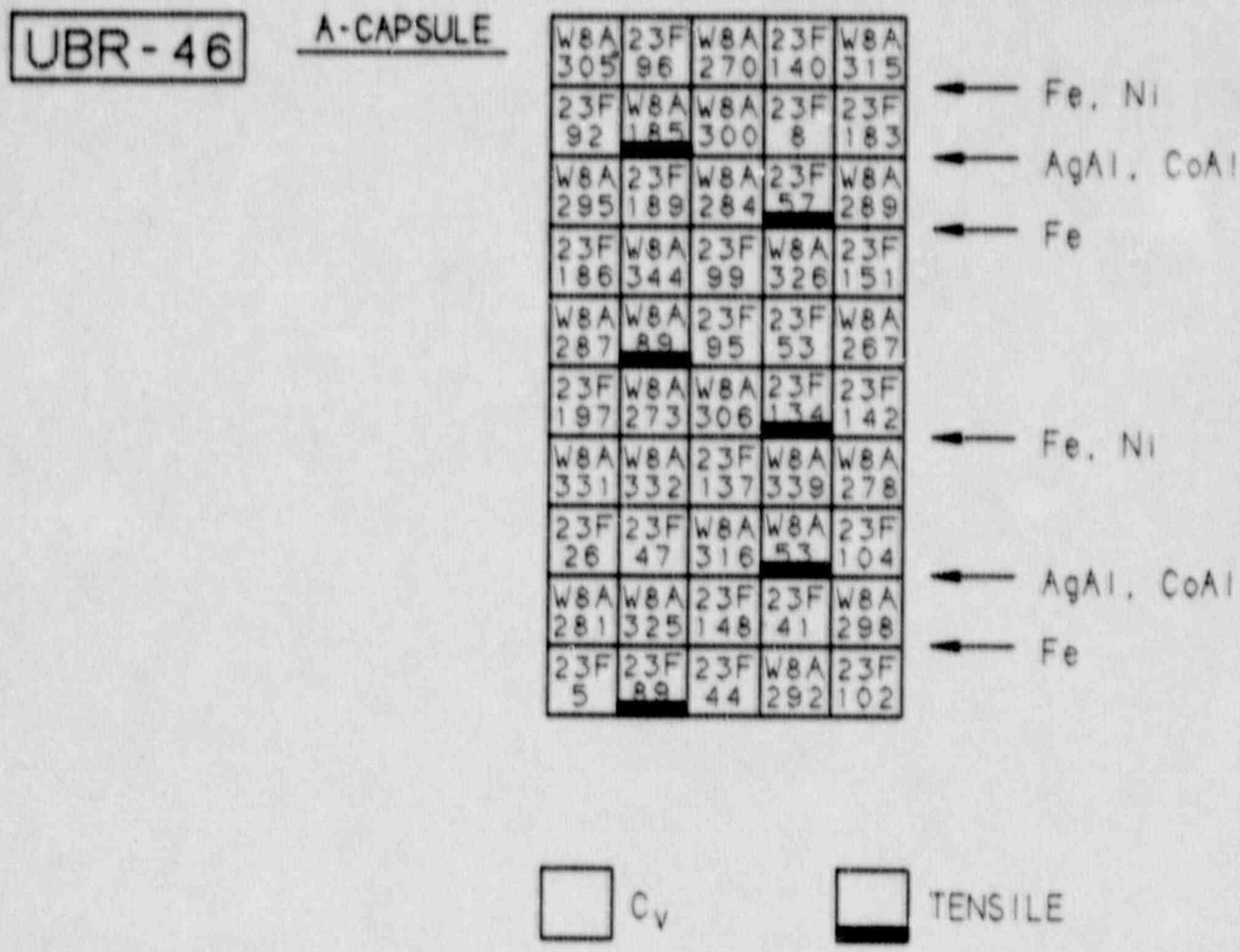

Fig. A-7 Irradiation Assembly UBR-46 (Capsule A) showing neutron fluence-rate monitor locations.

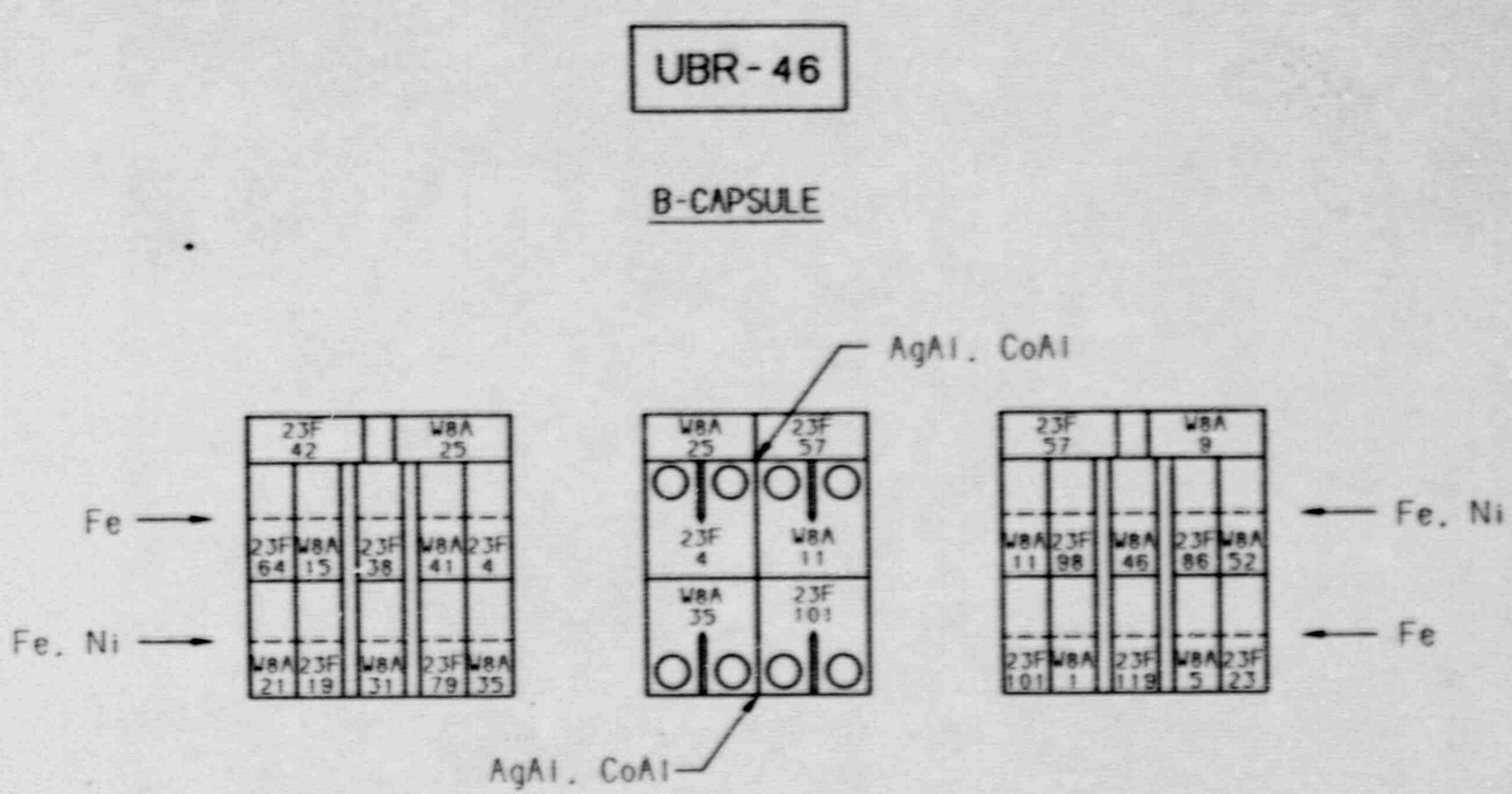

Fig. A-8 Irradiation Assembly UBR-46 (Capsule B) showing neutron fluence-rate monitor locations.

Table A-7 Irradiation Assembly UBR-46 Capsule A Fluence-Rate Monitor Results (Ref. 4)

Monitor/Segment[a]		Fluence Rate[b] x 10^{11} (Average)	Monitor Location in Specimen Array
A1	(Fe)	5.61	Between layers 1 and 2
	(Ni)	5.80	
A2	(AgCo)	12.20[c]	Between layers 2 and 3
A3	(Fe)	5.99	Between layers 3 and 4
A4	(Fe)	6.18	Between layers 6 and 7
	(Ni)	6.16	
A5	(AgCo)	10.20[c]	Between layers 8 and 9
A6	(Fe)	6.35	Between layers 9 and 10

[a] See Figure A-7 for monitor locii. The Fe and Ni results are based on > 1 MeV ^{235}U fission spectrum-averaged cross sections of 115.2 and 156.8 millibarns, respectively.

[b] Fission spectrum assumption; n/cm^2·s^{-1} (E > 1 MeV) unless noted.

[c] Thermal fluence rate corrected for epithermal neutron contributions based on ^{109}Ag and ^{59}Co reaction rates and their cross sections. Single determination value.

Total time of irradiation: 5,596.8 hours

Table A-8 Irradiation Assembly UBR-46 Capsule B Fluence-Rate Monitor Results (Ref. 4)

Monitor/Segment[a]		Fluence Rate[b] x 10^{11} (Average)	Monitor Location in Specimen Array
B23	(Fe)	6.77[c]	Specimens 23F-4 to 23F-64
B21	(Fe)	6.22	Specimens W8A-11 to W8A-52
	(Ni)	4.89(?)	
B20	(Fe)	7.11	Specimens W8A-35 to W8A-21
	(Ni)	7.62	
B19	(Fe)	5.90	Specimens 23F-101 to 23F-23
B22	(AgCo)	11.40[c,d]	Between specimens W8A-25 and 23F-57 and between specimens 23F-42 and W8A-9
B24	(AgCo)	10.90[c,d]	On capsule centerline immediately below specimen layer.

[a] See Figure A-8 for monitor locii. The Fe and Ni results are based on > 1 MeV ^{235}U fission spectrum-averaged cross sections of 115.2 and 156.8 millibarns, respectively.

[b] Fission spectrum assumption; n/cm^2·s^{-1} (E > 1 MeV) unless noted.

[c] Single determination value.

[d] Thermal fluence rate corrected for epithermal neutron contributions based on ^{109}Ag and ^{59}Co reaction rates and their cross sections.

Total time of irradiation: 5,631.4 hours

Neutron Fluence-Rate Determinations

Based on Fission Spectrum Assumption

For Assembly UBR-65 (In-Core Irradiation)

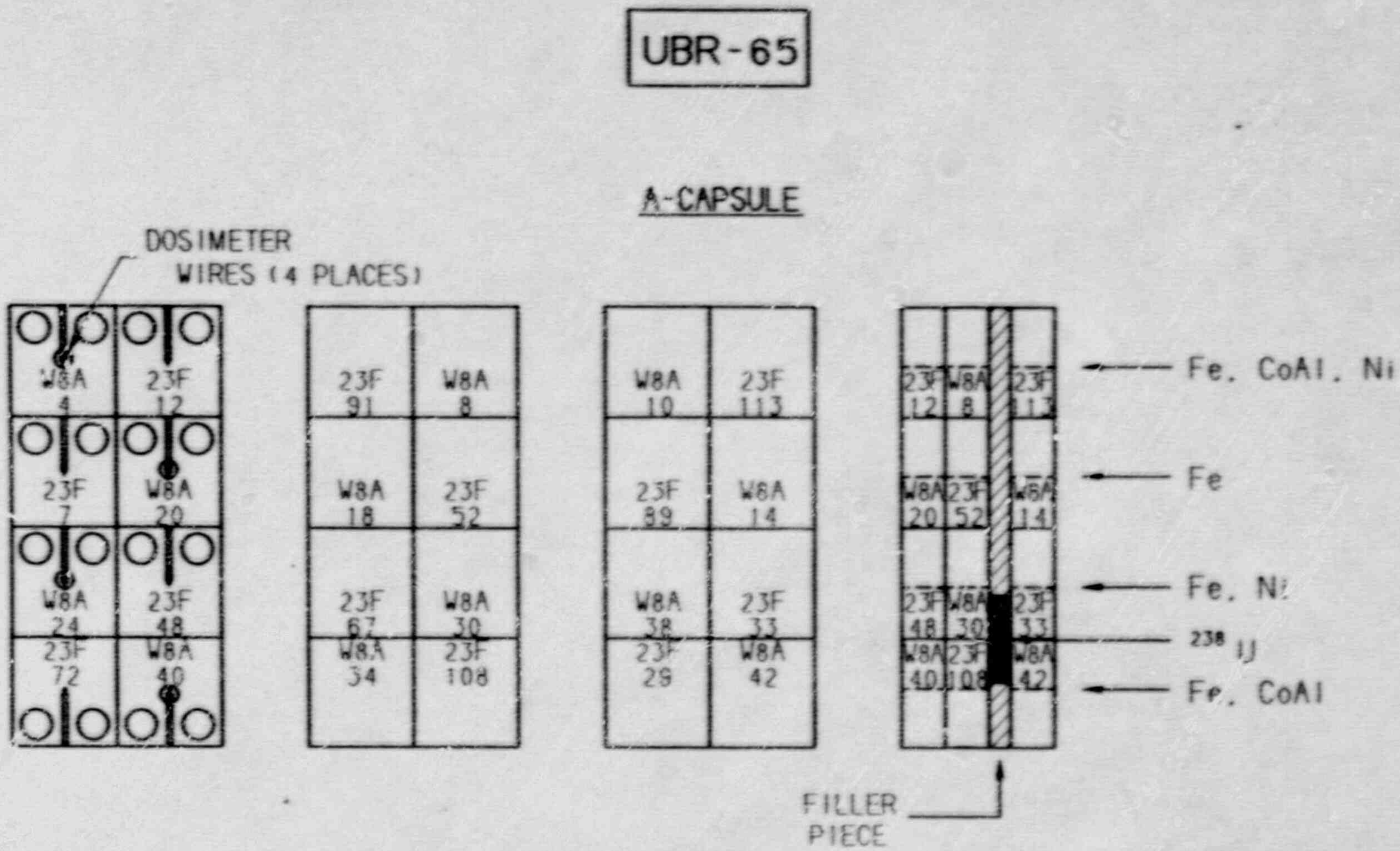

Fig. A-9 Irradiation Assembly UBR-65 (Capsule A) showing neutron fluence-rate monitor locations.

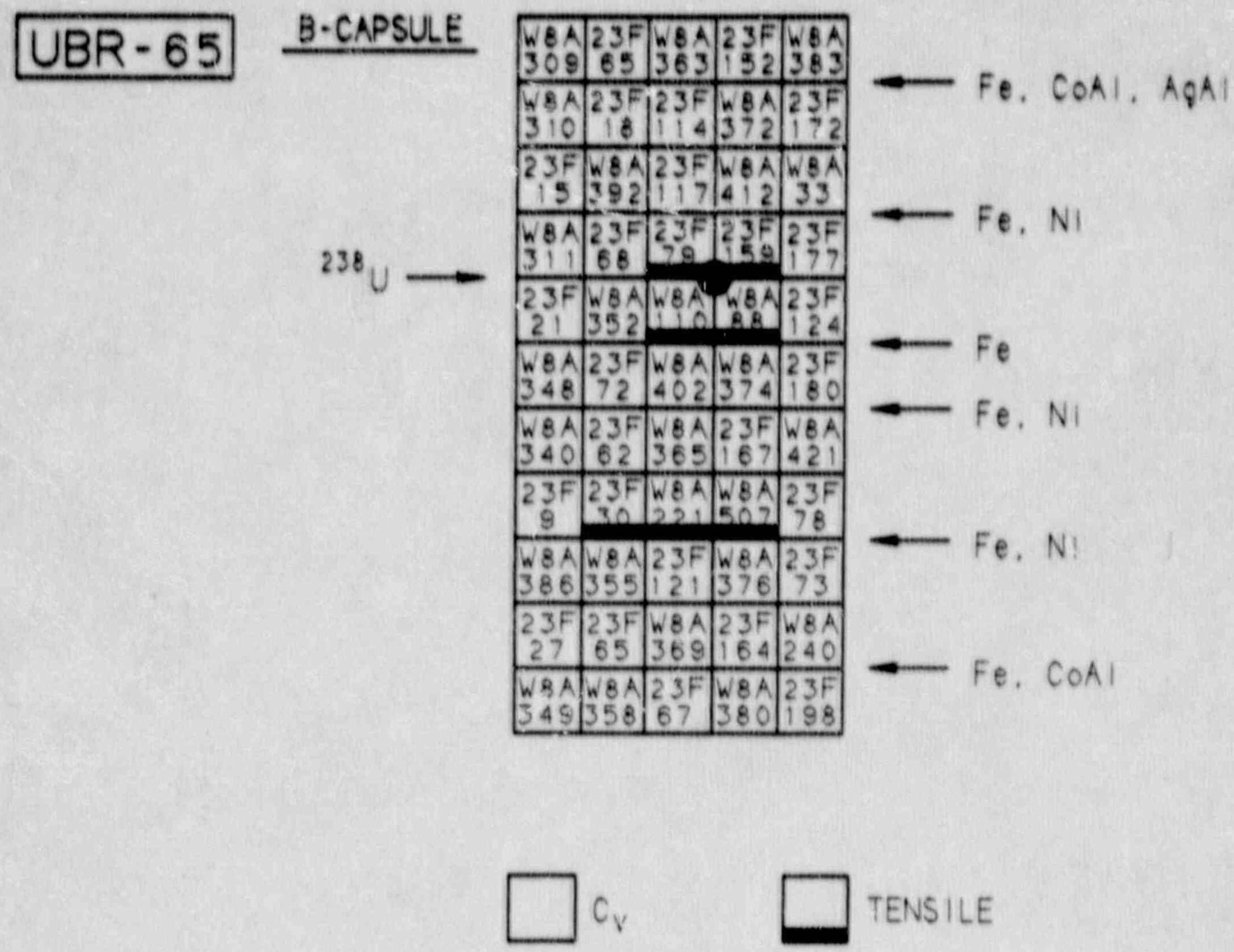

Fig. A-10 Irradiation Assembly UBR-65 (Capsule B) showing neutron fluence-rate monitor locations.

Table A-9 Irradiation Assembly UBR-65 Capsule A Fluence-Rate Monitor Results (Ref. 5)

Monitor/Segment[a]		Fluence Rate[b] x 10^{12} (Average)	Monitor Location in Specimen Array
A1	(Fe)	5.83	Specimens W8A-4 to W8A-10
	(Ni)	5.87	
	(AgCo)	3.64[c]	
A2	(Fe)	6.76	Specimens W8A-20 to W8A-14
A3	(Fe)	6.98	Specimens W8A-24 to W8A-38
	(Ni)	6.90	
A4	(Fe)	7.64	Specimens W8A-40 to W8A-428
	(AgCo)	5.11[c]	
Vial	(^{238}U)	8.26[d]	Specimens W8A-30 and W8A-38 and between specimens 23F-67 and 23F-33 (diagonally)
		9.42[e]	
	(Fe)	7.11	
	(Ni)	7.10	

[a] See Figure A-9 for monitor locii. The Fe, Ni and ^{238}U results are based on > 1 MeV ^{238}U fission spectrum-averaged cross sections of 115.2, 156.8 and 441 millibarns, respectively.

[b] Fission spectrum assumption; $n/cm^2 \cdot s^{-1}$ (E > 1 MeV) unless noted.

[c] Thermal fluence rate corrected for epithermal neutron contributions based on ^{109}Ag and ^{59}Co reaction rates and their cross sections.

[d] Determination from ^{137}Cs, ^{103}Ru, $^{140}BaLa$ and ^{95}Zr results.

[e] Calculated spectrum value.

Total time of irradiation: 154.22 hours

Table A-10 Irradiation Assembly UBR-65 Capsule B Fluence-Rate Monitor Results (Ref. 5)

Monitor/Segment[a]		Fluence Rate[b] x 10^{12} (Average)	Monitor Location in Specimen Array
B-1	(Fe)	7.51	Between layers 1 and 2
	(AgCo)	3.75[c]	
B-2	(Fe)	7.19	Between layers 3 and 4
	(Ni)	7.15	
B-3	(Fe)	7.10	Between layers 5 and 6
B-4	(Fe)	7.00	Between layers 6 and 7
	(Ni)	6.92	
B-5	(Fe)	6.80	Between layers 8 and 9
	(Ni)	6.75	
B-6	(Fe)	6.62	Between layers 10 and 11
	(AgCo)	3.08[c]	
Vial	(^{238}U)	8.65[d]	Between layers 4 and 5
		(9.86)[e]	
	(Fe)	7.02	
	(Ni)	6.97	

[a] See Figure A-10 for monitor locii. The Fe, Ni and ^{238}U results are based on > 1 MeV ^{238}U fission spectrum-averaged cross sections of 115.2, 156.8 and 441 millibarns, respectively.

[b] Fission spectrum assumption; $n/cm^2 \cdot s^{-1}$ (E > 1 MeV) unless noted.

[c] Thermal fluence rate corrected for epithermal neutron contributions based on ^{109}Ag and ^{59}Co reaction rates and their cross sections.

[d] Determination from ^{137}Cs, ^{103}Ru, $^{140}BaLa$ and ^{95}Zr results.

[e] Calculated spectrum value.

Total time of irradiation: 154.22 hours

Neutron Fluence-Rate Determinations

Based on Fission Spectrum Assumption

For Assembly UBR-75 (In-Core Irradiation)

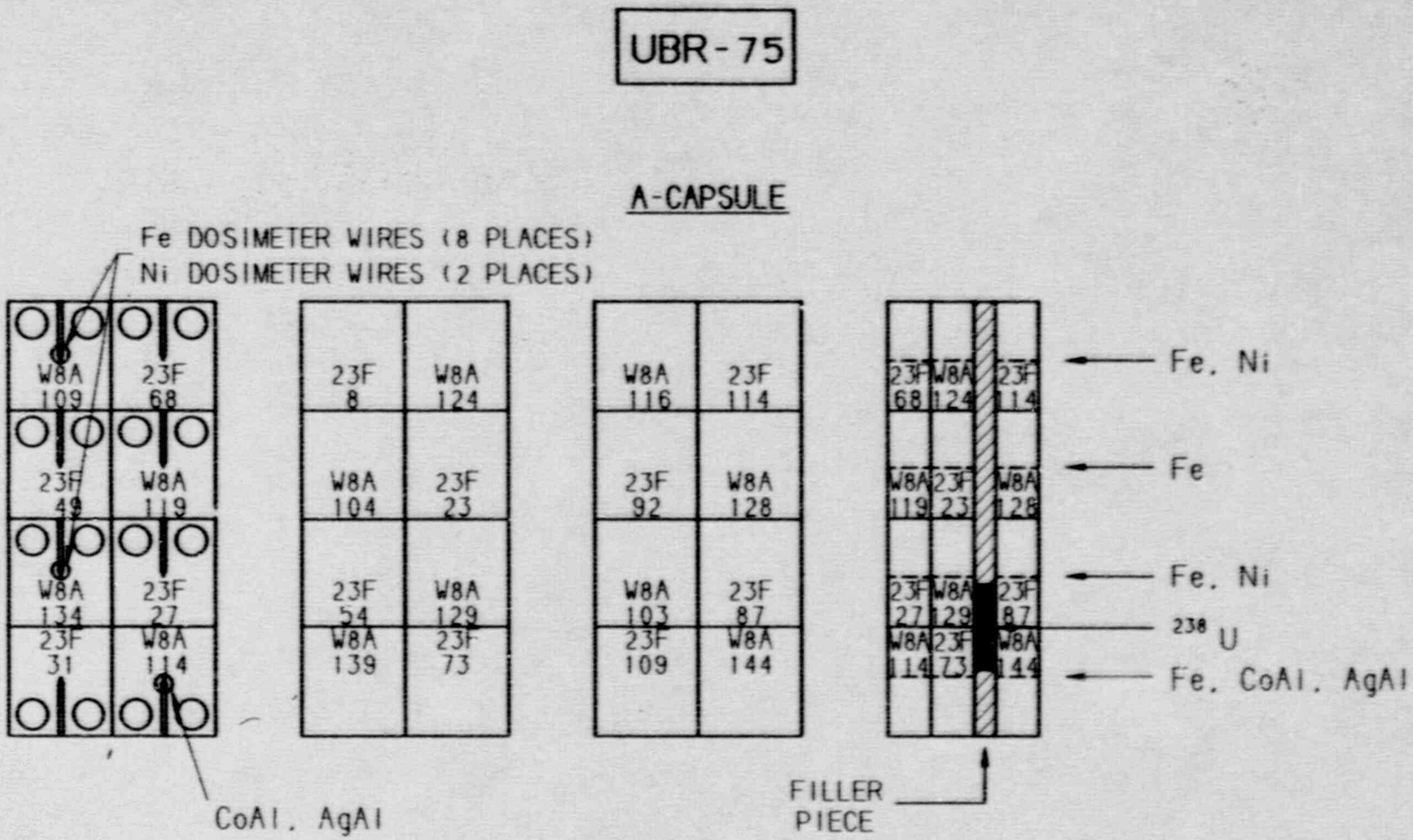

Fig. A-11 Irradiation Assembly UBR-75 (Capsule A) showing neutron fluence-rate monitor locations.

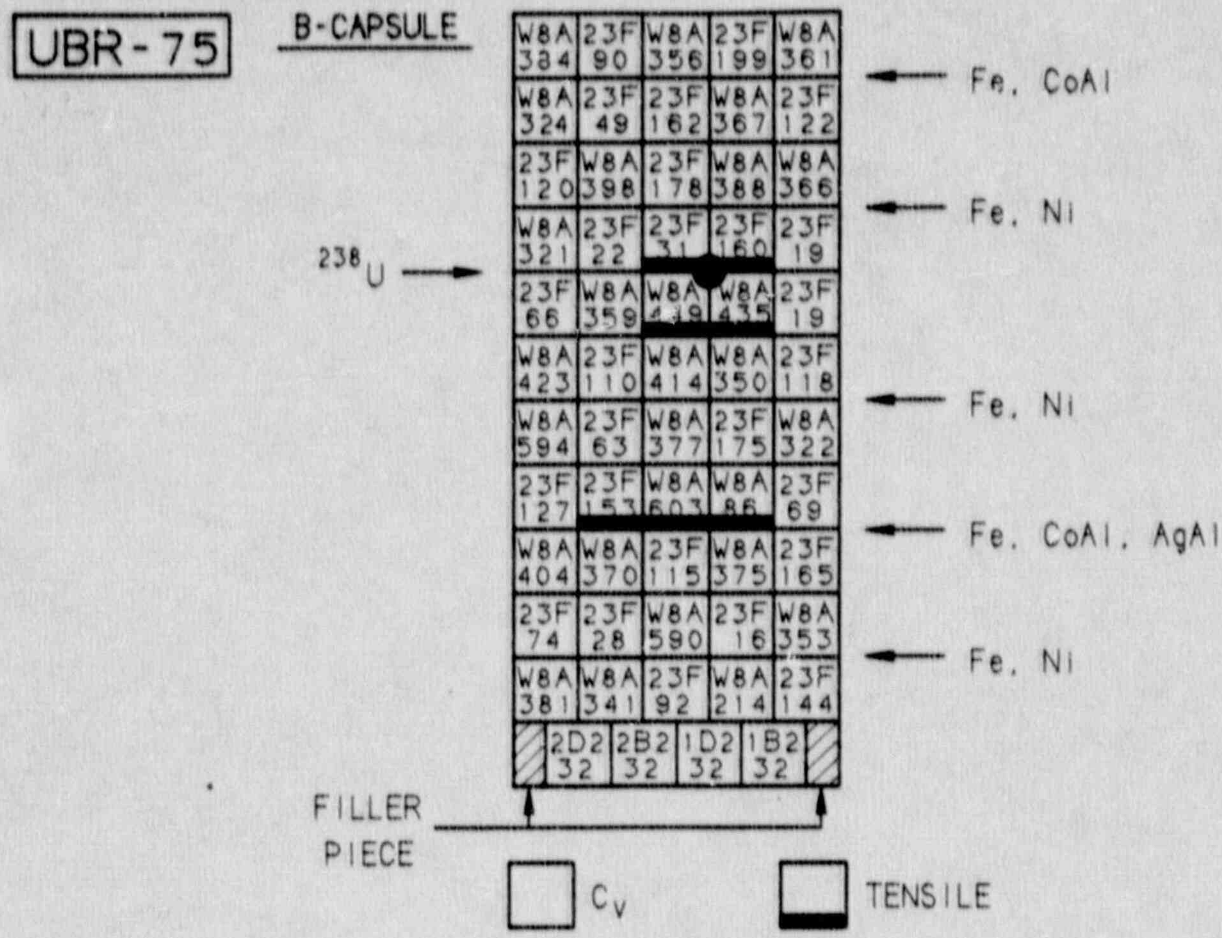

Fig. A-12 Irradiation Assembly UBR-75 (Capsule B) showing neutron fluence-rate monitor locations.

Table A-11 Irradiation Assembly UBR-75 Capsule A Fluence-Rate Monitor Results (Ref. 6)

Monitor/Segment[a]		Fluence Rate[b] x 10^{12} (Average)	Monitor Location in Specimen Array
A16	(Fe)	5.73	Specimens W8A-109 to W8A-116
	(Ni)	5.45	
A17	(Fe)	5.66	Specimens 23F-68 to 23F-114
A18	(Fe)	6.29	Specimens 23F-49 to 23F-92
A19	(Fe)	6.21	Specimens W8A-119 to W8A-128
A20	(Fe)	6.62	Specimens W8A-134 to W8A-103
	(Ni)	6.28	
A21	(Fe)	6.65	Specimens 23F-27 to 23F-87
A22	(Fe)	7.05	Specimens 23F-31 to 23F-109
A23	(Fe)	7.07	Specimens W8A-114 to W8A-144
	(AgCo)	4.86[c]	
Vial	(^{238}U)	8.13[d] (9.27)[e]	Between specimens 23F-54 and 23F-87 and between specimens W8A-129 and W8A-103 (diagonally)
	(Fe)	6.58	
	(Ni)	6.48	

[a] See Figure A-11 for monitor locii. The Fe, Ni and ^{238}U results are based on > 1 MeV ^{235}U fission spectrum-averaged cross sections of 115.2, 156.8 and 441 millibarns, respectively.

[b] Fission spectrum assumption; n/cm^2-s^{-1} (E > 1 MeV) unless noted.

[c] Thermal fluence rate corrected for epithermal neutron contributions based on ^{109}Ag and ^{59}Co reaction rates and their cross sections.

[d] Determination from ^{137}Cs, ^{103}Ru, $^{140}BaLa$ and ^{95}Zr results.

[e] Calculated spectrum value.

Total time of irradiation: 308.22 hours

Table A-12 Irradiation Assembly UBR-75 Capsule B Fluence-Rate Monitor Results (Ref. 6)

Monitor/Segment[a]		Fluence Rate[b] x 10^{12} (Average)	Monitor Location in Specimen Array
B25	(Fe)	6.85	Between layers 1 and 2
	(AgCo)	3.72[c]	
B26	(Fe)	6.67	Between layers 3 and 4
	(Ni)	6.44	
B27	(Fe)	6.58	Between layers 6 and 7
	(Ni)	6.27	
B28	(Fe)	6.35	Between layers 8 and 9
	(AgCo)	3.13[c]	
B29	(Fe)	6.29	Between layers 10 and 11
	(Ni)	6.05	
B30	(Fe)	6.25	Below layer 12
	(Ni)	5.98	
Vial	(^{238}U)	8.33[d] (9.50)[e]	Between layers 4 and 5
	(Fe)	6.63	
	(Ni)	6.56	

[a] See Figure A-12 for monitor locii. The Fe, Ni and ^{238}U results are based on > 1 MeV ^{235}U fission spectrum-averaged cross sections of 115.2, 156.8 and 441 millibarns, respectively.

[b] Fission spectrum assumption; $n/cm^2 \cdot s^{-1}$ (E > 1 MeV) unless noted.

[c] Thermal fluence rate corrected for epithermal neutron contributions based on ^{109}Ag and ^{59}Co reaction rates and their cross sections.

[d] Determination from ^{137}Cs, ^{103}Ru, $^{140}BaLa$ and ^{95}Zr results.

[e] Calculated spectrum value.

Total time of irradiation: 308.22 hours

Neutron Fluence-Rate Determinations

Based on Fission Spectrum Assumption

For Assembly UBR-76 (In-Core Irradiation)

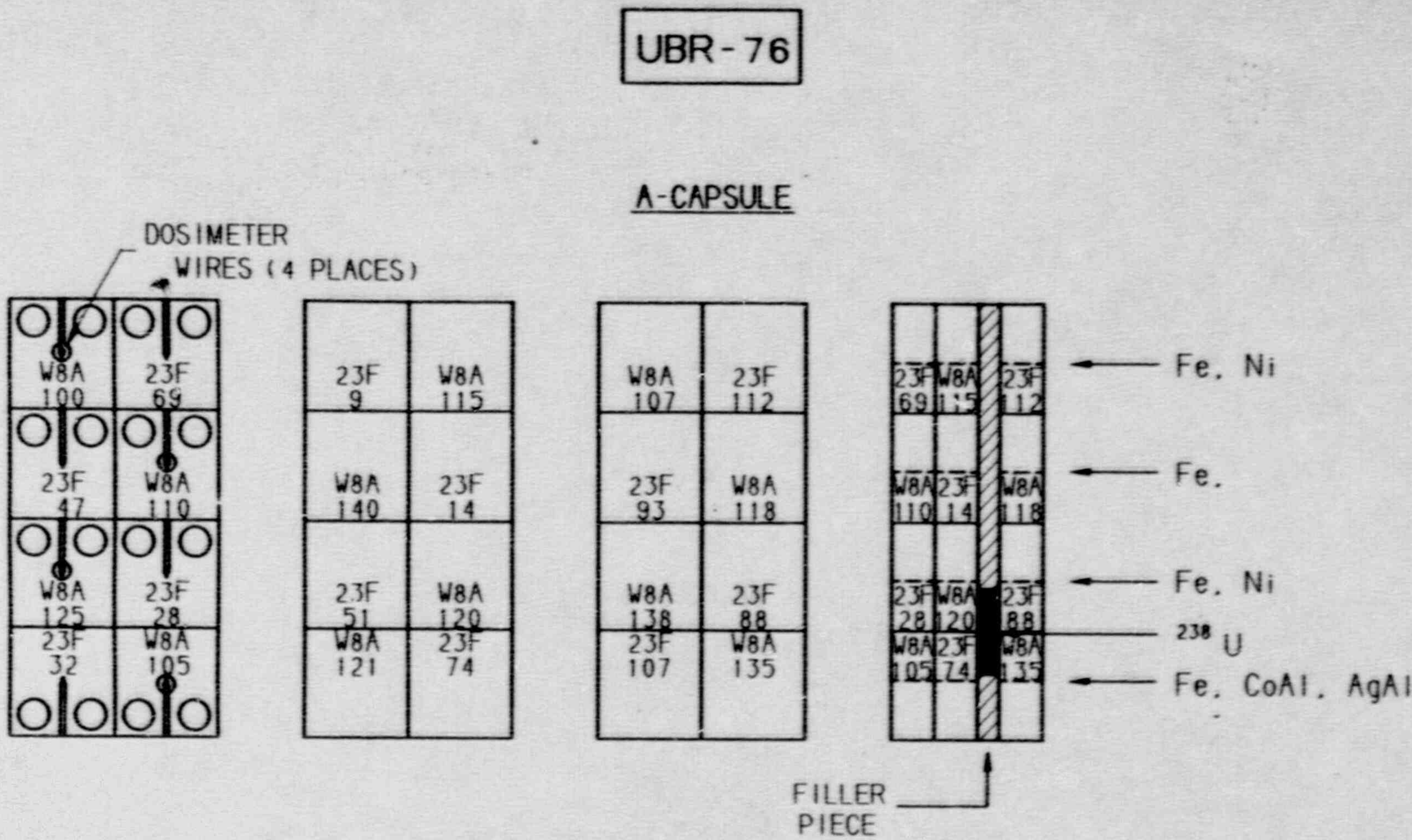

Fig. A-13 Irradiation Assembly UBR-76 (Capsule A) showing neutron fluence-rate monitor locations.

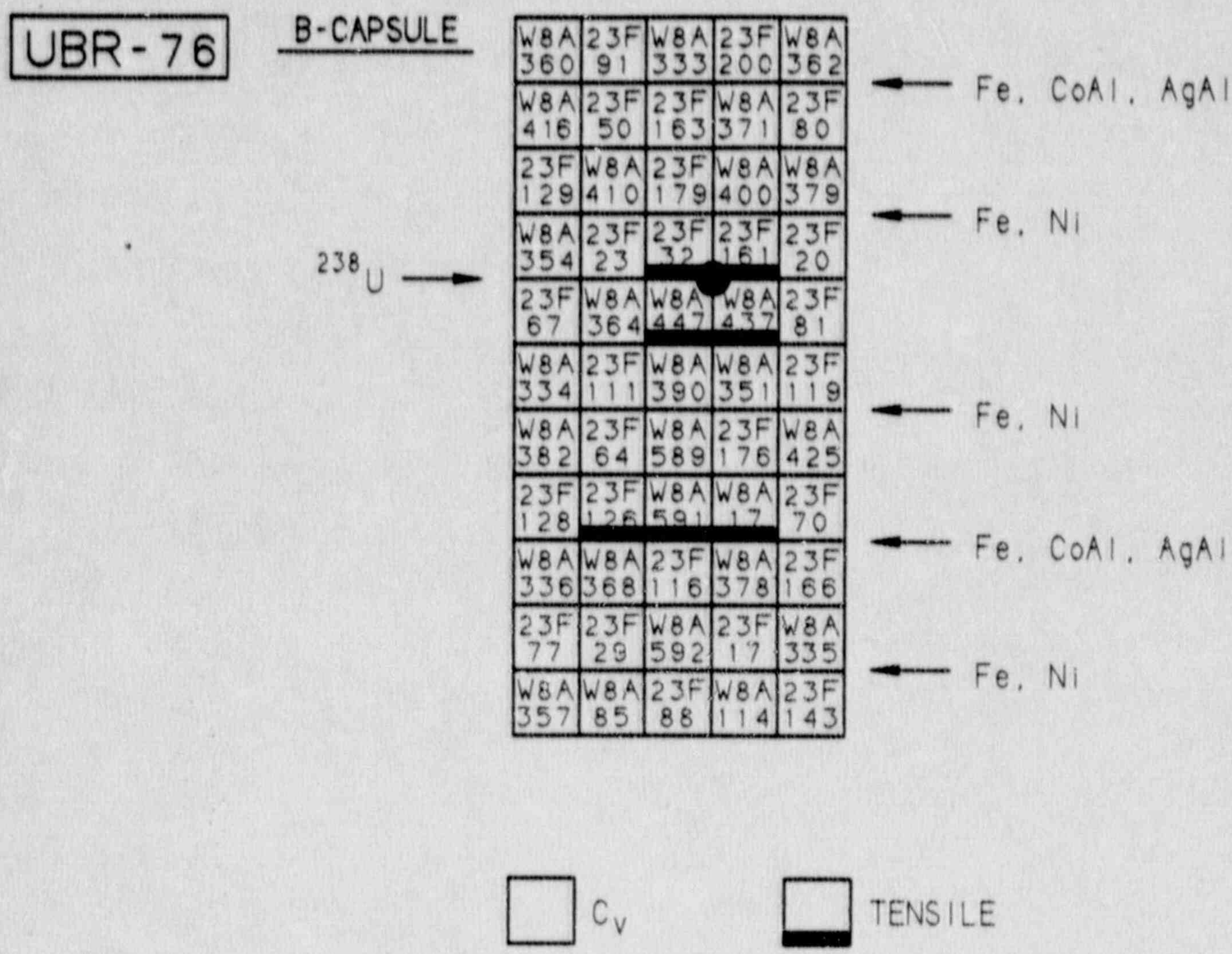

Fig. A-14 Irradiation Assembly UBR-76 (Capsule B) showing neutron fluence-rate monitor locations.

Table A-13 Irradiation Assembly UBR-76 Capsule A Fluence-Rate Monitor Results (Ref. 6)

Monitor/Segment[a]		Fluence Rate[b] x 10^{12} (Average)	Monitor Location in Specimen Array
A32	(Fe)	5.33	Specimens W8A-100 to W8A-107
	(Ni)	5.00	
A33	(Fe)	5.21	Specimens 23F-69 to 23F-112
A35	(Fe)	5.95	Specimens 23F-47 to 23F-93
A36	(Fe)	5.88	Specimens W8A-110 to W8A-118
A38	(Fe)	6.51	Specimens W8A-125 to W8A-138
	(Ni)	6.22	
A37	(Fe)	6.44	Specimens 23F-28 to 23F-88
A39	(Fe)	7.07	Specimens W8A-105 to W8A-135
	(AgCo)	4.08[c]	
Vial	(^{238}U)	8.25[d] (9.41)[e]	Between specimens W8A-120 and W8A-138 and between specimens 23F-51 and 23F-88
	(Fe)	6.51	
	(Ni)	6.43	

[a] See Figure A-13 for monitor locii. The Fe, Ni and ^{238}U results are based on > 1 MeV ^{235}U fission spectrum-averaged cross sections of 115.2, 156.8 and 441 millibarns, respectively.

[b] Fission spectrum assumption; $n/cm^2 \cdot s^{-1}$ (E > 1 MeV) unless noted.

[c] Thermal fluence rate corrected for epithermal neutron contributions based on ^{109}Ag and ^{59}Co reaction rates and their cross sections.

[d] Determination from ^{137}Cs, ^{103}Ru, $^{140}BaLa$ and ^{95}Zr results.

[e] Calculated spectrum value.

Total time of irradiation: 616.04 hours

Table A-14 Irradiation Assembly UBR-76 Capsule B Fluence-Rate Monitor Results (Ref. 6)

Monitor/Segment[a]		Fluence Rate[b] x 10^{12} (Average)	Monitor Location in Specimen Array
B1	(Fe)	7.32	Between layers 1 and 2
	(AgCo)	4.57[c,d]	
B2	(Fe)	7.10	Between layers 3 and 4
	(Ni)	6.87	
B3	(Fe)	7.02	Between layers 6 and 7
	(Ni)	6.70	
B4	(Fe)	6.92	Between layers 8 and 9
	(AgCo)	2.86[c]	
B5	(Fe)	6.75	Between layers 10 and 11
	(Ni)	6.57	
Vial	(^{238}U)	9.20[e] (10.45)[f]	Between layers 4 and 5
	(Fe)	7.00	
	(Ni)	6.95	

[a] See Figure A-14 for monitor locii. The Fe, Ni and ^{238}U results are based on > 1 MeV ^{238}U fission spectrum-averaged cross sections of 115.2, 156.8 and 441 millibarns, respectively.

[b] Fission spectrum assumption; $n/cm^2 \cdot s^{-1}$ (E > 1 MeV) unless noted.

[c] Thermal fluence rate corrected for epithermal neutron contributions based on ^{109}Ag and ^{59}Co reaction rates and their cross sections.

[d] Single determination value.

[e] Determination from ^{137}Cs, ^{103}Ru, $^{140}BaLa$ and ^{95}Zr results.

[f] Calculated spectrum value.

Total time of irradiation: 616.04 hours

Neutron Fluence-Rate Determinations

Based on Fission Spectrum Assumption

For Assembly UBR-77 (In-Core Irradiation)

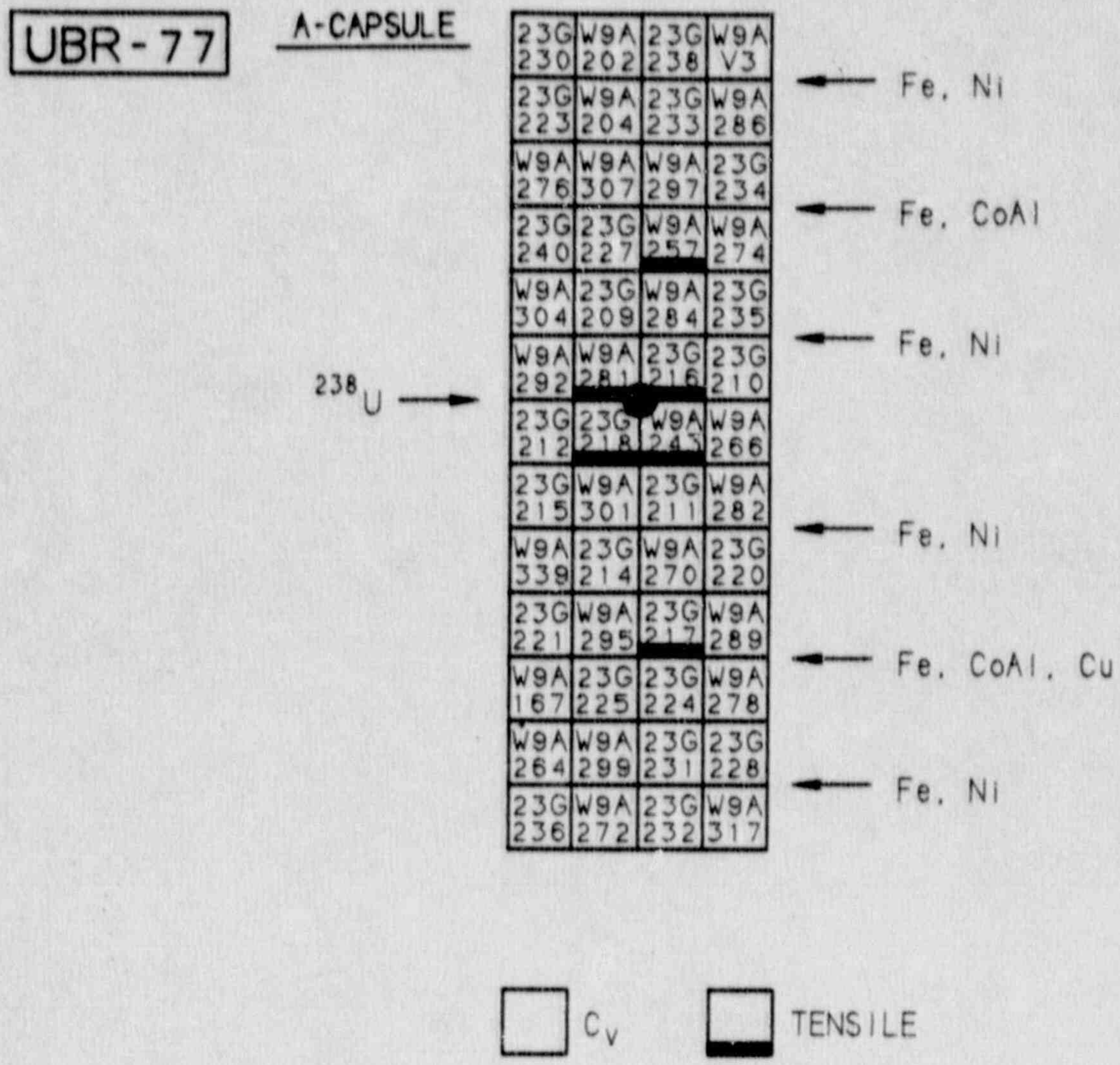

Fig. A-15 Irradiation Assembly UBR-77 (Capsule A) showing neutron fluence-rate monitor locations.

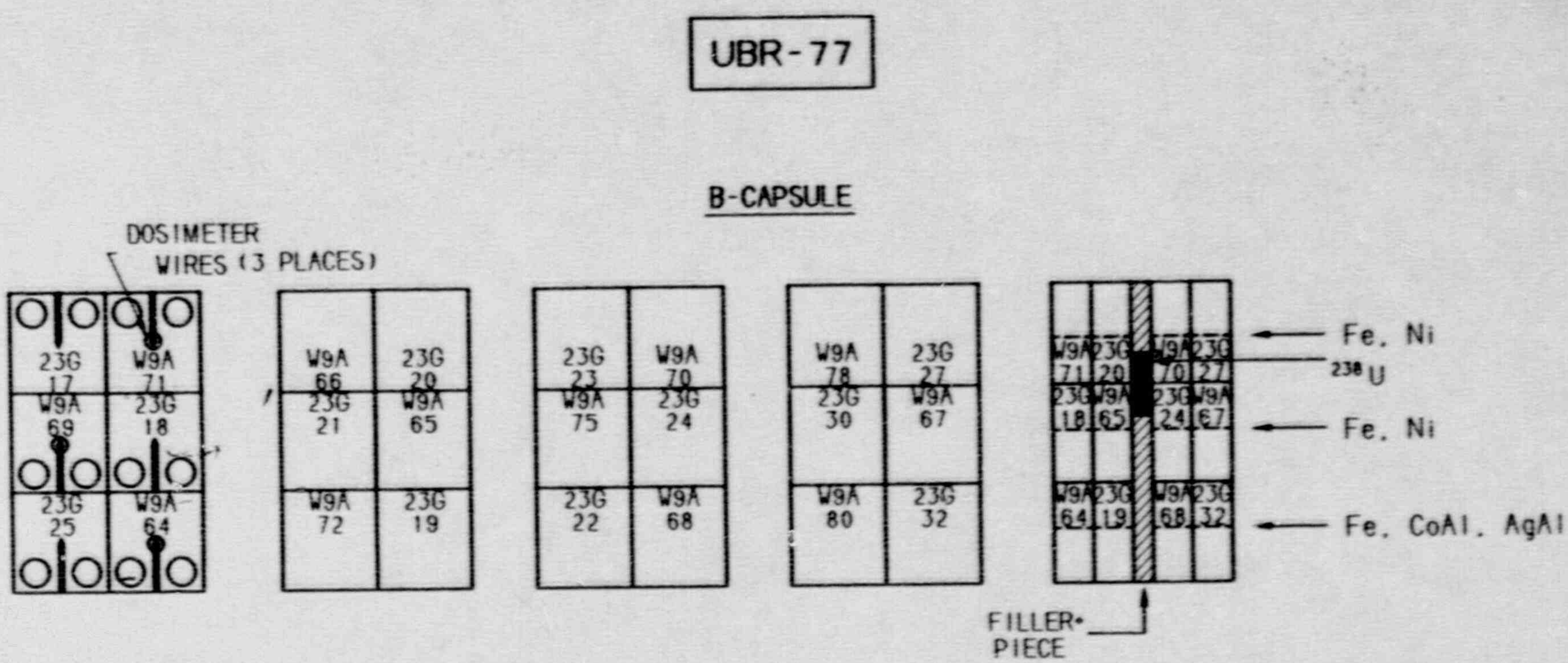

Fig. A-16 Irradiation Assembly UBR-77 (Capsule B) showing neutron fluence-rate monitor locations.

Table A-15 Irradiation Assembly UBR-77 Capsule A Fluence-Rate Monitor Results (Ref. 7)

Monitor/Segment[a]		Fluence Rate[b] x 10^{12} (Average)	Monitor Location in Specimen Array
A1	(Fe)	5.75	Between layers 1 and 2
	(Ni)	5.66	
A2	(Fe)	5.96	Between layers 3 and 4
	(AgCo)	2.75[c]	
A3	(Fe)	6.03	Between layers 5 and 6
	(Ni)	5.97	
A4	(Fe)	6.38	Between layers 8 and 9
	(Ni)	6.25	
A5	(Fe)	6.50	Between layers 10 and 11
	(AgCo)	2.92[c]	
	(Cu)	5.46	
A6	(Fe)	6.71	Between layers 12 and 13
	(Ni)	6.59	
Vial	(^{238}U)	7.64[d]	Between layers 6 and 7
		(8.71)[e]	
	(Fe)	6.33	
	(Ni)	6.26	

[a] See Figure A-15 for monitor locii. The Fe, Ni, Cu and ^{238}U results are based on > 1 MeV ^{238}U fission spectrum-averaged cross sections of 115.2, 156.8, 0.867 and 441 millibarns, respectively.

[b] Fission spectrum assumption; $n/cm^2 \cdot s^{-1}$ (E > 1 MeV) unless noted.

[c] Thermal fluence rate corrected for epithermal neutron contributions based on ^{109}Ag and ^{59}Co reaction rates and their cross sections.

[d] Determination from ^{137}Cs, ^{103}Ru, $^{140}BaLa$ and ^{95}Zr results.

[e] Calculated spectrum value.

Total time of irradiation: 139.00 hours

Table A-16 Irradiation Assembly UBR-77 Capsule B Fluence-Rate Monitor Results (Ref. 7)

Monitor/Segment[a]		Fluence Rate[b] x 10^{12} (Average)	Monitor Location in Specimen Array
B8	(Fe)	6.88	Specimens W9A-71 to 23G-27
	(Ni)	6.71	
B9	(Fe)	6.54	Specimens W9A-69 to 23G-30
	(Ni)	6.43	
B10	(Fe)	6.19	Specimens W9A-64 to 23G-32
	(AgCo)	2.71[c]	
Vial	(^{238}U)	7.64[d]	Between specimens W9A-65 and W9A-75 and between specimens 23G-219 and 23G-24 (diagonally)
		(8.71)[e]	
	(Fe)	6.39	
	(Ni)	6.30	

[a] See Figure A-16 for monitor locii. The Fe, Ni and ^{238}U results are based on > 1 MeV ^{235}U fission spectrum-averaged cross sections of 115.2, 156.8 and 441 millibarns, respectively.

[b] Fission spectrum assumption; $n/cm^2 \cdot s^{-1}$ (E > 1 MeV) unless noted.

[c] Thermal fluence rate corrected for epithermal neutron contributions based on ^{109}Ag and ^{59}Co reaction rates and their cross sections.

[d] Determination from ^{137}Cs, ^{103}Ru, $^{140}BaLa$ and ^{95}Zr results.

[e] Calculated spectrum value.

Total time of irradiation: 139.00 hours

REFERENCES

1. J. W. Rogers, "Neutron Fluence Rates for MEA-UBR Experiments," Letter Report JWR-52-87, EG&G Idaho, Inc., Idaho Falls, ID, 6 November 1987.

2. J. W. Rogers, "Neutron Fluence Rates for MEA-UBR Experiments," Letter Report JWR-22-85, EG&G Idaho, Inc., Idaho Falls, ID, 28 May 1985.

3. J. W. Rogers, "Neutron Fluence Rates for MEA-UBR Experiments," Letter Report JWR-16-87, EG&G Idaho, Inc., Idaho Falls, ID, 27 May 1987.

4. J. W. Rogers, "Neutron Fluence Rates for MEA-UBR Experiments," Letter Report JWR-22-86, EG&G Idaho, Inc., Idaho Falls, ID, 28 August 1986.

5. J. W. Rogers, "Neutron Fluence Rates for MEA-UBR Experiments," Letter Report JWR-14-87, EG&G Idaho, Inc., Idaho Falls, ID, 15 May 1987.

6. J. W. Rogers, "Neutron Fluence Rates for MEA-UBR Experiments," Letter Report JWR-36-88, EG&G Idaho, Inc., Idaho Falls, ID, 1 September 1988.

7. J. W. Rogers, "Neutron Fluence Rates for MEA-UBR Experiments," Letter Report JWR-39-87, EG&G Idaho, Inc., Idaho Falls, ID, 22 September 1987.

APPENDIX B

Reactor Operations History:
Irradiation Assemblies UBR-38, UBR-44, UBR-45, UBR-46
UBR-65, UBR-75, UBR-76, AND UBR-77

EXPOSURE HISTORY: UBR 38

DATE IN	TIME IN	DATE OUT	TIME OUT	EXPOSURE HOURS	SIGMA HOURS	CORE POSITION	NOTES
2-21-83	1715	2-22-83	0919	16.07	16.07	Reflector	6" S.P.
2-22-83	1048	2-23-83	1800	31.20	47.27		
2-23-83	1843	2-25-83	0830	37.78	85.05		
2-27-83	1720	2-28-83	0850	15.50	100.55		
2-28-83	0917	2-28-83	1827	9.17	109.72		
2-28-83	1854	3-1-83	1414	19.33	129.05		
3-1-83	1443	3-1-83	2342	8.98	138.03		
3-2-83	0010	302083	1300	12.83	150.86		
3-2-83	1345	3-4-83	1015	44.50	195.36		
3-6-83	1702	3-7-83	1040	17.63	212.99		
3-7-83	1040	3-7-83	2000	8.40	221.39		
3-7-83	2000	3-7-83	2100	0.95	222.34		
3-7-83	2100	3-7-83	2330	2.50	224.84		
3-7-83	2330	3-8-83	0100	1.35	226.19		
3-8-83	0100	3-8-83	1215	11.25	237.44		
3-8-83	1215	3-8-83	1345	1.35	238.79		
3-8-83	1345	3-11-83	0800	66.25	305.04		
3-11-83	0828	3-11-83	1123	1.46	306.50		
3-11-83	1149	3-11-83	1227	0.32	306.82		
3-13-83	1721	3-13-83	2209	4.80	311.62		
3-13-83	2313	3-14-83	1348	14.58	326.20		
3-14-83	1427	3-18-83	1052	92.42	418.62		
3-20-83	1705	3-24-83	1200	90.92	509.54		
3-27-83	1616	3-28-83	0945	17.48	527.02		
3-28-83	1106	3-28-83	1320	2.23	529.25		
3-28-83	1418	4-1-83	1200	93.70	622.95		
4-5-83	1054	4-8-83	1200	73.10	696.05		
4-10-83	1655	4-11-83	1930	26.58	722.63		
4-11-83	2017	4-15-83	0830	84.22	806.85		
4-17-83	1712	4-18-83	1300	19.80	826.65		
4-18-83	1355	4-19-83	2103	31.13	857.78		
4-19-83	2217	4-20-83	1024	12.12	869.90		
4-20-83	1054	4-22-83	1300	50.10	920.00		
4-24-83	1701	4-26-83	1630	47.48	967.48		
4-26-83	1740	4-28-83	1248	43.13	1010.61		
4-28-83	1530	4-29-83	1000	18.50	1029.11		

EXPOSURE HISTORY: UBR 38

DATE IN	TIME IN	DATE OUT	TIME OUT	EXPOSURE HOURS	SIGMA HOURS	CORE POSITION	NOTES
5-1-83	1707	5-2-83	0930	16.38	1045.49		
5-2-83	0954	5-6-83	1000	96.10	1141.59		
5-8-83	1653	5-13-83	0900	112.12	1253.71		
5-15-83	1630	5-18-83	2300	78.5	1332.21		
5-22-83	1655	5-26-83	0223	81.47	1413.68		
5-26-83	0213	5-27-83	1030	31.78	1445.46		
5-31-83	1345	6-3-83	0043	58.97	1504.43		
6-3-83	0204	6-3-83	1100	8.93	1513.36		
6-5-83	1643	6-10-83	0800	111.28	1624.64		
6-12-83	1654	6-16-83	1400	93.1	1717.74		
6-19-83	1718	6-24-83	0900	111.7	1829.44		
6-26-83	1720	7-1-83	1200	114.7	1944.14		
7-5-83	0054	7-7-83	1634	64.46	2008.60		
7-7-83	1726	7-8-83	1045	17.32	2025.92		
7-10-83	1756	7-15-83	1200	114.10	2140.02		
7-17-83	1703	7-20-83	1015	65.20	2205.22		
7-20-83	1100	7-22-83	1200	49.00	2254.22		
7-24-83	1700	7-26-83	1800	49.00	2303.22		
7-26-83	1836	7-27-83	1100	16.40	2319.62		
7-27-83	1202	7-29-83	1200	48.00	2367.62		
7-31-83	1705	8-5-83	0800	110.92	2478.54		
8-5-83	1214	8-5-83	1240	0.43	2478.97		
8-7-83	1714	8-11-83	0800	86.77	2565.74		
8-11-83	0937	8-12-83	1200	26.38	2592.12		
8-14-83	1700	8-19-83	1000	113.00	2709.12		
8-21-83	1700	8-25-83	1506	94.10	2803.22		
8-28-83	1743	8-31-83	1526	69.71	2891.52	South Reflector	
8-31-83	1600	9-1-83	1130	19.50	2911.02		
9-1-83	1237	9-2-83	0150	13.22	2924.24		
9-2-83	0300	9-2-83	1000	7.00	2931.24		
		180° ROTATION					
9-6-83	0050	9-9-83	0800	79.17	3010.41		
9-11-83	1712	9-16-83	1200	114.8	3125.21		
9-18-83	1659	9-23-83	0900	112.00	3237.21		
9-25-83	1608	9-30-83	0900	111.86	3349.07		
10-2-83	1700	10-5-83	1030	65.50	3414.57		

EXPOSURE HISTORY: UBR 38

DATE IN	TIME IN	DATE OUT	TIME OUT	EXPOSURE HOURS	SIGMA HOURS	CORE POSITION	NOTES
10-5-83	1159	10-7-83	1045	46.77	3461.34		
10-9-83	1723	10-11-83	0800	110.55	3571.89		
10-16-83	1715	10-21-83	0830	111.25	3683.14		
10-23-83	1648	10-28-83	0800	111.20	3794.34		
10-30-83	1709	11-4-83	0900	111.85	3906.19		
11-6-83	1710	11-7-83	1200	18.83	3925.02		
11-7-83	1342	11-10-83	1400	72.30	3997.32		
11-13-83	1700	11-14-83	0845	15.75	4013.07		
11-14-83	0938	11-17-83	0250	65.20	4078.27		
11-17-83	0312	11-17-83	1600	12.80	4091.07		
11-17-83	1655	11-18-83	0900	16.08	4107.15		
11-27-83	1653	11-30-83	1630	71.62	4178.77		
12-1-83	0035	12-2-83	1000	21.42	4200.19		
12-4-83	1710	12-6-83	1109	42.00	4242.19		
12-6-83	1544	12-7-83	1130	29.77	4271.96		
12-7-83	1200	12-9-83	0800	44.00	4315.96		
12-11-83	1900	12-16-83	1000	111.00	4426.96		
12-18-83	1713	12-20-83	0218	33.90	4460.86		
12-20-83	0307	12-23-83	0900	77.88	4538.74		
12-26-83	1623	12-29-83	2330	79.12	4617.86		
1-2-84	1604	1-4-84	2400	55.93	4673.79		
1-5-84	1013	1-5-84	1940	9.45	4683.24		
1-5-84	2043	1-6-84	1300	16.28	4699.52		
1-8-84	1651	1-9-84	1000	17.15	4716.67		
1-9-84	1035	1-13-84	1100	96.83	4813.50		
1-15-84	1653	1-16-84	0000	7.12	4820.62		
1-16-84	0000	1-19-84	1509	87.15	4907.77		
1-19-84	1600	1-20-84	1030	18.50	4926.27		
1-22-84	1641	1-27-84	0800	111.32	5037.59		
1-29-84	1652	1-30-84	1700	24.13	5061.72		
1-30-84	1838	2-3-84	1230	89.86	5151.59		
2-5-84	1655	2-10-84	1200	115.08	5266.67		
2-12-84	1647	2-17-84	1002	113.25	5379.92		
2-20-84	1648	2-23-84	1450	70.03	5449.95		
2-23-84	1544	2-24-84	1030	18.76	5468.72		

EXPOSURE HISTORY: UBR 38

DATE IN	TIME IN	DATE OUT	TIME OUT	EXPOSURE HOURS	SIGMA HOURS	CORE POSITION	NOTES
2-26-84	1705	2-28-84	0700	37.90	5506.62		
2-29-84	1106	2-29-84	1900	7.90	5514.52		
2-29-84	2002	3-2-84	1500	42.97	5557.49		
3-4-84	1712	3-5-84	1000	16.80	5574.29		
3-5-84	1022	3-6-84	0800	21.63	5595.92		
3-6-84	0826	3-8-84	2200	61.57	5657.49		
3-8-84	2240	3-9-84	1000	11.33	5668.82		
		ROTATED	180° 3-9-84				
3-11-84	1700	3-16-84	0830	111.5	5780.32		
3-13-84	1700	3-21-84	1518	70.3	5850.62		
3-21-84	1710	3-22-84	1330	20.33	5870.95		
3-22-84	1429	3-23-84	0840	18.183	5889.14		
3-25-84	1659	3-30-84	0830	111.52	6000.66		
4-1-84	1659	4-2-84	1500	22.00	6022.66		
4-2-84	1535	4-6-84	0800	88.42	6111.08		
4-8-84	1639	4-10-84	0800	39.35	6150.43		
4-10-84	0830	4-15-84	0900	72.50	6222.93		
4-15-84	1649	4-20-84	0800	111.18	6334.11		
4-22-84	1650	4-27-84	0800	111.17	6445.28		
4-29-84	1650	5-2-84	1500	70.83	6516.11		
5-2-84	1527	5-4-84	0800	40.55	6556.66		
5-4-84	1319	5-4-84	1410	0.85	6557.51		
5-6-84	1654	5-9-84	0000	55.10	6612.61		
5-9-84	0019	5-10-84	0800	31.68	6644.29		
5-10-84	1726	5-10-84	1830	1.07	6645.36		
5-11-84	1230	5-11-84	1240	0.17	6645.53		
5-13-84	1700	5-17-84	0800	87.00	6732.53		
5-18-84	1453	5-18-84	1533	0.67	6733.20		
5-20-84	1705	5-20-84	1749	0.73	6733.93		
5-20-84	1827	5-23-84	0230	56.05	6789.98		
5-23-84	0254	5-23-84	2200	19.10	6809.08		
5-29-84	1026	6-1-84	0800	69.56	6878.64		
6-3-84	1643	6-7-84	2200	101.28	6979.92		
6-10-84	1646	6-15-84	0800	111.23	7091.15		
6-17-84	1705	6-17-84	1745	0.67	7091.82		
6-17-84	1817	6-18-84	0123	7.20	7099.02		

EXPOSURE HISTORY: UBR 38

DATE IN	TIME IN	DATE OUT	TIME OUT	EXPOSURE HOURS	SIGMA HOURS	CORE POSITION	NOTES
6-18-84	0154	6-18-84	1312	11.30	7110.32		
6-18-84	1340	6-20-84	1745	52.08	7162.40		
6-20-84	1906	6-21-84	2400	28.90	7191.30		
6-24-84	1657	6-29-84	0118	105.25	7296.55		
7-1-84	1653	7-3-84	2300	54.12	7350.67		
7-5-84	0054	7-6-84	1423	37.48	7388.15		
7-8-84	1730	7-10-84	2053	51.38	7439.53		
7-10-84	2150	7-13-84	1200	62.17	7501.70		
7-15-84	1706	7-19-84	2300	101.90	7603.60		
7-22-84	1654	7-27-84	1200	115.10	7718.70		
7-29-84	1654	8-3-84	0900	111.90	7830.60		
8-5-84	1739	8-9-84	1900	97.35	7927.95		
8-9-84	2053	8-10-84	0815	11.37	7939.32		
8-10-84	1049	8-10-84	1219	1.50	7940.82		
8-12-84	1654	8-12-84	2000	3.10	7943.92		
8-12-84	2040	8-16-84	1400	89.33	8033.25		
8-16-84	1538	8-16-84	1752	2.23	8035.48		
8-22-84	1300	8-24-84	1515	50.25	8085.73		
8-26-84	1700	8-31-84	1223	115.38	8201.11		
9-4-84	0052	9-7-84	1400	85.13	8286.24		
9-9-84	1649	9-13-84	0020	80.15	8366.39		
9-13-84	0511	9-14-84	0900	27.82	8394.21		
9-16-84	1653	9-21-84	0800	111.12	8505.33		
9-23-84	1730	9-27-84	1230	91.00	8596.33		
9-27-84	1400	9-28-84	1141	21.68	8618.01		
9-30-84	1701	10-1-84	0930	16.50	8634.51		
10-1-84	1121	10-5-84	0800	92.65	8727.16		
10-7-84	1658	10-10-84	2130	76.53	8803.69		
10-10-84	2339	10-12-84	1500	39.35	8843.04		
10-14-84	1709	10-15-84	1300	19.85	8862.89		
10-15-84	1341	10-15-84	1400	0.32	8863.21		
10-15-84	1434	10-18-84	1300	70.43	8933.64		
10-18-84	1418	10-19-84	1400	24.30	8957.94		
10-21-84	1657	10-26-84	0800	111.03	9068.97		
10-26-84		ROTATED	180°				
10-28-84	1653	10-30-84	1900	50.12	9119.09		

EXPOSURE HISTORY: UBR 38

DATE IN	TIME IN	DATE OUT	TIME OUT	EXPOSURE HOURS	SIGMA HOURS	CORE POSITION	NOTES
10-30-84	2030	11-2-84	1115	62.75	9181.84		
11-4-84	1717	11-9-84	1130	114.22	9296.06		
11-11-84	1808	11-12-84	1339	19.52	9315.58		
11-12-84	1402	11-16-84	0800	89.97	9405.55		
11-18-84	1738	11-21-84	2300	77.37	9482.92		
11-25-84	1731	11-30-84	1200	114.48	9597.40		
12-2-84	1725	12-4-84	0714	37.81	9635.21		
12-4-84	1005	12-5-84	1119	25.24	9660.45		
12-5-84	1140	12-6-84	1415	26.58	9687.03		
12-6-84	1440	12-7-84	1233	21.88	9708.91		
12-9-84	1758	12-14-84	0800	110.03	9818.94		
12-16-84	1750	12-21-84	0800	110.16	9929.10		
1-2-85	0054	1-4-85	0900	56.10	9985.20		
1-6-85	1743	1-11-85	1000	113.28	10098.48		
1-13-85	1746	1-16-85	1900	73.23	10171.71		
1-16-85	2006	1-17-85	1300	16.90	10188.61		
1-17-85	1530	1-17-85	1715	1.75	10190.36		
1-17-85	1745	1-18-85	1200	18.25	10208.61		
1-25-85	0627	1-25-85	0945	3.30	10211.91		
1-25-85	1015	1-25-85	1520	5.08	10216.99		
1-27-85	1658	1-28-85	0830	15.53	10232.52		
1-28-85	0948	2-1-85	1300	99.20	10331.72		
2-3-85	1721	2-8-85	1300	115.65	10447.37		
2-10-85	1718	2-11-85	1100	17.70	10465.07		
2-11-85	1130	2-15-85	1530	100.00	10565.07		
2-17-85	1802	2-22-85	1000	112.00	10677.07		
2-24-85	1644	2-26-85	1300	44.27	10721.34		
2-26-85	1408	2-27-85	0109	11.02	10732.36		
2-27-85	0136	2-27-85	0544	4.13	10736.49		
2-27-85	0604	2-27-85	1105	5.02	10741.51		
2-27-85	1356	2-27-85	1717	3.35	10744.86		
2-27-85	1758	2-28-85	1100	17.03	10761.89		
2-28-85	1215	3-1-85	1010	21.61	10783.50		
3-3-85	1725	3-8-85	0900	111.58	10895.08		
3-8-85	1110	3-8-85	1125	0.25	10895.33		

EXPOSURE HISTORY: UBR 38

DATE IN	TIME IN	DATE OUT	TIME OUT	EXPOSURE HOURS	SIGMA HOURS	CORE POSITION	NOTES
3-8-85	1237	3-8-85	1509	2.53	10897.86		
3-10-85	1720	3-15-85	0800	110.66	11008.52		
3-17-85	1726	3-18-85	0254	15.46	11023.98		
3-18-85	1036	3-18-85	2045	10.15	11034.13		
3-18-85	2200	3-21-85	2025	71.62	11105.75		
3-21-85	2137	3-22-85	0600	8.38	11114.13		
3-22-85	1454	3-22-85	1511	0.28	11114.41		
3-24-85	1721	3-28-85	0457	83.60	11198.01		
3-28-85	0518	3-28-85	1045	5.45	11203.46		
3-28-85	1149	3-29-85	1100	23.18	11226.64		
3-31-85	1725	4-3-85	0700	61.58	11288.22		
4-3-85	1114	4-5-85	0900	45.77	11333.99		
4-7-85	1700	4-10-85	0815	63.25	11397.24		
4-10-85	1054	4-11-85	0900	22.10	11419.34		
4-11-85	1220	4-12-85	1100	22.67	11442.01		
4-13-85	0058	4-13-85	0133	0.58	11442.59		
4-14-85	1730	4-19-85	0913	111.72	11554.31		
4-19-85	2009	4-19-85	2021	0.20	11554.51		
4-21-85	1725	4-24-85	0836	63.18	11617.69		
4-24-85	0908	4-25-85	2042	35.57	11653.26		
4-25-85	2122	4-26-85	0640	9.30	11662.56		
4-28-85	1732	5-3-85	0700	109.47	11772.03		
5-3-85	1257	5-3-85	1336	0.65	11772.68		
5-5-85	1640	5-6-85	1551	23.18	11795.86		
5-6-85	2209	5-9-85	0830	58.35	11854.21		
5-9-85	1055	5-10-85	0721	20.43	11874.64		
5-10-85	1650	5-10-85	1716	0.87	11875.51		
5-12-85	1741	5-16-85	1200	90.32	11965.83		
5-19-85	1653	5-24-85	0900	112.15	12077.98		
5-28-85	0100	5-30-85	1400	61.00	12138.98		
5-30-85	1733	5-30-85	1913	1.67	12140.65		
5-30-85	2000	5-31-85	1440	18.67	12159.32		
6-2-85	1800	6-7-85	0900	111.00	12270.32		
6-9-85	1720	6-11-85	0715	37.92	12308.24		
6-11-85	0824	6-13-85	1500	54.60	12362.84		
6-13-85	1600	6-14-85	0830	16.50	12379.34		

EXPOSURE HISTORY: UBR 38

DATE IN	TIME IN	DATE OUT	TIME OUT	EXPOSURE HOURS	SIGMA HOURS	CORE POSITION	NOTES
6-16-85	1837	6-18-85	1000	39.38	12418.72		
6-18-85	1035	6-21-85	1015	71.67	12490.39		
6-23-85	1732	6-28-85	0900	111.47	12601.86		
6-30-85	1726	7-3-85	2300	77.58	12679.44		
7-7-85	1736	7-10-85	1030	64.90	12744.34		
7-10-85	1110	7-12-85	0830	45.33	12789.67		
7-12-85	1852	7-12-85	1910	0.30	12789.97		
7-14-85	1657	7-18-85	1127	90.50	12880.47		
7-18-85	1210	7-19-85	1120	23.16	12903.63		
7-21-85	1709	7-21-85	2006	2.95	12906.58		
7-21-85	2039	7-24-85	1535	66.93	12973.51		
7-24-85	1827	7-26-85	1430	44.05	13017.56		
7-28-85	1717	7-30-85	0438	35.35	13052.91		
7-30-85	0500	8-2-85	1200	67.00	13119.91		
8-4-85	1742	8-9-85	0800	110.30	13230.21		
8-11-85	1651	8-11-85	2020	3.48	13233.69		
8-11-85	2048	8-16-85	0930	108.70	13342.39		
		ROTATED	180°				
8-18-85	1658	8-23-85	1000	113.03	13455.42		
8-23-85		PULLED BACK FROM CORE (HEATER FAILURE)					
12-22-85		BACK IN FLUX					
12-22-85	1716	12-24-85	1130	42.20	13497.65		
12-26-85	0833	12-27-85	1200	27.45	13525.10		
12-27-85	1200	12-27-85	1508	1.57	13526.67		
12-29-85	1709	12-31-85	1500	45.85	13572.52		
1-5-86	1710	1-10-86	1400	116.83	13689.35		
1-12-86	1651	1-13-86	0900	16.15	13705.50		
1-19-86	1700	1-24-86	1000	113.00	13818.50		
1-26-86	1700	1-28-86	0800	39.00	13857.50		
1-28-86	0928	1-31-86	1000	72.53	13930.03		
2-2-86	1648	2-7-86	1200	115.20	14045.23		
2-9-86	1708	2-11-86	0809	39.02	14084.25		
2-11-86	0840	2-14-86	0900	72.33	14156.58		
2-17-86	1649	2-21-86	0900	88.18	14244.76		
2-23-86	1709	2-28-86	0800	110.85	14355.61		

EXPOSURE HISTORY: UBR 38

DATE IN	TIME IN	DATE OUT	TIME OUT	EXPOSURE HOURS	SIGMA HOURS	CORE POSITION	NOTES
3-2-86	1658	3-3-86	1030	17.53	14373.14		
3-3-86	1306	3-4-86	2224	33.30	14406.44		
3-4-86	2314	3-5-86	1906	19.87	14426.31		
3-5-86	1937	3-7-86	1241	41.07	14467.38		
3-9-86	1641	3-14-86	0900	112.32	14579.70		
3-16-86	1702	3-17-86	0850	15.80	14595.50		
3-17-86	1020	3-20-86	1200	73.67	14669.17		
3-23-86	1700	3-25-86	0704	38.07	14707.24		
3-25-86	0745	3-28-86	0930	73.75	14780.99		
3-30-86	1700	4-4-86	1200	115.00	14895.99		
4-6-86	1658	4-7-86	1123	18.41	14914.40		
4-7-86	1342	4-7-86	2217	8.58	14922.98		
4-7-86	2249	4-8-86	1400	15.18	14938.16		
4-8-86	1431	4-11-86	0900	66.48	15004.64		
4-13-86	1653	4-16-86	1100	66.12	15070.76		
4-16-86	1152	4-18-86	1130	47.63	15118.39		
4-20-86	1700	4-23-86	0000	55.00	15173.39		
4-23-86	0028	4-23-86	1545	15.28	15188.67		
4-23-86	1642	4-25-86	0945	41.05	15229.72		
4-27-86	2030	5-2-86	0900	108.50	15338.22		
5-4-86	1711	5-9-86	1300	115.82	15454.04		
5-11-86	1644	5-16-86	1450	118.10	15572.14		
5-18-86	1720	5-19-86	0830	15.16	15587.30		
5-19-86	0910	5-23-86	1300	99.67	15686.97		
5-26-86	1643	5-26-86	1650	0.12	15687.09		
5-26-86	1710	5-30-86	2103	99.88	15786.97		
6-1-86	1700	6-2-86	1300	20.00	15806.97		
6-2-86	1314	6-4-86	1000	44.77	15851.74		
6-4-86	1050	6-5-86	1000	23.17	15874.91		
6-5-86	1141	6-6-86	0700	19.32	15894.23		
6-6-86	1359	6-6-86	1407	0.13	15894.36		
6-6-86	1436	6-6-86	1508	0.53	15894.89		
6-8-86	1726	6-8-86	2100	3.57	15898.46		
6-8-86	2158	6-12-86	0700	81.03	15979.49		
6-12-86	0742	6-13-86	1200	28.30	16007.79		
6-13-86		ROTATED	180°				

EXPOSURE HISTORY: UBR 38

DATE IN	TIME IN	DATE OUT	TIME OUT	EXPOSURE HOURS	SIGMA HOURS	CORE POSITION	NOTES
6-15-86	1709	6-16-86	1544	22.58	16030.37		
6-16-86	1611	6-20-86	0900	88.82	16119.19		
6-22-86	1707	6-27-86	1300	115.88	16235.07		
6-29-86	1722	7-3-86	0200	80.63	16315.70		
7-3-86	0225	7-3-86	2145	19.33	16335.03		
7-6-86	1602	7-7-86	0800	15.97	16351.00		
7-21-86	1104	7-25-86	0800	92.93	16443.93		
7-27-86	1730	8-1-86	1200	114.50	16558.43		
8-3-86	1710	8-5-86	1400	44.83	16603.26		
8-5-86	1435	8-8-86	1000	67.42	16670.68		
8-10-86	1654	8-11-86	2226	29.53	16700.21		
8-15-86	1550	8-15-86	2312	7.37	16707.58		
8-17-86	1656	8-19-86	1330	44.57	16752.15		
8-19-86	1516	8-22-86	0800	64.73	16816.88		
8-24-86	1707	8-28-86	2300	101.88	16918.76		
9-2-86	0115	9-2-86	1102	9.78	16928.54		
9-2-86	1121	9-5-86	0700	67.65	16996.19		
9-7-86	1658	9-10-86	0845	63.78	17059.97		
9-10-86	1114	9-11-86	1300	25.77	17085.74		
9-11-86	1341	9-12-86	0800	18.31	17104.05		
9-14-86	1738	9-19-86	0900	111.37	17215.42		
9-21-86	1717	9-26-86	0800	110.72	17326.14		
9-28-86	1654	10-2-86	1200	91.10	17417.24		
						DISCHARGED	

EXPOSURE HISTORY

UBC 44 A & B

date in	time in	date out	time out	2MW exposure hours	2MW sigma hours	core position	
4·26·83	1740	4·28·83	1248	43.13	43.13	REFLECTOR	
4·28·83	1530	4·29·83	1000	18.50	61.63		
5·1·83	1707	5·2·83	0930	16.38	78.01		
5·2·83	0954	5·6·83	1000	96.10	174.11		
5·8·83	1653	5·13·83	0900	112.12	286.23		
5·15·83	1630	5·18·83	2300	78.50	364.73		
5·22·83	1655	5·26·83	0223	81.47	446.20		
5·26·83	0243	5·27·83	1030	31.78	477.98		
5·31·83	1345	6·3·83	0043	58.97	536.95		
6·3·83	0204	6·3·83	1100	8.93	545.88		
6·5·83	1643	6·10·83	0800	111.28	657.16		
6·12·83	1654	6·16·83	1400	93.10	750.26		
6·19·83	1718	6·24·83	0900	111.70	861.96		
6·26·83	1720	7·1·83	1200	114.70	976.66		
7·5·83	0054	7·7·83	1634	64.46	1041.12		
7·7·83	1726	7·8·83	1045	17.32	1058.44		
7·10·83	1756	7·15·83	1200	114.10	1172.54		
7·17·83	1703	7·20·83	1015	65.20	1237.74		
7·20·83	1100	7·22·83	1200	49.00	1286.74		
7·24·83	1700	7·26·83	1800	49.00	1335.74		
7·26·83	1836	7·27·83	1100	16.40	1352.14		
7·27·83	1202	7·29·83	1200	48.00	1400.14		
7·31·83	1705	8·5·83	0800	110.92	1511.06		
8·5·83	1214	8·5·83	1240	0.43	1511.49		
8·7·83	1714	8·11·83	0800	86.77	1598.26		
8·11·83	0937	8·12·83	1200	26.38	1624.64		

EXPOSURE HISTORY

UBR44A&B

date in	time in	date out	time out	2MW exposure hours	2MW sigma hours	core position	
——	FROM PAGE 1 ——			——	1624.64	REFLECTOR	
44 A&B	REMOVED	FROM ∅	8.12.83, REPLACED		12.9.83	——	
12.11.83	1900	12.16.83	1000	111.00	1735.64		
12.18.83	1713	12.20.83	0218	33.90	1769.54		
12.20.83	0307	12.23.83	0900	77.88	1847.42		
12.26.83	1623	12.29.83	2330	79.12	1926.54		
1.2.84	1604	1.4.84	2400	55.93	1982.47		
1.5.84	1013	1.5.84	1940	9.45	1991.92		
1.5.84	2043	1.6.84	1300	16.28	2008.20		
1.8.84	1651	1.9.84	1000	17.15	2025.35		
1.9.84	1035	1.13.84	1100	96.83	2122.18		
1.15.84	1653	1.16.84	0000	7.12	2129.30		
1.16.84	0000	1.19.84	1509	87.15	2216.45		
1.19.84	1600	1.20.84	1030	18.50	2234.95		
1.22.84	1641	1.27.84	0800	111.32	2346.27		
1.29.84	1652	1.30.84	1700	24.13	2370.40		
1.30.84	1838	2.3.84	1230	89.86	2460.26		
2.5.84	1655	2.10.84	1200	115.08	2575.34		
2.12.84	1647	2.17.84	1002	113.25	2688.59		
2.20.84	1648	2.23.84	1450	70.03	2758.62		
2.23.84	1544	2.24.84	1030	18.76	2777.38		
44 A&B	DISCHARGED		——	——	——	——	

EXPOSURE HISTORY

UBR 45 A,B

date in	time in	date out	time out	exposure hours	sigma hours	core position	
4-10-83	1655	4-11-83	1930	26.58	26.58		
4-11-83	2017	4-15-83	0830	84.22	110.80		
4-17-83	1712	4-18-83	1300	19.80	130.60		
4-18-83	1355	4-19-83	2103	31.13	161.73		
4-19-83	2217	4-20-83	1024	12.12	173.85		
4-20-83	1054	4-22-83	1300	50.10	223.95		
4-24-83	1701	4-26-83	1630	47.48	271.43		
4-26-83	1740	4-28-83	1248	43.13	314.56		
4-28-83	1530	4-29-83	1000	18.50	333.06		
5-1-83	1707	5-2-83	0930	16.38	349.44		
5-2-83	0954	5-6-83	1000	96.10	445.54		
5-8-83	1653	5-13-83	0900	112.12	557.66		
5-15-83	1630	5-18-83	2300	78.5	636.16		
5-22-83	1655	5-26-83	0223	81.47	717.63		
5-26-83	0243	5-27-83	1030	31.78	749.41		
5-31-83	1345	6-3-83	0043	58.97	808.38		
6-3-83	0204	6-3-83	1100	8.93	817.31		
6-5-83	1643	6-10-83	0800	111.28	928.59		
6-12-83	1654	6-16-83	1600	93.1	1021.69		
6-19-83	1718	6-24-83	0900	111.7	1133.39		
6-26-83	1720	7-1-83	1200	114.7	1248.09		
7-5-83	0054	7-7-83	1634	64.46	1312.55		
7-7-83	1726	7-8-83	1045	17.32	1329.87		
7-10-83	1756	7-15-83	1200	114.10	1443.97		
7-17-83	1703	7-20-83	1015	65.20	1509.17		
7-20-83	1100	7-22-83	1200	49.00	1558.17		

EXPOSURE HISTORY

UBR 45 A,B

date in	time in	date out	time out	exposure hours	sigma hours	core position	
7-24-83	1700	7-26-83	1800	49.00	1607.17		
7-26-83	1836	7-27-83	1100	16.40	1623.57		
7-27-83	1202	7-29-83	1200	48.00	1671.57		
7-31-83	1705	8-5-83	0800	110.92	1782.49		
8-5-83	1214	8-5-83	1240	0.43	1782.92		
8-7-83	1716	8-11-83	0800	86.77	1869.69		
8-11-83	0937	8-12-83	1200	26.38	1896.07	out of flux	
12-9-83		CAPSULE LOADED INTO REFLECTOR			1896.07		
12-11-83	1900	12-16-83	1000	111.00	2007.07		
12-18-83	1713	12-20-83	0218	33.90	2040.97		
12-20-83	0307	12-23-83	0900	77.88	2118.85		
12-26-83	1623	12-29-83	2330	79.12	2197.97		
1-2-84	1604	1-4-84	2400	55.93	2253.90		
1-5-84	1013	1-5-84	1940	9.45	2263.35		
1-5-84	2043	1-6-84	1300	16.28	2279.63		
1-8-84	1651	1-9-84	1000	17.13	2296.78		
1-9-84	1035	1-13-84	1100	96.83	2393.61		
1-15-84	1653	1-16-84	0000	7.12	2400.73		
1-16-84	0000	1-19-84	1509	87.15	2487.88		
1-19-84	1600	1-20-84	1030	18.50	2506.38		
1-22-84	1641	1-27-84	0800	111.32	2617.70		
1-29-84	1652	1-30-84	1700	24.13	2641.83		
1-30-84	1838	2-3-84	1230	89.86	2731.70		
2-5-84	1655	2-10-84	1200	115.08	2846.78		
2-12-84	1647	2-17-84	1002	113.25	2960.03		
2-20-84	1648	2-23-84	1450	70.03	3030.06		

EXPOSURE HISTORY

UBR 45 A,B

date in	time in	date out	time out	exposure hours	sigma hours	core position	
2-23-84	1544	2-24-84	1030	18.76	3048.83		
2-26-84	1705	2-28-84	0700	37.90	3086.73		
2-29-84	1106	2-29-84	1900	7.90	3094.63		
2-29-84	2002	3-2-84	1500	42.97	3137.60		
3-4-84	1712	3-5-84	1000	16.80	3154.40		
3-5-84	1022	3-6-84	0800	21.63	3176.03		
3-6-84	0826	3-8-84	2200	61.57	3237.6		
3-8-84	2240	3-9-84	1000	11.33	3248.93		
3-11-84	1700	3-16-84	0830	111.5	3360.43		
3-18-84	1700	3-21-84	1518	70.3	3430.73		
3-21-84	1710	3-22-84	1330	20.33	3451.06		
3-22-84	1429	3-23-84	0840	18.183	3469.243		
7-22-84	1654	7-27-84	1200	115.10	3584.343		
7-29-84	1654	8-3-84	0900	111.90	3696.243		
8-5-84	1739	8-9-84	1900	97.35	3793.59		
8-9-84	2053	8-10-84	0815	11.37	3804.96		
8-10-84	1049	8-10-84	1219	1.50	3806.46		
8-12-84	1654	8-12-84	2000	3.10	3809.56		

(Continues)

EXPOSURE HISTORY

UBR 45 A,B

date in	time in	date out	time out	exposure hours	sigma hours	core position	
8/12/84	2040	8/16/84	1400	89.33	3898.89		
8/16/84	1539	8/16/84	1752	2.23	3901.12		
8/22/84	1300	8/24/84	1515	50.25	3951.37		
8/26/84	1700	8/31/84	1223	115.38	4066.75		
9/4/84	0052	9/7/84	1400	85.13	4151.88		
9/9/84	1649	9/13/84	0020	80.15	4232.03		
9/13/84	0511	9/14/84	0900	27.82	4259.85		
9/16/84	1653	9/21/84	0400	111.12	4370.97		
9/23/84	1730	9/27/84	1230	91.00	4461.97		
9/27/84	1400	9/28/84	1141	21.68	4483.65		
9/30/84	1701	10/1/84	0930	16.50	4500.15		
10/1/84	1121	10/5/84	0800	92.65	4592.80		
0/7/84	1658	10/10/84	2130	76.53	4669.33		
0/10/84	2339	10/12/84	1500	39.35	4708.68		
0/14/84	1709	10/15/84	1300	19.85	4728.53		
0/15/84	1341	10/15/84	1400	0.32	4728.85		
0/15/84	1434	10/18/84	1300	70.43	4799.28		
0/18/84	1418	10/19/84	1400	24.30	4823.58		
0/21/84	1657	10/26/84	0800	111.03	4934.61		
0/28/84	1653	10/30/84	1900	50.12	4984.73		
0/30/84	2030	11/2/84	1115	62.75	5047.48		
1/4/84	1717	11/9/84	1130	114.22	5161.70		
1/11/84	1808	11/12/84	1339	19.52	5181.22		
1/12/84	1402	11/16/84	0800	89.97	5271.19		
1/18/84	1735	11/21/84	2300	77.37	5348.56		
1/25/84	1731	11/30/84	1200	114.48	5463.04		
2/2/84	1725	12/4/84	0714	37.81	5500.85		
2/4/84	1005	12/5/84	1119	25.24	5526.09		

EXPOSURE HISTORY

UBR 45 A,B

date in	time in	date out	time out	exposure hours	sigma hours	core position	
12/5/84	1140	12/6/84	1415	26.58	5552.67		
12/6/84	1440	12/7/84	1233	21.88	5574.55		
12/9/84	1758	12/14/84	0400	110.03	5684.58		
12/16/84	1750	12/21/84	0800	110.16	5794.74		
1/2/85	0054	1/4/85	0900	56.10	5850.84		
1/6/85	1743	1/11/85	1000	113.28	5964.12		
1/13/85	1746	1/16/85	1900	73.23	6037.35		
1/16/85	2006	1/17/85	1300	16.90	6054.25		
1/17/85	1530	1/17/85	1715	1.75	6056.00		
1/17/85	1745	1/18/85	1200	18.25	6074.25		
/25/85	0627	1/25/85	0945	3.30	6077.55		
/25/85	1015	1/25/85	1520	5.08	6082.63		
/27/85	1658	1/28/85	0830	15.53	6098.16		
/28/85	0948	1/31/85	1520	77.53	6175.69		
/31/85	1520	2/1/85	1300	21.66	6197.35		
2/3/85	1721	2/8/85	1300	115.65	6313.00		
2/10/85	1718	2/11/85	1100	17.70	6330.70		
2/11/85	1130	2/12/85	0852	21.37	6352.07		
2/12/85	0852	2/15/85	1530	78.63	6430.70		
2/17/85	1802	2/17/85	2200	4.00	6434.70		
2/17/85	2200	2/22/85	1000	108.00	6542.70		
2/24/85	1644	2/26/85	1300	44.27	6586.97		
2/26/85	1404	2/27/85	0109	11.02	6597.99		
[illegible]	0136	2/27/85	0544	4.13	6602.12		
2/27/85	0604	2/27/85	0923	3.32	6605.44		

EXPOSURE HISTORY

UBR 45 A,B

date in	time in	date out	time out	exposure hours	sigma hours	core position	
2/27/85	0923	2/27/85	1105	1.70	6607.14		
[redacted]	1356	2/27/85	1717	3.35	6610.49		
2/27/85	1758	2/28/85	1100	17.03	6627.52		
2/28/85	1215	3/1/85	1010	21.61	6649.13		
3/3/85	1725	3/8/85	0900	111.58	6760.71		
3/8/85	1110	3/8/85	1125	0.25	6760.96		
3/8/85	1237	3/8/85	1509	2.53	6763.49		

(Continues)

EXPOSURE HISTORY

UBR 45 A,B

date in	time in	date out	time out	exposure hours	'sigma' hours	core position	
3/10/85	1720	3/15/85	0400	110.66	6874.15		
3/17/85	1726	3/18/85	0854	15.46	6889.61		
3/18/85	1036	3/18/85	2045	10.15	6899.76		
3/18/85	2200	3/21/85	2025	71.62	6971.38		
3/21/85	2137	3/22/85	0600	8.38	6979.76		
3/22/85	1454	3/22/85	1511	0.28	6979.48		
3/24/85	1721	3/28/85	0457	83.60	7063.08		
3/28/85	0518	3/28/85	1045	5.45	7068.53		
3/28/85	1149	3/29/85	1100	23.18	7091.71		
3/31/85	1735	4/3/85	0700	61.58	7153.29		
4/3/85 .	1114	4/5/85	0900	45.77	7199.06		
4/7/85	1700	4/10/85	0815	63.25	7263.31		
4/10/85	1054	4/11/85	0900	22.10	7284.41		
4/11/85	1320	4/12/85	1100	22.67	7307.08		
4/12/85	0058	4/13/85	0133	0.58	7307.66		
4/14/85	1730	4/19/85	0913	111.72	7419.38		
4/19/85	2009	4/19/85	2021	0.20	7419.58		
4/21/85	1725	4/24/85	0836	63.18	7482.76		
4/24/85	0908	4/25/85	2042	35.57	7518.33		
4/25/85	2122	4/26/85	0640	9.30	7527.63		
4/28/85	1732	5/3/85	0700	109.47	7637.10		
5/3/85	1257	5/3/85	1336	0.65	7637.75		
5/5/85	1640	5/6/85	1551	23.18	7660.93		
5/6/85	2309	5/9/85	0830	58.35	7719.28		
5/9/85	1055	5/10/85	0721	20.43	7739.71		

EXPOSURE HISTORY

UBR 45 A,B

date in	time in	date out	time out	exposure hours	sigma hours		
5/10/85	1650	5/10/85	1716	0.43	7740.58		
5/13/85	1741	5/16/85	1200	90.32	7830.90		
5/19/85	1653	5/24/85	0900	112.15	7943.05		
5/28/85	0100	5/30/85	1400	61.00	8004.05		
5/30/85	1733	5/30/85	1913	1.67	8005.72		
5/30/85	2000	5/31/85	1440	18.67	8024.39		
6/2/85	1800	6/7/85	0900	111.00	8135.39		
6/9/85	1720	6/11/85	0715	37.82	8173.21		
6/11/85	0824	6/13/85	1500	54.60	8227.91		
6/13/85	1600	6/14/85	0830	16.50	8244.41		
6/16/85	1837	6/18/85	1000	39.38	8283.79		
6/18/85	1035	6/21/85	1015	71.67	8355.46		
6/23/85	1732	6/28/85	0900	111.47	8466.93		
6/30/85	1726	7/3/85	2300	77.58	8544.51		
7/7/85	1736	7/10/85	1030	64.90	8609.41		
7/10/85	1110	7/12/85	0830	45.33	8654.74		
7/12/85	1852	7/12/85	1910	0.30	8655.04		
7/14/85	1657	7/18/85	1137	90.50	8745.54		
7/18/85	1210	7/19/85	1120	23.16	8768.70		
7/21/85	1709	7/21/85	2006	2.95	8771.65		
7/21/85	2039	7/24/85	1535	66.93	8838.58		
7/24/85	1827	7/26/85	1430	44.05	8882.63		
7/28/85	1717	7/30/85	0438	35.35	8917.98		
7/30/85	0500	8/1/85	1253	43.88	8961.86		
8/1/85	1253	8/2/85	1200	23.12	8984.98		

EXPOSURE HISTORY

UBR 45 A,B

date in	time in	date out	time out	exposure hours	sigma hours	core position	
8/4/85	1742	8/9/85	0900	110.30	9095.28		
8/11/85	1651	8/11/85	2020	3.48	9098.76		
8/11/85	2048	8/16/85	0930	108.70	9207.46		
8/18/85	1658	8/23/85	1000	113.03	9320.49		
8/25/85	1716	8/30/85	1300	115.73	9436.22		
9/3/85	0100	9/5/85	0400	51.00	9487.22		
9/5/85	1138	9/6/85	2315	35.62	9522.84		
9/8/85	1734	9/13/85	1200	114.43	9637.27		
9/15/85	1653	9/20/85	0800	111.11	9748.38		
9/20/85	0800	9/20/85	1100	1.50	9749.88		* @ 1 Mw
9/22/85	1654	9/25/85	1520	70.44	9820.32		
9/29/85	1728	10/1/85	2307	53.65	9873.97		
10/2/85	0113	10/4/85	1300	59.78	9933.75		
10/6/85	1652	10/10/85	1312	92.33	10026.08		
10/10/85	1336	10/10/85	1700	3.40	10029.44		
10/10/85	2012	10/11/85	1010	13.96	10043.44		
10/13/85	1708	10/18/85	0800	110.87	10154.31		
		rotated	180°				
10/20/85	1700	10/25/85	0433	112.55	10266.86		
10/27/85	1717	11/1/85	0900	111.72	10378.58		
11/3/85	1655	11/7/85	1313	92.30	10470.88		
11/7/85	1335	11/8/85	1100	21.42	10492.30		
11/10/85	1713	11/15/85	0600	108.78	10601.08		
11/15/85	1130	11/15/85	1406	2.60	10603.68		
11/17/85	1715	11/21/85	1620	95.08	10698.76		

EXPOSURE HISTORY

UBR 45 A,B

date in	time in	date out	time out	exposure hours	sigma hours	core position	
11/21/85	1714	11/22/85	0900	15.77	10714.53		
11/24/85	1637	11/25/85	0912	16.58	10731.11		
11/25/85	0912	11/26/85	1739	32.45	10808.49		
11/26/85	1739	11/27/85	2200	28.35	10836.84		
12/1/85	1707	12/3/85	1429	45.36	10882.20		
12/3/85	1429	12/6/85	1000	67.50	10949.70		
12/8/85	1713	12/10/85	1500	45.78	10995.48		
12/10/85	1544	12/12/85	1312	45.47	11040.95		
12/12/85	1354	12/13/85	1100	21.10	11062.05		
12/15/85	1709	12/18/85	1052	65.72	11127.77		
12/18/85	1132	12/20/85	0900	45.47	11173.24		
12/20/85	0900	12/20/85	1207	1.56	11174.80		
	45A	+B OUT	OF REP.		END		T.C.

MEA UBR 46 A

date in	time in	date out	time out	2 MW exposure hours	2 MW sigma hours	core position	
4-8-83	LOADED	46 A				REFLECTOR	
4-10-83	1655	4-11-83	1930	26.58	26.58		
4-11-83	2017	4-15-83	0830	84.22	110.80		
4-17-83	1712	4-18-83	1300	19.80	130.60		
4-18-83	1355	4-19-83	2103	31.13	161.73		
4-19-83	2217	4-20-83	1026	12.12	173.85		
4-20-83	1054	4-22-83	1300	50.10	223.95		
4-24-83	1701	4-26-83	1630	47.48	271.43		
4-26-83	1740	4-28-83	1248	43.13	314.56		
4-28-83	1530	4-29-83	1000	18.50	333.06		
5-1-83	1707	5-2-83	0930	16.38	349.44		
5-2-83	0954	5-6-83	1000	96.10	445.54		
5-8-83	1653	5-13-83	0900	112.12	557.66		
5-15-83	1630	5-18-83	2300	78.5	636.16		
5-22-83	1655	5-26-83	0223	81.47	717.63		
5-26-83	0243	5-27-83	1030	31.78	749.41		
5-31-83	1345	6-3-83	0043	58.97	808.38		
6-3-83	0204	6-3-83	1100	8.93	817.31		
6-5-83	1643	6-10-83	0800	111.28	928.59		
6-12-83	1654	6-16-83	1400	93.1	1021.69		
6-19-83	1718	6-24-83	0900	111.7	1133.39		
6-26-83	1720	7-1-83	1200	116.7	1248.09		

EXPOSURE HISTORY

MEA UBR 46 A

date in	time in	date out	time out	2MW exposure hours	2MW sigma hours	core position	
7-5-83	0054	7-7-83	1634	64.46	1312.55	REFLECTOR	
7-7-83	1726	7-8-83	1045	17.32	1329.87		
7-10-83	1756	7-15-83	1200	114.10	1443.97		
7-17-83	1703	7-20-83	1015	65.20	1509.17		
7-20-83	1100	7-22-83	1200	49.00	1558.17		
7-24-83	1700	7-26-83	1800	49.00	1607.17		
7-26-83	1836	7-27-83	1100	16.40	1623.57		
7-27-83	1202	7-29-83	1200	48.00	1671.57		
7-31-83	1705	8-5-83	0800	110.92	1782.49		
8-5-83	1214	8-5-83	1240	0.43	1782.92		
8-7-83	1714	8-11-83	0800	86.77	1869.69		
8-11-83	0937	8-12-83	1200	26.38	1896.07		
12-9-83	LOADED 46	BACK INTO	REFLECTOR		1897.07		
12-11-83	1900	12-26-83	1000	111.00	2007.07		
12-18-83	1713	12-20-83	0218	33.90	2040.97		
12-20-83	0307	12-23-83	0900	77.88	2118.85		
12-26-83	1623	12-29-83	2330	79.12	2197.97		
1-2-84	1604	1-4-84	2400	55.93	2253.90		
1-5-84	1013	1-5-84	1940	9.45	2263.35		
1-5-84	2043	1-6-84	1300	16.28	2279.63		
1-8-84	1651	1-9-84	1000	17.15	2296.78		
1-9-84	1035	1-13-84	1100	96.83	2393.61		
1-15-84	1653	1-16-84	0000	7.12	2400.73		
1-16-84	0000	1-19-84	1509	87.15	2487.88		

EXPOSURE HISTORY

MEA UBR 46 A

date in	time in	date out	time out	2MW exposure hours	2MW sigma hours	core position	
1-19-84	1600	1-20-84	1030	18.50	2306.38	REFLECTOR	
1-22-84	1641	1-27-84	0800	111.32	2617.70		
1-29-84	1652	1-30-84	1700	24.13	2641.83		
1-30-84	1838	2-3-84	1230	89.86	2731.70		
2-5-84	1655	2-10-84	1200	115.08	2846.78		
2-12-84	1647	2-17-84	1002	113.25	2960.03		
2-20-84	1648	2-23-84	1450	70.03	3030.06		
2-23-84	1544	2-24-84	1030	18.76	3048.83		
2-26-84	1705	2-28-84	0700	37.90	3086.73		
2-29-84	1106	2-29-84	1900	7.90	3094.63		
2-29-84	2002	3-2-84	1500	42.97	3137.60		
3-4-84	1712	3-5-84	1000	16.80	3154.40		
3-5-84	1022	3-6-84	0800	21.63	3176.03		
3-6-84	0826	3-8-84	2200	61.57	3237.6		
3-8-84	2240	3-9-84	1000	11.33	3248.93		
3-11-84	1700	3-16-84	0830	111.5	3360.43		
3-18-84	1700	3-21-84	1518	70.3	3430.73		
3-21-84	1710	3-22-84	1330	20.33	3451.06		
3-22-84	1429	3-23-84	0840	18.183	3469.243		
7-22-84	1654	7-27-84	1200	115.10	3584.343		
7-29-84	1654	8-3-84	0900	111.90	3696.243		
8-5-84	1739	8-9-84	1900	97.35	3793.59		
8-9-84	2053	8-10-84	0815	11.37	3804.96		

EXPOSURE HISTORY

MEA UBR 46 A

date in	time in	date out	time out	2MW exposure hours	2MW sigma hours	core position	
8-10-84	1049	8-10-84	1219	1.50	3806.46	REFLECTOR	
8-12-84	1654	8-12-84	2000	3.10	3809.56		
8-12-84	UBR 46 A	OUT -					
1-31-85	UBR 46 A	RETURNED TO FLUX			3809.56		
1-31-85	1520	2-1-85	1300	21.66	3831.22		
2-3-85	1721	2-8-85	1300	115.65	3946.87		
2-8-85	UBR 46 A	OUT					
2-12-85	UBR 46 A	IN					
2-12-85	0852	2-15-85	1530	78.63	4025.50		
2-17-85	1802	2-17-85	2200	4.00	4029.50		
2-17-85	UBR 46 A	OUT					
2-27-85	UBR 46 A	IN					
2-27-85	0923	2-27-85	1105	1.70	4031.20		
2-27-85	1356	2-27-85	1717	3.35	4034.55		
2-27-85	1758	2-28-85	1100	17.03	4051.58		
2-28-85	1215	3-1-85	1010	21.61	4073.19		
3-3-85	172[illegible]	3-8-85	0900	111.58	4184.77		
3-8-85	1110	3-8-85	1125	0.25	4185.02		
3-8-85	1237	3-8-85	1509	2.53	4187.55		
3-10-85	1720	3-15-85	0800	110.66	4298.21		
3-17-85	1726	3-18-85	0854	15.46	4313.67		
3-18-85	1036	3-18-85	2045	10.15	4323.82		
3-18-85	2200	3-21-85	2025	71.62	4395.44		
3-21-85	2137	3-22-85	0600	8.38	4403.82		

EXPOSURE HISTORY

MEA UBR 46 A

date in	time in	date out	time out	2mw exposure hours	2mw sigma hours	core position	
3-22-85	1454	3-22-85	1511	0.28	4404.10	REPLACED	
3-24-85	1721	3-28-85	0457	83.60	4487.70		
3-28-85	0518	3-28-85	1045	5.45	4493.15		
3-28-85	1149	3-29-85	1100	23.18	4516.33		
	UBR 46 A	OUT					
8-1-85	UBR 46 A	IN - ON TOP OF 36 B					
8-1-85	1253	8-2-85	1200	23.12	4539.45		
8-4-85	1742	8-9-85	0800	110.30	4649.75		
8-11-85	1651	8-11-85	2020	3.48	4653.23		
8-11-85	2048	8-16-85	0930	108.70	4761.93		
8-18-85	1658	8-23-85	1000	113.03	4874.96		
8-25-85	1716	8-30-85	1300	115.73	4990.69		
9-3-85	0100	9-5-85	0400	51.00	5041.69		
9-5-85	1138	9-6-85	2315	35.62	5077.31		
9-8-85	1734	9-13-85	1200	114.43	5191.74		
9-15-85	1653	9-20-85	0800	111.11	5302.85		
9-20-85	0800	9-20-85	1100	1.50	5304.35 @	1 Kw	
9-22-85	1654	9-25-85	1520	70.44	5374.79		
9-29-85	1728	10-1-85	2307	53.65	5428.44		
10-2-85	0113	10-4-85	1300	59.78	5488.22		
10-6-85	1652	10-10-85	1312	92.33	5580.55		
10-10-85	1336	10-10-85	1700	3.40	5583.95		
10-10-85	2012	10-11-85	1010	13.96	5597.91		
	UBR 46 A	OUT			END		

EXPOSURE HISTORY

UBR 46 B

date in	time in	date out	time out	exposure hours	sigma hours	core position	
4-10-83	1655	4-11-83	1930	26.58	26.58		
4-11-83	2017	4-15-83	0830	84.22	110.80		
4-17-83	1712	4-18-83	1300	19.80	130.60		
4-18-83	1355	4-19-83	2103	31.13	161.73		
4-19-83	2217	4-20-83	1024	12.12	173.85		
4-20-83	1054	4-22-83	1300	50.10	223.95		
4-24-83	1701	4-26-83	1630	47.48	271.43		
4-26-83	1740	4-28-83	1248	43.13	314.56		
4-28-83	1530	4-29-83	1000	18.50	333.06		
5-1-83	1707	5-2-83	0930	16.38	349.44		
5-2-83	0954	5-6-83	1000	96.10	445.54		
5-8-83	1653	5-13-83	0900	112.12	557.66		
5-15-83	1630	5-18-83	2300	78.5	636.16		
5-22-83	1655	5-26-83	0223	81.47	717.63		
5-26-83	0243	5-27-83	1030	31.78	749.41		
5-31-83	1345	6-3-83	0043	58.97	808.38		
6-3-83	0204	6-3-83	1100	8.93	817.31		
6-5-83	1643	6-10-83	0800	111.28	928.59		
6-12-83	1654	6-16-83	1400	93.1	1021.69		
6-19-83	1718	6-24-83	0900	111.7	1133.39		
6-26-83	1720	7-1-83	1200	114.7	1248.09		
7-5-83	0054	7-7-83	1634	64.46	1312.55		
7-7-83	1726	7-8-83	1045	17.32	1329.87		
7-10-83	1756	7-15-83	1200	114.10	1443.97		
7-17-83	1703	7-20-83	1015	65.20	1509.17		
7-20-83	1100	7-22-83	1200	49.00	1558.17		

EXPOSURE HISTORY

UBR 46 B

date in	time in	date out	time out	exposure hours	sigma hours	core position	
7-24-83	1700	7-26-83	1800	49.00	1607.17		
7-26-83	1836	7-27-83	1100	16.40	1623.57		
7-27-83	1202	7-29-83	1200	48.00	1671.57		
7-31-83	1705	8-5-83	0800	110.92	1782.49		
8-5-83	1214	8-5-83	1240	0.43	1782.92		
8-7-83	1714	8-11-83	0800	86.77	1869.69		
8-11-83	0937	8-12-83	1200	26.38	1896.07	out of flux	
12-9-83		CAPSULE LOADED INTO REFLECTOR			1896.07		
12-11-83	1900	12-16-83	1000	111.00	2007.07		
12-18-83	1713	12-20-83	0218	33.90	2040.97		
12-20-83	0307	12-23-83	0900	77.88	2118.85		
12-26-83	1623	12-29-83	2330	79.12	2197.97		
1-2-84	1604	1-4-84	2400	55.93	2253.90		
1-5-84	1013	1-5-84	1940	9.45	2263.35		
1-5-84	2043	1-6-84	1300	16.28	2279.63		
1-8-84	1651	1-9-84	1000	17.15	2296.78		
1-9-84	1035	1-13-84	1100	96.83	2393.61		
1-15-84	1653	1-16-84	0000	7.12	2400.73		
1-16-84	0000	1-19-84	1509	87.15	2487.88		
1-19-84	1600	1-20-84	1030	18.50	2506.38		
1-22-84	1641	1-27-84	0800	111.32	2617.70		
1-29-84	1652	1-30-84	1700	24.13	2641.83		
1-30-84	1838	2-3-84	1230	89.86	2731.70		
2-5-84	1655	2-10-84	1200	115.08	2846.78		
2-12-84	1647	2-17-84	1002	113.25	2960.03		
2-20-84	1648	2-23-84	1450	70.03	3030.06		

EXPOSURE HISTORY

UBR 46 B

date in	time in	date out	time out	exposure hours	sigma hours	core position	
2-23-84	1544	2-24-84	1030	18.76	3048.83		
2-26-84	1705	2-28-84	0700	37.90	3086.73		
2-29-84	1106	2-29-84	1900	7.90	3094.63		
2-29-84	2002	3-2-84	1500	42.97	3137.60		
3-4-84	1712	3-5-84	1000	16.80	3154.40		
3-5-84	1022	3-6-84	0800	21.63	3176.03		
3-6-84	0826	3-8-84	2200	61.57	3237.6		
3-8-84	2240	3-9-84	1000	11.33	3248.93		
3-11-84	1700	3-16-84	0830	111.5	3360.43		
3-18-84	1700	3-21-84	1518	70.3	3430.73		
3-21-84	1710	3-22-84	1330	20.33	3451.06		
3-22-84	1429	3-23-84	0840	18.183	3469.243		
7-22-84	1654	7-27-84	1200	115.10	3584.343		
7-29-84	1654	8-3-84	0900	111.90	3696.243		
8-5-84	1739	8-9-84	1900	97.35	3793.59		
8-9-84	2053	8-10-84	0815	11.37	3804.96		
8-10-84	1049	8-10-84	1219	1.50	3806.46		
8-12-84	1654	8-12-84	2000	3.10	3809.56		
	CAPSULE	REMOVED					
1-31-85	CAPSULE	RETURNED TO	FLUX				
1-31-85	1520	2-1-85	1300	21.66	3831.22		
2-3-85	1721	2-8-85	1300	115.65	3946.87		
2-12-85	0852	2-15-85	1530	78.63	4025.50		
2-17-85	1802	2-17-85	2200	4.00	4029.50		
2-27-85	0923	2-27-85	1105	1.70	4031.20		
2-27-85	1356	2-27-85	1717	3.35	4034.55		

EXPOSURE HISTORY

UBR 46 B

date in	time in	date out	time out	exposure hours	sigma hours	core position	
2-27-85	1758	2-28-85	1100	17.03	4051.58		
2-28-85	1215	3-1-85	1010	21.61	4073.19		
3-3-85	1725	3-8-85	0900	111.58	4184.77		
3-8-85	1110	3-8-85	1125	0.25	4185.02		
3-8-85	1237	3-8-85	1509	2.53	4187.55		
3-10-85	1720	3-15-85	0800	110.66	4298.21		
3-17-85	1726	3-18-85	0854	15.46	4313.67		
3-18-85	1036	3-18-85	2045	10.15	4323.82		
3-18-85	2200	3-21-85	2025	71.62	4395.44		
3-21-85	2137	3-22-85	0600	8.38	4403.82		
3-22-85	1454	3-22-85	1511	0.28	4404.10		
3-24-85	1721	3-28-85	0457	83.60	4487.70		
3-28-85	0518	3-28-85	1045	5.45	4493.15		
3-28-85	1149	3-29-85	1100	23.18	4516.33		
11-25-85	0912	11-26-85	1739	32.45	4548.78		
12-3-85	1429	12-6-85	1000	67.50	4616.28		
12-8-85	1713	12-10-85	1500	45.78	4662.06		
12-10-85	1544	12-12-85	1312	45.47	4707.53		
12-12-85	1354	12-13-85	1100	21.10	4728.63		
12-15-85	1709	12-18-85	1052	65.72	4794.35		
12-18-85	1132	12-20-85	0900	45.47	4839.82		
12-20-85	0900	12-20-85	1207	1.56	4841.38		
12-22-85	1716	12-24-85	1130	42.20	4883.58		
12-26-85	0833	12-27-85	1200	27.45	4911.03		
12-27-85	1200	12-27-85	1508	1.57	4912.60		

EXPOSURE HISTORY

UBR 46 B

date in	time in	date out	time out	exposure hours	sigma hours	core position	
12-29-85	1709	12-31-85	1500	45.85	4958.45		
1-5-86	1710	1-10-86	1400	116.83	5075.28		
1-12-86	1651	1-13-86	0900	16.15	5091.43		
1-19-86	1700	1-24-86	1000	113.00	5204.43		
1-26-86	1700	1-28-86	0800	39.00	5243.43		
1-28-86	0928	1-31-86	1000	72.53	5315.96		
2-2-86	1648	2-7-86	1200	115.20	5431.16		
2-9-86	1708	2-11-86	0809	39.02	5470.18		
2-11-86	0840	2-14-86	0900	72.33	5542.51		
2-17-86	1649	2-21-86	0900	88.18	5630.69		
		CAPSULE	DISCHARGED				

EXPOSURE HISTORY

MEA UBR 65 A,B

DATE IN	TIME IN	DATE OUT	TIME OUT	EXPOSURE HOURS	SIGMA HOURS	CORE POSITION	NOTES
1-31-86	65 A & B into B - 4					B-4	6 3/8"
2-2-86	1648	2-7-86	1200	115.20	115.20		Spacer
2-9-86	1708	2-1-86	0809	39.02	154.22		
	65 A & B OUT OF CORE						

EXPOSURE HISTORY: MEA 75 A & B

DATE IN	TIME IN	DATE OUT	TIME OUT	EXPOSURE HOURS	SIGMA HOURS	CORE POSITION	NOTES
7-25-86	75 A & B	into C-2				C-2	
7-27-86	1730	8-1-86	1200	114.5	114.5		
8-3-86	1710	8-5-86	1400	44.83	159.33		
	ROTATED	180°					
8-5-86	1435	8-8-86	1000	67.42	226.75		
8-10-86	1654	8-11-86	2226	29.53	256.28		
8-15-86	1550	8-15-86	2312	7.37	263.65		
8-17-86	1656	8-19-86	1330	44.57	308.22		
	END OF EXPOSURE						

EXPOSURE HISTORY: UBR76A, B

DATE IN	TIME IN	DATE OUT	TIME OUT	EXPOSURE HOURS	SIGMA HOURS	CORE POSITION	NOTES
7/23/86	76A, B INTO B-4						
						B-4	
7/27/86	1730	8/1/86	1200	114.5	114.5		
8/3/86	1710	8/5/86	1400	44.83	159.33		
8/5/86	1435	8/8/86	1000	67.42	226.75		
8/10/86	1654	8/11/86	2226	29.53	256.28		
8/15/86	1550	8/15/86	2312	7.37	263.65		
8/17/86	1656	8/19/86	1330	44.57	308.22		
		180° ROTATION					
8/19/86	1516	8/22/86	0800	64.73	372.95		
8/24/86	1707	8/28/86	2300	101.88	474.83		
9/2/86	0115	9/2/86	1102	9.78	484.61		
9/2/86	1121	9/5/86	0700	67.65	552.26		
9/7/86	1658	9/10/86	0845	63.78	616.04		
		END OF EXPERIMENT					

EXPOSURE HISTORY

UBR 77 A,B

DATE IN	TIME IN	DATE OUT	TIME OUT	EXPOSURE HOURS	SIGMA HOURS	CORE POSITION	NOTES
5-31-87	1702	6-3-87	1400	68.97	68.97	B-4	Rotated 180°
6-3-87	1506	6-5-87	0907	42.02	110.99		
6-7-87	1729	6-8-87	2130	28.02	139.01		Discharged

APPENDIX C

Tabulations of Charpy-V Notch Ductility Test Results

Charpy-V Data from Unirradiated Condition Tests

A 302-B Plate 23F (Unirradiated Condition; L-T Orientation)

No.	Specimen Number	Layer	Capsule	Test Temp. (°C)	Test Temp. (°F)	Energy (J)	Energy (ft-lb)	Lat. Exp. (mm)	Lat. Exp. (mils)	Shear (%)
1	145	1	---	-29	-20	29.8	22.0	0.56	22	<100
2	38	1	---	-23	-10	32.5	24.0	0.71	28	<100
3	174	1	---	-7	20	55.6	41.0	0.89	35	<100
4	1	1	---	-1	30	51.5	38.0	0.89	35	<100
5	191	1	---	16	60	81.3	60.0	1.32	52	<100
6	2	1	---	38	100	113.9	84.0	1.83	72	<100
7	173	1	---	93	200	127.4	94.0	1.88	74	100
8	37	1	---	204	400	124.7	92.0	1.96	77	100
9	192	1	---	204	400	124.7	92.0	1.83	72	100

(ND) - Not Determined
(NT) - Not Tested

A 533-B Plate 23G (Unirradiated Condition; T-L Orientation)*

No.	Specimen Number	Layer	Capsule	Test Temp. (°C)	Test Temp. (°F)	Energy (J)	Energy (ft-lb)	Lat. Exp. (mm)	Lat. Exp. (mils)	Shear (%)
1	TA-6	1a	---	-62	-80	10.8	8.0	0.13	5	<100
2	TA-15	1	---	-62	-80	6.8	5.0	0.10	4	<100
3	TA-5	1	---	-40	-40	38.0	28.0	0.53	21	<100
4	TA-19	1	---	-40	-40	33.9	25.0	0.64	25	<100
5	TA-4	1	---	-18	0	66.4	49.0	0.99	39	<100
6	TA-17	1	---	-18	0	48.8	36.0	0.76	30	<100
7	TA-7	1	---	-1	30	92.2	68.0	1.37	54	<100
8	TA-14	1	---	-1	30	75.9	56.0	1.14	45	<100
9	TA-3	1	---	27	80	132.9	98.0	1.65	65	<100
10	TA-18	1	---	27	80	141.0	104.0	1.75	69	<100
11	TA-61	1	---	71	163	131.5	97.0	1.83	72	100
12	TA-80	1	---	71	160	158.6	117.0	1.91	75	100
13	TA-1	1	---	93	200	143.7	106.0	1.78	70	100
14	TA-16	1	---	93	200	158.6	117.0	1.85	73	100
15	TA-8	1	---	121	250	150.5	111.0	1.91	75	100
16	TA-2	1	---	160	320	127.4	94.0	1.75	69	100
17	TA-13	1	---	160	320	153.2	113.0	1.88	74	100
18	TA-20	1	---	160	320	166.8	123.0	2.01	79	100
19	TA4-8	3	---	-40	-40	14.9	11.0	0.28	11	<100
20	TA4-1	2b	---	-18	0	61.0	45.0	0.94	37	<100
21	TA4-5	2	---	27	80	109.8	81.0	1.55	61	<100
22	TA4-4	3c	---	204	400	134.2	99.0	1.63	64	100
23	TA4-9	2	---	204	400	151.9	112.0	1.85	73	100

* - Also MEA Code TA.
a - One layer above 1/4 T plane.
b - One layer above 3/4 T plane.
c - One layer below 3/4 T plane.

Code W8A (Unirradiated Condition)

No.	Specimen Number	Layer	Capsule	Test Temp. (°C)	Test Temp. (°F)	Energy (J)	Energy (ft-lb)	Lat. Exp. (mm)	Lat. Exp. (mils)	Shear (%)
1	4	4	---	-40	-40	19.0	14.0	0.33	13	5
2	11	11	---	-40	-40	24.4	18.0	0.43	17	5
3	30	6	---	-23	-10	35.3	26.0	(ND)	(ND)	----
4	9A	9	---	-23	-10	43.4	32.0	(ND)	(ND)	----
5	5	5	---	-18	0	48.8	36.0	0.94	37	----
6	12	12	---	-18	0	43.4	32.0	0.79	31	20
7	18	6	---	4	40	52.9	39.0	(ND)	(ND)	----
8	3	3	---	27	80	56.9	42.0	1.09	43	45
9	10	10	---	27	80	40.7	30.0	0.74	29	35
10	6	6	---	49	120	70.5	52.0	1.27	50	80
11	1	1	---	49	120	63.7	47.0	1.19	47	60
12	2	2	---	93	200	81.3	60.0	1.55	61	100
13	9	9	---	93	200	75.9	56.0	1.47	58	100
14	15	3	---	204	400	78.6	58.0	1.68	66	100
15	22	10	---	204	400	78.6	58.0	1.52	60	100

Code W9A (Unirradiated Condition)

No.	Specimen Number	Layer	Capsule	Test Temp. (°C)	Test Temp. (°F)	Energy (J)	Energy (ft-lb)	Lat. Exp. (mm)	Lat. Exp. (mils)	Shear (%)
1	5	5	---	-62	-80	39.3	29.0	0.71	28	20
2	15	3	---	-62	-80	38.0	28.0	0.64	25	10
3	3	3	---	-46	-50	71.9	53.0	1.09	43	50
4	19	7	---	-46	-50	67.8	50.0	1.07	42	20
5	18	7	---	24	75	130.2	96.0	1.85	73	95
6	27	3	---	24	75	149.1	110.0	1.96	77	99
7	6	6	---	71	160	154.6	114.0	2.18	86	100
8	16	4	---	204	400	169.5	125.0	2.21	87	100
9	29	5	---	204	400	169.5	125.0	2.21	87	100
10	35	11	---	204	400	168.1	124.0	2.16	85	100

Charpy-V Data from Irradiation Assembly UBR-38

(Reflector Region Irradiation)

A 302-B (UBR-38, Capsule A, As-Irradiated) [IP-1]

No.	Specimen Number	Layer	Capsule	Test Temp. (°C)	Test Temp. (°F)	Energy (J)	Energy (ft-lb)	Lat. Exp. (mm)	Lat. Exp. (mils)	Shear (%)
1	169		38-A	4	40	20.3	15.0	0.46	18	<100
2	168		38-A	21	70	19.0	14.0	0.36	14	<100
3	58		38-A	29	85	36.6	27.0	0.69	27	<100
4	106		38-A	32	90	38.0	28.0	0.64	25	<100
5	155		38-A	38	100	36.6	27.0	0.71	28	<100
6	130		38-A	46	115	62.4	46.0	0.91	36	<100
7	108		38-A	54	130	63.7	47.0	1.02	40	<100
8	109		38-A	60	140	63.7	47.0	1.19	47	<100
9	11		38-A	66	150	58.3	43.0	1.02	40	<100
10	171		38-A	74	165	120.7	89.0	1.55	61	100
11	133		38-A	82	180	97.6	72.0	1.55	61	<100
12	12		38-A	93	200	112.5	83.0	1.68	66	<100
13	36		38-A	138	280	118.0	87.0	2.01	79	<100
14	170		38-A	182	360	111.2	82.0	1.98	78	100
15	131		38-A	204	400	115.2	85.0	1.65	65	100

(ND) - Not Determined
(NT) - Not Tested

A 533-B Plate 23 G (UBR-38, Capsule A, As-Irradiated) [IP-1]

No.	Specimen Number	Capsule	Test Temp. (°C)	Test Temp. (°F)	Energy (J)	Energy (ft-lb)	Lat. Exp. (mm)	Lat. Exp. (mils)	Shear (%)
1	195	38-A	-18	0	10.8	8.0	(ND)	(ND)	<100
2	196	38-A	4	40	32.5	24.0	0.46	18	<100
3	182	38-A	10	50	27.1	20.0	0.41	16	<100
4	183	38-A	16	60	35.3	26.0	0.61	24	<100
5	202	38-A	21	70	32.5	24.0	0.61	24	<100
6	198	38-A	24	75	54.2	40.0	0.76	30	<100
7	181	38-A	32	90	56.9	42.0	0.86	34	<100
8	186	38-A	38	100	50.2	37.0	0.81	32	100
9	206	38-A	52	125	77.3	57.0	1.12	44	<100
10	188	38-A	66	150	81.3	60.0	1.12	44	<100
11	189	38-A	71	160	69.1	51.0	1.04	41	<100
12	200	38-A	88	190	97.8	72.1	1.75	69	<100
13	192	38-A	149	300	142.4	105.0	1.60	63	100
14	204	38-A	177	350	135.6	100.0	2.36	93	100
15	194	38-A	204	400	139.6	103.0	2.03	80	100

(ND) - Not Determined
(NT) - Not Tested

Charpy-V Data from Irradiation Assembly UBR-44

(Core-Edge Irradiation)

A 302-B (UBR-44, Capsule A, As-Irradiated) [CE-1]

No.	Specimen Number	Layer	Capsule	Test Temp. (°C)	Test Temp. (°F)	Energy (J)	Energy (ft-lb)	Lat. Exp. (mm)	Lat. Exp. (mils)	Shear (%)
1	*149		44-A	(NT)	(NT)					
2	* 13		44-A	(NT)	(NT)					
3	195		44-A	-7	20	5.4	4.0	0.03	1	<100
4	42		44-A	4	40	13.6	10.0	0.23	9	<100
5	141		44-A	21	70	31.2	23.0	0.66	26	<100
6	100		44-A	27	80	21.7	16.0	0.43	17	<100
7	93		44-A	43	110	40.7	30.0	0.69	27	<100
8	54		44-A	49	120	50.2	37.0	0.81	32	<100
9	135		44-A	66	150	56.9	42.0	1.04	41	<100
10	3		44-A	88	190	75.9	56.0	1.24	49	<100
11	181		44-A	93	200	99.0	73.0	1.50	59	<100
12	39		44-A	121	250	105.8	78.0	1.70	67	<100
13	*184		44-A			(NT)	(NT)	(ND)	(ND)	<100
14	105		44-A	182	360	100.3	74.0	1.96	77	100
15	90		44-A	204	400	113.9	84.0	2.21	87	100

* Reserved for postirradiation anneal.
(ND) - Not Determined
(NT) - Not Tested

Weld W8A (UBR-44, Capsule A, As-Irradiated) [CE-1]

No.	Specimen Number	Layer	Capsule	Test Temp. (°C)	Test Temp. (°F)	Energy (J)	Energy (ft-lb)	Lat. Exp. (mm)	Lat. Exp. (mils)	Shear (%)
1	*279	3	44-A	(NT)	(NT)					
2	*290	2	44-A	(NT)	(NT)					
3	*307	7	44-A	(NT)	(NT)					
4	*274	10	44-A	(NT)	(NT)					
5	*301	1	44-A	(NT)	(NT)					
6	265	1	44-A	49	120	10.8	8.0	0.15	6	<100
7	317	5	44-A	66	150	19.0	14.0	0.30	12	<100
8	327	3	44-A	88	190	24.4	18.0	0.43	17	<100
9	299	11	44-A	88	190	32.5	24.0	0.51	20	<100
10	271	7	44-A	104	220	48.8	36.0	0.86	34	<100
11	268	4	44-A	104	220	46.1	34.0	0.71	28	<100
12	282	6	44-A	110	230	35.3	26.0	0.58	23	<100
13	285	9	44-A	121	250	52.9	39.0	0.94	37	<100
14	296	8	44-A	204	400	54.4	40.1	1.02	40	100
15	293	5	44-A	204	400	50.3	37.1	0.79	31	98

* Reserved for postirradiation anneal.
(ND) - Not Determined
(NT) - Not Tested

Charpy-V Data from Irradiation Assembly UBR-45

(Core-Edge Irradiation)

A 302-B Plate 23 F (UBR-45, Capsule A, As-Irradiated)[CE-3]

No.	Specimen Number	Capsule	Test Temp. (°C)	Test Temp. (°F)	Energy (J)	Energy (ft-lb)	Lat. Exp. (mm)	Lat. Exp. (mils)	Shear (%)
1	40	45-A	16	60	9.5	7.0	0.18	7	<100
2	185	45-A	21	70	28.5	21.0	0.56	22	<100
3	94	45-A	38	100	24.4	18.0	0.51	20	<100
4	43	45-A	49	120	32.5	24.0	0.58	23	<100
5	150	45-A	60	140	33.9	25.0	0.74	29	<100
6	4	45-A	60	140	38.0	28.0	0.74	29	<100
7	14	45-A	71	160	58.3	43.0	0.99	39	<100
8	182	45-A	77	170	84.1	62.0	1.40	55	<100
9	48	45-A	82	180	56.9	42.0	0.99	39	<100
10	188	45-A	85	185	92.2	68.0	1.45	57	<100
11	25	45-A	93	200	77.3	57.0	1.30	51	<100
12	196	45-A	121	250	89.5	66.0	1.52	60	<100
13	136	45-A	177	350	101.7	75.0	1.65	65	<100
14	101	45-A	204	400	97.6	72.0	1.63	64	100
15	91	45-A	260	500	97.6	72.0	1.78	70	100

(ND) - Not Determined
(NT) - Not Tested

Weld W8A (UBR-45, Capsule A, As-Irradiated) [CE-3]

No.	Specimen Number	Layer	Capsule	Test Temp. (°C)	Test Temp. (°F)	Energy (J)	Energy (ft-lb)	Lat. Exp. (mm)	Lat. Exp. (mils)	Shear (%)
1	*303	3	45-A	(NT)	(NT)					
2	*269	5	45-A	(NT)	(NT)					
3	*319	7	45-A	(NT)	(NT)					
4	266	2	45-A	71	160	14.9	11.0	0.28	11	<100
5	291	3	45-A	88	190	12.2	9.0	0.23	9	<100
6	297	9	45-A	93	200	32.5	24.0	0.51	20	<100
7	277	1	45-A	104	220	23.0	17.0	0.38	15	<100
8	280	4	45-A	107	225	28.5	21.0	0.61	24	<100
9	12	8	45-A	121	250	43.4	32.0	0.79	31	<100
10	286	10	45-A	121	250	34.0	25.1	0.53	21	<100
11	329	5	45-A	138	280	40.7	30.0	0.66	26	<100
12	275	11	45-A	160	320	46.1	34.0	0.84	33	<100
13	283	7	45-A	204	400	40.7	30.0	0.79	31	<100
14	294	6	45-A	204	400	43.4	32.0	0.69	27	100
15	313	1	45-A	288	550	46.1	34.0	0.87	34	100

* Reserved for postirradiation anneal.
(ND) - Not Determined
(NT) - Not Tested

Charpy-V Data from Irradiation Assembly UBR-46

(Core-Edge Irradiation)

A 302-B Plate 23 F (UBR-46, Capsule A, As-Irradiated) [CE-2]

No.	Specimen Number	Capsule	Test Temp. (°C)	Test Temp. (°F)	Energy (J)	Energy (ft-lb)	Lat. Exp. (mm)	Lat. Exp. (mils)	Shear (%)
1	96	46-A	10	50	8.1	6.0	0.20	8	<100
2	95	46-A	21	70	20.3	15.0	0.38	15	<100
3	140	46-A	27	80	24.4	18.0	0.41	16	<100
4	104	46-A	32	90	38.0	28.0	0.64	25	<100
5	151	46-A	38	100	32.5	24.0	0.69	27	<100
6	41	46-A	54	130	46.1	34.0	0.76	30	<100
7	142	46-A	60	140	46.1	34.0	0.79	31	<100
8	186	46-A	71	160	69.1	51.0	1.09	43	<100
9	26	46-A	82	180	56.9	42.0	0.99	39	<100
10	92	46-A	88	190	82.7	61.0	1.37	54	<100
11	5	46-A	104	220	105.8	78.0	1.63	64	97
12	197	46-A	138	280	104.4	77.0	1.55	61	97
13	102	46-A	177	350	97.6	72.0	1.57	62	98
14	44	46-A	260	500	111.2	82.0	1.55	61	100
15	183	46-A	260	500	105.8	78.0	1.80	71	98

(ND) - Not Determined
(NT) - Not Tested

Weld W3A (UBR-46, Capsule A, As-Irradiated) [CE-2]

No.	Specimen Number	Layer	Capsule	Test Temp. (°C)	Test Temp. (°F)	Energy (J)	Energy (ft-lb)	Lat. Exp. (mm)	Lat. Exp. (mils)	Shear (%)
1	*315	3	46-A			(NT)	(NT)			
2	*331	7	46-A			(NT)	(NT)			
3	305	5	46-A	43	110	6.8	5.0	0.15	6	<100
4	298	10	46-A	60	140	19.0	14.0	0.38	15	<100
5	278	2	46-A	82	180	24.4	18.0	0.48	19	<100
6	289	1	46-A	88	190	28.5	21.0	0.46	18	<100
7	281	5	46-A	93	200	24.4	18.0	0.38	15	<100
8	267	3	46-A	104	220	33.9	25.0	0.58	23	<100
9	287	11	46-A	104	220	43.4	32.0	0.69	27	<100
10	325	1	46-A	110	230	38.0	28.0	0.64	25	<100
11	284	8	46-A	121	250	48.8	36.0	0.99	39	98
12	273	9	46-A	121	250	48.8	36.0	0.97	38	98
13	292	4	46-A	204	400	50.2	37.0	0.89	35	100
14	270	6	46-A	204	400	48.8	36.0	0.94	37	100
15	295	7	46-A	288	550	44.7	33.0	1.42	56	100

* Reserved for postirradiation anneal.
(ND) - Not Determined
(NT) - Not Tested

Charpy-V Data from Irradiation Assembly UBR-65

(In-Core Irradiation)

A 302-B Plate 23 F (UBR-65, Capsule B, As-Irradiated) [IC-1]

No.	Specimen Number	Capsule	Test Temp. (°C)	Test Temp. (°F)	Energy (J)	Energy (ft-lb)	Lat. Exp. (mm)	Lat. Exp. (mils)	Shear (%)
1	121	65-B	-4	25	20.3	15.0	0.43	17	<100
2	152	65-B	4	40	16.3	12.0	0.36	14	<100
3	68	65-B	16	60	32.5	24.0	0.71	28	<100
4	72	65-B	27	80	28.5	21.0	0.56	22	<100
5	21	65-B	27	80	43.4	32.0	0.84	33	<100
6	67	65-B	32	90	39.3	29.0	0.86	34	<100
7	78	65-B	38	100	56.9	42.0	1.02	40	<100
8	15	65-B	43	110	48.8	36.0	0.94	37	<100
9	198	65-B	49	120	61.0	45.0	1.07	42	<100
10	164	65-B	49	120	71.9	53.0	1.17	46	<100
11	9	65-B	71	160	89.5	66.0	1.42	56	<100
12	65	65-B	71	160	97.6	72.0	1.83	72	<100
13	65	65-B	71	160	93.6	69.0	1.50	59	<100
14	124	65-B	138	280	108.5	80.0	1.65	65	100
15	114	65-B	177	350	100.3	74.0	1.70	67	100
16	172	65-B	204	400	115.2	85.0	1.91	75	100
17	27	65-B	260	500	109.8	81.0	2.01	79	100

(ND) - Not Determined
(NT) - Not Tested

Weld W8A (UBR-65, Capsule B, As-Irradiated) [IC-1]

No.	Specimen Number	Layer	Capsule	Test Temp. (°C)	Test Temp. (°F)	Energy (J)	Energy (ft-lb)	Lat. Exp. (mm)	Lat. Exp. (mils)	Shear (%)
1	*376	4	65-B	(NT)	(NT)					
2	363	3	65-B	16	60	10.8	8.0	0.25	10	<100
3	340	4	65-B	27	80	8.1	6.0	0.36	14	<100
4	380	8	65-B	41	105	38.0	28.0	0.71	28	<100
5	369	9	65-B	49	120	38.0	28.0	0.71	28	<100
6	309	9	65-B	60	140	38.0	28.0	0.69	27	<100
7	311	11	65-B	66	150	29.8	22.0	0.53	21	<100
8	374	2	65-B	71	160	33.9	25.0	0.66	26	<100
9	355	7	65-B	82	180	48.8	36.0	1.02	40	<100
10	352	4	65-B	93	200	42.0	31.0	0.79	31	<100
11	365	5	65-B	93	200	40.7	30.0	0.86	34	<100
12	372	12	65-B	104	220	55.6	41.0	1.04	41	<100
13	33	9	65-B	121	250	55.6	41.0	1.04	41	99
14	358	10	65-B	121	250	56.9	42.0	1.17	46	97
15	349	1	65-B	204	400	59.7	44.0	1.12	44	100
16	383	11	65-B	204	400	61.0	45.0	1.12	44	98
17	240	12	65-B	288	550	61.0	45.0	1.32	52	100

* Reserved for postirradiation anneal
(ND) - Not Determined
(NT) - Not Tested

Charpy-V Data from Irradiation Assembly UBR-75

(In-Core Irradiation)

A 302-B Plate 23 F (UBR-75, Capsule B, As-Irradiated) [IC-2]

No.	Specimen Number	Capsule	Test Temp. (°C)	Test Temp. (°F)	Energy (J)	Energy (ft-lb)	Lat. Exp. (mm)	Lat. Exp. (mils)	Shear (%)
1	74	75-B	-1	30	13.6	10.0	0.23	9	<100
2	162	75-B	4	40	19.0	14.0	0.38	15	<100
3	22	75-B	27	80	24.4	18.0	0.46	18	<100
4	127	75-B	32	90	35.3	26.0	0.69	27	<100
5	120	75-B	49	120	43.4	32.0	0.79	31	<100
6	110	75-B	49	120	40.7	30.0	0.76	30	<100
7	69	75-B	63	145	66.4	49.0	1.17	46	<100
8	66	75-B	71	160	58.3	43.0	1.02	40	<100
9	16	75-B	79	175	90.8	67.0	1.40	55	<100
10	28	75-B	82	180	96.3	71.0	1.63	64	<100
11	24	75-B	93	200	85.4	63.0	1.57	62	<100
12	115	75-B	121	250	105.8	78.0	1.78	70	100
13	199	75-B	138	280	100.3	74.0	1.63	64	100
14	90	75-B	204	400	115.2	85.0	2.26	89	<100
15	144	75-B	204	400	103.0	76.0	1.85	73	100
16	122	75-B	288	550	105.8	78.0	1.75	69	100
17	92	75-B	288	550	118.0	87.0	1.63	64	100

(ND) - Not Determined
(NT) - Not Tested

Weld W8A (UBR-75, Capsule B, As-Irradiated) [IC-2]

No.	Specimen Number	Layer	Capsule	Test Temp. (°C)	Test Temp. (°F)	Energy (J)	Energy (ft-lb)	Lat. Exp. (mm)	Lat. Exp. (mils)	Shear (%)
1	341	5	75-B	24	75	8.1	6.0	0.10	4	<100
2	381	9	75-B	32	90	25.8	19.0	0.49	19	<100
3	375	3	75-B	49	120	21.7	16.0	0.41	16	<100
4	594	10	75-B	60	140	29.8	22.0	0.53	21	<100
5	359	11	75-B	71	160	29.8	22.0	0.53	21	<100
6	377	5	75-B	82	180	27.1	20.0	0.53	21	<100
7	590	2	75-B	82	180	32.5	24.0	(ND)	(ND)	<100
8	367	7	75-B	88	190	44.7	33.0	0.84	33	<100
9	370	10	75-B	99	210	40.7	30.0	0.74	29	<100
10	350	2	75-B	104	220	46.1	34.0	0.76	30	<100
11	366	6	75-B	110	230	40.7	30.0	0.71	28	<100
12	361	1	75-B	127	260	44.7	33.0	0.91	36	<100
13	214	10	75-B	138	280	55.6	41.0	0.91	36	<100
14	321	4	75-B	149	300	52.9	39.0	0.91	36	100
15	356	8	75-B	204	400	56.9	42.0	1.07	42	100
16	353	5	75-B	204	400	54.2	40.0	1.02	40	100
17	384	12	75-B	288	550	52.9	39.0	1.12	44	100

(ND) - Not Determined
(NT) - Not Tested

Charpy-V Data from Irradiation Assembly UBR-76

(In-Core Irradiation)

A 302-B Plate 23F (UBR-76, Capsule B, As-Irradiated) [IC-3]

No.	Specimen Number	Capsule	Test Temp. (°C)	Test Temp. (°F)	Energy (J)	Energy (ft-lb)	Lat. Exp. (mm)	Lat. Exp. (mils)	Shear (%)
1	29	76-B	4	40	6.8	5.0	0.15	6	<100
2	77	76-B	4	40	6.8	5.0	0.15	6	<100
3	163	76-B	27	80	23.0	17.0	0.46	18	<100
4	143	76-B	32	90	19.0	14.0	0.38	15	<100
5	128	76-B	49	120	33.9	25.0	0.64	25	<100
6	23	76-B	49	120	35.3	26.0	0.71	28	<100
7	67	76-B	57	135	42.0	31.0	0.74	29	<100
8	70	76-B	60	143	52.9	39.0	0.94	[illegible]	<100
9	129	76-B	74	165	55.6	41.0	0.94	[illegible]	<100
10	111	76-B	82	180	73.2	54.0	1.27	50	<100
11	91	76-B	88	190	70.5	52.0	1.37	54	<100
12	17	76-B	104	220	105.8	78.0	1.70	67	<100
13	81	76-B	121	250	110.0	81.1	1.63	64	100
14	80	76-B	149	300	105.8	78.0	1.83	72	100
15	77	76-B	204	400	96.3	71.0	1.78	70	100
16	200	76-B	288	550	94.9	70.0	2.03	80	100
17	88	76-B	288	550	93.6	69.0	2.13	84	100

(ND) - Not Determined
(NT) - Not Tested

Weld W8A (UBR-76, Capsule B, As-Irradiated) [IC-3]

No.	Specimen Number	Layer	Capsule	Test Temp. (°C)	Test Temp. (°F)	Energy (J)	Energy (ft-lb)	Lat. Exp. (mm)	Lat. Exp. (mils)	Shear (%)
1	*114	6	76-B	(NT)	(NT)					
2	*360	12	76-B	(NT)	(NT)					
3	354	6	76-B	49	120	13.6	10.0	(ND)	(ND)	<100
4	357	9	76-B	60	140	28.5	21.0	0.54	21	<100
5	351	3	76-B	66	150	20.3	15.0	0.36	14	<100
6	85	1	76-B	68	155	24.4	18.0	0.43	17	<100
7	589	1	76-B	82	180	27.1	20.0	0.61	24	<100
8	362	2	76-B	98	208	27.1	20.0	0.74	29	<100
9	378	6	76-B	99	210	35.3	26.0	0.58	23	<100
10	364	4	76-B	110	230	47.5	35.0	0.84	33	<100
11	371	11	76-B	110	230	43.4	32.0	0.79	31	<100
12	382	10	76-B	121	250	40.7	30.0	0.79	31	<100
13	379	7	76-B	127	260	46.1	34.0	0.84	33	100
14	368	8	76-B	149	300	52.9	39.0	0.97	38	<100
15	333	9	76-B	204	400	55.6	41.0	(ND)	(ND)	100
16	592	4	76-B	204	400	48.8	36.0	0.94	37	100
17	335	11	76-B	288	550	51.5	38.0	0.97	38	100

* Reserved for postirradiation anneal.
(ND) - Not Determined
(NT) - Not Tested

Charpy-V Data from Irradiation Assembly UBR-77

(In-Core Irradiation)

A 533-B Plate 23G (UBR-77, Capsule A, As-Irradiated) [IC-4]

No.	Specimen Number	Layer	Capsule	Test Temp. (°C)	Test Temp. (°F)	Energy (J)	Energy (ft-lb)	Lat. Exp. (mm)	Lat. Exp. (mils)	Shear (%)
1	220		77-A	-29	-20	32.5	24.0	0.61	24	<100
2	238		77-A	-7	20	36.6	27.0	0.74	29	<100
3	221		77-A	-1	30	44.7	33.0	0.74	29	<100
4	236		77-A	2	35	9.5	7.0	0.15	6	<100
5	212		77-A	4	40	46.1	34.0	0.74	29	<100
6	227		77-A	21	70	40.7	30.0	0.76	30	<100
7	232		77-A	21	70	51.5	38.0	0.84	33	<100
8	224		77-A	27	80	75.9	56.0	1.27	50	<100
9	214		77-A	38	100	100.3	74.0	1.83	72	<100
10	233		77-A	49	120	105.8	78.0	1.57	62	<100
11	230		77-A	66	150	113.9	84.0	1.75	69	<100
12	228		77-A	149	300	131.5	97.0	1.91	75	100
13	234		77-A	204	400	141.0	104.0	2.26	89	100
14	240		77-A	204	400	126.1	93.0	2.31	91	100

(ND) - Not Determined
(NT) - Not Tested

Weld W9A (UBR-77, Capsule A, As-Irradiated) [IC-4]

No.	Specimen Number	Layer	Capsule	Test Temp. (°C)	Test Temp. (°F)	Energy (J)	Energy (ft-lb)	Lat. Exp. (mm)	Lat. Exp. (mils)	Shear (%)
1	274	10	77-A	-32	-25	24.4	18.0	0.33	13	<100
2	272	8	77-A	(NT)	(NT)					----
3	276	12	77-A	-12	10	29.8	22.0	0.53	21	<100
4	292	4	77-A	-7	20	32.5	24.0	0.56	22	<100
5	167	11	77-A	4	40	48.8	36.0	0.69	27	<100
6	295	7	77-A	10	50	58.3	43.0	0.89	35	<100
7	289	1	77-A	16	60	51.5	38.0	0.84	33	<100
8	339	3	77-A	16	60	36.6	27.0	0.99	39	<100
9	202	10	77-A	27	80	66.4	49.0	1.04	41	<100
10	V3	Vee	77-A	43	110	88.1	65.0	1.35	53	<100
11	317	5	77-A	49	120	85.4	63.0	1.30	51	<100
12	266	2	77-A	66	150	100.3	74.0	1.52	60	<100
13	297	9	77-A	93	200	132.9	98.0	2.24	88	100
14	299	11	77-A	149	300	123.4	91.0	1.83	72	100
15	270	6	77-A	204	400	122.0	90.0	2.01	79	100
16	204	12	77-2	204	400	113.9	84.0	1.78	70	<100

(ND) - Not Determined
(NT) - Not Tested

APPENDIX D

Computer Curve-Fits of Charpy-V Test Results
(Specimen Energy Absorption vs. Temperature)

OVERVIEW

The data curve fitting procedure employed the hyperbolic tangent (Tanh) curve fitting method as given by:

$$C_v = A + B \tanh \frac{T - T_o}{C}$$

Parameters A, B, C and T_o are determined from non-linear regression analysis.

The quality of the fit to each data set generally depends upon the number of specimens tested and the availability of data defining the upper shelf and lower shelf for the data set. For many of the present data sets, both requirements are satisfied and an acceptable curve fit results. In other cases, either few tests were conducted or the data did not adequately define the lower shelf for the data set. For such cases, the lower shelf from a standard Tanh fit gives a lower shelf which is either above 27 J (20 ft-lb) or negative. Since such results are not satisfactory from either engineering or aesthetic standpoints, two modified curve fits can be applied. One (Case A) is illustrated for certain data sets of the plate Code 68B, 5C and 6A materials.

Case A is the result obtained when four fictitious data points with 7 J (5 ft-lb) of energy absorption are added at a temperature that is 28°C (50°F) below the intercept with the abscissa, of a line representing a linearized transition region. The line in this case is an eyeball fit to the data; the choice of a larger temperature shift (up to 56°C or 100°F) was found not to infuence the result appreciably. Case B represents use of a fixed lower shelf of 7 J (5 ft-lb); this lower shelf is attained at a temperature of -∞.

The use of the modified curve fits serve to force the curves to a reasonably low, positive value in the lower shelf region. This device is particularly useful for those cases where data are lacking in the lower shelf region for guiding the computer in its setting of bounding conditions. It should be noted that the American Society for Testing and Materials has not issued a standard method or a standard guide for curve-fitting C_v data for the irradiated condition.

Within this appendix, the curvefit sheet immediately following the data table represents a standard evaluation using the Tanh equation. The second curvefit sheet if present, gives the Case A results. For Case A, the fictitious data points are denoted by "O" on the graph and "*" in the data tabulation on the curvefit sheet. Table D-1 compares the 41-J temperatures indicated by the hand-drawn curves. (See main text.)

Table D-1 Comparison of Charpy-V Transition Temperature Indications From Two Data Curve Fitting Methods

Irradiation Assembly	Material	C_v 41-J Transition Temperature (°C) Hand-Drawn Curve (a)	Computer-Fit Curve (b)	Difference (a-b)
(Unirrad.)	23F	-15	-13.9	-1.1
	23G	-34	-28.9	-5.1
	W8A	-23	-17.0	-6.0
	W9A	-62	-61.3	-0.7
UBR-38	23F	38	38.2	-0.2
	23G	21	20.7	0.3
UBR-44	23F	43	43.1	0.1
	W8A	102	101.3	0.7
UBR-45	23F	63	59.5	3.5
	W8A	127	131.7	-4.7
UBR-46	23F	49	48.7	0.3
	W8A	107	109.3	-2.3
UBR-65	23F	29	31.0	-2.0
	W8A	82	71.3	10.7
UBR-75	23F	46	45.2	0.8
	W8A	96	97.7	-1.7
UBR-76	23F	57	55.4	1.6
	W8A	104	110.1	-6.1
UBR-77	23G	4	11.4	-7.4
	W9A	-1	3.1	-4.1

Computer Curve Fittings of Unirradiated Condition Data

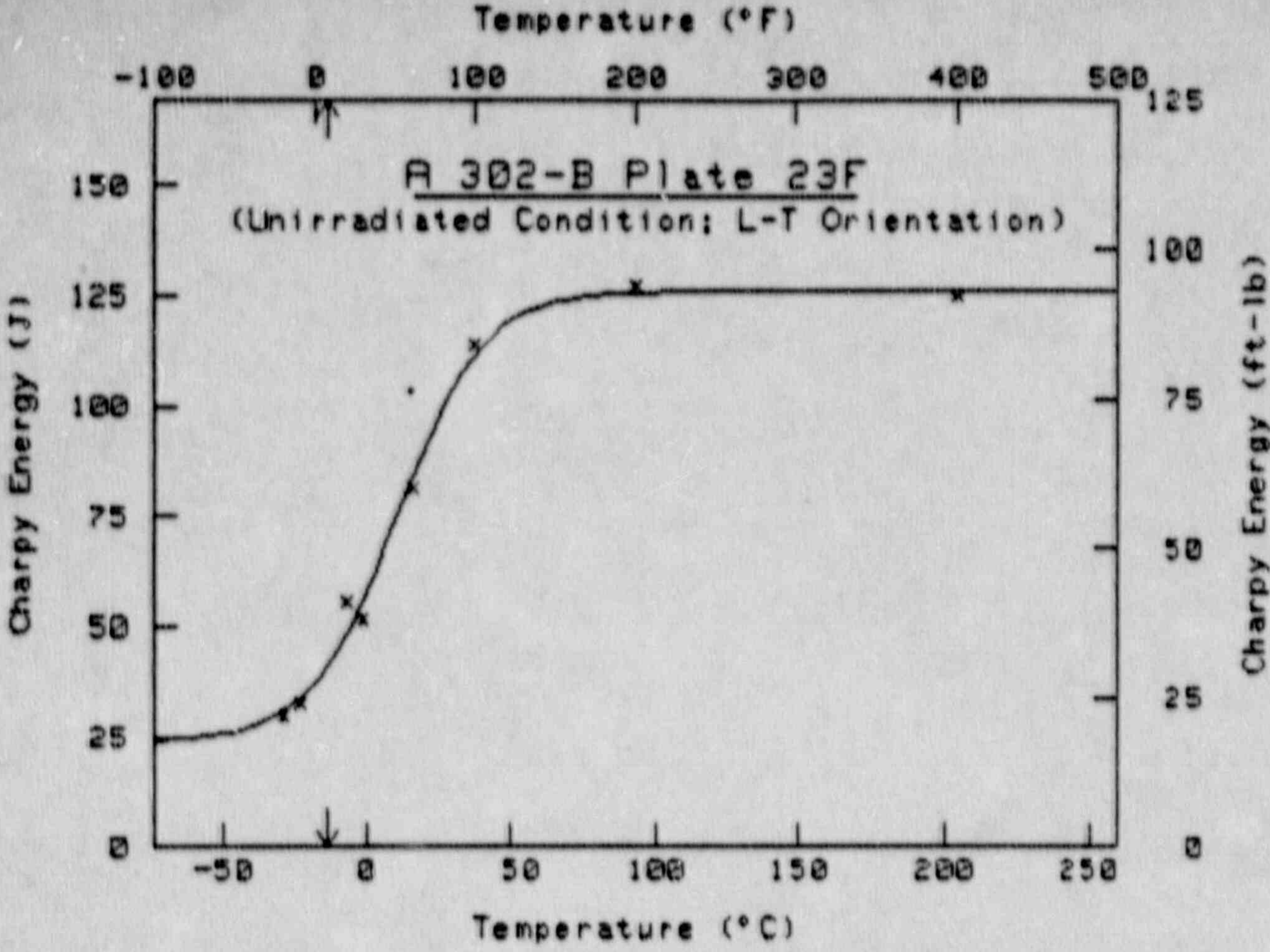

$$Cv = A + B \tanh[(T - To)/C]$$

		English	Metric
A	=	55.33 ft-lb	75.02 J
B	=	37.67 ft-lb	51.08 J
C	=	54.17 °F	30.09 °C
To	=	51.21 °F	10.67 °C
Cv = 30 ft-lb (41 J) at T	=	7.1 °F	-13.9 °C
Upper Shelf Energy	=	93.0 ft-lb	126.1 J

PT #	Temp (°F)	Energy (ft-lb)
1	-20	22.0
2	-10	24.0
3	20	41.0
4	30	38.0
5	60	60.0
6	100	84.0
7	200	94.0
8	400	92.0
9	400	92.0

O = Fictitious Point Added   * = Test Point Not Included

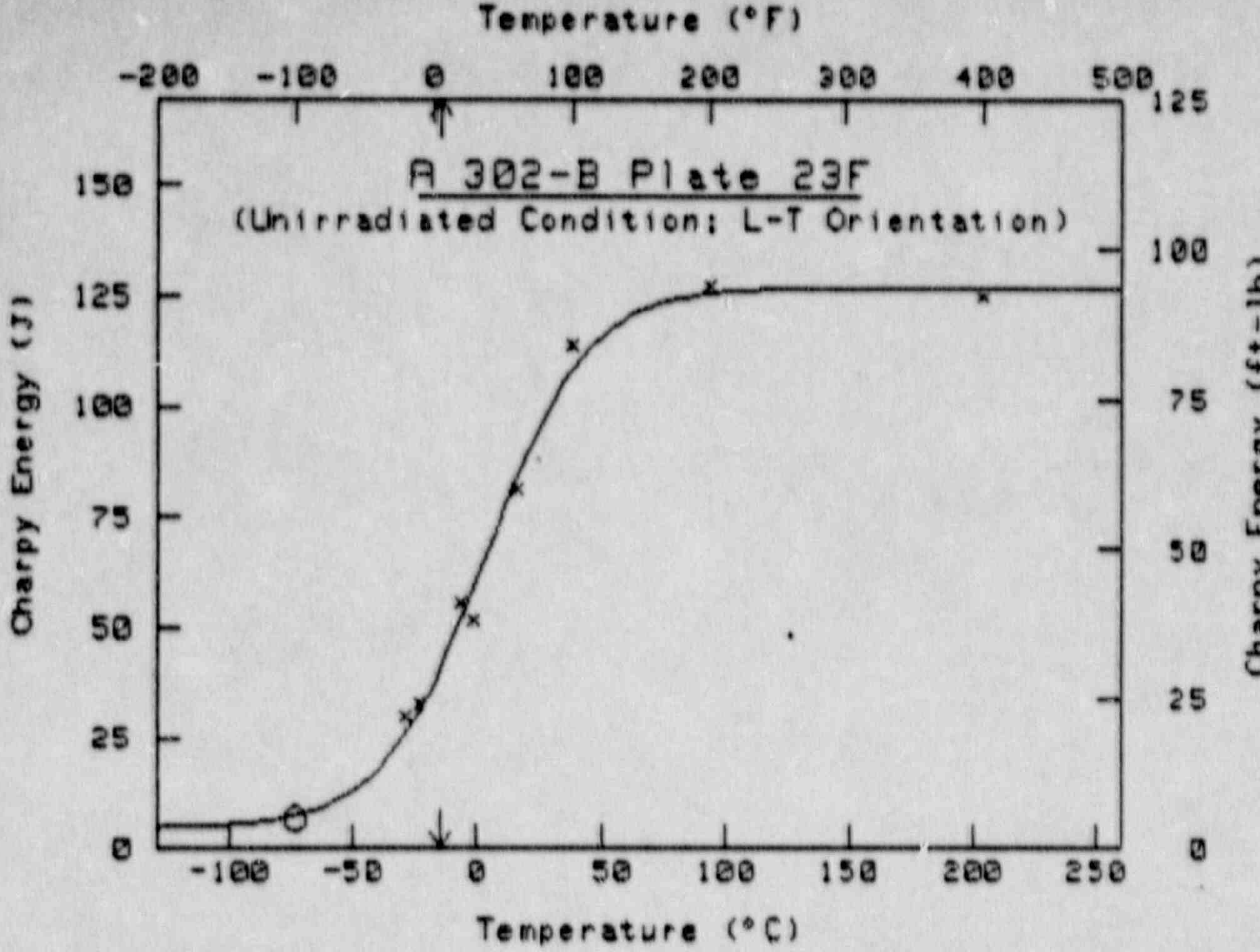

$$C_v = A + B \tanh[(T - T_o)/C]$$

		English	Metric
A	=	48.51 ft-lb	65.77 J
B	=	45.08 ft-lb	61.12 J
C	=	73.53 °F	40.85 °C
To	=	37.55 °F	3.08 °C

Cv = 30 ft-lb (41 J) at T	=	5.5 °F	-14.7 °C
Upper Shelf Energy	=	93.6 ft-lb	126.9 J

PT #		Temp (°F)	Energy (ft-lb)
1		-26	22.0
2		-10	24.0
3		20	41.0
4		30	38.0
5		60	60.0
6		100	84.0
7		200	94.0
8		400	92.0
9		400	92.0
10	O	-100	5.0
11	O	-100	5.0
12	O	-100	5.0
13	O	-100	5.0

O = Fictitious Point Added   * = Test Point Not Included

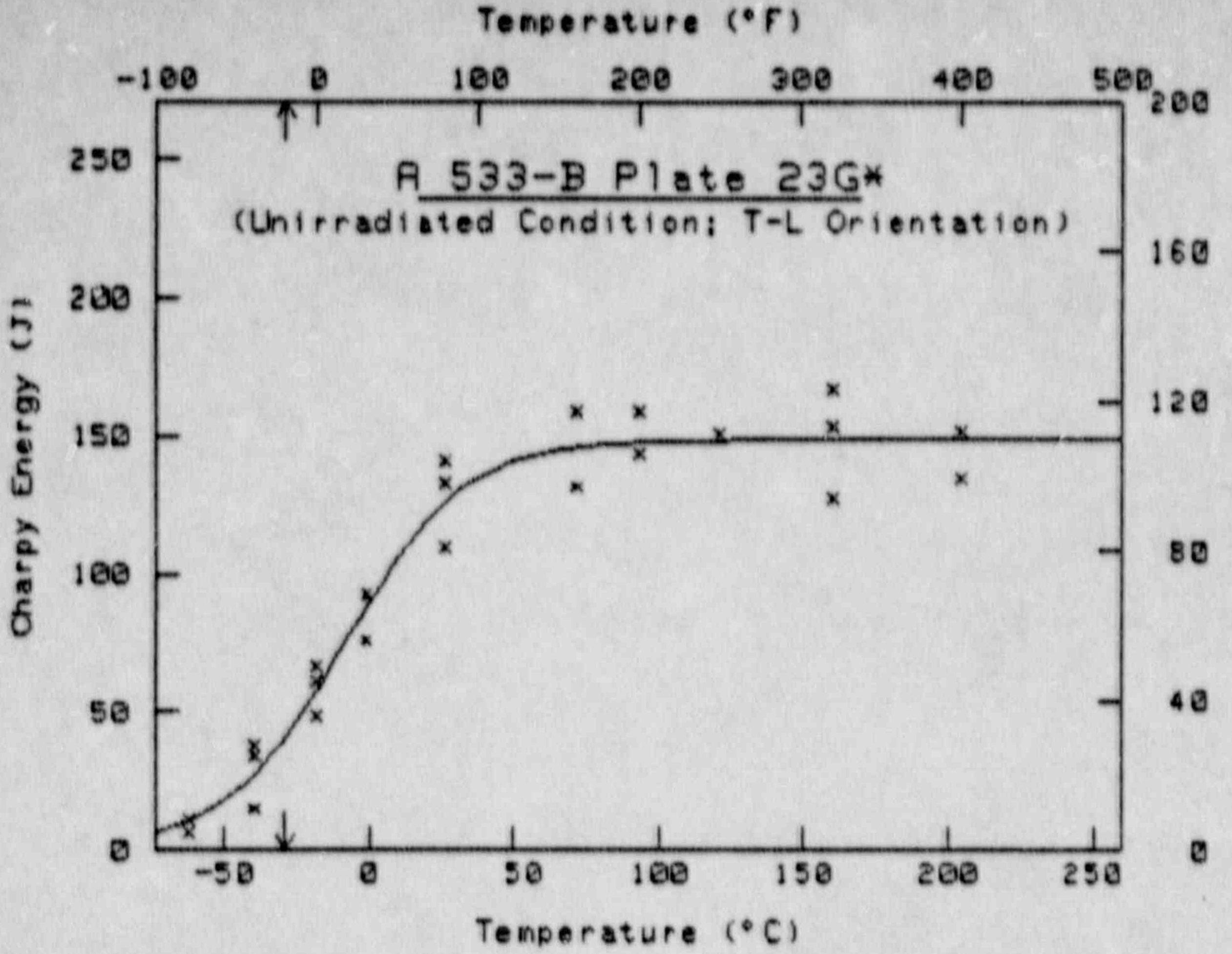

****

$C_v = A + B \tanh[(T - T_o)/C]$

		English	Metric
A	=	55.11 ft-lb	74.72 J
B	=	54.57 ft-lb	73.98 J
C	=	74.06 °F	41.14 °C
To	=	16.83 °F	-8.43 °C

Cv = 30 ft-lb (41 J) at T	=	-20.0 °F	-28.9 °C
Upper Shelf Energy	=	109.7 ft-lb	148.7 J

****

PT #	Temp (°F)	Energy (ft-lb)	PT #	Temp (°F)	Energy (ft-lb)
1	-80	8.0	13	80	81.0
2	-80	5.0	14	160	97.0
3	-40	28.0	15	160	117.0
4	-40	25.0	16	200	117.0
5	-40	11.0	17	200	106.0
6	0	36.0	18	250	111.0
7	0	49.0	19	320	94.0
8	0	45.0	20	320	123.0
9	30	68.0	21	320	113.0
10	30	56.0	22	400	99.0
11	80	98.0	23	400	112.0
12	80	104.0			

O = Fictitious Point Added   * = Test Point Not Included

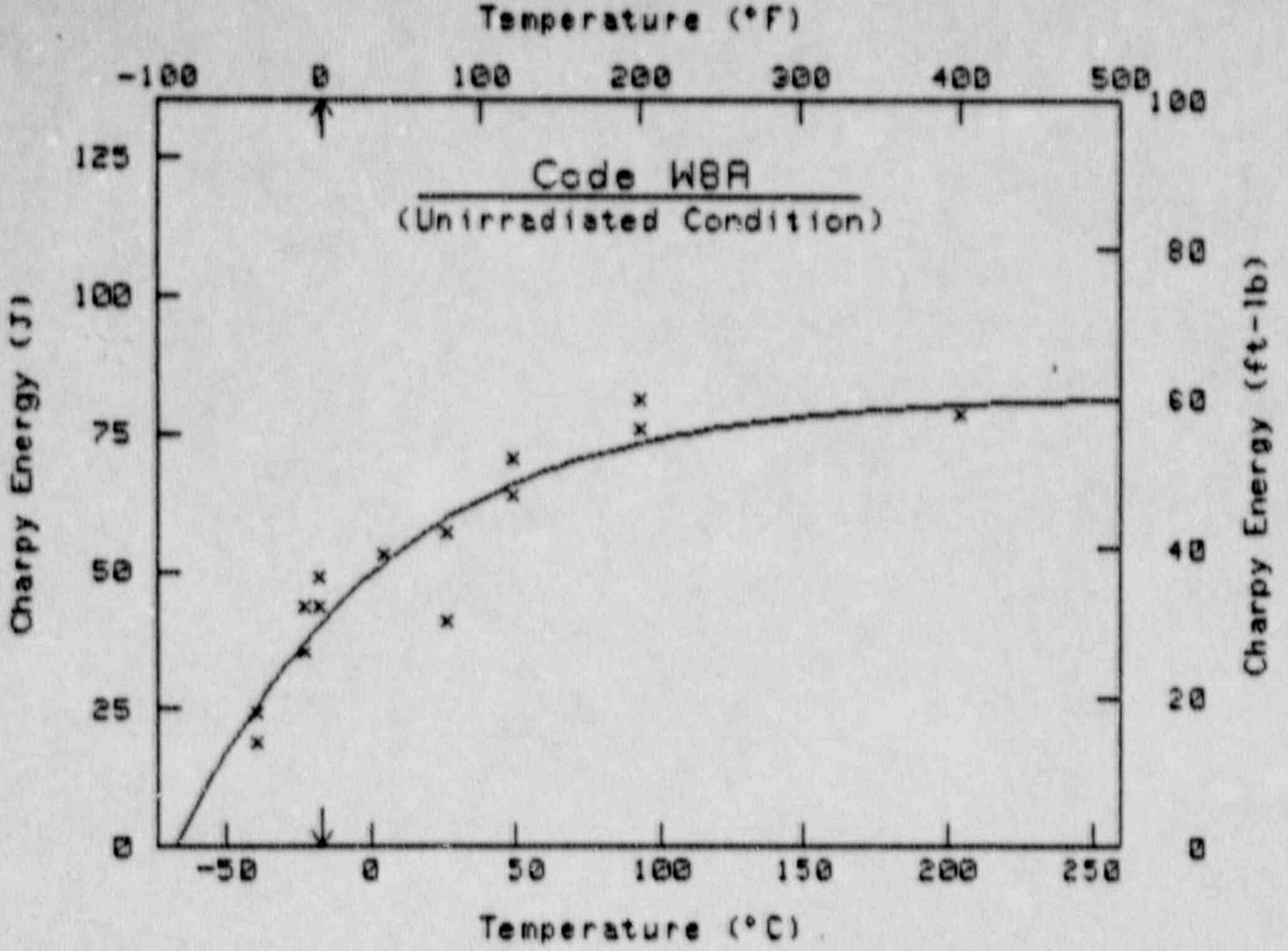

$$C_v = A + B \tanh[(T - T_o)/C]$$

		English	Metric
A	=	-355.03 ft-lb	-481.36 J
B	=	415.53 ft-lb	563.39 J
C	=	251.15 °F	139.53 °C
To	=	-408.93 °F	-244.96 °C

	English	Metric
Cv = 30 ft-lb (41 J) at T =	1.4 °F	-17.0 °C
Upper Shelf Energy =	60.5 ft-lb	82.0 J

PT #	Temp (°F)	Energy (ft-lb)
1	-40	14.0
2	-40	18.0
3	-10	26.0
4	-10	32.0
5	0	36.0
6	0	32.0
7	40	39.0
8	80	42.0
9	80	30.0
10	120	52.0
11	120	47.0
12	200	60.0
13	200	56.0
14	400	58.0
15	400	58.0

O = Fictitious Point Added * = Test Point Not Included

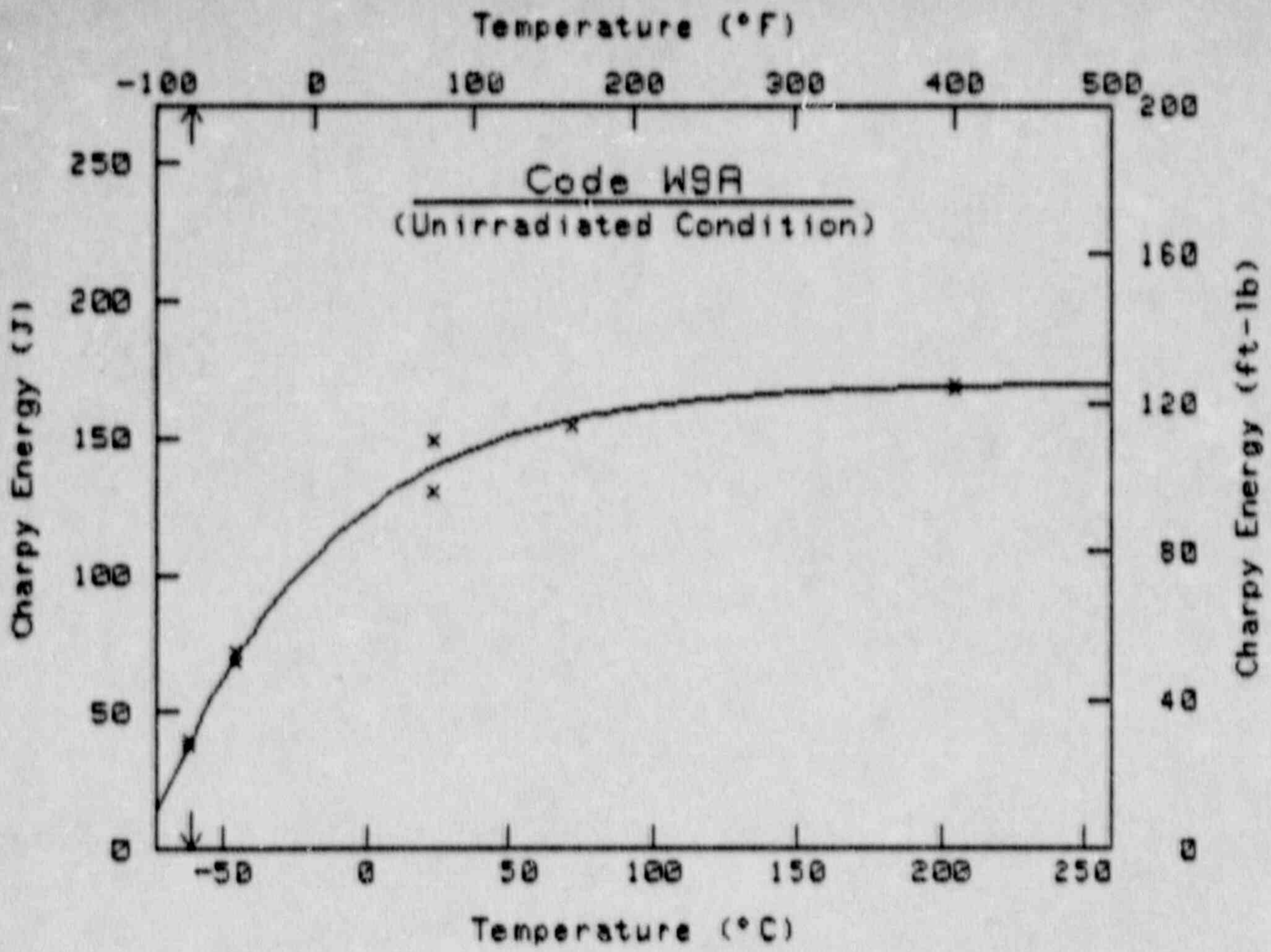

$$Cv = A + B \tanh[(T - To)/C]$$

	English	Metric
A =	-395.47 ft-lb	-536.18 J
B =	520.90 ft-lb	706.25 J
C =	204.01 °F	113.34 °C
To =	-312.32 °F	-191.29 °C
Cv = 30 ft-lb (41 J) at T =	-78.3 °F	-61.3 °C
Upper Shelf Energy =	125.4 ft-lb	170.1 J

PT #	Temp (°F)	Energy (ft-lb)
1	-80	29.0
2	-80	28.0
3	-50	53.0
4	-50	50.0
5	75	96.0
6	75	110.0
7	160	114.0
8	400	125.0
9	400	125.0
10	400	124.0

D = Fictitious Point Added   * = Test Point Not Included

Computer Curve Fittings of Data from Irradiation Assembly UBR-38

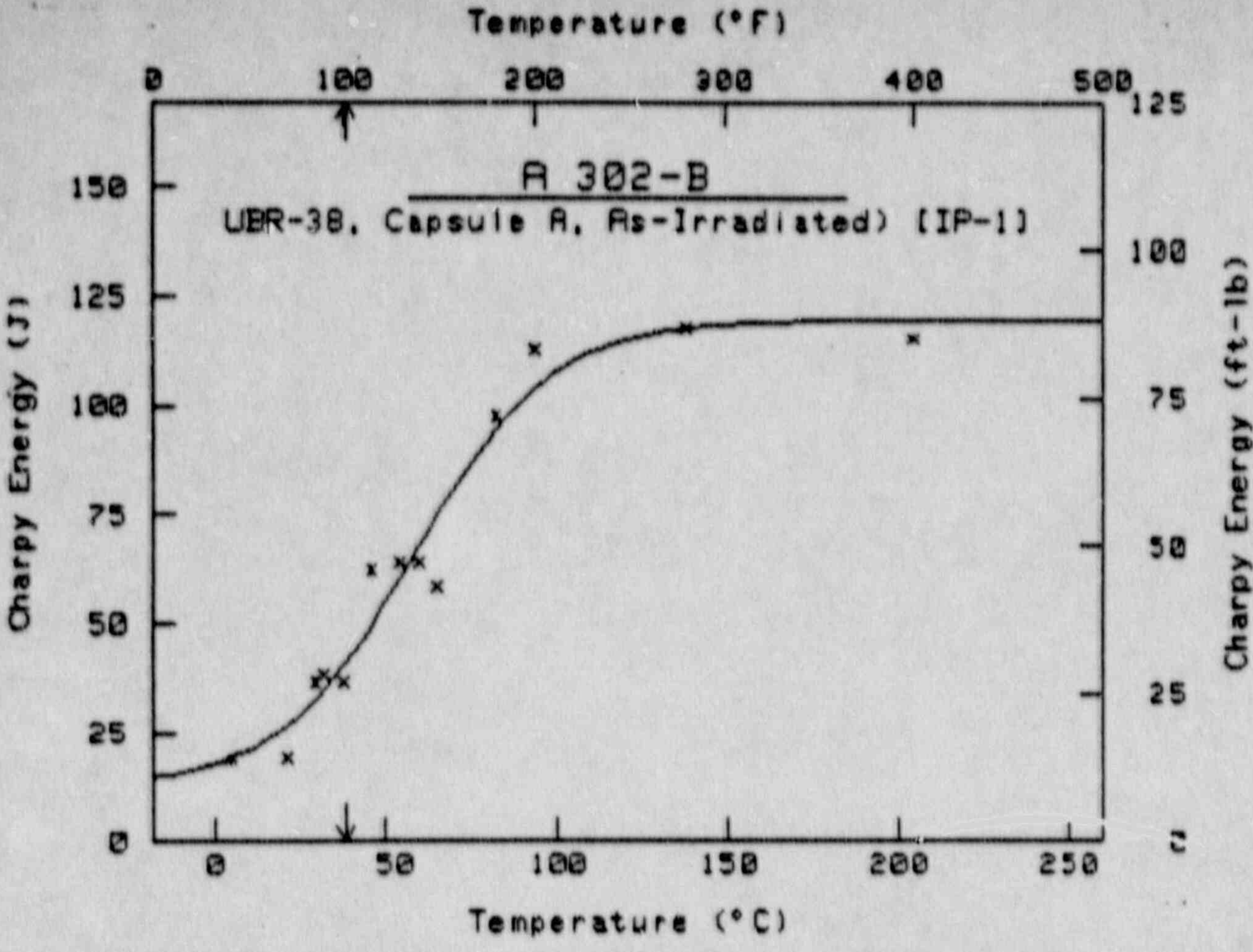

****

Cv = A + B tanh[(T - To)/C]

		English	Metric
A	=	48.71 ft-lb	66.04 J
B	=	39.47 ft-lb	53.51 J
C	=	71.78 °F	39.88 °C
To	=	137.80 °F	58.78 °C

Cv = 30 ft-lb (41 J) at T	=	100.8 °F	38.2 °C
Upper Shelf Energy	=	88.2 ft-lb	119.6 J

****

PT #		Temp (°F)	Energy (ft-lb)
1	*	40	15.0
2		70	14.0
3		85	27.0
4		90	28.0
5		100	27.0
6		115	46.0
7		130	47.0
8		140	47.0
9		150	43.0
10	*	165	89.0
11		180	72.0
12		200	83.0
13		280	87.0
14	*	360	82.0
15		400	85.0

O = Fictitious Point Added * = Test Point Not Included

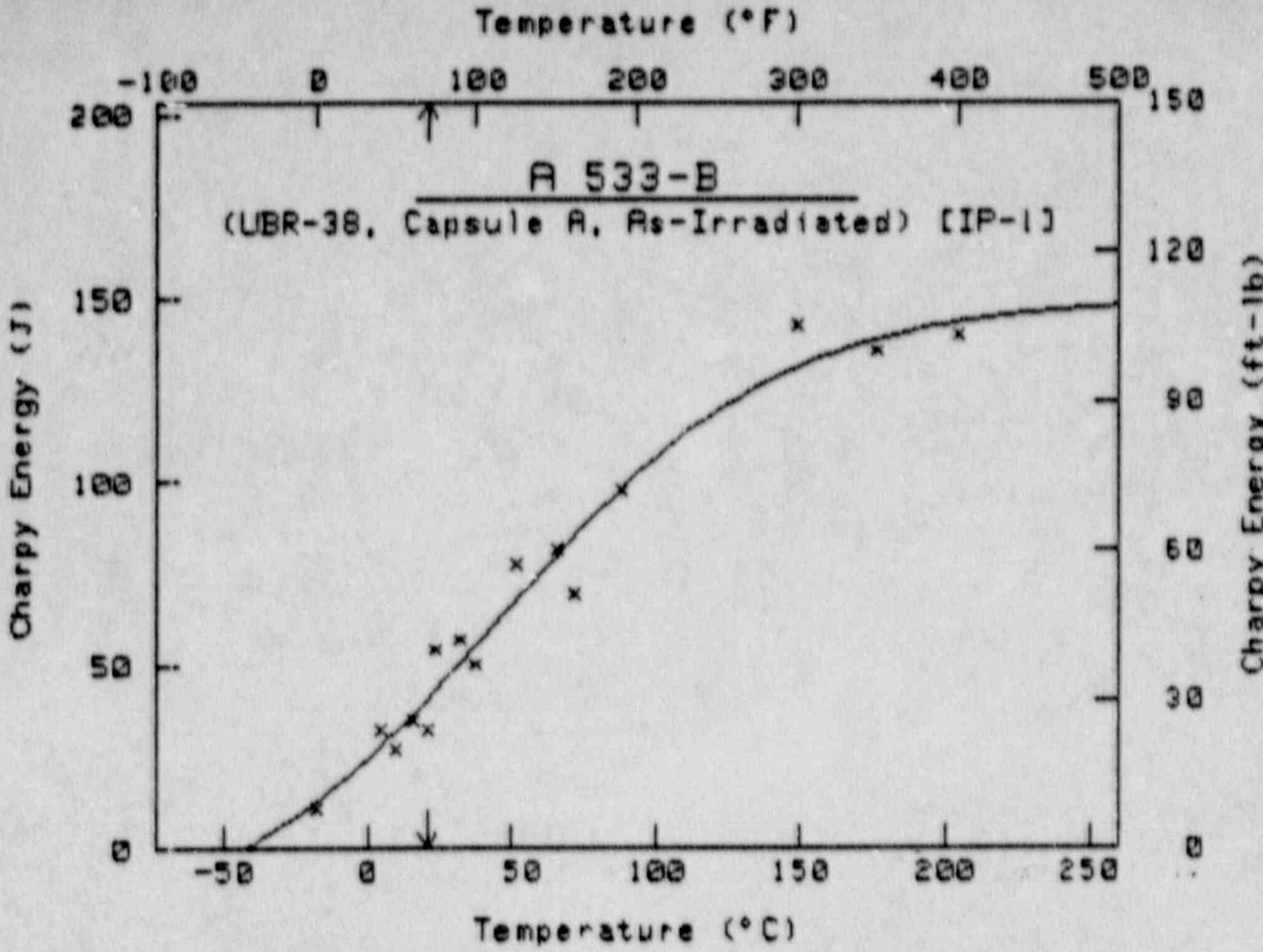

$Cv = A + B \tanh[(T - To)/C]$

	English	Metric
A =	46.24 ft-lb	62.69 J
B =	64.36 ft-lb	87.25 J
C =	175.95 °F	97.75 °C
To =	114.65 °F	45.92 °C
Cv = 30 ft-lb (41 J) at T =	69.3 °F	20.7 °C
Upper Shelf Energy =	110.6 ft-lb	149.9 J

PT #	Temp (°F)	Energy (ft-lb)
1	0	8.0
2	40	24.0
3	50	20.0
4	60	26.0
5	70	24.0
6	75	40.0
7	90	42.0
8	100	37.0
9	125	57.0
10	150	60.0
11	160	51.0
12	190	72.1
13	300	105.0
14	350	100.0
15	400	103.0

O = Fictitious Point Added   * = Test Point Not Included

Computer Curve Fittings of Data from Irradiation Assembly UBR-44

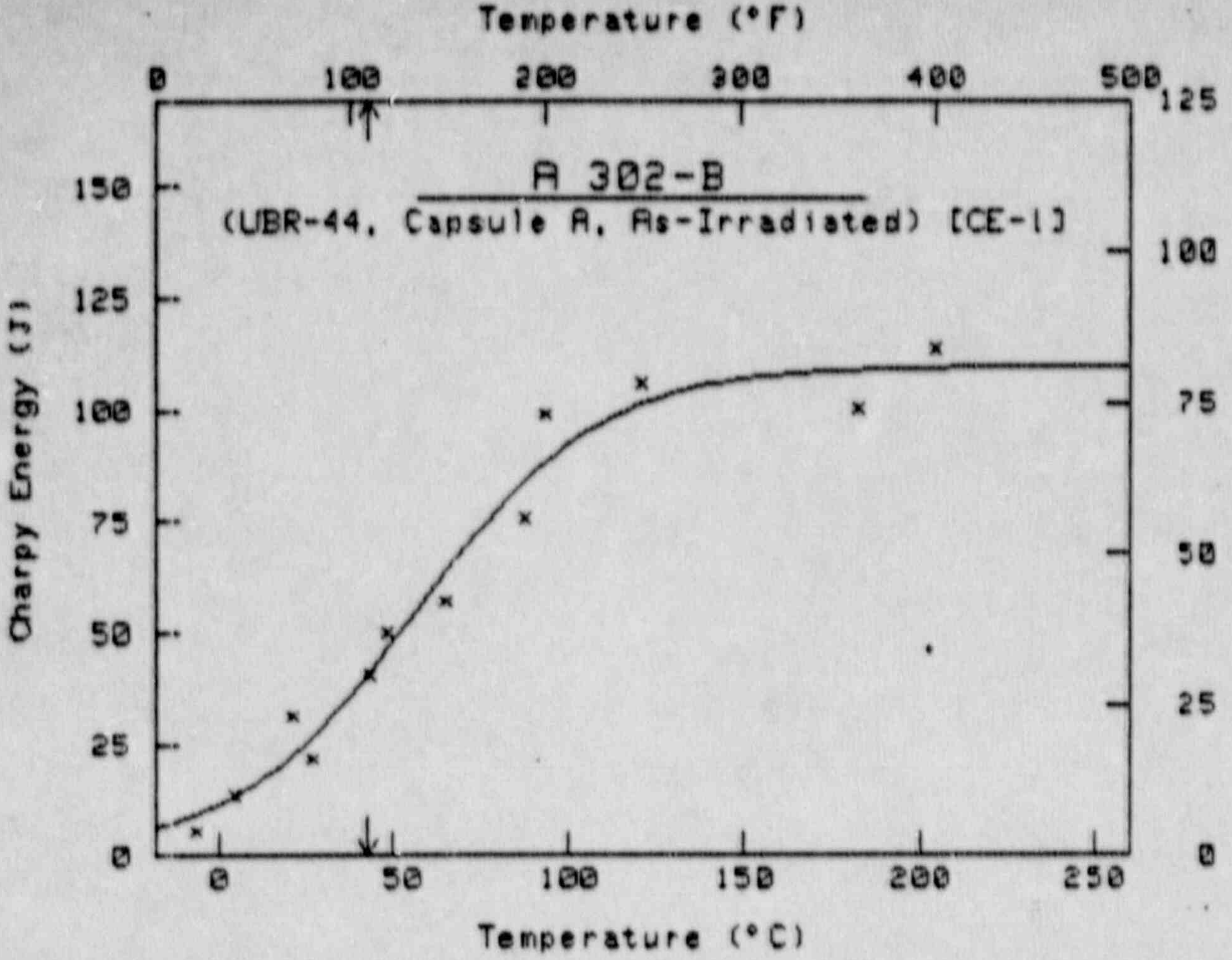

****

Cv = A + B tanh[(T - To)/C]

	English	Metric
A =	40.76 ft-lb	55.27 J
B =	40.30 ft-lb	54.64 J
C =	93.30 °F	51.83 °C
To =	135.11 °F	57.28 °C
Cv = 30 ft-lb (41 J) at T =	109.6 °F	43.1 °C
Upper Shelf Energy =	81.1 ft-lb	109.9 J

****

PT #	Temp (°F)	Energy (ft-lb)
1	20	4.0
2	40	10.0
3	70	23.0
4	80	16.0
5	110	30.0
6	120	37.0
7	150	42.0
8	190	56.0
9	200	73.0
10	250	78.0
11	360	74.0
12	400	84.0

0 = Fictitious Point Added   * = Test Point Not Included

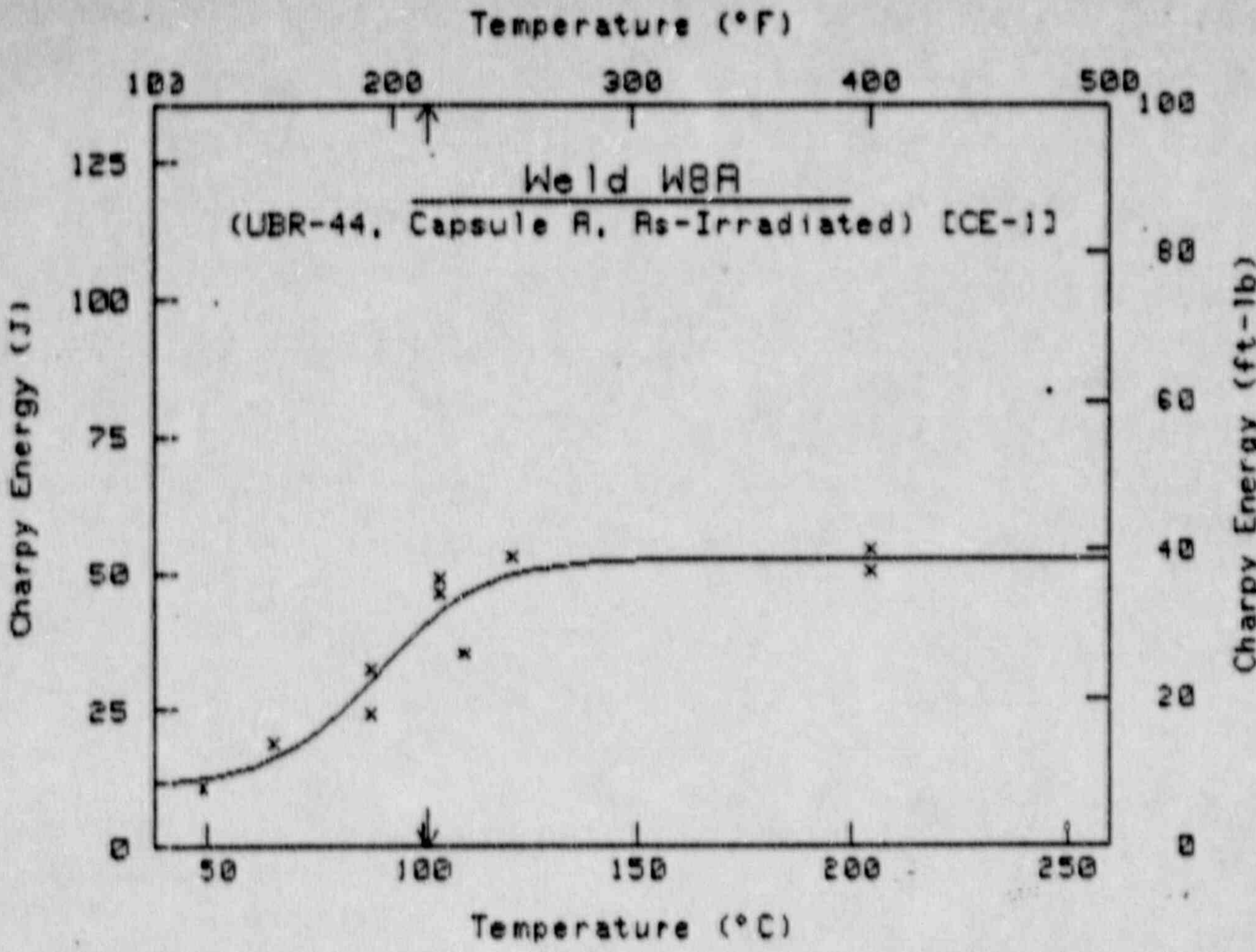

****

$Cv = A + B \tanh[(T - To)/C]$

		English	Metric
A	=	23.45 ft-lb	31.79 J
B	=	15.38 ft-lb	20.86 J
C	=	45.16 °F	25.09 °C
To	=	193.82 °F	89.90 °C

Cv = 30 ft-lb (41 J) at T	=	214.4 °F	101.3 °C
Upper Shelf Energy	=	38.8 ft-lb	52.7 J

****

PT #	Temp (°F)	Energy (ft-lb)
1	120	8.0
2	150	14.0
3	190	18.0
4	190	24.0
5	220	36.0
6	220	34.0
7	230	26.0
8	250	39.0
9	400	40.1
10	400	37.1

O = Fictitious Point Added   * = Test Point Not Included

Computer Curve Fittings of Data from Irradiation Assembly UBR-45

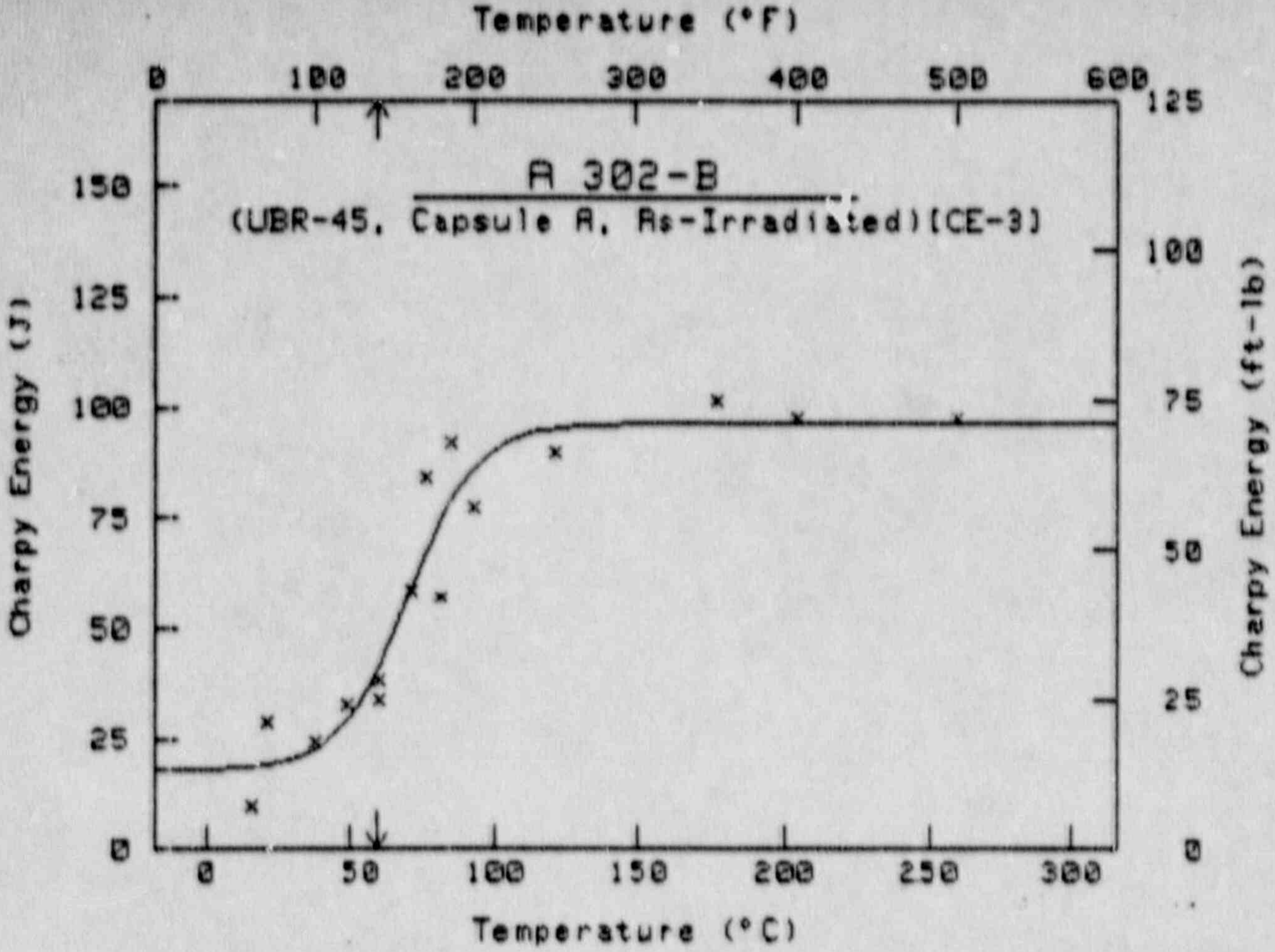

****

$$Cv = A + B \tanh[(T - To)/C]$$

		English	Metric
A	=	42.12 ft-lb	57.11 J
B	=	28.95 ft-lb	39.25 J
C	=	43.56 °F	24.20 °C
To	=	158.59 °F	70.33 °C
Cv = 30 ft-lb (41 J) at T	=	139.2 °F	59.5 °C
Upper Shelf Energy	=	71.1 ft-lb	96.4 J

****

PT #	Temp (°F)	Energy (ft-lb)
1	60	7.0
2	70	21.0
3	100	18.0
4	120	24.0
5	140	25.0
6	140	28.0
7	160	43.0
8	170	62.0
9	180	42.0
10	185	68.0
11	200	57.0
12	250	66.0
13	350	75.0
14	400	72.0
15	500	72.0

O = Fictitious Point Added   * = Test Point Not Included

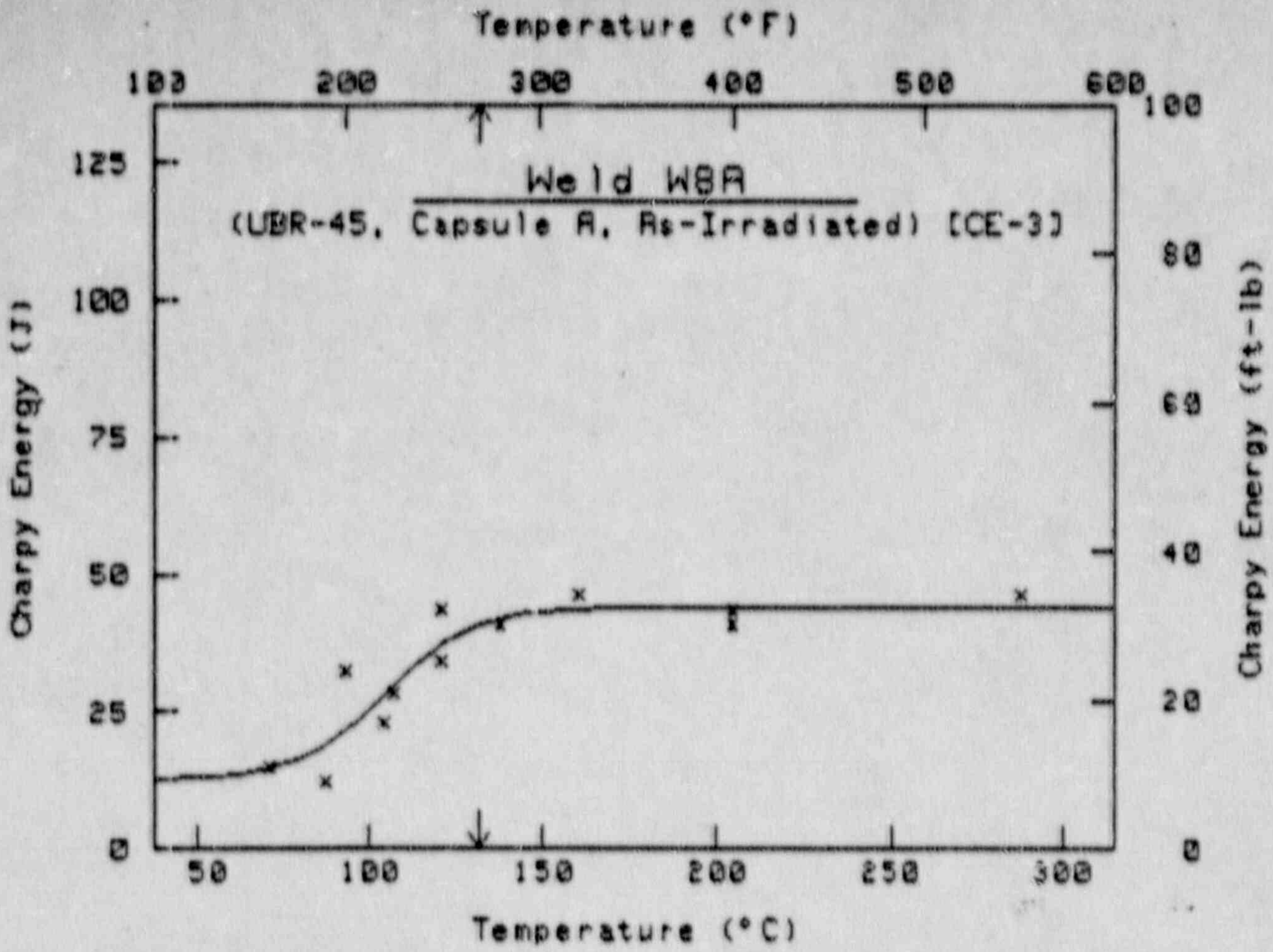

****

$Cv = A + B \tanh[(T - To)/C]$

	English	Metric
A =	20.90 ft-lb	28.34 J
B =	11.63 ft-lb	15.76 J
C =	45.81 °F	25.45 °C
To =	220.80 °F	104.89 °C
Cv = 30 ft-lb (41 J) at T =	269.0 °F	131.7 °C
Upper Shelf Energy =	32.5 ft-lb	44.1 J

****

PT #	Temp (°F)	Energy (ft-lb)
1	160	11.0
2	190	9.0
3	200	24.0
4	220	17.0
5	225	21.0
6	250	32.0
7	250	25.1
8	280	30.0
9	320	34.0
10	400	30.0
11	400	32.0
12	550	34.0

O = Fictitious Point Added   * = Test Point Not Included

Computer Curve Fittings of Data from Irradiation Assembly UBR-46

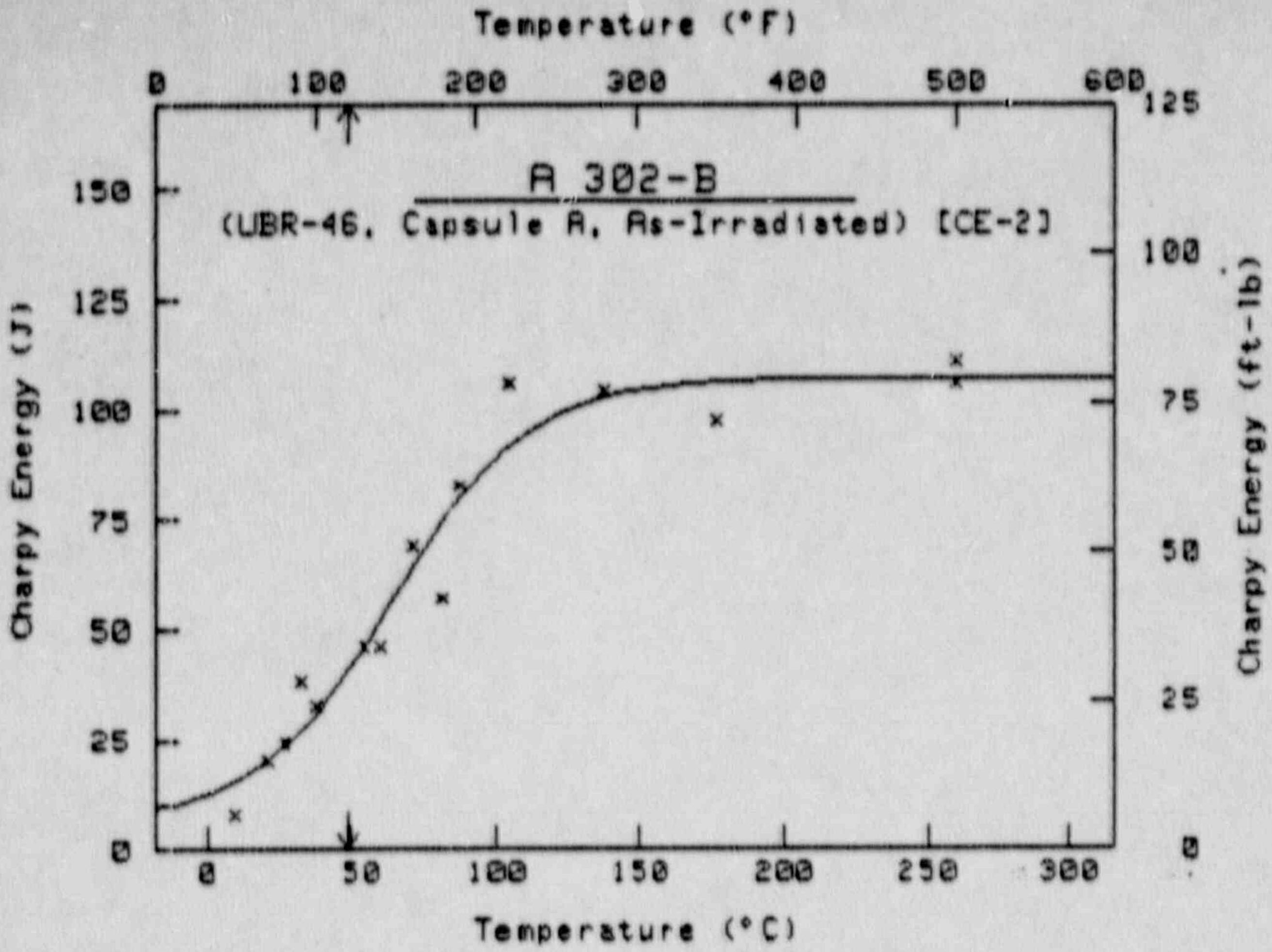

****

Cv = A + B tanh[(T - To)/C]

	English	Metric
A =	41.92 ft-lb	56.84 J
B =	37.21 ft-lb	50.45 J
C =	85.81 °F	47.67 °C
To =	148.24 °F	64.58 °C

Cv = 30 ft-lb (41 J) at T =	119.7 °F	48.7 °C
Upper Shelf Energy =	79.1 ft-lb	107.3 J

****

PT #	Temp (°F)	Energy (ft-lb)
1	50	6.0
2	70	15.0
3	80	18.0
4	90	28.0
5	100	24.0
6	130	34.0
7	140	34.0
8	160	51.0
9	180	42.0
10	190	61.0
11	220	78.0
12	280	77.0
13	350	72.0
14	500	82.0
15	500	78.0

O = Fictitious Point Added * = Test Point Not Included

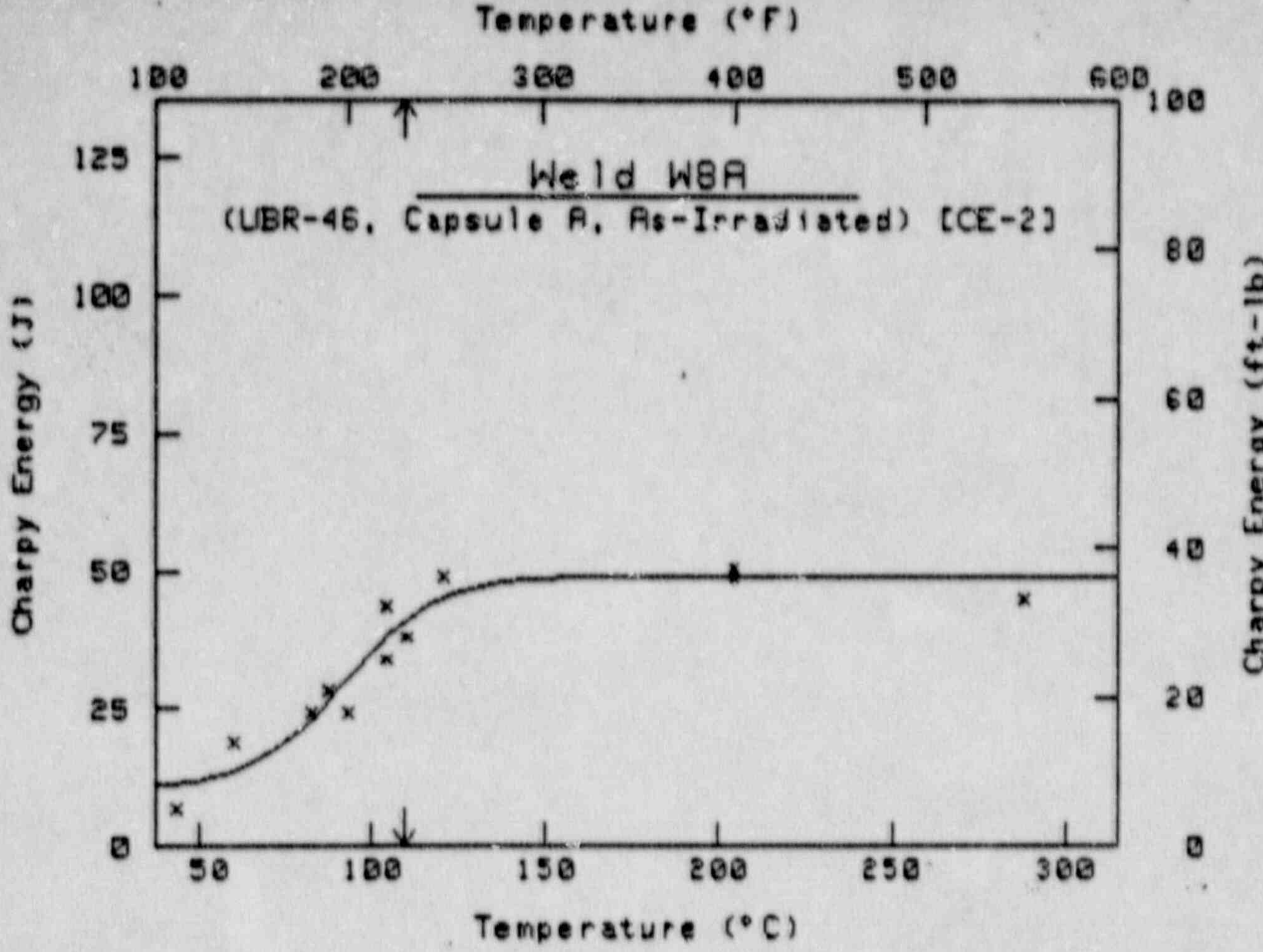

$$Cv = A + B \tanh[(T - To)/C]$$

		English	Metric
A	=	21.98 ft-lb	29.80 J
B	=	14.24 ft-lb	19.30 J
C	=	48.14 °F	26.75 °C
To	=	198.10 °F	92.28 °C

Cv = 30 ft-lb (41 J) at T	=	228.8 °F	109.3 °C
Upper Shelf Energy	=	36.2 ft-lb	49.1 J

PT #	Temp (°F)	Energy (ft-lb)
1	110	5.0
2	140	14.0
3	180	18.0
4	190	21.0
5	200	18.0
6	220	25.0
7	220	32.0
8	230	28.0
9	250	36.0
10	250	36.0
11	400	36.0
12	400	37.0
13	550	33.0

0 = Fictitious Point Added * = Test Point Not Included

Computer Curve Fittings of Data from Irradiation Assembly UBR-65

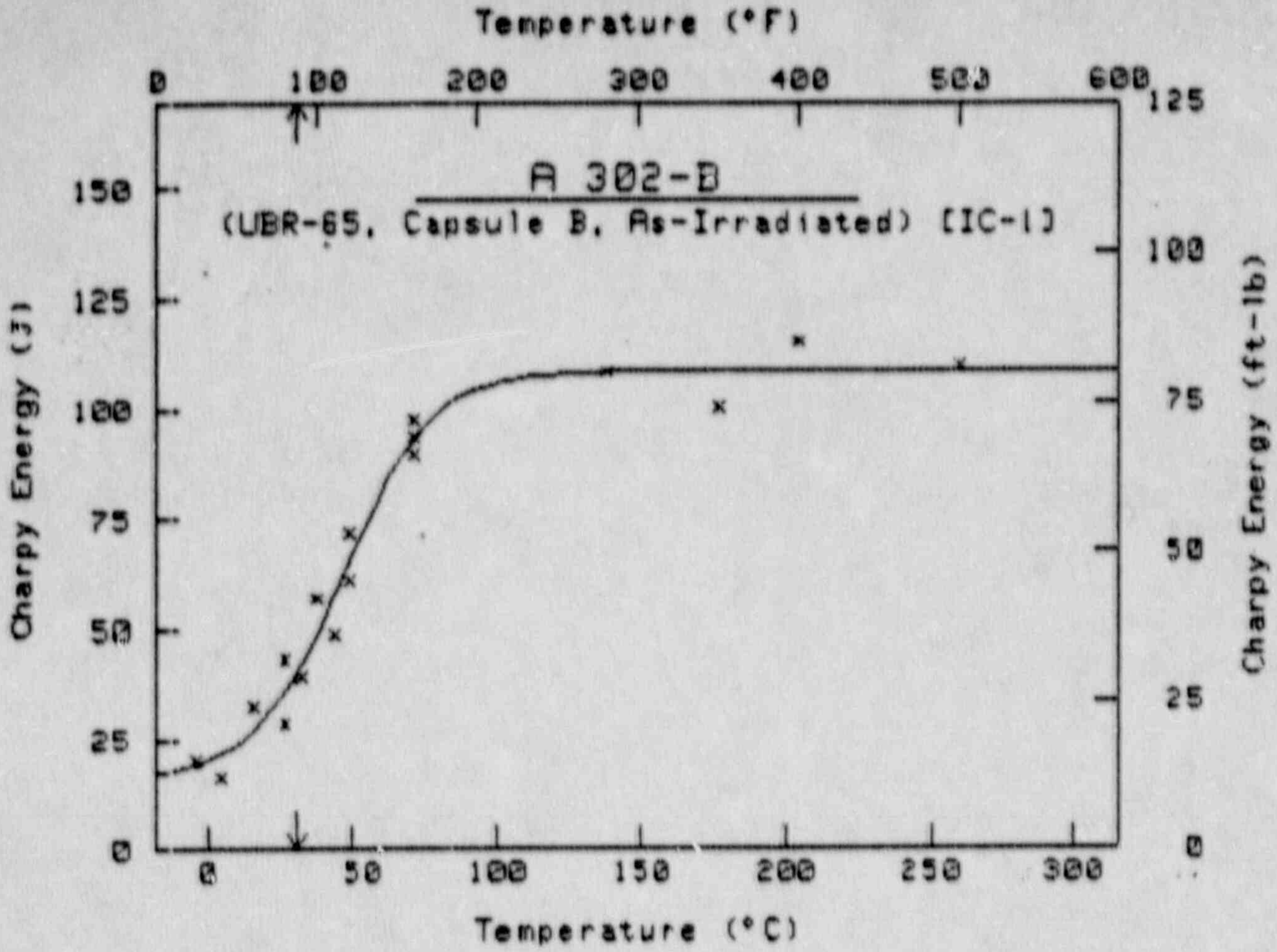

$$Cv = A + B \tanh[(T - To)/C]$$

		English	Metric
A	=	45.97 ft-lb	62.33 J
B	=	34.24 ft-lb	46.42 J
C	=	55.71 °F	30.95 °C
To	=	115.95 °F	46.64 °C

Cv = 30 ft-lb (41 J) at T	=	87.8 °F	31.0 °C
Upper Shelf Energy	=	80.2 ft-lb	108.7 J

PT #	Temp (°F)	Energy (ft-lb)	PT #	Temp (°F)	Energy (ft-lb)
1	25	15.0	10	120	53.0
2	40	12.0	11	160	66.0
3	60	24.0	12	160	72.0
4	80	21.0	13	160	69.0
5	80	32.0	14	280	80.0
6	90	29.0	15	350	74.0
7	100	42.0	16	400	85.0
8	110	36.0	17	500	81.0
9	120	45.0			

O = Fictitious Point Added * = Test Point Not Included

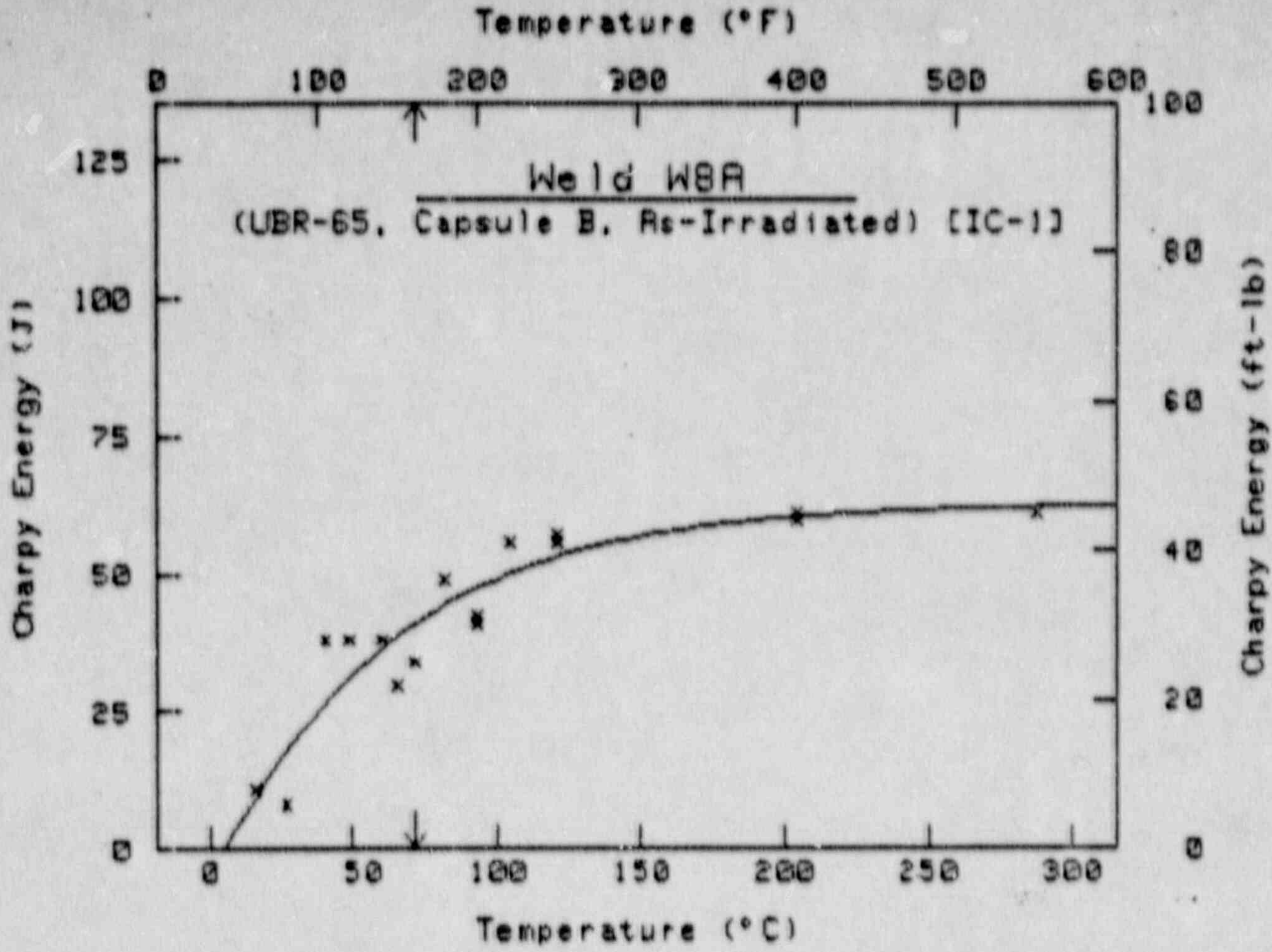

$Cv = A + B \tanh[(T - To)/C]$

		English	Metric
A	=	-192.93 ft-lb	-261.58 J
B	=	239.22 ft-lb	324.34 J
C	=	214.24 °F	119.02 °C
To	=	-198.09 °F	-127.83 °C

	English	Metric
Cv = 30 ft-lb (41 J) at T =	160.3 °F	71.3 °C
Upper Shelf Energy =	46.3 ft-lb	62.8 J

PT #	Temp (°F)	Energy (ft-lb)	PT #	Temp (°F)	Energy (ft-lb)
1	60	8.0	9	200	30.0
2	80	6.0	10	200	31.0
3	105	28.0	11	220	41.0
4	120	28.0	12	250	41.0
5	140	28.0	13	250	42.0
6	150	22.0	14	400	44.0
7	160	25.0	15	400	45.0
8	180	36.0	16	550	45.0

0 = Fictitious Point Added   * = Test Point Not Included

Computer Curve Fittings of Data from Irradiation Assembly UBR-75

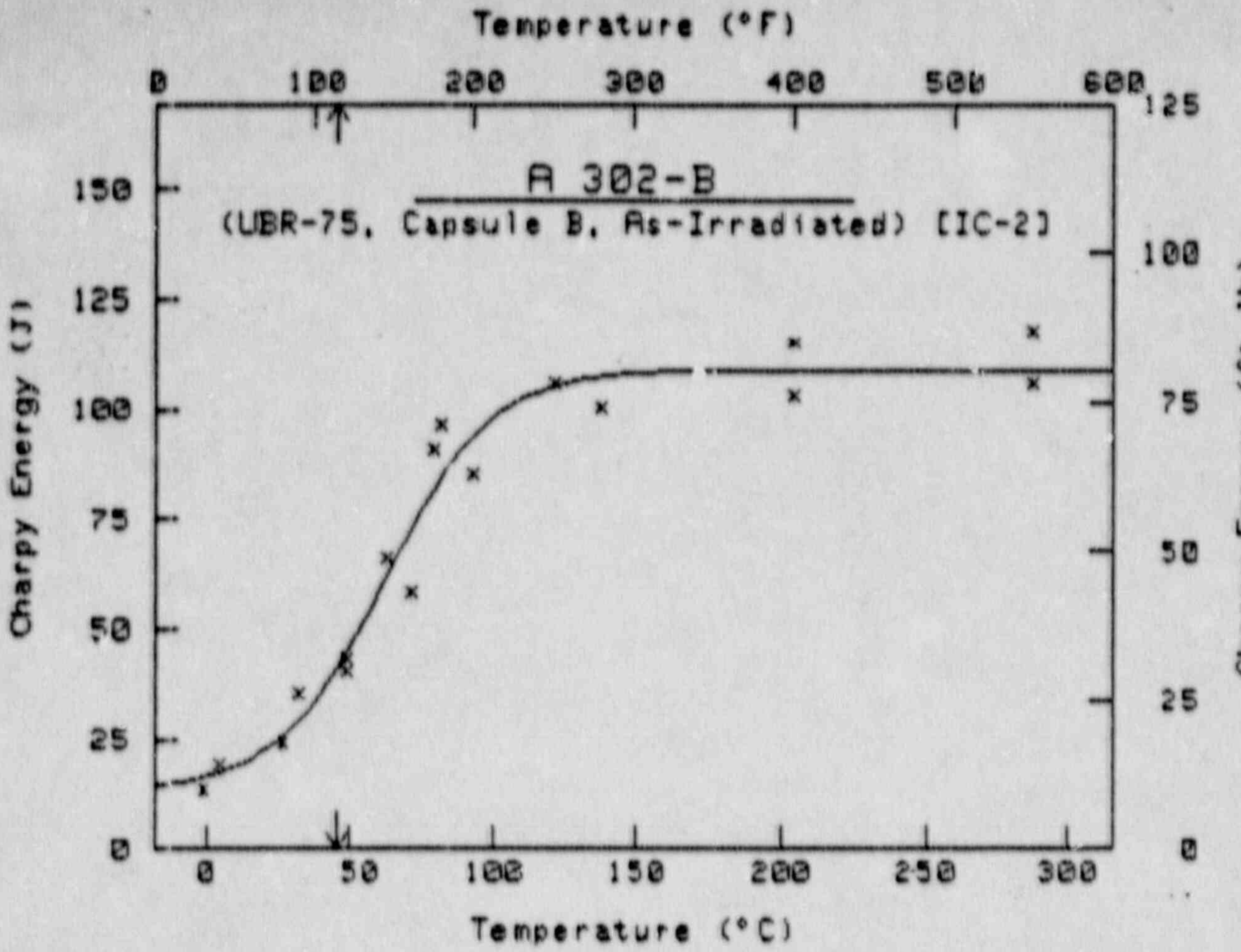

$$C_v = A + B \tanh[(T - T_o)/C]$$

		English	Metric
A	=	45.07 ft-lb	61.10 J
B	=	35.33 ft-lb	47.91 J
C	=	66.98 °F	37.21 °C
To	=	143.78 °F	62.10 °C
Cv = 30 ft-lb (41 J) at T	=	113.3 °F	45.2 °C
Upper Shelf Energy	=	80.4 ft-lb	109.0 J

PT #	Temp (°F)	Energy (ft-lb)	PT #	Temp (°F)	Energy (ft-lb)
1	30	10.0	10	180	71.0
2	40	14.0	11	200	63.0
3	80	18.0	12	250	78.0
4	90	26.0	13	280	74.0
5	120	32.0	14	400	85.0
6	120	30.0	15	400	76.0
7	145	49.0	16	550	78.0
8	160	43.0	17	550	87.0
9	175	67.0			

O = Fictitious Point Added   * = Test Point Not Included

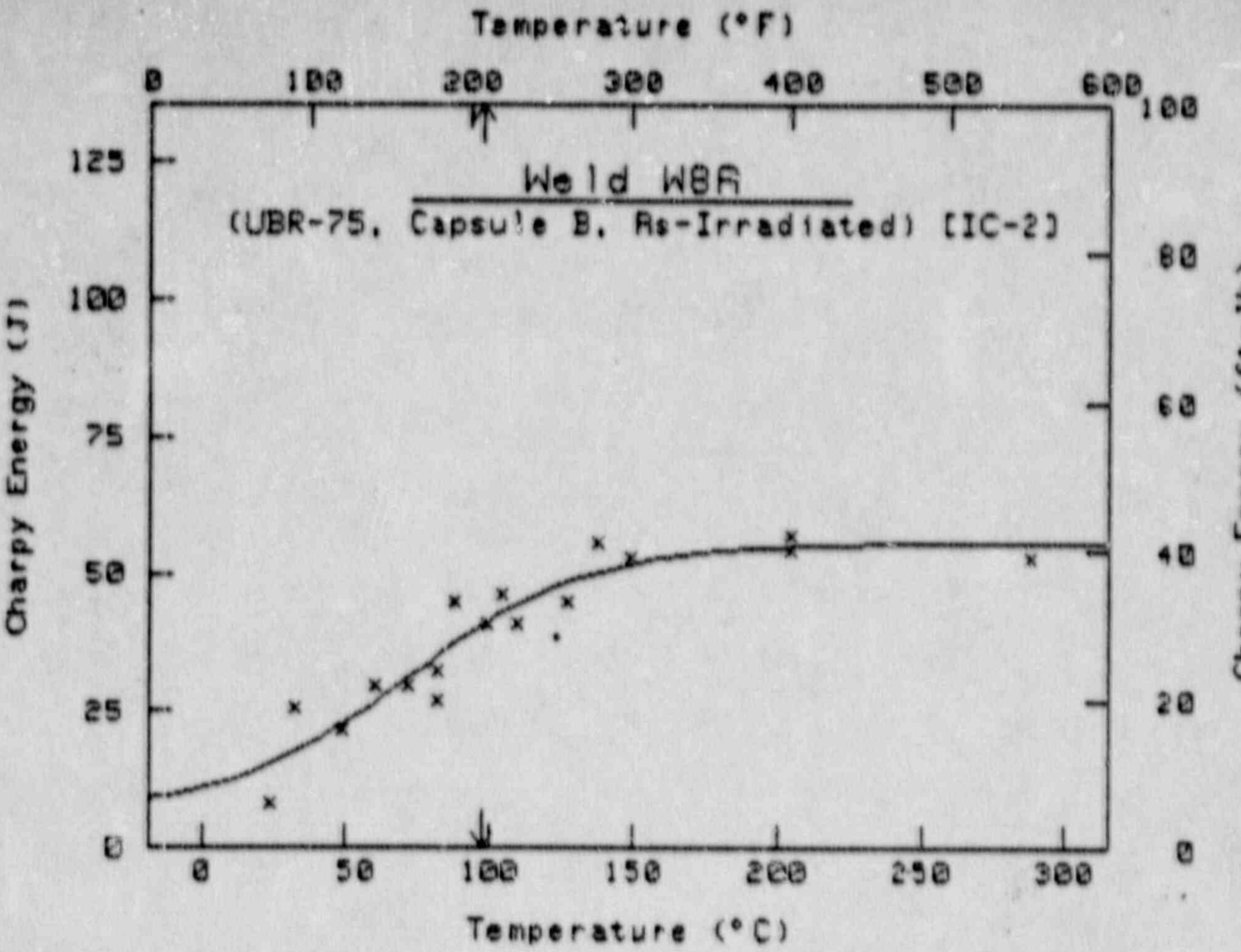

$$Cv = A + B \tanh[(T - To)/C]$$

		English	Metric
A	=	22.84 ft-lb	30.96 J
B	=	18.27 ft-lb	24.77 J
C	=	114.29 °F	63.50 °C
To	=	160.55 °F	71.41 °C

	English	Metric
Cv = 30 ft-lb (41 J) at T =	207.9 °F	97.7 °C
Upper Shelf Energy =	41.1 ft-lb	55.7 J

PT #	Temp (°F)	Energy (ft-lb)	PT #	Temp (°F)	Energy (ft-lb)
1	75	6.0	10	220	34.0
2	90	19.0	11	230	30.0
3	120	16.0	12	260	33.0
4	140	22.0	13	280	41.0
5	160	22.0	14	300	39.0
6	180	20.0	15	400	42.0
7	180	24.0	16	400	40.0
8	190	33.0	17	550	39.0
9	210	30.0			

O = Fictitious Point Added   * = Test Point Not Included

Computer Curve Fittings of Data from Irradiation Assembly UBR-76

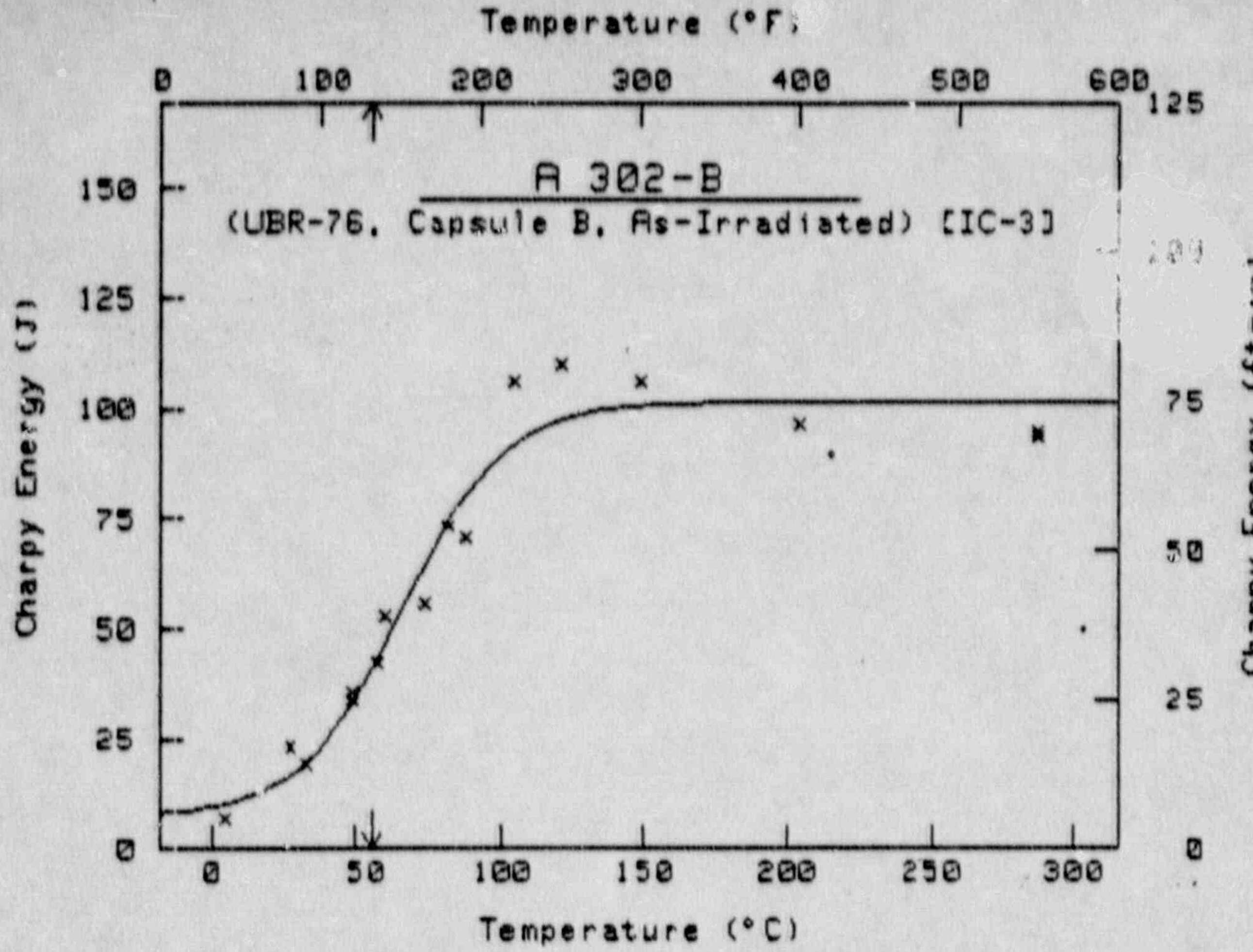

$$Cv = A + B \tanh[(T - To)/C]$$

	English	Metric
A =	40.09 ft-lb	54.35 J
B =	34.74 ft-lb	47.10 J
C =	64.13 °F	35.63 °C
To =	150.87 °F	66.04 °C
Cv = 30 ft-lb (41 J) at T =	131.7 °F	55.4 °C
Upper Shelf Energy =	74.8 ft-lb	101.5 J

PT #	Temp (°F)	Energy (ft-lb)	PT #	Temp (°F)	Energy (ft-lb)
1	40	5.0	10	180	54.0
2	40	5.0	11	190	52.0
3	80	17.0	12	220	78.0
4	90	14.0	13	250	81.1
5	120	25.0	14	300	78.0
6	120	26.0	15	400	71.0
7	135	31.0	16	550	70.0
8	140	39.0	17	550	69.0
9	165	41.0			

O = Fictitious Point Added * = Test Point Not Included

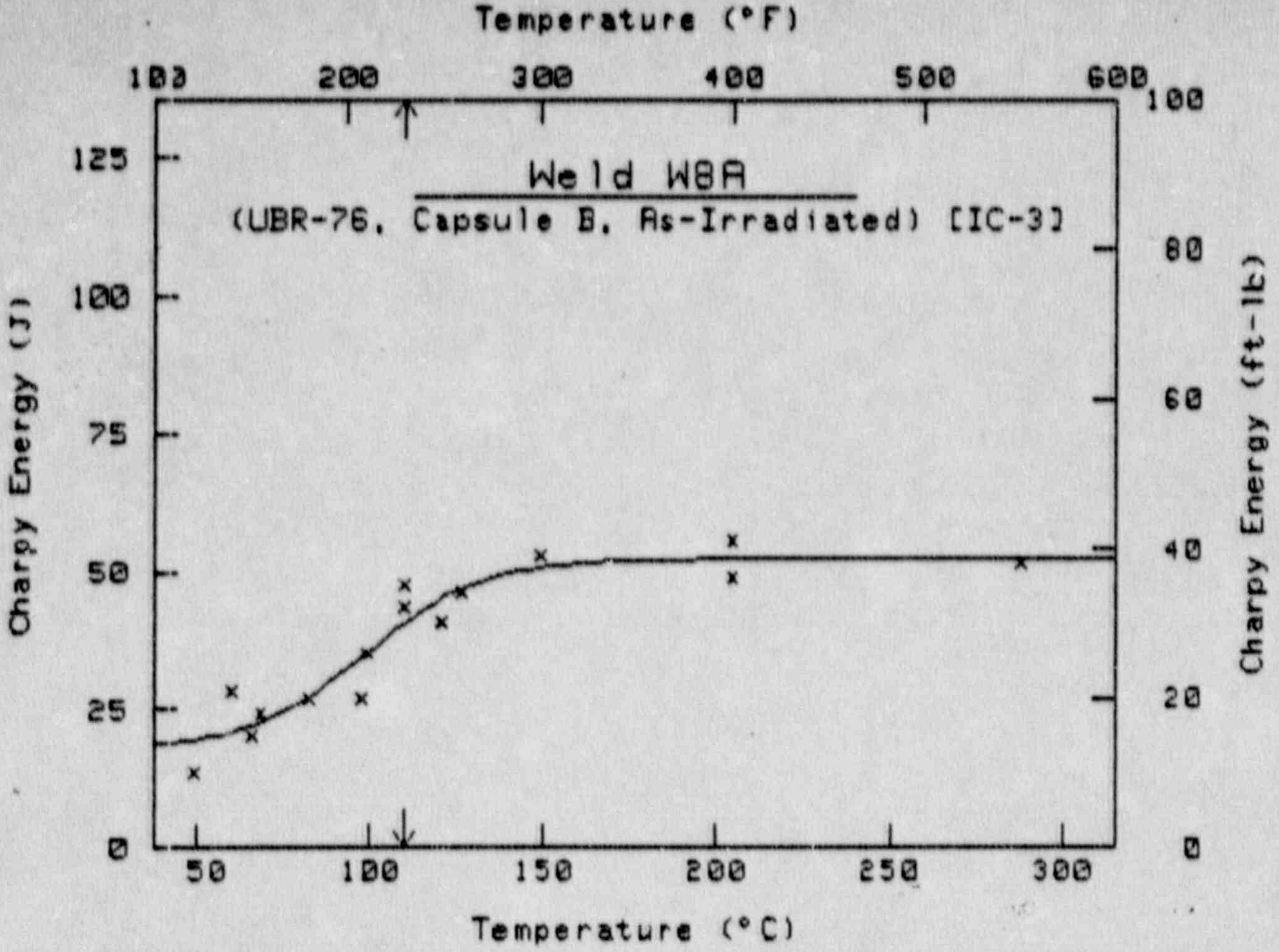

****

Cv = A + B tanh[(T - To)/C]

	English	Metric
A =	25.90 ft-lb	35.11 J
B =	12.75 ft-lb	17.29 J
C =	60.17 °F	33.43 °C
To =	210.12 °F	98.95 °C
Cv = 30 ft-lb (41 J) at T =	230.2 °F	110.1 °C
Upper Shelf Energy =	38.6 ft-lb	52.4 J

****

PT #	Temp (°F)	Energy (ft-lb)
1	120	10.0
2	140	21.0
3	150	15.0
4	155	18.0
5	180	20.0
6	208	20.0
7	210	26.0
8	230	35.0
9	230	32.0
10	250	30.0
11	260	34.0
12	300	39.0
13	400	36.0
14	400	41.0
15	550	38.0

0 = Fictitious Point Added * = Test Point Not Included

Computer Curve Fittings of Data from Irradiation Assembly UBR-77

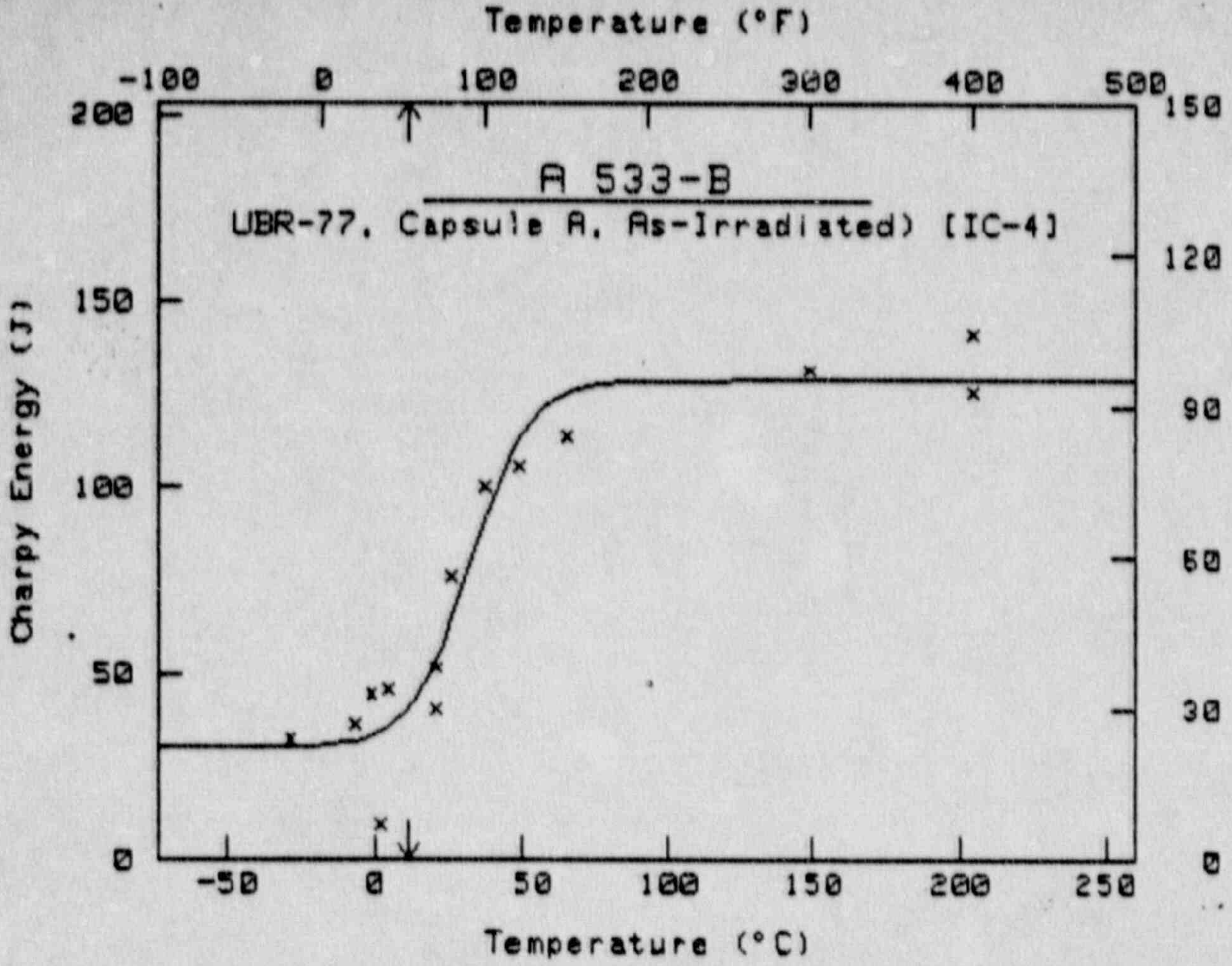

****

Cv = A + B tanh[(T - To)/C]

	English	Metric
A =	58.61 ft-lb	79.47 J
B =	36.42 ft-lb	49.38 J
C =	35.90 °F	19.94 °C
To =	90.49 °F	32.49 °C
Cv = 30 ft-lb (41 J) at T =	52.4 °F	11.4 °C
Upper Shelf Energy =	95.0 ft-lb	128.9 J

****

PT #	Temp (°F)	Energy (ft-lb)
1	-20	24.0
2	20	27.0
3	30	33.0
4	35	7.0
5	40	34.0
6	70	30.0
7	70	38.0
8	80	56.0
9	100	74.0
10	120	78.0
11	150	84.0
12	300	97.0
13	400	104.0
14	400	93.0

O = Fictitious Point Added   * = Test Point Not Included

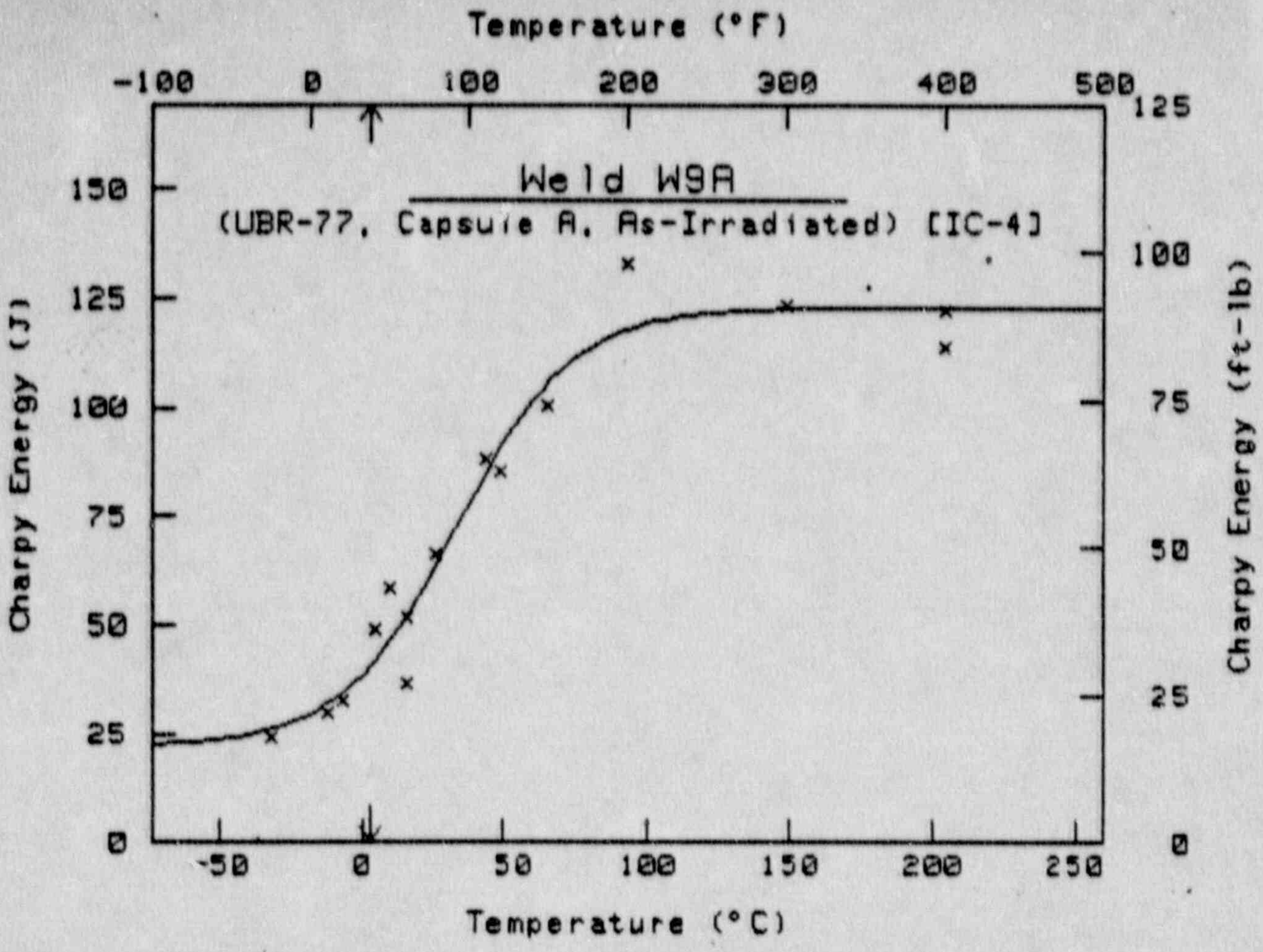

****

Cv = A + B tanh[(T - To)/C]

	English	Metric
A =	53.47 ft-lb	72.49 J
B =	37.20 ft-lb	50.44 J
C =	73.66 °F	40.92 °C
To =	92.33 °F	33.52 °C
Cv = 30 ft-lb (41 J) at T =	37.6 °F	3.1 °C
Upper Shelf Energy =	90.7 ft-lb	122.9 J

****

PT #	Temp (°F)	Energy (ft-lb)
1	-25	18.0
2	10	22.0
3	20	24.0
4	40	36.0
5	50	43.0
6	60	27.0
7	60	38.0
8	80	49.0
9	110	65.0
10	120	63.0
11	150	74.0
12	200	98.0
13	300	91.0
14	400	90.0
15	400	84.0

0 = Fictitious Point Added

* = Test Point Not Included

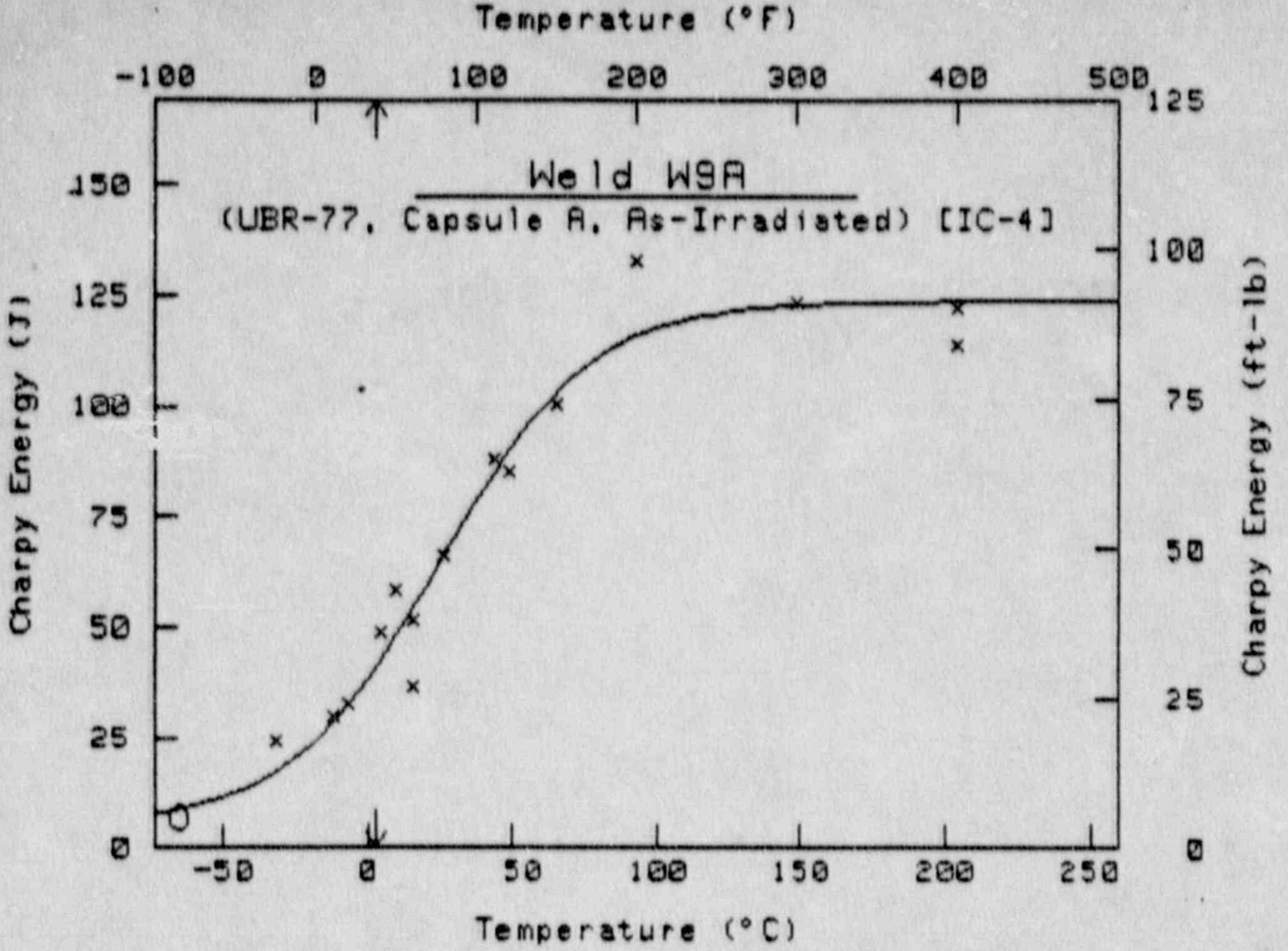

****

Cv = A + B tanh[(T - To)/C]

	English	Metric
A =	47.48 ft-lb	64.37 J
B =	43.80 ft-lb	59.39 J
C =	93.92 °F	52.18 °C
To =	76.47 °F	24.71 °C
Cv = 30 ft-lb (41 J) at T =	36.8 °F	2.7 °C
Upper Shelf Energy =	91.3 ft-lb	123.8 J

****

PT #	Temp (°F)	Energy (ft-lb)	PT #	Temp (°F)	Energy (ft-lb)
1	-25	18.0	11	150	74.0
2	10	22.0	12	200	98.0
3	20	24.0	13	300	91.0
4	40	36.0	14	400	90.0
5	50	43.0	15	400	84.0
6	60	38.0	16 O	-85	5.0
7	60	27.0	17 O	-85	5.0
8	80	49.0	18 O	-85	5.0
9	110	65.0	19 O	-85	5.0
10	120	63.0			

O = Fictitious Point Added   * = Test Point Not Included

APPENDIX E

Fracture Toughness Determinations

Appendix E

FRACTURE TOUGHNESS DETERMINATIONS

1. SPECIMEN DESIGN

The fracture toughness determinations were made using 0.5T-CT specimens with a thickness of 12.7 mm (Fig. E-1). This design is similar to the specimen recommended in ASTM E 813-81 (Ref. E-1) where load-line displacement is measured on the specimen. This specimen size was considered acceptable based upon results from a size effect study, as discussed in Section 7.4 of Ref. E-2. As illustrated in Fig. E-2 for a Linde 0091 weld (code E24), the 0.5T-CT specimen design gives similar J_M-R curves to 1T-CT specimens, but lower J_D levels at large crack growth levels (i.e., $\Delta a > 1$ mm).

Precracking was performed in the preirradiation condition for all tests, with K_{max} below 22 MPa$\sqrt{m}$ for the last 1 mm (0.04 in.). Side grooves were applied only to those specimens for which ductile failure (i.e., J-R curve development) was anticipated. (All specimens of capsule UBR-38 were side-grooved by 20% prior to irradiation.) The side grooving was targeted to a total depth of 2.54 mm, 1.27 mm per side, or 20% of the gross specimen thickness. Side grooving of the irradiated specimens was generally performed prior to irradiation. Razor blades were spot welded to the flats located on the load line, to allow accurate measurement of the load-line displacement.

2. TEST PROCEDURES

Although definition of upper shelf (ductile, J-R curve) and transition (cleavage, K_{Ic} or K_J) behavior was desired in this program, the testing procedures for both types of tests were identical. Specifically, a 50-kN (110-kip) servohydraulic test frame was used, with either a strain-gaged clip gage or a capacitance-type clip gage used for displacement measurements. In all cases, a computerized data acquisition system was used, with digital load-displacement pairs stored on magnetic media for later retrieval or analysis. In addition, an analog load-displacement trace was recorded for each test. The $\dot{K}$ for these tests was ~ 44 MPa$\sqrt{m}$/min, with monotonic loading of the specimen until the ASTM E 399 (Ref. E-3) 5% secant line was intersected, at which time the single specimen compliance (SSC) technique was utilized to track the crack length during the remainder of the test (Refs. E-4 to E-6). Successive crack length determinations were made at intervals sufficient to accurately characterize the J-R curve behavior of the specimen.

After completion of the J-R curve tests, the specimens were heat tinted at ~ 300°C to mark the end of the stable growth, cooled to liquid nitrogen temperature, and then fractured. This procedure allows for an undistorted characterization of the fracture surface, as it was upon test termination. For the unirradiated tests, the resultant crack lengths (initial and final) were measured using a microscope and an X-Y table (accurate to 0.025 mm). The irradiated

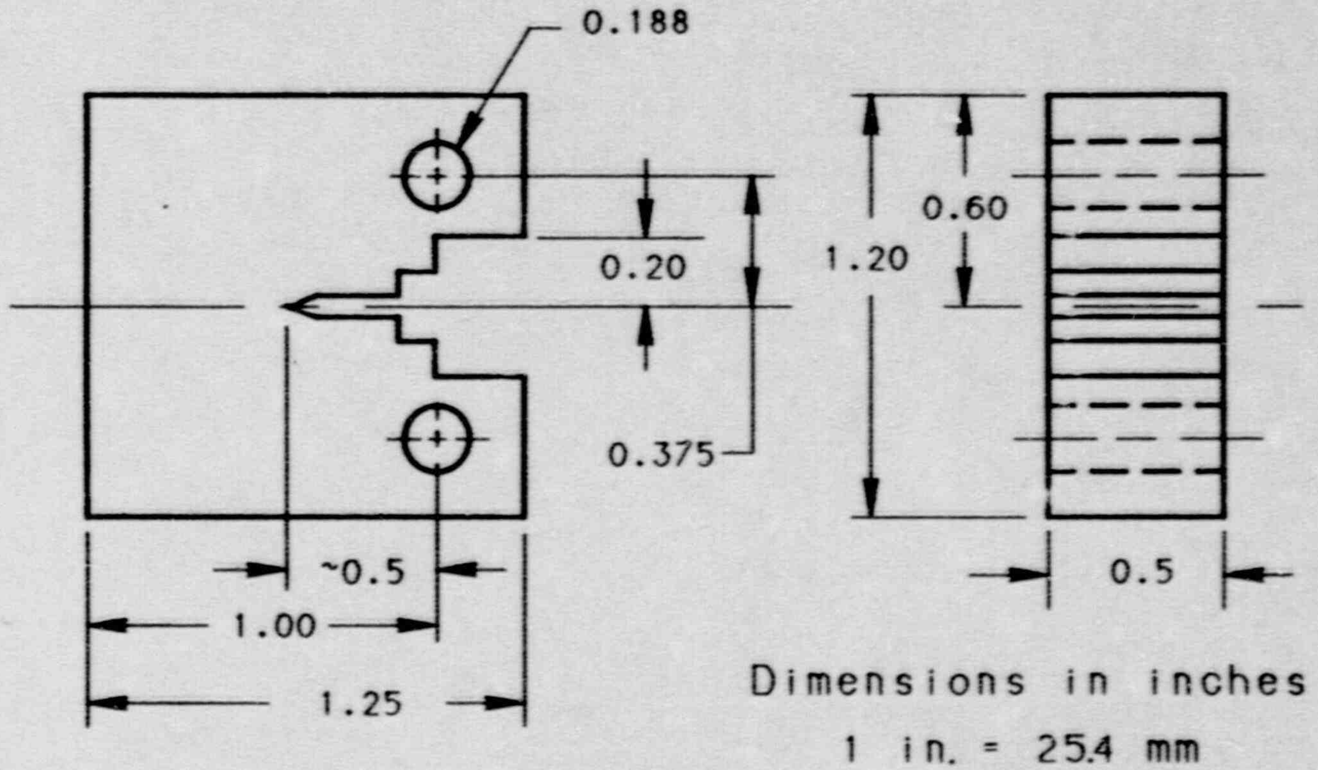

Fig. E-1 The 0.5T-CT specimen design used for the fracture toughness determination.

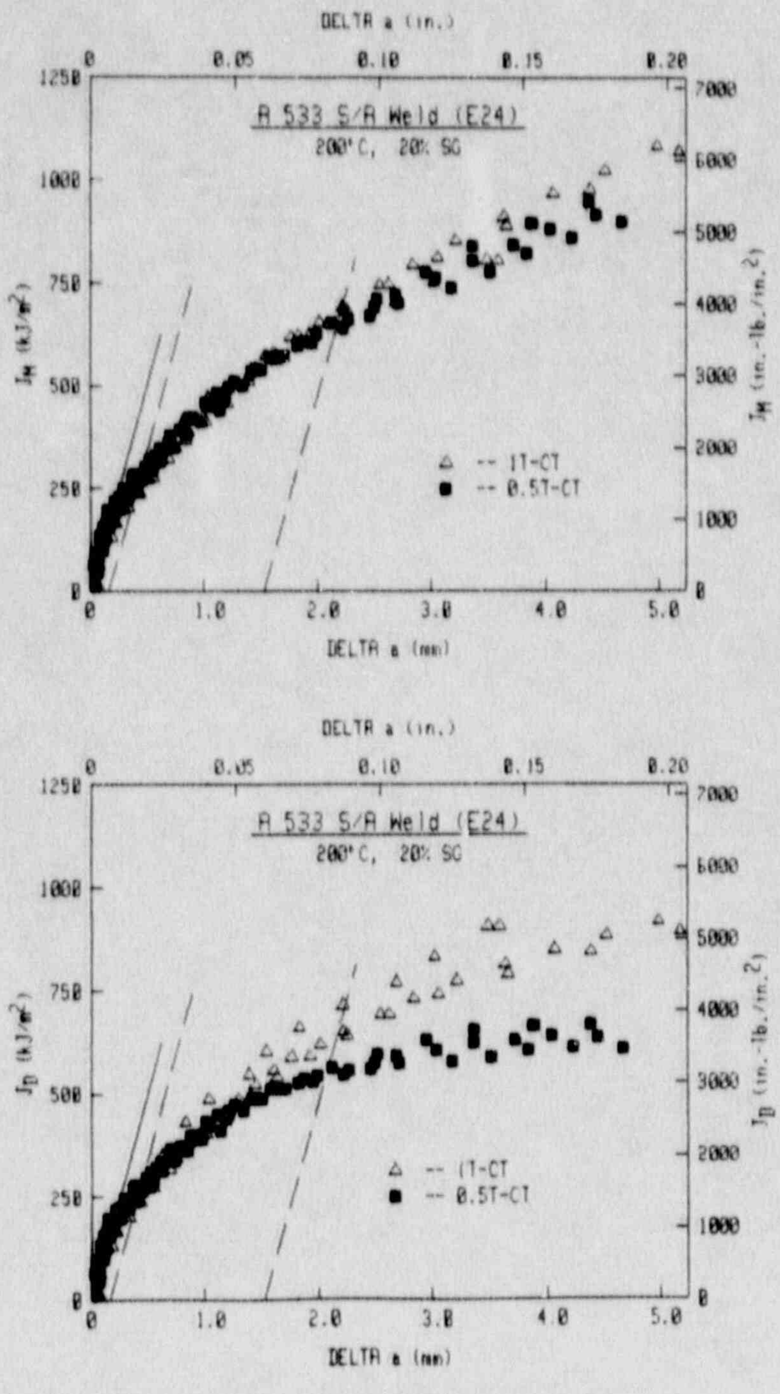

Fig. E-2 The 0.5T-CT specimens give similar J_D and J_M levels to those from 1T-CT specimens at low Δa levels (Δa < 0.5 mm).

fracture surfaces were photographed, with the crack lengths then digitized using an X-Y digitizer. The latter technique has been found accurate to within 0.05 mm, based on optical and photographic measurements of unirradiated fracture surfaces.

3. DATA ANALYSIS PROCEDURES

3.1 Cleavage/No Stable Crack Growth

For those tests resulting in cleavage failure with no stable crack growth, an ASTM E 399 (Ref. E-3) analysis was performed to determine K_Q, and to assess if $K_Q = K_{Ic}$.

In addition, the J integral was used to calculate toughness for these tests. The form of the J integral used was the ASTM E 813-81 (Ref. E-1) form developed by Merkle and Corten (Ref. E-7), as simplified in Ref. E-8:

$$J = \frac{A}{B_N b_o} \; f(a_o/W) \qquad \text{(E-1)}$$

with

$f(a_o/W) = 2(1 + \alpha) / (1 + \alpha^2)$

$\alpha \quad = [(2a_o/b_o)^2 + 2\,(2a_o/b_o) + 2]^{1/2} - (2a_o/b_o + 1)$

$A \quad$ = total area under the load-load line displacement curve

$B_N \quad$ = net specimen thickness

$a_o \quad$ = initial (precrack) crack length

$b_o \quad = W - a_o$

Specifically, the J value at the cleavage point was termed J_{Crit}, and a K_{Jc} value was calculated from

$$K_{Jc} = \sqrt{E\, J_{Crit} / (1 - \nu^2)} \qquad \text{(E-2)}$$

where E is the modulus of elasticity and ν is Poisson's ratio, taken to be 0.3 in all cases. (In the data tables, the J_{Crit} values are listed under J_{Ic}.)

Since the specimens used here were small and precluded the determination of valid K_{Ic} values above 60 $MPa\sqrt{m}$, the K_{Jc} values were adjusted using the Irwin β_{Ic} procedure (Ref. E-9). As recommended by Merkle (Ref. E-10), these tests were conducted in displacement control, cleavage was the failure mode in every case, and conditions at the cleavage point were used to calculate the unadjusted fracture toughness values. The adjusted fracture toughness values, termed $K_{\beta c}$ and thought to provide a better approximation to K_{Ic}, were calculated from:

$$\beta_c = \beta_{Ic} + 1.4\,\beta_{Ic}^{3} \qquad \text{(E-3)}$$

where

$$\beta_c = \frac{1}{B}\left(\frac{K_c}{\sigma_y}\right)^2$$

$$\beta_{Ic} = \frac{1}{B}\left(\frac{K_{\beta c}}{\sigma_y}\right)^2$$

and

σ_y = 0.2% offset yield strength at temperature

K_c = "non-plane strain fracture toughness" = K_{Jc}

$K_{\beta c}$ = to be solved for

Rearranged, Eq. E-3 gives:

$$\beta_{Ic}^{3} + (5/7)\,\beta_{Ic} - (5/7)\,\beta_c = 0 \qquad \text{(E-4)}$$

Several parameters can be defined

$$m = (5/14)\,\beta_c$$

$$A_1 = \sqrt{m^2 + \frac{(5/7)^3}{27}} + m$$

$$A_2 = A_1 - 2m$$

β_{Ic} can be calculated from

$$\beta_{Ic} = A_1^{1/3} - A_2^{1/3}$$

and finally $K_{\beta c} = \sigma_y \sqrt{B\,\beta_{Ic}}$.

Since the magnitude of the β_{Ic} adjustment is inversely proportional to the yield strength, unirradiated data are adjusted significantly more than irradiated data, due to strengthening typically associated with irradiation embrittlement. This in turn results in irradiation-induced transition temperature increases (ΔT's) which should be lower (by definition) than ΔT's from K_{Jc} data. While the β_{Ic} data are reported in the data tables, no other use of the data are made in this report.

3.2 Ductile/Stable Crack Growth

The J integral resistance curve (J-R curve) was used for upper shelf characterizations. The test procedure used was in general conformance with ASTM Standard E 1152-87 (Ref. E-11) and the J_{Ic} test procedure, ASTM E 813-81 (Ref. E-1).

As noted previously, the unloading compliance technique was used for crack length (and crack growth) determinations. For J-integral calculations, the modified J integral, J_M, was used (Ref. E-12):

$$J_M = J_D - \int_{a_o}^{a} \left(\frac{\partial (J_D - G)}{\partial a}\right)_{\delta_{pl}} da \qquad \text{(E-5)}$$

with

- J_D = deformation theory J
- G = Griffith linear elastic energy release rate
- a_o, a = the initial and current crack lengths, respectively
- δ_{Pl} = the plastic part of the displacement

Reference E-6 gives a detailed listing of the computations required to calculate J_M. Additionally, Refs. E-6 and E-12 provide justification for the use of this non-path independent integral whereby small specimen data using J_M are seen to give better corresondence with large specimen data (using path independent J_D or J_M) than do small specimen data using J_D. Since one intent of this study is to develop data relevant to structural integrity applications, J_M is considered the appropriate formulation of the J integral.

The format for the presentation and analysis of these J-R curves is illustrated in Fig. E-3. The left most J_{Ic} value is determined using ASTM E 813-81 procedures (Ref. E-1), whereby selected data are fit to a linear equation, which is then extrapolated back to the blunting line (as given by $J = 2\,\sigma_f\,\Delta a$, with σ_f the flow strength, the average of the yield and ultimate strengths). The intersection of the linear equation and the blunting line is defined as J_Q, which becomes J_{Ic} if various validity criteria are satisfied.

In a similar fashion, the power-law definition of J_{Ic} used in this report is the intersection of the 0.15-mm exclusion line with a power-law fit to the test data. The power law is given by

$$J = C\,\Delta a^n \qquad \text{(E-6)}$$

with C and n determined through regression analysis. This power-law method is considered preferable to the ASTM linear method in that the actual J-R curve behavior is modeled better using the power law than using a linear equation, and power-law intersection represents a true intersection and not an extrapolated intersection. In addition, the cited power law method gives J_{Ic} values which are generally within 10% of the E 813-81 values, instead of the larger differences found with the power law method given in E 813-87, which uses a 0.2 mm offset to define J_{Ic}.

Another parameter used to define J-R curves is the tearing modulus (T), as given by (Ref. E-13):

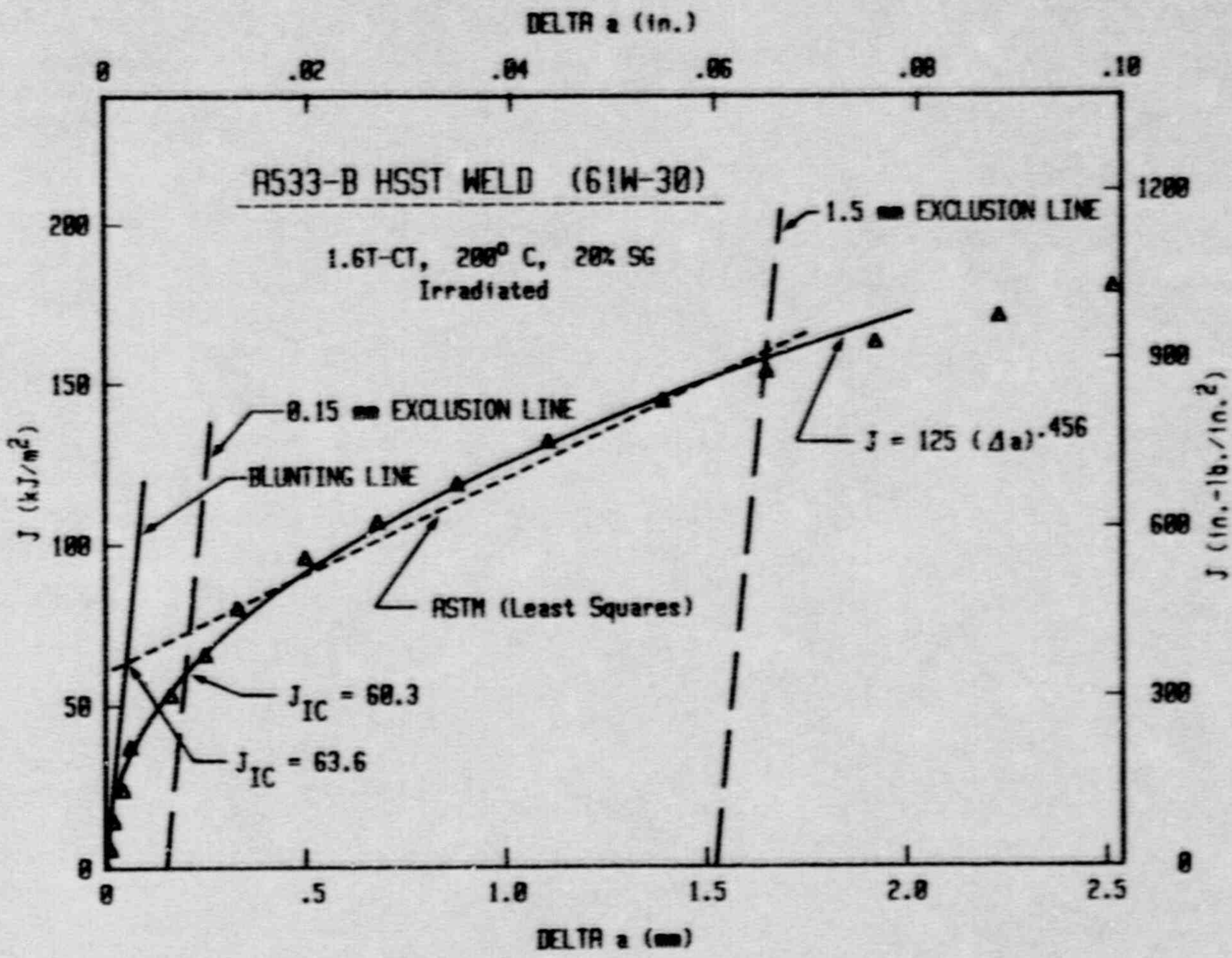

Fig. E-3 The format used for analysis of the J-R curve data.

$$T = \frac{E}{\sigma_f^2} \frac{dJ}{da} \qquad (E\text{-}7)$$

where dJ/da is the slope of the J-R slope. While T changes continuously with crack growth, an average value of T between the 0.15- and 1.5-mm exclusion lines, T_{avg}, has been defined (in Appendix H of Ref. E-6) for use in referencing fracture toughness differences.

4. FRACTURE TOUGHNESS RESULTS

The fracture toughness data will be treated on a material-by-material basis, with comparison of the transition region and upper shelf data made. Each of the irradiation capsules contains specimens from two materials. In all cases the specimens are randomized within the capsule such that there is no fluence bias for one material vis a vis the other.

As a note, validity of fracture toughness data and evaluation of J_{Ic} and T_{avg} require the use of tensile properties, specifically the yield strength (σ_y) and the flow strength (σ_f). For the unirradiated condition, full curves of strength as a function of temperature were made. In contrast, limited testing was possible for the irradiated conditions. To provide strength data at each test temperature, the strength results for the unirradiated condition were fit to a quadratic equation. For the irradiated conditions, the same overall curvature of the strength vs. temperature curve was used (i.e., the same quadratic equation), with the constant (either A_3 or B_3) adjusted to account for differences in strengths between the unirradiated condition and each irradiated condition. The following equations were used for yield (σ_y) and ultimate (σ_u) strength:

$$\sigma_y = A_1 \times T^2 + A_2 \times T + A_3 \text{ MPa}$$

$$\sigma_u = B_1 \times T^2 + B_2 \times T + B_3 \text{ MPa}$$

where T is the test temperature in °C and the resultant strengths are in MPa. The constants A_1, A_2, A_3, B_1, B_2 and B_3 are given for each material and each irradiation capsule in Table E-1.

The transition region fracture toughness data have been curve-fit to an exponential equation of the form:

$$K = D_1 + D_2 \text{ EXP } [(T-T_o)/D_3] \qquad (E\text{-}8)$$

with D_1, D_2 and D_3 constants for each data set as determined through a non-linear regression analysis, and T_o is 0°C or 32°F. Data sheets from this curve-fitting are given in Appendix F for each data set, with the overall results summarized in Table E-2. Included on each sheet are tabulations of the data points used for each fit, along with upper and lower bounds (95%-95% confidence bounds). Although the ideal situation would involve using only those data points exhibiting

Table E-1 Strength Results for Program Materials

		Yield Strength ($\sigma_y = A_1 \times T^2 + A_2 \times T + A_3$)			Ultimate Strength ($\sigma_u = B_1 \times T^2 + B_2 \times T + B_3$)		
Capsule	UBR-	A_1 ($MPa/^{\circ}C^2$)	A_2 ($MPa/^{\circ}C$)	A_3 (MPa)	B_1 ($MPa/^{\circ}C^2$)	B_2 ($MPa/^{\circ}C$)	B_3 (MPa)
				A 302-B Plate (23F)			
Unirrad.	--	0.002651	-0.9574	468.50	0.003063	-0.9838	619.90
CE-1	44	0.002651	-0.9574	529.86	0.003063	-0.9838	697.06
CE-2	46	0.002651	-0.9574	533.89	0.003063	-0.9838	699.83
CE-3	45	0.002651	-0.9574	547.11	0.003063	-0.9838	707.67
IC-1	65	0.002651	-0.9574	502.57	0.003063	-0.9838	663.34
IC-2	75	0.002651	-0.9574	520.37	0.003063	-0.9838	681.90
IC-3	76	0.002651	-0.9574	540.78	0.003063	-0.9838	699.36
IP-1	38	0.002651	-0.9574	508.69	0.003063	-0.9838	669.32
				Linde 80 Weld (W8A)			
Unirrad.	--	0.001987	-0.8086	500.70	0.002431	-0.8158	627.20
CE-1	44	0.001987	-0.8086	646.39	0.002431	-0.8158	743.94
CE-2	46	0.001987	-0.8086	652.82	0.002431	-0.8158	754.18
CE-3	45	0.001987	-0.8086	682.49	0.002431	-0.8158	768.46
IC-1	65	0.001987	-0.8086	606.07	0.002431	-0.8158	707.88
IC-2	75	0.001987	-0.8086	633.48	0.002431	-0.8158	729.95
IC-3	76	0.001987	-0.8086	662.54	0.002431	-0.8158	750.17
				A 533-B Plate (23G)			
Unirrad.	--	0.001381	-0.5984	449.40	0.002822	-0.9007	608.00
IP-1	38	0.001381	-0.5984	549.65	0.002822	-0.9007	698.67
IC-4	77	0.001381	-0.5984	501.38	0.002822	-0.9007	655.56
				Linde 0091 Weld (W9A)			
Unirrad.	--	0.002542	-1.1200	589.40	0.002214	-0.8457	672.50
IC-4	77	0.002542	-1.1200	698.22	0.002214	-0.8457	764.21

Table E-2 Transition Temperature Curve-Fit Results

Capsule	Fluence (b)	$K = D_0 + D_1 \, EXP[(T-T_o)/D_2]$[a] D_0 $(MPa\sqrt{m})$	D_1 $(MPa\sqrt{m})$	D_2 $(^\circ C)$	Temperature at 100 $MPa\sqrt{m}$ Mean Curve $(^\circ C)$	Lower Bound $(^\circ C)$	Shift at 100 $MPa\sqrt{m}$ $(^\circ C)$
				A 302-B Plate (23F)			
Unirrad.	----	34.31	211.21	37.31	-44	-37	--
IP-1	0.57	64.71	16.64	21.25	16	21	60
CE-1	0.88	62.37	5.06	15.66	31	37	75
CE-2	1.64	4.90	70.51	109.48	33	40	77
CE-3	4.01	-21.45	94.06	118.56	30	46	74
IC-1	0.53	-94.80	209.40	175.56	-13	2	31
IC-2	1.02	-41.11	129.66	103.43	9	21	53
IC-3	1.95	37.03	26.47	46.09	40	--[c]	84
				Linde 80 Weld (W8A)			
Unirrad.	----	-30.21	188.13	164.52	-61	-41	---
CE-1	0.88	45.32	10.88	42.56	69	75	130
CE-2	1.64	44.49	12.18	52.99	80	--	141
CE-3	4.01	51.10	7.49	34.95	66	--	127
IC-1	0.53	25.58	48.46	50.23	22	40	83
IC-2	1.02	44.93	13.89	36.91	51	61	112
IC-3	1.95	-49.78	93.48	154.78	73	97	134
				A 533-B Plate (23G)			
Unirrad.	----	29.21	276.59	60.83	-83	-75	--
IP-1	0.57	41.25	51.03	50.92	7	26	90
IC-4	0.47	30.60	131.34	84.53	-54	-38	29
				Linde 0091 Weld (W9A)			
Unirrad.	----	22.40	519.22	44.24	-84	-77	--
IC-4	0.47	13.69	91.27	94.29	-5	-1	79

a T_o is $0^\circ C$ or $32^\circ F$

b 10^{19} n/cm^2 (E > 1 MeV)

c Lower bound does not reach this level

cleavage fracture with no ductile crack growth in this curve-fitting, in some cases one or more of the tests exhibiting ductile crack growth are also used to provide an improved fit. In all cases, the trend curves illustrated with the K_{Jc} data are from curve-fitting to Eq. E-8.

4.1 A 302-B Plate (23F)

This plate was tested in all three fluence rate levels, with one IP, three CE, and three IC conditions. Detailed data for all of these irradiation conditions and the unirradiated condition are given in Table E-3.

Comparison of the J-R curves for the unirradiated condition of this plate are illustrated in Fig. E-4. As expected, increasing the test temperature tends to result in reduced J levels, although two curves at 288°C exhibit moderate differences and bound the curve at 200°C.

In addition to the post-irradiation data included in this report, several other sets of irradiated data for this plate are reported in Refs. E-14 and E-15. From Ref. E-14 (the NRC's LWR-SDIP), Simulated Surveillance Capsules (SSC) were irradiated at a fluence rate of ~ 7 x 10^{12} $n/cm^2 \cdot s^{-1}$, slightly lower than the fluence rate of ~ 9 x 10^{12} $n/cm^2 \cdot s^{-1}$ for the IC irradiations. The In-Wall capsules were irradiated at a fluence rate of 2-8 x 10^{11} $n/cm^2 \cdot s^{-1}$, bounding the 5-6 x 10^{11} $n/cm^2 \cdot s^{-1}$ for the CE irradiations. The irradiated data from Ref. E-15 for this plate is also from an in-core irradiation at UBR. These previous irradiation data were from the plate 1/4T and 3/4T thickness locations, in contrast to the 1/2T location used for these fluence rate assessments.

4.1.1 High Fluence Rate (IC)

Comparisons of the K_{Jc} data for the IC conditions and the unirradiated condition are illustrated in Fig. E-5. As expected, increasing the fluence results in a higher transition temperature shift, as illustrated in Fig. E-6. In contrast, the upper shelf K_{Jc} data do not demonstrate similar ordering.

The J-R curves for each irradiation condition are compared in Figs. E-7 to E-9. Tests at temperatures below 200°C were made with plane-sided specimens, resulting in somewhat of an artificial elevation of those curves in comparison to those from side-grooved specimens. In each case, higher test temperature tends to result in reduced J levels, with tests at 200°C and 288°C generally yielding similar trends. Comparisons of the J-R curves for all three irradiation conditions at 200°C and 288° (Figs. E-10 and E-11) indicate no consistent trends, as all three conditions yield similar J levels to those for the unirradiated condition (all conditions give curves which appear to be from a common scatter band).

(text continues on pg. E-24)

Table E-3 Fracture Toughness Data for A 302-B Plate (23F) (continued)

Specimen Number	Test Temp (°C)	$(a/W)_o$ [a]	Δa_m [b] (mm)	Δa_p [c] (mm)	$\Delta a_p - \Delta a_m$ (mm)	J_{Ic} P.L. (kJ/m^2)	J_{Ic} ASTM (kJ/m^2)	K_{Jc} P.L. ($MPa\sqrt{m}$)	K_{Jc} ASTM ($MPa\sqrt{m}$)	$K_{\beta c}$ ($MPa\sqrt{m}$)	K_{max} ($MPa\sqrt{m}$)	T_{avg}	σ_f (MPa)	σ_y (MPa)
IRRADIATED CE-1 (UBR-44)														
23F-2	-75	0.542	—	—	—	12.7	—	54.3	55.5	47.5	55.5	—	702.3	616.6
23F-83	-20	0.506	—	—	—	19.7	—	67.1	49.4	51.8	63.5	—	634.0	550.1
23F-39	10	0.511	—	—	—	34.9	—	89.0	49.7	58.1	77.5	—	604.0	520.6
23F-77	20	0.512	—	—	—	20.4	—	68.0	52.8	50.4	64.4	—	595.2	511.8
23F-102	29	0.538	—	—	—	39.2	—	94.1	57.4	58.6	81.4	—	587.7	504.3
23F-62	31	0.518	— [g]	— [g]	— [g]	143.7	—	180.1	—	—	—	—	586.1	502.7
23F-43	44	0.518	— [g]	— [g]	— [g]	165.9	—	193.2	—	—	—	—	576.3	492.9
23F-117	45	0.504	—	—	—	103.7	—	152.8	57.9	70.6	91.0	—	575.6	492.1
23F-24	60	0.496	2.96	2.80	-0.16	151.0	131.5 [f]	183.9	171.6	—	—	114	565.5	482.0
23F-99 [d]	80	0.517	6.66	6.17	-0.49	136.3	151.8 [f]	174.2	183.9	—	—	55	554.1	470.2
23F-17 [d]	288	0.524	6.60	6.23	-0.37	82.2	87.0 [f]	131.3	135.1	—	—	32	570.9	474.0
23F-58 [d]	288	0.515	5.91	5.72	-0.19	58.4	53.8 [f]	110.6	106.2	—	—	42	570.9	474.0
IRRADIATED CE-2 (UBR-46)														
23F-19	-100	0.507	—	—	—	3.9	—	30.4	29.4 [g]	29.8	29.4	—	742.5	656.1
23F-98	-40	0.515	—	—	—	15.3	—	59.4	52.0	49.2	55.4	—	660.3	576.4
23F-64	0	0.533	—	—	—	28.2	—	80.2	53.8	56.0	76.4	—	616.9	539.9
23F-42	20	0.492	—	—	—	27.8	—	79.4	46.9	54.8	69.2	—	598.6	515.8
23F-119	28	0.513	—	—	—	37.9	—	92.6	42.3	58.5	82.7	—	591.9	509.2
23F-38	45	0.527	—	—	—	59.7	—	115.9	51.2	63.5	88.2	—	579.0	496.2
23F-4	47	0.519	—	—	—	58.3	—	114.5	48.7	63.1	87.6	—	577.5	494.7
23F-101	50	0.533	5.69	4.83	-0.86	145.5	104.2	180.8	153.0	—	—	152	575.5	492.6
23F-86	70	0.518	4.98	4.82	-0.16	91.0	61.4 [f]	142.6	117.0	—	—	131	562.9	479.9
23F-23 [d]	90	0.526	6.90	6.13	-0.77	147.5	145.8 [f]	181.0	179.9	—	—	54	552.6	469.2
23F-57 [d]	288	0.531	6.90	6.42	-0.48	87.1	87.6 [f]	135.2	135.5	—	—	31	574.3	478.0
23F-79 [d]	288	0.529	7.37	6.91	-0.46	87.2	87.1 [f]	135.2	135.1	—	—	37	574.3	478.0

[a] Pre-test a/W.
[b] Optically-measured crack growth.
[c] Crack growth predicted by compliance.
[d] Side grooved.
[e] Valid K_{Ic} per ASTM E 399.
[f] Valid J_{Ic} per ASTM E 813-81.
[g] Cleavage failure precluded determination of this quantity.

Specimen Number	Test Temp (°C)	$(a/W)_o$[a]	Δa_m[b] (mm)	Δa_p[c] (mm)	$\Delta a_p - \Delta a_m$ (mm)	P.L. (kJ/m^2)	ASTM (kJ/m^2)	P.L. ($MPa\sqrt{m}$)	ASTM ($MPa\sqrt{m}$)	K_{Bc} ($MPa\sqrt{m}$)	K_{max} ($MPa\sqrt{m}$)	T_{avg}	σ_f (MPa)	σ_y (MPa)
UNIRRADIATED														
23F-1	-129	0.522	—	—	—	4.5	—	32.4	32.3[e]	31.6	32.3	—	705.5	638.1
23F-104	-96	0.506	—	—	—	12.3	—	53.6	46.8	46.6	51.3	—	662.3	596.6
23F-84	-73	0.531	—	—	—	23.9	—	74.5	47.6	55.7	67.4	—	635.0	570.3
23F-66	-57	0.525	—	—	—	38.1	—	93.9	44.4	61.5	74.6	—	617.4	553.2
23F-16	-43	0.517	—	—	—	32.9	—	87.1	45.2	58.6	71.6	—	603.0	539.1
23F-60	-37	0.521	—	—	—	40.6	—	96.6	35.6	61.1	75.1	—	597.0	533.3
23F-34	-34	0.508	—	—	—	58.6	—	116.1	43.0	66.1	79.7	—	594.1	530.5
23F-100	-26	0.519	—	—	—	103.4	—	154.0	44.1	73.5	81.2	—	586.6	523.1
23F-30	-18	0.515	—[g]	—[g]	—[g]	238.7	—	233.7	—	—	—	—	579.3	515.9
23F-5[d]	-1	0.512	—[g]	—[g]	—[g]	191.2	—	208.7	—	—	—	—	564.8	501.5
23F-80[d]	93	0.526	6.18	5.27	-0.5[illegible]	115.6	118.1[f]	160.2	161.9	—	—	89	507.5	442.7
23F-94[d]	204	0.535	6.79	6.12	-0.6[illegible]	90.6	91.9[f]	139.5	140.5	—	—	62	490.2	418.4
23F-46[d]	288	0.526	6.68	6.15	-0.53	92.4	91.8[f]	139.2	138.8	—	—	54	513.3	432.6
23F-110[d]	288	0.528	6.38	6.20	-0.18	86.5	84.2[f]	134.6	132.9	—	—	51	513.3	432.6
IRRADIATED IP-1 (UBR-38)														
23F-115[d]	-50	0.507	—	—	—	22.6	—	72.2	52.1	51.6	65.4	—	644.7	563.2
23F-55[d]	-25	0.515	—	—	—	16.5	—	61.4	49.8	46.3	57.3	—	615.1	534.3
23F-35[d]	0	0.510	—	—	—	26.3	—	77.4	52.0	50.7	68.0	—	589.0	508.7
23F-25[d]	10	0.509	—	—	—	45.3	—	101.4	51.8	56.5	81.2	—	579.6	499.4
23F-15[d]	20	0.514	—	—	—	49.4	—	105.8	52.2	56.9	83.8	—	570.7	490.6
23F-105[d]	31	0.504	—	—	—	78.7	—	133.3	52.8	61.7	91.3	—	561.7	481.6
23F-85[d]	42	0.507	—	—	—	65.6	—	121.6	53.6	58.9	86.7	—	553.3	473.2
23F-45[d]	50	0.522	—[g]	—[g]	-1.05	155.6	169.0	186.9	194.8	—	—	94	547.6	467.4
23F-75[d]	55	0.502	6.54	5.99	-0.55	141.1	135.7[f]	177.9	174.5	—	—	87	544.6	464.4
23F-6[d]	200	0.514	7.29	6.19	-1.10	103.7	102.6	149.4	148.6	—	—	48	509.2	423.2
23F-65[d]	288	0.521	6.05	5.76	-0.29	88.0	84.3[f]	135.8	132.9	—	—	42	546.4	452.8

a Pre-test a/W.
b Optically-measured crack growth.
c Crack growth predicted by compliance.

d Side grooved.
e Valid K_{Ic} per ASTM E 399.
f Valid J_{Ic} per ASTM E 813-81.

g Cleavage failure precluded determination of this quantity.

Crack growth predicted by compliance.

Valid K_{Ic} per ASTM E 399.
f Valid J_{Ic} per ASTM E 813-81.

Cleavage failure precluded determination of this quantity.

Table E-3 Fracture Toughness Data for A 302-B Plate (23F) (continued)

Specimen Number	Test Temp (°C)	$(a/W)_o$ [a]	Δa_m [b] (mm)	Δa_p [c] (mm)	$\Delta a_p - \Delta a_m$ (mm)	J_{Ic} P.L. (kJ/m^2)	J_{Ic} ASTM (kJ/m^2)	K_{Jc} P.L. (MPa$\sqrt{m}$)	K_{Jc} ASTM (MPa$\sqrt{m}$)	$K_{\beta c}$ (MPa$\sqrt{m}$)	K_{max} (MPa$\sqrt{m}$)	T_{avg}	σ_f (MPa)	σ_y (MPa)
IRRADIATED CE-3 (UBR-45)														
23F-37	-40	0.530	—	—	—	9.7	—	47.3	48.0	42.6	48.0	—	670.8	589.6
23F-118	-20	0.530	—	—	—	9.7	—	47.2	47.3	42.0	47.3	—	647.9	567.3
23F-82	0	0.531	—	—	—	33.5	—	87.4	40.8	59.1	74.4	—	627.4	547.1
23F-59	25	0.524	—	—	—	31.9	—	85.0	49.4	57.1	76.2	—	604.9	524.8
23F-103	40	0.524	—	—	—	91.4	—	143.5	51.4	70.7	93.2	—	593.1	513.1
23F-18	45	0.508	—	—	—	45.2	—	100.9	47.4	60.8	81.7	—	589.5	509.4
23F-3	50	0.513	—	—	—	42.7	—	98.0	47.4	59.8	81.3	—	586.0	505.9
23F-97	65	0.524	6.35	5.22	-1.13	102.3	67.5	151.3	122.9	—	—	133	576.4	496.1
23F-44	70	0.513	7.09	5.77	-1.32	108.2	56.5	155.4	112.3	—	—	120	573.4	493.1
23F-22	80	0.533	5.58	5.32	-0.26	132.0	72.7[f]	171.4	127.2	—	—	103	568.0	487.5
23F-63[d]	204	0.520	6.17	5.80	-0.37	85.8	89.4[f]	135.8	138.5	—	—	45	548.3	462.1
23F-78[d]	288	0.527	7.04	6.17	-0.87	61.0	56.4[f]	113.1	108.7	—	—	24	584.8	491.3
IRRADIATED IC-1 (UBR-65)														
23F-12	-80	0.492	—	—	—	6.8	—	39.7	37.7	37.3	37.7	—	678.9	596.1
23F-33	-45	0.492	—	—	—	17.4	—	63.4	52.2	50.2	57.5	—	632.4	551.0
23F-52	-20	0.505	—	—	—	40.1	—	95.9	48.2	60.3	79.2	—	603.5	522.8
23F-29	-5	0.498	—	—	—	42.7	—	98.7	47.6	60.0	77.0	—	587.9	507.4
23F-89	5	0.503	—	—	—	87.5	—	141.1	50.7	68.9	89.2	—	578.2	497.8
23F-48	10	0.509	—	—	—	45.5	—	101.7	48.0	59.9	82.7	—	573.5	493.3
23F-108	20	0.496	—[g]	—[g]	—[g]	132.3	—[g]	173.1	—[g]	—	—	—	564.7	484.5
23F-7	26	0.504	—	—	—	72.2	—	127.8	51.0	64.8	85.7	—	560.5	480.3
23F-72	50	0.505	5.08	3.89	-1.19	148.6	90.9	182.7	142.9	—	—	186	541.6	461.7
23F-91[d]	204	0.504	6.57	6.25	-0.32	92.7	84.3[f]	141.1	134.6	—	—	60	503.8	417.6
23F-67[d]	288	0.521	6.49	6.12	-0.37	78.3	95.8[f]	128.1	141.7	—	—	35	540.4	446.7
23F-113[d]	288	0.511	6.97	6.31	-0.66	87.8	91.0[f]	135.7	138.1	—	—	44	540.4	446.7

[a] Pre-test a/W.
[b] Optically-measured crack growth.
[c] Crack growth predicted by compliance.
[d] Side grooved.
[e] Valid K_{Ic} per ASTM E 399.
[f] Valid J_{Ic} per ASTM E 813-81.
[g] Cleavage failure precluded determination of this quantity.

Table E-3 Fracture Toughness Data for A 302-B Plate (23F) (continued)

Specimen Number	Test Temp (°C)	$(a/W)_o$[a]	Δa_m[b] (mm)	Δa_p[c] (mm)	$\Delta a_p - \Delta a_m$ (mm)	J_{Ic} P.L. (kJ/m^2)	J_{Ic} ASTM (kJ/m^2)	K_{Jc} P.L. ($MPa\sqrt{m}$)	K_{Jc} ASTM ($MPa\sqrt{m}$)	K_{Bc} ($MPa\sqrt{m}$)	K_{max} ($MPa\sqrt{m}$)	T_{avg}	σ_f (MPa)	σ_y (MPa)
IRRADIATED IC-2 (UBR-75)														
23F-8	-50	0.498	—	—	—	4.0	—	30.6	30.3[e]	29.7	30.3	—	656.8	574.9
23F-73	-20	0.505	—	—	—	20.4	—	68.3	49.9	51.9	63.1	—	621.7	540.6
23F-49	-18	0.504	—	—	—	34.1	—	88.4	53.0	59.0	73.8	—	619.5	538.5
23F-31	5	0.506	—	—	—	46.6	—	103.0	53.9	61.7	82.7	—	596.4	515.6
23F-13	12	0.489	—	—	—	18.2	—	64.2	50.9	48.8	58.6	—	589.9	509.3
23F-87[d]	21	0.500	—	—	—	73.6	—	129.1	43.0	62.5	90.1	—	582.0	501.4
23F-68	32	0.487	—	—	—	78.4	—	133.1	56.0	66.9	89.3	—	573.0	492.4
23F-54	45	0.493	9.81	6.50	-3.31	149.2	126.7	183.1	168.8	—	—	140	563.2	482.7
23F-92	50	0.511	—[g]	—[g]	—[g]	105.3	—[g]	153.8	—[g]	—	—	—	559.7	479.1
23F-114	55	0.500	8.08	6.64	-1.44	167.4	122.6	193.8	165.8	—	—	163	556.4	475.7
23F-109[d]	200	0.507	6.68	6.08	-0.60	101.2	99.8[f]	147.6	146.5	—	—	53	521.3	434.9
23F-27[d]	288	0.512	6.58	5.67	-0.91	84.2	86.2[f]	132.8	134.4	—	—	37	558.6	464.5
IRRADIATED IC-3 (UBR-76)														
23F-9	-25	0.505	—	—	—	12.2	—	52.9	50.8	45.4	52.1	—	646.1	566.4
23F-28	0	0.503	—	—	—	19.7	—	66.9	48.9	51.3	60.9	—	620.1	540.8
23F-93	25	0.497	—	—	—	30.1	—	82.5	52.0	55.9	72.5	—	597.6	518.5
23F-69	32	0.495	—	—	—	25.1	—	75.2	49.1	53.2	69.8	—	591.9	512.9
23F-107	41	0.498	—	—	—	37.9	—	92.4	48.5	58.2	80.3	—	585.1	506.0
23F-74	50	0.489	7.86	6.01	-1.85	126.2	83.8	168.4	137.2	—	—	139	578.7	499.5
23F-112	55	0.505	—	—	—	37.1	—	91.3	52.4	57.3	80.3	—	575.3	496.1
23F-51	65	0.497	7.44	5.76	-1.68	140.9	107.9	177.5	155.3	—	—	140	569.1	489.7
23F-47	65	0.499	7.52	6.30	-1.22	150.3	123.4	183.3	166.1	—	—	134	569.1	489.7
23F-14	75	0.508	7.45	6.25	-1.20	146.8	111.7	180.9	157.6	—	—	155	563.3	485.9
23F-66[d]	200	0.510	6.05	5.86	-0.19	106.4	95.7[f]	151.3	143.5	—	—	36	540.2	455.3
23F-32[d]	288	0.527	6.11	6.07	-0.04	123.5	120.8[f]	160.9	159.1	—	—	36	577.5	484.9

a Pre-test a/W.
b Optically-measured crack growth.
c Crack growth predicted by compliance.
d Side grooved.
e Valid K_{Ic} per ASTM E 399.
f Valid J_{Ic} per ASTM E 813-81.
g Cleavage failure precluded determination of this quantity.

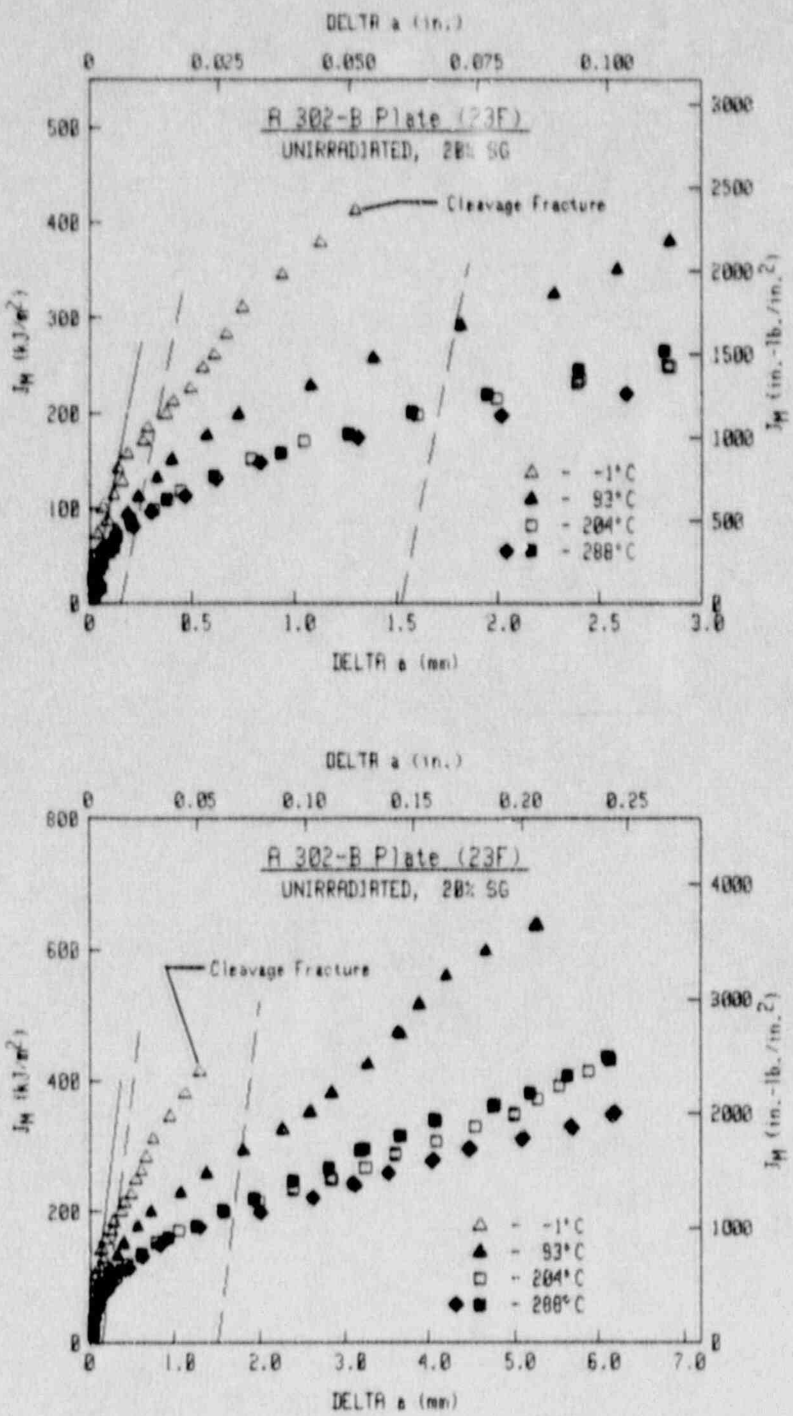

Fig. E-4 J-R curves for the unirradiated condition of A 302-B Plate 23F.

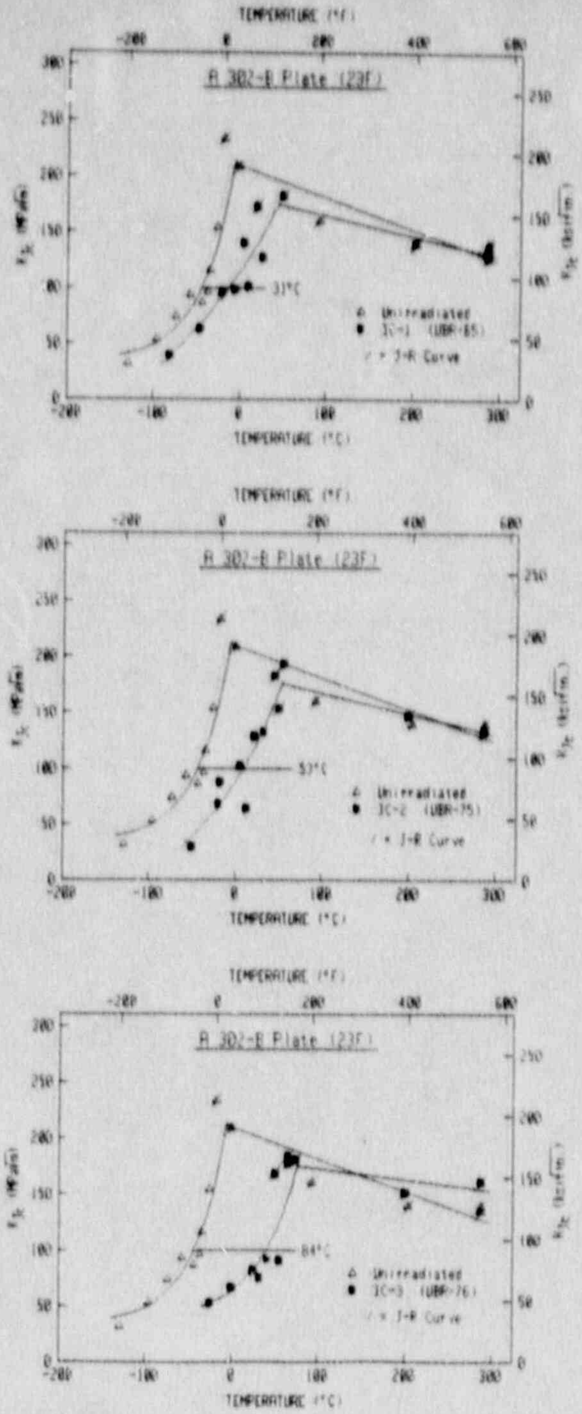

Fig. E-5 Comparisons of K_{Jc} data for the unirradiated condition and the high fluence rate (IC) irradiated conditions of the A 302-B Plate 23F.

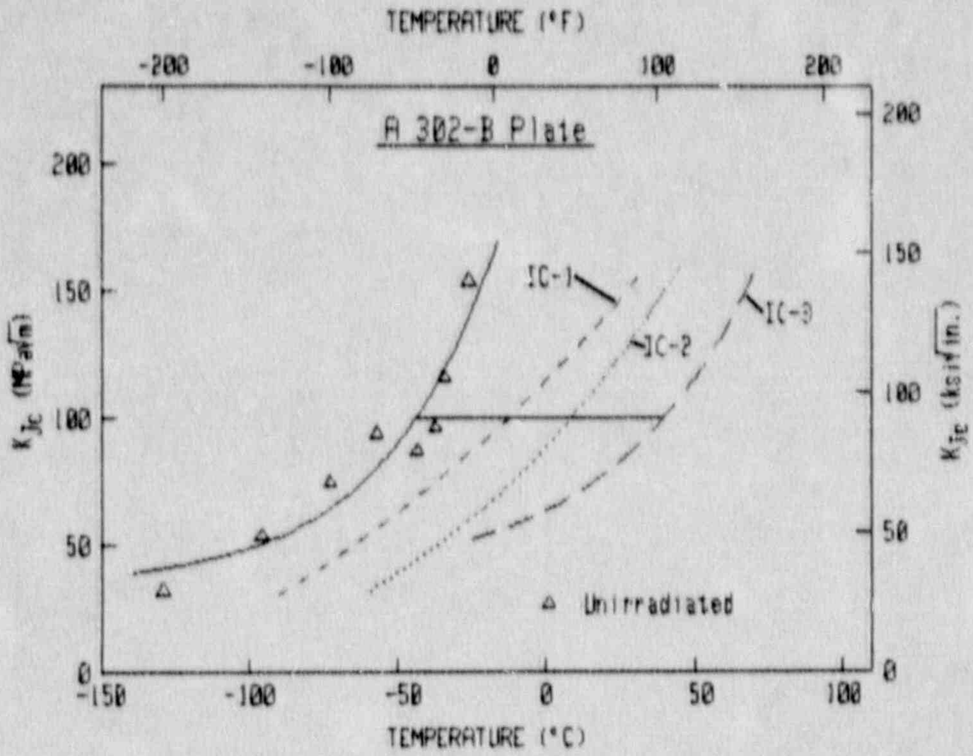

Fig. E-6 Comparison of the curve-fit results for the three high fluence rate (IC) irradiated conditions.

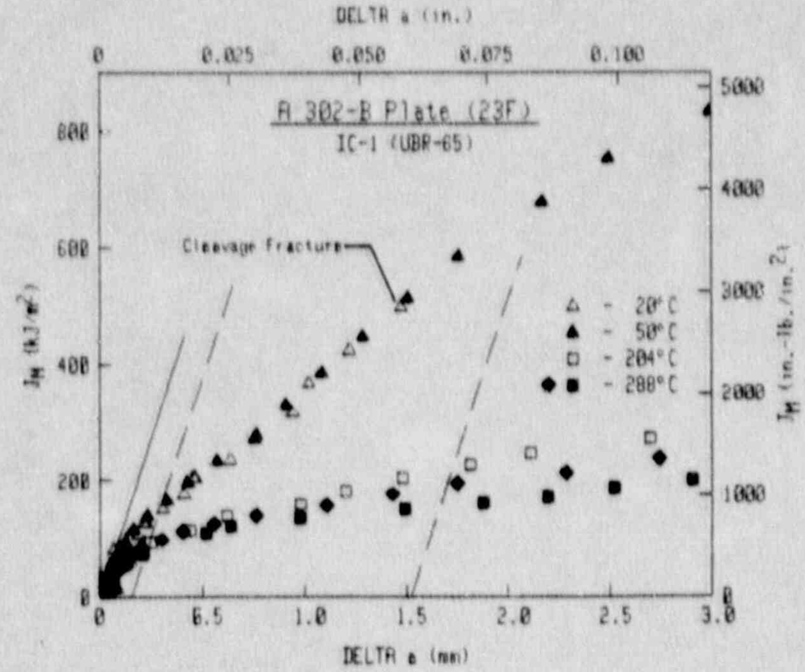

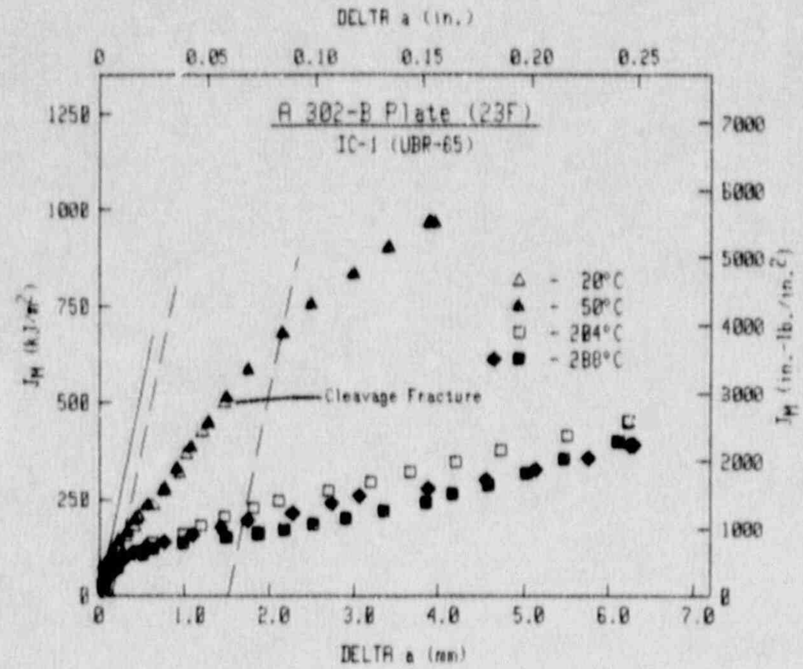

Fig. E-7 J-R curves for the IC-1 (UBR-65) irradiated condition of A 302-B Plate 23F.

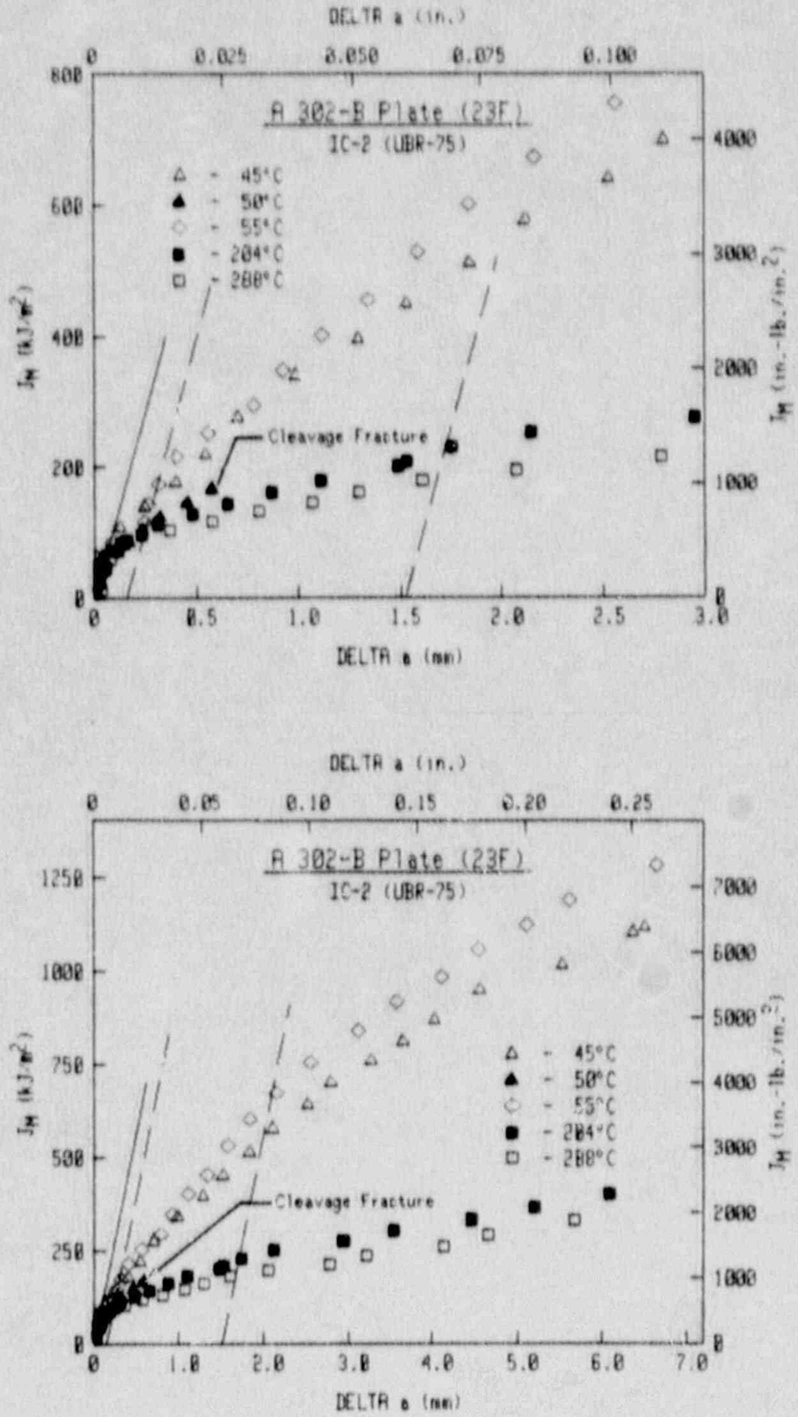

Fig. E-8 J-R curves for the IC-2 (UBR-75) irradiated condition of A 302-B Plate 23F.

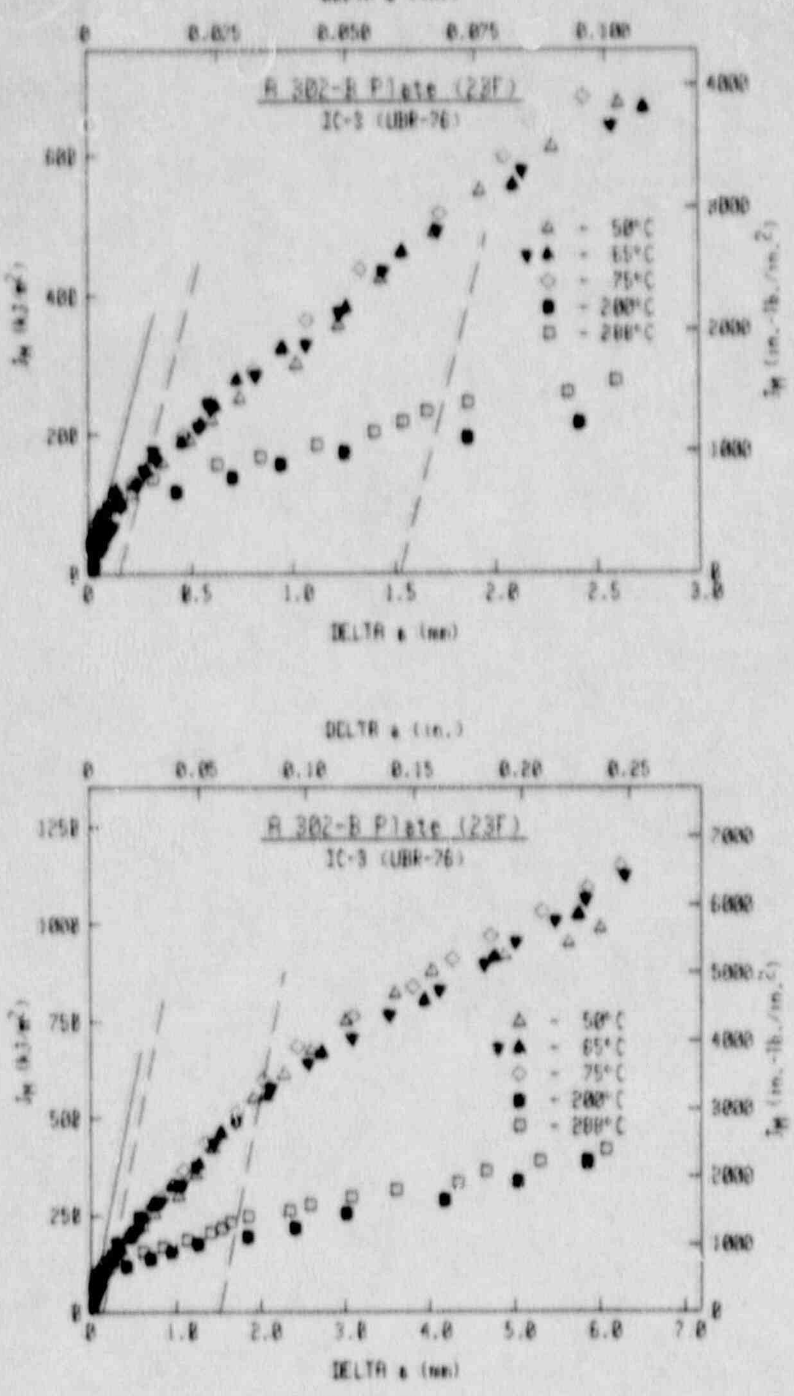

Fig. E-9 J-R curves for the IC-3 (UBR-76) irradiated condition of A 302-B Plate 23F.

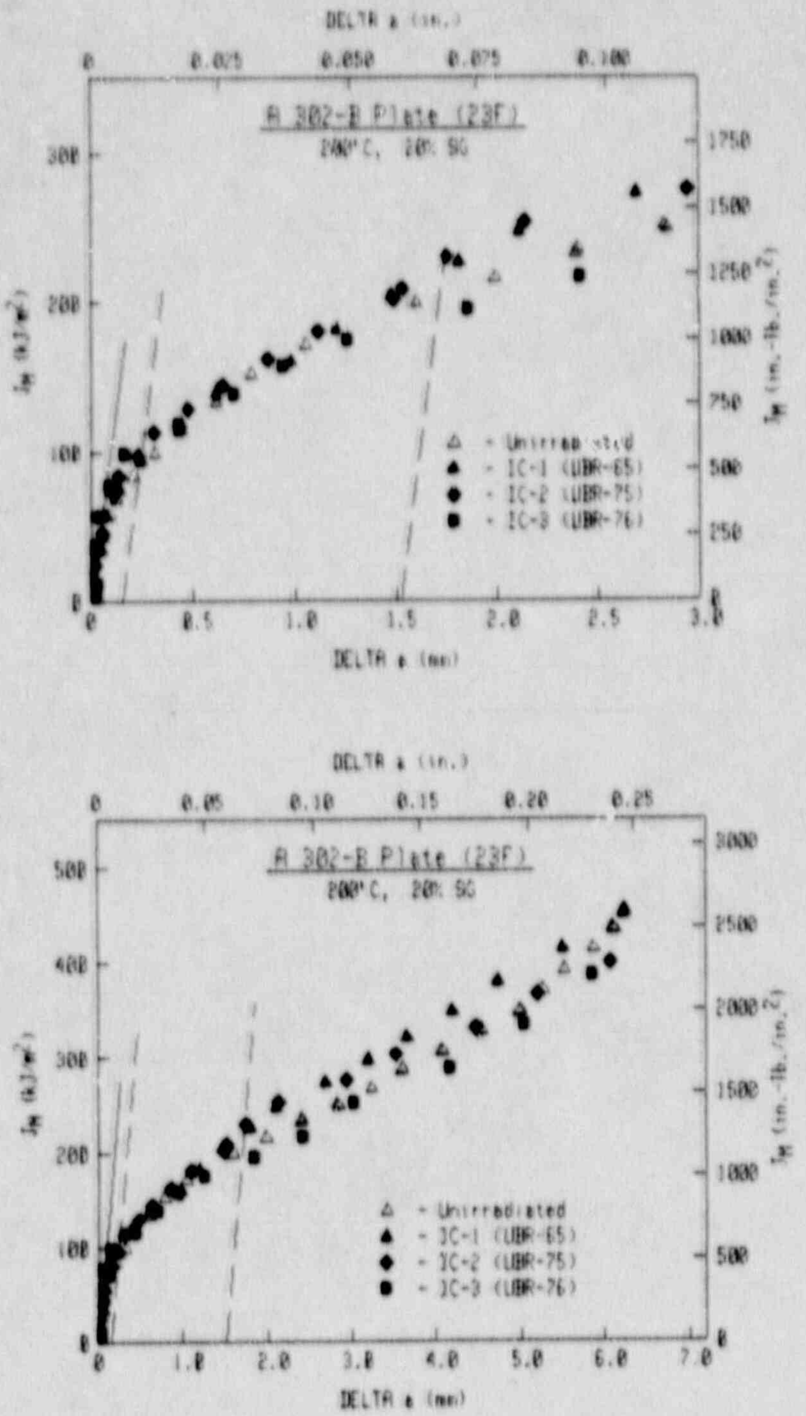

Fig. E-10 Comparison of J-R curves at 200°C from the unirradiated condition and the high fluence rate (IC) irradiated conditions of the A 302-B Plate 23F.

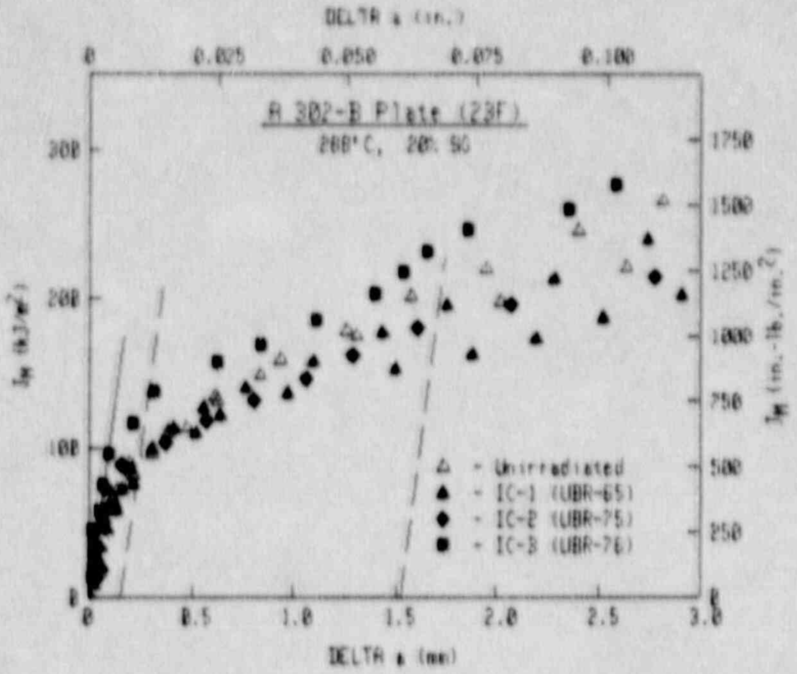

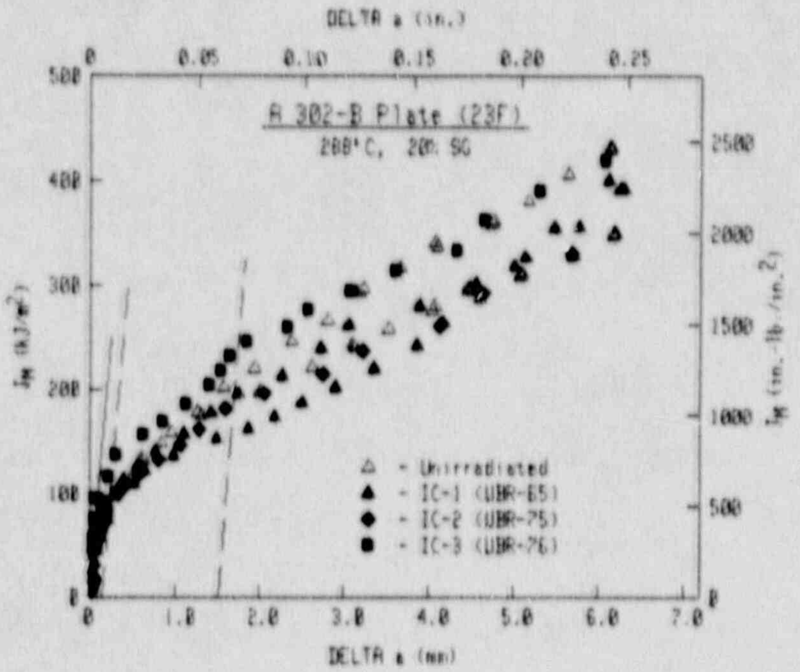

Fig. E-11 Comparison of J-R curves at 288 °C from the unirradiated condition and the high fluence rate (IC) irradiated conditions of the A 302-B Plate 23F.

4.1.2 Intermediate Fluence Rate (CE)

In contrast to the generally consistent results evident for the high fluence rate (IC) data, data for the intermediate fluence rate (CE) are not as well-behaved. Comparisons of the K_{Jc} data for each of the CE conditions and the unirradiated condition are illustrated in Fig. E-12, with all of the irradiated conditions compared in Fig. E-13. All three of the CE data sets demonstrate similar trends within the transition region (indicative of an embrittlement-saturation "plateau" phenomenon), surprising given the large fluence differences among the three capsules (a factor of 4 between CE-1 and CE-3). Data scatter is not too severe, even for CE-1 (UBR-44) where the fluence varies by a factor of ~ 2 for the extremes in the capsule (this capsule was not rotated at mid-exposure as the others were).

The indicated saturation of embrittlement for this plate is not expected, given previous results with similar or higher fluence rates at higher fluences (Ref. E-14). One consequence of the CE-1 data is a very rapid initial embrittlement for this plate, with minimal additional embrittlement after subsequent irradiation time. The irradiations themselves appear to have been performed in a satisfactory fashion, except for CE-1, UBR-44, which has a large fluence gradient. Additional irradiations at this fluence rate to low and high total fluences similar to those of CE-1 and CE-3 would help to confirm the trend fully.

The J-R curve trends for the CE conditions (Figs. E-14 to E-16) are similar to those for the IC conditions, where higher test temperatures result in reduced J levels. Comparison of data for the three CE conditions (Figs. E-17 to E-19) is likewise generally consistent with the observations for the IC conditions, where data for the irradiated conditions are similar to those for the irradiated conditions. One difference is at 288°C (Fig. E-19), where data from CE-3 has the lowest overall J levels. However, data for CE-1 and CE-2 exhibit only minor differences with the unirradiated data.

4.1.3 Low Fluence Rate (IP)

K_{Jc} data for IP-1 are illustrated in Fig. E-20. As with the other irradiation conditions, data scatter is not too severe for the K_{Jc} data. On the upper shelf, increasing the test temperature results in generally lower J levels (Fig. E-21). Toughness reductions due to irradiation are minimal for the IP-1 condition (Figs. E-22 and E-23).

4.1.4 Comparisons of Different Fluence Rates

Since comparisons of data from different fluence rates cannot be made in all cases on a 1:1 basis due to fluence differences, transition temperature comparisons will be made by looking at overall trends as a function of fluence. As illustrated in Fig. E-24, the highest fluence rates (IC from this program, SSC-1 and SSC-2 from Ref. E-14, and UBR-31 from Ref. E-15) tend to give the lowest embrittlement at low fluence levels and the highest embrittlement at high fluence levels. In contrast, the intermediate fluence rates (CE in this program and

(text continues on pg. E-38)

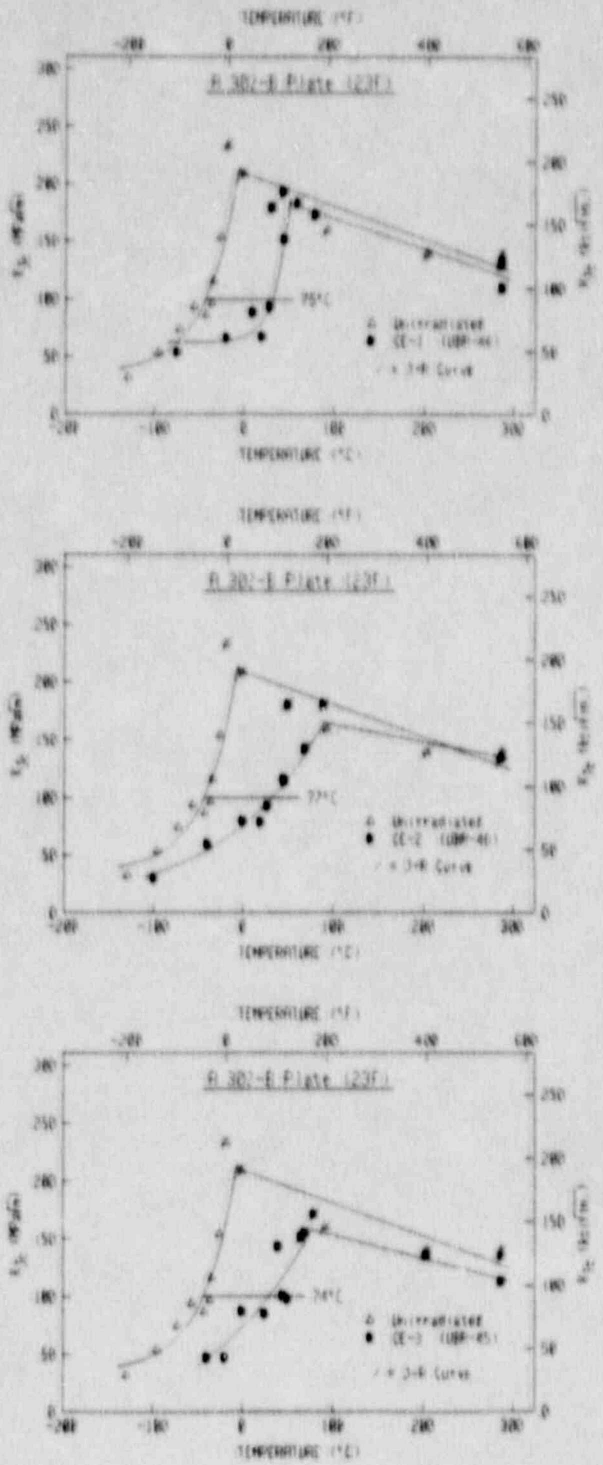

Fig. E-12 Comparisons of K_{Jc} data for the unirradiated condition and the intermediate fluence rate (CE) irradiated conditions of the A 302-B Plate 23F.

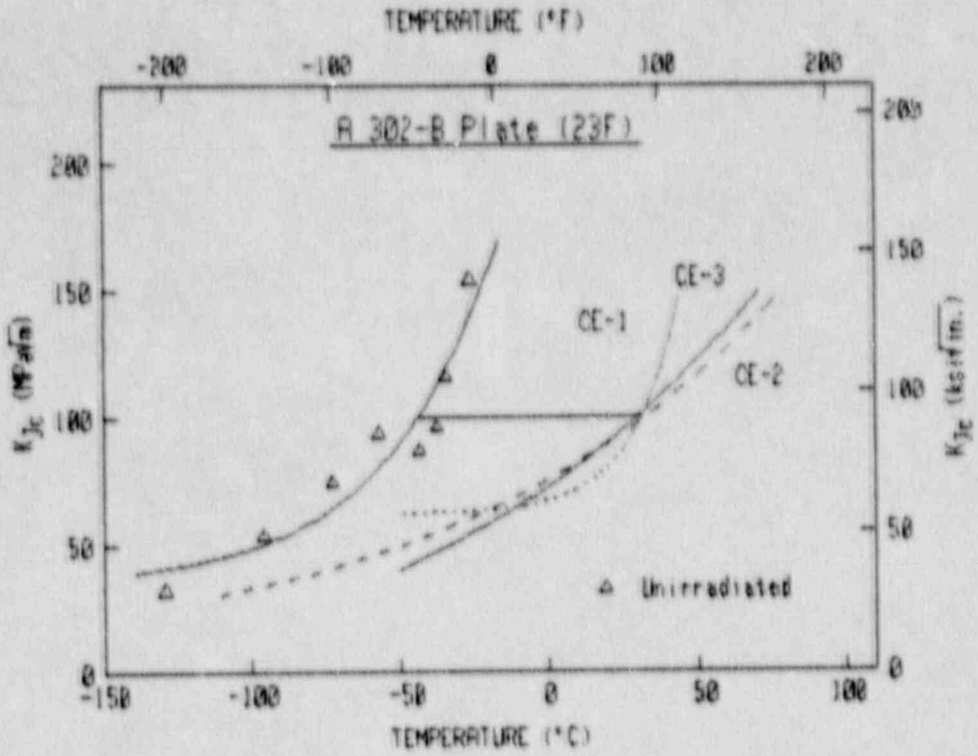

Fig. E-13 Comparison of the curve-fit results for the three intermediate fluence rate (CE) irradiated conditions.

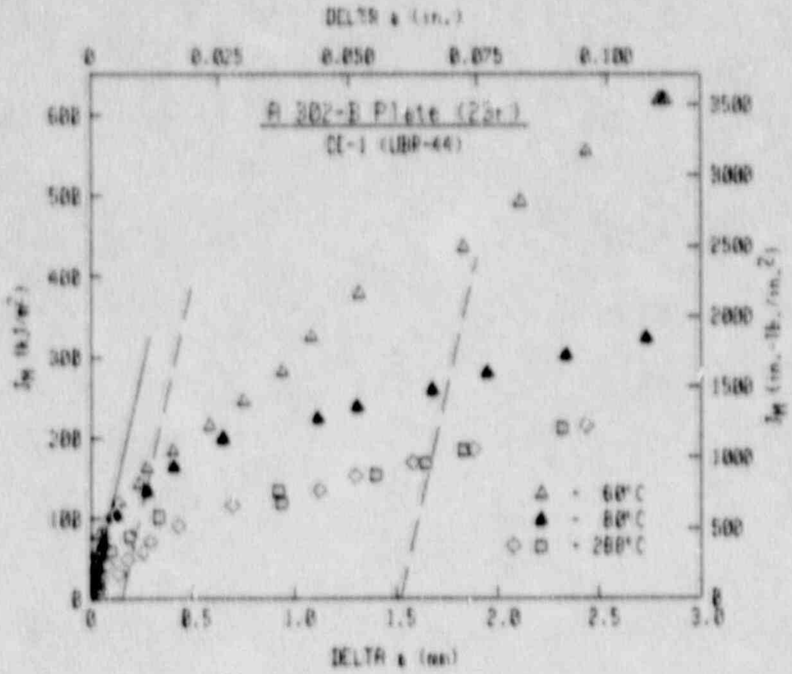

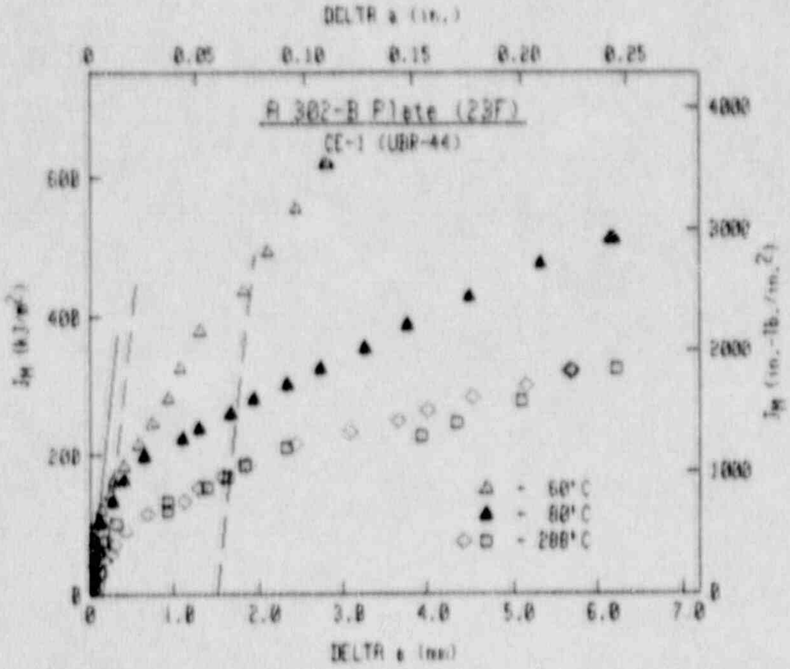

Fig. E-14 J-R curves for the CE-1 (UBR-44) irradiated condition of A 302-B Plate 23F.

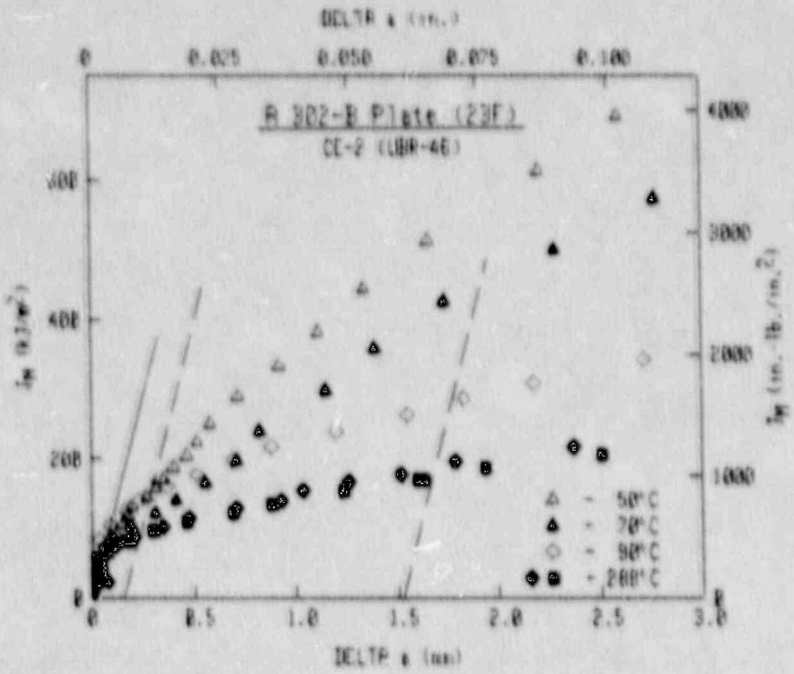

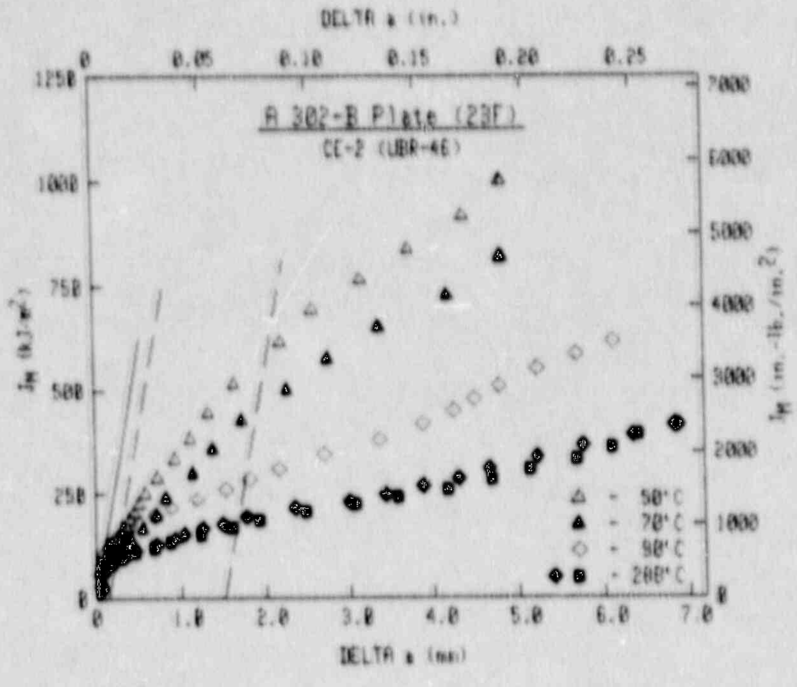

Fig. E-15 J-R curves for the CE-2 (UBR-46) irradiated condition of A 302-B Plate 23F.

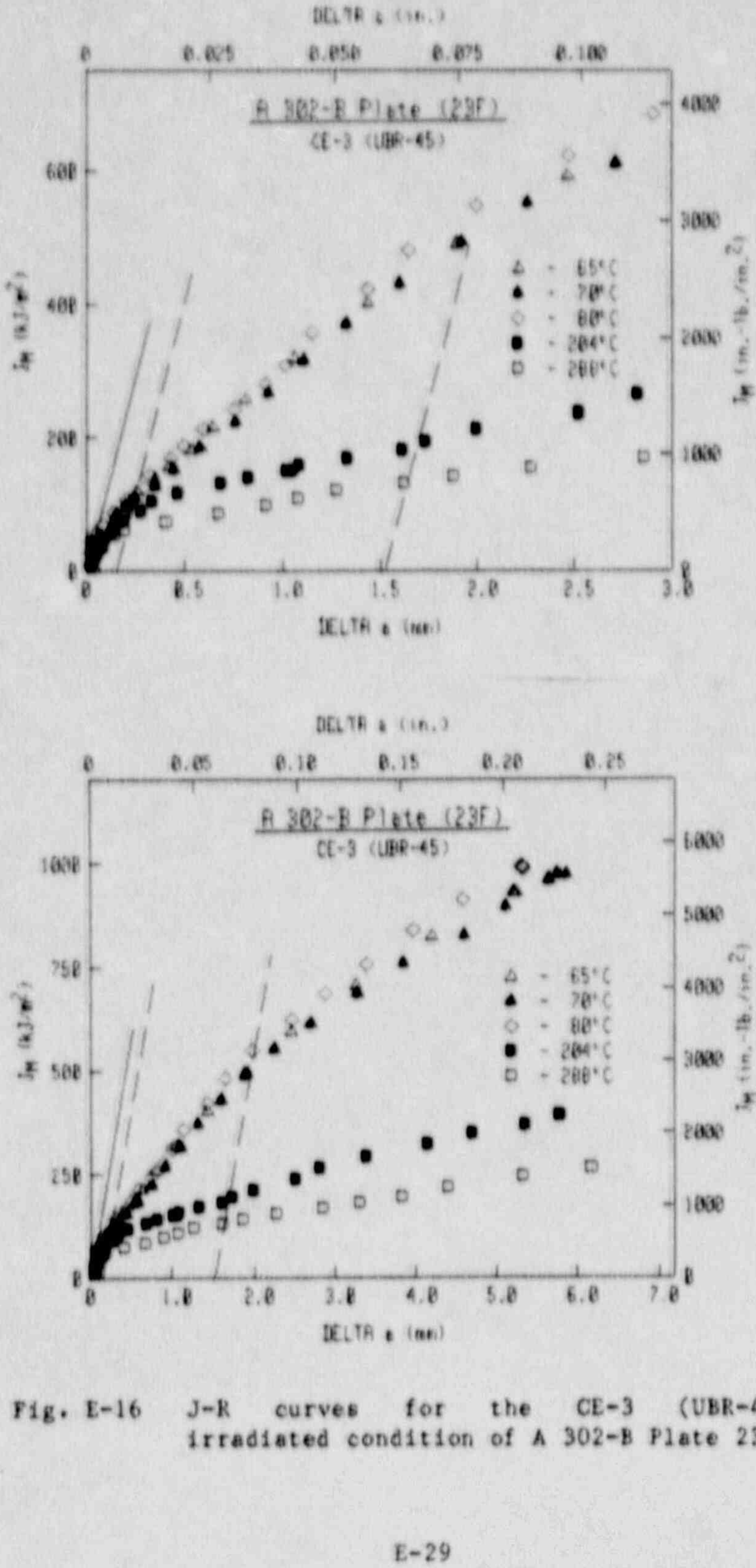

Fig. E-16 J-R curves for the CE-3 (UBR-45) irradiated condition of A 302-B Plate 23F.

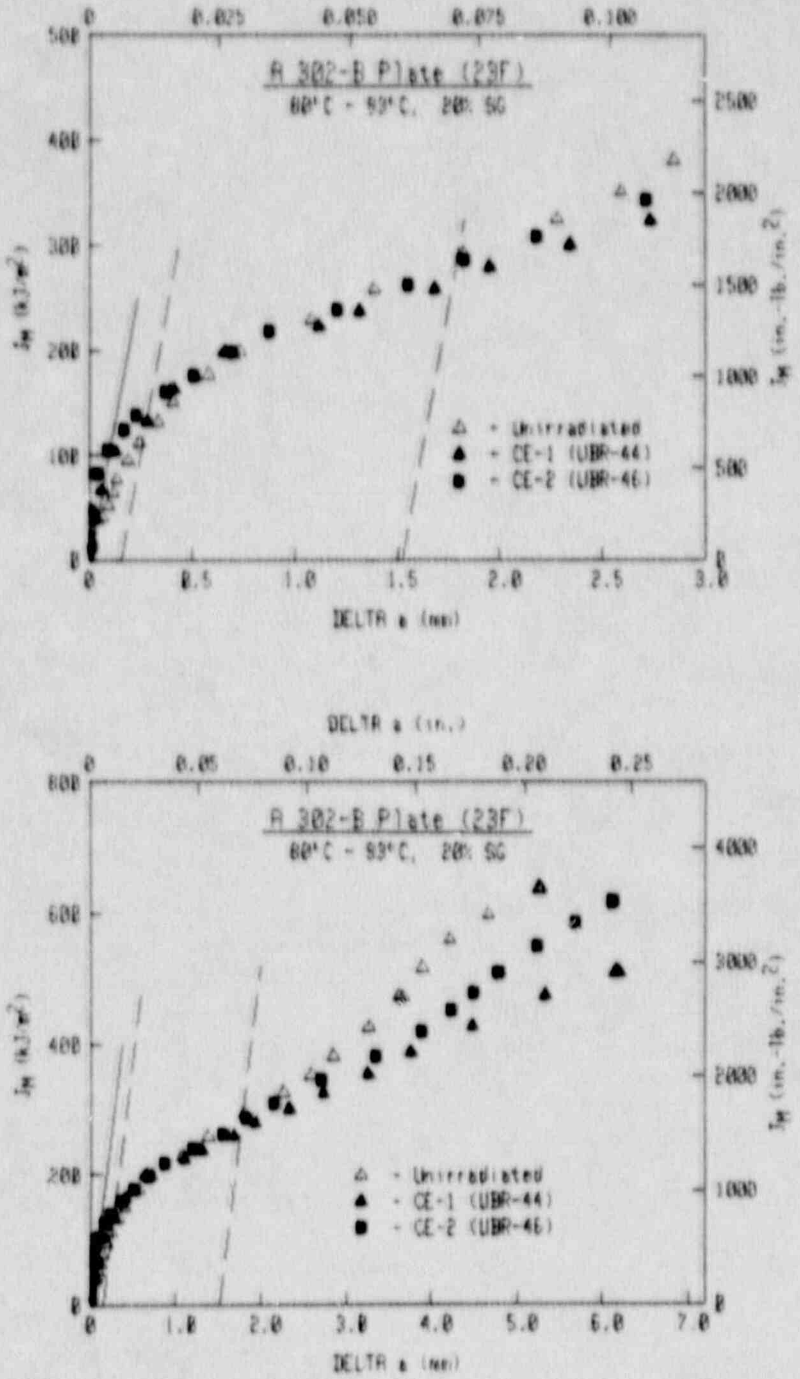

Fig. E-17 Comparison of J-R curves at 80°C to 93°C from the unirradiated condition and the intermediate fluence rate (CE) irradiated conditions of the A 302-B Plate 23F.

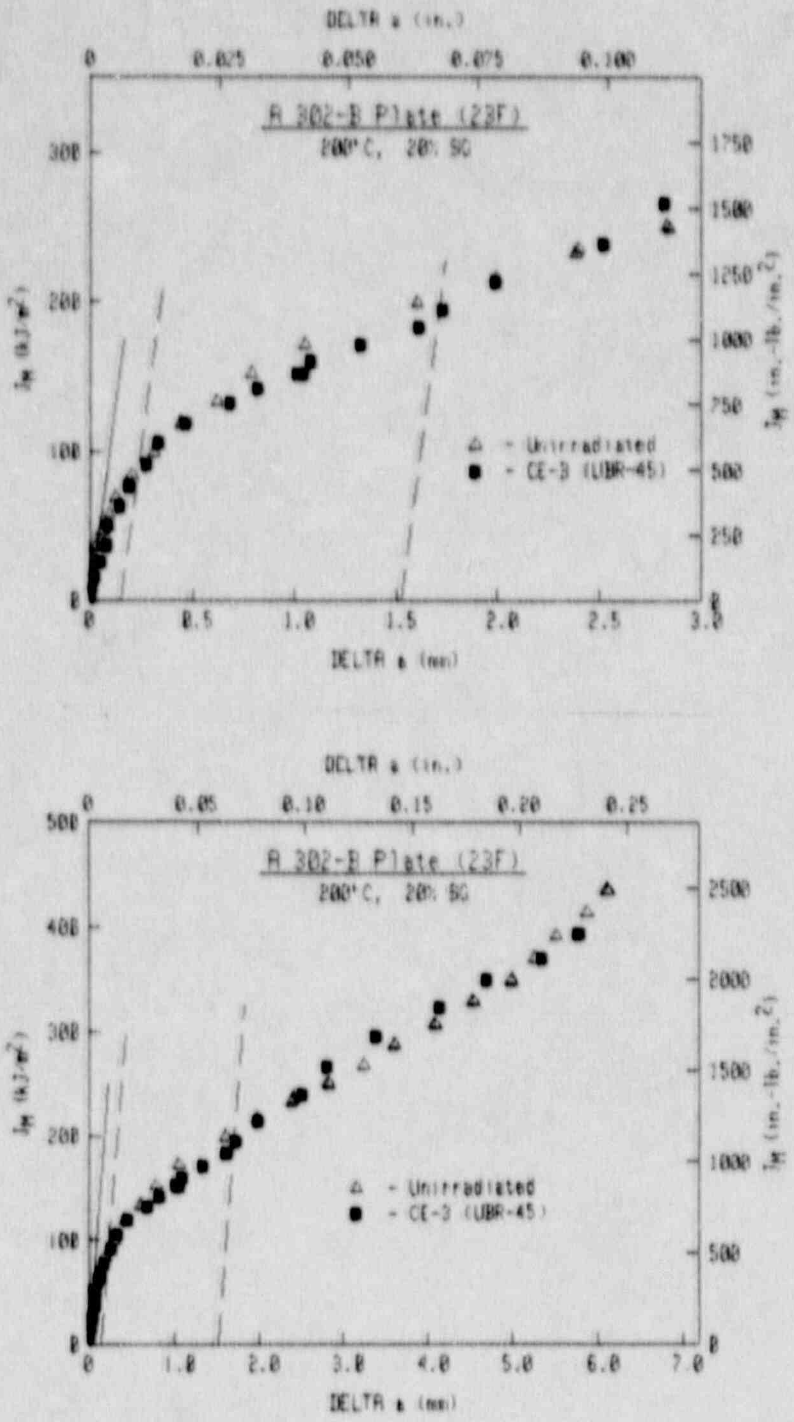

Fig. E-18 Comparison of J-R curves at 200°C from the unirradiated condition and the intermediate fluence rate (CE) irradiated conditions of the A 302-B Plate 23F.

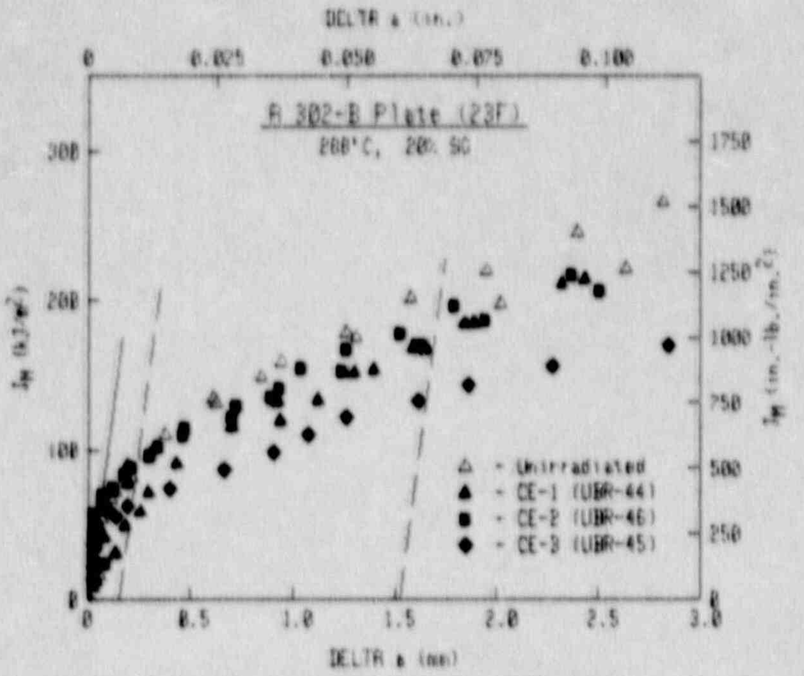

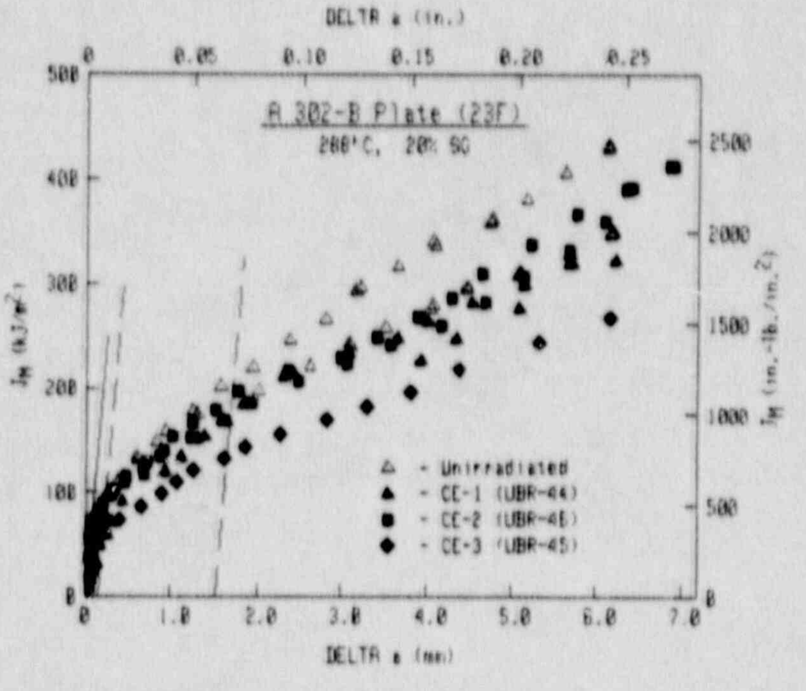

Fig. E-19 Comparison of J-R curves at 288 °C from the unirradiated condition and the intermediate fluence rate (CE) irradiated conditions of the A 302-B Plate 23F.

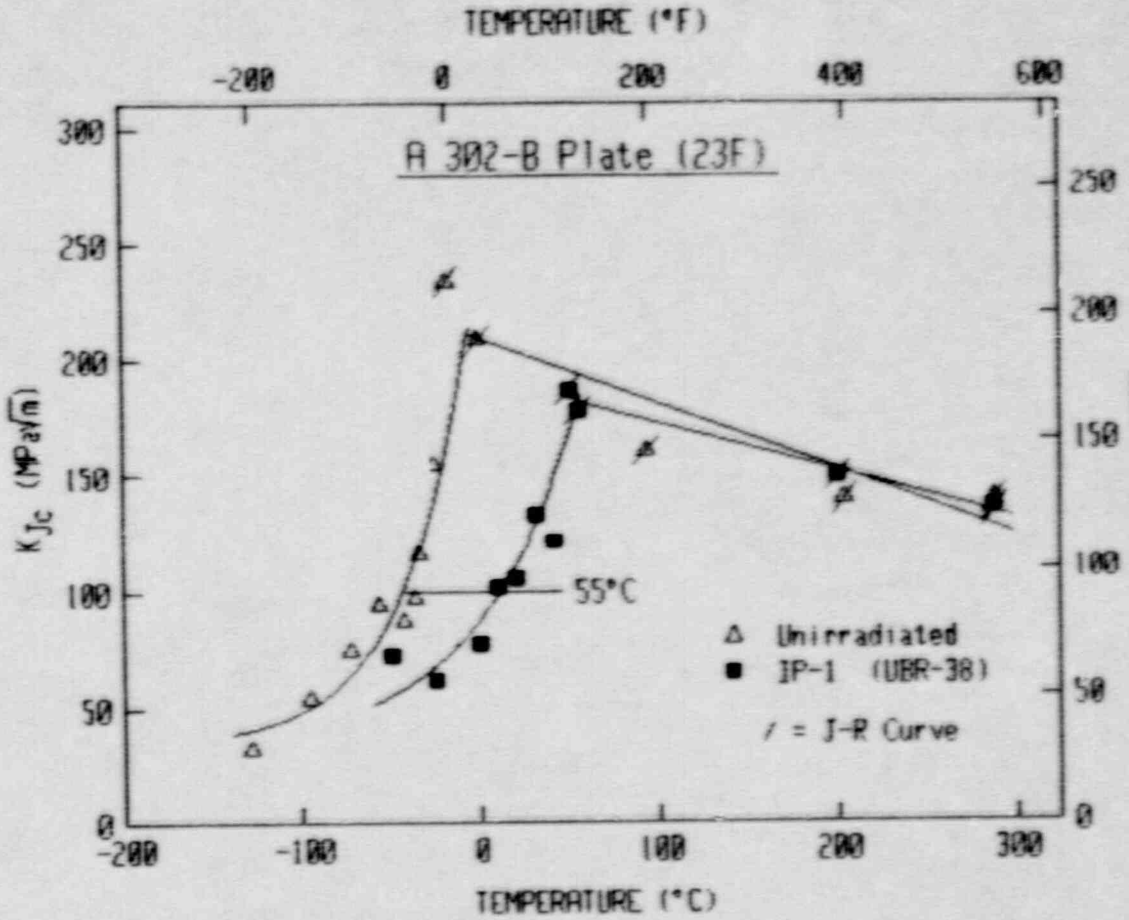

Fig. E-20 Comparison of K_{Jc} data for the unirradiated condition and the low fluence rate (IP) irradiated condition of A 302-B Plate 23F.

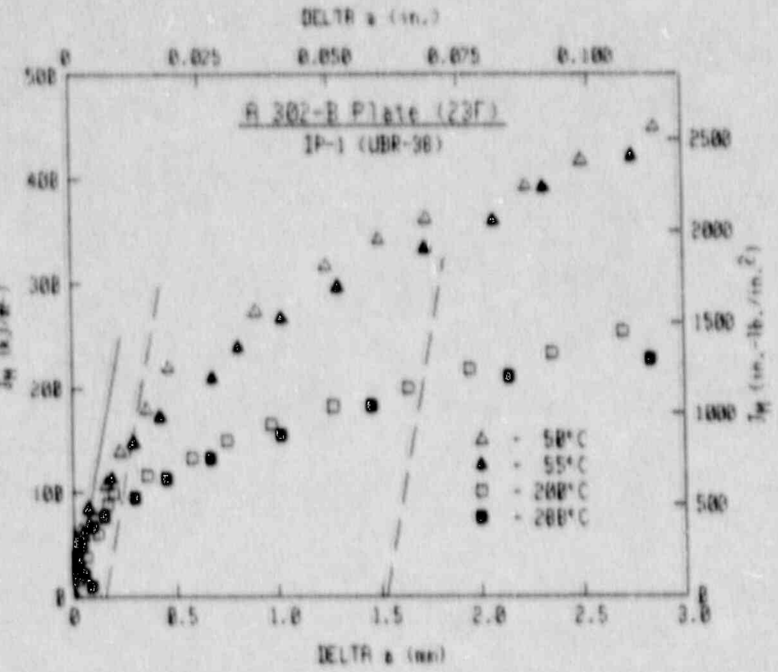

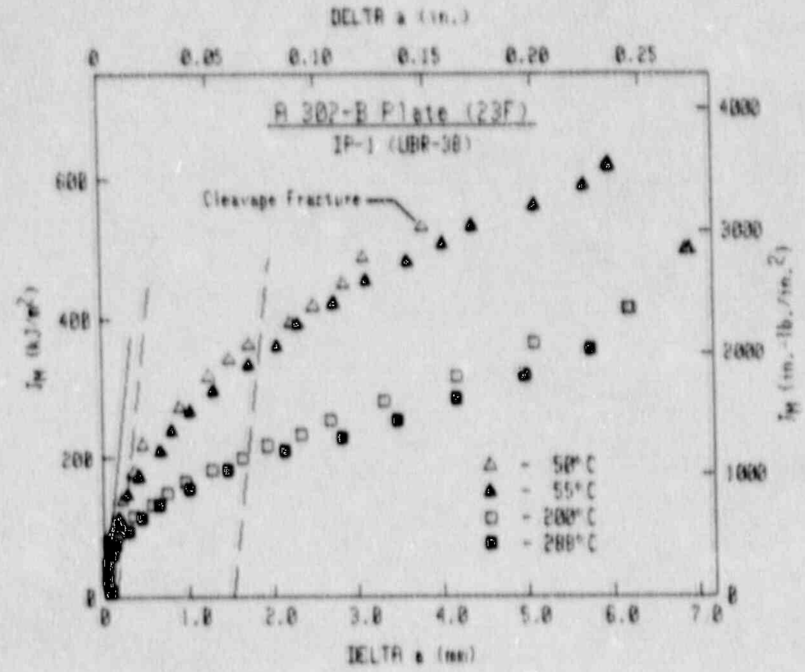

Fig. E-21 J-R curves for the IP-1 (UBR-38) irradiated condition of A 302-B Plate 23F.

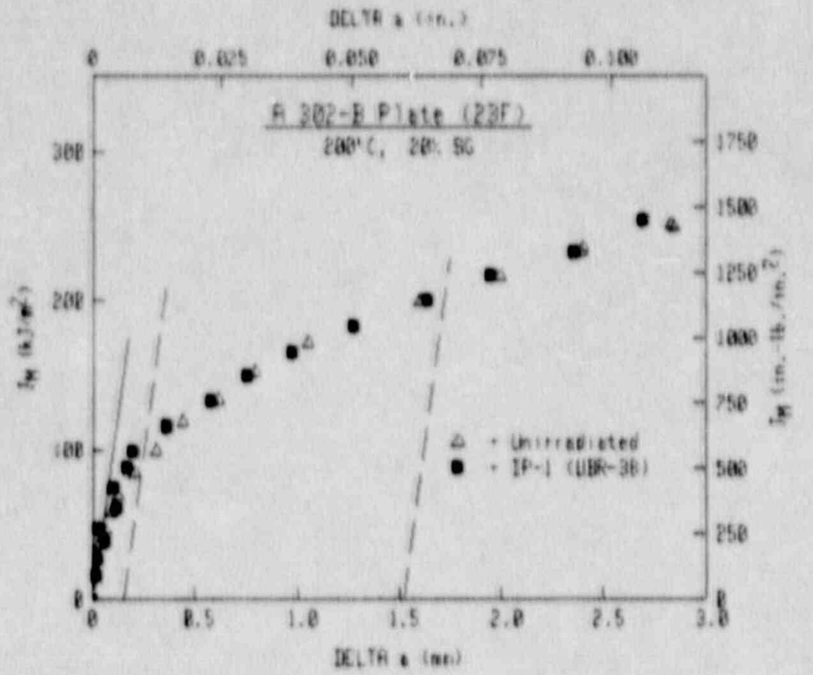

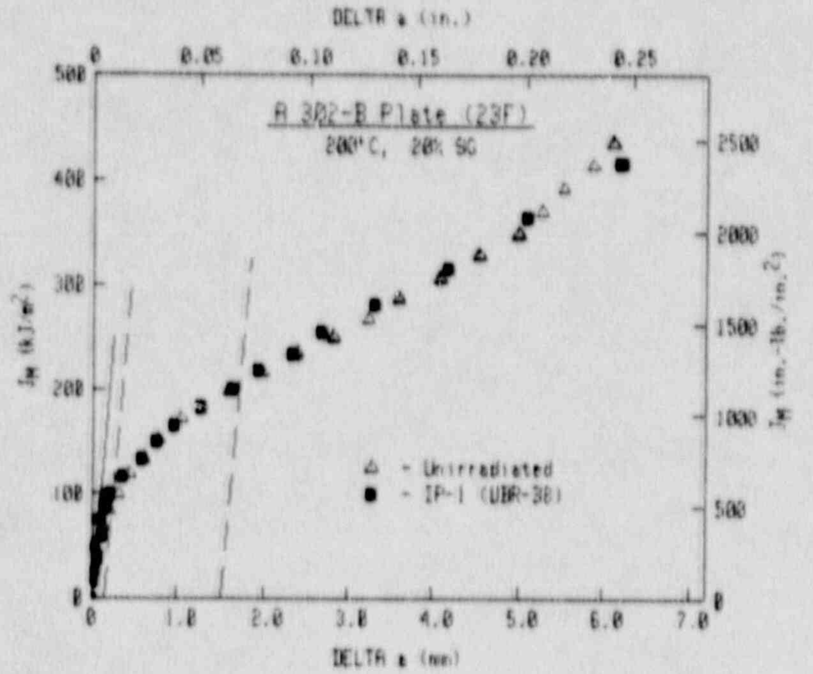

Fig. E-22 Comparison of J-R curves at 200°C from the unirradiated condition and the low fluence rate (IP) irradiated condition of the A 302-B Plate 23F.

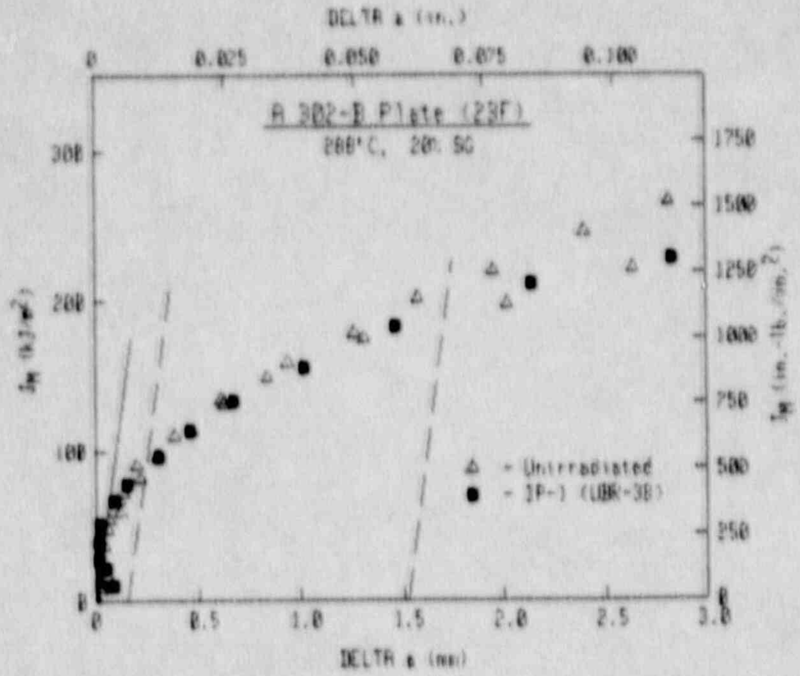

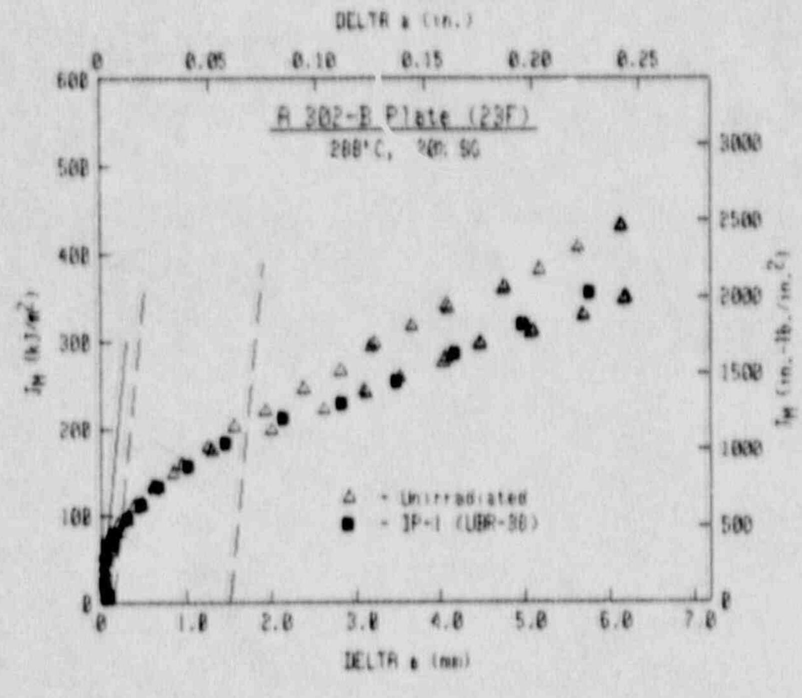

Fig. E-23 Comparison of J-R curves at 288°C from the unirradiated condition and the low fluence rate (IP) irradiated condition of the A 302-B Plate 23F.

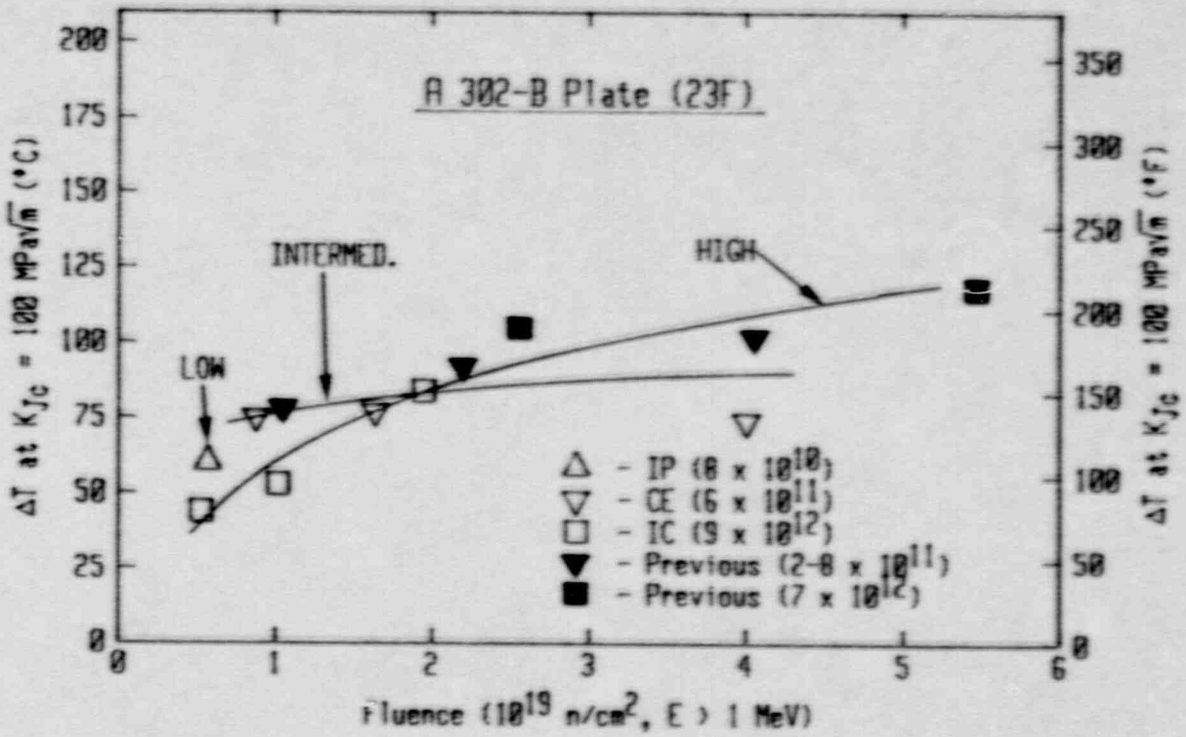

Fig. E-24 Transition temperature shifts as a function of fluence for the A 302-B Plate 23F.

the In-Wall Capsules 1, 2, and 3 in Ref. E-14) give the highest embrittlement at low fluence levels and lower embrittlement at high fluence levels. Trends for the high and the intermediate fluence rates cross at a fluence of ~ 2 x 10^{19} n/cm^2. At the lowest fluence rate (IP from this program), the single data point at a very low fluence is located midway between the trends for the CE and the IC fluence rates.

J-R curves for this plate at 288°C are illustrated in Fig. E-25. At low Δa levels (< 3 mm), the curve for IC-3 is higher than most of the curves and the curve for CE-3 is much lower than most of the curves. In other respects, the remaining curves are quite similar to one another.

4.2 Linde 80 Weld (W8A)

This weld was tested at three fluences each of the intermediate (CE) and the high (IC) fluence rates. Detailed data for these irradiation conditions and the unirradiated condition are given in Table E-4. Data for the unirradiated condition have been treated previously in Ref. E-2.

Comparison of the J-R curves for the unirradiated condition are illustrated in Fig. E-26. As expected, increasing the test temperature results in lower J levels, with a large drop evident from 200°C to 288°C. The latter is in contrast to the A 302-B plate (Fig. E-4), where two curves at 288°C bounded a curve at 200°C.

Besides the data reported here, two additional sets of post-irradiation data from in-core irradiations are used for comparison purposes (Ref. E-2).

4.2.1 High Fluence Rate (IC)

Comparison of the K_{Jc} data for the IC conditions and the unirradiated condition are given in Fig. E-27. As expected, increasing the fluence results in greater transition temperature shifts for the IC irradiations (Fig. E-28). For this weld, data scatter in the transition region appears to be greater than that for the A 302-B plate (23F). At least a partial cause of this appearance is the lower upper shelf toughness for this weld and an apparent magnification effect of the scatter resulting from the reduced toughness range exhibited by this weld. A second cause is undoubtably the somewhat large scatter inherent to the weld metal, as indicated by data for the unirradiated condition.

In terms of upper shelf toughness, comparisons of the J-R curves for each of the irradiation conditions are illustrated in Figs. E-29 to E-31. Tests at temperature below 200°C are somewhat elevated in comparison to those at higher temperatures due to the use of plane-sided specimens for the low temperature tests. Comparisons of the curves for all three irradiation conditions at 200°C and 288°C (Figs. E-32 and E-33) indicate fairly large reductions in J levels after

(text continues on pg. E-52)

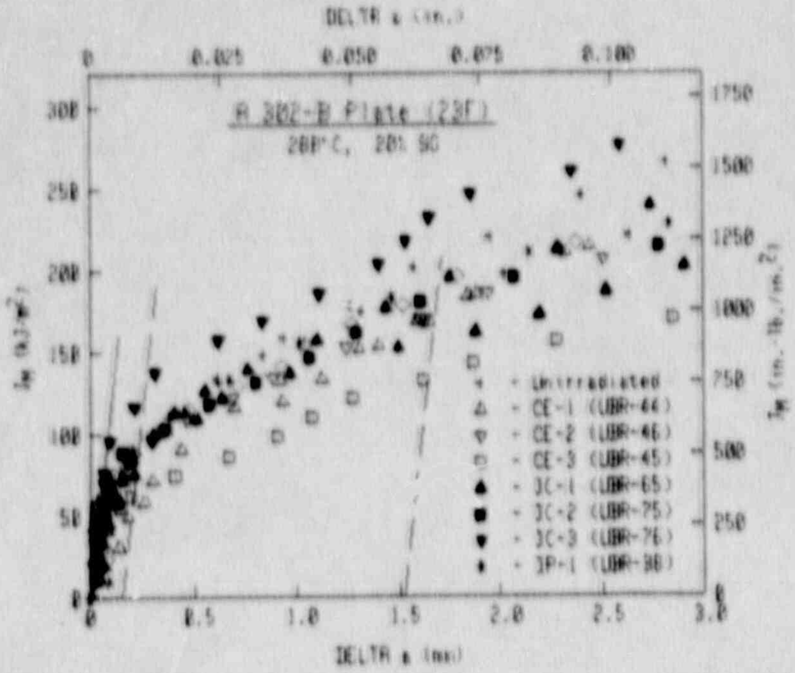

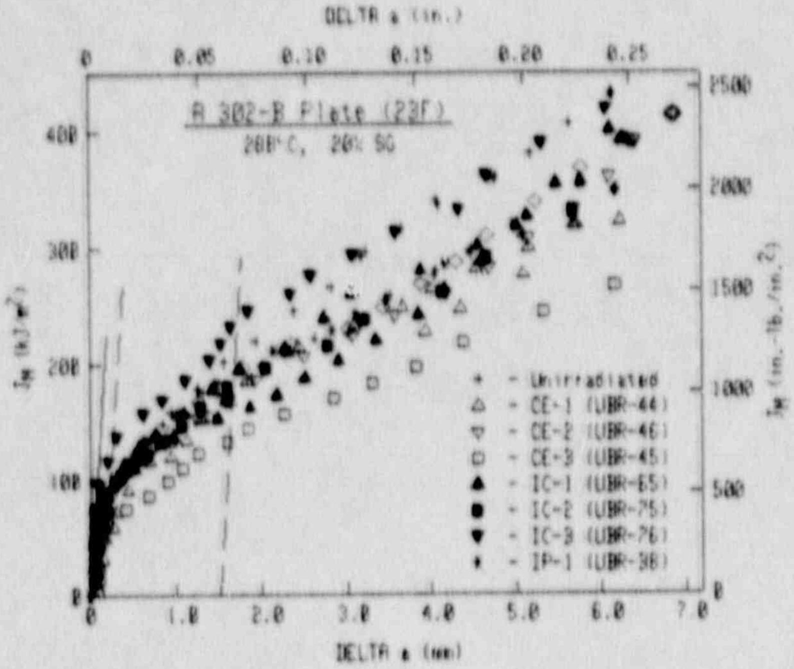

Fig. E-25 Comparison of J-R curves at 288°C for the A 302-B Plate 23F.

Table E-4 Fracture Toughness Data for Linde 80 Weld (WBA)

Specimen Number	Test Temp (°C)	$(a/W)_o$[a]	Δa_m[b] (mm)	Δa_p[c] (mm)	$\Delta a_p - \Delta a_m$ (mm)	J_{Ic} P.L. (kJ/m^2)	J_{Ic} ASTM (kJ/m^2)	K_{Jc} P.L. ($MPa\sqrt{m}$)	K_{Jc} ASTM ($MPa\sqrt{m}$)	K_{Bc} ($MPa\sqrt{m}$)	K_{max} ($MPa\sqrt{m}$)	T_{avg}	f (MPa)	y (MPa)
UNIRRADIATED														
WBA-99	-150	0.511	—	—	—	6.7	—	40.0	40.3[e]	38.5	40.3	—	754.5	703.6
WBA-93	-110	0.519	—	—	—	12.7	—	54.6	53.2	48.4	53.2	—	697.2	645.5
WBA-122	-110	0.503	—	—	—	26.3	—	78.6	57.1	60.7	71.5	—	697.2	645.5
WBA-6	-100	0.509	—	—	—	35.4	—	90.9	55.3	64.9	80.1	—	683.9	632.0
WBA-98	-70	0.513	—	—	—	31.5	—	85.5	49.4	61.0	74.2	—	646.9	594.0
WBA-48	-50	0.509	—	—	—	43.5	—	100.2	53.4	64.5	78.3	—	624.4	570.8
WBA-91	-50	0.518	—	—	—	28.7	—	81.5	55.9	58.4	72.1	—	624.4	570.8
WBA-44	-35	0.511	—	—	—	78.7	—	134.5	48.2	72.1	86.7	—	608.7	554.5
WBA-7	-25	0.516	—	—	—	128.1	—	171.4	43.6	78.5	84.7	—	598.8	544.2
WBA-92	-15	0.523	—	—	—	60.0	—	117.2	53.8	66.6	83.5	—	589.2	534.2
WBA-95	0	0.518	6.02	5.98	-0.04	102.9	104.4[f]	153.1	154.2	—	—	72	575.9	520.1
WBA-45[d]	75	0.516	6.41	6.39	-0.02	94.2	94.4[f]	144.9	145.1	—	—	81	524.0	463.6
WBA-97[d]	200	0.522	5.87	5.70	-0.17	80.2	79.7[f]	131.4	131.0	—	—	57	492.7	421.5
WBA-141[d]	200	0.504	6.11	5.91	-0.20	89.1	89.6[f]	138.5	138.8	—	—	54	492.7	421.5
WBA-96[d]	288	0.521	5.83	5.92	+0.09	54.2	58.6[f]	106.6	110.8	—	—	34	512.2	431.0
IRRADIATED CE-1 ([illegible]-44)														
WBA-28	-20	0.509	—	—	—	7.8	—	42.4	42.8[e]	40.1	42.8	—	712.3	663.3
WBA-51	15	0.508	—	—	—	20.4	—	68.0	59.3	55.4	66.3	—	683.5	634.7
WBA-50	29	0.514	—	—	—	29.5	—	81.7	60.4	61.0	76.6	—	673.4	624.6
WBA-22	50	0.525	—	—	—	25.5	—	75.6	58.8	57.9	74.6	—	660.1	610.9
WBA-26	60	0.491	—	—	—	29.0	—	80.6	53.7	59.7	[illegible]	—	654.4	605.0
WBA-47	65	0.521	—	—	—	38.1	—	92.4	56.8	63.8	85.[illegible]	—	651.7	602.2
WBA-2	72	0.512	—	—	—	49.5	—	105.2	54.4	67.7	90.5	—	648.1	598.4
WBA-32	85	0.500	4.36	2.98	-1.38	75.3	59.7	129.5	115.2	—	—	44	642.1	592.0
WBA-12[d]	93	0.522	6.91	6.23	-0.68	55.8	—[g]	113.3	—[g]	—	—	—	638.7	588.3
WBA-36	100	0.509	4.03	2.60	-1.43	79.2	80.1	132.4	133.2	—	—	33	636.0	585.4
WBA-54	204	0.516	7.38	6.09	-1.29	49.7	34.3	103.4	85.9	—	—	18	621.4	564.1
WBA-16[d]	288	0.518	6.36	6.28	-0.08	50.5	47.8[f]	102.9	100.1	—	—	14	644.4	578.3

[a] Pre-test a/W.
[b] Optically-measured crack growth.
[c] Crack growth predicted by compliance.
[d] Side grooved.
[e] Valid K_{Ic} per ASTM E 399.
[f] Valid J_{Ic} per ASTM E 813-81.
[g] Cleavage failure precluded determination of this quantity.

Table E-4 Fracture Toughness Data for Linde 80 Weld (WBA) (continued)

Specimen Number	Test Temp (°C)	$(a/W)_o$[a]	Δa_m[b] (mm)	Δa_p[c] (mm)	$\Delta a_p - \Delta a_m$ (mm)	J_{Ic} P.L. (kJ/m²)	J_{Ic} ASTM (kJ/m²)	K_{Jc} P.L. (MPa√m)	K_{Jc} ASTM (MPa√m)	$K_{\beta c}$ (MPa√m)	K_{max} (MPa√m)	T_{avg}	f (MPa)	y (MPa)
IRRADIATED CE-2 (UBR-46)														
WBA-52	-40	0.515	—	—	—	11.9	—	52.3	56.5	47.7	51.5	—	739.5	688.3
WBA-15	-20	0.503	—	—	—	15.2	—	59.0	54.6	51.6	54.6	—	720.6	669.8
WBA-11	27	0.525	—	—	—	11.9	—	51.8	55.2	46.3	55.2	—	683.2	632.4
WBA-35	40	0.511	—	—	—	14.5	—	57.1	55.8	49.3	55.8	—	674.5	623.7
WBA-41	65	0.501	—[g]	—[g]	—[g]	65.1	—[g]	120.6	—[g]	—	—	—	660.0	608.7
WBA-46	66	0.516	—	—	—	28.1	—	79.3	79.5	59.3	79.5	—	659.5	608.1
WBA-31	90	0.517	—	—	—	44.2	—	99.1	60.2	65.7	87.9	—	648.3	596.1
WBA-25	98	0.512	4.23	2.69	-1.54	70.1	43.3	124.7	97.9	—	—	42	645.1	592.7
WBA-1[d]	120	0.532	6.30	6.32	+0.02	60.5	70.1	115.4	124.3	—	—	16	637.8	584.4
WBA-5	120	0.509	8.98	6.81	-2.17	61.7	47.6	116.6	102.4	—	—	43	637.8	584.4
WBA-21[d]	204	0.512	5.89	6.09	+0.20	42.7	45.4[f]	95.7	98.8	—	—	15	629.7	570.6
WBA-9[d]	288	0.520	6.69	6.47	-0.22	45.4	43.5[f]	97.6	95.5	—	—	12	652.8	584.7
IRRADIATED CE-3 (UBR-45)														
WBA-29	-40	0.509	—	—	—	11.6	—	51.7	50.5	47.8	50.5	—	761.5	718.0
WBA-19	0	0.514	—	—	—	15.7	—	59.8	57.4	52.4	58.8	—	725.5	682.5
WBA-23	40	0.522	—	—	—	27.7	—	79.0	59.0	61.2	74.8	—	696.5	653.3
WBA-17	50	0.504	—	—	—	21.3	—	69.2	56.2	56.5	66.0	—	690.4	647.0
WBA-33	60	0.512	5.78	5.83	+0.05	63.6	—[g]	119.4	—[g]	—	—	—	684.7	641.1
WBA-49	70	0.518	—[g]	—[g]	—[g]	29.5	—	81.1	54.5	—	—	—	679.4	635.6
WBA-43	80	0.522	8.85	5.14	-3.71	79.7	53.9	133.2	109.6	—	—	33	674.6	630.5
WBA-39	110	0.515	7.64	6.42	-1.22	39.2	—[g]	93.1	—[g]	—	—	49	662.9	617.6
WBA-13	130	0.504	7.31	6.30	-1.01	49.9	43.3[f]	104.7	97.5	—	—	39	657.2	611.0
WBA-3[d]	288	0.518	6.09	6.19	+0.10	35.9	36.1[f]	86.8	87.0	—	—	13	674.8	614.4
WBA-27[d]	288	0.524	5.72	6.02	+0.30	38.7	39.8[f]	90.1	91.4	—	—	12	674.8	614.4

a Pre-test a/W.
b Optically-measured crack growth.
c Crack growth predicted by compliance.
d Side grooved.
e Valid K_{Ic} per ASTM E 399.
f Valid J_{Ic} per ASTM E 813-81.
g Cleavage failure precluded determination of this quantity.

Table E-4 Fracture Toughness Data for Linde 80 Weld (WRA) (continued)

Specimen Number	Test Temp (°C)	$(a/W)_o$[a]	Δa_m[b] (mm)	Δa_p[c] (mm)	$\Delta a_p - \Delta a_m$ (mm)	J_{Ic} P.L. (kJ/m^2)	J_{Ic} ASTM (kJ/m^2)	K_{Jc} P.L. ($MPa\sqrt{m}$)	K_{Jc} ASTM ($MPa\sqrt{m}$)	K_c ($MPa\sqrt{m}$)	K_{max} ($MPa\sqrt{m}$)	T_{avg}	f (MPa)	y (MPa)
IRRADIATED IC-1 (UBR-65)														
WBA-4	-60	0.501	—	—	—	7.1	—	40.5	38.5	38.6	38.5	—	713.4	661.7
WBA-8	-40	0.513	—	—	—	7.3	—	41.1	40.1	38.9	40.1	—	693.0	641.6
WBA-42	-18	0.503	—	—	—	17.2	—	62.7	55.8	52.3	59.1	—	672.0	621.3
WBA-34	0	0.508	—	—	—	41.9	—	97.7	58.0	65.8	85.1	—	657.0	606.1
WBA-20	10	0.524	—	—	—	20.3	—	68.0	57.7	54.1	65.8	—	649.1	598.2
WBA-38	10	0.505	—	—	—	19.5	—	66.6	55.1	53.4	61.5	—	649.1	598.2
WBA-24	20	0.515	—	—	—	80.7	—	135.3	54.3	75.0	96.1	—	641.6	590.7
WBA-40	28	0.505	—	—	—	27.3	—	78.6	52.3	58.0	70.9	—	636.0	585.0
WBA-14	42	0.517	4.64	6.22	+1.58	94.1	75.3	145.5	130.2	—	—	79	626.8	575.6
WBA-18	60	0.521	—[g]	—[g]	—[g]	62.4	—[g]	118.2	—[g]	—	—	—	616.2	564.7
WBA-10[d]	204	0.514	5.40	5.80	+0.40	49.6	49.2[f]	103.2	102.9	—	—	23	583.2	523.8
WBA-30[d]	288	0.509	6.25	6.31	+0.06	41.7	46.8	93.5	99.0	—	—	21	606.3	538.0
IRRADIATED IC-2 (UBR-75)														
WBA-116	-12	0.498	—	—	—	7.8	—	42.2	41.8	39.7	41.8	—	691.8	643.5
WBA-114	0	0.483	—	—	—	18.1	—	64.2	51.2	53.5	60.0	—	681.7	633.5
WBA-124	12	0.509	—	—	—	30.9	—	83.7	46.9	61.8	74.3	—	672.3	624.1
WBA-119	32	0.492	—	—	—	24.0	—	73.5	53.9	57.0	66.8	—	658.0	609.6
WBA-129	38	0.497	—	—	—	17.9	—	63.6	53.5	52.2	58.9	—	654.0	605.6
WBA-144	46	0.470	—	—	—	50.6	—	106.7	61.3	68.2	89.6	—	649.0	600.5
WBA-128	55	0.505	—	—	—	48.9	—	104.7	58.3	67.3	89.3	—	643.7	595.0
WBA-103	65	0.481	—	—	—	71.8	—	126.7	56.4	72.8	92.9	—	638.3	589.3
WBA-104	75	0.498	8.29	6.44	-1.85	64.3	55.8	119.8	111.6	—	—	71	633.2	584.0
WBA-134[d]	200	0.503	6.93	6.75	-0.18	53.6	53.7	107.4	107.5[f]	—	—	24	607.6	551.2
WBA-139[d]	288	0.512	6.28	6.05	-0.23	48.2	52.9	100.5	105.3[f]	—	—	16	631.0	565.4

a Pre-test a/W.
b Optically-measured crack growth.
c Crack growth predicted by compliance.
d Side grooved.
e Valid K_{Ic} per ASTM E 399.
f Valid J_{Ic} per ASTM E 813-81.
g Cleavage failure precluded determination of this quantity.

Table E-4 Fracture Toughness Data for Linde 80 Weld (WBA) (continued)

Specimen Number	Test Temp (°C)	$(a/W)_o$ [a]	a_m [b] (mm)	a_p [c] (mm)	$a_p - a_m$ (mm)	J_{Ic} P.L. (kJ/m²)	J_{Ic} ASTM (kJ/m²)	K_{Jc} P.L. (MPa √m)	K_{Jc} ASTM (MPa √m)	K_c (MPa √m)	K_{max} (MPa √m)	T_{avg}	f (MPa)	y (MPa)
IRRADIATED IC-3 (UBR-76)														
WBA-115	-12	0.494	—	—	—	5.1	—	34.3	34.0	33.4	40.8	—	716.4	672.5
WBA-107	10	0.495	—	—	—	17.6	—	63.3	57.5	53.6	58.4	—	698.4	654.6
WBA-100	32	0.498	—	—	—	12.8	—	53.7	51.7	47.8	51.7	—	688.1	644.3
WBA-118	38	0.499	—	—	—	[illegible].7	—	59.6	56.3	51.0	56.3	—	678.7	634.[illegible]
WBA-110	46	0.508	—	—	—	21.8	—	70.1	57.0	56.2	65.5	—	673.7	629.5
WBA-120	55	0.498	—	—	—	43.8	—	99.2	67.7	67.3	87.5	—	668.4	624.1
WBA-138	65	0.502	—	—	—	33.3	—	86.3	59.2	62.5	81.7	—	662.9	618.4
WBA-140	75	0.509	7.38	6.26	-1.12	77.2	40.8	131.2	95.4	—	—	56	657.9	613.1
WBA-135	80	0.494	—	—	—	33.8	—	86.8	56.5	62.3	77.9	—	655.5	610.6
WBA-105	95	0.499	6.85	5.59	-1.26	66.2	55.2	121.1	110.6	—	—	59	649.1	603.7
WBA-125[d]	200	0.497	6.63	6.76	+0.13	61.7	60.1[f]	115.2	113.7	—	—	16	632.3	580.3
WBA-121[d]	288	0.509	5.90	5.72	-0.18	48.0	48.6[f]	100.4	101.0	—	—	12	655.7	594.5

a Pre-test a/W.
b Optically-measured crack growth.
c Crack growth predicted by compliance.
d Side grooved.
e Valid K_{Ic} per ASTM E 399.
f Valid J_{Ic} per ASTM E 813-81.
g Cleavage failure precluded determination of this quantity.

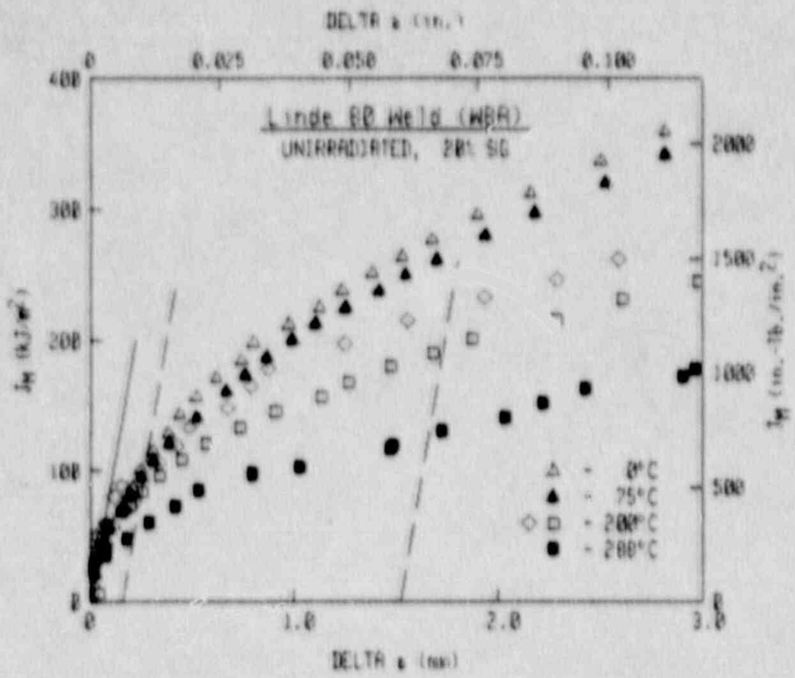

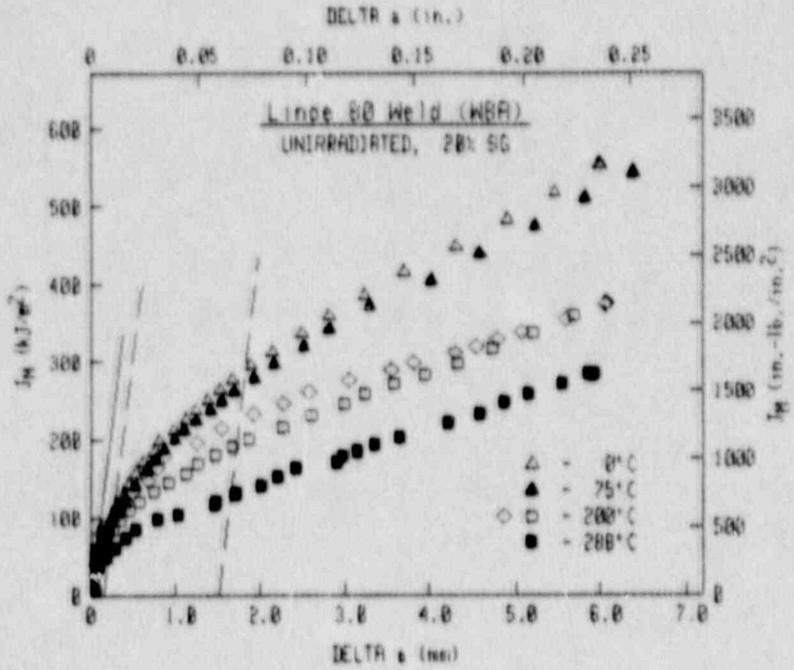

Fig. E-26 J-R curves for the unirradiated condition of the Linde 80 Weld W8A.

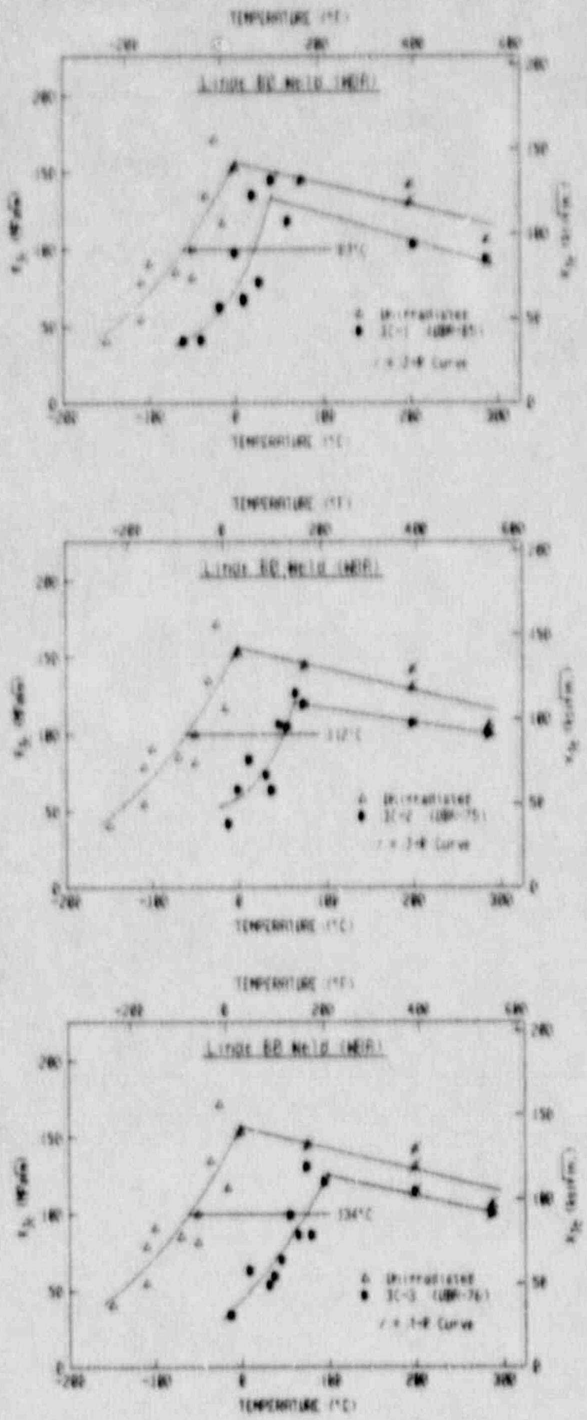

Fig. E-27 Comparisons of K_{Jc} data for the unirradiated condition and the high fluence rate (IC) irradiated conditions of the Linde 80 Weld W8A.

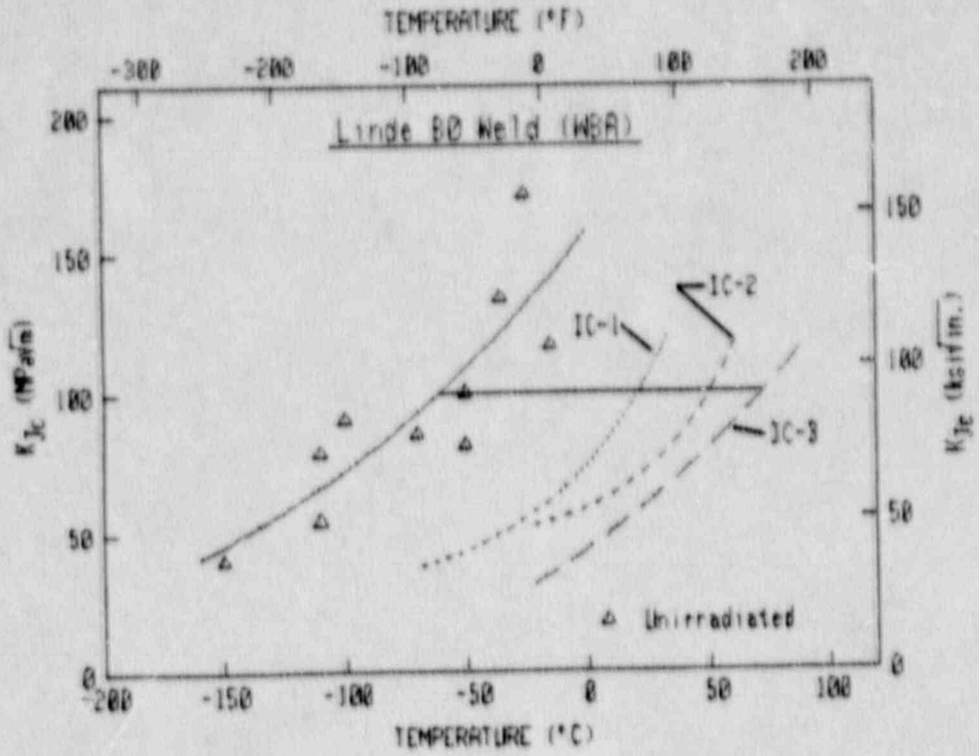

Fig. E-28 Comparison of the curve-fit results for the three high fluence rate (IC) irradiated conditions.

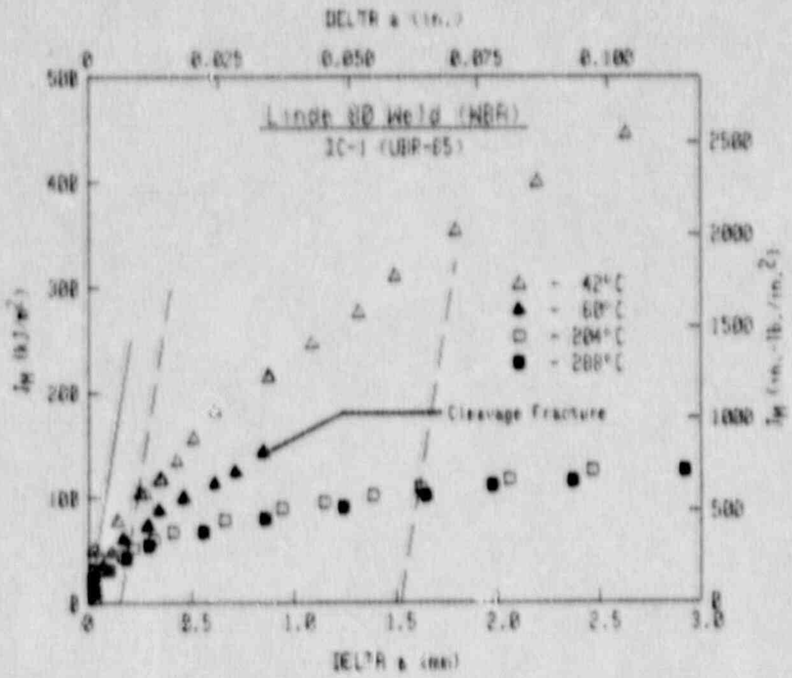

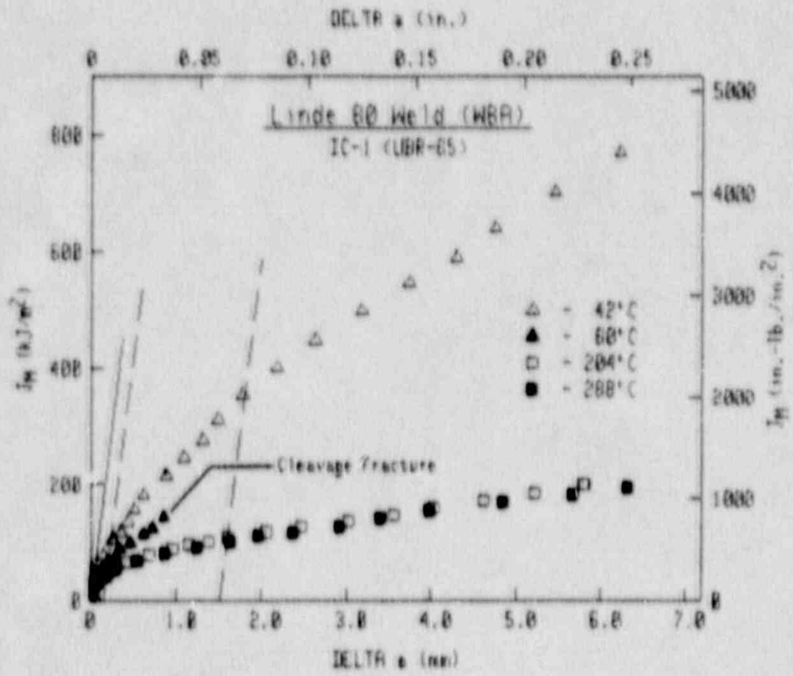

Fig. E-29 J-R curves for the IC-1 (UBR-65) irradiated condition of Linde 80 Weld WBA.

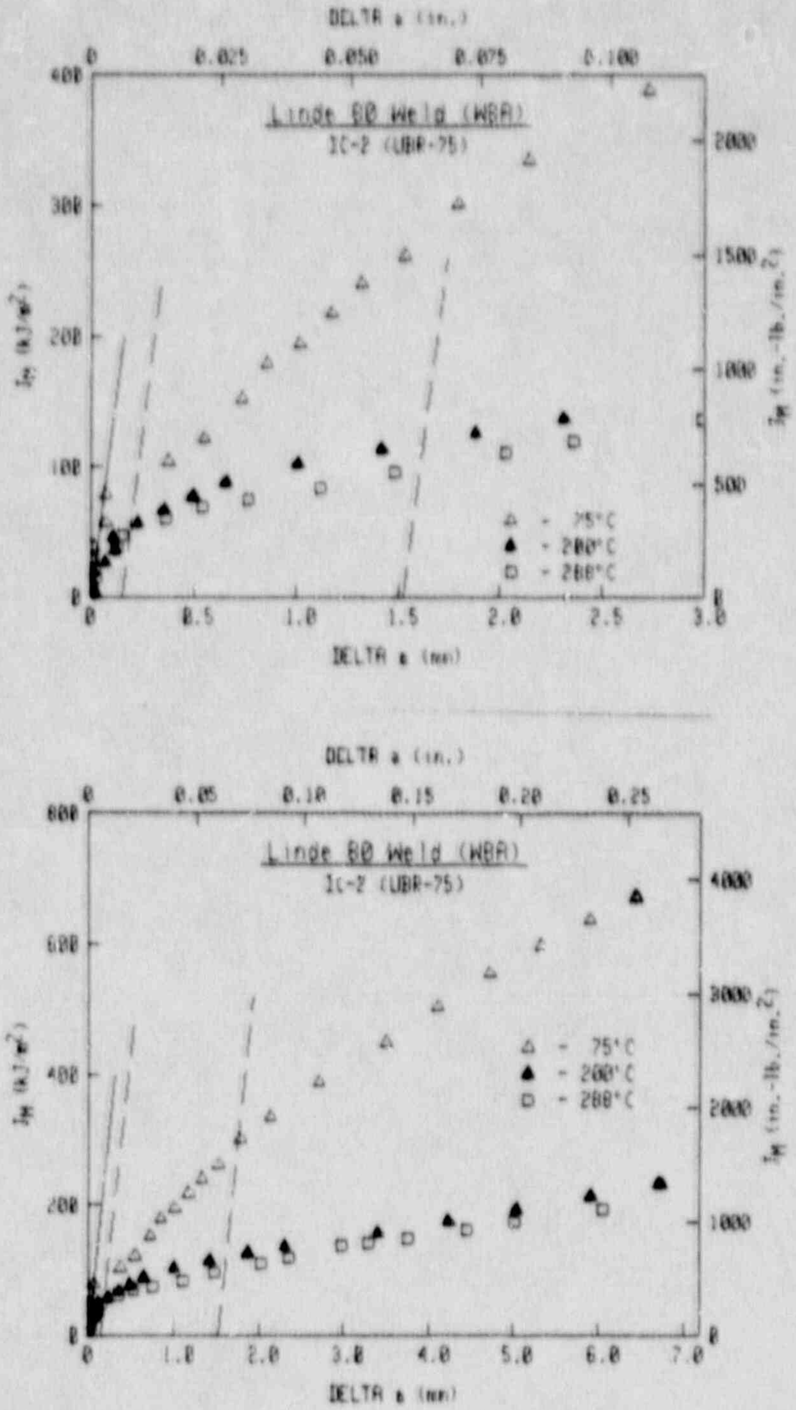

Fig. E-30 J-R curves for the IC-2 (UBR-75) irradiated condition of Linde 80 Weld W8A.

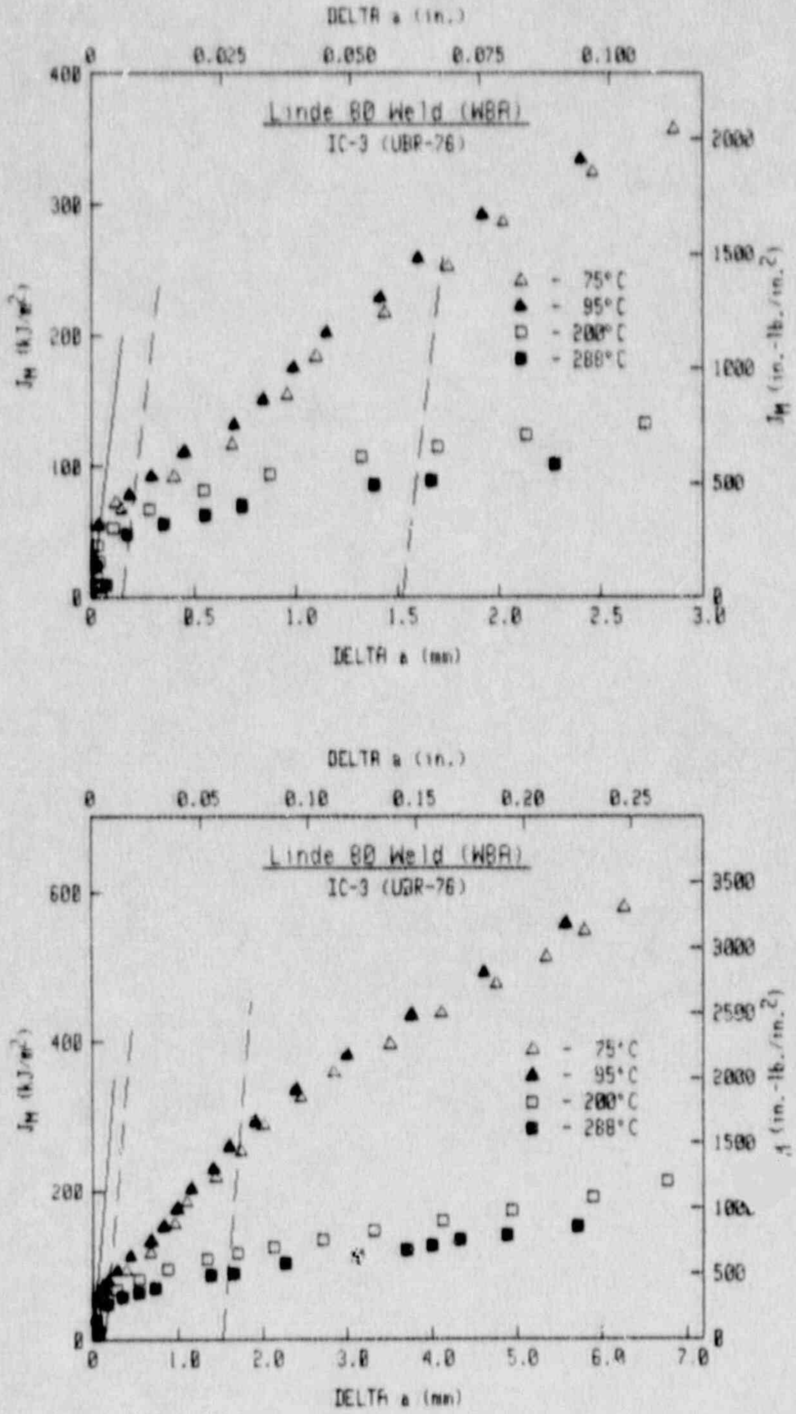

Fig. E-31 J-R curves for the IC-3 (UBR-76) irradiated condition of Linde 80 Weld W8A.

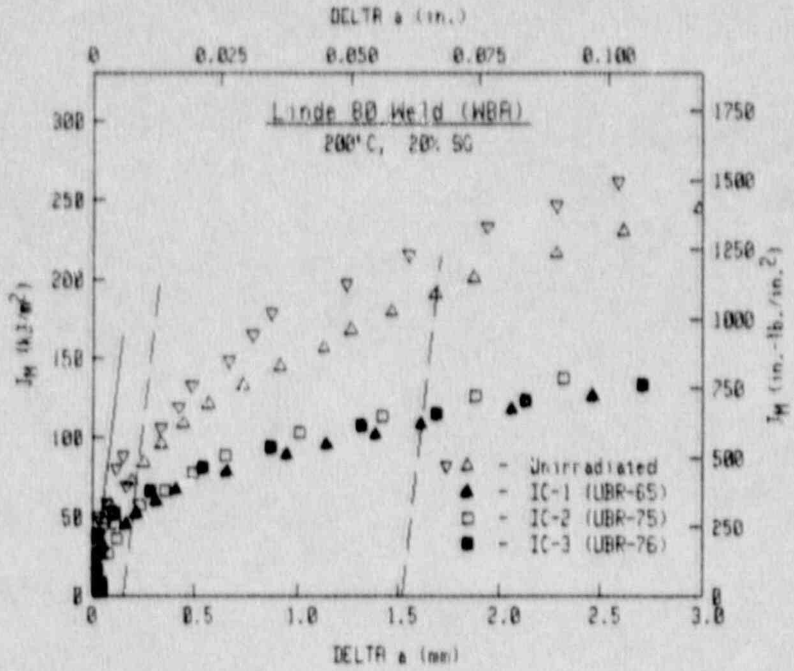

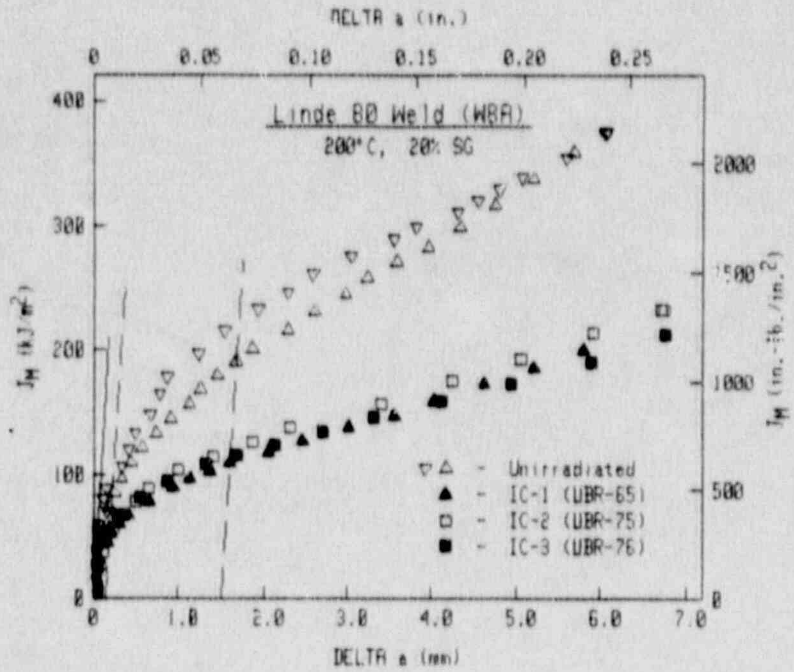

Fig. E-32 Comparison of J-R curves at 200°C from the unirradiated condition and the high fluence rate (IC) irradiated conditions of the Linde 80 Weld W8A.

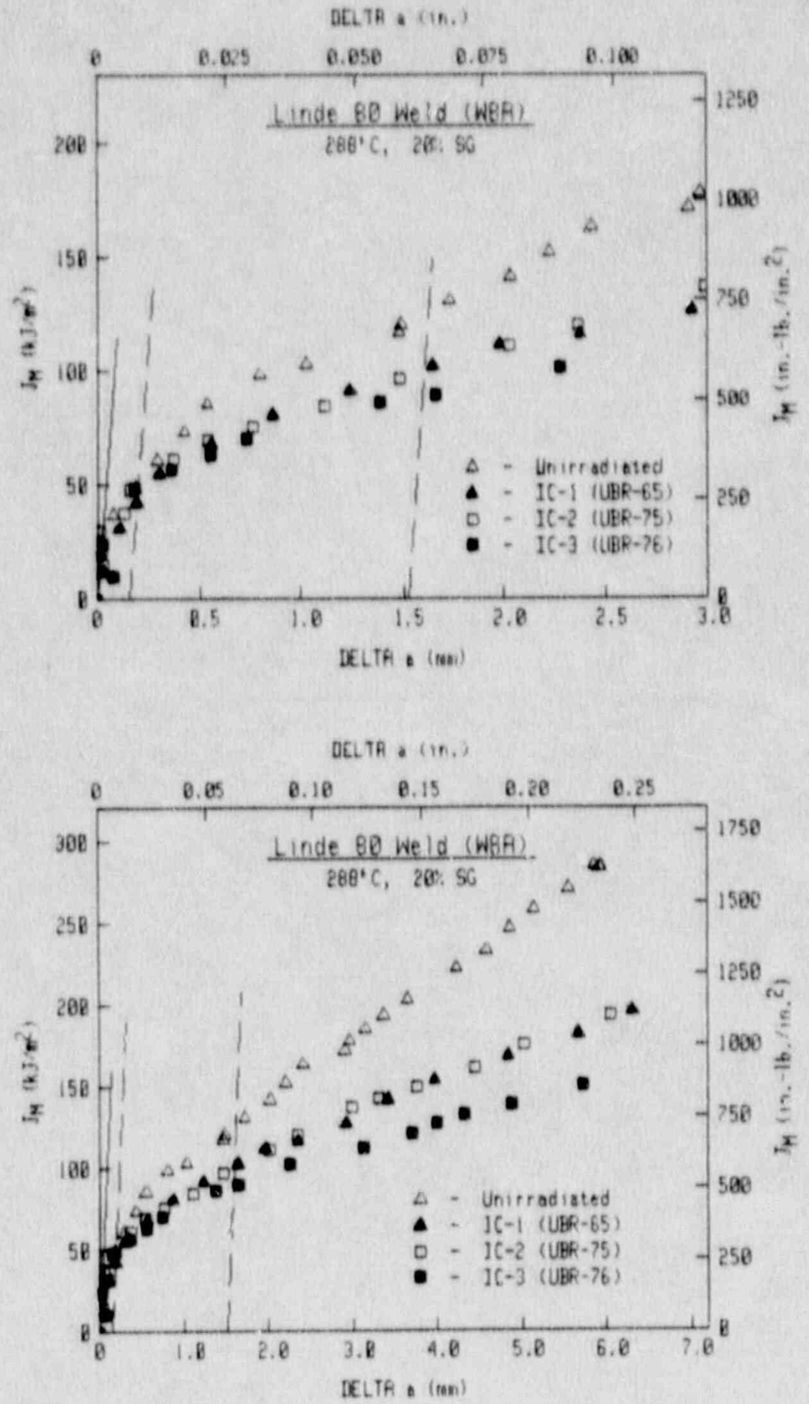

Fig. E-33 Comparison of J-R curves at 288°C from the unirradiated condition and the high fluence rate (IC) irradiated conditions of the Linde 80 Weld W8A.

irradiation. At 200°C (Fig. E-32), all three IC conditions exhibit similar J levels, whereas at 288°C the curve for IC-3 is lower than the other IC conditions.

Comparisons of these IC data with previous in-core irradiaton data are illustrated in Fig. E-34 at 200°C and 288°C. In general higher fluence tends to results in lower J-R curve levels, with the lowest curves from UBR-48 in Ref. E-2.

4.2.2 Intermediate Fluence Rate (CE)

K_{Jc} data for the CE conditions of the Linde 80 weld are illustrated in Figs. E-35. In contrast to the well-behaved nature of the IC data, the CE data do not indicate a consistent trend with fluence (Fig. E-36). Specifically, all three CE conditions indicate similar data in the transition temperature region. This trend is remarkably consistent with that exhibited by the A 302-B plate. The same discussion given in Section 4.1.2 on possible saturation of embrittlement for the A 302-B plate is also pertinent here.

Upper shelf (J-R curve) data for this weld are illustrated in Figs. E-37 to E-39. An example of the effect of side-grooves on J-R curves for this weld can be found in Fig. E-38 for CE-2. Of the two tests at 120°C, the higher curve is from a plane-sided specimen, whereas the lower curve is from a side-grooved specimen. In this case, the effect of side-grooving (ignoring all other variables such as fluence and irradiation temperature) is quite striking. In contrast, two side-grooved specimens from CE-3 tested at 288°C exhibit nearly identical J-R curves (Fig. E-39).

Comparisons of the curves for all three CE conditions at 288°C (Fig. E-40) are similar to those for the IC conditions. Specifically, large reductions in toughness are evident for the post-irradiation conditions, with the highest fluence yielding the lowest J levels overall.

4.2.3 Comparisons of Different Fluence Rates

Transition temperature increases as a function of fluence are compared in Fig. E-41 for all of the irradiation conditions. Data for the highest fluence rates include the IC conditions and two other in-core irradiations reported in Ref. E-2. For reasons yet unknown, fracture toughness data for the IC conditions and that from Ref. E-2 indicate somewhat different trends.

The data for the CE conditions within themselves do not indicate a consistent trend. Whereas CE-1 and CE-2 give an expected trend of increasing ΔT with increasing fluence, CE-3, which had the highest overall fluence of the CE irradiations, indicates the lowest overall ΔT of the three CE conditions. A satisfactory cause of this discrepancy is not readily identified; specimens for all three CE irradiations were from the same portion of the weld. One rationale is that the inherent scatter in the toughness data, in combination with fluence and irradiation temperature differences, may be masking a trend towards an embrittlement plateau.

(text continues on pg. E-61)

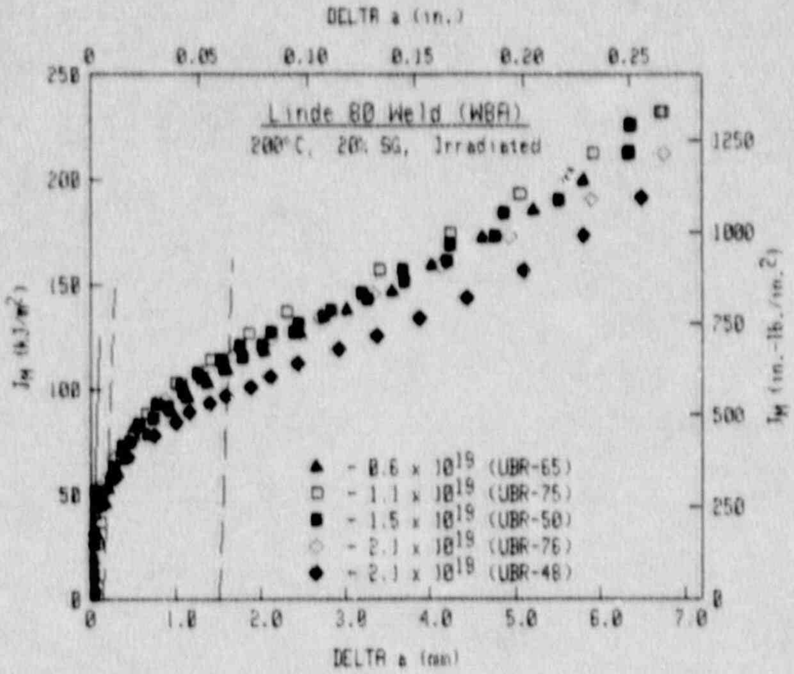

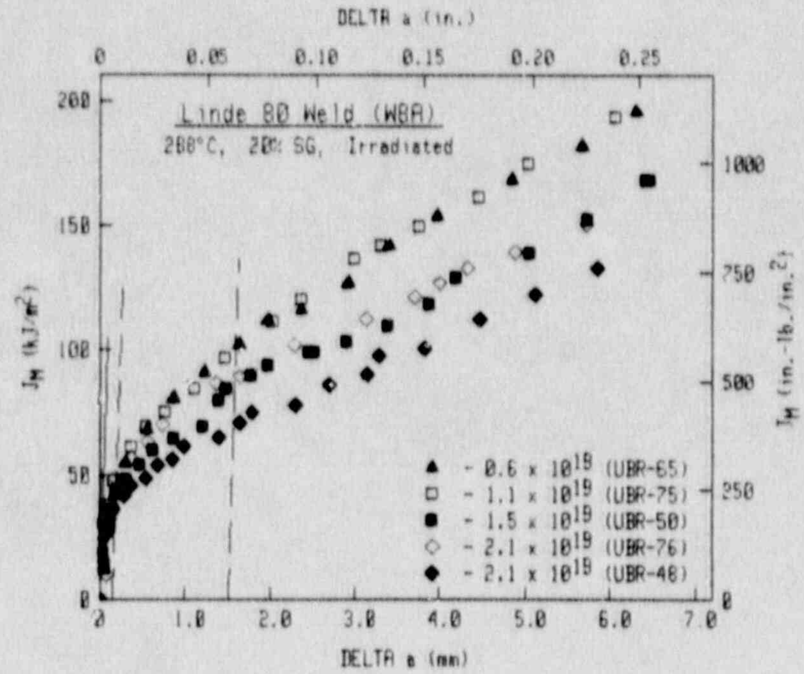

Fig. E-34 Comparison of J-R curves at 200°C and 288°C from the IC irradiations with those from previous in-core irradiations.

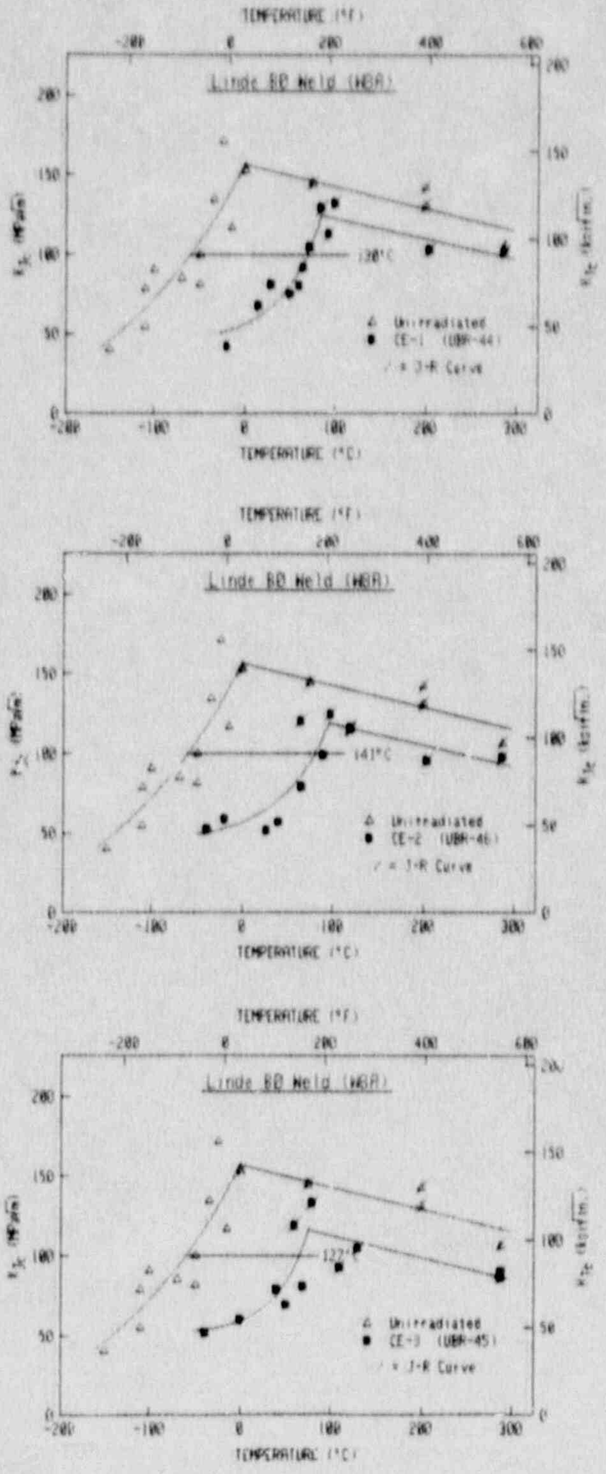

Fig. E-35 Comparisons of K_{Jc} data for the unirradiated condition and the intermediate fluence rate (CE) irradiated conditions of the Linde 80 Weld W8A.

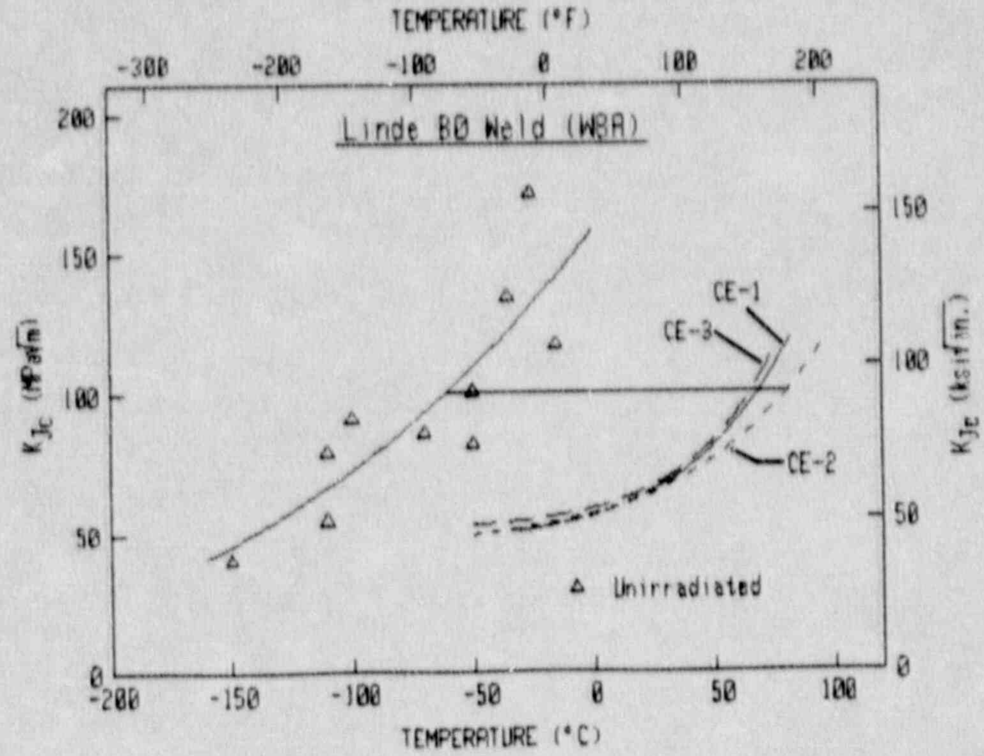

Fig. E-36 Comparison of the curve-fit results for the three intermediate fluence rate (CE) irradiated conditions.

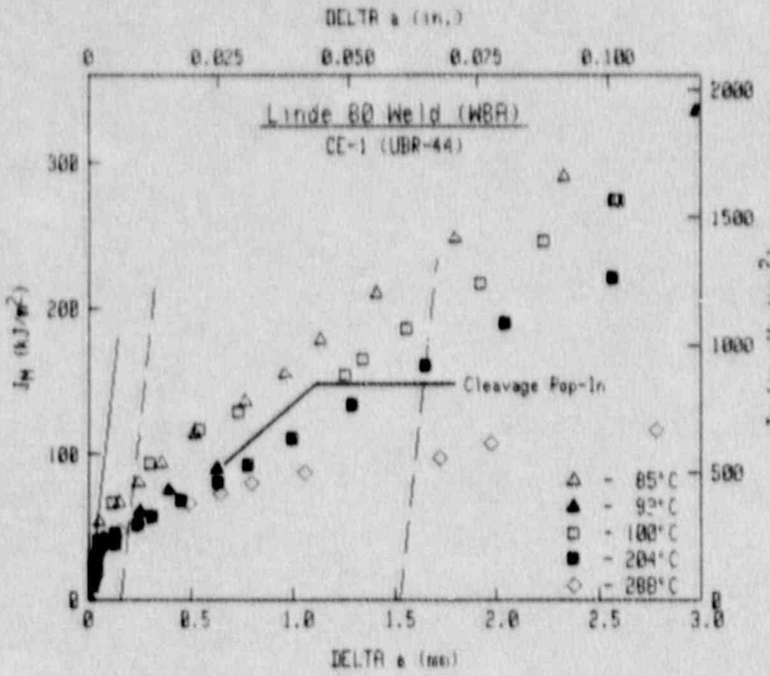

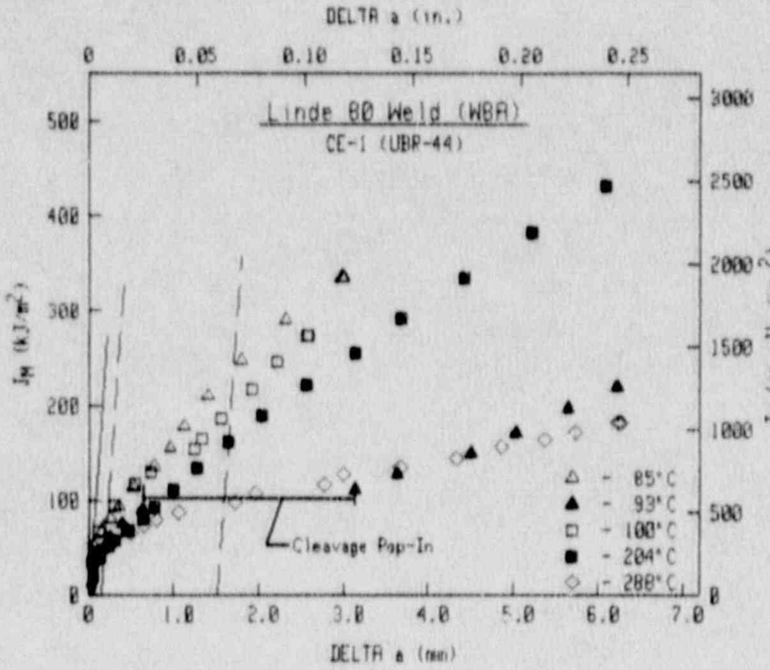

Fig. E-37 J-R curves for the CE-1 (UBR-44) irradiated condition of Linde 80 Weld W8A.

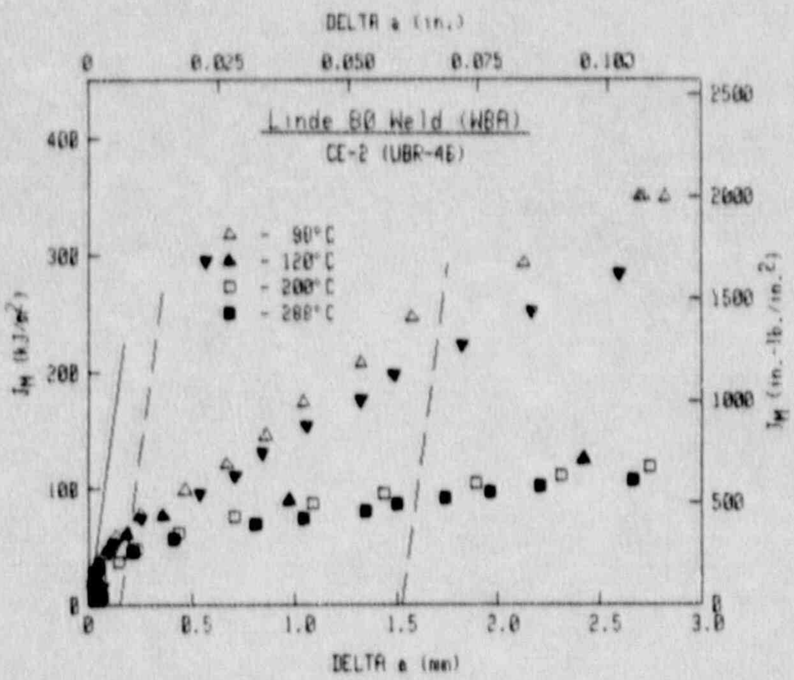

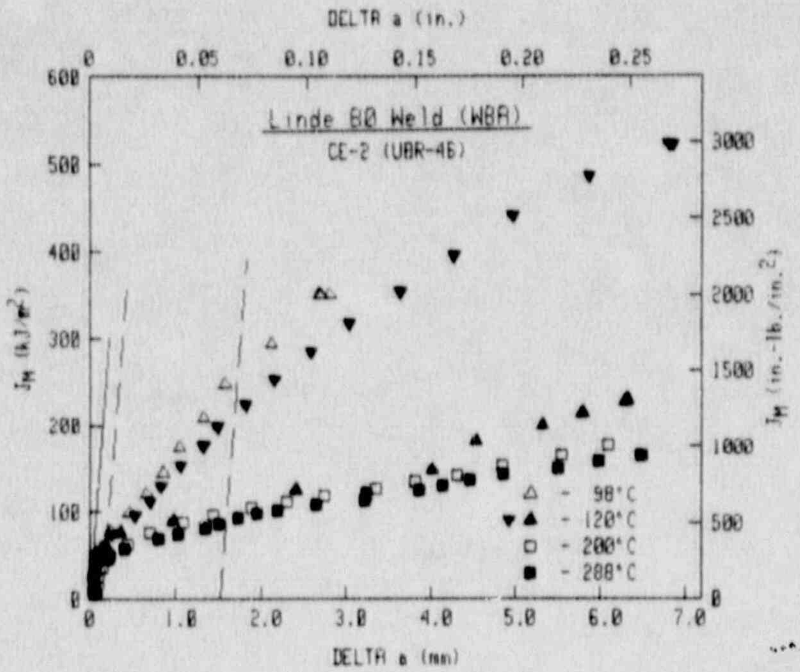

Fig. E-38 J-R curves for the CE-2 (UBR-46) irradiated condition of Linde 80 Weld W8A.

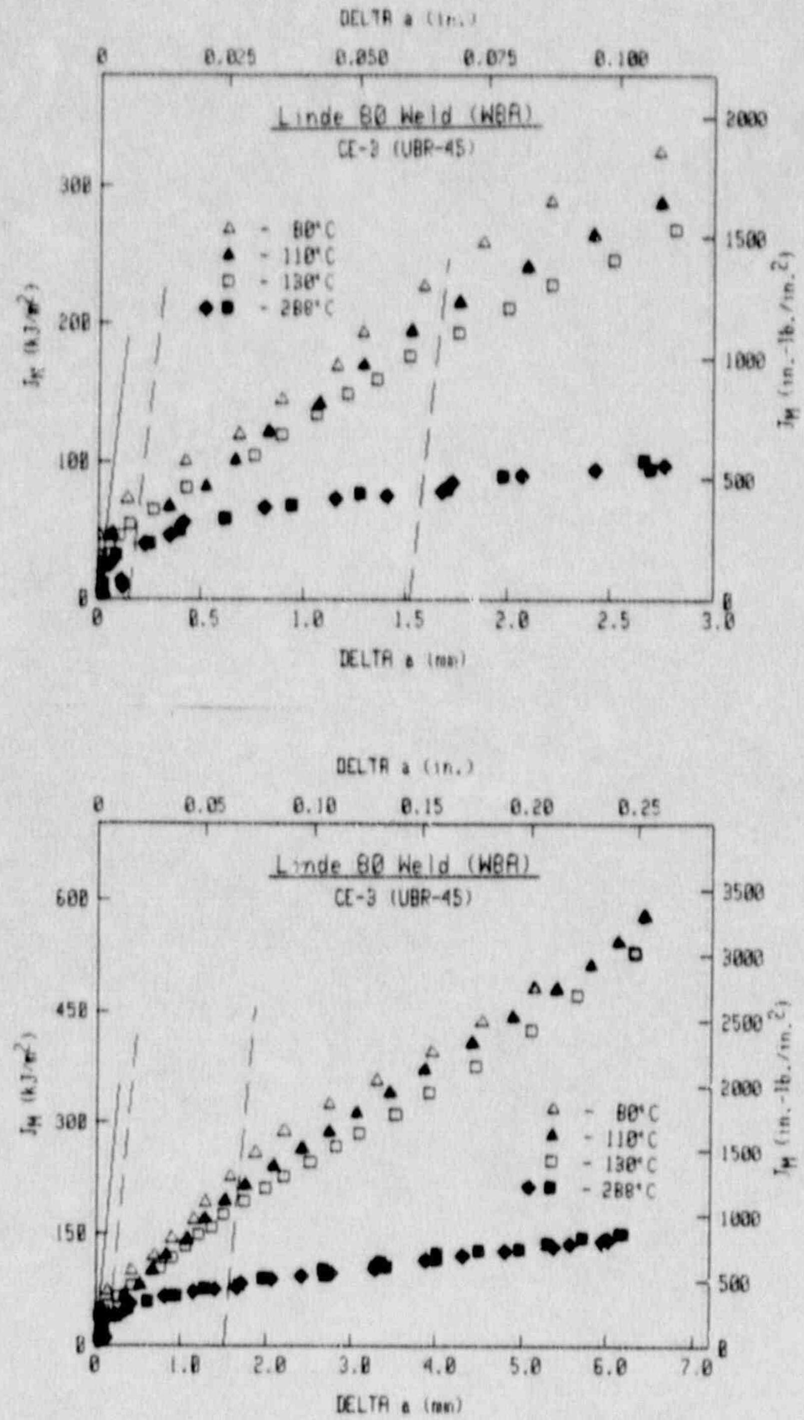

Fig. E-39 J-R curves for the CE-3 (UBR-45) irradiated condition of Linde 80 Weld W8A.

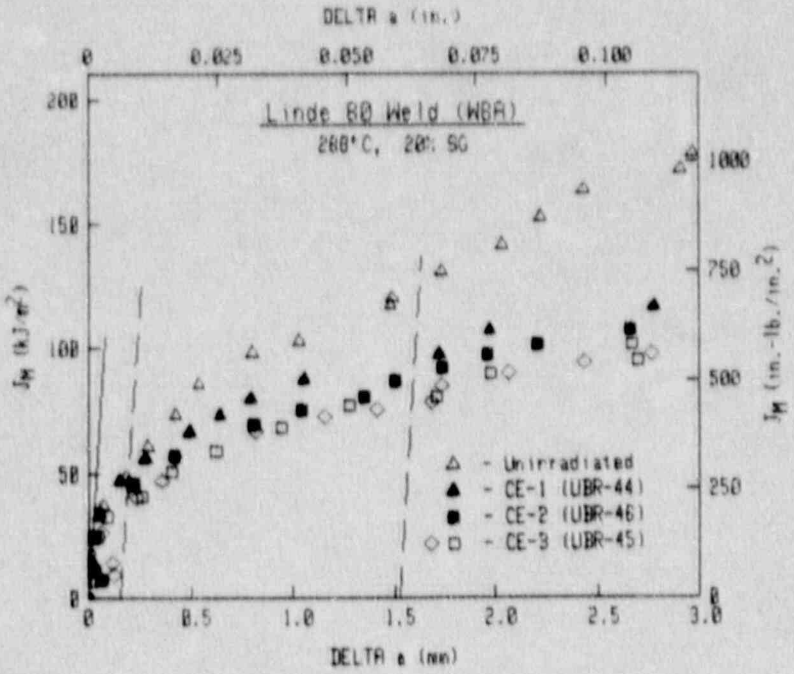

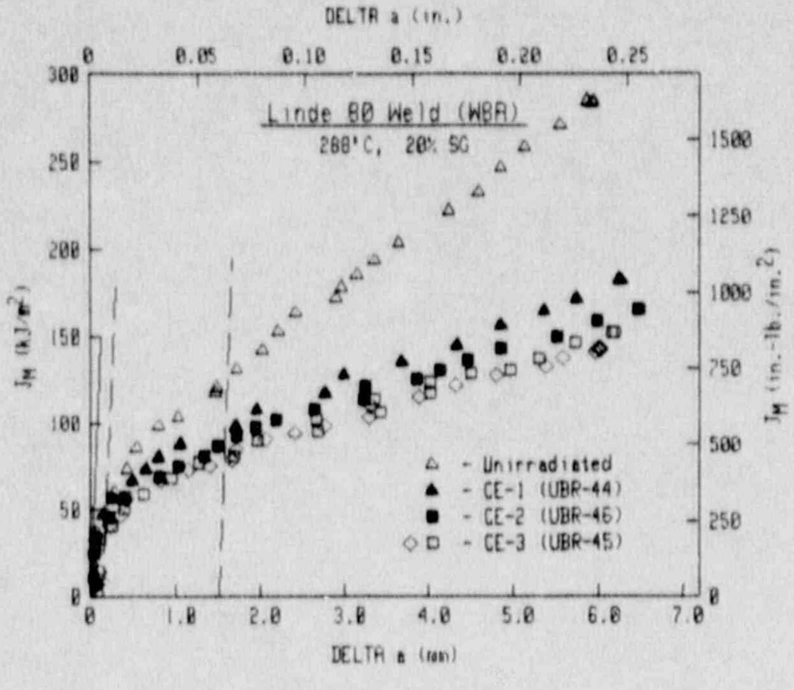

Fig. E-40 Comparison of J-R curves at 288 °C from the CE irradiations.

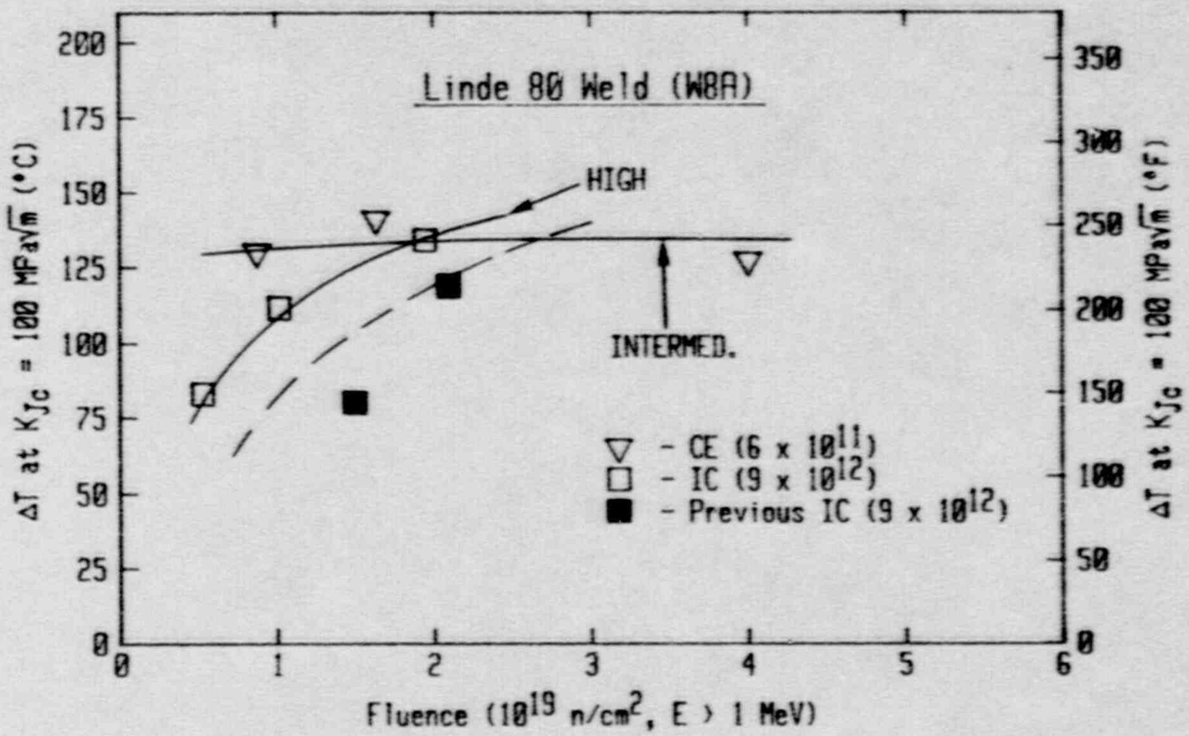

Fig. E-41 Transition temperature shifts as a function of fluence for the Linde 80 Weld W8A.

Overall, data for the IC conditions exhibit lower embrittlement than the CE conditions at low fluence. A cross-over in embrittlement for the two fluence rates occurs near 2×10^{19} n/cm^2, similar to the trend found for the A 302-B plate.

In terms of the upper shelf (J-R curve) trends, data for the irradiated conditions only are illustrated in Fig. E-42 for 200°C and 288°C. The comparisons at 200°C are only useful from the standpoint of CE-2 and the IC conditions, since no data is available for CE-3 and the specimen tested from CE-1 was plane-sided, resulting in a large elevation in the J levels. At 288°C, the highest curves are from IC-1 and IC-3, whereas the lowest curves are from CE-3. Comparison of the curves from IC-3 and CE-2 at 288°C indicates close agreement, which is also indicated by the fluences. Therefore, the upper shelf data are consistent with the transition region data, in that the IC condition at low fluences indicates less embrittlement than the CE condition, but at a fluence of ~ 2×10^{19} the two fluence rates give similar J-R curve trends.

4.3 <u>A 533-B Plate (23G)</u>

This plate was tested in one IC condition (IC-4) and one IP condition (IP-1). Detailed data for all of these conditions are given in Table E-5.

Comparisons of the J-R curves for the unirradiated condition are illustrated in Fig. E-43. Tests at 200°C and 288°C indicate excellent agreement at those temperatures.

4.3.1 High Fluence Rate (IC)

K_{Jc} data for the IC condition are compared to data for the unirradiated condition in Fig. E-44. Near the arbitrary index of 100 MPa$\sqrt{m}$, data for the irradiated condition indicate only a small shift (29°C) from that for the unirradiated condition. There is some variability in the data for the irradiated condition near 100 MPa$\sqrt{m}$, although the indicated mean curve bisects the data at that fracture toughness level.

J-R curve data for the IC condition are illustrated in Fig. E-45. As with the unirradiated condition, data at 200°C and 288°C are coincident. Comparisons of the J-R curves for the IC condition with those for the unirradiated condition (Figs. E-46 and E-47) at 200°C and 288°C indicate no loss in upper shelf toughness due to the irradiation exposure.

4.3.2 Low Fluence Rate (IP)

K_{Jc} data for the IP condition are compared to those for the unirradiated condition in Fig. E-48. In contrast to the IC data in Fig. E-44 and IP data for the A 302-B plate (23F) in Fig. E-20, considerable scatter is obvious in the data for the IP condition of the A 533-B plate. No simple explanation for the scatter in the IP data is at hand. The transition temperature shift is also much larger for the A 533-B plate than for the A 302-B Plate 23F.

(text continues on pg. E-71)

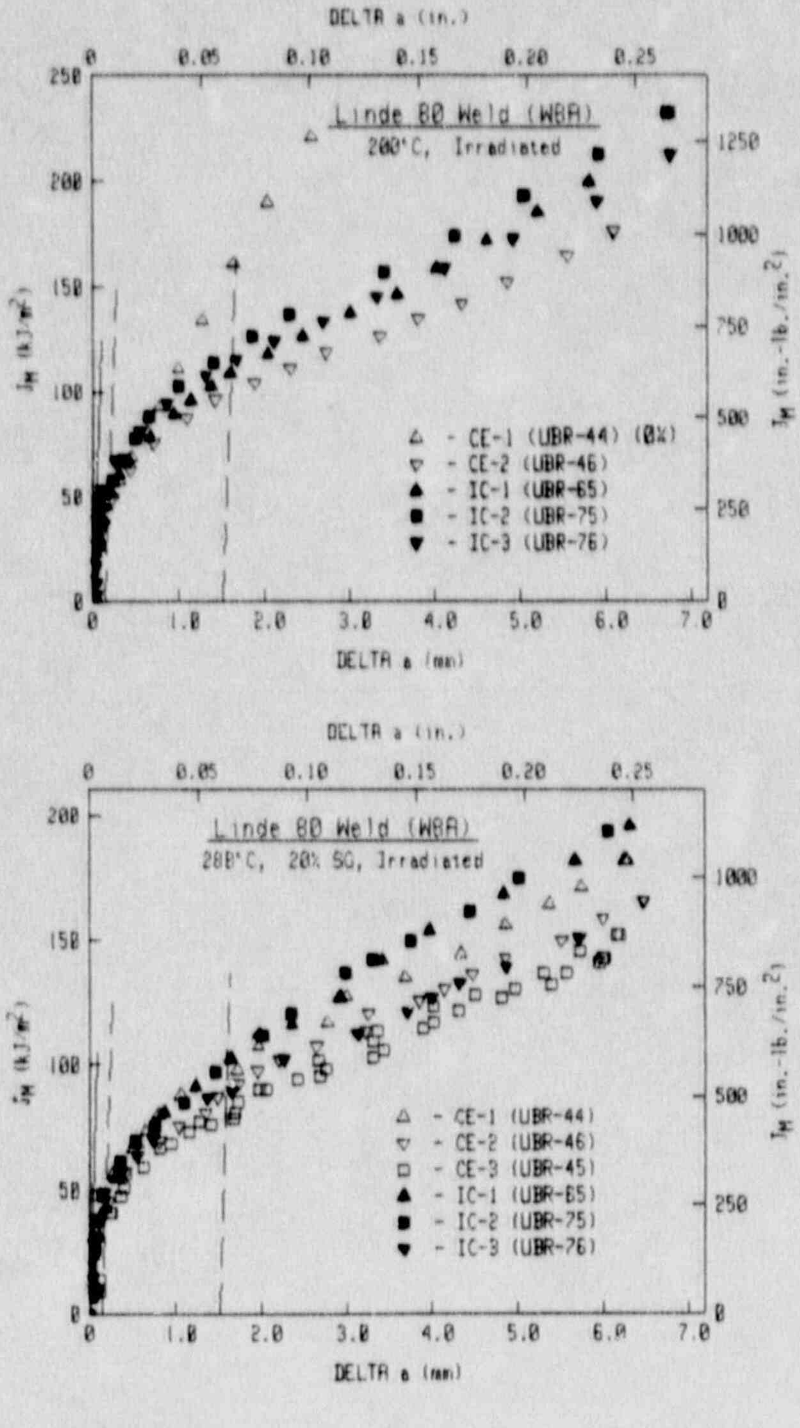

Fig. E-42 Comparison of J-R curves at 200 °C and 288 °C from the irradiation conditions of the Linde 80 Weld W8A.

Table E-5 Fracture Toughness Data for A 533-B Plate (23G)

Specimen Number	Test Temp (°C)	$(a/W)_o$ [a]	a_m [b] (mm)	a_p [c] (mm)	$a_p - a_m$ (mm)	J_{Ic} P.L. (kJ/m^2)	J_{Ic} ASTM (kJ/m^2)	K_{Jc} P.L. (MPa $\sqrt{m}$)	K_{Jc} ASTM (MPa $\sqrt{m}$)	K_c (MPa $\sqrt{m}$)	K_{max} (MPa $\sqrt{m}$)	T_{avg}	f (MPa)	y (MPa)
UNIRRADIATED														
23G-28	-171	0.519	—	—	—	6.4	—	39.0	39.3[e]	36.7	39.3	—	718.3	592.1
TA4-14	-140	0.555	—	—	—	1[illegible].2	—	58.0	56.1	47.9	56.1	—	674.8	560.2
23G-16	-110	0.508	—	—	—	31.3	—	85.7	46.7	57.7	75.3	—	636.6	531.9
TA4-16	-95	0.509	—	—	—	32.5	—	87.2	47.1	57.4	76.6	—	618.9	518.7
23G-31	-80	0.539	—	—	—	39.5	—	96.0	35.0	59.2	81.8	—	602.1	506.1
TA4-15	-65	0.534	—	—	—	82.8	—	138.5	45.1	68.1	80.1	—	586.3	494.4
23G-29	-50	0.518	—	—	—	86.2	—	141.1	46.9	67.1	84.8	—	571.4	482.[illegible]
TA4-17	-35	0.515	—	—	—	132.3	—	174.4	41.9	72.4	80.1	—	557.5	47[illegible].0
23G-15	-20	0.511	—	—	—	243.5	—	236.2	54.2	79.8	89.0	—	544.5	[illegible]61.9
23G-8[d]	24	0.516	5.63	5.29	-0.34	267.3	195.1	245.8	210.0	—	—	200	511.[illegible]	435.8
TA4-13[d]	200	0.514	6.14	5.96	-0.18	164.5	157.3[f]	188.0	183.9	—	—	122	462.8	385.0
TA4-18[d]	288	0.516	6.86	6.69	-0.17	195.4	188.6[f]	202.4	198.8	—	—	91	487.1	391.6
23G-14[d]	288	0.517	6.29	6.11	-0.18	153.1	146.0[f]	179.2	174.9	—	—	114	487.1	391.6
IRRADIATED IP-1 (UBR-38)														
23G-13[d]	-90	0.524	—	—	—	15.7	—	60.5	52.3	48.8	55.8	—	708.6	614.7
23G-7[d]	-55	0.519	—	—	—	10.7	—	49.7	47.3	42.4	47.3	—	671.7	586.7
23G-5[d]	-30	0.508	—	—	—	30.3	—	83.4	51.9	55.7	73.2	—	648.5	568.8
23G-11[d]	-10	0.515	—	—	—	11.1	—	50.3	47.0	41.9	47.0	—	631.9	555.8
23G-10[d]	15	0.507	—	—	—	32.5	—	85.9	50.2	54.9	74.1	—	613.4	541.0
23G-2[d]	22	0.508	—	—	—	130.6	—	171.9	51.4	72.8	98.6	—	608.7	537.1
23G-3[d]	28	0.520	—	—	—	73.0	—	128.4	55.5	64.8	95.7	—	604.8	534.0
23G-12[d]	50	0.518	—	—	—	125.6	—	168.0	53.7	71.0	97.9	—	591.9	523.2
23G-9[d]	70	0.510	—[g]	—[g]	—[g]	258.7	265.1	240.3	243.3	—	—	—	582.0	514.5
23G-4[d]	100	0.520	6.60	6.29	-0.31	237.9	244.1	229.5	232.5	—	—	97	570.2	503.6
23G-6[d]	200	0.533	6.48	6.32	-0.16	196.4	183.7[f]	205.6	198.8	—	—	102	558.3	485.2
23G-1[d]	288	0.517	7.11	5.80	-1.31	150.9	147.4	177.9	175.8	—	—	62	582.6	491.9

[a] Pre-test a/W.
[b] Optically-measured crack growth.
[c] Crack growth predicted by compliance.
[d] Side grooved.
[e] Valid K_{Ic} per ASTM E 399.
[f] Valid J_{Ic} per ASTM E 813-81.
[g] Cleavage failure precluded determination of this quantity.

Table E-5 Fracture Toughness Data for A 533-B Plate (23G) (continued)

Specimen Number	Test Temp (°C)	$(a/W)_o$ [a]	a_m [b] (mm)	a_p [c] (mm)	$a_p - a_m$ (mm)	J_{Ic} P.L. (kJ/m^2)	J_{Ic} ASTM (kJ/m^2)	K_{Jc} P.L. ($MPa\sqrt{m}$)	K_{Jc} ASTM ($MPa\sqrt{m}$)	K_c ($MPa\sqrt{m}$)	K_{max} ($MPa\sqrt{m}$)	T_{avg}	f (MPa)	y (MPa)
IRRADIATED IC-4 (UBR-77)														
23G-21	-130	0.513	—	—	—	—	—	—	34.0 [e]	—	34.0	—	711.4	602.5
23G-19	-100	0.515	—	—	—	11.3	—	51.5	41.5	44.8	49.5	—	674.4	575.0
23G-24	-75	0.514	—	—	—	41.4	—	98.1	52.4	62.8	83.8	—	646.5	554.0
23G-17	-60	0.509	—	—	—	53.2	—	110.9	51.4	65.6	87.3	—	631.0	542.3
23G-22	-35	0.508	—	—	—	45.1	—	101.9	49.9	62.0	83.0	—	607.3	524.0
23G-30	-22	0.513	—	—	—	87.0	—	141.2	49.6	70.4	92.5	—	596.0	515.2
23G-27	-10	0.517	—	—	—	103.8	—	153.9	48.8	72.2	89.7	—	586.2	507.5
23G-18	10	0.510	—	—	—	147.4	—	182.8	47.0	76.0	92.0	—	571.2	495.5
23G-25	30	0.515	—	—	—	156.9	—	188.2	48.3	75.7	90.9	—	557.9	484.7
23G-23	50	0.525	— [g]	— [g]	— [g]	356.7	— [g]	283.0	— [g]	—	—	—	546.2	474.9
23G-32 [d]	200	0.524	6.78	6.09	-0.69	173.0	175.8 [f]	192.9	194.5	—	—	87	512.6	436.9
23G-20 [d]	288	0.529	6.59	6.13	-0.46	163.3	144.3 [f]	185.0	174.0	—	—	86	536.9	443.6

[a] Pre-test a/W.
[b] Optically-measured crack growth.
[c] Crack growth predicted by compliance.
[d] Side grooved.
[e] Valid K_{Ic} per ASTM E 399.
[f] Valid J_{Ic} per ASTM E 813-81.
[g] Cleavage failure precluded determination of this quantity.

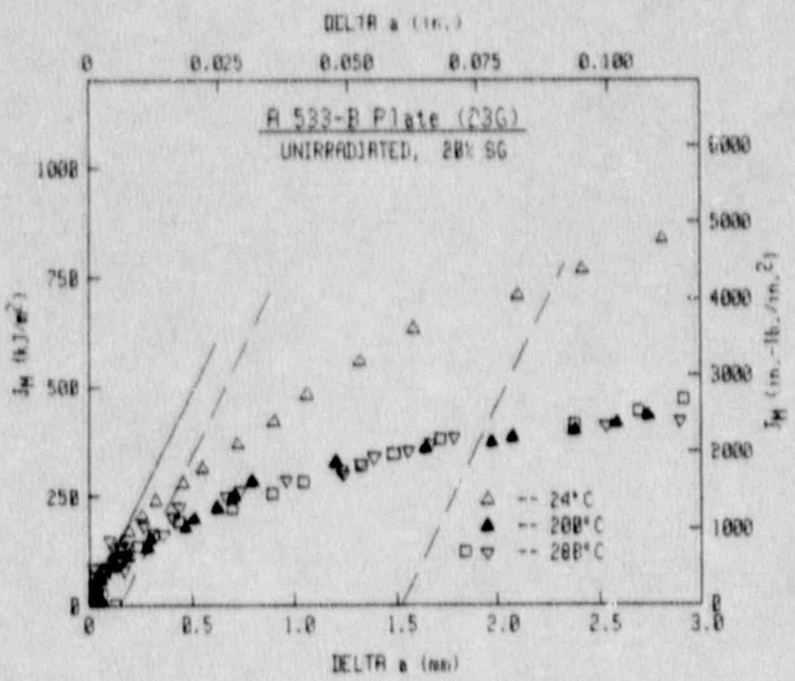

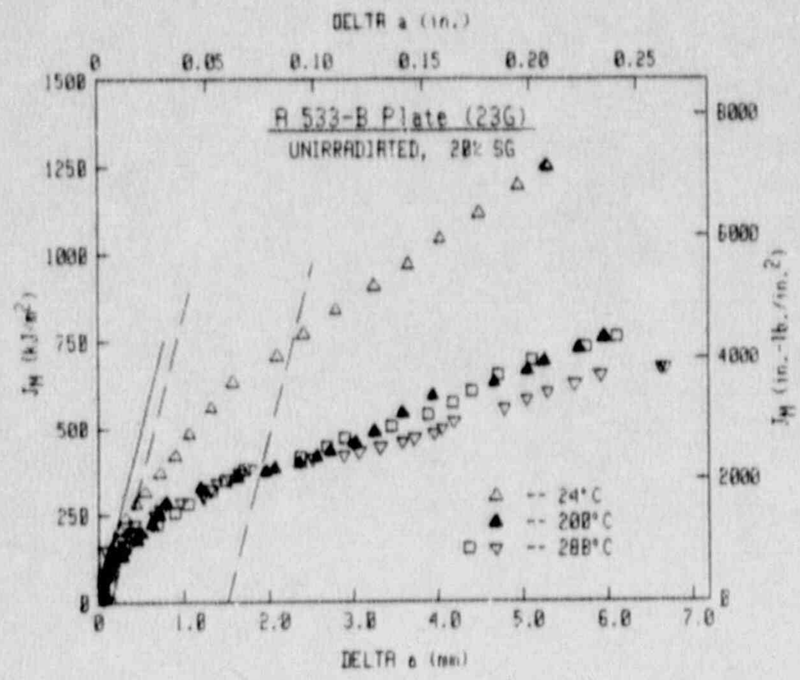

Fig. E-43 J-R curves for the unirradiated condition of the A 533-B Plate 23G.

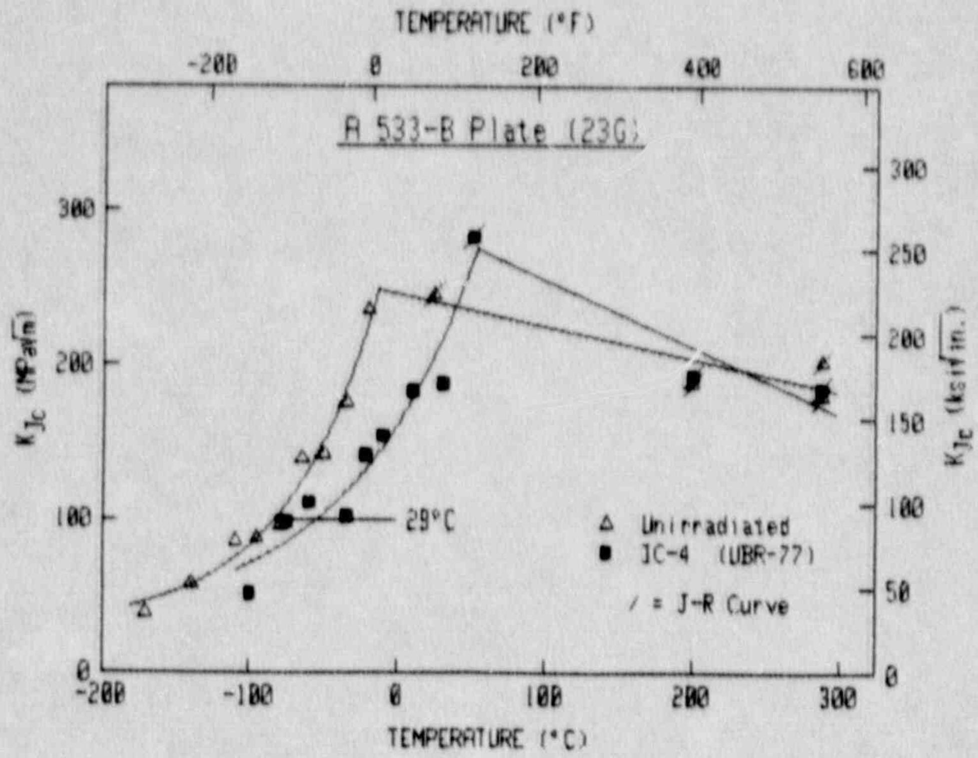

Fig. E-44 Comparisons of K_{Jc} data for the unirradiated condition and the high fluence rate (IC) irradiated condition of the A 533-B Plate 23G.

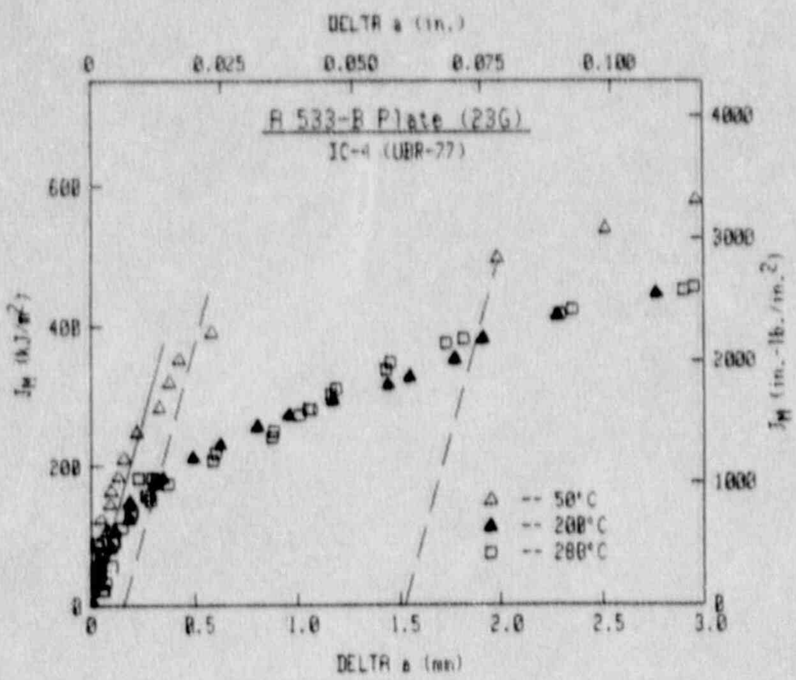

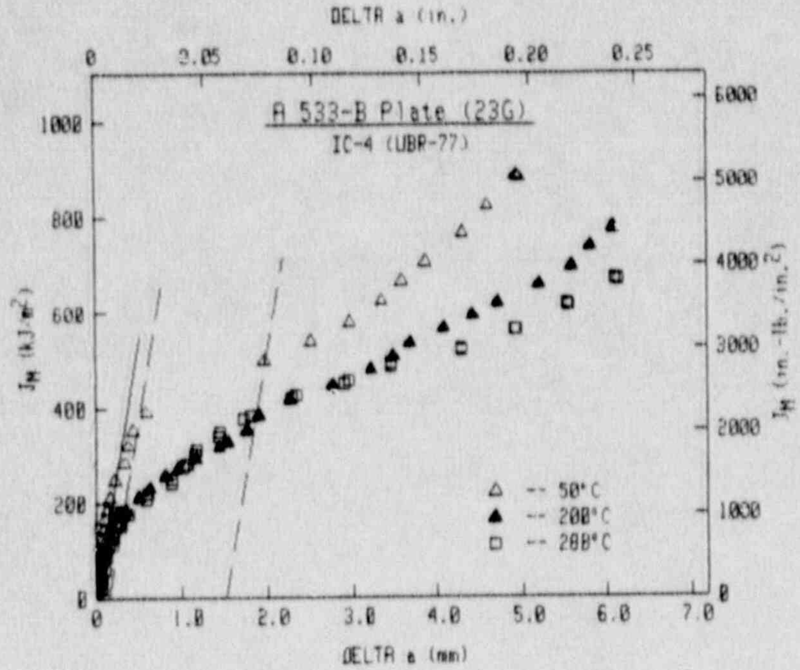

Fig. E-45 J-R curves for the IC-4 (UBR-77) irradiated condition of A 533-B Plate 23G.

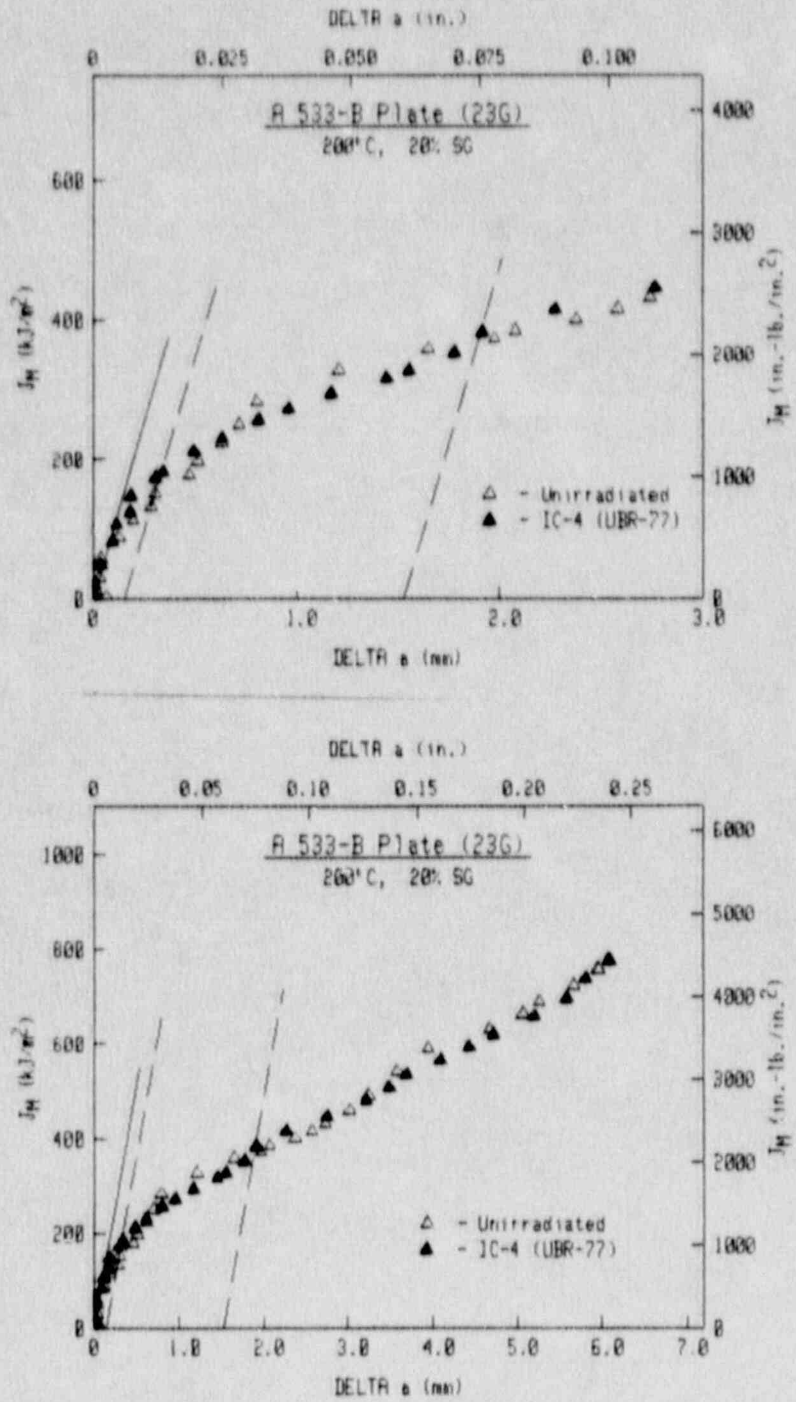

Fig. E-46 Comparison of J-R curves at 200 °C from the unirradiated condition and the high fluence rate (IC) irradiated condition of the A 533-B Plate 23G.

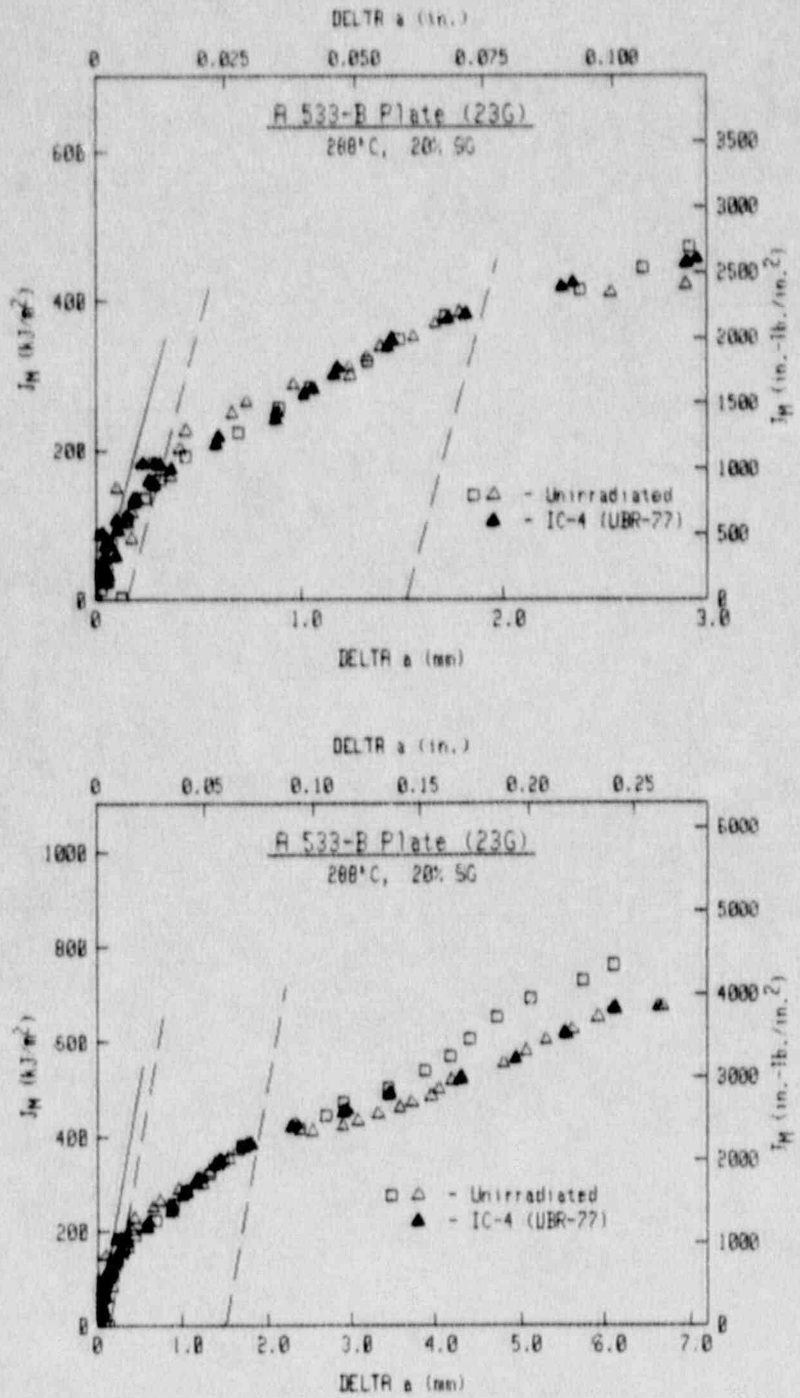

Fig. E-47 Comparison of J-R curves at 288 °C from the unirradiated condition and the high fluence rate (IC) irradiated condition of the A 533-B Plate 23G.

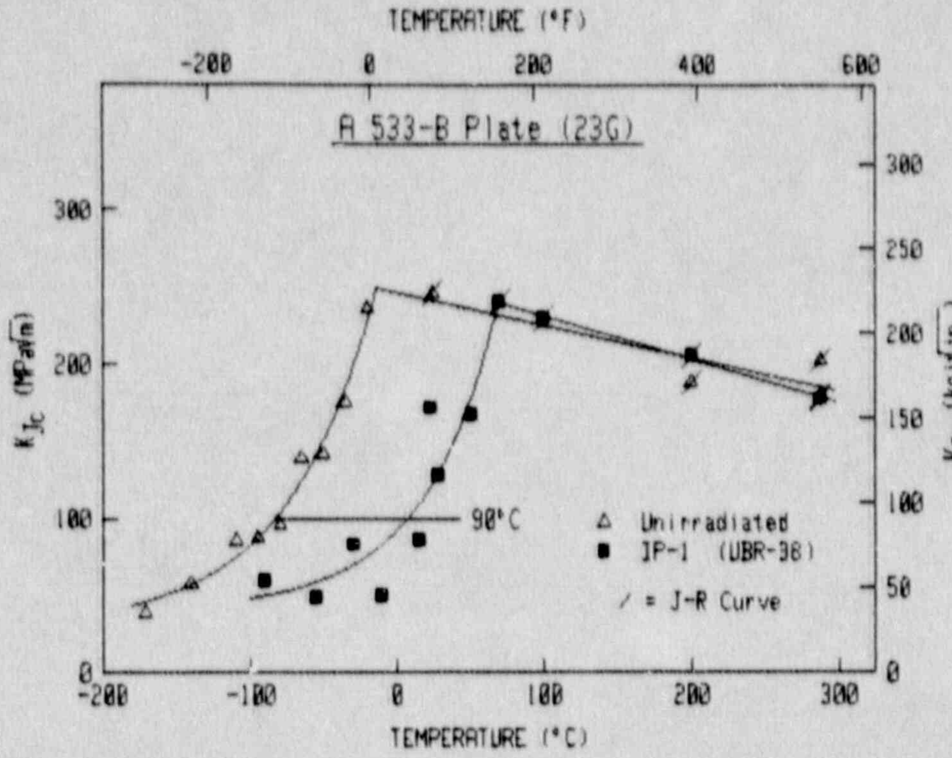

Fig. E-48 Comparison of K_{Jc} data for the unirradiated condition and the low fluence rate (IP) irradiated condition of the A 533-B Plate 23G.

J-R curves for the IP condition are also somewhat unusual for this plate, as the test at 200°C yields much higher J levels than the test at 288°C (Fig. E-49). As expected, data for the IP condition at 200°C indicate no loss in toughness due to irradiation (Fig. E-50). However, data for the IP condition at 288°C indicate slightly higher toughness than the unirradiated condition (Fig. E-51).

4.3.3 Comparisons of Different Fluence Rates

Since the fluences of the IC and the IP conditions are relatively close (within ±10%), K_{Jc} data for these two conditions can be directly compared. As illustrated in Fig. E-52, data for the IP condition indicate a much larger shift than do the data for the IC condition. While this trend is consistent with that found with the A 302-B plate (23F), the magnitude of the differences is much greater than that found with the A 302-B plate. Although data scatter does tend to magnify the apparent differences, even the upper bound data for the IP condition are only close to but not within the data scatter for the IC condition.

In terms of the upper shelf trends (Fig. E-53), data for both irradiated conditions indicate similar toughness to the unirradiated condition at 288°C, whereas the IP condition exhibits somewhat higher toughness at 200°C.

4.4 Linde 0091 Weld (W9A)

At this point, irradiated data for this weld are available for an IC condition (IC-4) only. (Data for an IP condition, IP-2, will be developed in follow-on work.) Previous data from in-core irradiations are also available (Ref. E-2).

Detailed data for this weld in the unirradiated condition and the IC condition (IC-4) are given in Table E-6. K_{Jc} data for these conditions are compared in Fig. E-54. Data scatter is remarkably low for this weld. The transition temperature shift at 100 MPa$\sqrt{m}$ (79°C) is similar to that for the Linde 80 Weld W8A for the IC-1 condition (81°C), with similar fluences.

For each condition, J-R curves are illustrated in Figs. E-55 and E-56. In each case, increased test temperature results in lower J levels, and tests at 288°C give only slightly lower J levels than those at 200°C. Comparing data for these two conditions with that from previous in-core irradiations (Ref. E-2), a consistent trend emerges whereby higher fluence results in lower J levels (Figs. E-57 to E-59). This trend is most pronounced at 75°C (Fig. E-57) and 288°C (Fig. E-59).

Transition temperature shifts (ΔT) from K_{Jc} data as a function of fluence are illustrated in Fig. E-60. The previous data from in-core irradiations illustrate somewhat less embrittlement with fluence than does the data from IC-4.

(end of text)

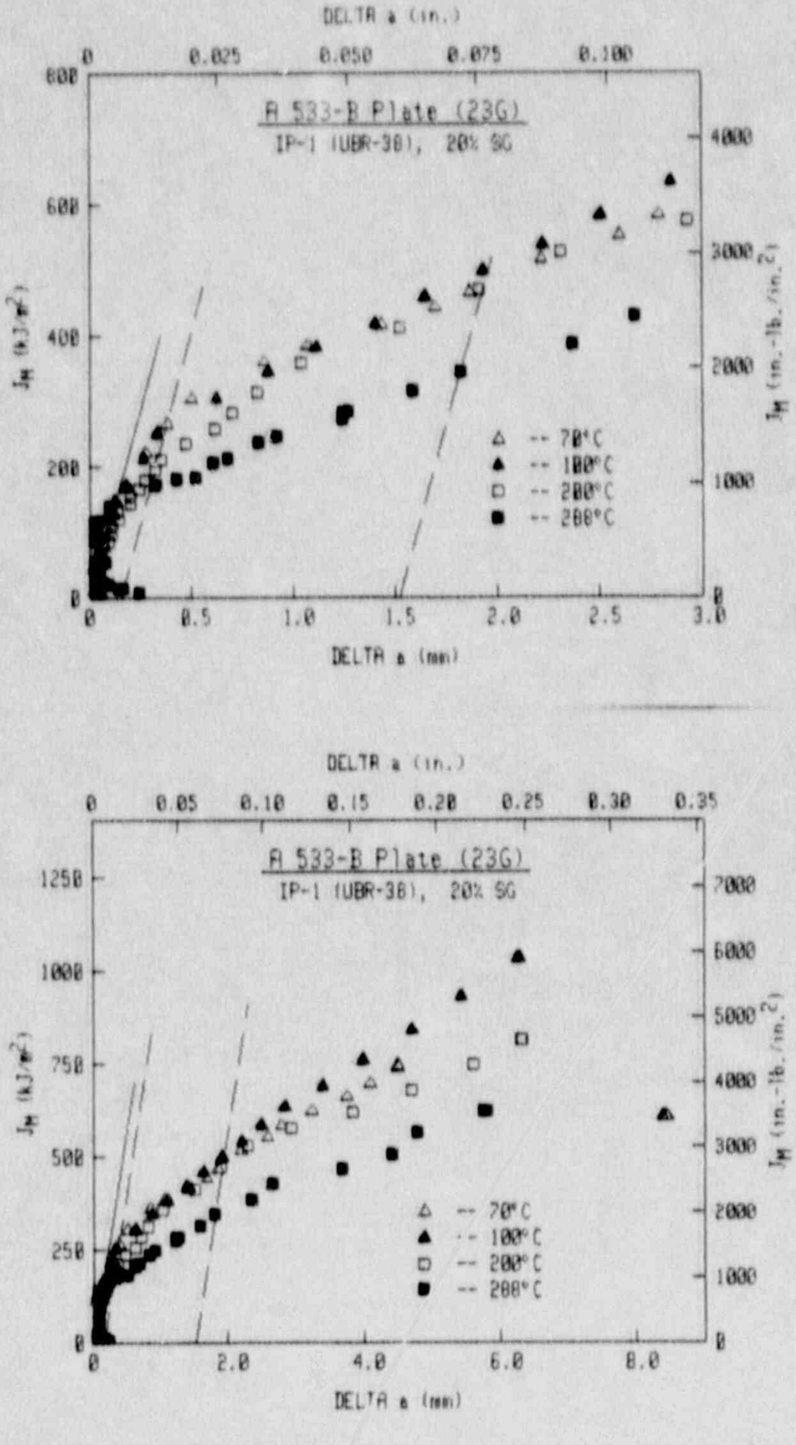

Fig. E-49 J-R curves for the IP-1 (UBR-38) irradiated condition of A 533-B Plate 23G.

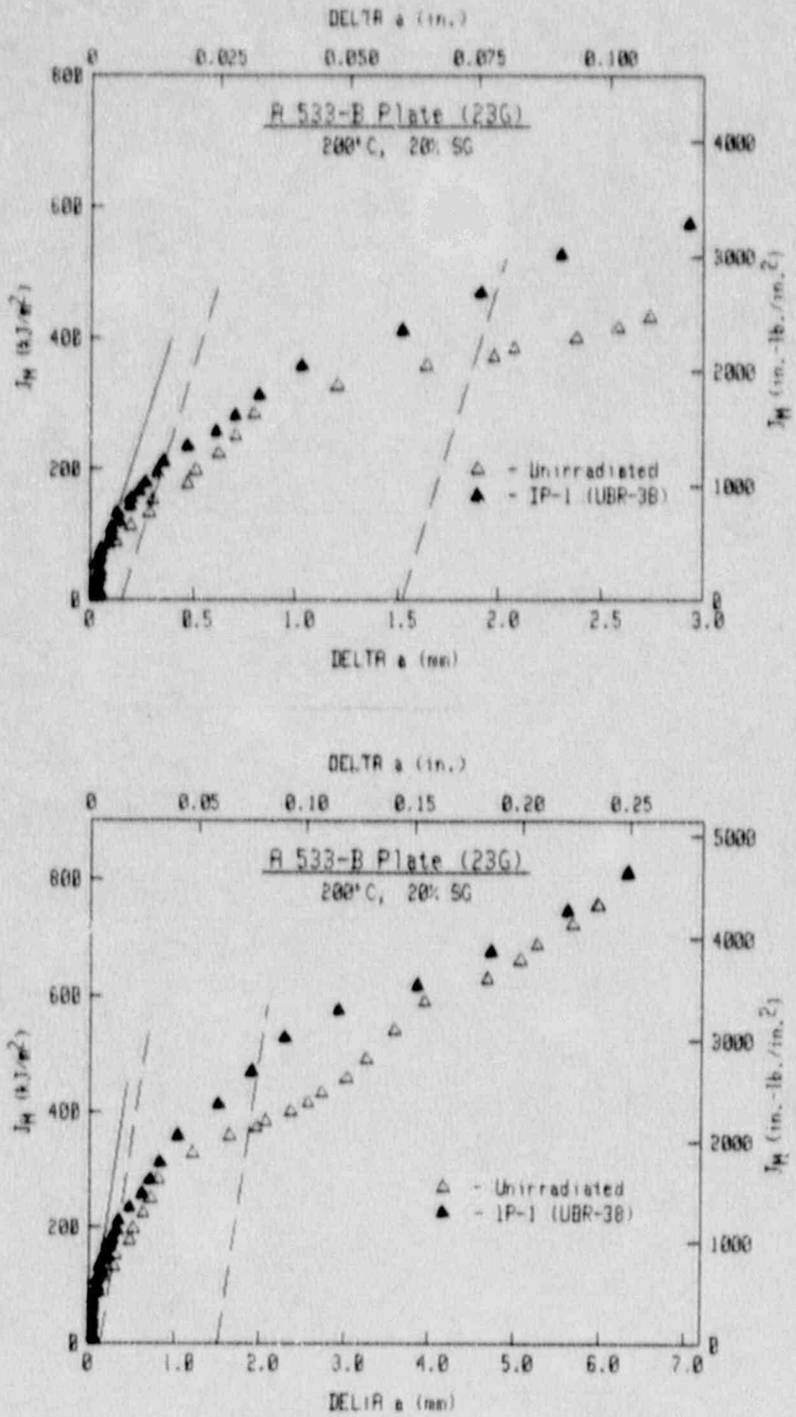

Fig. E-50 Comparison of J-R curves at 200 °C from the unirradiated condition and the low fluence rate (IP) irradiated condition of the A 533-B Plate 23G.

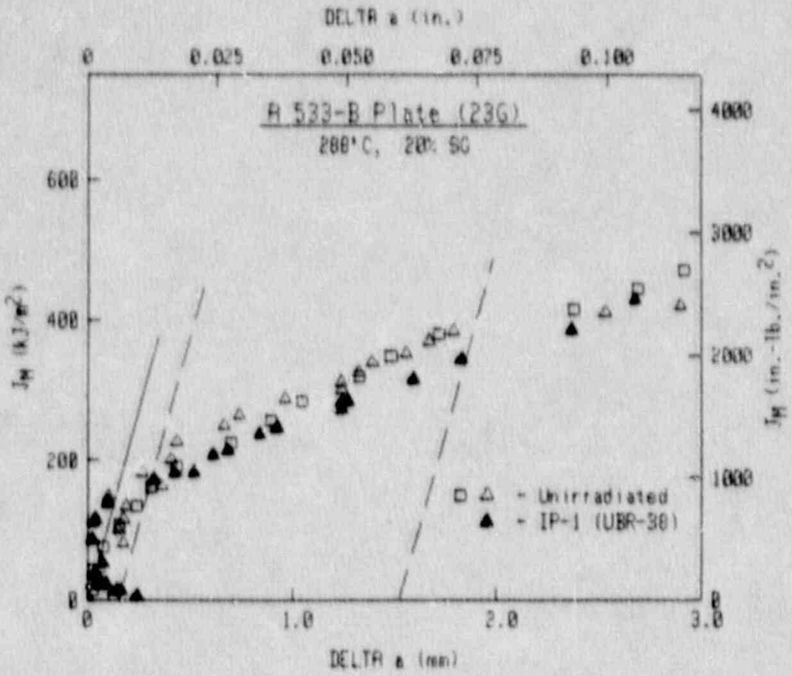

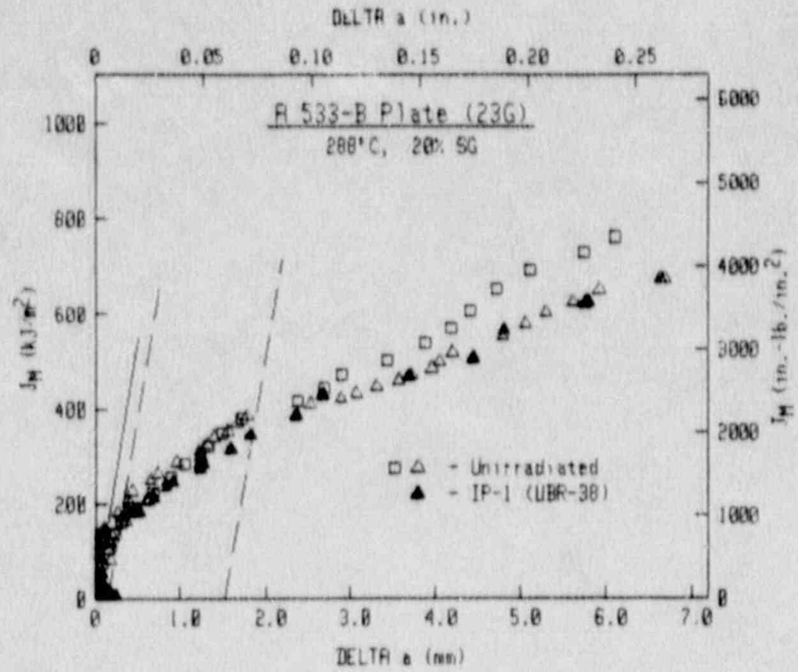

Fig. E-51 Comparison of J-R curves at 288 °C from the unirradiated condition and the low fluence rate (IP) irradiated conditions of the A 533-B Plate 23G.

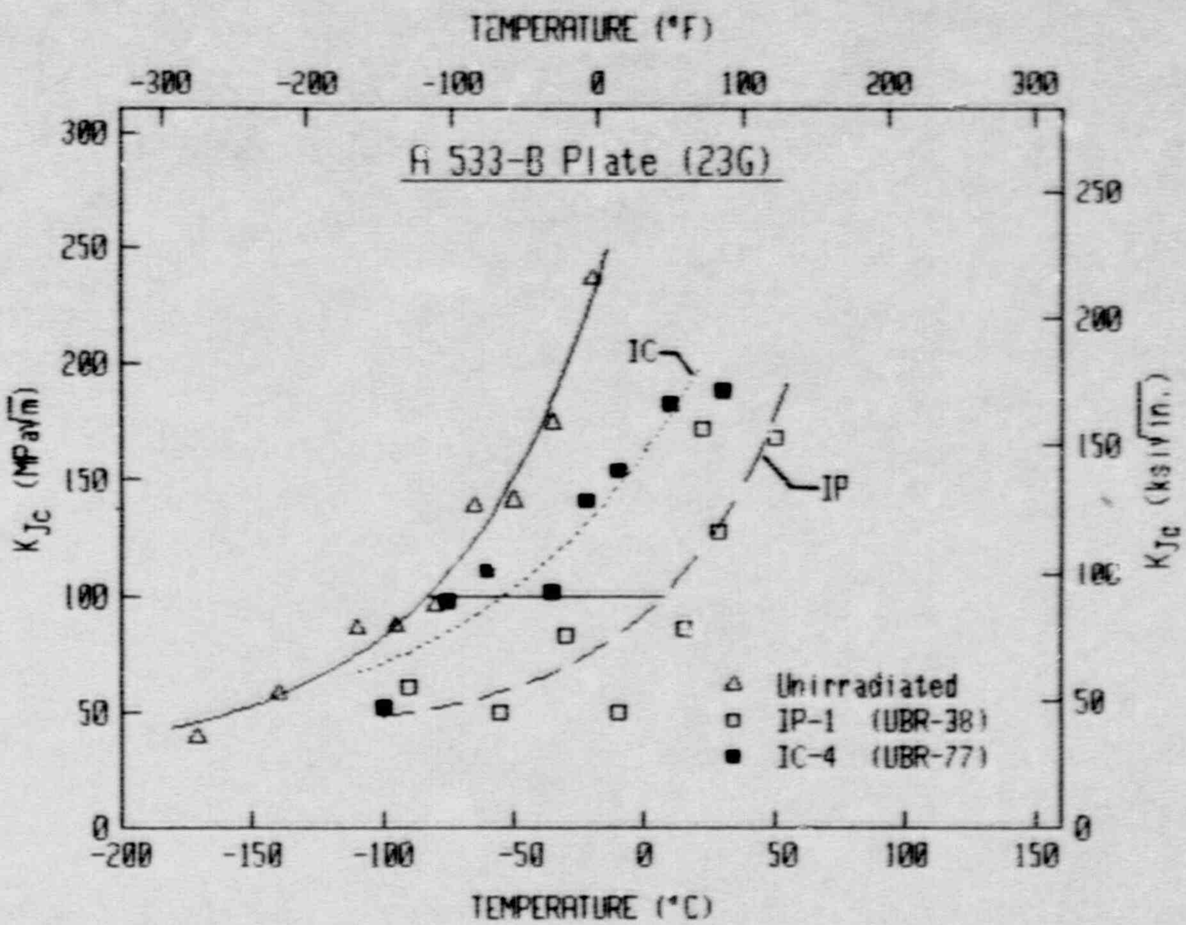

Fig. E-52 Comparison of transition regime data from low fluence rate (IP) and high fluence rate (IC) irradiations of the A 533-B Plate 23G.

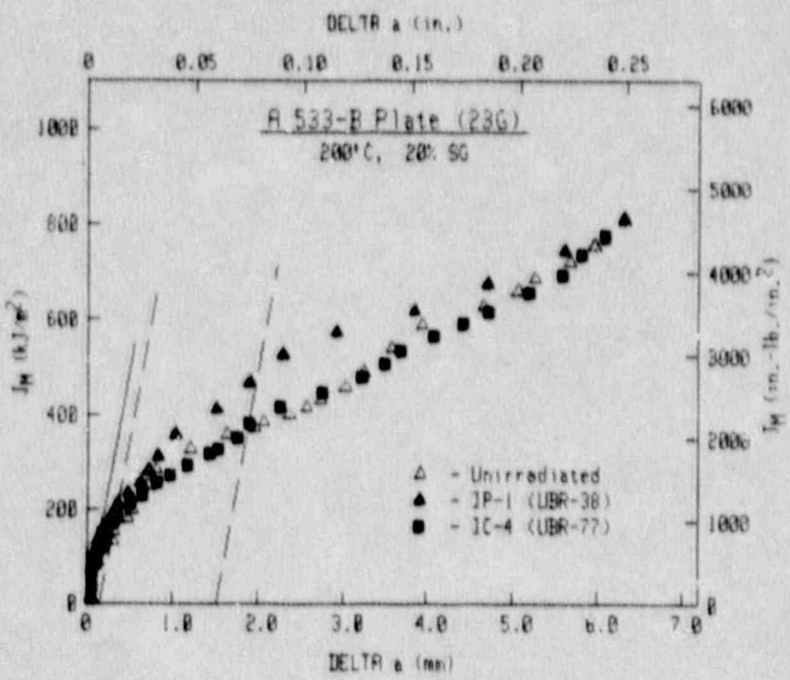

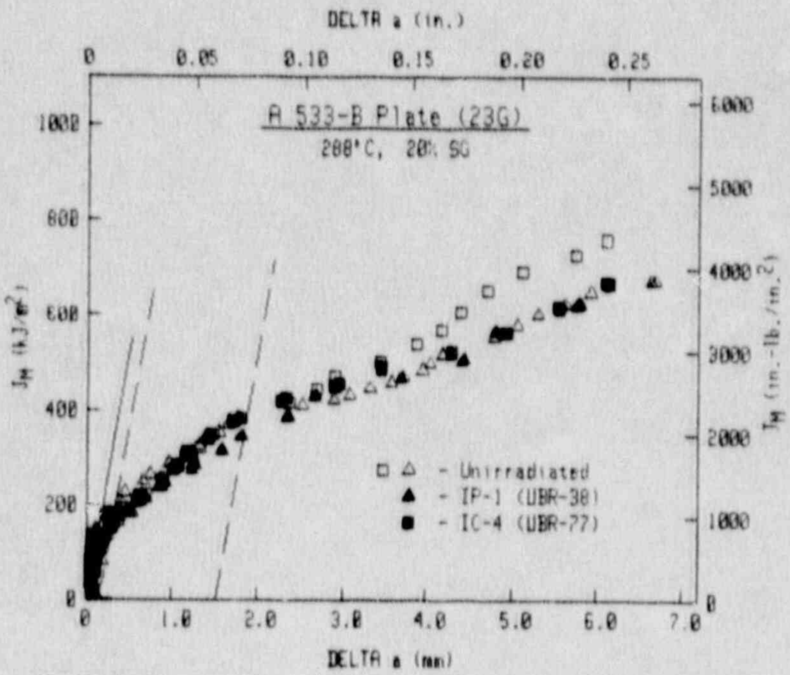

Fig. E-53 Comparison of J-R curves at 200°C and 288°C for the A 533-B Plate 23G.

Table E-6 Fracture Toughness Data for Linde 0091 Weld (W9A)

Specimen Number	Test Temp (°C)	$(a/W)_o$[a]	a_m[b] (mm)	a_p[c] (mm)	$a_p - a_m$ (mm)	J_{Ic} P.L. (kJ/m^2)	J_{Ic} ASTM (kJ/m^2)	K_{Jc} P.L. (MPa $\sqrt{m}$)	K_{Jc} ASTM (MPa $\sqrt{m}$)	K_c (MPa $\sqrt{m}$)	K_{max} (MPa $\sqrt{m}$)	T_{avg}	f (MPa)	y (MPa)
UNIRRADIATED														
W9A-43	-150	0.505	—	—	—	5.3	—	35.4	35.2[e]	34.9	35.2	—	830.8	813.2
W9A-46	-110	0.510	—	—	—	22.5	—	72.7	64.3	61.3	68.9	—	766.3	742.1
W9A-39	-90	0.513	—	—	—	40.8	—	97.6	53.1	71.2	85.3	—	736.9	709.6
W9A-54	-75	0.509	—	—	—	48.7	—	106.4	62.0	73.1	92.2	—	716.1	686.5
W9A-49	-65	0.503	—	—	—	73.0	—	130.1	57.5	79.3	100.6	—	702.9	671.8
W9A-[illegible]	-60	0.506	—	—	—	123.8	—	169.3	56.9	88.2	106.3	—	696.4	664.6
W9A-44	-40	0.506	—[g]	—[g]	—[g]	397.1	207.4	302.4	218.5	—	—	—	671.9	637.2
W9A-45[d]	0	0.517	5.21	4.98	-0.23	267.4	255.0[f]	246.7	241.0	—	—	173	628.6	588.5
W9A-51[d]	75	0.514	5.26	5.10	-0.16	230.4	195.9[f]	226.6	209.0	—	—	170	568.2	519.0
W9A-42[d]	200	0.512	5.39	5.21	-0.18	161.7	147.9[f]	186.5	178.4	—	—	130	526.0	466.8
W9A-52[d]	288	0.510	6.31	5.97	-0.34	111.4	92.9	152.8	139.6	—	—	120	545.1	477.8
W9A-40[d]	288	0.518	6.65	6.45	-0.20	131.6	116.0[f]	166.1	156.0	—	—	97	545.1	477.8
IRRADIATED IC-4 (UBR-77)														
W9A-72	-90	0.503	—	—	—	11.0	—	50.6	48.3[e]	48.2	48.9	—	838.9	819.6
W9A-71	-45	0.518	—	—	—	18.7	—	65.7	59.9	57.7	62.1	—	780.3	753.8
W9A-69	-20	0.512	—	—	—	34.1	—	88.4	65.0	68.0	81.6	—	751.8	721.6
W9A-70	0	0.516	—	—	—	50.8	—	107.5	65.4	74.1	92.4	—	731.2	698.2
W9A-67	10	0.504	—	—	—	61.3	—	118.0	61.0	76.8	98.4	—	721.6	687.3
W9A-75	20	0.526	—	—	—	66.9	—	123.1	63.0	77.7	103.9	—	712.5	676.8
W9A-64	25	0.517	—[g]	—[g]	—[g]	130.0	—[g]	171.4	—[g]	—	—	—	708.1	671.8
W9A-65	38	0.501	4.53	3.88	-0.65	165.9	126.9[f]	193.4	169.1	—	—	120	697.3	659.3
W9A-78	50	0.528	5.88	4.25	-1.63	146.8	79.8	181.6	133.9	—	—	125	688.0	648.6
W9A-68[d]	75	0.517	6.01	5.66	-0.35	176.1	168.6[f]	198.2	193.9	—	—	71	670.9	628.5
W9A-80[d]	200	0.529	6.20	6.07	-0.13	133.7	117.1	169.6	158.8	—	—	56	629.8	575.9
W9A-66[d]	288	0.521	6.46	6.16	-0.30	116.3	113.4[f]	156.2	154.2	—	—	67	645.4	586.5

[a] Pre-test a/W.
[b] Optically-measured crack growth.
[c] Crack growth predicted by compliance.
[d] Side grooved.
[e] Valid K_{Ic} per ASTM E 399.
[f] Valid J_{Ic} per ASTM E 813-81.
[g] Cleavage failure precluded determination of this quantity.

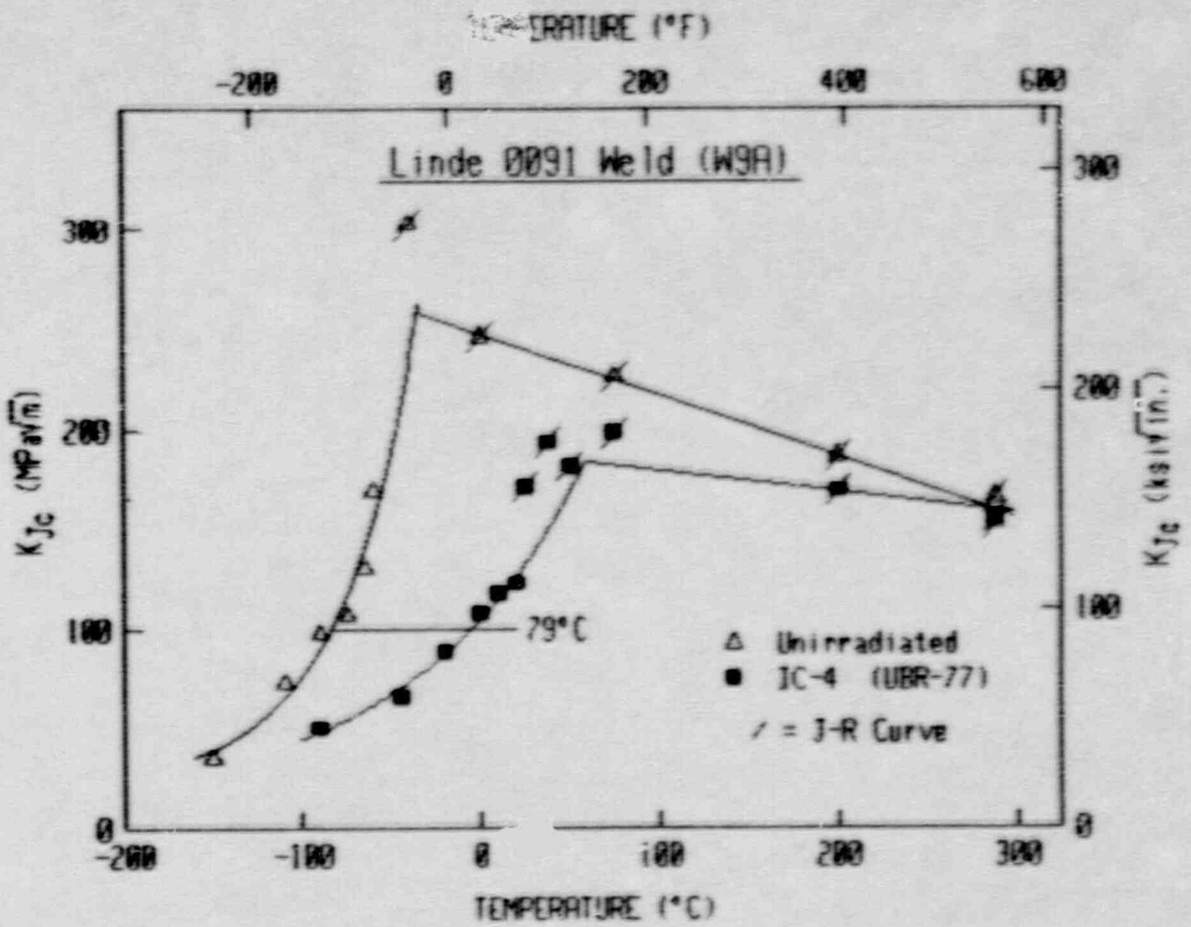

Fig. E-54 Comparison of K_{Jc} data for the unirradiated condition and the IC-4 (UBR-77) irradiated condition of the Linde 0091 Weld W9A.

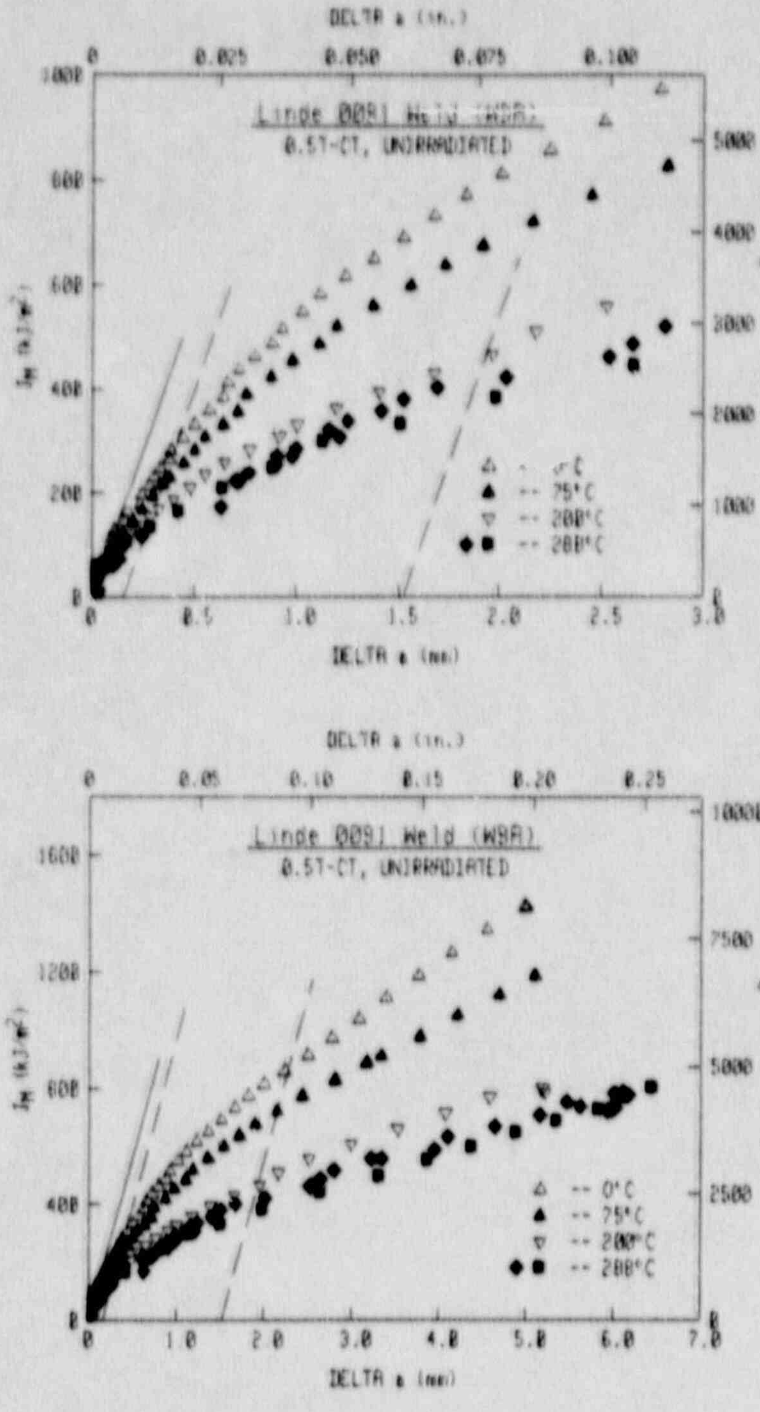

Fig. E-55 J-R curves for the unirradiated condition of the Linde 0091 Weld W9A.

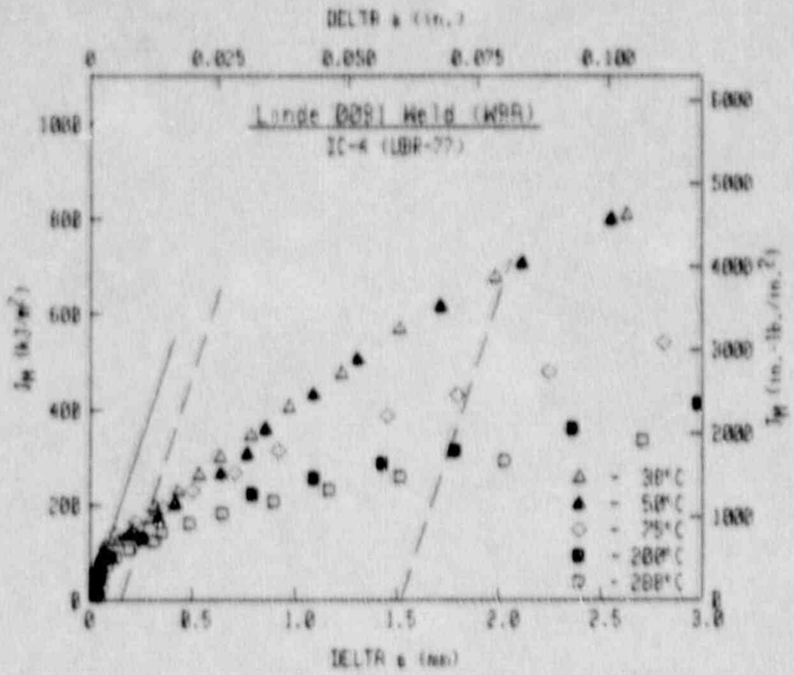

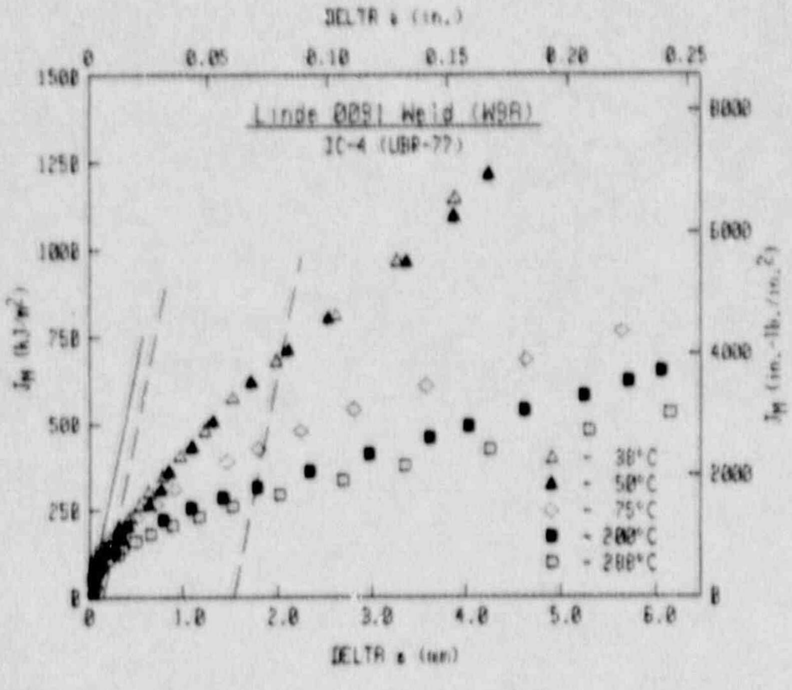

Fig. E-56 J-R curves for the IC-4 (UBR-77) irradiated condition of the Linde 0091 Weld W9A.

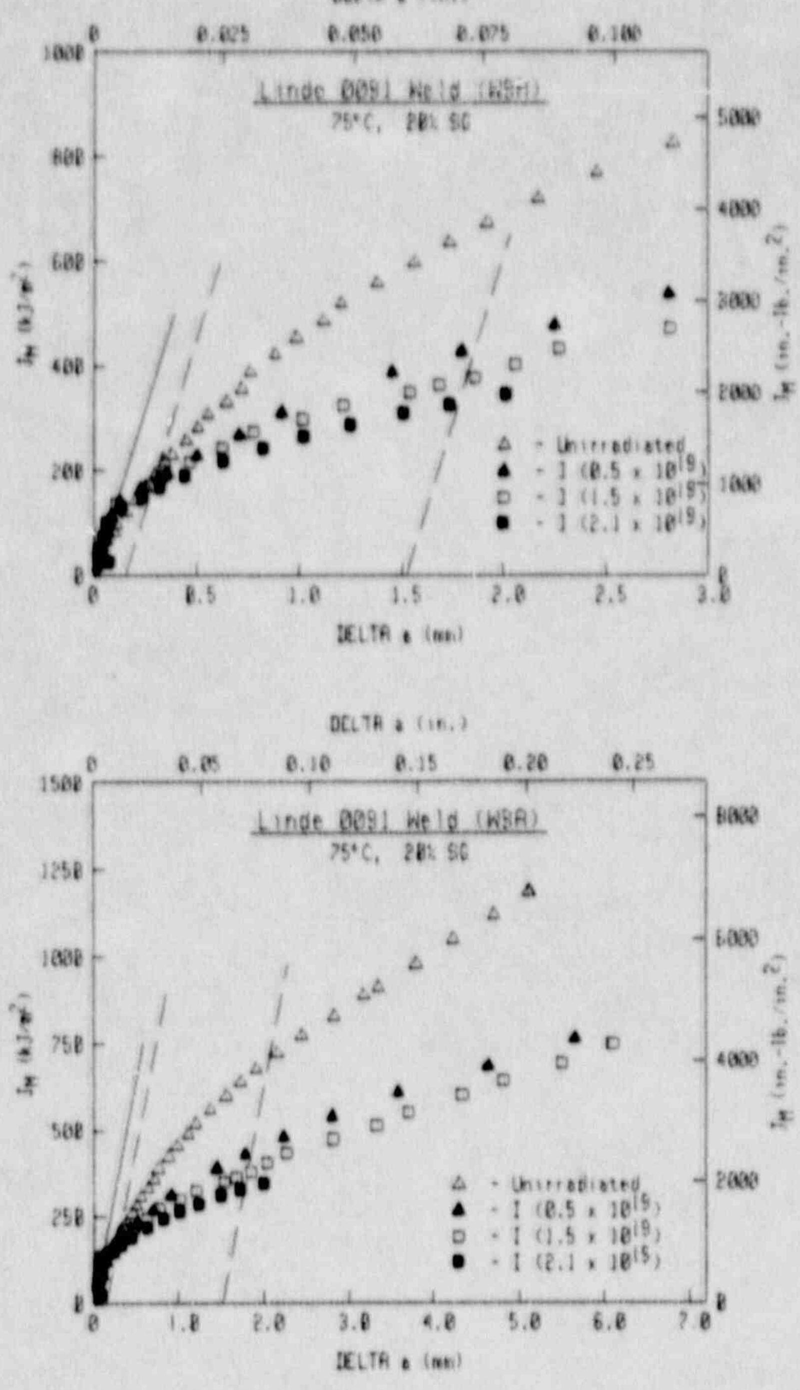

Fig. E-57 Comparison of J-R curves at 75°C from high fluence rate (IC) irradiations of the Linde 0091 Weld W9A.

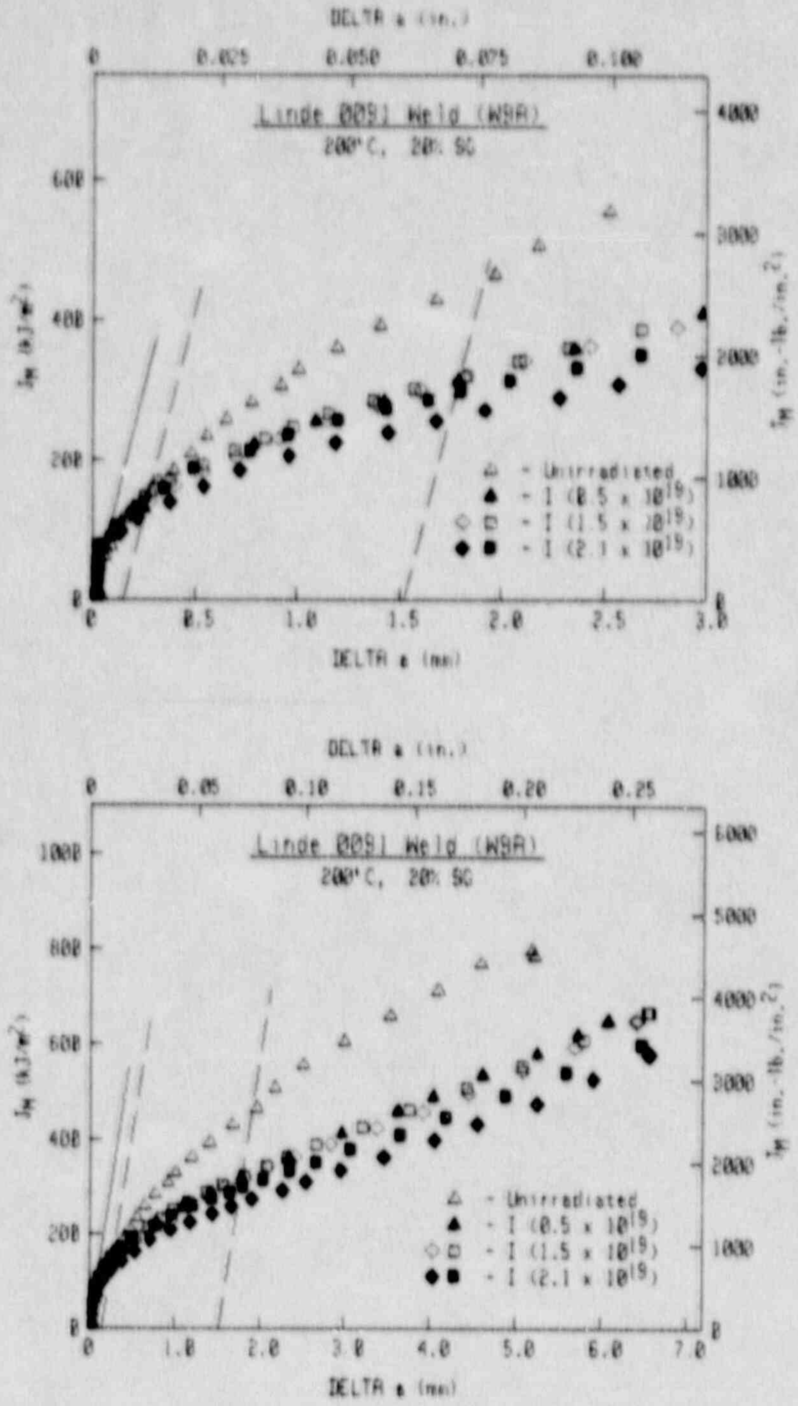

Fig. E-58 Comparison of J-R curves at 200°C from high fluence rate (IC) irradiations of the Linde 0091 Weld W9A.

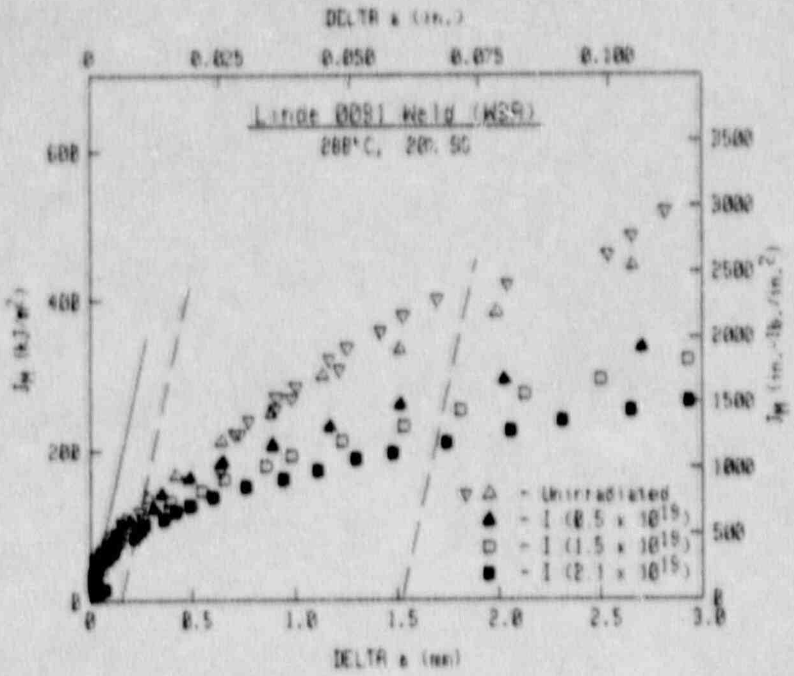

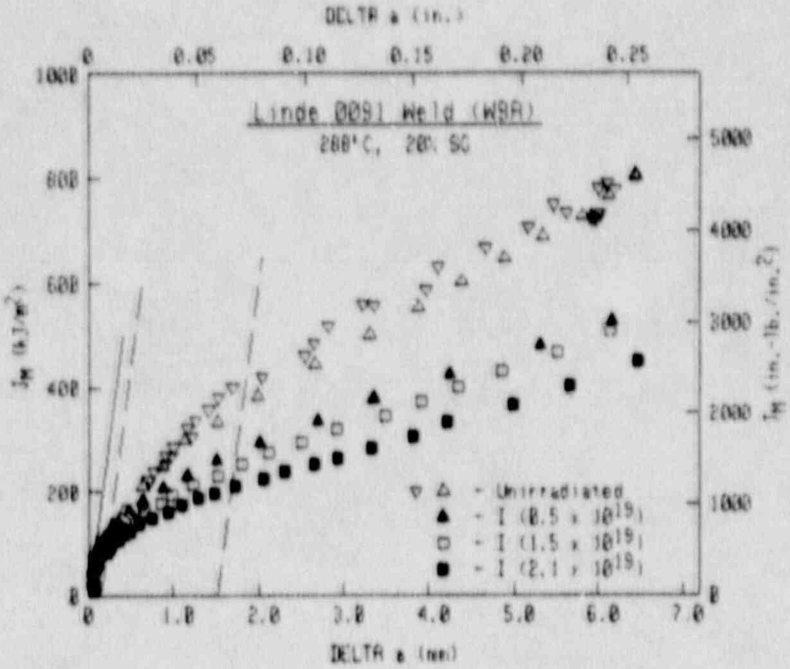

Fig. E-59 Comparison of J-R curves at 288°C from high fluence rate (IC) irradiations of the Linde 0091 Weld W9A.

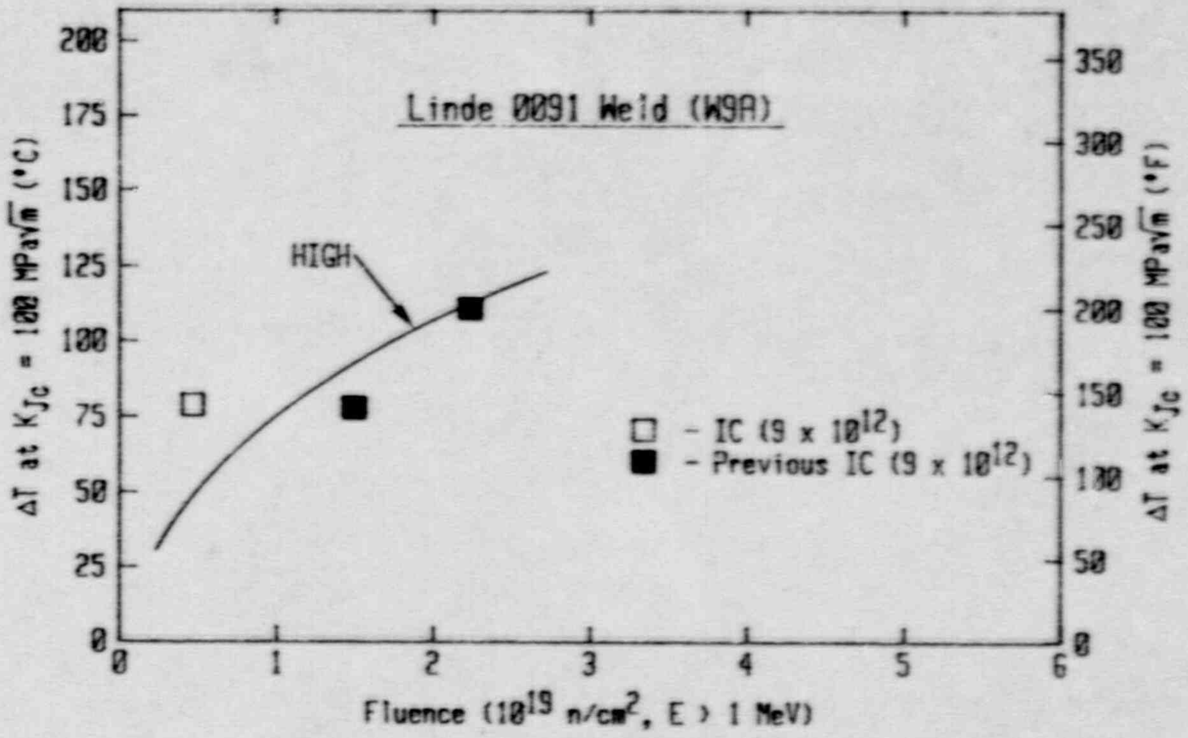

Fig. E-60 Transition temperature shifts as a function of fluence for the Linde 0091 Weld W9A. All data are from in-core irradiations at UBR.

5. SUMMARY

Overall the trends from these data are reasonably consistent. Specifically, the A 302-B Plate 23F and the Linde 80 Weld W8A indicate similar trends for the same fluences and fluence rates, indicative of the success from randomizing the specimens within each capsule. Such cases are for the intermediate (CE) fluence rate experiments where each material indicates an embrittlement plateau, and the high (IC) fluence rate experiments where each material illustrates increased embrittlement with increased fluence.

Comparison of trends for the plates and the welds are consistent for each product form. Specifically, the A 533-B Plate 23G and the Linde 0091 Weld W9A exhibit similar transition temperature shifts as the A 302-B Plate 23F and the Linde 80 Weld W8A, respectively, for the same low fluence (~0.5 x 10^{19} n/cm^2) at the high fluence rate (IC). In addition, the plates consistently demonstrate limited or no loss of upper shelf toughness with irradiation, whereas the welds demonstrate considerable loss of upper shelf toughness after irradiation.

The one inconsistent result is the high transition temperature shift found for the A 533-B Plate 23G with the low fluence rate (IP) exposure at low fluence. This high shift is much greater (90°C vs. 29°C) than that for a similar fluence at a high fluence rate (IC), and also much greater than that (60°C) found for the A 302-B Plate 23F in the IP condition.

REFERENCES

E-1. ASTM E 813-81, "Standard Test for J_{Ic}, A Measure of Fracture Toughness," ASTM Book of Standards, Part 10, 1981, pp. 810-828.

E-2. J. R. Hawthorne and A. L. Hiser, "Investigations of Irradiation-Anneal-Reirradiation (IAR) Properties Trends of RPV Welds: Phase 2 Final Report," USNRC Report NUREG/CR-5492, Dec. 1989.

E-3. ASTM E 399-81, "Standard Test Method for Plane-Strain Fracture Toughness of Metallic Materials," ASTM Book of Standards, Part 10, 1981, p. 589.

E-4. F. J. Loss, B. H. Menke and R. A. Gray, "Development of J-R Curve Procedures," in The NRL-EPRI Research Program (RP886-2), Evaluation and Prediction of Neutron Embrittlement in Reactor Pressure Vessel Materials Annual Report for CY 1978, Naval Research Laboratory, Report 8327, Aug. 30, 1979, pp. 30-57.

E-5. F. J. Loss, et al., "J-R Curve Characterization of Irradiated and Annealed Weld Deposits," in Structural Integrity of Water Reactor Pressure Boundary Components, Annual Report, FY 1979, USNRC Report NUREG/CR-1128, Dec. 31, 1979, pp. 4-36.

E-6. A. L. Hiser, F. J. Loss and B. H. Menke, "J-R Curve Characterization of Irradiated Low Upper Shelf Welds," USNRC Report NUREG/CR-3506, April 1984.

E-7. J. G. Merkle and H. T. Corten, "A J Integral Analysis for the Compact Specimen, Considering Axial Force as Well as Bending Effects," Trans. ASME, Journal of Pressure Vessel Technology, Nov. 1974, pp. 286-292.

E-8. G. A. Clarke and J. D. Landes, "Evaluation of J for the Compact Specimen," Journal of Testing and Evaluation, Vol. 7(5), Sept. 1979, pp. 264-269.

E-9. G. R. Irwin, "Fracture Mode Transition for a Crack Traversing a Plate," J. of Basic Eng., ASME, Vol. 82(2), 1960, pp. 417-425.

E-10. J. G. Merkle, "An Examination of the Size Effect and Data Scatter Observed in Small-Specimen Cleavage Fracture Toughness Testing," ORNL/TM-9800, USNRC Report NUREG/CR-3672, April 1984.

E-11. ASTM E 1152-87, "Standard Test Method for Determining J-R Curves," Annual Book of ASTM Standards, Volume 03.01, 1989, pp. 814-824.

E-12. H. A. Ernst, "Material Resistance and Instability Beyond J-Controlled Crack Growth," Elastic-Plastic Fracture, ASTM STP 803 Vol. 1, Phila., Pa., 1983, pp. 191-213.

E-13. P. C. Paris, H. Tada, A. Zahoor, and H. Ernst, "The Theory of Instability of the Tearing Mode of Elastic-Plastic Crack Growth," Elastic-Plastic Fracture, ASTM STP 668, March 1979, pp. 5-36.

E-14. J. R. Hawthorne, B. H. Menke and A. L. Hiser, "Notch Ductility and Fracture Toughness Degradation of A 302-B and A 533-B Reference Plates from PSF Simulated Surveillance and Through-Wall Irradiation Capsules," USNRC Report NUREG/CR-3295 Vol. 1, Apr. 1984.

E-15. J. R. Hawthorne, et al., "Evaluation and Prediction of Neutron Embrittlement in Reactor Pressure Vessel Materials," EPRI NP-2782, Electric Power Research Institute, Dec. 1982.

APPENDIX F

Computer Curve-Fits of
Transition Regime Fracture Toughness Data

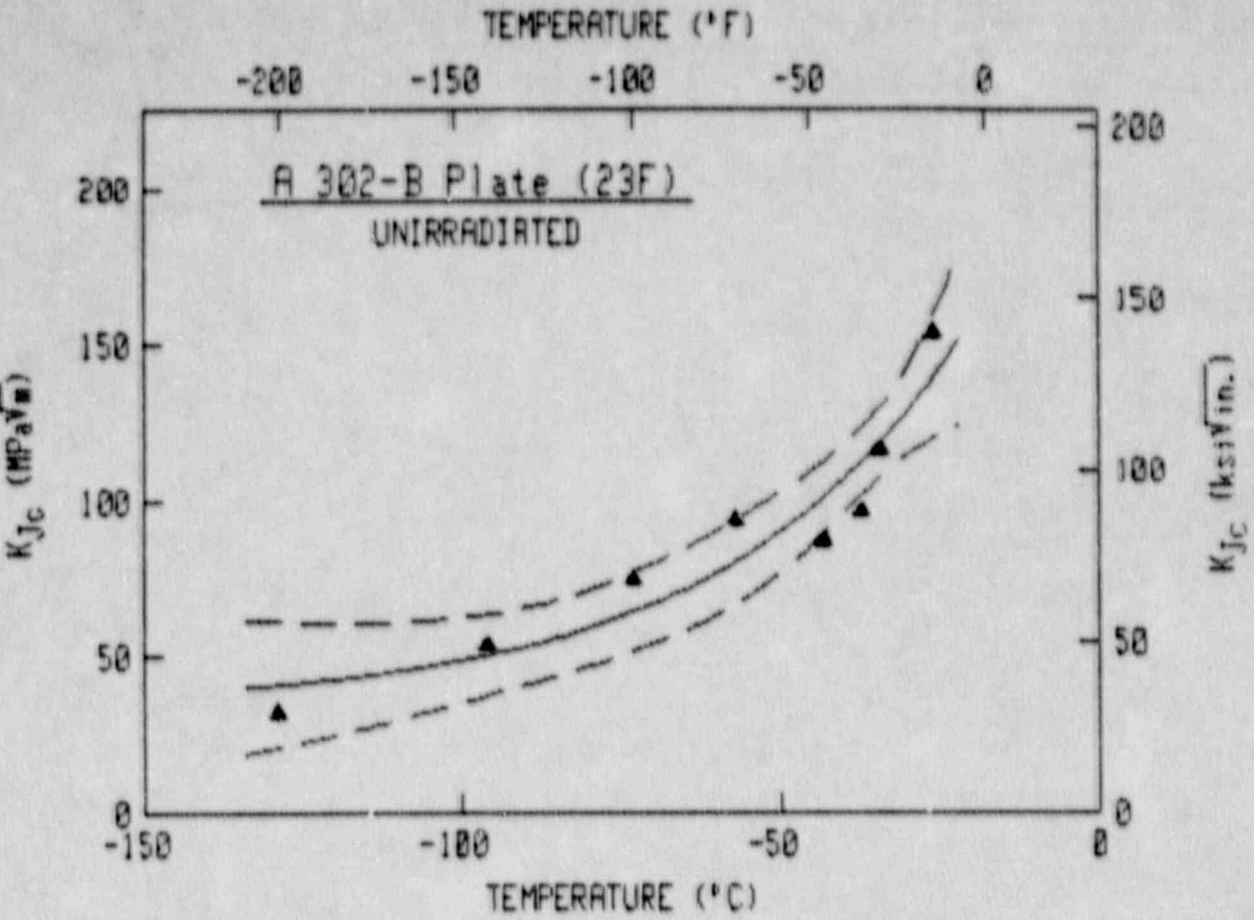

****

Kjc = A + B exp [(T-To)/C)]

	Metric	English
A =	34.31 MPa√m	31.23 ksi√in
B =	211.21 MPa√m	192.21 ksi√in
C =	37.31°C	67.16°F
To =	0.00°C	32.00°F

	Temperature at 100 MPa√m	
Upper Bound =	-51°C	-60°F
Mean Curve =	-44°C	-46°F
Lower Bound =	-37°C	-35°F

****

Pt #	Temperature	Kjc
1	-129	32.4
2	-96	53.6
3	-73	74.5
4	-57	93.9
5	-43	87.1
6	-37	96.6
7	-34	116.1
8	-26	154.0

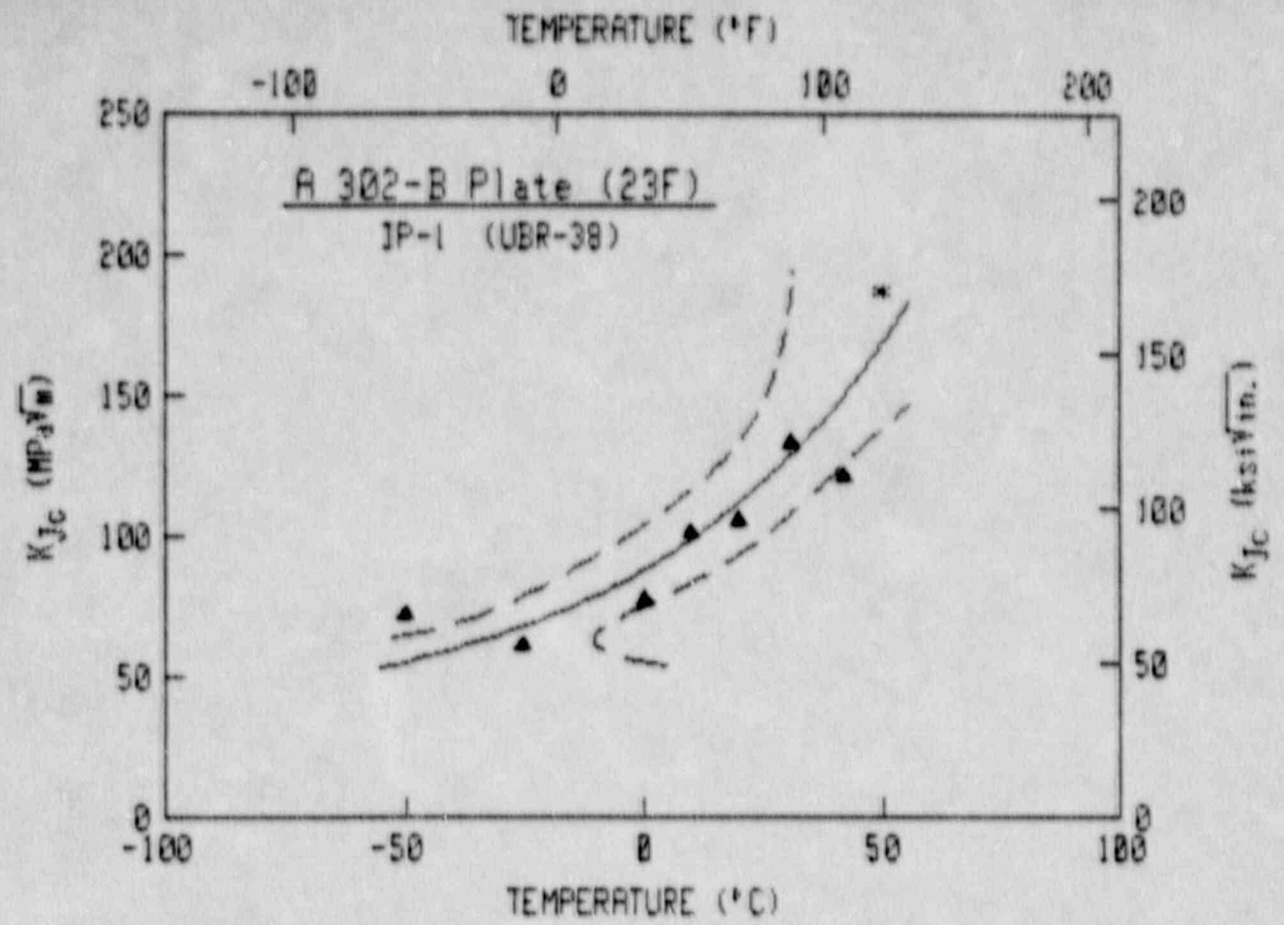

$$K_{jc} = A + B \exp[(T-T_o)/C]$$

	Metric	English
A =	33.34 MPa√m	30.34 ksi√in
B =	54.49 MPa√m	49.59 ksi√in
C =	55.01°C	99.02°F
To =	0.00°C	32.00°F

	Temperature at 100 MPa√m	
Upper Bound =	-3°C	26°F
Mean Curve =	11°C	52°F
Lower Bound =	25°C	78°F

Pt #	Temperature	Kjc
1	-50	72.2
2	-25	61.4
3	0	77.4
4	10	101.4
5	20	105.8
6	31	133.3
7	42	121.6
8 *	50	186.9

* = Upper Shelf Data Point

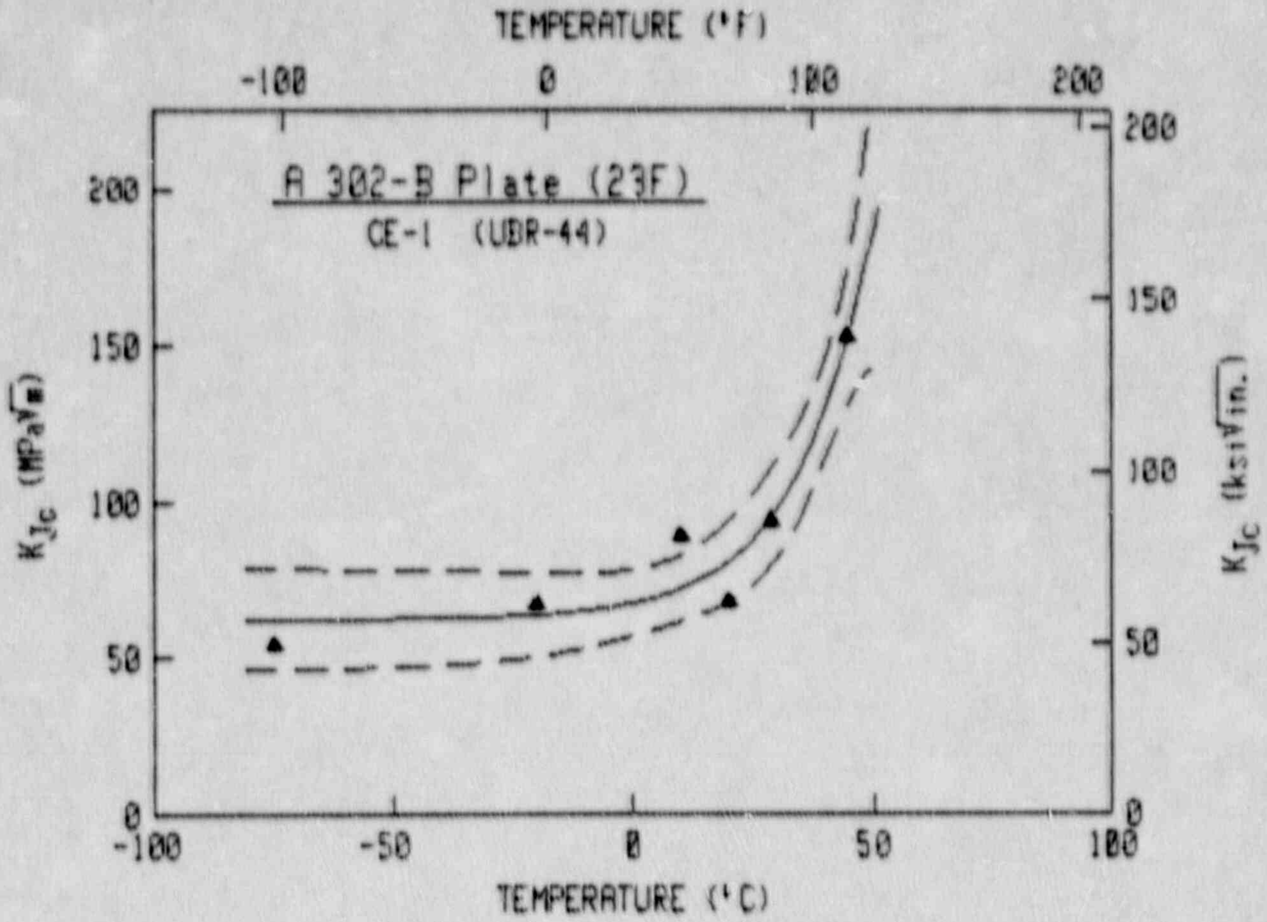

$$Kjc = A + B \exp[(T-To)/C)]$$

	Metric	English
A =	62.37 MPa$\sqrt{m}$	56.76 ksi$\sqrt{in}$
B =	5.06 MPa$\sqrt{m}$	4.61 ksi$\sqrt{in}$
C =	15.66°C	28.19°F
To =	0.00°C	32.00°F

	Temperature at 100 MPa$\sqrt{m}$	
Upper Bound =	25°C	77°F
Mean Curve =	31°C	89°F
Lower Bound =	37°C	99°F

Pt #	Temperature	Kjc
1	-75	54.3
2	-20	67.1
3	10	89.0
4	20	68.0
5	29	94.0
6	45	152.8

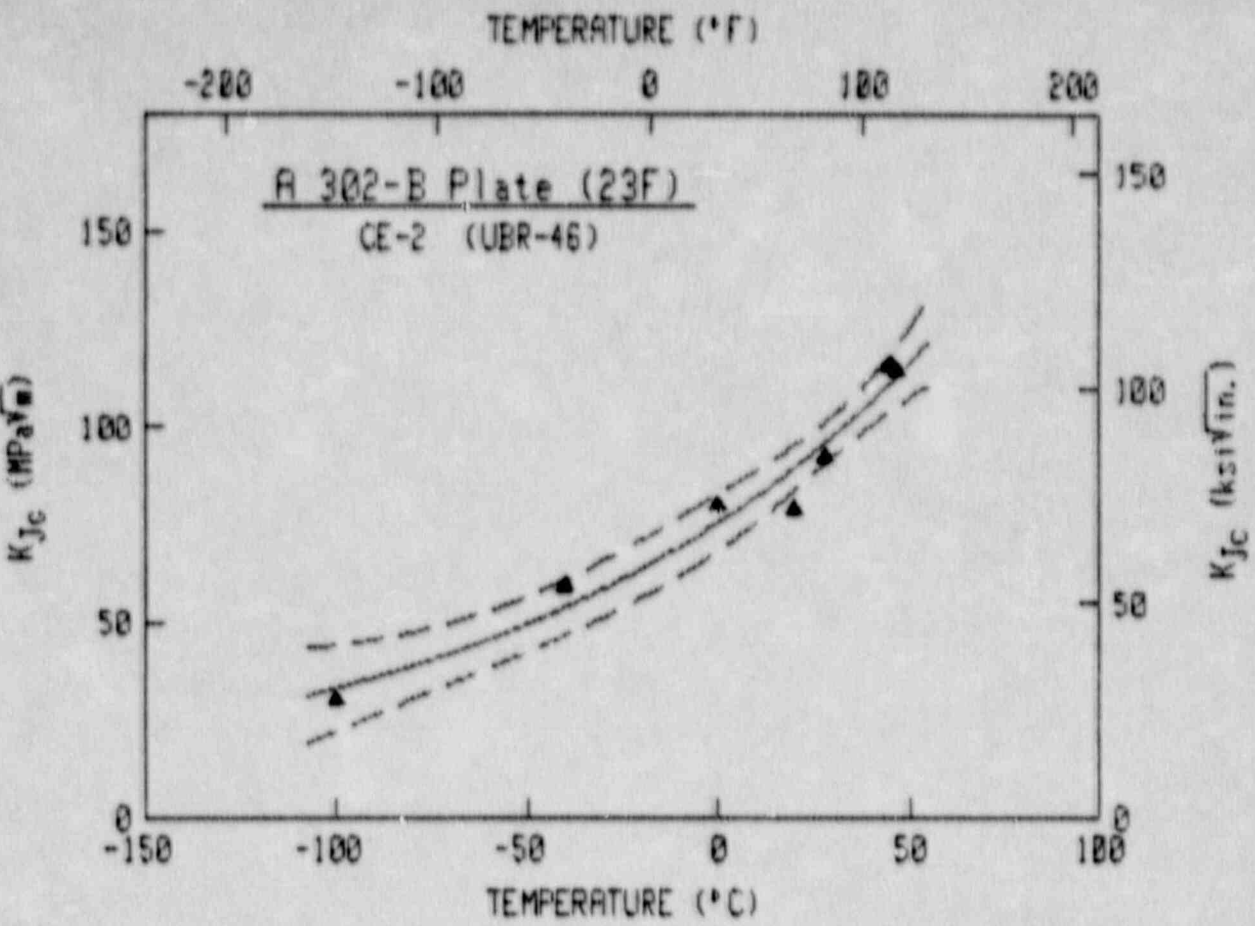

****

Kjc = A + B exp [(T-To)/C)]

		Metric	English
A	=	4.90 MPa√m	4.46 ksi√in
B	=	70.51 MPa√m	64.17 ksi√in
C	=	109.48°C	197.06°F
To	=	0.00°C	32.00°F

	Temperature at 100 MPa√m	
Upper Bound =	27°C	81°F
Mean Curve =	33°C	91°F
Lower Bound =	40°C	104°F

****

Pt #	Temperature	Kjc
1	-100	30.4
2	-40	59.4
3	0	80.2
4	20	79.4
5	28	92.6
6	45	115.9
7	47	114.5

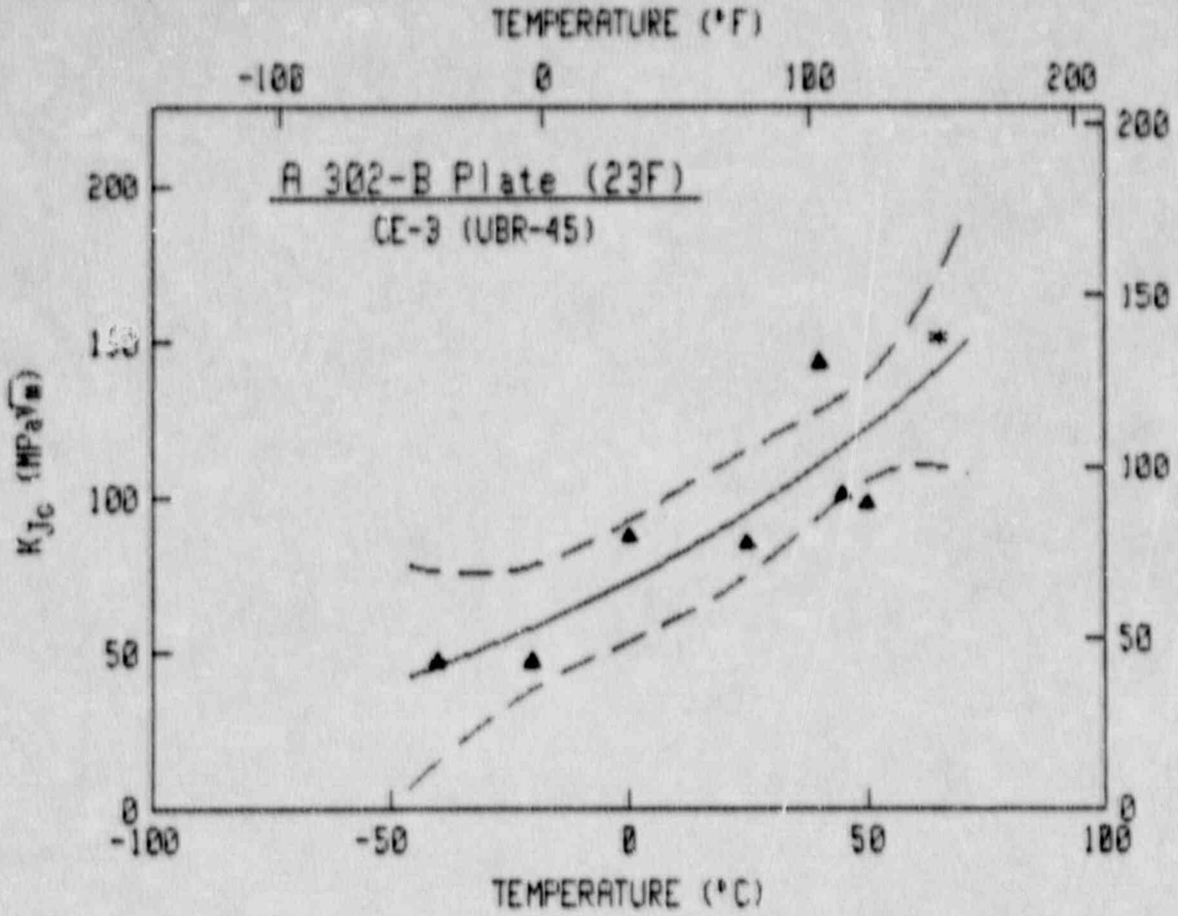

****

Kjc = A + B exp [(T-To)/C)]

		Metric	English
A	=	-21.45 MPa√m	-19.52 ksi√in
B	=	94.06 MPa√m	85.60 ksi√in
C	=	118.56°C	213.41°F
To	=	0.00°C	32.00°F

		Temperature at 100 MPa√m	
Upper Bound	=	9°C	48°F
Mean Curve	=	30°C	87°F
Lower Bound	=	46°C	115°F

****

Pt #	Temperature	Kjc
1	-40	47.3
2	-20	47.2
3	0	87.4
4	25	85.0
5	40	143.5
6	45	100.9
7	50	98.0
8 *	65	151.3

* = Upper Shelf Data Point

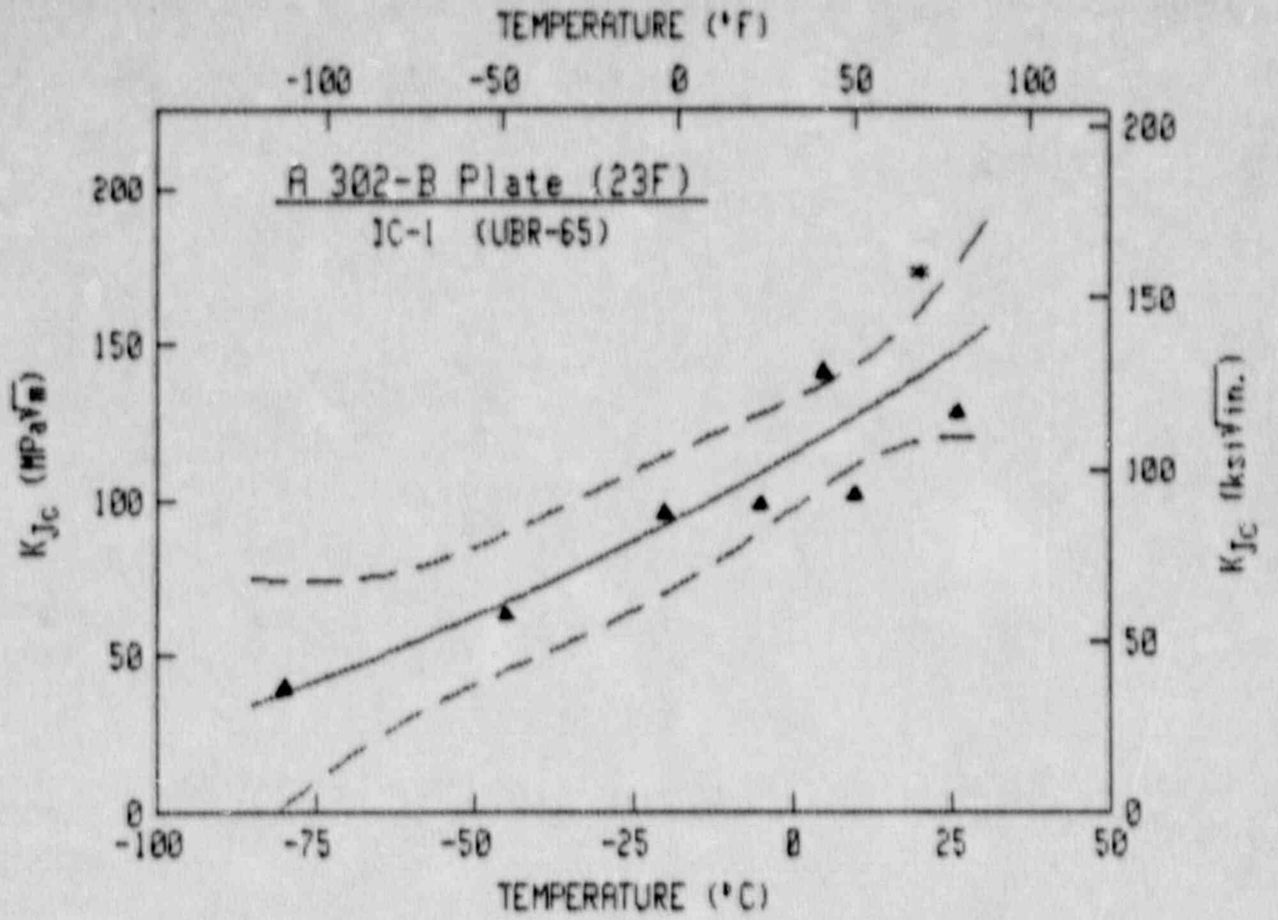

****

Kjc = A + B exp [(T-To)/C)]

		Metric	English
A	=	-94.80 MPa√m	-86.27 ksi√in
B	=	209.40 MPa√m	190.56 ksi√in
C	=	175.56°C	316.01°F
To	=	0.00°C	32.00°F

		Temperature at 100 MPa√m	
Upper Bound	=	-34°C	-29°F
Mean Curve	=	-13°C	9°F
Lower Bound	=	2°C	36°F

****

Pt #	Temperature	Kjc
1	-80	39.7
2	-45	63.4
3	-20	95.9
4	-5	98.7
5	5	141.1
6	10	101.7
7	26	127.8
8 *	20	173.1

* = Upper Shelf Data Point

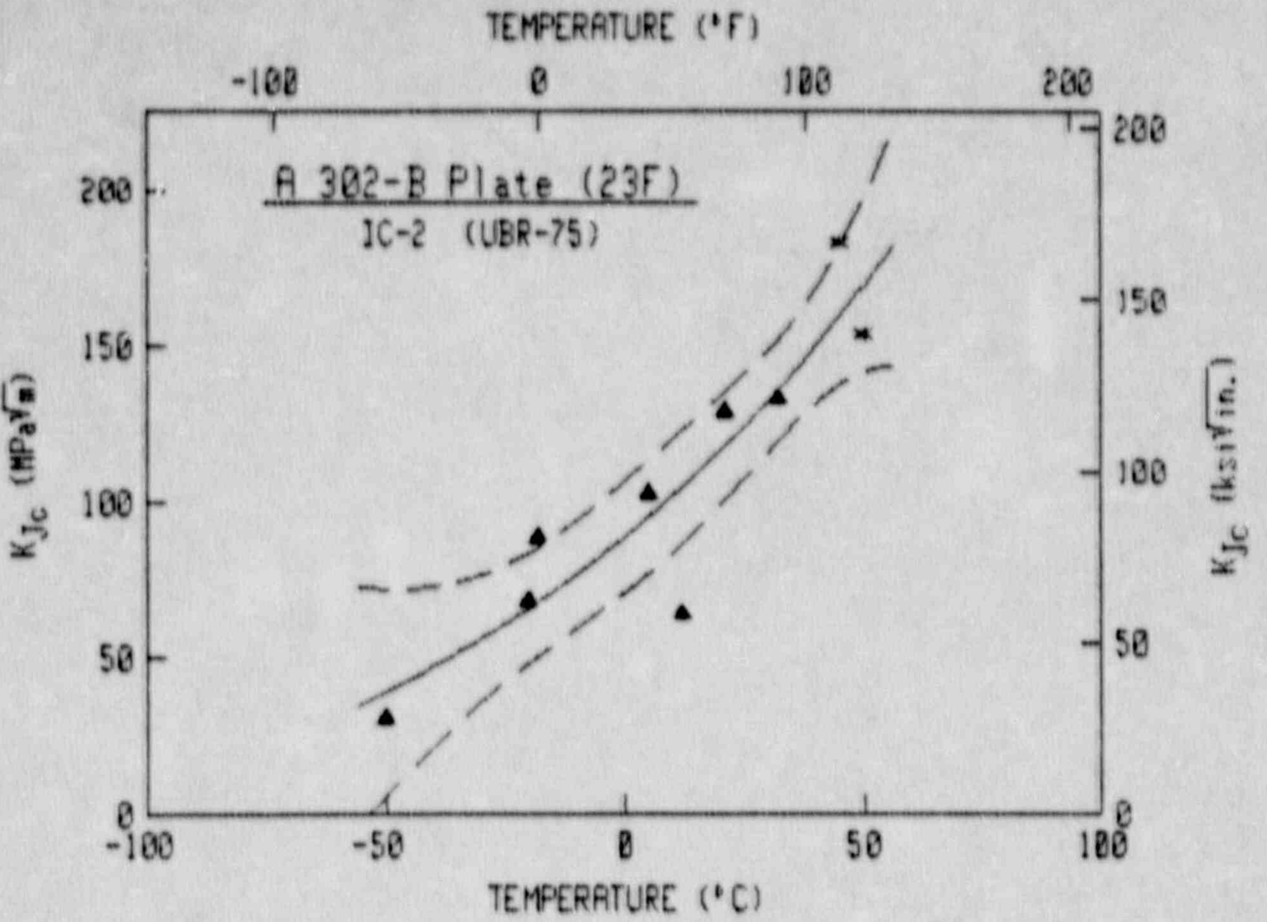

****

$$K_{jc} = A + B \exp[(T-T_o)/C]$$

	Metric	English
A =	-41.11 MPa$\sqrt{m}$	-37.41 ksi$\sqrt{in}$
B =	129.66 MPa$\sqrt{m}$	118.00 ksi$\sqrt{in}$
C =	103.43°C	186.17°F
To =	0.00°C	32.00°F

	Temperature at 100 MPa$\sqrt{m}$	
Upper Bound =	-4°C	25°F
Mean Curve =	9°C	48°F
Lower Bound =	21°C	70°F

****

Pt #	Temperature	Kjc
1	-50	30.6
2	12	64.2
3	-18	88.4
4	32	133.1
5	21	129.1
6	-20	68.3
7	5	103.0
8 *	45	183.1
9 *	50	153.8

* = Upper Shelf Data Point

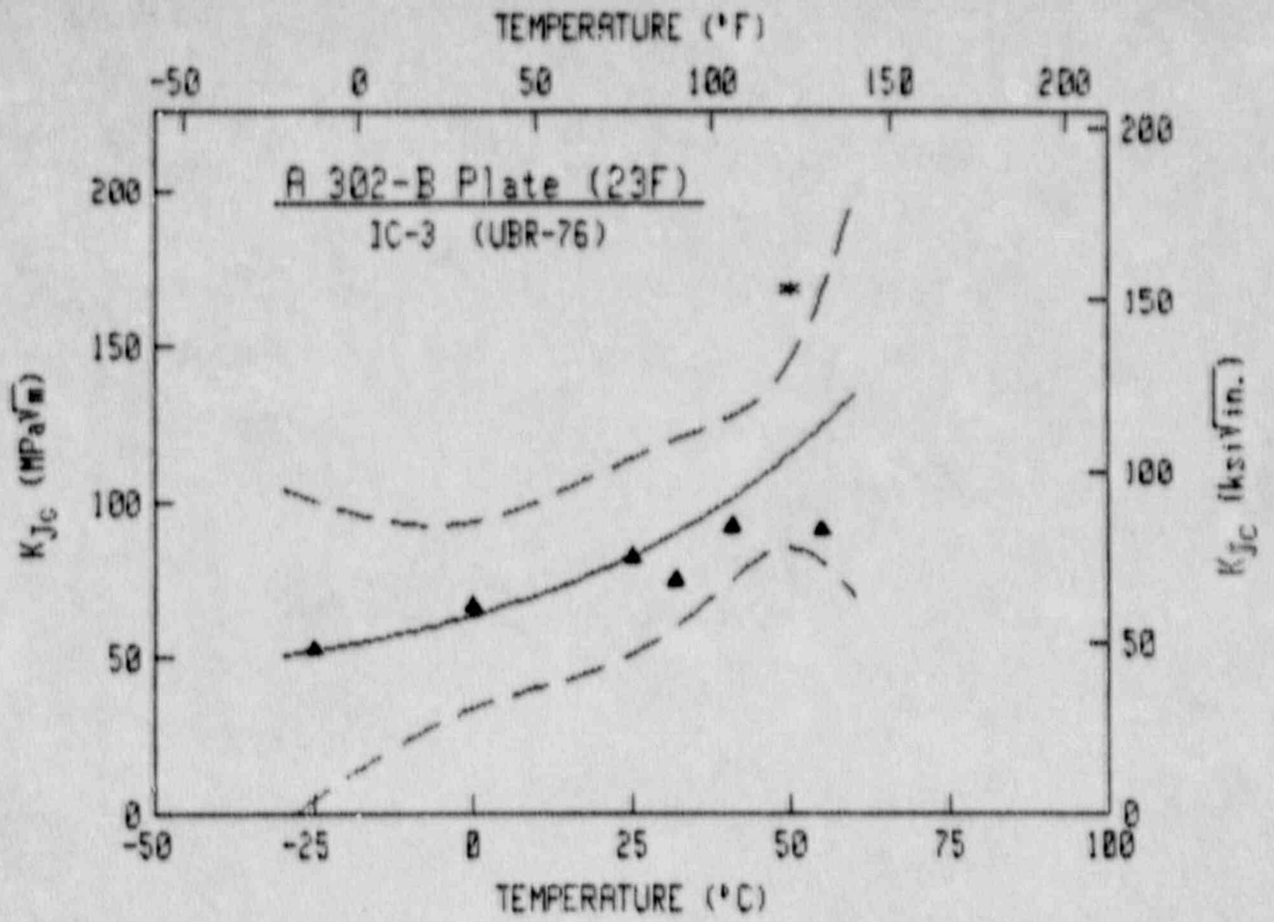

$$Kjc = A + B \exp[(T-To)/C)]$$

	Metric	English
A =	37.03 MPa$\sqrt{m}$	33.70 ksi$\sqrt{in}$
B =	26.47 MPa$\sqrt{m}$	24.09 ksi$\sqrt{in}$
C =	46.09°C	82.97°F
To =	0.00°C	32.00°F

	Temperature at 100 MPa$\sqrt{m}$	
Upper Bound =	-30°C	-22°F
Mean Curve =	40°C	104°F

Pt #	Temperature	Kjc
1	-25	52.9
2	0	66.9
3	25	82.5
4	32	75.2
5	41	92.4
6	55	91.3
7 *	50	168.4

* = Upper Shelf Data Point

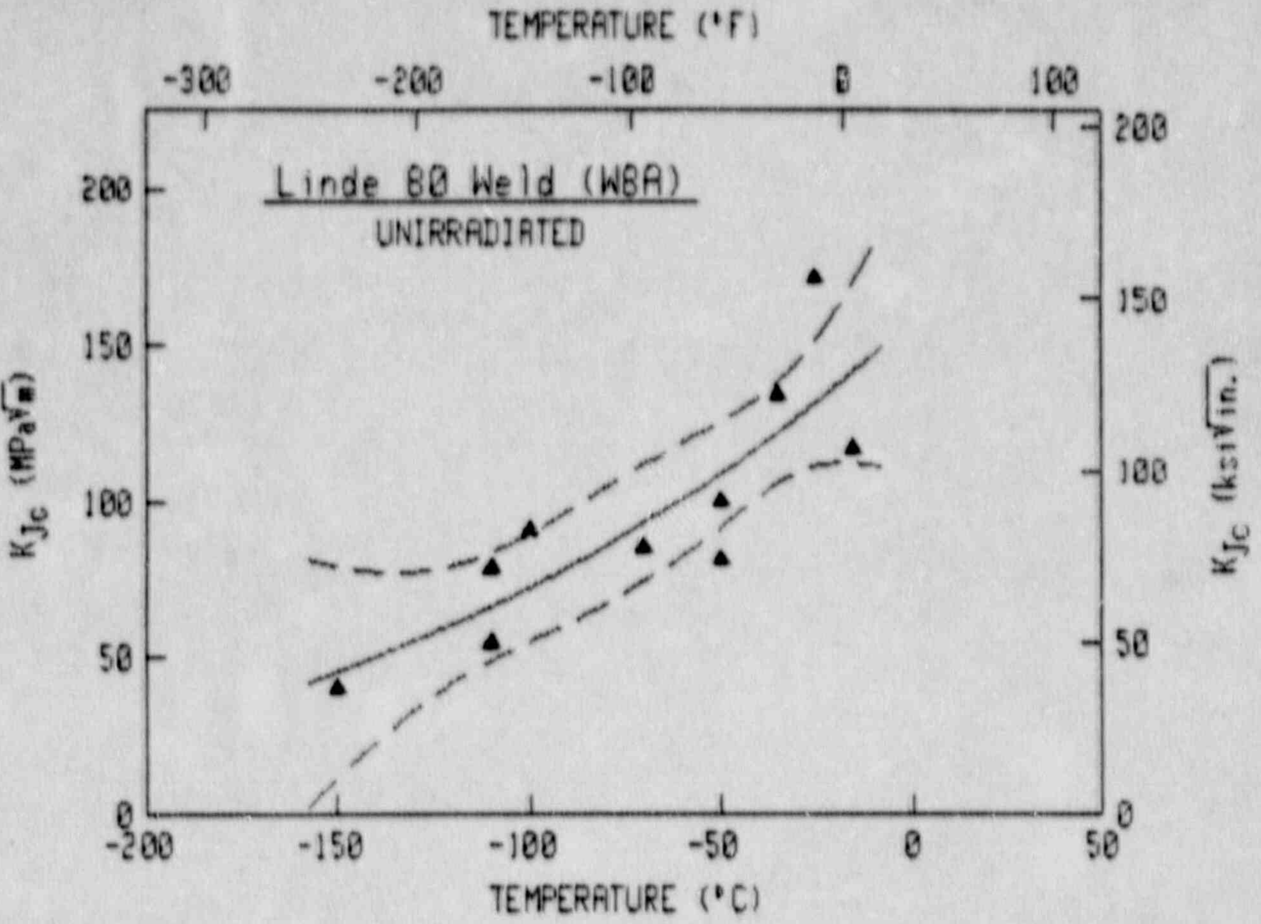

****

Kjc = A + B exp [(T-To)/C)]

	Metric	English
A =	-30.21 MPa√m	-27.50 ksi√in
B =	188.13 MPa√m	171.21 ksi√in
C =	164.52°C	296.13°F
To =	0.00°C	32.00°F

	Temperature at 100 MPa√m	
Upper Bound =	-85°C	-121°F
Mean Curve =	-61°C	-77°F
Lower Bound =	-41°C	-42°F

****

Pt #	Temperature	Kjc
1	-150	40.3
2	-110	54.6
3	-110	78.6
4	-100	90.9
5	-70	85.5
6	-50	100.2
7	-50	81.5
8	-35	134.5
9	-25	171.4
10	-15	117.2

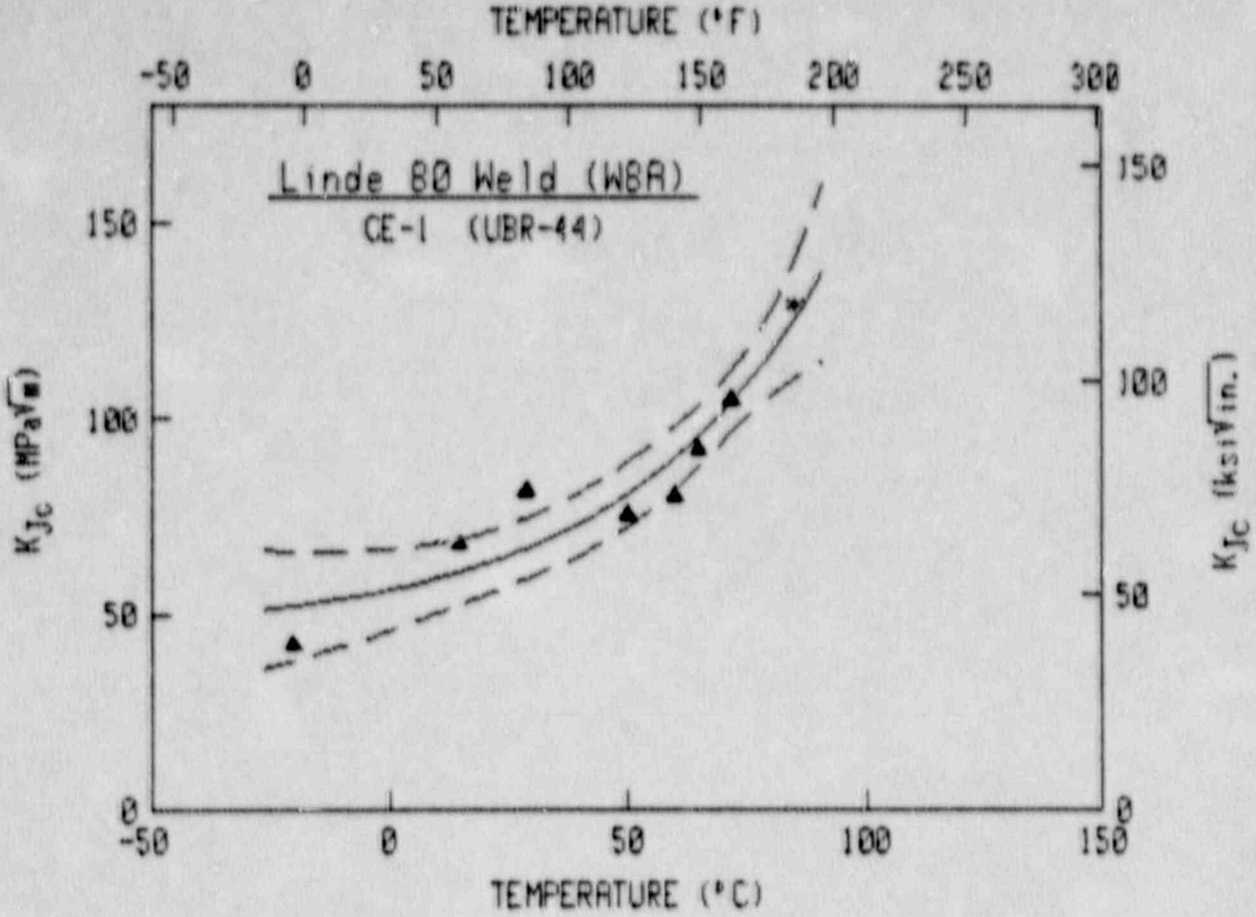

****

Kjc = A + B exp [(T-To)/C)]

	Metric	English
A =	45.32 MPa√m	41.25 ksi√in
B =	10.88 MPa√m	9.90 ksi√in
C =	42.56°C	76.61°F
To =	0.00°C	32.00°F

	Temperature at 100 MPa√m	
Upper Bound =	63°C	145°F
Mean Curve =	69°C	156°F
Lower Bound =	75°C	167°F

****

Pt #	Temperature	Kjc
1	-20	42.4
2	15	68.0
3	29	81.7
4	50	75.6
5	60	80.6
6	65	92.4
7	72	105.2
8 *	85	129.5

* = Upper Shelf Data Point

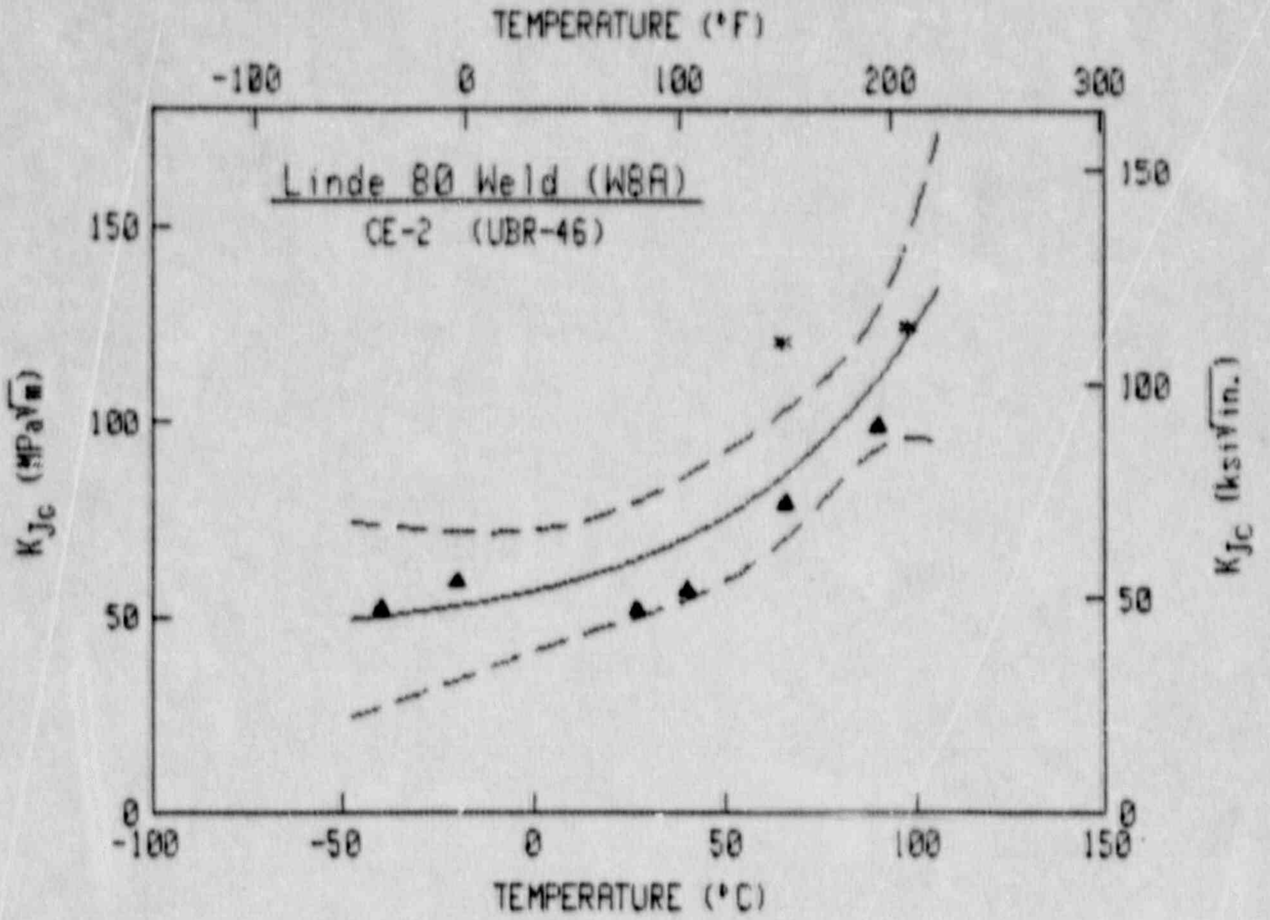

****

$$K_{jc} = A + B \exp[(T-T_o)/C)]$$

	Metric	English
A =	44.49 MPa√m	40.48 ksi√in
B =	12.18 MPa√m	11.08 ksi√in
C =	52.99°C	95.38°F
To =	0.00°C	32.00°F

	Temperature at 100 MPa√m	
Upper Bound =	62°C	144°F
Mean Curve =	80°C	177°F

****

Pt #	Temperature	Kjc
1	-40	52.3
2	-20	59.0
3	27	51.8
4	40	57.1
5	66	79.3
6	90	99.1
7 *	65	120.6
8 *	98	124.7

* = Upper Shelf Data Point

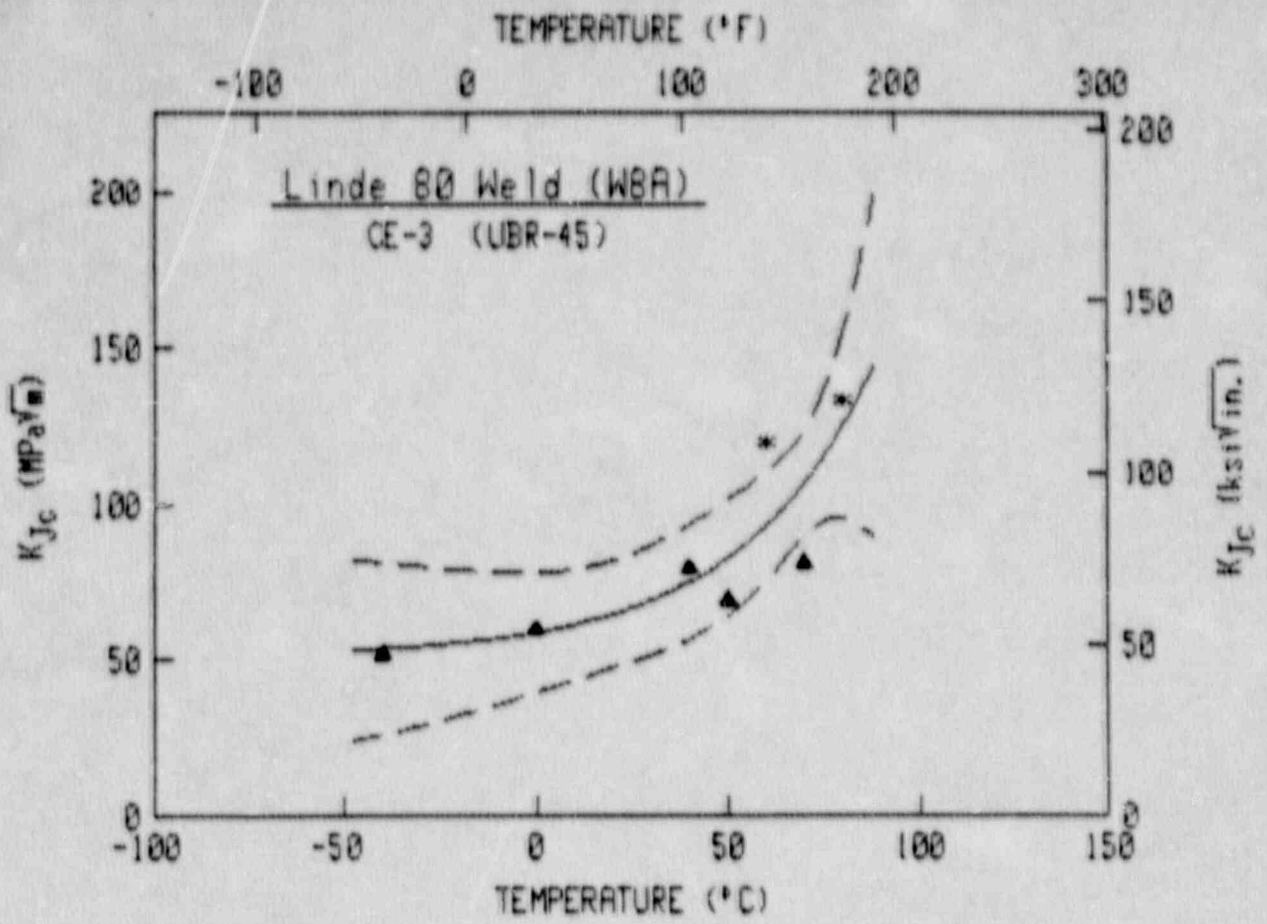

****

Kjc = A + B exp [(T-To)/C)]

	Metric	English
A =	51.10 MPa√m	46.50 ksi√in
B =	7.49 MPa√m	6.82 ksi√in
C =	34.96°C	62.92°F
To =	0.00°C	32.00°F

	Temperature at 100 MPa√m	
Upper Bound =	49°C	120°F
Mean Curve =	66°C	150°F

****

Pt #	Temperature	Kjc
1	-40	51.7
2	0	59.8
3	40	79.0
4	50	69.2
5	70	81.1
6 *	60	119.4
7 *	80	133.2

* = Upper Shelf Data Point

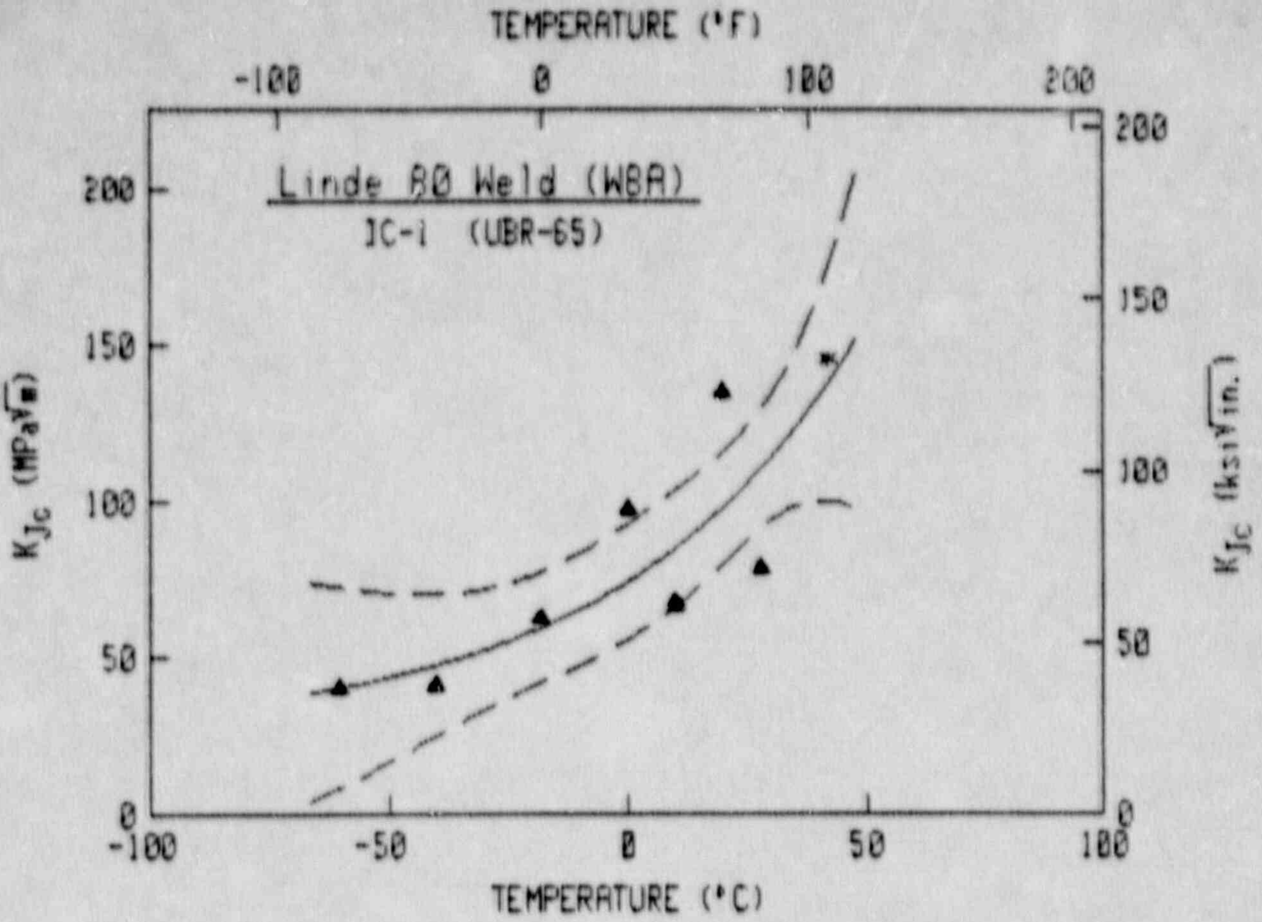

$$K_{jc} = A + B \exp[(T - T_o)/C]$$

	Metric	English
A =	25.58 MPa$\sqrt{m}$	23.28 ksi$\sqrt{in}$
B =	48.46 MPa$\sqrt{m}$	44.10 ksi$\sqrt{in}$
C =	50.23°C	90.41°F
To =	0.00°C	32.00°F

	Temperature at 100 MPa$\sqrt{m}$	
Upper Bound =	7°C	45°F
Mean Curve =	22°C	71°F
Lower Bound =	40°C	104°F

Pt #	Temperature	Kjc
1	-60	40.5
2	-40	41.1
3	-18	62.7
4	0	97.7
5	10	68.0
6	10	66.6
7	20	135.3
8	28	78.6
9 *	42	145.5

* = Upper Shelf Data Point

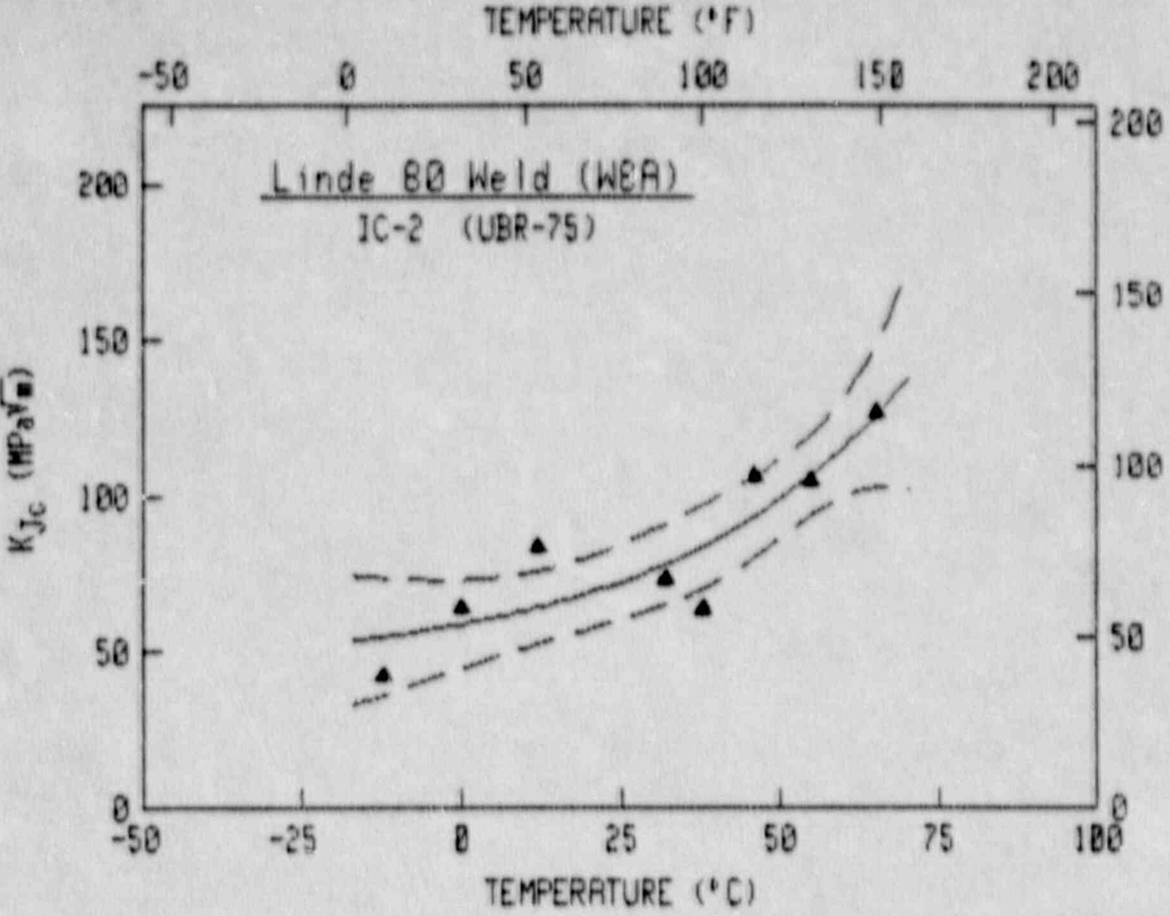

****

Kjc = A + B exp [(T-To)/C)]

	Metric	English
A =	44.93 MPa√m	40.89 ksi√in
B =	13.89 MPa√m	12.64 ksi√in
C =	36.91°C	66.44°F
To =	0.00°C	32.00°F

	Temperature at 100 MPa√m	
Upper Bound =	41°C	106°F
Mean Curve =	51°C	124°F
Lower Bound =	61°C	142°F

****

Pt #	Temperature	Kjc
1	-12	42.2
2	0	64.2
3	12	83.7
4	32	73.5
5	38	63.6
6	46	106.7
7	55	104.7
8	65	126.7

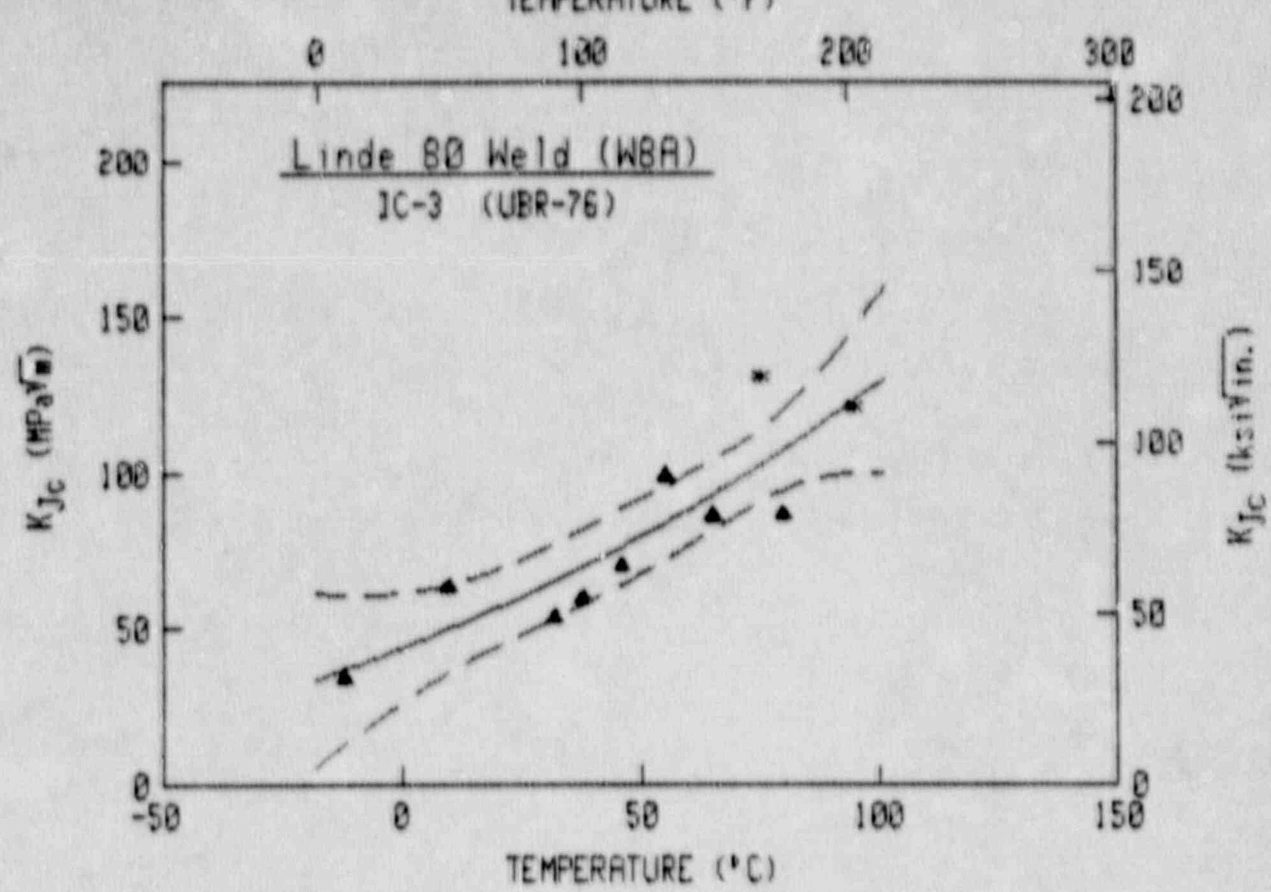

$$K_{Jc} = A + B \exp[(T-T_o)/C]$$

	Metric	English
A =	-49.78 MPa√m	-45.30 ksi√in
B =	93.48 MPa√m	85.07 ksi√in
C =	154.78°C	278.60°F
To =	0.00°C	32.00°F

	Temperature at 100 MPa√m	
Upper Bound =	61°C	142°F
Mean Curve =	73°C	163°F
Lower Bound =	97°C	207°F

Pt #	Temperature	Kjc
1	-12	34.3
2	10	63.3
3	32	53.7
4	38	59.6
5	46	70.1
6	55	99.2
7	65	86.3
8	80	86.8
9 *	75	131.2
10 *	95	121.1

* = Upper Shelf Data Point

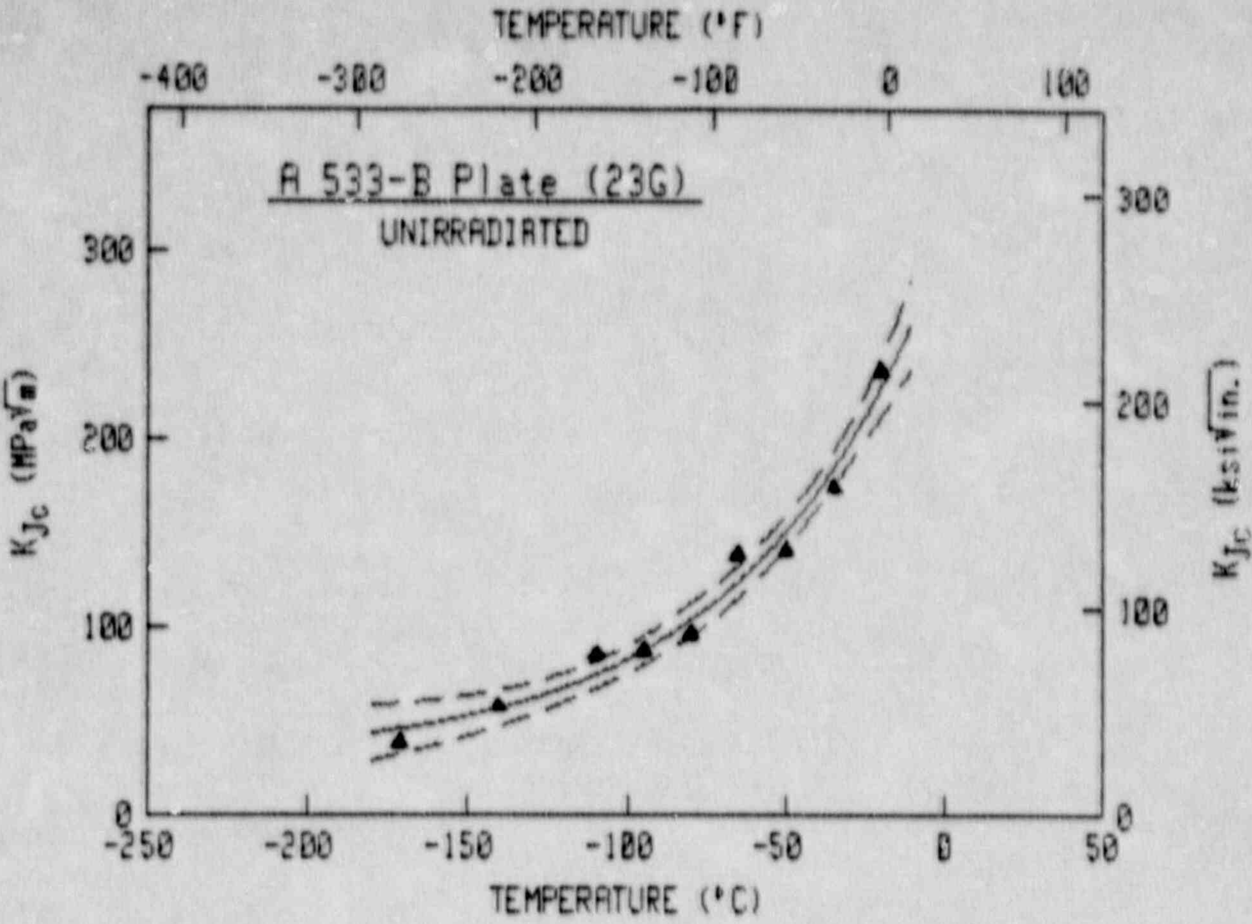

****

$$Kjc = A + B \exp[(T-To)/C)]$$

		Metric	English
A	=	29.21 MPa√m	26.59 ksi√in
B	=	276.59 MPa√m	251.71 ksi√in
C	=	60.83°C	109.49°F
To	=	0.00°C	32.00°F

	Temperature at 100 MPa√m	
Upper Bound =	-90°C	-130°F
Mean Curve =	-83°C	-117°F
Lower Bound =	-75°C	-103°F

****

Pt #	Temperature	Kjc
1	-171	39.0
2	-140	58.0
3	-110	85.7
4	-95	87.2
5	-80	96.0
6	-65	138.5
7	-50	141.1
8	-35	174.4
9	-20	236.2

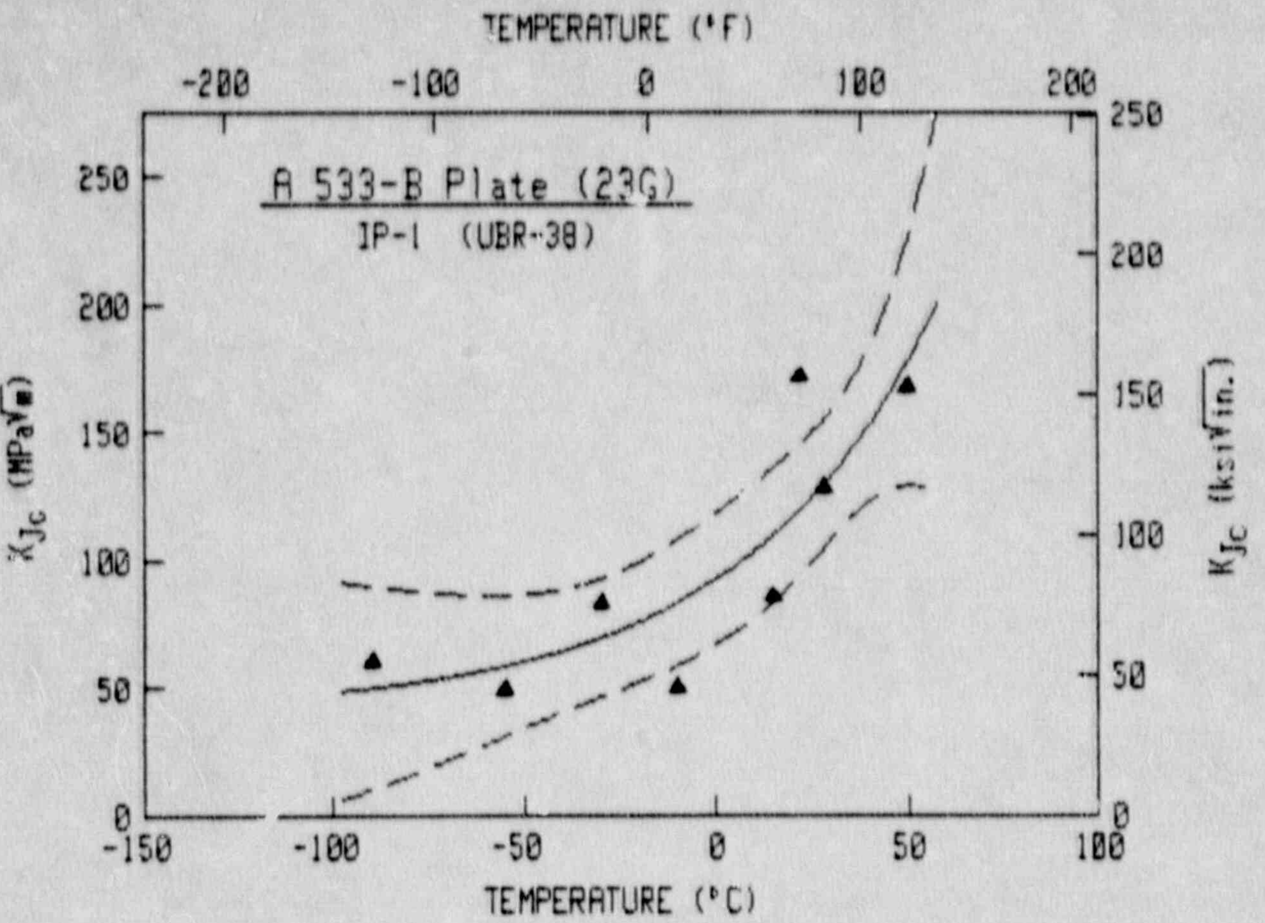

$$Kjc = A + B \exp[(T-To)/C)]$$

	Metric	English
A =	41.25 MPa$\sqrt{m}$	37.54 ksi$\sqrt{in}$
B =	51.03 MPa$\sqrt{m}$	46.44 ksi$\sqrt{in}$
C =	50.92°C	91.65°F
To =	0.00°C	32.00°F

	Temperature at 100 MPa$\sqrt{m}$	
Upper Bound =	-19°C	-2°F
Mean Curve =	7°C	45°F
Lower Bound =	26°C	79°F

Pt #	Temperature	Kjc
1	-90	60.5
2	-55	49.7
3	-30	83.4
4	-10	50.3
5	15	85.9
6	22	171.9
7	28	128.4
8	50	168.0

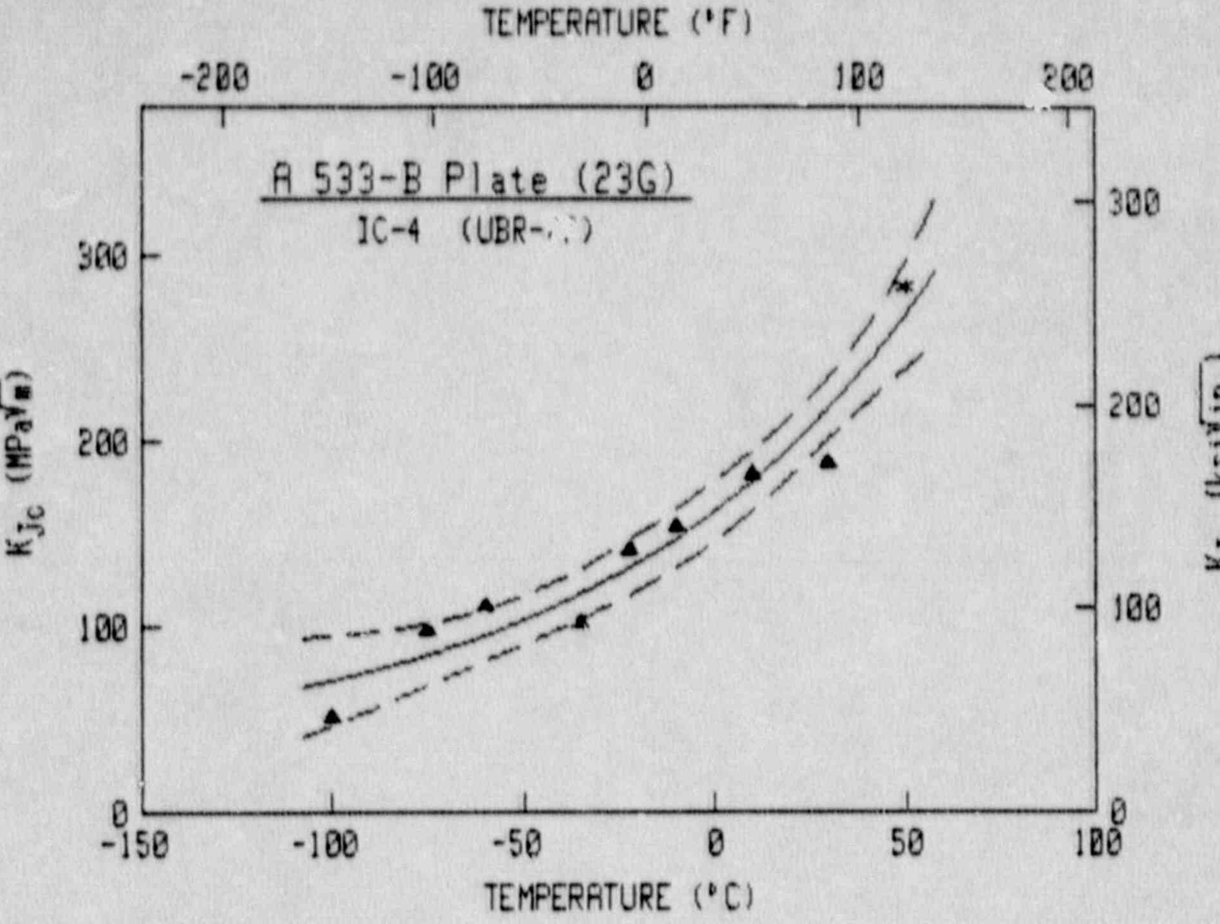

****

Kjc = A + B exp [(T-To)/C)]

	Metric	English
A =	30.60 MPa√m	27.85 ksi√in
B =	131.34 MPa√m	119.53 ksi√in
C =	84.53°C	152.16°F
To =	0.00°C	32.00°F

	Temperature at 100 MPa√m	
Upper Bound =	-78°C	-108°F
Mean Curve =	-54°C	-65°F
Lower Bound =	-38°C	-36°F

****

Pt #	Temperature	Kjc
1	-100	51.5
2	-75	98.1
3	-60	110.9
4	-35	101.9
5	-22	141.2
6	-10	153.9
7	10	182.8
8	30	188.2
9 *	50	283.0

* = Upper Shelf Data Point

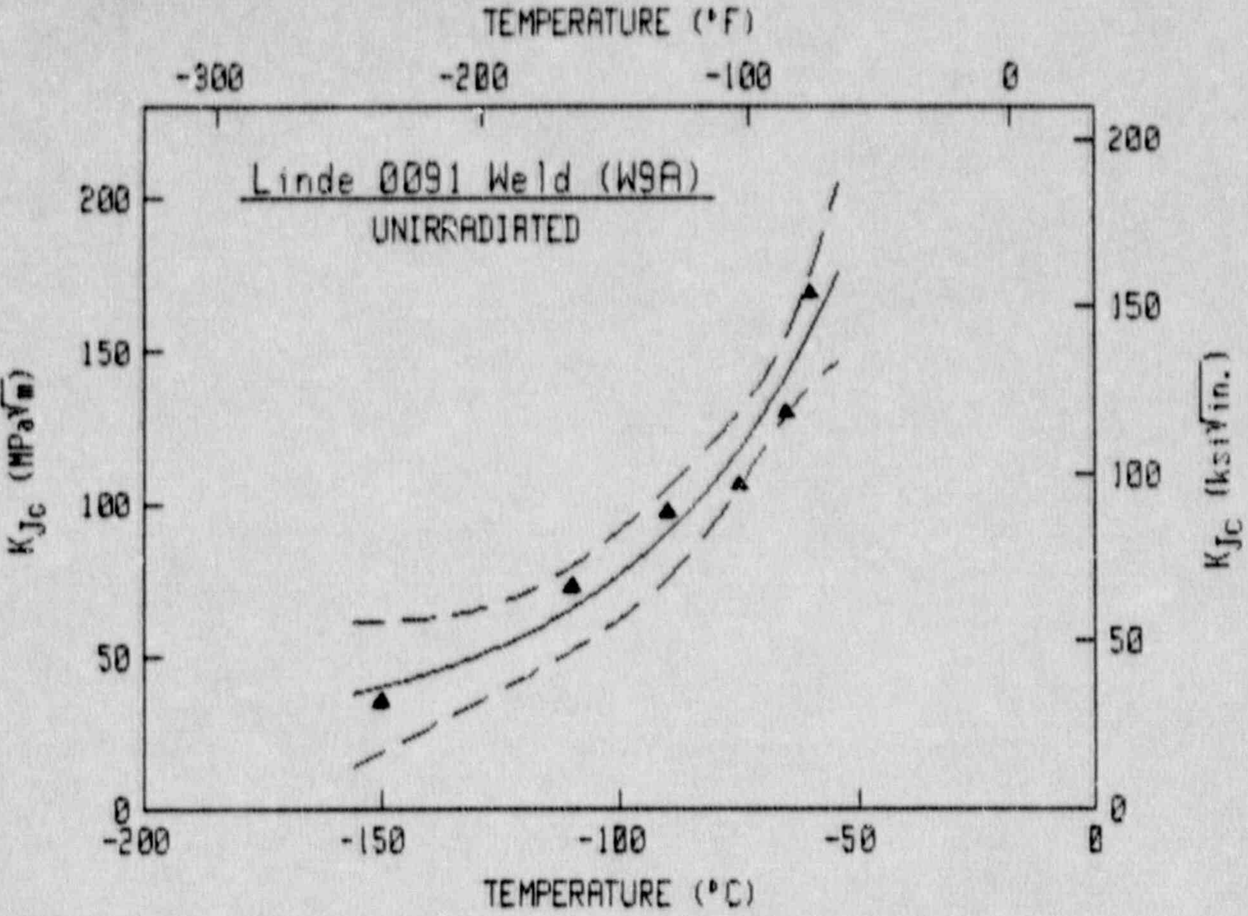

****

$$K_{jc} = A + B \exp[(T - T_o)/C]$$

		Metric	English
A	=	22.40 MPa√m	20.38 ksi√in
B	=	519.22 MPa√m	472.51 ksi√in
C	=	44.24°C	79.63°F
To	=	0.00°C	32.00°F

	Temperature at 100 MPa√m	
Upper Bound =	-93°C	-135°F
Mean Curve =	-84°C	-119°F
Lower Bound =	-77°C	-107°F

****

Pt #	Temperature	Kjc
1	-150	35.4
2	-110	72.7
3	-90	97.6
4	-75	106.4
5	-60	169.3
6	-65	130.1

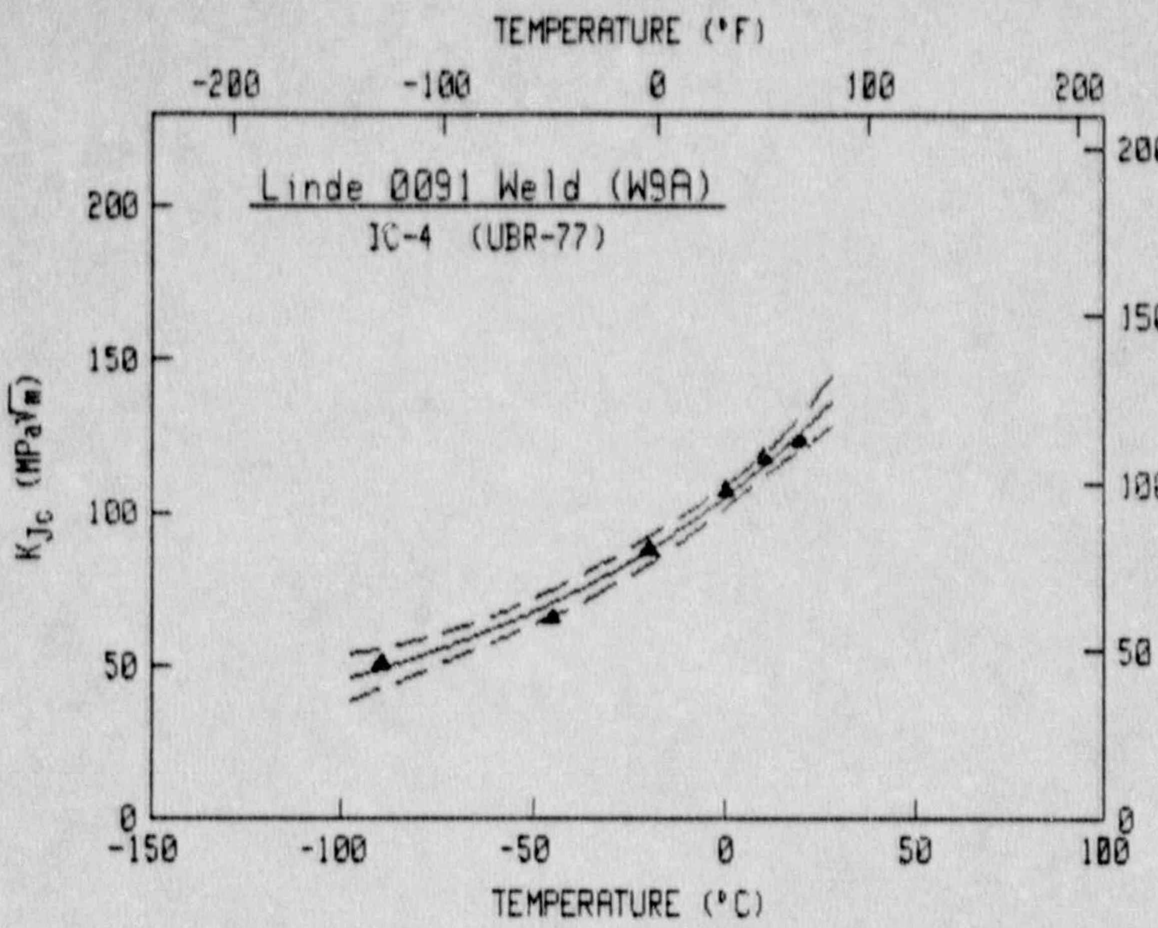

****

$$K_{jc} = A + B \exp[(T-T_o)/C]$$

	Metric	English
A =	13.69 MPa√m	12.45 ksi√in
B =	91.27 MPa√m	83.06 ksi√in
C =	94.29°C	169.72°F
To =	0.00°C	32.00°F

	Temperature at 100 MPa√m	
Upper Bound =	-9°C	16°F
Mean Curve =	-5°C	23°F
Lower Bound =	-1°C	30°F

****

Pt #	Temperature	Kjc
1	-90	50.6
2	-45	65.7
3	-20	88.4
4	0	107.5
5	10	118.0
6	20	123.1

NRC FORM 335 (2-89) NRCM 1102, 3201, 3202

U.S. NUCLEAR REGULATORY COMMISSION

BIBLIOGRAPHIC DATA SHEET

(See instructions on the reverse)

1. REPORT NUMBER (Assigned by NRC. Add Vol., Supp., Rev., and Addendum Numbers, if any.)
NUREG/CR-5493
MEA-2376

2. TITLE AND SUBTITLE
Influence of Fluence Rate on Radiation-Induced Mechanical Property Changes in Reactor Pressure Vessel Steels

Final Report on Exploratory Experiments

3. DATE REPORT PUBLISHED
MONTH: March YEAR: 1990

4. FIN OR GRANT NUMBER
B8900

5. AUTHOR(S)
J. R. Hawthorne, A. L. Hiser

6. TYPE OF REPORT
Technical

7. PERIOD COVERED (Inclusive Dates)

8. PERFORMING ORGANIZATION – NAME AND ADDRESS (If NRC, provide Division, Office or Region, U.S. Nuclear Regulatory Commission, and mailing address; if contractor, provide name and mailing address.)
Materials Engineering Associates, Inc.
9700-B Martin Luther King, Jr. Highway
Lanham, Maryland 20706-1837

9. SPONSORING ORGANIZATION – NAME AND ADDRESS (If NRC, type "Same as above"; if contractor, provide NRC Division, Office or Region, U.S. Nuclear Regulatory Commission, and mailing address.)
Division of Engineering
Office of Nuclear Regulatory Research
U. S. Nuclear Regulatory Commission
Washington, D.C. 20555

10. SUPPLEMENTARY NOTES

11. ABSTRACT (200 words or less)

This report describes a set of experiments undertaken using a 2 MW test reactor, the UBR, to qualify the significance of fluence rate to the extent of embrittlement produced in reactor pressure vessel steels at their service temperature. The test materials included two reference plates (A 302-B, A 533-B steel) and two submerged arc weld deposits (Linde 80, Linde 0091 welding fluxes). Charpy-V (C_v), tension and 0.5T-CT compact specimens were employed for notch ductility, strength and fracture toughness (J-R curve) determinations, respectively. Target fluence rates were 8×10^{10}, 6×10^{11} and 9×10^{12} n/cm^2-s^{-1}. Specimen fluences ranged from 0.5 to 3.8×10^{19} n/cm^2, E > 1 MeV.

The data describe a fluence-rate effect which may extend to power reactor surveillance as well as test reactor facilities now in use. The dependence of embrittlement sensitivity on fluence rate appears to differ for plate and weld deposit materials. Relatively good agreement in fluence-rate effects definition was observed among the three test methods.

12. KEY WORDS/DESCRIPTORS (List words or phrases that will assist researchers in locating the report.)
A 302-B steel, A 533-B steel, submerged arc welds, radiation effects, radiation embrittlement sensitivity, neutron fluence rate, dose rate effects, notch ductility, Charpy-V test, tension test, neutron irradiation, nuclear reactors, fracture toughness, J-R curves, correlations

13. AVAILABILITY STATEMENT
Unlimited

14. SECURITY CLASSIFICATION
(This Page) Unclassified
(This Report) Unclassified

15. NUMBER OF PAGES

16. PRICE